A theoretical study of the mechanism of (*S*) proline-catalysed aldol reactions

by

George Dhimba

Submitted in partial fulfillment of the requirements for the degree

Doctor of Philosophy

In the Faculty of Natural and Agricultural Sciences

University of Pretoria

Supervisor: Prof Ignacy Cukrowski

Co–supervisor Prof Darren Riley

Department of Chemistry

University of Pretoria

Declaration

I, George Dhimba declare that the thesis, which I hereby submit for the degree Doctor of philosophy at the University of Pretoria, is my own work and has not previously been submitted by me for a degree at this or any other tertiary institution.

SIGNATURE: g.Dhimba.……
DATE: ……21 December 2020…….

Outputs from this work

Conference Presentations:

George Dhimba, Dr Darren Riley, Prof Ignacy Cukrowski* New mechanistic insights for the role of DMSO in proline catalysed aldol. *CHPC conference* Pretoria 2017.

Publications

1. Cukrowski, I.; Dhimba, G.; Riley, D. L., A reaction energy profile and fragment attributed molecular system energy change (FAMSEC)-based protocol designed to uncover reaction mechanisms: a case study of the proline-catalysed aldol reaction. *Physical Chemistry Chemical Physics* **2019,** *21* (30), 16694-16705.

Abstract

In this study, the novel, reaction energy profile-fragment attributed molecular system energy change (REP-FAMSEC) was applied in studying mechanisms of chemical reactions. The applicability of the REP-FAMSEC protocol was tested for the mechanism of proline catalysed aldol reaction whereby several possible mechanisms have been debated for the past four decades. The approach quantifies and explains energy changes for each successive step along with the reaction profile. It mainly uses interaction energies between meaningful polyatomic fragments of a molecular system and generates energy contribution made by each fragment of a molecule. The fragments or atoms driving or opposing a change can easily be discovered and the reason for their (un)reactivity can be established. The relative stability and catalytic behaviour of (*S*) proline conformers including the zwitterion were fully explained at an atomic and molecular level. Though the zwitterion becomes the most dominant conformer in dimethyl sulfoxide (DMSO) solvent, it is not the active catalyst in proline catalysis. It forms very weak interactions with the ketone donor and will not form the active enamine catalyst.

The study shows that the first step of the catalytic reaction which was coined as the C–N bond formation using classical techniques, cannot be explained using the interaction of the $N^{\delta-}$,$C^{\delta+}$ atom pair but rather by the interaction of O-atom of acetone and the acidic H-atom of proline. Hence the first step is best described as the C–N bond formation/1st H-transfer. Based on this initial interaction the lowest energy conformer of proline is eliminated as a catalyst. When the REP is explored in the presence of an explicit solvent molecule of DMSO, FAMSEC shows that molecules of proline conformers (lowest **1a** and higher energy **1b**), acetone **2**, and DMSO **3** are involved in strong intermolecular interactions when they form 3-molecular complexes (3-MCs). The interactions formed by the molecule of DMSO weaken interactions between **1a** and **2** while strengthening those between **1b** and **2**, thereby eliminating **1a** as an inactive catalyst.

The zwitterion which becomes the most dominant in DMSO is converted to conformer **1a** through a low energy barrier intramolecular proton transfer. When formed conformer **1a** undergoes a puckering of the pyrrolidine ring resulting in its conversion to the catalytically active conformer **1b**. The presence of a molecule of acetone, DMSO, or a combination of the two molecules facilitates the structural change of proline from conformer **1a** to **1b**. This shows that there is no need to adhere to a specific sequence of reagent addition in proline catalysis. During the formation of the active enamine catalyst from an initial imine, it was found that the molecule of the eliminated water acts

as a medium for proton transfer relay while interaction involving the solvent molecule of DMSO is essential for decreasing the energy barrier and stabilising the resulting enamine catalyst.

Acknowledgements

Firstly, I give thanks and glory to God the Almighty and most High, in the name of Jesus Christ my Savior and Redeemer. The lord has been my strength and my habitation throughout my studies. I am very grateful to my supervisor, Prof. Ignacy Cukrowski for initiating this project, financial support, guidance, and constructive criticism. I thank my co-supervisor Prof Dareen Riley for his guidance, support, and supervision. I thank my wife Precious Nyaganga for her support, love, care, and sacrifice throughout my studies. Special appreciation goes to former and current students in the computational chemistry research group at the department of chemistry (University of Pretoria). I thank you guys for your support and companionship during my studies. To the leaders and brethren in the Lord I say thank you, your labour is not in vain, and you will surely receive your rewards. I would like to thank the University of Pretoria for providing a platform conducive for research and graduate studies and the National Research Foundation (NRF) for their financial support. I am very gratefully and acknowledge the Centre for High Performance Computing (CHPC), South Africa, for providing computational resources for this research project

Table of Contents

List of Figures

List of Tables

List of Abbreviations

AO–Atomic Orbital

BCPs–Bond critical points

BET–bonding evolution theory

B3LYP–Becke's three parameter hybrid exchange potential combined with Lee-Yang-Parr

DA–Dihedral angle

DFT–Density Functional Theory

ELF–Electron localisation function

FAMSEC–Fragment attributed molecular system energy

GD3–Grimme's empirical correction for dispersion

GTOs–Gaussian-type orbitals

HEC–Higher energy conformer

IQA–Interacting Quantum Atoms

IRC–Intrinsic reaction coordinate

LEC–Lowest energy conformers

LCAO–Linear Combination of Atomic Orbitals

MEDT–Molecular electron density theory

MO–Molecular Orbitals

MP2–Second order Møller-Plesset perturbation theory

NBO–Non-bonding orbitals

PES-Potential energy surface

QTAIM–Quantum Theory of Atoms in Molecules

REP–FAMSEC–Reaction energy profile-Fragment attributed molecular system energy

RCPs–Ring critical points

STOs-Slater-type orbitals

TSs–Transition states

Zw–Zwitterion

2-MC–Two molecular complex

3-MC–Three molecular complex

List of Uncommon Symbols Used

Terms applicable to entire molecular system (MS)

$E_{\text{int}}^{\text{MS}}$ Accounts for all possible intra and intermolecular interactions in a MS
$E_{\text{int}}^{\text{MS}} = {}_{\text{intra}}E_{\text{int}}^{\text{MS}} + {}_{\text{inter}}E_{\text{int}}^{\text{MS}}$

${}_{\text{intra}}E_{\text{int}}^{\text{MS}}$ Sum of all intramolecular interaction energies in a MS
${}_{\text{intra}}E_{\text{int}}^{\text{MS}} = {}_{\text{intra}}^{\text{C-B}}E_{\text{int}}^{\text{MS}} + {}_{\text{intra}}^{\text{L-D}}E_{\text{int}}^{\text{MS}}$

${}_{\text{intra}}^{\text{C-B}}E_{\text{int}}^{\text{MS}}$ Sum of interaction energies computed for all covalently bonded atom-pairs A,B individual molecules of a MS

${}_{\text{intra}}^{\text{L-D}}E_{\text{int}}^{\text{MS}}$ Sum of long-distance (L-D) intramolecular interaction energies computed for individu molecules in a MS

${}_{\text{inter}}E_{\text{int}}^{\text{MS}}$ Sum of all intermolecular interaction energies in a MS. Here MS = **1** (proline) + (acetone) + **3** (DMSO); hence, ${}_{\text{inter}}E_{\text{int}}^{\text{MS}} = {}_{\text{inter}}E_{\text{int}}^{\mathbf{1,2}} + {}_{\text{inter}}E_{\text{int}}^{\mathbf{1,3}} + {}_{\text{inter}}E_{\text{int}}^{\mathbf{2,3}}$

${}_{\text{inter}}E_{\text{int}}^{\text{mol-A,mol-B}}$ Sum of diatomic interactions energies computed between all atoms of molecule A and atoms of molecule B, e.g., ${}_{\text{inter}}E_{\text{int}}^{\mathbf{1,2}}$

Terms applicable to a molecule (mol)

$E_{\text{int}}^{\text{mol}}$ The total interaction energy computed for a molecule in an *n*-component MS. It is a su of intra and intermolecular contributions:
$E_{\text{int}}^{\text{mol}} = {}_{\text{intra}}E_{\text{int}}^{\text{mol}} + {}_{\text{inter}}E_{\text{int}}^{\text{mol}}$.

${}_{\text{intra}}E_{\text{int}}^{\text{mol}}$ Accounts for all intramolecular interactions:
${}_{\text{intra}}E_{\text{int}}^{\text{mol}} = {}^{\text{C-B}}E_{\text{int}}^{\text{mol}} + {}^{\text{L-D}}E_{\text{int}}^{\text{mol}}$.

${}_{\text{intra}}^{\text{C-B}}E_{\text{int}}^{\text{mol}}$ Sum of interaction energies computed for all covalently bonded atom-pairs A,B in individual molecule, e.g., ${}_{\text{intra}}^{\text{C-B}}E_{\text{int}}^{\mathbf{1}}$ describes combined strength of covalent bonds ir molecule numbered **1**, i.e., proline in this work.

${}_{\text{intra}}^{\text{L-D}}E_{\text{int}}^{\text{mol}}$ Sum of interaction energies computed for long-distance, L-D, covalently non-bond atom-pairs A,B in individual molecule.

${}_{\text{inter}}E_{\text{int}}^{\text{mol}}$ The total intermolecular interaction energy between atoms of the specified molecule a atoms of remaining molecules in a MS Here MS = **1** + **2** + **3**; hence, for acetone ${}_{\text{inter}}E_{\text{int}}^{\mathbf{2}} = {}_{\text{inter}}E_{\text{int}}^{\mathbf{1,2}} + {}_{\text{inter}}E_{\text{int}}^{\mathbf{2,3}}$

${}_{\text{inter}}E_{\text{int}}^{\mathbf{1a,(2,3)}}$ Sum of intermolecular interaction between atoms of a molecule (here LEC of proline **1** and atoms of other two molecules (here acetone **2** and DMSO **3**)
${}_{\text{inter}}E_{\text{int}}^{\mathbf{1a,(2,3)}} = {}_{\text{inter}}E_{\text{int}}^{\mathbf{1a,2}} + {}_{\text{inter}}E_{\text{int}}^{\mathbf{1a,3}}$

Chapter 1

Introduction

1.0 Proline in organocatalysis

The past few decades have witnessed a rapid progression in the use of organocatalysis as an active synthetic tool in organic chemistry.[1,2] This has largely been driven by the increasing demand of enantiomerically pure and multi–functionalised complex compounds which possess important biological activities.[3,4] Though transition metal complexes have been successfully employed in synthesising such compounds, the challenges of removing traces of toxic heavy metals and the demands for green chemistry have prompted the search for alternative strategies. Thus, organocatalysts are perfect substitutes owing to their notable advantages over metal-mediated approaches.[5–7] The term organocatalyst is often used to describe organic compounds of low molecular weights which in substoichiometric amounts can speed up the rate of synthetic reactions.[5]

The (*S*) proline-catalysed Hajos–Parrish–Eder–Sauer–Wiechert (HPESW) reactions represent the earliest examples of the utilisation of proline in organocatalysis.[8,9] The amino acid proline has been regarded as an enzyme mimic[10,11] and is remarkable owing to its ability to catalyse various organic transformations.[1,2] The pyrrolidine ring together with the carboxylic group has been cited to be essential for asymmetric induction. Though the success of the HPESW reactions triggered interests in the use of proline in organocatalysis, the area remained dormant for nearly four decades probably due to a bias towards metal catalysis. A rejuvenation was brought about in 2000 by List and Barbas when they reported that (*S*) proline and its derivatives can catalyse the direct aldol reaction between aldehydes and ketones with high yields and enantioselectivities.[12]

1.1 Proline catalysed aldol reactions and the importance of chirality

The aldol reaction represents one of the most fascinating C–C bond-forming reactions, both in nature e.g., in the metabolism of carbohydrates[13,14] and in synthetic chemistry.[10] Nature uses enzymes, usually aldolases, in typical aldol reactions during catabolism, anabolism, and metabolism of oxygenated metabolites.[15] For synthetic chemists, the aldol reaction is used in the synthesis of target molecules possessing predetermined chemical properties that are relevant to the academia and chemical industry. Since the reaction results in the formation of new chiral centres, control of the resulting absolute configuration is very essential.

In chemical sciences, chirality is a distinguishing feature of asymmetric and total synthesis, this has been evidenced by the current extensive research in this area. Importantly, most useful chemicals, drugs, pesticides, and food colorants or preservatives are chiral molecules, hence careful control is needed when synthesising such compounds. An important property of chiral

molecules is that when one enantiomer, for instance, displays desirable biological or pharmacological activity towards a target, its opposite pair may be inactive, toxic or in some cases inhibit such activity. To this effect, necessary deliberation on chirality is now the central focus of chemical development and research. The resuscitation of proline catalysis and it's analogues has enabled the construction of complex chiral molecular architectures from very simple prochiral molecules under mild conditions in one pot.

1.2 Advantages of direct aldol reactions

Asymmetric aldol reactions are generally classified into two main categories, one type involves pre-conversion of aldol donors (usually ketones and esters) into more reactive enol ethers or ketene acetals. This approach mainly utilises chiral Lewis acids and bases which generates unwanted waste by-products. On the contrary, the second approach is an atomically economic direct aldol reaction between unmodified ketones with aldehyde acceptors. The ability of organocatalysts to impart asymmetric induction in catalytic reactions is the reason for their recent prominence. The rapid shift towards organocatalysis is a result of their practical advantages offered to the synthetic chemist, academia and other beneficiaries of such technologies. For proline, its abundance and cost-effectiveness when used for conducting pilot reactions in the laboratory coupled with the possibility of opening new areas in academic research and investigation have made it an interesting molecule. In addition, its availability in both enantiomeric forms, ease of separation from products and ability to catalyse scores of organic reactions makes it an attractive catalyst.

Hence, its numerous catalytic applications in synthetic transformations have made it a prototype of asymmetric organocatalysis.[16] The presence of a chiral centre and the bifunctionality resulting from the proximity of the basic amine and the acidic carboxyl moiety are essential attributes leading to its efficiency in asymmetric catalysis. The two functional groups can act as both acids and bases following protonation or deprotonation, thereby facilitating synthetic transformation in concurrence as observed in enzyme catalysis.[17] The use of amino acids as catalysts, and more importantly proline, remains unrivalled by no class of chiral organocatalysts in terms of stability and accessibility.

The possibility of a simple organic molecule to act as an enzyme opens a wide range of synthetic alternatives to the existing asymmetric transformations. This would potentially allow the production of chemically useful chiral intermediates and building blocks at a lower cost.

Proline in particular has been shown to act as an enzyme mimic as demonstrated by List, Lerner, and Barbas[12] in their seminal paper.

1.3 Effect of solvents on the aldol reaction.

One of the most outstanding features of the proline-catalysed aldol reaction is its ability to tolerate a variety of solvents.[18] The reaction has been reported to proceed smoothly under protic[19] and aprotic solvents, including solvent mixtures. The use of anhydrous conditions was originally cited to be the most ideal condition.[12] Nevertheless, the presence of water in small quantities was reported to cause an enhancement of reaction yields with good enantioselectivity, indicating that strictly controlled anhydrous conditions are not necessary.[20–22] Alternative solvents including chlorinated solvents,[23] cyclic carbonates,[24] and ionic liquids[25] have also been reported to promote the reaction producing the aldol product in moderate to high yields and enantioselectivity.

1.4 Catalytic activity of *S*–proline conformers

In nature, the amino acid proline exists predominantly as an equilibrium between the zwitterion, and neutral conformers (Figure 1.1). The zwitterion has been reported to be lower in energy compared to the lower and higher energy conformers (LEC and HEC) by a magnitude of 2.6 and 8.6 kcal/mol, respectively.[26,27]

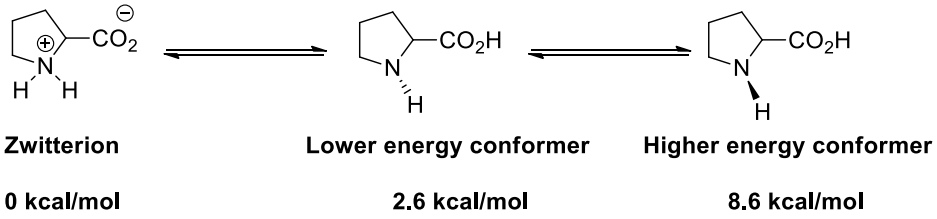

Figure 1.1. Equilibrium between the zwitterion and non-ionic conformers of proline

Arno and Domingo[26] reasoned that only the neutral forms (LEC or HEC) will result in the formation of the active enamine after a nucleophilic attack on the ring nitrogen. The two hydrogen atoms attached to the ring nitrogen in the zwitterion possibly hinder the approaching nucleophile and prevent the formation of a C–N bond between proline and the ketone coupling partner. In principle, the small energy difference between the zwitterion and the LEC allows an equilibrium to exist between the zwitterion and the neutral conformers.

1.5 Mechanism of the proline-catalysed aldol reaction

The study of reaction mechanism/s is one of the main focuses of synthetic organic chemistry. For optimisation, control or a possible scale-up, a detailed understanding of the reaction profile

needs to be fully understood. In many cases, the reaction profile consists of isolated reactants through adduct/s and transition state/s to products and sometimes unwanted side reactions. The mechanism of the proline-catalysed aldol reaction is a rather complex multi-step process and elucidating a reaction mechanism involving the formation of several adducts, complexes and intermediates often becomes too demanding for experimental tools alone. As a result, and due to the potential use of proline as a catalyst, several mechanisms were proposed over the years.[8, 27–31] The proline-catalysed aldol reaction was independently discovered by the groups of Hajos and Parrish[8] and Wiechert, Eder, and Sauer[9] in their efforts to synthesise steroids, (**3** and **6** in Figure 1.2) which are important building blocks in natural product synthesis. Under Wiechert's conditions, the aldol product **5** was not isolated but undergoes water elimination at high temperatures (80–100ºC) in the presence of an acid cocatalyst (HCl or $HClO_4$) to yield enedione **6**.

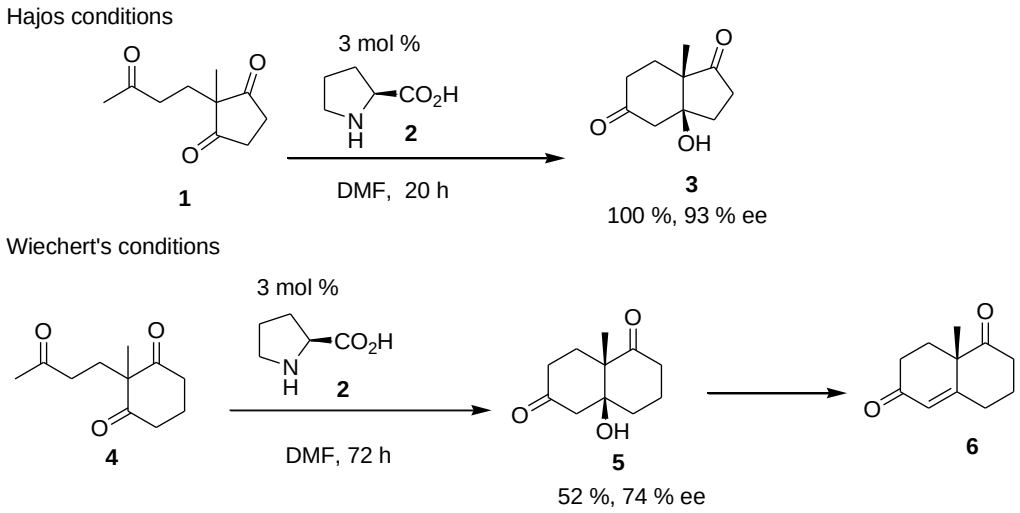

Figure 1.2. Hajos-Parrish-Eder-Sauer-Wiechert aldol reaction.

1.5.1 Chronicles of the mechanism of proline-catalysed aldol reactions

1.5.1.0 Mechanistic studies using experimental observations.

At its inception in the 70s, Hajos and Parrish tentatively proposed two mechanisms, the first involves an initial formation of a carbinolamine intermediate (**7** in Figure 1.3) between proline and triketone **1**. This is followed by the formation of an enol at the side chain ketone causing the displacement of proline and formation of intermediate **A**. The second involves an enamine intermediate (**8**) and nucleophile for the stereoselective C–C bond formation which is accompanied by a concomitant (N–H···O) proton transfer from the ring nitrogen to the carbonyl oxygen (**C** in Figure 1.3). The researchers eliminated mechanism **C** in favour of mechanism **A** based on ^{18}O labelled water experiment, in which there was no evidence of ^{18}O incorporation in the product.

This was in contradiction to earlier experimental studies by Spencer,[32] and Eschenmoser,[33] which showed evidence of enamine intermediates in amine and amino acid-catalysed aldol reactions.

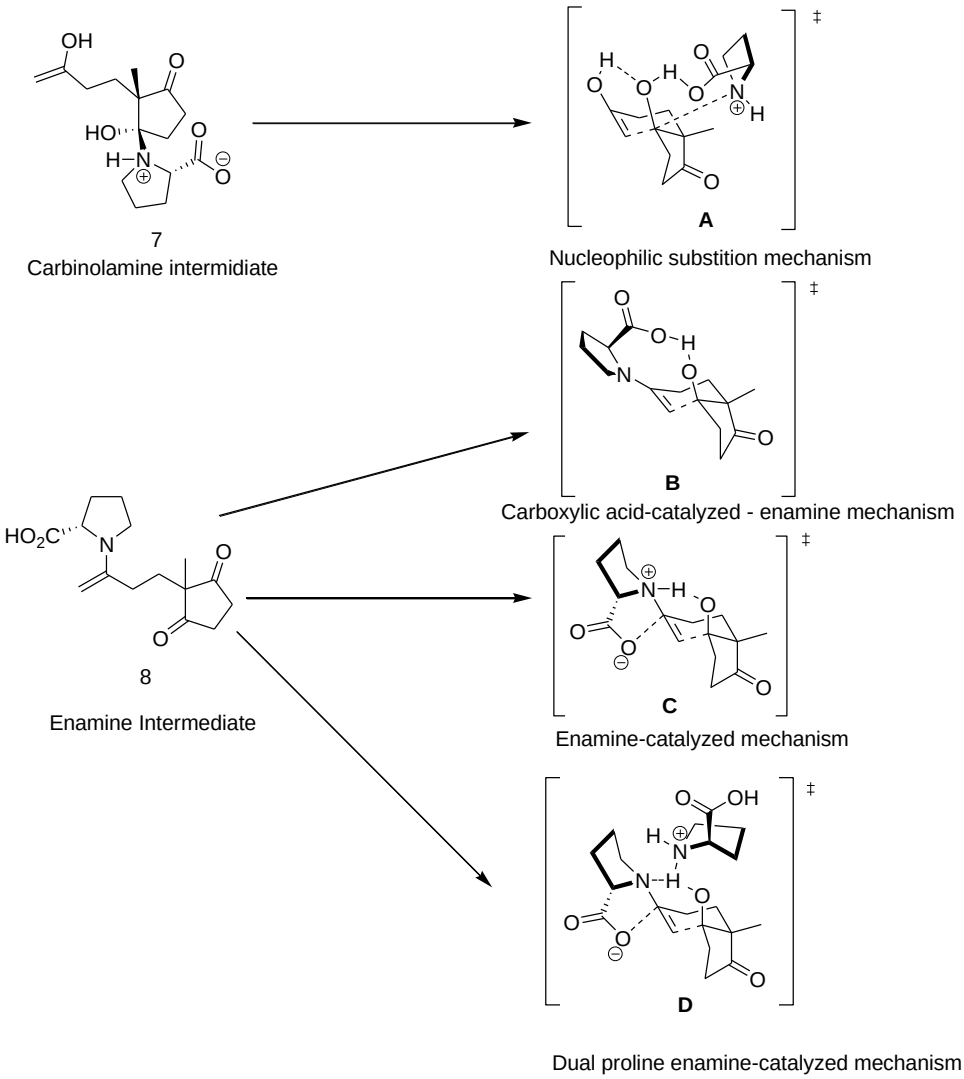

Figure 1.3. Proposed mechanism for the proline-catalysed intramolecular aldol reaction

No attention was given to mechanism **B** initially proposed in a review on annulation in the mid-70s.[34] It involves the C–C bond formation with concomitant proton transfer from the carboxylic group to the oxygen atom of the acceptor. However, mechanism **D** involving a second proline to facilitate the proton transfer process proposed in the 80s[31,35] became the generally accepted mechanism until the year 2000. It was supported by polarimetric studies that claimed minor nonlinear kinetic effects which demonstrated more than one proline molecule in the stereo controlling step. In their seminal paper, List and his group proposed a proline-catalysed intermolecular molecular aldol reaction which proceeds in a mechanism similar to **B** (Figure 1.4).[12]

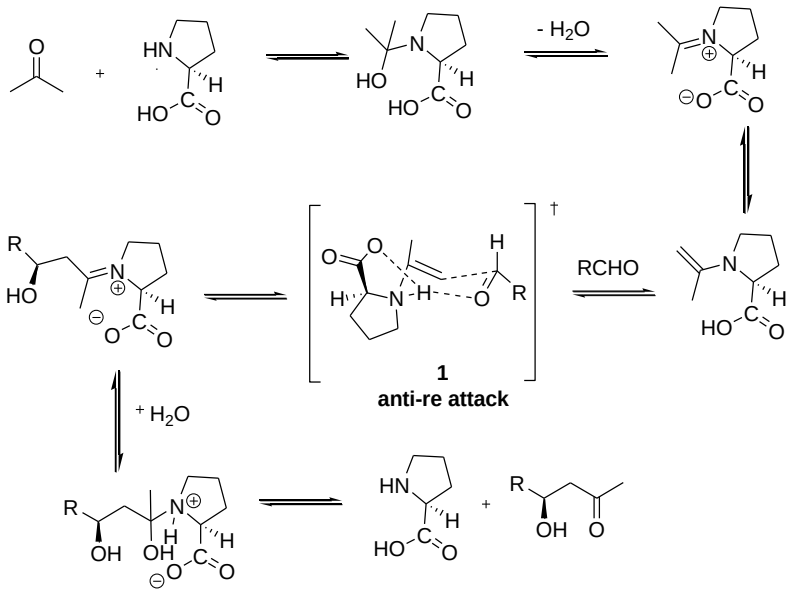

Figure 1.4. List mechanism for the intermolecular variant

In an effort to understand the details regarding the mechanism of the cyclisation of triketone **1**, List, Hoang, and Martin[36] revisited the reaction mechanism using the intramolecular variant. The report by Hajos and Parish that claimed no ^{18}O incorporation made the mechanism a mystery since it totally eliminated the enamine as a possible intermediate. As a result, List and co-workers repeated the ^{18}O labelled water experiment as outlined by Hajos and Parish but under carefully controlled conditions and observed efficient (> 90%) ^{18}O incorporation in the product as predicted by the enamine mechanism (Figure 1.5).

The observed non-linear effect reported by Agami was the remaining mechanistic puzzle that needed to be unlocked. For this reason, Hoang, Bahmanyar, and Houk re-investigated the mechanism of proline catalysed intramolecular cyclisation of triketone **1** and intermolecular addition reactions.[37] They observed that the reaction is first order with respect to proline which indicates the presence of only one proline molecule in the C–C bond formation. More evidence that reaffirms the enamine mechanism was provided by experimental studies by the group of Gschwind[38–40] who detected the presence of proline enamines *in situ*.

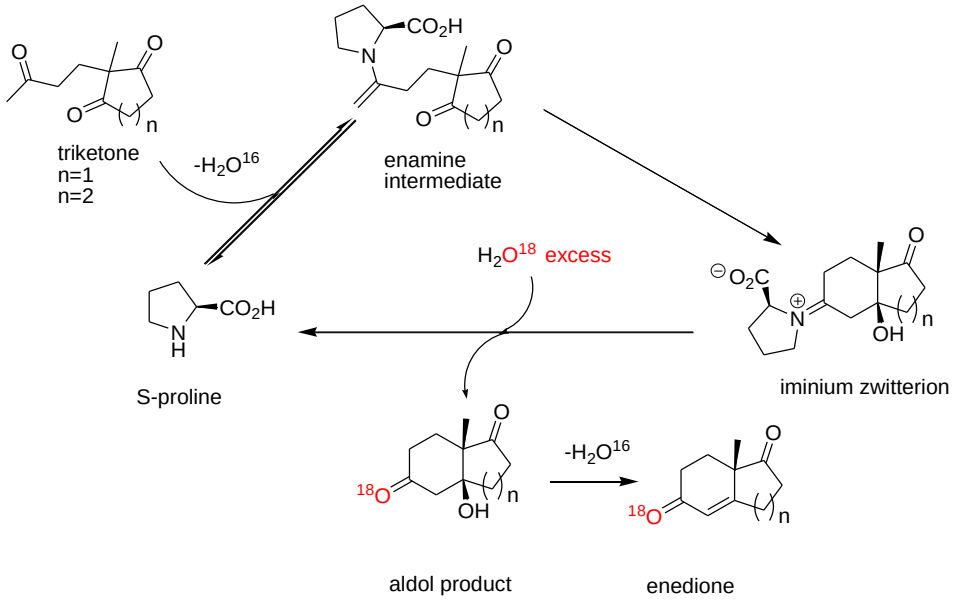

Figure 1.5. ^{18}O incorporation in the Hajos-Parish-Eder-Sauer-Wiechert reaction in the presence of ^{18}O enriched water.

1.5.1.1 Mechanistic studies using theoretical predictions.

In 2004 Clemente and Houk,[29] with the aid of density functional theory calculated the relative energies of all the proposed intermediates in Figure 1.3. Interestingly, their findings demonstrated that the carboxylic acid assisted enamine mechanism **B** is energetically the most favoured pathway. When compared to mechanism **B**, the carbinolamine (intermediate **7**) is 12 kcal/mol higher in energy at B3LYP/6-31+G(d,p) level while the enamine catalysed (intermediate **C**) is 30 kcal/mol higher in energy at the same level of theory. The group was, however, unable to locate the carbinolamine intermediate **A** suggested by Hajos and Parish. At present, the carboxylic acid assisted enamine mechanism is the most widely accepted mechanism for proline-catalysed aldol reaction.

1.6 Justification of the research

Although it is currently largely accepted that the proline-catalysed aldol reactions proceed via the carboxylic acid-mediated enamine intermediates, the mechanistic details of the intermolecular variant remain elusive. Many, if not most, of the computational reports[26, 29,41–45] concentrate on the later stages of the reaction mechanism (involving the already formed enamine catalyst), giving less attention to the crucial proline–acetone (Prl–Ac) adduct formation and the C–N bond formation, with only a few papers,[27,28,46,47] emphasizing importance of this fundamental initial step. What is striking is that these few papers are at variance with each other, indicating that a reasonable

convention is not yet achieved. For instance, Rankin *et al.*[28] who were the first to computationally study the mechanism of the intermolecular variant (between acetone and acetaldehyde), reported only two proline–acetone adducts. The first involves the LEC forming a transition state in a four-membered ring for the C–N bond formation step (Figure 1.6).

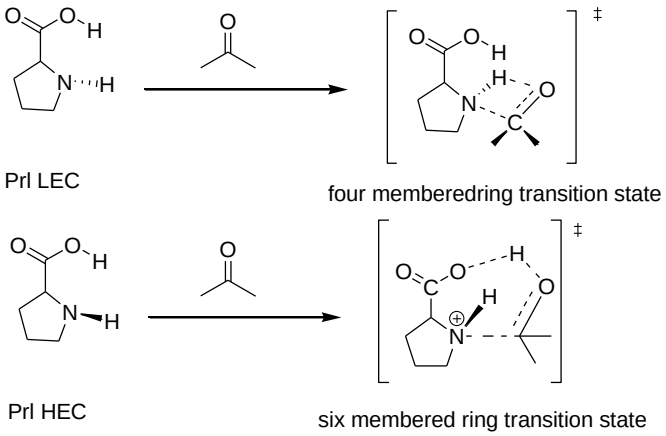

Figure 1.6. Boyd transition state for the C–N bond formation

This was computed in the gas phase and has an activation electronic energy of 171 kJ/mol at B3LYP/6-311+G(2df,p)//B3LYP/6–31G(d,p) level of theory. While the second involves the HEC forming a six-membered ring transition state in DMSO implicit solvation model and has an activation electronic energy of 40.7 kJ/mol. It is unclear why the reaction would follow a mechanism involving a four-membered ring in the gas phase and a six-membered ring in implicit solvent. One can easily undertake that the transition state involving a four-membered ring was not stable enough and is not a stationary point when optimised in DMSO implicit solvation model, hence the researchers assumed that it represented the gas phase transition state. The six-membered ring transition state could still be optimised in the gas phase and its transition energy determined; it will obviously be lower than 171 kJ/mol. Also, it is apparent that the high activation energy of 171 kJ/mol would hinder subsequent steps and the progress of the reaction.

In their quest to explore more Prl–Ac interaction modes Yang *et al.*[46] revisited the mechanism and reported six other Prl–Ac interaction modes in a DMSO implicit solvation model. Among them, only two led to the C–N bond formation but in both cases the activation electronic energy was much larger (either 136 or 86 kJ mol^{-1} for the two possible paths) when compared to the earlier reported transition state.[12] Interestingly and importantly, Ajitha *et al.*[17] reported that the HEC rather than the LEC should be the active catalyst in proline-catalysed aldol reactions. The mechanism involving the LEC could not proceed beyond the C–N bond formation due to the high energy demand of the proton transfer step.

The zwitterion has been previously reported to be an unreactive species in proline catalysis due to the quaternisation of the ring nitrogen which consequently removes its nucleophilicity.[26] Nonetheless, the use of the hygroscopic DMSO solvent in proline catalysis stabilizes the zwitterion to a large extent compared to neutral conformers, thereby making it more predominant.[48,49] For this reason, Yang and Zhou recently suggested that the zwitterion should be considered as the active catalyst in the proline-catalysed aldol reactions.[47] They proposed the formation of a complex between a water molecule, acetone, the zwitterion, and a DMSO solvent molecule. In their mechanism, a water molecule facilitated the transformation of the zwitterion into the HEC. However, this initial step has an activation electronic energy of 88.8 kJ mol^{-1} at the MP2/6-311++G(3df,2pd)//B3LYP/6–31+G(d,p) level of theory, which is higher than the one reported by Rankin using an implicit solvation model. The involvement of the HEC in their modelling is in agreement with earlier reports which suggest that the HEC is the active species in the proline catalysed aldol reaction but their computed energy for the initial step was by far higher than the previously reportedy.[27]

Very recently when this thesis was in preparation Nobahkt and Arshadi[50] reported that the enol rather than the enamine should be considered as the key intermediate and hence the preferred pathway in a proline-catalysed aldol reaction. This claim was based on theoretical calculations that show a preferential kinetic formation of oxazolidinone as opposed to the enamine. Nevertheless, experimental evidence supports the formation of oxazolidinone which can either undergo a reversible reaction back to reactants or be converted to the active enamine[38] as shown in Figure 1.7.

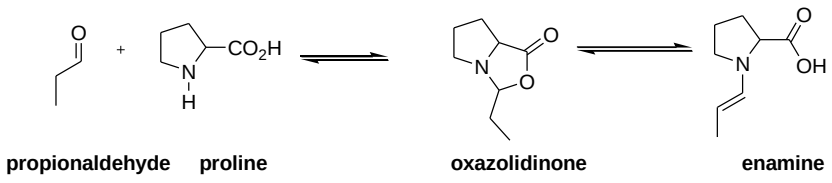

Figure 1.7. Reversible formation of oxazolidinone

Apart from the formation of the active enamine catalyst, the stereoselective C–C bond formation is one of the most critical steps in proline catalysed intermolecular aldol reactions, it involves the addition of aldehyde substrate to the *in-situ* formed active enamine.[26,51] Four possible and distinct transition state has been identified for this step – they correspond to *syn-re*, *syn-si*, *anti-re*, and *anti-si* where the prefix represents the nature of the enamine either *anti* or *syn* and the suffix represents the face of the prochiral aldehyde substrate being attacked (*re* or *si*).[27,45]

According to the Houk-List model,[45] the transition state structure with the lowest energy is considered the preferred pathway through which the reaction proceeds. Transition states arising from the *syn*-enamines are generally higher in energy than their *anti*-analogues and their prediction of the aldol outcome contradicts experimentally observed results.[26,36,51] As a result, the *syn*-enamine is considered inactive conformer in proline catalysed aldol reaction. On the other hand, the *anti*-enamine is regarded as the active catalyst in proline catalysis, the *anti-re* attack predicts the correct stereochemistry of the aldol product as obtained in experimental studies.

Although the Houk-List model has been successful in predicting the stereochemical outcomes of proline catalysed aldol reactions, the success was deemed coincidental.[52,53] It was successfully used to predict the selectivity of the reaction between cyclohexanone and benzaldehyde in excellent agreement with experiment.[51] However, subsequent comprehensive conformational searches resulted in transition states with lower energies, this potentially affects the predicted selectivity. In addition, experimental studies showed that the high selectivity obtained was a result of serendipitous involvement of water, which is not included in computational predictions.

Moreover, in most cases, the *anti-re* transition is only marginally lower in energy than the *anti-si* yet the two predict opposite enantiomers. The reaction between acetone and isobutyraldehyde is a perfect example in this regard, the experimental enantiomeric excess (ee) for this reaction was found to be 96%,[12] yet the *anti-re* transition state was calculated to be only 1.5 kcal/mol lower in $\Delta G_{298(\varepsilon=47)}$ than the *anti-si* transition state.[45] In another study, the *anti-re* transition state was reported to be lower in energy than the *anti-si* by 1.4 kcal/mol.[26] Surprisingly, it was reported in both cases that the calculations were in excellent agreement with experimental outcomes. Though it can be appreciated that computational calculations are meant to provide a predictive assessment the small energy difference observed could be interpreted as suggesting that the reaction would suffer from a poor enantiomeric excess (a mixture of both products). These calculations were conducted in the absence of dispersion correction D3 which is often needed for accurate energy optimisation of complex structures. Its inclusion will most likely further lower the energy differences, again suggesting poor enantiomeric excess.

Evidently, there should be some mechanistic aspects of the reaction that chemists are unaware of and the whole mechanism requires a revisit at least from a computational viewpoint.

1.7 Aim of the study

From this brief discussion, it is evident that there is no consensus reached regarding the earlier stages of the reaction. The roles played by conformers are not fully understood, as a result, we

will explore the mechanism using the zwitterion, the LEC and the HEC. Beyond identifying the (in)active conformer, we will explain why it is (in)active. Among most computational reports available in the literature (though they may agree to some degree regarding the preferred pathway) they use activation energies to eliminate/justify a given mechanism. But this approach is a classical protocol that lacks fundamental explanation on why a mechanism is (un)favoured.

This classical approach always lacks essential information regarding the origin of a mechanism for instance (i) the driving forces causing or preventing a mechanism to proceed to products, (ii) atoms/functional groups/fragments playing most significant role and why, (iii) molecular fragments energy change along the computationally predicted pathway, (iv) interacting energies between fragments participating in bond making/breaking (v) most strained or stabilised molecular fragments. Hence, classical methodologies cannot provide an understanding of the reaction mechanism on a fundamental atomic/molecular fragment level. As a result, one is not able to justify why a given mechanism takes precedence over another proposed mechanism. We will use computed density functional theory (DFT) energies, interacting quantum atoms (IQA), and fragment attributed molecular system energy change (FAMSEC) to uncover the issues around the early stages of the proline catalysed aldol reactions including the formation of the active enamine catalyst.

Meanwhile, it is well established that solvent molecules can play significant roles in catalytic reactions and their inclusion in modelling provides additional mechanistic insights unavailable from using implicit models alone.[54,55] As a result of this, we will model/study the influence of the DMSO explicit solvent molecule in the formation of adducts/complexes – global minimum energy structures and complexes pre-organised for the very first step of the catalytic reaction. We will also explore the role played by the explicit solvent molecule of DMSO in the formation of the active enamine catalyst including the role of the water molecule which is eliminated before the enamine is formed. Data obtained in the implicit solvation model will be compared with data obtained when an explicit solvent molecule of DMSO is present. By this, we hope to fully explore and explain the mechanistic details of the proline catalysed aldol reactions.

1.8 References

1. Mukherjee, S.; Yang, J. W.; Hoffmann, S.; List, B. *Chem. Rev.,* **2007**, *107* (12), 5471-5569.
2. List, B. *Tetrahedron* **2002,** *28* (58), 5573-5590.
3. Sunoj, R. B. *Wiley Interd. Rev. Comput. Mol. Sci.,* **2011**, *1* (6), 920-931.
4. Heravi, M. M.; Zadsirjan, V.; Dehghani, M.; Hosseintash, N. *Tetrahedron Asymmetry* **2017**, *28* (5), 587-707.
5. MacMillan, D. W. C. *Nature.,* **2008**, *455*, 304.
6. Bertelsen, S.; Jørgensen, K. A. *Chem. Soc. Rev.,* **2009**, *38* (8), 2178-2189.
7. Oliveira, V. d. G.; Cardoso, M. F. d. C.; Forezi, L. d. S. M., *Catalysts.,* **2018**, *8* (12), 605.
8. Hajos, Z. G.; Parrish, D. R. *J. Org. Chem.,* **1974**, *39* (12), 1615-1621.
9. Eder, U.; Sauer, G.; Wiechert, R. *Angew. Chem. Int. Ed.,* **1971**, *10* (7), 496-497.
10. Movassaghi, M.; Jacobsen, E. N. *Science.,* **2002,** *298* (5600), 1904-1905.
11. Gröger, H.; Wilken, J. *Angew. Chem. Int. Ed.,* **2001**, *40* (3), 529-532.
12. List, B.; Lerner, R. A.; Barbas, C. F. *J. Am. Chem., Soc.,* **2000**, *122* (10), 2395-2396.
13. Machajewski, T.; Wong, C. *Angew. Chem. Int. Ed.,* **2000**, *39* (8), 1352-1375.
14. Wong, C.-H.; Whitesides, G. M. *Enzymes in synthetic organic chemistry*. Academic Press: **1994**; Vol. 12.
15. Mlynarski, J.; Gut, B. *Chem. Soc. Rev.,* **2012,** *41* (2), 587-596.
16. Shinisha, C.; Sunoj, R. B. *Org. Bio. Chem.,* **2007**, *5* (8), 1287-1294.
17. Taylor, M. S.; Jacobsen, E. N. *Angew. Chem. Int. Ed.,* **2006**, *45* (10), 1520-1543.
18. Tang, Z.; Yang, Z.-H.; Cun, L.-F.; Gong, L.-Z.; Mi, A.-Q.; Jiang, Y.-Z. *Org. Lett.,* **2004**, *6* (13), 2285-2287.
19. Northrup, A. B.; MacMillan, D. W. *J. Am. Chem. Soc.,* **2002**, *124* (24), 6798-6799.
20. Zotova, N.; Franzke, A.; Armstrong, A.; Blackmond, D. G. *J. Am. Chem. Soc.* **2007**, *129* (49), 15100-15101.
21. Aratake, S.; Itoh, T.; Okano, T.; Usui, T.; Shoji, M.; Hayashi, Y. *Chem. Commun.,* **2007**, (24), 2524-2526.
22. Pihko, P. M.; Laurikainen, K. M.; Usano, A.; Nyberg, A. I.; Kaavi, J. A. *Tetrahedron* **2006,** *62* (2), 317-328.
23. Yang, H.; Zhang, X.; Li, S.; Wang, X.; Ma, J. *RSC Adv.,* **2014**, *4* (18), 9292-9299.
24. Clegg, W.; Harrington, R. W.; North, M.; Pizzato, F.; Villuendas, P. *Tetrahedron Asymmetry.,* **2010**, *21* (9), 1262-1271.

25. Porcar, R.; Burguete, M. I.; Lozano, P.; Garcia-Verdugo, E.; Luis, S. V. *ACS Sustain. Chem. Eng.*, **2016**, *4* (11), 6062-6071.

26. Arnó, M.; Domingo, L. R. *Theor. Chem. Acc.*, **2002**, *108* (4), 232-239.

27. Ajitha, M. J.; Suresh, C. H. *J. Mol. Catal. A: Chem.*, **2011**, *345* (1), 37-43.

28. Rankin, K. N.; Gauld, J. W.; Boyd, R. J. *J. Phys. Chem.: A* **2002,** *106* (20), 5155-5159.

29. Clemente, F. R.; Houk, K. *Angew. Chem.*, **2004**, *116* (43), 5890-5892.

30. Agami, C.; Meynier, F.; Puchot, C.; Guilhem, J.; Pascard, C. *Tetrahedron* **1984**, *40* (6), 1031-1038.

31. Agami, C.; Puchot, C.; Sevestre, H. *Tetrahedron Letters.*, **1986**, *27* (13), 1501-1504.

32. Spencer, T.; Neel, H.; Flechtner, T.; Zayle, R. *Tetrahedron letters.*, **1965**, *6* (43), 3889-3897.

33. Brown, K. L.; Damm, L.; Dunitz, J. D.; Eschenmoser, A.; Hobi, R.; Kratky, C. *Helv. Chim. Acta.*, **1978**, *61* (8), 3108-3135.

34. Jung, M. E. *Tetrahedron.*, **1976**, *32* (1), 3-31.

35. Agami, C. *Bull. Soc. Chim. Fr.*, **1988,** (3), 499-507.

36. List, B.; Hoang, L.; Martin, H. J. *Proc. Natl. Acad. Sci. U.S.A.*, **2004**, *101* (16), 5839-5842.

37. Hoang, L.; Bahmanyar, S.; Houk, K.; List, B. *J. Am. Chem. Soc.*, **2003**, *125* (1), 16-17.

38. Schmid, M. B.; Zeitler, K.; Gschwind, R. M. *Angew. Chem. Int. Ed.*, **2010**, *49* (29), 4997-5003.

39. Schmid, M. B.; Zeitler, K.; Gschwind, R. M. *Chem. Sci.*, **2011**, *2* (9), 1793-1803.

40. Schmid, M. B.; Zeitler, K.; Gschwind, R. M. *J. Org. Chem.* **2011**, *76* (9), 3005-3015.

41. Allemann, C.; Um, J. M.; Houk, K. *J. Mol. Catal. A: Chem.*, **2010,** *324* (1), 31-38.

42. Bahmanyar, S.; Houk, K. *J. Am. Chem. Soc.*, **2001**, *123* (51), 12911-12912.

43. Tang, Z.; Jiang, F.; Cui, X.; Gong, L.-Z.; Mi, A.-Q.; Jiang, Y.-Z.; Wu, Y.-D. *Proc. Natl. Acad. Sci. U.S.A.*,**2004**, *101* (16), 5755-5760.

44. Clemente, F. R.; Houk, K. *J. Am. Chem. Soc.*, **2005**, *127* (32), 11294-11302.

45. Bahmanyar, S.; Houk, K.; Martin, H. J.; List, B. *J. Am. Chem. Soc.* **2003**, *125* (9), 2475-2479.

46. Yang, G.; Yang, Z.; Zhou, L.; Zhu, R.; Liu, C. *J. Mol. Catal. A: Chem.*, **2010**, *316* (1), 112-117.

47. Yang, G.; Zhou, L. *Catal. Sci. Technol.*, **2016**, *6* (10), 3378-3385.

48. Yang, G.; Zhu, C.; Zhou, L. *Int. J. Quantum. Chem.*, **2015**, *115* (24), 1746-1752.

49. Yang, G.; Zhou, L.; Chen, Y. *SpringerPlus.*, **2016,** *5* (1), 19.

50. Nobakht, Y.; Arshadi, N. *J. Mol. Model.*, **2018**, *24* (12), 334.

51. Arnó, M.; Zaragozá, R. J.; Domingo, L. R. *Tetrahedron. Asymmetry.*, **2005**, *16* (16), 2764-2770.

52. Armstrong, A.; Boto, R. A.; Dingwall, P.; Contreras-García, J.; Harvey, M. J.; Mason, N. J.; Rzepa, H. S. *Chem. Sci.*, **2014**, *5* (5), 2057-2071.

53. Cheong, P. H.-Y.; Legault, C. Y.; Um, J. M.; Çelebi-Ölçüm, N.; Houk, K. *Chem. Rev.*, **2011,** *111* (8), 5042-5137.

54. Schaffer, C. L.; Thomson, K. T. *J. Phys. Chem. C.*, **2008**, *112* (33), 12653-12662.

55. Emamian, S. R.; Domingo, L. R.; Tayyari, S. F. *J. Mol. Graph. Model.*, **2014**, *49*, 47-54.

Chapter 2

Computational methods

2.0 Introduction

Computational chemistry or modeling is a powerful technique that has been effectively used to study the behaviour of molecules including interactions between atoms and molecules. Recently the method has been applied in rationalizing and predicting mechanisms of organic reactions with high accuracy.[1] Its success is indisputable, as evidenced by numerous publications on mechanistic insights otherwise unavailable to the organic chemist.[2] Such success can be traced to result from a rapid expansion in the field of computer science leading to increased computational power and accuracies. The corresponding increase in the field of software engineering leading to the development of efficient algorithms has also contributed to the recent evolution of this area. It is important to emphasize that success is mainly a result of the skills and techniques of the computational chemists rather than the strength of computer power alone.

In this chapter, highlights of computational chemistry methods and programs that were used to achieve the aims of this thesis are summarised. Only a short introduction of the utilised procedures is given. To ensure reproducibility of results, practical application of the methods is provided for selected calculations. The two main electronic structure methods utilised are namely ab initio and density functional theory (DFT). These were used for energy minimisations, transition state searches, IRC scans, and frequency calculations. In addition, topological methods such as interacting quantum atoms (IQA) and the quantum theory of atoms in molecules (QTAIM) were used to provide insights regarding the interaction of atoms and molecules involved in chemical reactions.

For in-depth details and clarification of quantum mechanics the reader is referred to *Essentials of Computational Chemistry: Theories and Models* by C Cramer[3] and *Computational chemistry: Introduction to the Theory and Applications of Molecular and Quantum Mechanics* by E Lewars.[4]

2.1 Theoretical models and theoretical model chemistry

Since the exact wave functions for a multi-electron system cannot be determined, a mathematical approximation of the wave functions is required. It can be assumed that the molecular properties obtained from solving the exact wave functions would match those from experiments. The use of approximate solutions to the Schrödinger equation means that the molecular properties would deviate from experimentally measured quantities. Due to the different theoretical approximations used in various theoretical models, it follows that each method will lead to a different result but comparable to experiments. Here a theoretical model is a set of approximations to the Schrödinger equation, while model chemistry is the results from a given theoretical model. A given theoretical model should fulfil the following conditions.

- It must converge to a distinct energy provided the kind of nuclei and the total number of paired and unpaired electrons is known.
- It must be unbiased and must not depend on chemical intuition resulting in certain molecules requiring special treatment than others.
- The calculation error generated must roughly increase in percentage with the size of the molecule being calculated.
- The energy obtained from the model should denote a bound to the exact energy (Schrödinger energy).
- A model must possess the ability to be used in real scientific problems of interest not only in ideal or small systems (needs to be practical).

When the above conditions are satisfied it becomes sensible to assume that reaction energy profiles are accurately represented.

2.3 Schrödinger Equation

Before getting into details of computational chemistry methods, it is important to understand the Schrödinger equation because it is the theoretical foundation for quantum chemistry. Quantum chemistry defines molecules based on the interactions between positively charged nuclei and negatively charged electrons, while molecular geometry is the arrangement of nuclei resulting in the lowest possible energy. The exact solutions to the Schrödinger equation for a hydrogen atom (a particle in three-dimensions) can be obtained.

$$\left[-\frac{1}{2}\nabla^2 - \frac{Z}{r}\right]\psi(\mathbf{r}) = \mathrm{E}\psi(\mathbf{r}) \qquad (2.1)$$

The energy term in square brackets is the potential and kinetic energy terms of an electron of charge Z (1 for hydrogen) and distance r from its nucleus, ψ is an electron coordinate function, and **r** is a wave function related to the motion of the electrons and *E* is the energy (electronic) in atomic units, ∇² is the Laplacian operator in Cartesian Coordinates, and is given by

$$\nabla^2 = \frac{\partial^2}{\partial x^2} + \frac{\partial^2}{\partial y^2} + \frac{\partial^2}{\partial z^2}. \qquad (2.2)$$

For the hydrogen atom, the wave function is represented by its atomic orbitals (s,p,d,f…,). The probability of finding an electron inside a given small volume is given by the square of the wave function multiplied by the small volume. This is typically called the electron density and resembles the X-ray diffraction determined electron density.

The Schrödinger equation for a many-electron and many nuclear systems can be generalised as,

$$\hat{H}\Psi=E\Psi \tag{2.3}$$

where Ψ is the multi-electron wave function, it's a function of the positions of nucleus and electrons which fully describes the properties of the system, $\hat{H}$ is the Hamiltonian operator of the associated observable energy, and E is the total energy of the system.

The Hamiltonian $\hat{H}$ is an operator consisting of all terms contributing to the energy of the system.

$$\hat{H} = \hat{T} + \hat{V} \tag{2.4}$$

where $\hat{T}$ and $\hat{V}$ are the kinetic and potential energy operators, respectively

$\hat{T}$ is the sum of $\hat{T}_e$ and $\hat{T}_n$ where $\hat{T}_e$ is kinetic energy due to motion of electrons and $\hat{T}_n$ arise from nuclei motion. Likewise, $\hat{V}$ is a sum of nuclei-nuclei repulsion $\hat{V}_{nn}$, nuclear-electron attraction $\hat{V}_{ne}$ and electron-electron repulsion $\hat{V}_{ee}$. Hence,

$$\hat{H} = \hat{T}_e + \hat{T}_N + \hat{V}_{eN} + \hat{V}_{ee} + \hat{V}_{NN} \tag{2.5}$$

$$H = -\frac{1}{2}\sum_{i=1}\nabla^2_i - \frac{1}{2}\sum_A \frac{1}{M_A}\nabla^2_i - \sum_{i=1}^{N}\sum_{A=1}^{M}\frac{Z_A}{r_{1A}} + \sum_{i=1}^{N}\sum_{j>i}^{N}\frac{1}{r_{ij}} + \sum_{i=1}^{N}\sum_{A=1}^{M}\frac{Z_A Z_B}{R_{AB}} \tag{2.6}$$

In Eq. 2.6, r_{iA} and r_{ij} are the distances between electron i and nucleus A and the separation of electrons i and j respectively. R_{AB} is the distance between nuclei A and B, while Z_A is the charge of nucleus A.

The exact solution to the Schrödinger equation for many-electron (even simple two-electron systems like helium and hydrogen molecule) is extremely difficult to solve. This is mainly because the Hamiltonian in Eq. 2.6 consists of pairs of attraction and repulsive terms, indicating that no particle moves independently of others (correlation is used to define their interdependency).

2.3.1 The Born-Oppenheimer approximation

The Born-Oppenheimer approximation assumes that the nuclei does not move since its motion is much slower compared to the motion of electrons (moves with the speed of light) hence the nucleus can be considered as being stationary. This approximation fixes the positions of the nuclei and there is no need for accounting the effect of the movement of nuclei on electrons. The Born-Oppenheimer approximation results in an electronic Schrödinger equation

$$\hat{H}^{el}\Psi^{el}=E^{el}\Psi^{el} \tag{2.7}$$

The electronic Hamiltonian $\hat{H}^{el}$ can be expressed as

$$\hat{H}^{el} = -\frac{1}{2}\sum_{i=1}\nabla^2_i - \sum_{i=1}^{N}\sum_{A=1}^{M}\frac{Z_A}{r_{iA}} + \sum_{i=1}^{N}\sum_{j>i}^{N}\frac{1}{r_{ij}} \quad (2.8)$$

In Eq. 2.8, the nuclear kinetic energy is zero and the repulsion between nuclei is constant and is added to the electronic energy to get the total energy E of the system.

$$E = E^{el} + \sum_{i=1}^{N}\sum_{A=1}^{M}\frac{Z_A Z_B}{R_{AB}} \quad (2.9)$$

2.4 Potential energy surface

The concept of potential energy surface (PES) is the cornerstone of computational chemistry. When the Born-Oppenheimer approximation is used in solving the Schrödinger equation it is assumed that the nuclei is immobile, and the energy obtained is the electronic energy E. When all the available nuclear positions are represented by a general coordinate R, the electronic energy E(R) obtained depends on the nuclei coordinates. If the nuclei position is changed and the Schrödinger equation is solved again a different electronic energy (ER_1) is obtained. A plot of the electronic energy E against the collective coordinate R gives a potential energy curve or the Potential energy surface, PES = E(R). A PES shows the graphical or mathematical relationship between the energy and geometry of a molecular system. Stationary points found on the PES are very useful in the studying of reaction mechanisms. For a Cartesian coordinate system, the PES consists of 3_N dimensions, where N is the number of atoms in the molecular system. The position of each atom in a 3D space is represented by the three dimensions (x, y and z).

2.4.1 Stationary points

The relationship between potential energy and molecular geometry can be understood by examining the structure of the PES. The primary focus of applied computational chemistry is to analyse the structure/geometry and relate it to the energy of molecules. A study of reaction mechanisms will thus involve studying the PES from adducts through transitions states to products/intermediates. Stationary points on a PES are points in which the surface is parallel to the horizontal axis, a ball placed on such points will remain stationary. At points other than the stationary point the ball will roll to minima (regions of lower potential energy).

The nature of the stationary point is very useful to the computational chemist, minima represent stable structures while first order maxima correspond to first order transition state structures.

Mathematically, stationary points are found where the first derivative (gradient) of the electronic energy *E* with respect to nuclei coordinate c_i is zero – Eq. 2.10,

$$\frac{dE_{el}}{dc_i} = 0 \text{ where } c_{1=}x_{i,}y_{i,}z_{i,} \; \forall \; (1 < I \leq n) \qquad (2.10)$$

A description of the nature of the stationary point is given by the second derivative of the electronic energy with respect to each coordinate. In a minimum, all the eigenvalues of $\frac{d^2E_{el}}{dc_i}$ are positive, whereas in a first order saddle point or transition state, one and only one eigenvalue of $\frac{d^2E_{el}}{dc_i}$ is less than zero, while the rest are positive. A saddle point links two energy minima together, while the lowest energy pathway linking the two minima through a transition state is called an intrinsic reaction coordinate (IRC).

2.4.2 Intrinsic reaction coordinate (IRC)

The reaction path of a chemical process is traced from a transition state or first-order saddle point using the IRC method.[5] The input or guess first-order saddle point should be a good approximation of the transition state. When the IRC path is properly computed, the final structures at both ends will represent the reactants and products. Its main use is to verify the validity of the obtained transition state structure by checking if it connects the reactants to products. It also helps in identifying any other reaction intermediates that might be available and yet not located.

The IRC path is a solution to Eq. 2.11

$$\frac{d\boldsymbol{q}(s)}{ds} = \boldsymbol{v}s \qquad (2.11)$$

q is called the mass-weighted Cartesian coordinates and s is the cartesian coordinate along the IRC path. The tangent vector $\boldsymbol{v}$ of IRC is normalised and represents the eigenvector coordinates which have a negative value at the transition structure where $s = 0$ The IRC method is well established for predicting and investigating the mechanisms of many reactions.[6,7]

2.5 Ab initio method

The word *ab initio* is Latin for "from scratch" in which the calculation is done using fundamental laws of quantum mechanics and physics without the need for experimental data. The method uses only mathematical approximations to the Schrödinger equation to predict molecular properties for a range of molecules ranging from small to very large organic molecules. It can be applied for the calculation of electron density, electronic energies, and thermochemical properties.

2.5.1 Hartree-Fock (HF) Approximation

The major objective of solving quantum mechanical problems is to obtain a wave function which is a solution to the Schrödinger equation – Eq. 2.3. This wave function contains a wealth of information as it provides a description of the motion of a single electron and the behaviour of all the remaining electrons within the molecular system. The Hartree product– a product of all the one-electron wave functions of the system is often used to construct such wave functions.[8.]

$$\psi_{(x)}=\psi_1(x_1)\,\psi_2(x_2)\cdots\,\psi_N(X_N) \tag{2.12}$$

Unfortunately, this method of representing the many-electron wave function is not applicable for electrons due to Pauli Exclusion Principle which states that "*in a quantum system, two or more fermions of the same kind cannot be in the same (pure) state*". This is called antisymmetry, a property which Eq. 2.11 does not have. Nevertheless, by mathematical permutations, the one-electron wave functions in Eq. 2.3, it is possible to formulate an antisymmetric many-electron wave function. The permutation is known as the Slater determinant ($\Phi_{SD)}$, Eq. 2.13,

$$\Psi_O \approx \Phi_{SD} = |\psi_1\psi_2 \ldots \psi_N| = \frac{1}{\sqrt{N!}}\begin{vmatrix} \psi_1(x_1) & \psi_1(x_2) & \ldots & \psi_1(x_N) \\ \psi_2(x_1) & \psi_2(x_2) & \ldots & \psi_2(x_N) \\ \vdots & \vdots & \ddots & \vdots \\ \psi_N(\psi_1) & \psi_N(x_2) & \ldots & \psi_N(x_N) \end{vmatrix}. \tag{2.13}$$

N is the number of electrons in the system, and the product of individual one-electron wave functions $\psi_1(x_1)$ is the molecular orbitals (MO).

This determinant can be re-written to involve only the diagonal elements of the matrix:

$$\Phi_{SD}= \frac{1}{\sqrt{N!}}\det\{\psi_1(x_1)\,\psi_2(x_2)\cdots\psi_N(x_N)\} \tag{2.14}$$

Individual one-electron wave functions $\psi_i(x_i)$ are called MO, hence the HF method resembles the molecular orbital approximation method. The wavefunction consists of a combination of MOs with spatial orbitals $\phi(r)$ with spin functions, $\alpha(s)$ or $\beta(s)$ hence they are commonly referred to as spin orbitals, i.e.,

$$\psi_i(x_i) = \varphi(r)\sigma(s), \text{ where } \sigma = \alpha, \beta. \tag{2.15}$$

The product of MO and electron spin functions α and β, defines the overall electronic wavefunction ψ and produce spin orbitals. The resulting spin orbitals are orthogonal since the orthogonal molecular orbitals were normalised, i.e.,

$$\int \Psi_i\Psi_j \,= \langle\Psi_i|\Psi_j\rangle = \delta_{ij} \tag{2.16}$$

δ_{ij} is the kronecker delta (which is equal to 1 if $i = j$, and zero otherwise). The antisymmetric nature of the exact wave function is preserved by the slater determinant because the determinant changes sign if two columns or rows are interchanged. This means that the HF wavefunction is an antisymmetric wave function expressed in terms of the one-electron molecular orbitals. Moreover, each of the MOs can be represented as a linear combination of atomic orbitals (LCAO) i.e.,

$$\Psi_i(r_i) = \sum C_{\mu i}\psi_\mu(r_i) \tag{2.17}$$

ψ_μ are atomic orbitals or basis functions and $C_{\mu i}$are MO coefficients.

If the wave function is normalized, the expectation value of the energy is given by:

$$E = \langle \psi | \hat{H} | \psi \rangle \tag{2.18}$$

In case of the HF wavefunction, the expectation value of the energy is given by:

$$E_{HF} = \sum_i H_i + \frac{1}{2}\sum_{ij}(j_{ij} - k_{ij}) \tag{2.19}$$

H_i collects all the one-electron terms arising from the kinetic energy of the electrons and the nuclear attraction energy. J_{ij} involves two-electron terms associated with the coulomb repulsion between the electrons and K_{ij} involves two-electron terms associated with the exchange of electronic coordinates.

The HF method neglect electron correlation which results in deviations from experimental observation, as a result, post HF method which address electron correlation were developed to address this pitfall.[9] However, the post HF methods are not included in this discussion. Density functional theory (DFT) methods were developed as alternative to HF and the method is briefly described in the next section.

2.6 Density functional theory

2.6.1 Early approximation of the DFT approach

The energy component of a system is divided into kinetic energy (T) and its potential energy (V). If a theory of evaluating the molecular energy using only the electron density as a variable is developed, the easiest method is to regard the system to be classical. From this follows that the V component of the system energy can easily be determined Eq. 2.20–2.21. The attraction between the electron density and the nuclei is given by Eq. 2.20,

$$V_{ne}[\rho(\mathbf{r})] = \sum_k^{nuclei} \int \frac{Z_k}{|\boldsymbol{r} - \boldsymbol{r}_k|}\rho(\boldsymbol{r})d\boldsymbol{r} \tag{2.20}.$$

The electron–electron repulsion component is given by Eq. 2.21,

$$V_{ee}[\rho(\mathbf{r})]=\frac{1}{2}\iint\frac{\rho(\boldsymbol{r}_1)\rho(\boldsymbol{r}_2)}{|\boldsymbol{r}_1-\boldsymbol{r}_2|}d\boldsymbol{r}_1 d\boldsymbol{r}_2 \quad (2.21)$$

r_1 and r_2 are dummy integration variables which run over all space.

Determining the kinetic energy component due to a continuous charge distribution is not straight forward. Hence, a fictitious substance (Jellium) which is a system component consisting of infinite number of electrons moving in an infinite volume of space surrounded by a uniformly distributed positive charge is introduced. The electron distribution is also called constant electron gas with uniform non-zero density Eq. 2.22,

$$V_{ueg}[\rho(\mathbf{r})]=\frac{1}{2}(3\pi^2)^{2/3}\int\rho^{\frac{5}{3}}(\boldsymbol{r})\,d\boldsymbol{r} \quad (2.22).$$

It can be noted that the T and V terms shown in Eq. 2.20–2.22 are functions of density while the density is a function of three-dimensional coordinates. By definition, a functional is a function whose argument is also function, hence, T and V are "density functionals". Hence, the energy of a system can be calculated using the Thomas–Fermi equations Eq. 2.20–2.22[10] and an assumed variational principle without using a wave function. The fundamental assumption of the Thomas–Fermi equation are inaccurate, and they are not useful in modern practical application. However, the simplicity of the equations opened avenues for the development of advanced density functional approaches. Hohenberg and Kohn proved two critical theorems which became the basis of establishing DFT as a genuine quantum mechanical methodology. In DFT methodology, there exist electron–electron interactions as well as interaction between electrons with an external potential. The external potential is a uniformly distributed positive charge, in molecules the external potential is attraction caused by the nucleus.

The prominence of density functional theory (DFT) methods can be ascribed to their less computationally demanding but comparable accuracies to methods that account for electron correlation.[11,12] Like the case of ab initio methods, the major objective of DFT methods is to solve the Schrodinger equation. While ab initio methods calculate the wave function of the Schrodinger equation directly, DFT methods use the electron density to get information on the properties of atoms and electrons. The cornerstone of DFT methods is that the ground-state electronic energy can be obtained entirely from the electron density ρ as proven by the Hohenberg and Kohn first theorem.[13,14] The electron density ρ is the "density" in density functional theory and is the foundation for methods

of atoms in molecules (AIM). An important property of the electron density is that it is measurable e.g., by electron diffraction or X-ray diffraction.

Hohenberg and Kohn theorem

The field of density functional theory centres around two theorems developed and proved by Kohn and Hohenberg. The theorems can be applied to any system where electrons flow under an external potential $v_{ext}(\boldsymbol{r})$

Theorem 1

All properties of a molecule in a ground electronic state are determined by the ground state electron density function $\rho_o(x, y, z)$

This implies that any ground state property like energy E_o can be calculated from the electron density $\rho_o(x, y, z)$, this can be written as

$$\rho_o(x, y, z) \rightarrow E_o \qquad (2.23)$$

Eq. 2.13 means E_o is a functional of ρ_o(x,y,z), a functional is simply a rule used to transform a function into a number.

The first Hohenberg–Kohn theorem can be restated as '*any ground state property of a molecule is a functional of the ground state electron density function*, i.e.,

$$E_o = F[\rho_0] = E[\rho_o] \qquad (2.24)$$

The theorem is termed an *existence theorem* because it states that a function F exists but does not describe how to find it, this is the major short fall for all DFT methods.

Theorem 2

Any trial electron density function will give an energy higher than the true ground state energy (or equal to, if it were exactly the true electron density function).

The DFT energy due to a trial electron density is the electronic energy of electrons flowing under the influence of atomic nuclei (which is regarded as an external nuclear potential). Using $v(\boldsymbol{r})$ to represent this nuclear potential, the electronic energy becomes E_v can be expressed as $E_v = E_v[\rho_o]$ which is the electronic energy functional of the ground state electron density.

Mathematically the second theorem can be written as

$$E_v[\rho_t] \geq E_o[\rho_o] \qquad (2.25)$$

Where ρ_t is a trial electron density and $E_o[\rho_o]$ a true ground state energy, the trial electron density must satisfy the differential equation in Eq. 2.26,

$$\int \rho_t(\boldsymbol{r}) d\boldsymbol{r} = n \tag{2.26}$$

Where n is the number of electrons in the system, and $\rho_t(\boldsymbol{r}) \geq 0 \quad \forall\, \boldsymbol{r}$.

2.6.2 Kohn–Shan Self Consistent Field Methodology

From the discussion above, the wave function is determined by the Hamiltonian which is determined by an external potential which is determined by the density. The energy of the system can therefore be computed from the Hamiltonian and the wavefunction. This method is not a simplification of the MO theory because the final step involves solving the Schrödinger equation and this is usually difficult in many instances. The difficulty is caused by the electron–electron interaction term in the Hamiltonian. The breakthrough came when Kohn and Shan[15] simplified the equations using one Hamiltonian operator for non–interaction electron systems. The Hamiltonian can then be expressed as a sum of one–electron operator and consist of eigenfunctions which are Slater determinants. The energy functional of such systems can then be divided into different components, – Eq. 2.27,

$$E[\rho(\boldsymbol{r})] = T_{ni}[\rho(r)] + V_{ne}[\rho(r)] + V_{ee}[\rho(r)] + \Delta T[\rho(r)] + \Delta V_{ee}[\rho(r)] \tag{2.27}.$$

The energy terms on the right-hand side of the equation refers to the kinetic energy of non–interacting electrons, nuclear–electron interactions, classical electron–electron repulsion, the correction of the kinetic energy caused by interacting electrons, and lastly the non–classical corrections due to electron–electron repulsion energy. The kinetic energy of a non–interacting system of electrons is the sum individual electronic kinetic energies. The density within an orbital can be given by Eq. 2.28,

$$E[\rho(\boldsymbol{r})] = \sum_{i}^{N} \left(\langle X_i \left| -\frac{1}{2} {\nabla_i}^2 \right| X_i \rangle - \langle X_i \left| \sum_{k}^{nuclei} \frac{Z_k}{|\boldsymbol{r}_i - \boldsymbol{r}_k|} \right| X_i \rangle \right) + \sum_{i}^{N} \langle X_i \left| \frac{1}{2} \int \frac{\rho(\boldsymbol{r}')}{|\boldsymbol{r}_i - \boldsymbol{r}'|} d\boldsymbol{r}' \right| X_i \rangle + E_{XC}\,[\rho(\boldsymbol{r})] \tag{2.28}.$$

N is the total number of electrons while the density is an exact eigenfunction for the non–interacting system which is given by Eq. 2.29,

$$\rho = \sum_{i=1}^{N} \langle X_i | X_i \rangle \tag{2.29}$$

The terms ΔT and ΔV_{ee} are combined in Eq. 2.28 to form a new term E_{EX} known as the exchange–correlation energy. It consists of quantum mechanical exchange and correlation correction for

classical self–interaction energy and the difference between the kinetic energy of the fictitious non–interacting system and the real one.

The orbitals *X* that minimize the energy *E* in Eq 2.28 should satisfy the pseudoeigenvalue equations

$$h_i^{KS} X_i = \varepsilon_i X_i \tag{2.30}$$

The Kohn–Sham (KS) one-electron operator is given by Eq. 2.31,

$$h_i^{KS} = -\frac{1}{2}\nabla_i^2 - \sum_k^{nuclei} \frac{Z_k}{[\mathbf{r_i}-\mathbf{r_k}]} + \int \frac{\rho(\boldsymbol{r}')}{|\boldsymbol{r_i}-\boldsymbol{r}'|} d\boldsymbol{r}' + V_{XC} \tag{2.31}$$

and $$V_{XC} = \frac{\delta E_{XC}}{\delta \rho} \tag{2.32}$$

V_{XC} is a functional derivative.

Advantages and disadvantages of Density Functional Theory

The most notable advantage of DFT methods is their higher computational accuracy without the additional increase in computing time. DFT methods are reliable in modelling organic molecules especially when dispersion influence is accounted for, and correct basis set are used. In this thesis Grimme's empirical correction for dispersion (GD3) will be used to calculate the effects of dispersion. The major disadvantage of DFT methods is the trial-and-error method used for determining the appropriate method for a new system.

2.7 Basis sets

Basis sets are sets of functions (basis functions) used to represent atomic orbitals (AOs), an approximate linear combination of atomic orbitals (LCAO) of these basis functions give the molecular orbitals (MO) φ

$$\phi = \sum_{i=1}^{N} \alpha_i \varphi_i \tag{2.33}$$

φ is the molecular orbital, and the sum of N functions φ_i is the basis set each having a characteristic scalar coefficient α_i.

Chemists would prefer to use atomic orbitals (AOs) as a representation of molecular orbitals MOs, however, mathematically, molecular orbitals are treated as functions only. This prevents being hypothetically partial on where and how to apply them. For instance, the square of the wave functions gives the probability density that is where the electrons are more likely to appear. Hence, the basis function should be flexible enough to allow electrons to flow to regions of lower energy and high density. An example is when p functions are used to describe the bonding of a hydrogen atom aligned in the axis of a bond in a bond between a carbon and hydrogen atom. This allows

effective localisation of the electron density along the bonding regions than when there are only σ functions.

2.7.1 Slater-type orbitals (STOs)

Slater-type orbitals (STOs) are used in systems where high accuracy is needed, and in cases where all three and four-centre integrals are ignored. The minimum basis set of STOs refers to the STOs in a molecule which is occupied by electrons. Larger basis set increases the accuracy by offering an improved approximation yet increases computational time. STOs consist of the following components

$$R(r) = Nr^{n-1}e^{-\zeta r} \tag{2.34}$$

N is the normalisation constant, n is a natural number, r is the distance of electrons from the nucleus and ς is a constant associate with the effective nuclear charge.

2.7.2 Double zeta orbitals

More than one STO can be used to represent one atomic orbital as shown in the below equation,

$$R_{2s}(r) = C_1 re^{-\zeta_1 r} + C_2 re^{-\zeta_2 r} \tag{2.35}$$

The function consisting of a smaller ζ value represent charges with a larger distance from the nucleus while larger ζ functions are very close to the nucleus; this is called double-zeta basis set. Double-zeta functions prevent the problem of having orbitals of the same type being considered to be identical in chemically inequivalent molecules. An example is the P_z orbital along the inter nuclear axis in acetylene, which is normally considered identical to the P_x and P_y. But with a double-zeta basis set the P_z orbital is not regarded to be in the same chemical environment as the P_x and P_y orbitals.

2.7.3 Gaussian orbitals

The computation of STOs type orbitals can be simplified by Gaussian-type orbitals (GTOs) which improves accuracy and description of molecules with Gaussian basis functions. While STO basis set improves the efficiency and accuracy of hydrogenic orbitals, Gaussian basis functions offer further improvement. Gaussian basis functions take the format of the below equation

$$G_{nlm}(r, \theta, \psi) = N_n r^{n-1} e^{-\alpha r^2} Y_l^m(\theta, \psi) \tag{2.36}$$

2.7.4 Nomenclature of basis sets

Basis sets are named based on the number of atomic orbitals per valence atomic orbitals used in constructing them. The STO-3G basis set is the Slater-type orbitals approximated by three Gaussian functions, also called 'minimal' basis set. This means only one basis function is used to represent each occupied atomic orbital (1s, 2s, $2P_x$, $2P_y$, $2P_z$). STO-3G basis set means that in the calculation the molecule is represented by STO equations, with the combination of 3 Gaussian primitives. In general, the number n in STO-nG represent Gaussian primitives used in building the STO equation, for higher accuracies bigger n values are used.

Since it is monotonous to calculate the equations for individual atomic orbitals, the orbital of interest can be approximated by a combination of expressions for orbitals smaller and larger than the one being considered, this is called 'Split-Valence' basis sets. This describes an orbital by combining two or more STOs. An example is a 3–21G basis set when used for carbon, means 3 Gaussian primitives for the core 1s, two Gaussians each for 2s and 2p plus one Gaussian each for 2s' and 2p'. For a further improvement in the accuracy of computational calculations, triple split-valence basis sets are used the most popular is the 6-311G* basis set. The number 6 denotes 6 Gaussian primitives used for the core s-shell, 3 is the number of GTOs for one of the sp-shells and each 1 denotes the number of GTOs for the remaining two sp-shells. The asterisk * represents that the d-shell is considered due to polarisation which occurs when two atoms are brought close together.

Diffuse functions are used when working with anions and atoms with lone electron pairs which likely cause an electron density far from the nucleus. They are also used for molecules in an excited state and when there is a greater presence of negative charge. Their presence is indicated by a + sign on the basis set eg 6-311++G. Sometimes basis sets that account for electron correlation cc-pVNZ, where N=D (double), T(triple), Q(quadruple) and 5(quintuple) zeta should be used. They also allow polarisation and diffuse effect to be added by the use of prefix "AUG"-

2.8 Solvation models

Most chemical reactions are conducted in the presence of solvents, since solvent properties such as (non)polarity, basicity, hydrogen-bond donating/accepting ability can influence reaction outcomes,[16] there is a need to incorporate solvent effects in theoretical modelling. Since there are a variety of solvents available to the chemist, the ability of computational chemistry programs and packages to evaluate solvent effects is amazing. Generally, the solvation models are classified into two broad types (i) implicit or continuum solvation models which perceives the solvent as a homogenous medium with a constant

dielectric constant and (ii) explicit solvation modes which provides a description of solvent as individual molecules.[17,18]

2.8.1 Implicit solvent model

In implicit or continuum solvation models, the continuum is used to represent the existence of solvent molecules as polarizable medium having a constant dielectric constant $\boldsymbol{\varepsilon}$, the algorithm puts the solute molecules inside a cavity where interaction between the solute molecules and cavity is calculated.[19] The solute molecules **M** are then introduced in a hole within the solvent medium, once inside the medium the distribution of electric charge in **M** will polarize the medium by induction. The free energy of solvation $\Delta G_{solvation}$ is decomposed into three components, – Eq. 2.37,

$$\Delta G_{solvation} = \Delta G_{cavity} + \Delta G_{dispersion} + \Delta G_{electrostatic}. \quad (2.37).$$

The cavity is created by a succession of overlapping spheres defined by the van der Waals radii of individual atoms. Reaction field is a term used to denote the continuous electric field that represents the solvent degrees of freedom after reaching thermal equilibrium with solute molecules.

2.8.2 The Poisson Equation

Almost all continuum solvation models depend on Poison equations which show the relationship between the electrostatic potential φ with respect to charge density ρ and dielectric constant of the medium $\boldsymbol{\varepsilon}$. The equation is valid only in cases where there is a linear relationship between the dielectric constant due to the surrounding medium and the charge, it is expressed as,

$$\nabla^2\phi(\mathbf{r}) = -\frac{4\pi\rho(\mathbf{r})}{\varepsilon} \quad (2.38).$$

In continuum models, when a solute is placed inside a homogeneous solvent medium it is assumed that there is a disruption of the uniformity of the homogeneous medium which creates two regions inside and outside the cavity, the overall Poison equation is expressed as

$$\nabla\varepsilon\,(\mathbf{r})\,.\nabla\phi\,(\mathrm{r}) = -\,4\pi\rho(\mathbf{r}) \quad (2.39)$$

The validity of the Poison equation depends on zero solvent ion strength, in cases where there are mobile ions which act as electrolytes then the Poison-Boltzmann equation is used

$$\nabla\varepsilon\,(\mathbf{r})\,.\nabla\phi(\boldsymbol{r}) - \varepsilon(\mathbf{r})\,\lambda\,(\mathbf{r})\kappa^2\,\frac{\kappa_B T}{q}\sin\left[\frac{q\phi(\boldsymbol{r})}{\kappa_{BT}}\right] = -\,4\pi\rho(\mathbf{r}) \quad (2.40)$$

where q is the charge of the electrolyte ions and λ is a switching parameter which can either be zero or 1 and k^2 is a Debye Hückel parameter given by:

$$\kappa^2 = \frac{8\pi q^2 I}{\varepsilon \kappa_B T} \quad (2.41)$$

where I is the is the electrolyte ionic strength and $\frac{1}{\kappa_B}$ is called the Debye length.

2.8.3 Explicit/hybrid solvation model

In explicit solvation model, the solvent molecules are represented atomistically (the coordinates of the solvent molecules are included in the modelling) this allows the effect of intermolecular interactions between solvent and solute to be determined. The number of explicit solvent molecules and the position with respect to the solute molecules where they should be placed is still a subject for discussion.[20] In practice, practical consideration of computational cost limits the number of explicit solvent molecules to as few as possible. Chemical intuition is often adopted in which solvent molecules are added to the most likely coordinating sites (one at a time) until subsequent addition results in no coordination to the solute molecules.

2.8.4 Hybrid micro solvation

To simulate the effect of solvent in implicit solvent models, a few numbers of solvent molecules are now being placed around the solute molecule at places where key interactions like hydrogen bonding are anticipated to occur.[21,22] This decreases the limitations of the implicit solvent model of not being able to account for hydrogen bonding and related interactions. This is usually referred to as micro solvation in which the explicit solvent molecules added are subjected to the same theoretical treatment as the solute molecules. In practice, this explicit solvent model is used in combination with an implicit continuum dielectric constant to account for long-range interactions, this solvent model is termed hybrid explicit-implicit solvation model.[23,24]

2.9 Fragment attributed molecular system energy change (FAMSEC)

In the FAMSEC concept, changes in the properties of atoms/molecules or atomic/molecular fragments are monitored when a chemical change occurs in a molecule from an initial or reference state (*ref*) to the final state (*fin*).[25] When applied in studying reaction mechanisms, the *ref* state may represent isolated conformers, complexes formed by two reactants and molecule/s of solvent or structures that are pre-arranged for bond formation. In principle, the *ref* state may represent structures of interest at any stage along the reaction profile while the *fin* state will be the structure at the subsequent stage or any other stage of interest along the same pathway. The FAMSEC concept can also be used to monitor and calculate the changes in properties (usually energy) of any two atoms of interest which are covalent or non-covalently bonded when a molecule or molecular system changes

from *ref* to *fin* state, for instance, from reactants to transition state. The approach is based on the understanding that for a given change in the 3D configuration of a molecule there is an associated change in the energy of the molecule and all its atoms. The FAMSEC protocol is deeply rooted in the IQA technique and method which uses IQA-defined one-body and two-body energy components of total molecular energy.[26,27]

2.9.1 Concept of the FAMSEC

The main objective of the FAMSEC protocol is to calculate the energy change of either a single molecule, entire molecular system or a molecular fragment caused by a new 3D placement of molecules. This is achieved using IQA principal energy components ($E^{\mathrm{A}}_{\mathrm{add}}$, $E^{\mathrm{A}}_{\mathrm{self}}$, $E^{\mathrm{A,B}}_{\mathrm{int}}$), which partitions the energy, *E*, of a molecular system. A molecular system can represent an isolated molecule, a complex formed by two or more reactants, transition state structures or products. In this regard, a molecular system consists of atoms which fills the whole region that the molecular system occupies without voids or overlapping areas inside the 3D space. This allows each atom to have its unique energy which depends on the kind of atom and the chemical environment it occupies. As a result, the IQA scheme recovers the computed energy *E* (electronic, or *ab initio*) by the addition of energies of individual atoms A, called total (or additive) atomic energies – Eq. 2.42,

$$E = E_{\mathrm{IQA}} = \sum_{\mathrm{A}} E^{\mathrm{A}}_{\mathrm{add}} \tag{2.42}$$

In the IQA concept, all atoms in a molecule are involved in either attractive or repulsive interactions with other atoms, thus they carry a unique interaction energy. It is important to stress that though classical chemists view atoms as being covalently bonded, hydrogen bonded or non-bonded, in IQA all atoms are treated on equal footing. Hence, the total atomic energy of an atom originates from two main contributions, i.e., the energy of the atom (itself) called the self-atomic energy $E^{\mathrm{A}}_{\mathrm{self}}$ and the sum of interaction energies $E^{\mathrm{A,X}}_{\mathrm{int}}$, atom A experience as a result of another other atom X in a molecule. In short, the energy of a molecular system is made up of all self-atomic energy and halved diatomic interactions. For the energy *E* of a molecular system to be recovered, total interaction energy related to distinct pairs of atoms is halved – Eq. 2.43.

$$E^{\mathrm{A}}_{\mathrm{add}} = E^{\mathrm{A}}_{\mathrm{self}} + 0.5\sum_{\mathrm{X}\neq\mathrm{A}} E^{\mathrm{A,X}}_{\mathrm{int}} . \tag{2.43}$$

Eq. 2.28 implies that total self-molecular energy can be obtained from the sum of all the self-atomic energies, Eq. 2.44

$$E_{\text{self}}^{\text{Tot}} = \sum_{\text{A}} E_{\text{self}}^{\text{A}} \,. \tag{2.44}$$

Similarly, the total interaction energy of a molecular system is obtained from the sum of all unique diatomic interaction energies between atoms A and B, Eq. 2.45

$$E_{\text{int}}^{\text{Tot}} = 0.5 \sum_{\text{A}} \sum_{\text{B}\neq\text{A}} E_{\text{int}}^{\text{A,B}} \,. \tag{2.45}$$

Finally, the electronic energy, *E*, of a molecular system is recovered from the total self-molecular energy and total interaction energy, Eq. 2.46,

$$E = E_{\text{IQA}} = E_{\text{self}}^{\text{Tot}} + E_{\text{int}}^{\text{Tot}} \tag{2.46}$$

IQA is an important tool that decomposes self-atomic and interaction energies into different contributions that are vital for fundamental understating of chemical processes. For example, the $E_{\text{int}}^{\text{A,B}}$ energy term measures the strength of diatomic interaction between any two pair of atoms. It can be extended to compare the strength of covalent bonding interaction between different systems by decomposing it into its components, Eq. 2.47

$$E_{\text{int}}^{\text{A,B}} = V_{\text{XC}}^{\text{A,B}} + V_{\text{cl}}^{\text{A,B}} \tag{2.47}$$

Thus, the interaction energy term $E_{\text{int}}^{\text{A,B}}$ is made of two unique contributions, i.e., the exchange-correlation ($V_{\text{XC}}^{\text{A,B}}$), which measures the degree of covalence and the classical ($V_{\text{cl}}^{\text{A,B}}$) term which is contribution from classical electrostatic Coulomb interaction. Hence, by decomposing the $E_{\text{int}}^{\text{A,B}}$ term, one can gain important information regarding the strength and nature of bonding. For a detailed knowledge on IQA-defined energy components which we will not use in this work the interested reader is referred to relevant literature on IQA

2.9.2 Basic concepts of the REP-FAMSEC method

The REP-FAMSEC method is an extension of the FAMSEC technique, the prefix REP stands for reaction energy profile which means it is the FAMSEC method applied in studying energy profiles of chemical reactions. In a chemical event, diatomic interaction energies change significantly (usually by more than an order of magnitude) compared to atomic energies. Thus, the fundamental concepts of the REP-FAMSEC method is based on, but not limited to, observing, measuring and interpreting changes in the interaction energies, i.e., the $E_{\text{int}}^{\text{A,B}}$ term and its components, namely, $V_{\text{cl}}^{\text{A,B}}$, and the $V_{\text{XC}}^{\text{A,B}}$. It is important to emphasise that even when a single atom in a molecule is slightly displaced there will be associated changes in all $E_{\text{int}}^{\text{A,B}}$ terms calculated for all unique atom pairs in

the molecule. As a result, calculation of $E_{\text{int}}^{\text{A,B}}$ terms in all unique pairs of atoms {A,B} will be conducted irrespective of whether the atoms are classically seen as chemically bonded or the size of internuclear distance between them. Typically for larger molecules it is just a handful of atoms that experience significant changes in their $E_{\text{int}}^{\text{A,B}}$ terms say greater than ±10 kcal/mol. Such atoms are regarded as the drivers of the chemical change in the REP-FAMSEC approach and their interaction energies along the reaction coordinate will be examined. For convenience, these atoms are regarded as an n-atom or atomic fragment $\mathcal{G}$ of a molecule or molecular system. In studying mechanisms of chemical reactions, each molecule will have its set of "key" atoms which drives a given chemical event and they are treated as distinct fragments. The $\Delta E_{\text{int}}^{\text{A,B}}$ terms are usually monitored at each subsequent step along the reaction coordinate in a stepwise manner, i.e., $\Delta E_{\text{int}} = {}^{\text{fin}}E_{\text{int}} - {}^{\text{ini}}E_{\text{int}}$, where *fin* and *ini* refer to the final or after a chemical event and initial or before a chemical event, respectively.

2.10 References

1. Allemann, C.; Gordillo, R.; Clemente, F. R.; Cheong, P. H.-Y.; Houk, K., *Acc. Chem. Res.*, **2004**, *37* (8), 558-569.
2. Balcells, D.; Maseras, F., *New. J. Chem.*, **2007,** *31* (3), 333-343.
3. Cramer, C. J., *Essentials of computational chemistry: theories and models*. John Wiley & Sons: **2013**.
4. Lewars, E. G., *Computational Chemistry: Introduction to the theory and applications of molecular and quantum mechanics*. Springer Science & Business Media: **2010**.
5. Fukui, K., *J. Phys. Chem.* **1970**, *74* (23), 4161-4163.
6. Niu, S.; Hall, M. B., *Chem. Rev.*, **2000**, *100* (2), 353-406.
7. Jensen, F., *Introduction to computational chemistry*. John wiley & sons: **2017**.
8. Hatree, D. R., *Proc. Cambridge Phil. Soc.*, **1928** (24) 111–132
9. Bartlett, R. J., *Annu. Rev. Phys. Chem.*, **1981**, *32* (1) 359–401.
10. March, N. H., The Thomas-Fermi approximation in quantum mechanics. *Adv. Phys.*, **1957** *6*. (21) 1–101.
11. Curtiss, L. A.; Raghavachari, K.; Redfern, P. C.; Pople, J. A., *Chem. Phys. Lett.*, **1997**, *270* (*6),* 419-426.
12. Oliphant, N.; Bartlett, R. J., *J. Chem. Phys.* **1994**, *100* (9), 6550-6561.
13 Hohenberg, P., Kohn, W., *Phys. Rev.*, **1964** *136*, B864.
14 Sham, L. J.; Kohn, W., *Phys. Rev.*, **1966** *145* (2), 561.
15 Kohn, W., Sham, L. J., *Phys. Rev.*, **1965** *140* (4A), A1133.
16. Dyson, P. J.; Jessop, P. G. *Catal. Sci. Technol.*, **2016**, *6* (10), 3302-3316.
17. Cramer, C. J.; Truhlar, D. G., *Chem. Rev.*, **1999**, *99* (8), 2161-2200.
18. Cramer, C. J.; Truhlar, D. G., *Acc. Chem. Res.*, **2008**, *41* (6), 760-768.
19. Roux, B.; Simonson, T., *Biophys. Chem.*, **1999**, *78* (*2*), 1-20.
20. Bachrach, S. M., *Wiley. Interdiscip. Rev. Comput. Mol. Sci.*, **2014**, *4* (5), 482-487.
21. Michel, C.; Auneau, F.; Delbecq, F.; Sautet, P., *ACS Catal.*, **2011**, *1* (10), 1430-1440.
22. Zaffran, J.; Michel, C.; Delbecq, F.; Sautet, P., *Catal. Sci. Technol.*, **2016**, *6* (17), 6615-6624.
23. Zhang, Q.; Asthagiri, A., *Catal. Today.*, **2019**, *323*, 35-43.
24. Garcia-Ratés, M.; García-Muelas, R.; López, N., *J. Phys. Chem. C.* **2017**, *121* (25), 13803-13809.
25. Cukrowski, I. *Comput, Theor, Chem.*, **2015**, *1066*, 62-75.

26. Blanco, M.; Martín Pendás, A.; Francisco, E., *J. Chem. Theory. Comput.*, **2005**, *1* (6), 1096-1109.
27. Francisco, E.; Martín Pendás, A.; Blanco, M., *J. Chem. Theory. Comput.*, **2006**, *2* (1), 90-102.

Chapter 3

Reaction energy profile and fragment attributed molecular system energy change (FAMSEC)-based protocol designed to uncover reaction mechanism: A case study of the proline catalysed aldol reaction

---

This chapter consist entirely of the paper published in *PCCP* **2019**, *21* (30), 16694-16705.

Abstract

A REP-FAMSEC (reaction energy profile-fragment attributed molecular system energy change) protocol designed to explain each consecutive energy change along the reaction pathway is reported. It mainly explores interactions between meaningful polyatomic fragments of a molecular system and, by quantifying energetic contributions, pin-points fragments (atoms) leading to or opposing a chemical change. Its usefulness is tested, as a case study, on the proline catalysed aldol reaction for which a number of mechanisms is being debated for over four decades. Relative stability of *S*-proline conformers, their catalytic (in)activity and superior affinity of the higher energy conformer to acetone is fully explained on an atomic and molecular fragment levels, but still appealing to general chemist knowledge. We found that (i) contrary to generally accepted view, the CN-bond formation cannot be explained by the $N^{\delta-}$,$C^{\delta+}$ atom pair but rather by O-atom of acetone and its strongest intermolecular attractive interactions with N-atom as well as C-atom of the COO group of proline (at this initial stage the lower energy conformer of proline is eliminated) and (ii) the following 'first' H-transfer from N to O atoms of proline moiety is nearly energy-free even though initially H-atom interacts three times stronger with N- than O-atom; a full explanation of this phenomenon is provided.

3.1. Introduction

The classic understanding of how bond formation and breaking occurs in organic reactions is intrinsically linked to two principles, the 3D-structure of the molecule as approximated by the linear combination of atomic orbitals and the electronic structure of the molecule.[1] Typically, in considering a multi-step chemical process a textbook approach will involve the identification of atoms of reactants with most negative ($A^{\delta-}$) and positive ($B^{\delta+}$) partial charge constituting a 2-atom fragment G = {A,B} of a molecular system with the expectation being that the large difference in electronegativity $\Delta\delta$(A,B), will lead to the formation of a new bond.[2–4] Although the movement of electrons from nucleophilic to electrophilic sites is successfully used to predict the formation (breaking) of covalent bonds in many instances,[5] this approach does not provide a deep understanding of processes taking place and does not guarantee that $\Delta\delta$(A,B) is the primary driving force. Moreover, in many instances the failure of reactions with the required structural and electronic features is challenging to predict (explain) by use of this approximate model.

Typically, by combining general knowledge, available experimental data and chemical intuition, a working hypothesis is put forward and used in drawing a reaction mechanism.[6,7] Clearly, it would be highly beneficial if such hypotheses could be supported (or otherwise) by computational modelling of at least most critical steps. This is then not surprising that computational/theoretical modelling of reaction mechanism and chemical reactivity has gained a lot of attention for decades and indeed it is still a very active area of research.[8–29] (and references therein). There are two general approaches used in gaining chemical insight from quantum chemical calculations, namely, making use of (i) orbitals (e.g., MO,[8–11] VB,[12–15] and NBO[16-18] methods) and (ii) topology of electron density using e.g., properties at BCPs and RCPs,[19-21] topology of the Laplacian,[22] the electron localisation function (ELF),[23] the bonding evolution theory (BET),[24,25] the molecular electron density theory (MEDT)[26,27] and concerted DFT-conceptual DFT-QTAIM approach.[28,29] Although classical orbital-based approach was successful in explaining many reaction mechanisms, the contemporary density-based approaches provide deeper insights that sometimes either do not support previous orbital-based models or are in direct conflict with them[26] (and reference therein).

The use of proline as an organic catalyst was first reported in the 1970's,[30,31] and the reagent can be used in either the L- or S-forms allowing enantioselective transformations most notably aldol condensations[32] and mechanistically related Michael, Robinson and Mannich reactions.[33–35] The mechanism of the proline catalysed aldol reaction (Figure 3.1) is still the target of both theoretical[33,36–38] and experimental investigations[39–41] and to date several contrasting mechanisms

have been proposed.[30,36-38,42–46] Most reports concentrated on the latter stages of the reaction mechanism[47–51] (they are at variance with each other) with less attention being given to initial proline–acetone adduct formation.[46] To date several conformers of proline have been reported but little to no attention has been paid to their role when the entire catalytic process is considered. That being said, there is a single recent report claiming that the active catalyst is the higher energy conformer,[37] with the lowest energy conformer being eliminated at the first H-transfer step.

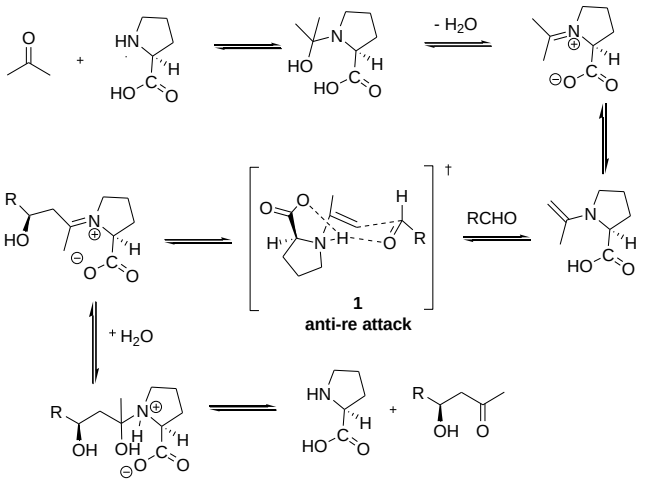

Figure 3.1. Proposed[32] mechanism of proline catalysed aldol reaction.

Clearly, prior to considering the entire process, it is of paramount importance to (dis)prove the catalytic form of *S*-proline using computational methods. Furthermore, in such modelling, when performed on an atomic and molecular fragment levels, many atoms of a molecular system should be considered as they might play subtle yet critical mechanistic roles. This, in turn, should provide a more in-depth mechanistic insight into how reactions proceed and why, e.g., 3D, substituent and electronic changes sometimes lead to dramatic variation in reactivity.

Hence, with a focus on the initial steps of the proline catalysed aldol reaction, we decided to go beyond the classical 2-atom approach and a standard analysis of energy profiles generated from computational studies. To explain every incremental step along the reaction pathway, we have developed a protocol that makes use of the energy terms computed within the interacting quantum atoms (IQA)[52,53] framework and a general concept of the fragment attributed molecular system energy change, FAMSEC,[54–56] method (computational details and coordinates for all structures are included in PART A1 of Appendix A). The main (but not exclusive) focus of the protocol is on interaction energies and their changes, ΔE_{int}, computed for each incremental step (with a specific increase/decrease in the electronic energy, ΔE) along the reaction pathway. The protocol is highly flexible as a chemist can (i) select any size of a fragment, from a single atom up to entire molecule, (ii) investigate inter and intrafragment interactions, (iii) analyse variations in long- and short-

distance interactions, or (iv) monitor a process of covalent bond's breaking/formation through $E_{\text{int}}^{\text{A,B}}$ computed for atoms A and B of interest. The wealth of data collected can then be used to rationalize computed ΔE values and identify fragments that either lead to or oppose the chemical change most.

3.2. Basic and relevant to this work concepts

3.2.1. Interacting quantum atoms method (IQA)

The IQA method is an energy partitioning scheme of a molecular system (e.g., a single molecule, adduct, or interacting molecules at a transition state) that recovers properties of atoms, such as (i) their energies confined within each atom's specific volume it occupies in a molecule and (ii) numerous interactions atoms are involved in and this also includes components atoms are made of (nuclei and electrons). Importantly, a molecular system is being considered as made of atoms that fill in the entire space occupied by the system. From this follows that there are no voids in 3D molecular space or regions of overlapping atoms. Hence, each atom has well-defined interatomic boundaries and, as consequence, its own energy that depends mainly on the kind of an atom and somewhat (to a much lesser degree) on its placement in a molecule. From this follows that the computed electronic (or *ab initio*) molecular energy E can be recovered in the IQA scheme by summing up energies of each atom A, called total (or additive, $E_{\text{add}}^{\text{A}}$) atomic energies – Eq. 3.1,

$$E = E_{\text{IQA}} = \sum_{\text{A}} E_{\text{add}}^{\text{A}} \tag{3.1}$$

In accord with a chemical intuition, all IQA atoms of a molecule are involved in interactions (either attractive or repulsive) with associated interaction energies. Importantly, regardless whether a classical chemist see atoms as covalently or otherwise (non)bonded, they all are treated on equal footing. From this follows that the total atomic energy must consist of two major components, namely the energy of an atom itself (often referred to as a self-atomic energy, $E_{\text{self}}^{\text{A}}$) and the sum of diatomic interaction energies, $E_{\text{int}}^{\text{A,B}}$, atom A is experiencing with each other atom B of a molecule. Note that to make an energy of an atom additive (in order to recover energy E of a system), the total interaction energy involving all possible unique atom pairs {A,B} is halved – Eq. 3.2,

$$E_{\text{add}}^{\text{A}} = E_{\text{self}}^{\text{A}} + 0.5\sum_{\text{X}\neq\text{A}} E_{\text{int}}^{\text{A,B}} \tag{3.2}$$

From the above it follows that by summing up all self-atomic energies one can compute the total self-molecular energy, Eq. 3.3

$$E_{\text{self}}^{\text{Tot}} = \sum_{\text{A}} E_{\text{self}}^{\text{A}} , \tag{3.3}$$

and by summing up all unique diatomic interaction energies between atoms A and B one obtains the total interaction energy of a molecular system, Eq. 3.4

$$E_{\text{int}}^{\text{Tot}} = 0.5 \sum_{\text{A}} \sum_{\text{B}\neq\text{A}} E_{\text{int}}^{\text{A,B}} . \tag{3.4}$$

Note that the total self-molecular energy and total interaction energy of a molecular system recovers the electronic energy of that system, Eq. 3.5,

$$E = E_{\text{IQA}} = E_{\text{self}}^{\text{Tot}} + E_{\text{int}}^{\text{Tot}} . \tag{3.5}$$

IQA is a powerful tool that partitions self-atomic and interaction energies into many important components that are extremely useful in theoretical studies, e.g., in understanding a nature and strength of chemical bonding. For instance, whereas $E_{\text{int}}^{\text{A,B}}$ quantifies strength of interaction or chemical bonding of any nature between two atoms A and B, by partitioning this energy term - Eq. 3.6

$$E_{\text{int}}^{\text{A,B}} = V_{\text{XC}}^{\text{A,B}} + V_{\text{cl}}^{\text{A,B}} \tag{3.6}$$

to the exchange-correlation ($V_{\text{XC}}^{\text{A,B}}$, the interaction energy due to purely quantum effects) and classical ($V_{\text{cl}}^{\text{A,B}}$, the classical electrostatic Coulomb interaction) components a chemists gains an instant quantitative description of bonding and its nature in terms of the degree of covalent (XC-term) or electrostatic contributions. To learn more about other IQA-defined energy components (we will not make use of them in this work) an interested reader is referred to relevant literature on IQA and its applications.

3.2.2. Fragment attributed molecular system energy change (FAMSEC)

It is trivial to state that it would be of great importance and assistance to a chemist if one was able to understand and quantify changes taking place throughout a molecular system when it is exposed to a new environment. A change of environment can be seen as a broad spectrum of chemically relevant events, such as:

(a) Conformational change (to understand relative stability of conformers and role played by intramolecular interactions as well steric clashes).

(b) Formation of adducts and clusters (what drives them to form, molecular fragments interacting strongest in adducts).

(c) Reaction pathway from reactants through a transition state to products (this covers inter and intramolecular interactions, bond breaking and new bond formation; all needed to explain reaction mechanism and preferential substitution sites).

(d) Formation of metal complexes and their relative stability (*e.g.* in terms of formation of 5- and 6-membered coordination rings and their influence on strength of coordination bonds), and many more.

Moreover, it would be highly beneficial to explain these changes in terms of classical thinking as it should be useful in designing a chemical process leading to a desired output (product). Clearly, to gain an insight on a complex chemical process, one must compare the properties of atoms, chemically meaningful molecular fragments or even entire molecules between two states of a molecular system, i.e., when it changes form a particular initial state (it can be used as a reference state, *ref*) to a state of a system that is of interest (final state, *fin*). Two major and useful for interpretation approaches are used in FAMSEC; they focus on:

(1) Properties confined to a 3D space occupied by a selected (on purpose) *n*-atom fragment G of a system and related to it energetic effects when the *ref* → *fin* structural transformation or chemical change takes place. This can be seen as focusing on a localised to within a fragment G event and *loc*-FAMSEC energy term applies

$$\textit{loc}\text{-FAMSEC} = \Delta E^{\mathcal{G}}_{\text{self}} + \Delta E^{\mathcal{G}}_{\text{int}} . \tag{3.7}$$

The $\Delta E^{\mathcal{G}}_{\text{self}}$ term accounts for self-fragment energy change, i.e., a sum of self-atomic energy changes of atoms constituting a molecular fragment G. The $\Delta E^{\mathcal{G}}_{\text{int}}$ term quantifies the intra-fragment interaction energy change and when G is made of two atoms it quantifies a diatomic interaction energy change. From this follows that *loc*-FAMSEC might be useful in identifying parts of a molecule that experienced most significant decrease/increase of their energies on a *ref* → fin environmental change that can be interpreted as being most stabilised/strained, respectively, in *fin* relative to *ref*.

(2) How changes in properties of G and remaining atoms of a molecule (typically treated as another molecular fragment H) impact on entire molecule when *ref* → *fin* occurs and what are energetic

consequences in terms of stability of a molecule. This can be seen as a global, on a molecular scale, event and it can be quantified by use of the *mol*-FAMSEC energy term,

$$\textit{mol}\text{-FAMSEC} = \textit{loc}\text{-FAMSEC} + \Delta E_{\text{int}}^{\mathcal{G},\mathcal{H}} \quad (3.8)$$

where the $\Delta E_{\text{int}}^{\mathcal{G},\mathcal{H}}$ energy term quantifies the interfragment interaction energy change between G (a fragment of interest) and H (remaining atoms of a molecular system).

Moreover, when $\Delta E_{\text{int}}^{\mathcal{G},\mathcal{H}} < 0$ then it implies that G found itself, relative to the *ref* state, in more attractive (stabilizing) molecular environment when in the *fin* state. The interplay between the two components, *loc*-FAMSEC and $\Delta E_{\text{int}}^{\mathcal{G},\mathcal{H}}$, decides whether the molecular fragment G has added to stability of the *fin* state of a molecular system (then *mol*-FAMSEC < 0) or contributed in a destabilizing manner.

It is important to stress that the *loc*- and *mol*-FAMSEC terms can be computed for all unique, 2-, 3-, …, *n*-atom, fragments. From that one can establish which fragments were most locally (de)stabilised and which ones (de)stabilised a molecule the most, *etc.* This is very useful information in interpreting many chemical phenomena and also puts the energies attributed to a selected fragment on a molecular-scale perspective.

3.2.3. FAMSEC-based protocol designed for the study of reaction mechanism

Firstly, let us point at several aspects that must be brought to the attention of a classical chemist and we will make use of adduct made of *S*-proline (lowest energy conformer) and acetone to illustrate points specified below:

1) The $E_{\text{self}}^{\text{Tot}}$ energy term always contributes most to molecular electronic energy *E* regardless of the level of theory used. The computed at a B3LYP/6-311++G(d,p) level of theory *E*(adduct) is –594.5415085 a.u. that translates to hundreds of thousands of kcal/mol, namely –373080.4 kcal/mol, of which 98.32 % comes from the total self-molecular energy, $E_{\text{self}}^{\text{Tot}}$(adduct). Very much comparable values apply to the components of adduct; 98.33 and 98.31% of the total energy of *S*-proline and acetone comes from $E_{\text{self}}^{\text{Tot}}$(*S*-proline) and $E_{\text{self}}^{\text{Tot}}$(acetone), respectively. It means that less than 1.7 % of *E* comes from all interactions and this also includes all covalent bonds! These %-fractions are typical in many molecular systems and do not very significantly with the level of theory.
2) When a synthetic process is considered (from reactants, through adduct formation, structural re-arrangements leading to a transition state, formation of intermediates, formation of a final product

and by-products) rather small changes in molecular system energy ΔE are observed when compared with the total energy of a system. Typically, ΔE does not exceed ±30 kcal/mol at a single step of a chemical process and this would constitute just 0.008% of this adduct energy.

3) Obviously, the expression $\Delta E = \Delta E_{\text{self}}^{\text{Tot}} + \Delta E_{\text{int}}^{\text{Tot}}$ holds at any point along reaction coordinates but the changes in self-atomic energies do not typically exceed ±10 kcal/mol for an individual atom. For instance, 22 (out of 27) atoms of adduct experienced $\left| \Delta E_{\text{self}}^{\text{A}} \right| < 2$ kcal/mol and the largest change found on the adduct formation was +8.3 kcal/mol.

4) The number of unique atom-pairs {A,B} in any molecular system is $(n \times (n\text{-}1))/2$ where n is the number of atoms (e.g., $n = 27$ in the *S*-proline adduct with acetone). Hence, not only there are many more diatomic interactions than atoms in a molecule (the number of unique diatomic pairs in the adduct is 351) but their interactions can vary extensively; the $\Delta E_{\text{int}}^{\text{A,B}}$ values are often over an order of magnitude larger when compared with either $\Delta E_{\text{self}}^{\text{A}}$ or $\Delta E_{\text{self}}^{\text{B}}$. To illustrate this point, the most significant changes $\Delta E_{\text{int}}^{\text{A,B}}$ were found to be –161.3 and +138.3 kcal/mol for {O19,C14} and {O18,14} atom pairs, respectively, on this adduct formation.

The above observations inspired us in designing a protocol where a general concept of FAMSEC, i.e., monitoring changes in selected on purpose energy terms (rather than values themselves) is used to explain ΔE for each consecutive step (hence the overall reaction mechanism) with a main focus on interaction energies as they vary most and can be seen as a driving force for a chemical change. This protocol can be seen as open-ended as one can pursue many strategies in monitoring and explaining a chemical process. To this effect, one can consider all possible 2,3,4-…*n*-atom fragments in order to identify parts of a molecule that play the leading role. Moreover, this protocol is perfectly suited for making best use of chemical intuition and general knowledge in selecting atoms constituting classical functional groups or specific fragments of molecules, or even entire molecules that interact with each other. Clearly, there is no specific protocol to follow as each synthetic route involving different reactants containing specific functionalities might require a unique set of descriptors needed to explain the role played by uniquely selected molecular fragments. However, as a good starting point, *n*-atomic fragments might/should be selected for which most significant change in the intra- and inter-fragment interaction energies were computed between consecutive steps. Furthermore, from a change in e.g., di-atomic interaction energies it is highly informative and useful to identify atoms of these fragments that facilitate or obstruct the progress of reaction most. To guide a chemist in selecting energy terms that might be most

appropriate in explaining the computed ΔE values for a particular step along the reaction coordinates, a set of approaches (far from being exhaustive) and what knowledge can be gained from them is included in PART A2 of Appendix A.

3.3. Results and discussion

There is a growing evidence that chemical bonding has a multicentre character not only in the case of classical intramolecular H-bonds but also in the case of typical covalent bonds, such as C–C, with numerous atom contributing to electron density into the inter-nuclear region where bond is thought to be formed.[57–62] Furthermore, diatomic interaction energies computed for all unique atom pairs show that many of them, even when considered as being non-bonded, are indeed involved in very strong interactions. We realised that more fruitful and informative approach should focus on molecular fragments containing atoms involved in most significant inter-fragment and intermolecular interactions. This concept is implemented in the present study and applied to each consecutive step identified from computational modelling of a reaction mechanism.

3.3.1. The origin of relative stability of *S*-proline conformers

Molecular graphs of *S*-proline conformers **1** reported in the literature[37] (Figure 3.2, part A) show the same kind of classical H-bond (O16–H17···N13) in **1a** and **1b** (lower and higher energy conformers, LEC and HEC, respectively); in each case a well-defined density bridge (or Bader's bond path) is linking N13 and H17. From MP2 data (E_{ZPVE}, H and G), **1a** is lower in energy by ~ –6.7 kcal/mol.

Classically, by an eye inspection of structural features, the higher stability of **1a** would be attributed to the presence of the significantly shorter H-bond (d(N13,H17) = 1.78637 Å in **1a**; ~ 0.3388 Å shorter than in **1b**) and/or (in)availability of the lone electron-pair on N13 to form an intramolecular H-bond with H17. This might be the case, but would have to be proven, and this is not an easy (if at all possible) task. Let us start then with the two-atom (classical) approach: we computed $E_{\text{int}}^{\text{N13,H17}}$ of –132.8 kcal/mol in **1a** that is stronger, by –33.5 kcal/mol, than in **1b.** In both conformers, the diatomic $E_{\text{int}}^{\text{N13,H17}}$ interaction energy is dominated, in accord with classical thinking, by the electrostatic component with $V_{\text{cl}}^{\text{N13,H17}}$ of –113.8 and –92.5 kcal/mol in **1a** and **1b**, respectively. Importantly, the exchange-correlation energy term, $V_{\text{XC}}^{\text{N13,H17}}$ = –19.1 kcal/mol, in **1a** is not only significant (it constitutes 14.3 % of the total interaction energy) but it is also stronger, by –12.2 kcal/mol, when compared with **1b**. This seems to correlate well with the

reviewer's comment on the better exposure of a free electron pair on N13 in **1a**, but it does not explain fully (as will be shown below) a relative stability of the two conformers.

Part A

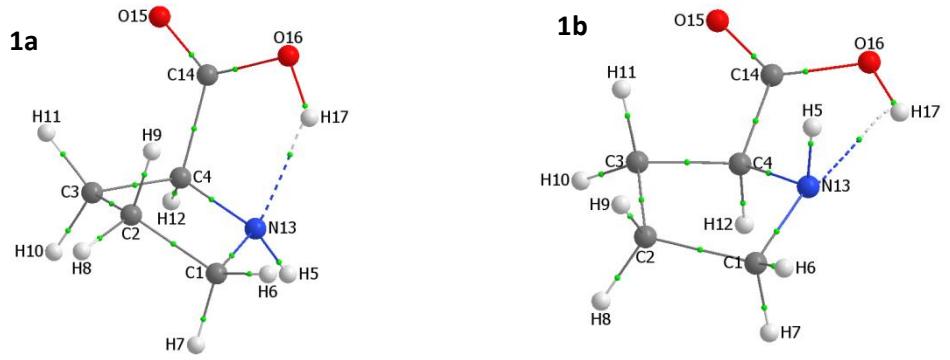

Part B

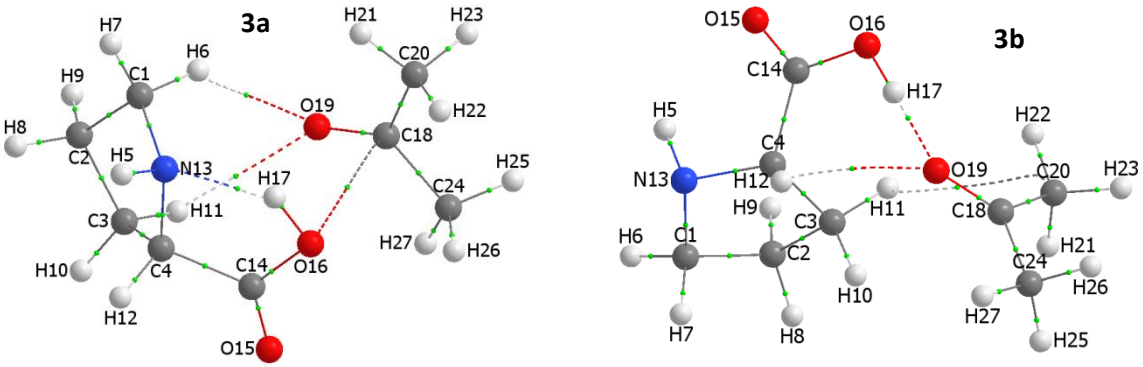

Figure 3.2. Molecular graphs of: part A - lower (**1a**) and higher (**1b**) energy conformers of *S*-proline; part B - the global minimum structures of adducts **3a** (**1a** and acetone, **2**) and **3b** (**1b** and **2**).

Hence, instead of focusing on a single interaction, we analysed entire molecules and relevant data are placed in PART A3 of Appendix A. Analysis of all 136 unique atom pairs (119 non-covalent interactions and 17 covalent bonds) shows that:

1 Covalent bonds (*Cov*-bonds) are stronger in **1a** by $\Delta E_{\text{int}}^{Cov\text{-bonds}}$ = –39.2 kcal/mol that is more significant than $\Delta E_{\text{int}}^{\text{N13,H17}}$. Moreover, the components of $\Delta E_{\text{int}}^{Cov\text{-bonds}}$, namely $\Delta V_{\text{XC}}^{Cov\text{-bonds}}$ = +15.0 kcal/mol and $\Delta V_{\text{cl}}^{Cov\text{-bonds}}$ = –54.2 kcal/mol show that, quite unexpectedly, an increase in strength of all covalent bonds in **1a** is entirely due to a large contribution of stabilizing nature made by these bonds' electrostatic (classical) components.

2 The sum of all (covalent and long distance) 136 diatomic interaction energies ($E_{\text{int}}^{\text{Tot}}$) is more negative in **1a,** by $\Delta E_{\text{int}}^{\text{Tot}}$ = –49.6 kcal/mol, with a classical component $\Delta V_{\text{cl}}^{\text{Tot}}$ of –49.8 kcal/mol,

meaning that the same set of interactions contributes to stability of the LEC much more then in HEC

3 Atoms of the {C14,N13} fragment are involved in the strongest attractive intramolecular diatomic interaction in both conformers, $E_{\rm int}^{\rm C14,N13}$ = –188.2 and –176.9 kcal/mol in **1a** and **1b**, respectively, with 96.8 % coming from the electrostatic nature of these interactions ($V_{\rm cl}^{\rm C14,N13}$ of –182.2 and –171.1 kcal/mol in **1a** and **1b**, respectively). The N13···H17 H-bond is only the second strongest interaction that is weaker, by 55.3 and 77.5 kcal/mol in **1a** and **1b**, respectively, when compared with the C14···N13 interaction. In accord with classical thinking, however, the intramolecular N13···H17 H-bonding interaction strengthened most (by –33.5 kcal/mol) among all di-atomic interactions on the **1b** → **1a** structural change closely followed by the covalently bonded {C14,O16} atom-pair with $\Delta E_{\rm int}^{\rm C14,O16}$ of –33.0 kcal/mol ($\Delta V_{\rm XC}^{\rm C14,O16}$ = –6.6 and $\Delta V_{\rm cl}^{\rm C14,O16}$ = –26.4 kcal/mol).

One can also gain an additional insight on relative stability of conformers by analysing changes in specific energy components on the structural transformation of **1b** (HEC) to **1a** (LEC). The FAMSEC method is perfectly suited for the purpose and it revealed that:

1) Out of 17 atoms of *S*-proline, 11 became involved in stronger intramolecular interactions as measured by the $E_{\rm int}^{\rm A,\mathcal{R}}$ term where R. is a molecular fragment made of all the atoms of *S*-proline except A. This means that most of atoms found molecular environment of the LEC of *S*-proline favourable with N13, C14, O16 and H17 strengthening their interactions most for which we obtained the $\Delta E_{\rm int}^{\rm A,\mathcal{R}}/\Delta V_{\rm cl}^{\rm A,\mathcal{R}}$ values of –45.8/–36.7, –27.2/–29.2, 21.9/–22.7 and –9.8/–9.6 kcal/mol, respectively. Notably, strengthening/weakening of most (but not all) interactions (regardless whether being considered as covalent bonds or long-distance) is predominantly due to changes in the electrostatic components as no new bonds are formed or broken on the **1b** → **1a** structural transformation.

2) The {H17,N13} fragment became most stabilised (*loc*-FAMSEC = –18.3 kcal/mol) whereas the {O16,N13} fragment stabilised the entire **1a** molecule the most (*mol*-FAMSEC = –49.7 kcal/mol). It is important to understand that there are two possible ways any *n*-atom fragment can stabilize the *fin* (here **1a**) relative to *ref* (here **1b**) state of a molecular system when interactions are considered: interactions can become either more attractive or less repulsive. To illustrate this let us first follow energy contributions made by an 'obvious' G = {H17,N13} fragment. Its di-atomic interaction

strengthened most (with $\Delta E_{\text{int}}^{\text{N13,H17}}$ of –33.5 kcal/mol) among all 136 atom-pairs, self-fragment energy increased ($\Delta E_{\text{self}}^{\text{N13,H17}}$ = 15.2 kcal/mol) and as a result this fragment became stabilised in **1a** (eq. 7) with *loc*-FAMSEC = –18.3 kcal/mol. New nuclear positions of N13 and H17 in **1a** resulted in the overall weakening of these atoms interactions with remaining atoms of *S*-proline treated as a fragment H ($\Delta E_{\text{int}}^{\mathcal{G},\mathcal{H}}$ =11.3 kcal/mol). Summing up *loc*-FAMSEC and $\Delta E_{\text{int}}^{\mathcal{G},\mathcal{H}}$ (eq. 8) gives *mol*-FAMSEC energy term of –7.0 kcal/mol showing that this atom-pair does indeed adds to overall stability of **1a** but its contribution is seven times smaller than that made by the G = {O16,N13} fragment. To explain this unexpected finding, we will follow the same protocol as for the intramolecular H-bond. Predictably, N13 and O16 are involved in highly repulsive interaction in **1b** ($E_{\text{int}}^{\text{N13,O16}}$ = 128.0 kcal/mol) that became even more repulsive in **1a** by +12.9 kcal/mol (with $\Delta V_{\text{XC}}^{\text{N13,O16}}$ and $\Delta V_{\text{cl}}^{\text{N13,O16}}$ of –5.0 and +17.9 kcal/mol, respectively) due to d(N13,O16) of 2.5535 Å in **1a** being shorter by 0.1577 Å than in **1b**. The self-fragment energy increased by $\Delta E_{\text{self}}^{\text{N13,O16}}$ = 30.8 kcal/mol and the sum of $\Delta E_{\text{int}}^{\text{N13,O16}}$ and $\Delta E_{\text{self}}^{\text{N13,O16}}$ gave *loc*-FAMSEC = +43.7 kcal/mol resulting in the G = {N13,O16} fragment being most destabilised on **1b** → **1a**. However, the new placement of these two atoms in **1a** facilitated these atoms interactions with the remaining atoms (fragment H) such that $\Delta E_{\text{int}}^{\mathcal{G},\mathcal{H}}$ = –93.5 kcal/mol was obtained. Clearly, the inter-fragment interactions strengthened much more when compared with an increased (i) repulsive interaction between the two atoms and (ii) their self-atomic energies. Summing up *loc*-FAMSEC and $\Delta E_{\text{int}}^{\mathcal{G},\mathcal{H}}$ terms we obtained the net energy contribution, *mol*-FAMSEC = –49.7 kcal/mol, made by this fragment to a molecular energy that is the most significant contribution of stabilizing nature among all unique atom pairs in **1a**.

The above observations (together with additional data in Appendix A) would not be easily predicted (most likely not even considered) by a classical organic chemist, but on the other hand they provide a wealth of information and, most importantly, fully explain the relative stability of the *S*-proline conformers (and molecular systems in general).

3.3.2. Proline-Acetone adduct formation

To understand reaction mechanism fully we have analysed all possible structural changes leading to consecutive steps and relevant energy profiles computed at two levels of theory are depicted in Figure 3.3 Such a detailed approach is not used in classical interpretations of reaction

mechanisms (see Figure 3.1); hence, they cannot explain, e.g., chemical reactivity of conformers or necessary structural re-arrangements as well as forces driving a chemical change. In sections that follow we will explain all energy changes along reaction coordinates as well as energy differences between consecutive steps computed for the lowest and higher energy conformers of *S*-proline.

S-proline **1** and acetone **2** readily form adducts **3**; the global minimum structures discovered, **3a** and **3b,** are shown in Figure 3.1, part B. Importantly, the energy of **3b** is only 2.5 kcal/mol higher relative to **3a** at the MP2 level (Figure 3.3).

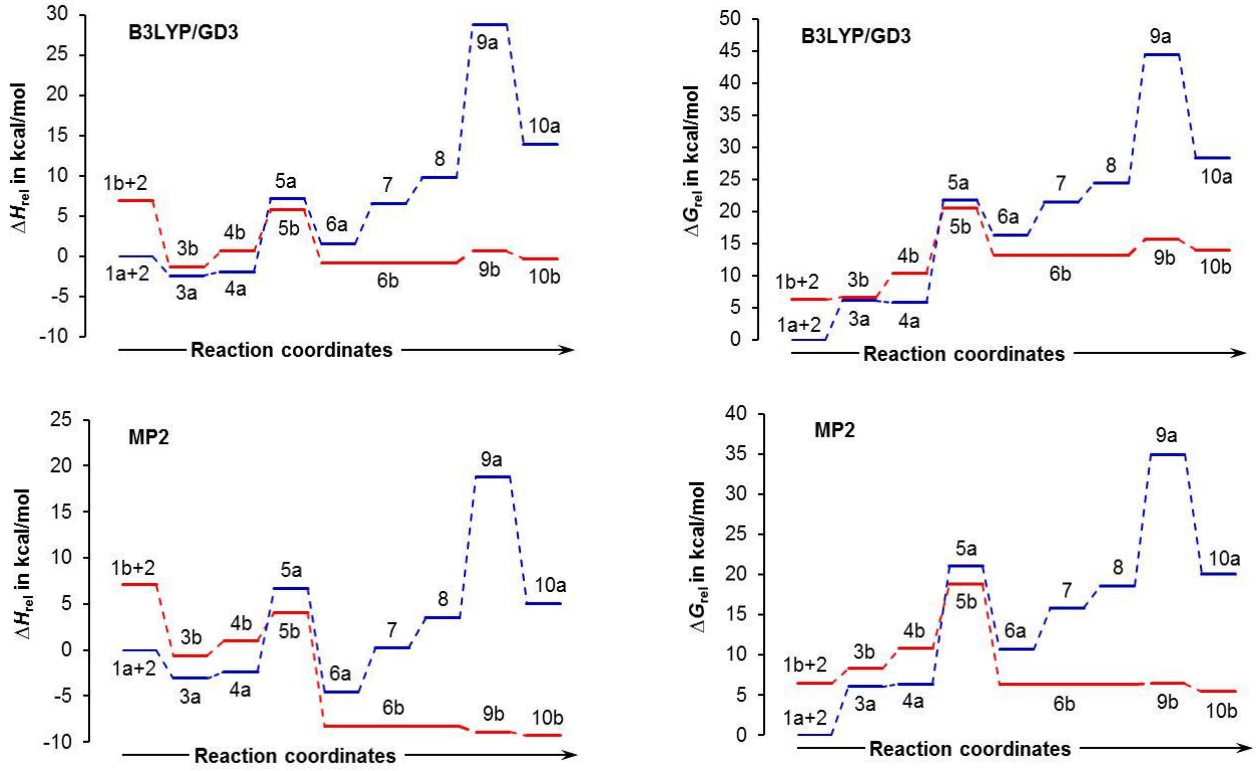

Figure 3.3. Relative to the initial states, either **1a**+**2** or **1b**+**2**, enthalpy and Gibbs free energy changes computed at the indicated levels of theory for all intermediate structures leading to the product of H-transfer, **10a** and **10b**.

Clearly, on the adduct formation, the energy of molecular system **3b** made of **1b**+**2** must have decreased more significantly relative to **3a**.

To explain this, let us focus on what we consider being most pertinent to a classical chemist (for more details and relevant data see PART A4 in Appendix A):

1) The two molecules, **1** and **2**, can be seen as molecular fragments of the molecular system **3**. These molecules show high affinity to each other as measured by the total intermolecular interaction

energy, $E_{\text{int}}^{\mathbf{1,2}}$, i.e., the sum of *intermolecular* diatomic interaction energies computed for all unique 170 atom-pairs. We found $E_{\text{int}}^{\mathbf{1a,2}}$ and $E_{\text{int}}^{\mathbf{1b,2}}$ of –34.3 (with $V_{\text{XC}}^{\mathbf{1a,2}}/V_{\text{cl}}^{\mathbf{1a,2}}$ = –26.7/–7.6 kcal/mol) and –53.6 kcal/mol (with $V_{\text{XC}}^{\mathbf{1b,2}}/V_{\text{cl}}^{\mathbf{1b,2}}$ = –40.7/–12.9 kcal/mol) in **3a** and **3b**, respectively. Therefore, the HEC interacts with **2** stronger by –19.3 kcal/mol with main contribution coming from the XC-term.

2) The combined intra and intermolecular diatomic interactions became stronger in **3**; hence, they stabilised both molecular systems but significantly more, by –24.8 kcal/mol, in the case of **3b**.

3) Molecular fragments G and H (4) containing atoms of **1** and **2**, respectively, can be seen as driving the adduct formation. This is because these atoms are involved in strongest diatomic intermolecular interactions in **3a** and **3b** with $\left|E_{\text{int}}^{\text{A,B}}\right|$ > 10 kcal/mol; among them, 10 and 5 atom-pairs are involved in very strong interactions with $\left|E_{\text{int}}^{\text{A,B}}\right|$ above 50 and 100 kcal/mol, respectively - see Tables A7–A9, PART A4 in Appendix A. The interfragment interaction energy, $E_{\text{int}}^{\mathcal{G},\mathcal{H}}$ of –5.3 and –43.2 kcal/mol computed for **3a** and **3b,** respectively, supports the much higher affinity between **1b** and **2**.

4) We have also identified individual atoms playing most significant role – Table A7 in PART A4 in Appendix A. The formation of adducts is driven mainly by attraction between entire fragment G of **1** and (i) C18 of **2** with $E_{\text{int}}^{\mathcal{G},\text{C18}}$ = –19.5 kcal/mol ($V_{\text{cl}}^{\mathcal{G},\text{C18}}$ = –17.4 kcal/mol) in **3a** and (ii) quite unexpectedly, O19 of **2** with over three times stronger interaction energy $E_{\text{int}}^{\mathcal{G},\text{O19}}$ of –62.0 kcal/mol ($V_{\text{XC}}^{\mathcal{G},\text{O19}}$ = –28.3 kcal/mol and $V_{\text{cl}}^{\mathcal{G},\text{O19}}$ = –33.7 kcal/mol) in **3b**.

5) The leading role of the {H17,O19} atom-pair destined to form a new covalent bond is already apparent on the adduct formation. Relative to **3a**, an order of magnitude larger $V_{\text{XC}}^{\mathcal{G},\text{O19}}$ in **3b** is mainly due to the exchange-correlation term $V_{\text{XC}}^{\text{H17,O19}}$ of –18.3 kcal/mol that is in contrast to ~0 kcal/mol (in both adducts, **3a** and **3b**) computed for the atom-pair destined to make a new C18–N13 bond.

To conclude, regardless of the approach taken, a consistent picture emerges pin-pointing the origin of a more significant energy decrease for the **3b** formation and the higher affinity of the HEC (**1b**) to **2**.

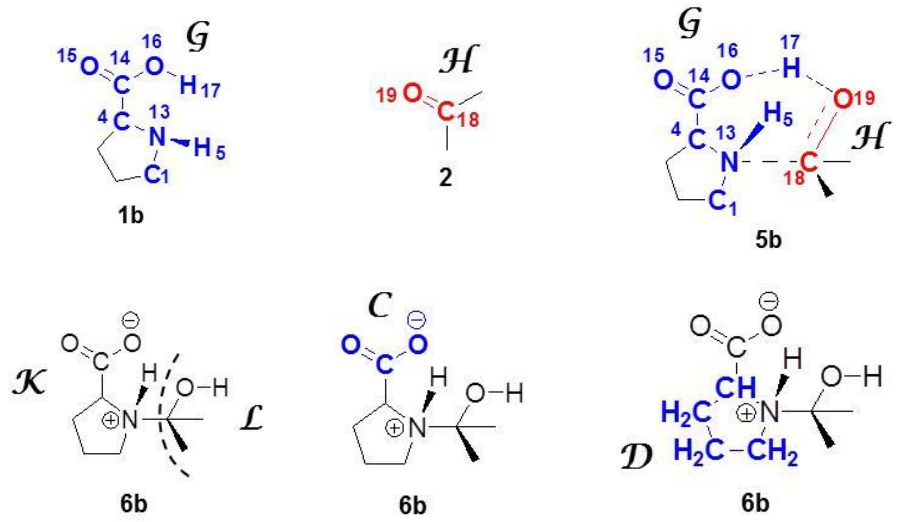

Figure 3.4. Schematic presentation of selected molecular fragments used in this study.

3.3.3. CN-bond formation

In a first step, proline-acetone adducts **3** must overcome an energy barrier of about 3 kcal/mol to form pre-organised structures **4** (Figure 3.5); a complete set of data pertaining to the CN bond formation is included in PART A5 of Appendix A. As found for **3**, **1** and **2** are also involved in overall attractive intermolecular interactions in **4** but nearly three times stronger in **4b** ($E_{\text{int}}^{1,2}$ = –70.3 kcal/mol). Surprisingly, however, the $E_{\text{int}}^{1,2}$ energy term changed in the opposite direction on the **3a** → **4a** and **3b** → **4b** structural re-arrangements as we found $\Delta E_{\text{int}}^{1,2}$ of +10.4 and –16.7 kcal/mol, respectively. Therefore, **1** and **2** interact much stronger in **4b** (by –46.4 kcal/mol) and **4b** appears to be much better pre-organised for progression of the reaction as (i) the interatomic distances d(N13,C18) and d(H17,O19) of 2.9278 and 1.6806 Å in **4b** are much shorter than in **4a** (by 0.41 and 0.64 Å, respectively). Moreover, considering the **3** → **4** structural re-arrangements we found that:

a) There are eight {A,B} atom-pairs involved in either attractive or repulsive interactions with $\left|E_{\text{int}}^{\text{A,B}}\right|$ > 10 kcal/mol in **3** and **4**; the same atoms also experienced the most significant change in interaction energies on the preorganization process. Therefore, relevant atoms of **1** (or **2**) were selected to constitute the G and H molecular fragments shown in – Tables A13-A15 in PART A5 of Appendix A.

b) Inter-molecular interactions between atoms of the {N13,C18} and {H17,O19} fragments in **3a** are highly attractive (–76.9 and –65.6 kcal/mol, respectively) but they are only fourth and fifth,

respectively, among most attractive interactions (the strongest interaction in **3a** was found between C14 and O19 atoms with $E_{\text{int}}^{\text{C14,O19}}$ = –161.3 kcal/mol).

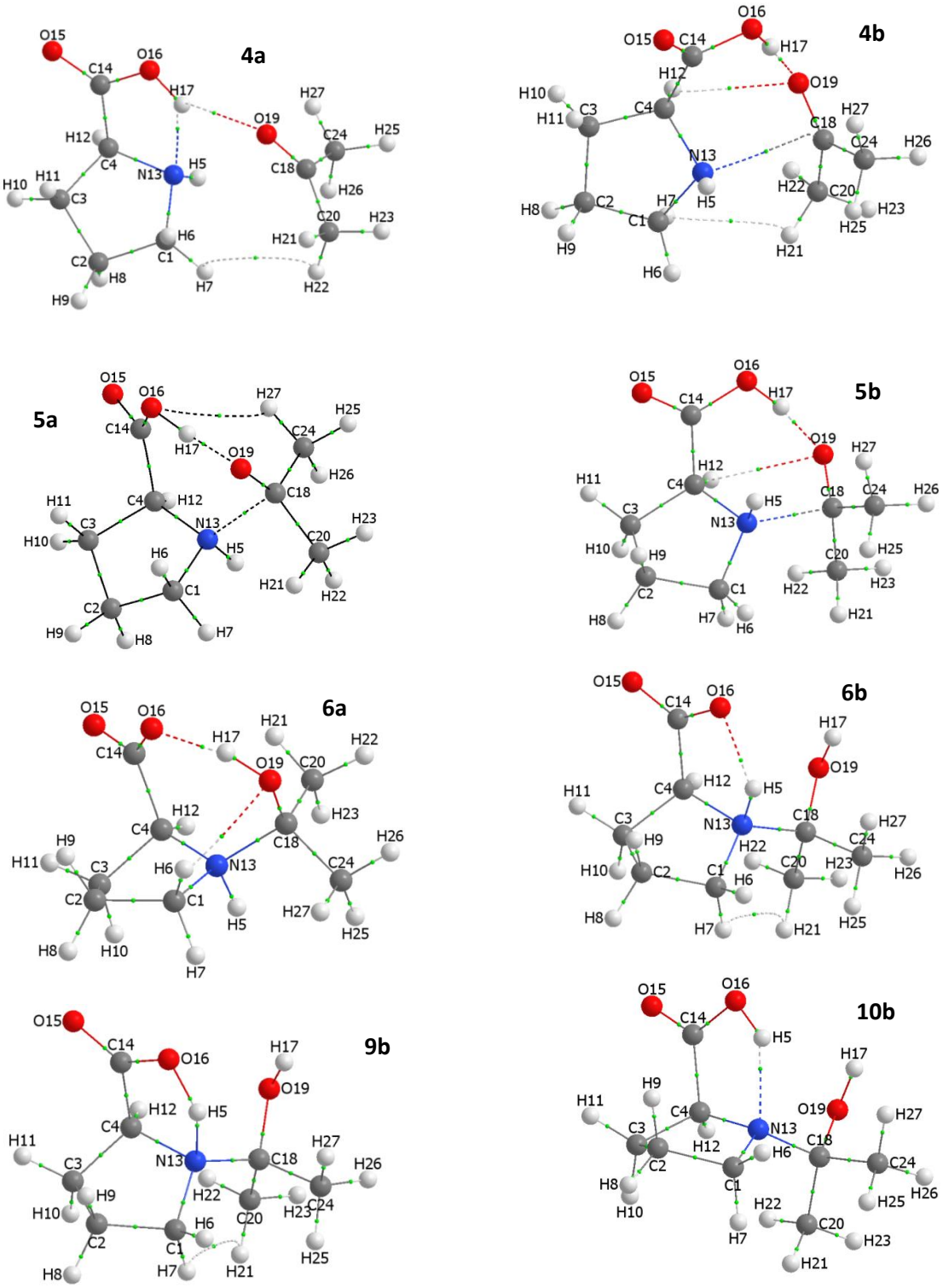

Figure 3.5. Molecular graphs of pre-organised adducts (**4a** and **4b**), TS structures for the CN-bond formation (**5a** and **5b**), products after the C–N bond formation (**6a** and **6b**), TS structure for the first H-transfer (**9b**) and product after the first H-transfer (**10b**).

c) Interactions between atoms of {N13,C18} and {H17,O19} became even stronger and of comparable strength in **4a** (with $E_{\text{int}}^{\text{A,B}}$ of about –103 kcal/mol) but $E_{\text{int}}^{\text{C14,O19}}$ of –139.6 kcal/mol is still the strongest. We also noted that $\Delta E_{\text{int}}^{\text{H17,O19}}$ of –37.1 kcal/mol was most significant among 170 intermolecular diatomic interaction changes on **3a** → **4a** and the {H17,O19} fragment became most stabilised in **4a** with *loc*-FAMSEC = –33.4 kcal/mol.

d) In **3b**, H17 and O19 are involved in an extremely strong interaction of $E_{\text{int}}^{\text{H17,O19}}$ = –143.9 kcal/mol that is (i) nearly three times stronger than that between N13 and C18 and (ii) second strongest as it is about 'only' 16 kcal/mol weaker than that found between C14 and O19. The interaction between N13 and C18 strengthened the most, by –54.1 kcal/mol when in **4b** ($E_{\text{int}}^{\text{N13,C18}}$ = –112.2 kcal/mol) but it is still 34.3 kcal/mol weaker when compared with the {H17,O19} fragment. Here again, atoms of the {C14,O19} fragment are involved in the strongest interaction of –165.3 kcal/mol.

From the above, which can be seen as a picture recovered from the diatomic intermolecular interaction perspective, it is obvious that (i) the interaction between N13 and C18 cannot be seen as the leading driver in forming either **4a** or **4b** and (ii) between the {H17,O19} and {N13,C18} atom pairs, the former plays by far more important role in leading to **4b**.

An additional and important insight one can gain from a single atom A perspective when its interactions with entire oncoming molecule are considered, either $E_{\text{int}}^{\text{A,1}}$ or $E_{\text{int}}^{\text{A,2}}$. To this effect we discovered (Table A16 in PART A5 of Appendix A) that on **3** → **4**:

a) Totally unexpectedly, C18 that is destined to form a covalent bond with N13 of **1**, is involved in most significant overall repulsive interactions dominated by electrostatic repulsion as we obtained $E_{\text{int}}^{\text{C18,1}}/V_{\text{cl}}^{\text{C18,1}}$ of +7.8/+9.8 and +11.2/+17.2 kcal/mol in **4a** and **4b**, respectively; hence, it is opposing oncoming **1a** and **1b**. Even more surprising is the fact that C18 interactions with **1** changed from slightly attractive in **3a** to repulsive in **4a.** In contrast, O19 that is destined to form a covalent bond with H17 of **1**, is involved in most attractive interactions with about

b) 50% covalent contribution; we obtained $E_{\text{int}}^{\text{O19,1}}/V_{\text{XC}}^{\text{O19,1}}$ of –25.8/–13.3 and –69.3/–35.6 kcal/mol in **4a** and **4b**, respectively. Hence O19 facilitates the process leading to the formation of these two bonds most among atoms of **2**.

c) Focusing on **1**, there are three atoms that attract oncoming **2** most, namely N13, H17 and C14. H17 of both *S*-proline conformers is involved in the strongest attractive interactions that are predominantly of electrostatic nature in **4a** but showing 50% covalent character in **4b** ($E_{\text{int}}^{\text{H17,2}}/V_{\text{XC}}^{\text{H17,2}}$

of –17.0/–4.0 (in **4a**) and –38.4/–19.2 (in **4b**) kcal/mol). Interactions involving N13 and **2** are stronger in **4b** and are dominated by the XC-term ($E_{\text{int}}^{\text{N13,2}}/V_{\text{XC}}^{\text{N13,2}}$ of –5.8/–7.3 (in **4a**) and –24.6/–15.2 (in **4b**) kcal/mol). This illustrates an important role played by H17 in both conformers of *S*-proline and N13 in the HEC that, as discussed above, shows much higher overall affinity to **2**.

Let us discus a picture that immerged on the **4** → **5** step (i.e., reaching the TS) starting from the intermolecular diatomic interactions. As one would expect, atoms of the {N13,C18} and {H17,O19} fragments are involved in strongest interactions in **5** (Table A19 in PART A5 of Appendix A). However, $E_{\text{int}}^{\text{H17,O19}}$ of –217.0 kcal/mol is still stronger (by –9.4 kcal/mol) than that involving N13 and C18 in **5a**. In contrast, $E_{\text{int}}^{\text{N13,C18}}$ of –224.8 kcal/mol is now stronger (by –26.7 kcal/mol) than that involving H17 and O19 in **5b**. Notably, only at the TS the covalent contribution to interaction between N13 and C18 became larger ($V_{\text{XC}}^{\text{N13,C18}}$ = –74.2 kcal/mol) relative to the that found for the {H17,O19} atom-pair ($V_{\text{XC}}^{\text{H17,O19}}$ = –44.9 kcal/mol). Interestingly, the new bonds formed, C18N13 and O19H17, are of comparable strength in **6b**, as indicated by interaction energies of –311.9±0.1 kcal/mol, but the O19H17 bond in **6a** is stronger by –30.4 kcal/mol.

From the 1-atom perspective, interactions between C18 and **1** changed from overall repulsive to attractive ($E_{\text{int}}^{\text{C18,1}}$ of –32.3 and –43.4 kcal/mol were computed in TSs **5a** and **5b**, respectively, Table A21 in PART A5 of Appendix A) and they are several times weaker when compared with interactions between O19 and **1** for which we found $E_{\text{int}}^{\text{O19,1}}$ of –174.9 and –167.6 kcal/mol in **5a** and **5b**, respectively. Furthermore, from the classical electrostatic component point of view, C18 is strongly obstructing oncoming **1** in the TSs as $V_{\text{cl}}^{\text{C18,1}}$ became more repulsive from +9.8/+17.2 to +47.8/+48.3 kcal/mol in **4a**/**5a** and **4b**/**5b**, respectively. In contrast, O19 interactions with **1** are characterised by largely strengthened electrostatic attractions that changed from –12.5/–33.8 kcal/mol in **4a**/**4b** to –93.1/-94.5 kcal/mol in **5a**/**5b**.

Considering atoms of **1**, the interactions between either N13 or H17 and **2** are by far the strongest as we found $E_{\text{int}}^{\text{N13,2}}$ of –120.0/–131.9 kcal/mol and $E_{\text{int}}^{\text{H17,2}}$ of –100.0/–93.8 kcal/mol in **5a**/**5b**. Importantly, these atoms attractive nature of electrostatic interactions with **2** strengthened and particularly so in the case of H17 as $V_{\text{cl}}^{\text{H17,2}}$ changed from –12.8/–19.2 (in **4a**/**4b**) to –53.8/–56.8 (in **5a**/**5b**) kcal/mol.

From the above and data in the Appendix A we came to several important conclusions:

1. This stage of the catalytic process is always reflected as the CN-bond formation implying that it is driven by the interacting $\{N^{\delta-}\cdots C^{\delta+}\}$ atom pair. Our results contradict this generally accepted view as they conclusively showed that many diatomic and atom-molecule interactions (excluding those involving C18) can be seen as responsible for relative orientation of *S*-proline (**1**) and acetone (**2**) already on the adduct (**3**) formation and its better pre-organised structure (**4**) leading to the TS. As a matter of fact, C18 is involved in repulsive classical interactions with an on-coming **1** even at the TS. Hence, we have concluded that binding of *S*-proline and acetone via the C18–N13 bond formation can be seen as kind of a 'by-product' of other and much stronger, hence leading interactions.

2. From the perspective of a single atom interacting with an oncoming molecule it follows that: (i) O19 of **2** (due to interactions with atoms of oncoming **1**, either **1a** or **1b**) and (ii) N13 and H17 of **1** (due to these atoms interactions with atoms of oncoming **2**) drive the process from **4** to **6**.

3. From the 2-atom perspective we discovered that the interaction between C14 and O19 is the strongest in **3** and **4** and is closely followed by strength of interaction between H17 and O19 in **3b** and **4b**. Hence, the $\{C14^{\delta+}\cdots O19^{\delta-}\}$ fragment (with $\Delta\delta$(C14,O19) = 2.69*e* in **4b**) can be seen as a driving force that is highly assisted by the $\{H17^{\delta+}\cdots O19^{\delta-}\}$ fragment (with $\Delta\delta$(H17,O19) = 1.79*e* in **4b**) in process leading to the CN as well as OH bonds formation in **6**.

4. It is evident that O19 plays a very special and decisive role at this stage of a catalytic process as it is a major player regardless of the perspective taken.

5. It is apparent that **2** should preferentially form CN and OH bonds with **1b** rather than **1a**.

Let us briefly discuss an energy difference between transition states **5a** and **5b**. The energy barrier, when moving from **4** to TSs **5,** is much lower (by ~6 kcal/mol) for **5b** resulting in **5b** having a lower energy than **5a** by ~2.5 kcal/mol (MP2 data). The lower energy barrier computed for **5b** can be attributed to **4b** being better pre-organised when compared with **4a**, as discussed above. A slightly lower energy of **5b** relative to **5a** can be explained from the total self-molecular energy, $E_{\text{self}}^{\text{Tot}}$, and the total interaction energy of the molecular system, $E_{\text{int}}^{\text{Tot}}$. Since $E_{\text{self}}^{\text{Tot}}$ increased in **5**, relative to **4**, by about the same value of 26 kcal/mol, the lower energy of **5b** when compared with **5a** must be attributed to the change in $E_{\text{int}}^{\text{Tot}}$ (recall that energy of a system is the sum of $E_{\text{self}}^{\text{Tot}}$ and $E_{\text{int}}^{\text{Tot}}$). Indeed, the overall change in all interaction energies was found to be –8.5 and –11.0 kcal/mol for **5a** and **5b**, respectively, and this compares very well with the difference in the energy barrier at the TS being ~2.5 kcal/mol lower in the case of **5b**. Clearly, the small energy difference between

5a and **5b** is, in this instance, a result of combined large increases and decreases in interaction energies between many atoms on the **4** → **5** step.

Finally, combined MP2 data (for details see Table A4 in PART A4 and Table A8 in PART A5 in Appendix A) shows that the energy of **6b** is lower, relative to **1b+2**, by ΔH = –15.4 kcal/mol and ΔG = –0.2 kcal/mol. In contrast, a small decrease in H and significant increase in G of –4.6 and +10.6 kcal/mol, respectively, was computed for **6a**. From this, one can conclude that on the CN-bond formation the reaction path involving **1a** should be eliminated. In other words, any molecular system that has two equivalent (chemistry-wise) states will proceed towards the lower energy structure, here **6b**, provided this does not require overcoming a large energy barrier as is indeed the case for the **1b**+**2** pathway. As this work has demonstrated, a selection based on relative energies of conformers or molecules in general (a common practice in the field[6]) in considering their involvement in synthetic rout might lead to wrong conclusions.

3.3.4. First proton transfer

Energy profile diagrams in Figure 3.3 show that **6a**, even if it were present in the reaction environment, cannot be involved in consecutive steps. This is because (i) **1a+2** would have to overcome (ΔG_{rel} at the MP2 level) a total energy barrier of ~35 kcal/mol to reach **9a** (TS) and (ii) the product of H-transfer **10a** is higher in energy than **1a**+**2** by 20 kcal/mol (note significantly larger values at B3LYP/GD3). From the ΔG_{rel} perspective, a reverse process is thermodynamically driven, from **10a**, via quite small 15 kcal/mol energy barrier at **9a**, to initial reactants **1a**+**2**.

A very different and significantly more favourable energy profile is observed for the path involving **1b**+**2**. These reactants must overcome a small energy barrier (from **1b**+**2** to **5b**) of 12.3 kcal/mol (ΔG_{rel} at MP 2) to form **6b** and the proton transfer is essentially 'energy-free' (ΔG_{rel} at MP2 between **6a** and **9b** is 0.1 kcal/mol). Hence, our overall interpretation is as follows. We found an energy barrier of 10.8 kcal/mol (at B3LYP/GD3) applicable to the **1a** → **1b** conformational re-arrangement. This means that starting from **1a**+**2** it is less energy demanding to reach **5b** via **1b** than **5a** via **3a** and **4a**. Furthermore, ΔE_{rel}(**6b**) << ΔE_{rel}(**6a**) regardless of whether ΔG_{rel} or ΔH_{rel} at MP2 is considered. It is then clear that **1a** is eliminated from the reaction environment already at the first major step of this catalytic process; nonetheless, for those interested we have provided relevant data to explain step-wise hypothetical changes from **6a** to **10a** in Appendix A.

Typically, the energy profiles shown in Figure 3.3, together with accompanied analysis of energy differences between consecutive steps, would fully satisfied a physical organic chemist in interpreting (i) relative catalytic properties of *S*-proline and (ii) the proton transfer as nearly a spontaneous process, hence not rate determining step. However, having all diatomic interactions at hand, we noticed with a great concern that H5 is attracted much more to N13 (by –135 kcal/mol) than to O16 in **6b**. Then why does H5 leave N13 as easily as revealed by the enthalpy and Gibbs free energy changes shown in Figure 3.3? Clearly, the related energy profile cannot be explained by way of classical thinking and it was of paramount importance to analyse molecular system from **6b**, *via* **9b** (TS) to **10b**.

Looking at computed diatomic interactions we established that H5 is involved in attractive interactions only with 4 atoms, namely: N13 to which it is bonded to in **6b**, O15 and O16 of the COO functional group of molecular fragment K and O19 of the L fragment (see Figure 3.4). Due to the fact that on a proton transfer process H5 is heading not only towards O16 but rather in the direction of the entire COO group, it makes perfect sense to partition K into two fragments, one containing COO atoms (we will call it C) and remaining atoms of K with exclusion of N13 (let us call it D). We decided to make use of our approach to gain an insight on a plausible origin of the proton transfer. To this effect, we considered specifically selected for the purpose interactions:

a) The interaction energies $E_{\text{int}}^{\text{H5,N13}}$ and $E_{\text{int}}^{\text{H5,O16}}$ are –254.3 and –119.1 kcal/mol in **6b**, respectively. Clearly, this cannot lead to an energy 'free' transfer of H5 to O16.

b) H5 is being attracted by atoms of the C fragment with $E_{\text{int}}^{\text{H5},\mathcal{C}}$ of –65.5 (in **6b**) and –148.0 (in **9b**) kcal/mol and this is not sufficient for the spontaneous proton transfer either because $E_{\text{int}}^{\text{H5,N13}}$ = –203.8 kcal/mol was obtained in **9b**. Therefore, there must be other interactions that facilitate the chemical event leading to the TS **9b**.

c) Notably, H5 is being repelled by atoms of L with $E_{\text{int}}^{\text{H5},\mathcal{L}}$ of +46.2 (in **6b**) and +43.5 (in **9b**) kcal/mol. One must stress that the computed $E_{\text{int}}^{\text{H5},\mathcal{L}}$ term includes the attractive interaction between H5 and O19 in L of –68.1 and –75.8 kcal/mol in **6b** and **9b**, respectively.

d) H5 is also being repelled by atoms of D with $E_{\text{int}}^{\text{H5},\mathcal{D}}$ of +85.3 (in **6b**) and +86.7 (in **9b**) kcal/mol. Importantly, these repulsive interactions, $E_{\text{int}}^{\text{H5},\mathcal{L}}$ and $E_{\text{int}}^{\text{H5},\mathcal{D}}$, do not change significantly on **6b** → **9b** and, by repelling H5, can be seen as counteracting the H5 attraction to N13 by 'pushing' H5 towards O16 (or C in general); hence, atoms of L and D facilitate H5 transfer. One can get a

rough estimate of the corrected (for repulsive contributions) interaction energy ${}^{\text{corr}}E_{\text{int}}^{\text{H5,N13}}$ between H5 and N13 by summing up $E_{\text{int}}^{\text{H5,N13}}$, $E_{\text{int}}^{\text{H5},\mathcal{L}}$ and $E_{\text{int}}^{\text{H5},\mathcal{D}}$; it gives a product of –122.8 (in **6b**) and –73.7 kcal/mol in **9b**. Finally, accounting for the attraction of H5 to the C fragment (${}^{\text{corr}}E_{\text{int}}^{\text{H5,N13}} - E_{\text{int}}^{\text{H5},C}$) gives us –57.3 and +74.3 kcal/mol of the net interaction energies between N13 and H5 in **6b** and **9b**. This shows that a small movement of H5 between N13 and O16, e.g., due to numerous vibrational modes, will change the balance from being attracted more either to N13 or to O16.

Finally, the computed ${}^{\text{corr}}E_{\text{int}}^{\text{H5,N13}}$ and $E_{\text{int}}^{\text{H5},C}$ interaction energy terms in **10b** of –16.4 and –223.3 kcal/mol, respectively, show that the proton transfer from **6b** to **10b** can be seen as overall favourable. Furthermore, one must note that (i) **10b** is perfectly pre-organised for the next step, i.e., water elimination and (ii) according to our study, H5 must be on O16 for the water elimination to take place. From this follows that even when one assumes some kind of equilibrium N13 ← H5 → O16 with H5 oscillating between N13 and O16 in **6b**, **9b** and **10b**, the reaction will proceed with ease due to **10b** being used up by the water elimination process.

3.4. Conclusions

The reaction energy profile (REP) computed for the assumed reaction mechanism illustrates how the energy of a molecular system varies along the reaction coordinates. Small (or large) energy differences between consecutive steps are typically used in support (or rejection) of the proposed mechanism but they provide no insight on the origin of processes taking place. In order to identify atoms and molecular fragments leading to a chemical change (with the associated computed an energy change of a molecular system) we have implemented the general concept of the fragment attributed molecular system energy change (FAMSEC) method combined with analysis of interactions between fragment of different sizes (they range between a single atom to entire molecule). Hence, a new method is proposed (called the REP-FAMSEC method) that represents a shift from a commonly used 2-atom approach (involving interacting atoms of reactants with most negative $A^{\delta-}$ and positive $B^{\delta+}$ partial charges) to interacting poly-atomic fragments of a molecular system. Focusing on initial steps of the proline catalysed aldol reaction (used here as a case study), we have (i) identified atoms and molecular fragments that lead to every incremental step along the reaction pathway and (ii) quantified their energy contributions in terms of relevant intra- and inter-fragment/molecular interaction energies and their changes between consecutive stages of the reaction progression. The proposed REP-FAMSEC approach proved to

be of general nature as we were able to fully explain (i) relative stability of the *S*-proline conformers, (ii) why only higher energy conformer (HEC) can act as a catalyst; it has been demonstrated that the involvement of the lower energy conformer (LEC) in the proline catalysed aldol reaction is terminated already in the first major step commonly called the CN-bond formation, (iii) the CN-bond formation mechanism showing that it is not driven by the interacting $\{N^{\delta-}\cdots C^{\delta+}\}$ atom pair but rather the O-atom of acetone plays a very special and deceive role at this stage of a catalytic process, (iv) nearly energy-free the intramolecular proton transfer (taking place after the CN-bond formation) from N to O atoms of proline moiety even though initially H-atom interacts three times stronger with N- than O-atom as well as (v) small differences in the ΔE values computed for reaction pathways involving LEC and HEC.

It has been shown recently[63] that the FAMSEC energy terms (more generally, changes in the IQA-defined energy terms) computed at the computationally affordable B3LYP/IQA combination produced exact qualitative description of relative stability of glycol conformers and, quantitatively, perfectly comparable values with CCSD/BBC1/IQA data. This, together with the protocol described in this work, paves the way for studying many reaction mechanisms even when a significant number of atoms is involved.

3.5. References

1 R. Koch, and T. Clark, *Linear Combination of Atomic Orbitals*, The Chemist's Electronic Book of Orbitals. Springer, Berlin, Heidelberg 1999, pp. 5–22.

2 C. Jonathan, N. Grevees, S. Warren, and P. Wothers, *Organic Chemistry*, 1st ed., Oxford University Press 2001, pp. 123–133

3 W. O. Kermack, R. Robinson, *J. Chem. Soc. Trans.*, 1922, **121**, 427–440.

4 N. P. Grove, M. M. Cooper, and K. M. Rush, *J. Chem. Edu.*, 2012, **89**, 844–849.

5 G. Abhik, and B. Steffen, *Arrow Pusshing in Inorganic Chemistry*, A logical Approach to the Chemistry of Main Group Elements. John Wiley & Sons 2014.

6 L. Jarrige, D Glavač, G. Levitre, P. Retailleau, G. Bernadat, L. Neuville and G. Masson, *Chem. Sci*., 2019, **10**, 3765–3769.

7 H. Mitsunuma, S. Tanabe, H. Fuse, K. Ohkubo and M. Kanai, *Chem. Sci*., 2019, **10**, 3459–3465.

8 R. B. Woodward and R. Hoffmann, *J. Am. Chem. Soc.*, 1965, **87**, 395–397.

9 R. B. Woodward and R. Hoffmann, *J. Am. Chem. Soc.*, 1965, **87**, 2511–2513.

10 R. Hoffmann and R. B. Woodward, *Acc. Chem. Res*., 1968, **1**, 17–22.

11 K. Fukui, *Acc. Chem. Res*., 1971, **4**, 57–64.

12 R. D. Harcourt, *J. Mol. Struct.*, (THEOCHEM) 1997, **398**, 93–100.

13 A. C. Pavão, C. A. Taft, T. C. F. Guimarães, M. B. C Leão, J. R. Mohallem and W. A. Lester, Jr., *J. Phys. Chem. A*, 2001, **105**, 5–11.

14 S. Shaik and P. C. Hiberty, Valence bond theory, its history, fundaments, and applications: A primer. In *Reviews in Computational Chemistry*; K. B. Lipkowitz, R. Larter and T. R. Cundari, Eds.; Wiley-VCH: Hoboken, New Jersey, 2004, Vol. 20, Chapter 1.

15 P. C. Hiberty and S. Shaik, *J. Comput. Chem*., 2007, **28**, 137–151.

16 E. D. Glendening and F. Weinhold, *J. Comput. Chem.*, 1998, **19**, 593–609.

17 E. D. Glendening and F. Weinhold, *J. Comput. Chem.*, 1998, **19**, 610–627.

18 E. D. Glendening, J. K. Badenhoop and F. Weinhold, *J. Comput. Chem*. 1998, 19, 628–646.

19 X. Li, Y. Zeng, L. Meng and S. Zheng, *J. Phys. Chem. A*, 2007, **111**, 1530–1535.

20 X. Li, H. Fan, L. Meng, Y. Zeng and S Zheng, *J. Phys. Chem. A*, 2007, **111**, 2343–2350.

21 P. Macchi and A. Sironi, *Coord. Chem. Rev.*, 2003, **238**, 383–412.

22 N. O. J. Malcolm and P. L. A. Popelier, *J. Phys. Chem. A*, 2001, **105**, 7638–7645.

23 J. Andrés, S. Berski, M. Feliz, R. Llusar, F. Sensato and B. Silvi, *C. R. Chimie*, 2005, **8**, 1400–1412.

24 L. R. Domingo, *RSC Adv.*, 2014, **4**, 32415–32428.

25 J. Andrés, S. Berski, L. R. Domingo, V. Polo and B. Silvi, *Current Org. Chem.*, 2011, **15**, 3566–3575.

26 L. R. Domingo, M. Ríos-Gutiérrez, B. Silvi and P. Pérez, *Eur. J. Org. Chem*., 2018, **9**, 1107–1120.

27 L. R. Domingo, *Molecules*, 2016, **21**, 1319.

28 V. Tognetti, S. Bouzbouz and L. Joubert, *J. Mol. Model.*, 2017, **23**, 5.

29 R. Inostroza-Rivera, M Yahia-Ouahmed, V. Tognetti, L. Joubert, B. Herrera and A. Toro-Labbé, *Phys. Chem. Chem. Phys.*, 2015, **17**, 17797–17808.

30 Z. G. Hajos and D. R. Parrish, *J. Org. Chem.*, 1974, **39**, 1615–1621.

31 U. Eder, G. Sauer and R. Wiechert, *Angew. Chem., Int. Ed.*, 1971, **10**, 496–497.

32 B. List, R. A. Lerner and C. F. Barbas, *J. Am. Chem. Soc.*, 2000, **122**, 2395–2396.

33 R. B. Sunoj, *Wiley. Interdiscip. Rev. Comput. Mol. Sci.*, 2011, **1**, 920–931.

34 M. M. Heravi, V. Zadsirjan, M. Dehghani and N. Hosseintash, *Tetrahedron: Asymmetry*. 2017, **28**, 587–707.

35 T. D. Machajewski and C. H. Wong, *Angew. Chem., Int. Ed.*, 2000, **39**, 1352–1375.

36 Y. Nobakht and N. Arshadi, *J. Mol. Model.*, 2018, **24**, 334.

37 M. J. Ajitha and C. H. Suresh, *J. Mol. Catal. A: Chem.*, 2011, **345**, 37–43.

38 G. Yang, and L. Zhou, *Catal. Sci. Technol.*, 2016, **6**, 3378–3385.

39 W. Notz and B. List, *J. Am. Chem. Soc.*, 2000, **122**, 7386–7387.

40 S. Mukherjee, J. W. Yang, S. Hoffmann and B. List, *Chem. Rev.*, 2007, **107**, 5471–5569.

41 H. Yang, X. Zhang, S. Li, X. Wang and J. Ma, *RSC Adv.*, 2014, **4**, 9292–9299.

42 C. Agami, C. Puchot and H. Sevestre, *Tetrahedron Lett.*, 1986, **27**, 1501–1504.

43 L. Hoang, S. Bahmanyar, K. Houk and B. List, *J. Am. Chem. Soc.*, 2003, **125**, 16–17.

44 B. List, L. Hoang and H. J. Martin, *Proc. Natl. Acad. Sci. U. S. A.* 2004, **101**, 5839–5842.

45 K. N. Rankin, J. W. Gauld and R. J. Boyd, *J. Phys. Chem. A.*, 2002, **106**, 5155–5159.

46 G. Yang, Z. Yang, L. Zhou, R. Zhu and C. Liu, *J. Mol. Catal. A: Chem.*, 2010, **316**, 112–117.

47 M. Arnó and L. R. Domingo, *Theor. Chem. Acc.*, 2002, **108**, 232-239.

48 M. Arnó, R. J. Zaragozá and L. R. Domingo, *Tetrahedron: Asymmetry.*, 2005, **16**, 2764–2770.

49 C. Allemann, J. M. Um and K. Houk, *J. Mol. Catal. A: Chem.*, 2010, **324**, 31–38.

50 S. Bahmanyar and K. Houk, *J. Am. Chem. Soc.*, 2001, **123**, 12911–12912.

51 F. R. Clemente and K. Houk, *J. Am. Chem. Soc.*, 2005, **127**, 11294–11302.

52 M. Blanco, M. A. Pendás and E. Francisco, *J. Chem. Theory Comput.*, 2005, **1**, 1096–1109.

53 E. Francisco, M. A. Pendás and M. A. Blanco, *J. Chem. Theory. Comput.*, 2006, **2**, 90–102.

54 I. Cukrowski, *Comput. Theoret. Chem.*, 2015, **1066**, 62–75.

55 I. Cukrowski, F. Sagan and M. P. Mitoraj, *J. Comput. Chem.*, 2016, **37**, 2783–2798.

56 I. Cukrowski, D. M. E. van Niekerk and J. H. de Lange, *Struct. Chem.*, 2017, **28**, 1429–1444.

57 B. Silvi, *J. Mol. Struct.*, 2002, **614**, 3–10.

58 L. R. Lavine and W. N. Lipscomb, *J. Chem. Phys.*, 1954, **22**, 614–620.

59 J. S. Miller, and J. J. Novoa, *Acc. Chem. Res.*, 2007, **40**, 189–196.

60 R. Ponec, G. Lendvay and J. Chaves, *J. Comput. Chem.*, 2008, **29**, 1387–1398.

61 W. Wang, Y. Kan, L. Wang, S. Sun and Y. Qiu, *J. Phys. Chem. C.*, 2014, **118**, 28746–28756.

62 J. H. de Lange, D. M. E. van Niekerk and I. Cukrowski, *J. Comp. Chem.*, 2018, **39**, 973–985.

63 I. Cukrowski, *Phys. Chem. Chem. Phys.*, 2019, **21**, 10244–10260.

Chapter 4

Facilitating role played by a DMSO solvent molecule in the proline catalysed aldol reaction

---

Abstract

From a qualitative and quantitative examining of different modes of interactions along the reaction coordinates and interpreting those in combination with a reaction energy profile (REP) we explored a reaction mechanism in the presence of a DMSO solvent molecule. Interactions between two molecules, a set of molecules, fragments of molecules, or just selected atoms, allows fragment attributed molecular system energy change (FAMSEC) to be explored from which major players driving a chemical change can be identified. Using the principles of the REP-FAMSEC approach we found that proline conformers (lowest **1a** and higher energy **1b**), acetone **2** and DMSO **3** instantly became involved in strong interactions upon the formation of 3-molecular complexes (3-MCs). These interactions mainly involve the HN-C-COOH (of **1**), CO (of **2**) and SO (of **3**) fragments that lead 3-MCs to the global minimum structures (GMSs) and subsequently the first step in this multi-step catalytic aldol reaction, i.e., the first H-transfer and CN-bond formation. The presence of DMSO, through its interactions with **1** and **2**, strongly promotes **1b** and essentially eliminates **1a** as an active catalyst. For instance, interaction (i) combined intra and intermolecular weakened for **1a** and strengthened for **1b** on the input-to-GMS rearrangement of 3-MCs (they are 2.5 more stronger in **1b**-GMS), (ii) between **1** and **2** are 5 times stronger in **1b**-GMS, (iii) involving HN-C-COOH and CO are nearly neutral and highly attractive (–63 kcal/mol) in **1a**-GMS and **1b**-GMS, respectively. The presence of DMSO also improved the REP for **1b**-containing 3-MCs.

4.1. Introduction

Organocatalysts have historically been utilised to catalyse a range of non-asymmetrical organic transformations, most notably Knoevenagel condensations, esterifications, Baylis-Hillman reactions and Stetter reactions.[1,2] Attempts to develop organocatalysed asymmetrical transformations led to the development of the Hajos-Parrish-Eder-Sauer-Wiechert reaction in the 1970s.[3,4] However, following this breakthrough, the development in the field remained largely limited until the late 1990's.[2] In the past two decades, the increasing demand for pure and optically active compounds in chemical industries and academia and a growing drive for greener metal-free catalytic processes has prompted a renaissance in the field of asymmetric organocatalysis.[2,5–7] As a result, one can now access vast libraries of organocatalysts that can be utilised for a multitude of different chemical transformations. Notably, the use of proline and related analogues in asymmetric synthesis has continued to see development, becoming one of the most widely utilised classes of organocatalysts.[8–11]

One of the more important transformations catalysed by proline is the economic direct aldol reaction wherein a C–C bond is formed between simple carbonyls,[12–14] allowing access to enantiomerically rich intermediates. Proline has been shown to exhibit a similar effect to that of type 1 aldolase enzymes,[12,15] wherein the C–C bond formation is preceded by the formation of a key enamine intermediate.[12,16,17] Proline's efficiency as an organocatalyst in the aldol reaction has in turn led to several investigations aimed at elucidating the mechanistic details of the transformation.[17–19]

Computational modelling provides valuable information required to uncover the mechanisms of complex reactions otherwise unavailable when only employing synthetic studies. For example, computational modelling can allow one to rationalise the roles played by different conformers in (i) the formation of adducts with reactants, (ii) moving from global minimum structures (GMS) to structures pre-arranged for bond formation and (iii) transformation from pre-arranged structures to transition states. An assessment of such parameters ultimately provides a clearer picture of the reactivity of the conformers involved.

As pertaining to the proline catalysed aldol reaction, Ajitha and Suresh proposed in 2011, based on a density functional theory (DFT) study, that the lowest energy conformer (LEC) of (*S*) proline was inactive with its reaction pathway not proceeding beyond an initial proton transfer step.[20] In 2019, we confirmed these findings using the Reaction Energy Profile – Fragment Attributed Molecular System Energy Change (REP-FAMSEC) technique.[21] This approach goes beyond the

classical use of reaction energies by identifying atoms, group of atoms treated as molecular fragments, and molecules which either drive or inhibit the progression of a reaction.[21]

In previously reported computational modelling of the aldol reaction,[15,19–24] an implicit solvent model, which "pre-averages" solvent behaviours with a dielectric continuum, has been explicitly used. This is despite the fact that (i) the aldol reaction was reported to proceed better when performed in dimethyl sulfoxide (DMSO),[12,15,25] (ii) incorporating an explicit solvent molecules produced more reliable computed activation free energy barriers in modelling of numerous reaction mechanisms[26,27] and (iii) discrete solvent molecules can capture solvent dynamics[28] and may play a significant role in chemical reactions that implicit solvation models fail to capture.[29,30]

To the best of our knowledge, no prior report is available describing the mechanistic role played by DMSO molecules in the aldol catalysed reactions. Hence, the aim of this work is to explore and explain (i) the reaction mechanism by examining the effects of an explicit solvent molecule of DMSO using a hybrid (explicit + implicit) solvation model in which solvent molecule/s are typically added at sites where specific interactions, like H-bonding, are anticipated to occur and (ii) a role played by the carboxylic group of proline (called a cocatalyst[12]) with a special focus on the initial step described by List et al[12] as 'the nucleophilic attack of the amino group' that leads to a CN-bond formation. List et al[12] hypothesised that 'This cocatalyst may facilitate each individual step of the mechanism, including the nucleophilic attack of the amino group' but were not able to support it. This initial step is of critical importance because it fixes the in-coming molecule, e.g., acetone, through the newly formed CN-bond with proline and this is a pre-requisite for consecutive steps to proceed successfully. To achieve our aims we will take advantage of the recently reported REP-FAMSEC technique; computational details and coordinates of all optimised structures are included in Part B1 of appendix B Information. Finally, there are several important questions we hoped to address, among them:

(i) Do the mechanisms obtained in implicit and hybrid solvation models differ significantly and does the explicit DMSO solvent molecule facilitate catalytic process in general?

(ii) Does a DMSO molecule promote or obstruct the reaction pathway of the lower energy conformer of proline? In other words, is the LEC catalytically active or inactive in the presence of the explicit DMSO molecule?

(iii) Are free energy barriers lowered (or otherwise) and is the impact of a solvent molecule on catalytic properties of both conformers of proline the same?

(iv) Which atoms of proline and acetone play leading and decisive roles in the presence of DMSO?

(v) Which atoms of DMSO have decisive impact (if any) on the catalytic properties of proline?

4.2. Basic concepts of REP-FAMSEC method applicable to this work

A detailed account of the concept and potential applicability of the REP-FAMSEC method have been described previously.[21] Hence, to aid the interpretation of generated energy trends, only basic ideas and expressions relevant to molecular systems of interest to this work will be presented and explained.

We consider a molecular system (MS) as a 3D assembly of any number of atoms that are mathematically treated on equal footing using an Interacting Quantum Atoms (IQA)[31,32] energy partitioning scheme. All atoms of a MS interact with each other and, as we have explained in detail previously,[21] the interatomic interactions are influenced by far more (often by more than an order of magnitude) than just atomic energies when a chemical event occurs. Monitoring, quantifying and interpreting of mainly, but not exclusively, changes in interaction energies is the fundamental concept incorporated in the REP-FAMSEC method. The main inputs come from a diatomic interaction energy term, $E_{\mathrm{int}}^{\mathrm{A,B}}$, and its components (a Coulomb or classical term, $V_{\mathrm{cl}}^{\mathrm{A,B}}$, and an exchange-correlation term, $V_{\mathrm{XC}}^{\mathrm{A,B}}$, that is commonly used as a measure of the degree of covalent contribution). These terms will be computed for each unique atom-pair A,B in a MS regardless of (i) the internuclear distance between them, d(A,B), or whether atoms are considered as being chemically bonded. One must stress that even the smallest displacement of one (or more) atoms within a MS will always change all $E_{\mathrm{int}}^{\mathrm{A,B}}$ values computed for a full set of unique atom-pairs. Naturally, the significance of the interaction energy change, $\Delta E_{\mathrm{int}}^{\mathrm{A,B}}$, depends on the extent of the atoms' displacement due to a chemical event and is largest for atom-pairs containing displaced atoms and their immediate (closest) neighbours.

From a classical perspective, atoms of a MS might belong to a single molecule or several molecules where a molecule is considered as a constellation of atoms linked by a network of mainly, but not exclusively, covalent bonds. In a larger MS, typically, only a few atoms will experience a significant diatomic interaction energy variation on a chemical event, *e.g.* more than ±10 kcal/mol. These atoms are considered in the REP-FAMSEC approach as most responsible for, or as driving a chemical change; interactions they are involved in will be monitored and analysed along the reaction coordinates. It is then appropriate and convenient to consider them as a molecular *n*-atom fragment $\mathcal{G}$ of a MS. Each molecule may have a set of most 'influential' atoms, when a mechanism of a reaction is considered, and they will be treated as separate fragments. Moreover, there may be more than one molecular fragment in a single molecule. Typically, changes in

interaction energies are monitored in a step-wise fashion along the reaction coordinates as $\Delta E_{int} = {}^{fin}E_{int} - {}^{ini}E_{int}$, where *fin* and *ini* refer to the final (after a chemical change) and initial (prior a chemical change) structure (or 3D placement of atoms) of a MS. The ΔE_{int} term might provide invaluable insight at any stage of a process under investigation, e.g., (i) a formation of a poly-molecular complex from separate molecules – from this one can learn how and why molecules arrange themselves relative to each other, and which atoms drive such arrangement, (ii) inclusion of a solvent molecule to a poly-molecular complex – does this impact relative placement of molecules in the complex, what is the solvent molecule's preferred site and why, (iii) can molecules re-arrange themselves 'freely' within a complex and which atoms drive the molecules to attain their lowest, or global minimum structure, and (iv) what drives molecules to better pre-organisation required for subsequent bond formation or breaking, *etc*.

To gain a full picture and understand the reaction mechanism we will analyse many interaction energy terms, such as intra and intermolecular, covalent and long-distance interactions, all of them computed for either a single molecule or grouped molecules. This requires a specific, purposeful grouping of diatomic interaction energy $E_{int}^{A,B}$ terms. As a consequence, numerous and not commonly encountered expressions quantifying such energy terms will be introduced; for convenience they are placed, together with descriptions, in an Appendix at the end of the manuscript. As already mentioned above, in the REP-FAMSEC approach all interactions are accounted for and to appreciate the extent of computation required it is worth mentioning that, e.g., for a medium-sised MS (37 atoms in total) made of proline (**1**), acetone (**2**) and a DMSO solvent molecule (**3**) one has to compute interaction energy $E_{int}^{A,B}$ terms for all 666 unique atom-pairs for both, *ini* and *fin*, states at several stages of a catalytic process. The 666 number is made of 35 covalent bonds, 631 non-covalent (or long-distance, L-D) interactions in total, among them there are 191 and 440 intra and intermolecular L-D interactions, respectively.

4.3. Results and discussion

4.3.1. Formation of three-molecule complexes (3-MCs): proline-acetone-DMSO.

Constructing initial (input) 3-MCs for computational modelling.

When implementing an explicit solvation model, in which discrete molecule/s of solvent are included in the computational modelling, the number of solvent molecules to be added and their positioning relative to the solute molecules is still a subject of debate.[33] Considering an initial placement of a DMSO molecule, we started with the global minimum structures (GMSs) of adducts

(2-MC between proline **1** and acetone **2**) as they are expected to be most dominant in solution and likely to be preferentially solvated. We decided to place a single DMSO solvent molecule (**3**) such that its O37 interacted with proline **1** through H5 – see **4_inp** structures in Table 4.1. We hypothesised that (i) a major impact, in terms of direct interactions between a solvent molecule and those of solute, will be made by DMSO molecules occupying an inner solvation sphere, (ii) since DMSO is a polar solvent, in this case intermolecular H-bond interactions must be mainly considered, and (iii) the initial placement of a DMSO molecule alongside the 2-MC should be such that the interaction between H17 of proline **1** and O19 of acetone **2** should be influenced the least. This is because according to our previous studies,[21] this interaction leads to the transfer of H17 from proline **1** to acetone **2** that, in turn, facilitates the CN-bond formation occurring between N13 (in proline **1**) and C18 (in acetone **2**).

The manually prepared 3-MCs were energy-optimised and, as predicted, the H5···O37 interaction appeared to be strong enough to keep the DMSO molecule in close proximity to proline **1** – see the **4A_inp** and **4B_inp** 3-MCs in Table 4.1. However, the analysis of net atomic charges (see commented Tables B1-B2, Part B2 of Appendix B) revealed that H17 carries a significantly larger positive charge than H5 (both in proline **1**). Having such knowledge, most of orthodox organic chemists would expect that DMSO should in fact preferentially interact with H17. It was then of paramount importance to computationally establish the preferred mode of interaction between proline **1** and DMSO **3**. To achieve that, we placed DMSO **3** with O37 in close proximity to H17 in **1a** as a test. At the same time O19 of acetone **2** was facing H17 as this is required for the H17 transfer to acetone **2**. This means that the prepared structure – see 3-MC called **4A_inp*** in Table 4.1 – allowed for a 'free' competition for the H17 between two H-bond type interactions involving O37 of DMSO **3** and O19 of acetone **2**. The DMSO molecule duly migrated to face the H5 atom during the energy-optimisation process, (see the **4A_LM-3** 3-MC in Table 4.1) affording a 3-MC displaying the relative orientations that we originally hypothesised were necessary.

Re-arrangement from initial to GMS 3-MCs

It is a common practice to search for the lowest energy or global minimum structure (GMS) of a molecule (or molecular system) prior to modelling of any stage of a synthetic organic reaction. This is because the GMS is the most abundant form of a MS in solution. Moreover, and importantly, analysis of structural re-arrangement, from the input to the GMS, should allow the identification of atoms driving the process through intermolecular interactions. Finally, it was also of importance to establish whether the GMS represents the best pre-organised arrangement of molecules for the subsequent H-transfer and CN-bond formation. If not, it would be necessary to establish if the three

molecules can re-arrange themselves 'freely' or at what cost to attain most suitable configuration for reaction to proceed. A detailed description of the protocol used in the search for the GMS as well as a full set of energies (i.e., electronic (*E*), zero-point vibrational energy corrected electronic energy (E_{ZPVE}), enthalpy (*H*) and Gibbs free energy, *G*) are included in Part B3 of Appendix B. These energies were computed for the 3-MCs considered, from the input structures, through the intermediate local minima (LM) to global minimum structures; they are shown in Table 4.1 for both the LEC and HEC of proline.

Table 4.1. Ball-and-stick representation of: part A - **4A** 3-MCs involving **1a** (LEC of proline), **2** (acetone) and **3** (DMSO solvent molecule) and part B – 4B 3-MCs made of **1b** (HEC of proline), **2** and **3**.
Part A

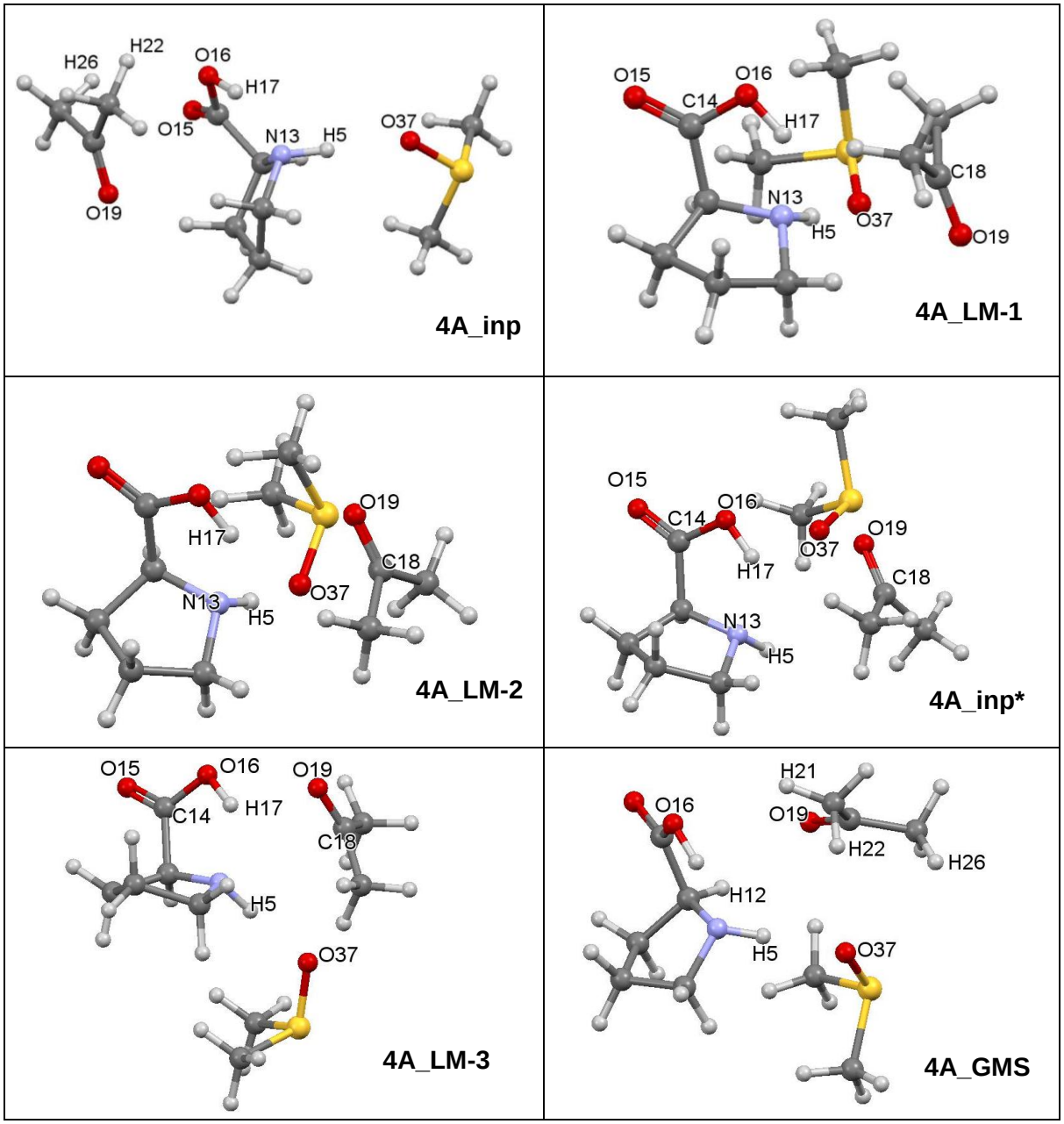

Part B

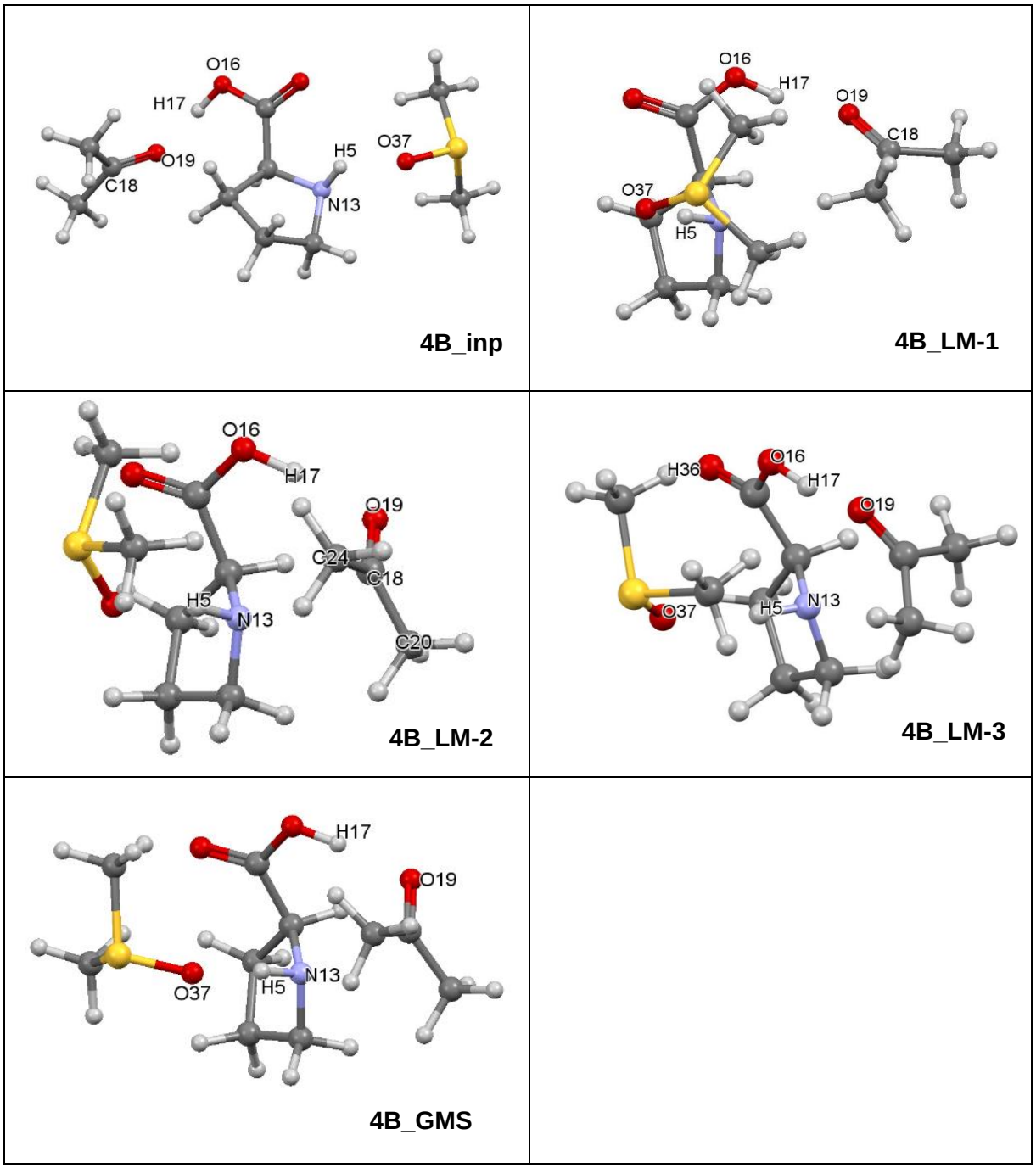

Figure 4.1 shows that in both cases, the formation of 3-MC is energetically favourable when the electronic energy of 3-MCs is considered; note that, relative to separate components, ΔE_{ZPVE} decreased by –9.3 and –12.6 kcal/mol for the **4A_inp** and **4B_inp** MSs, respectively. Furthermore, energetic changes (ΔE_{ZPVE} and ΔG) do not vary much throughout the **4_inp** → **4_GMS** rearrangement, are relatively small and highly comparable for both MSs; relative to the input 3-MCs, a small decrease in the E_{ZPVE} of –2.5 kcal/mol was found for both GMSs.

It is then clear that a classical analysis, based on trends in the ΔE / ΔG values, cannot provide any significant information on what drives molecular systems towards a GMS and the subsequent first stage of a catalytic process. Remarkably, a trend in the change in the total interaction energies, i.e., the $\Delta E_{\text{int}}^{\text{MS}}$ energy term incorporating intra and intermolecular contributions computed for entire molecular systems, follows the overall trend observed in the ΔE_{ZPVE}, but the $\Delta E_{\text{int}}^{\text{MS}}$ values are nearly an order of magnitude more significant. Molecules instantly became involved in strong interactions upon the formation of 3-MCs as $\Delta E_{\text{int}}^{\text{MS}}$ = –62.7 (**4A_inp**) and –72.9 (**4B_inp**) kcal/mol is seen in Figure 4.1.

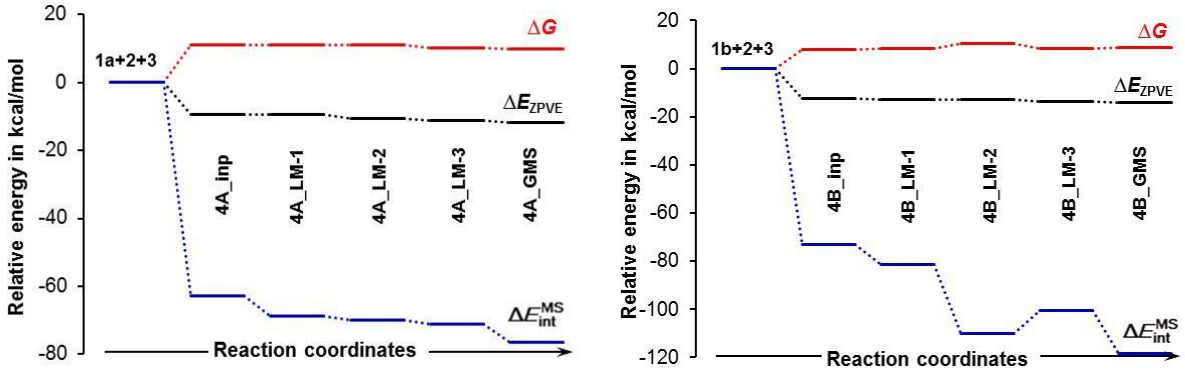

Figure 4.1. Relative to the energy of reactants **1** (proline, either **1a** or **1b**), **2** (acetone) and **3** (DMSO solvent molecule), energy changes (ΔE_{ZPVE}, ΔG and $\Delta E_{\text{int}}^{\text{MS}}$) computed at the 6-311++G(d,p)/GD3 level for 3-MCs shown in Table 4.1.

Notably, they are stronger, by about –10 kcal/mol, in the case of the HEC-containing input 3-MC. These interactions became even stronger in both GMSs and were found to be –118.2 kcal/mol in **4B_GMS** that, relative to **4A_GMS**, is over –40 kcal/mol more significant. One might conclude that (i) the interactions drive the 3-MCs formation in the first place and (ii) strengthening of interactions is a leading force in the **4_inp** → **4_GMS** structural re-arrangement.

Intra and intermolecular interaction energies computed for individual molecules in 3-MCs

The total interaction energy computed for a MS, $E_{\text{int}}^{\text{MS}} = {}_{\text{intra}}^{\text{C-B}}E_{\text{int}}^{\text{MS}} + {}_{\text{intra}}^{\text{L-D}}E_{\text{int}}^{\text{MS}} + {}_{\text{inter}}E_{\text{int}}^{\text{MS}}$, comprises the sum of energy contributions made by (i) all intramolecular interactions within each constituent molecule (i.e., between covalently bonded atoms, ${}_{\text{intra}}^{\text{C-B}}E_{\text{int}}^{\text{MS}}$, and long-distance (L-D) interactions between all the atoms in a molecule, ${}_{\text{intra}}^{\text{L-D}}E_{\text{int}}^{\text{MS}}$) and (ii) the intermolecular interactions between atoms of all molecules making up a MS, ${}_{\text{inter}}E_{\text{int}}^{\text{MS}}$. We decided to decompose the values of $E_{\text{int}}^{\text{MS}}$ computed for 3-MCs in a step-wise manner, with the hope of uncovering the role played

by a DMSO molecule **3** as well as gaining a unique understanding of the molecules' responses to changes in their relative placement in the 3-MCs on conversion from **4_inp** → **4_GMS**. The approach should then provide us with an understanding of what drives the molecules within complexes to attain **4_GMSs**. As far as we know, such an approach has not been reported previously but the concept of the REP-FAMSEC method provides all necessary tools to achieve this.

Our focus now is on the sum of intra and intermolecular interaction energies computed for a single molecule, i.e., the $E_{\text{int}}^{\text{mol}}$ energy term. This term is comprised of contributions derived from covalently bonded and non-bonded L-D intramolecular interactions as well as intermolecular interactions between atoms of a selected molecule and atoms of all remaining molecules. Trends in the $\Delta E_{\text{int}}^{\text{mol}}$ terms computed for each constituent molecule of the 3-MCs considered, are shown in Figure 4.2. They were computed relative to individual molecules (**1a**, **2** and **3**) when they are not involved in any intermolecular interactions.

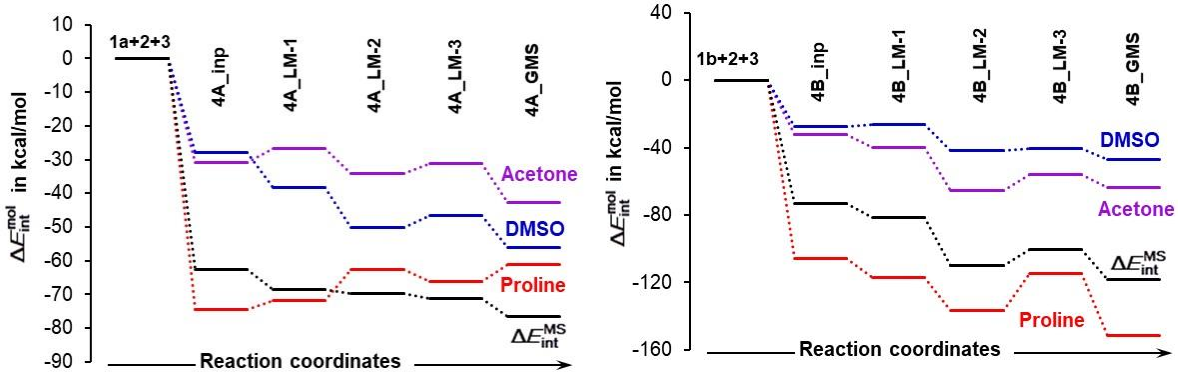

Figure 4.2. Relative to interaction energies computed for separate molecules, changes, $\Delta E_{\text{int}}^{\text{mol}}$, in the sum of intra and intermolecular interaction energies computed for the indicated individual molecules constituting a MS (either **1a**+**2**+**3** or **1b**+**2**+**3**, **4A** or **4B** 3-molecular complexes (3-MCs), respectively) undergoing a structural change. Inp, LM and GMS stands for input, local minimum and global minimum structures of 3-MCs. For comparison, a trend in $\Delta E_{\text{int}}^{\text{MS}}$ (it accounts for all interactions in a MS) is also shown.

Hence, as an example, for the LEC of proline **1a**, $\Delta E_{\text{int}}^{\mathbf{1a}} = {}_{\text{intra}}\Delta E_{\text{int}}^{\mathbf{1a}} + {}_{\text{inter}}E_{\text{int}}^{\mathbf{1a,2}} + {}_{\text{inter}}E_{\text{int}}^{\mathbf{1a,3}}$ applies, where the first term accounts for the change in the intramolecular interactions in proline **1a** on complex formation and the latter two terms account for intermolecular interaction energies between atoms of proline **1a** and all atoms of the other two molecules in the 3-MCs, i.e., **2** (acetone) and **3** (a DMSO solvent molecule). From Figure 4.2, on moving from the input to the GMS structures of the 3-MCs, we found that:

a) Quite surprisingly, the $\Delta E_{\text{int}}^{\mathbf{1a}}$ term computed for the LEC of proline (**1a**) in the 3-MC increased, from –74.5 to –61.1 kcal/mol. Notably, and importantly, **1a** is the only molecule for which an increase in the $\Delta E_{\text{int}}^{\text{mol}}$ term is observed in the **4A_GMS**. This is in total contrast to complexes of the HEC (**1b**) for which the interactions strengthened immensely, from –105.9 (in **4B_inp**) to –151.6 (in **4B_GMS**) kcal/mol; hence, the trends in $\Delta E_{\text{int}}^{\text{mol}}$ values obtained for **1a** and **1b** are opposite.

b) Considering **4A_GMS**, the $\Delta E_{\text{int}}^{\mathbf{1a}}$ value is less significant than the $\Delta E_{\text{int}}^{\text{MS}}$ value. In contrast, just the opposite is observed for the HEC of proline; the trace computed for proline **1b**, i.e., the $\Delta E_{\text{int}}^{\mathbf{1b}}$ term, is consistently below the trend obtained for entire molecular system ($\Delta E_{\text{int}}^{\text{mol}}$) throughout entire **4B_inp** → **4B_GMS** structural re-arrangement.

c) Significant variation in the $\Delta E_{\text{int}}^{\text{mol}}$ term is also observed for acetone **2** and DMSO **3**, but the trends obtained are different in the 3-MCs with **1a** and **1b**. The interactions that the DMSO molecule experiences in **1a**-containing 3-MCs are stronger than those computed for acetone, whereas the opposite trend is observed for **1b**-containing 3-MCs.

d) Using common sense and chemical intuition, one would expect a good catalyst to be involved in stronger interactions than any other molecule in a given molecular system. This is exactly observed in Figure 4.2 but only for the HEC for which $\Delta E_{\text{int}}^{\mathbf{1b}}$ is about 2.5 times more significant than the relevant values obtained for acetone and DMSO.

Intermolecular interactions

From the above analysis of trends that are shown in Figure 4.2 and visual-inspection of **4_GMSs** shown in Table 4.1 one might speculate that the 3-MC with **1b** should be more reactive; hence, a smaller energy barrier at a transition state (TS) on, e.g., the CN-bond formation, could be expected.

To verify this hypothesis, we first analysed the intermolecular interactions for the entire MSs. We found that trends in ${}_{\text{inter}}E_{\text{int}}^{\text{MS}}$ follow the trends in $\Delta E_{\text{int}}^{\text{MS}}$ (combined, inter and intramolecular interactions) but the ${}_{\text{inter}}E_{\text{int}}^{\text{MS}}$ values are more significant (i.e., more negative) - see Figure B7, Part B3 of Appendix B. Most importantly, the intermolecular interactions ${}_{\text{inter}}E_{\text{int}}^{\text{MS}}$ of –144.2 kcal/mol in **4B_GMS** are much stronger, by –61 kcal/mol, than in **4A_GMS**.

To gain further insight, we analysed intermolecular interactions between each unique molecule-pair – Figure 4.3. We start from **1** and **2** as one would assume that proline and acetone should play the most decisive and leading role in driving the reaction forward.

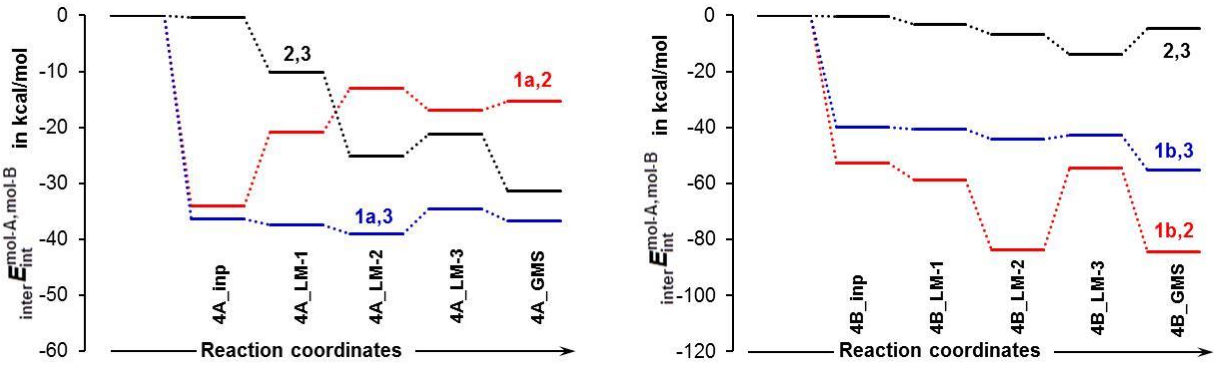

Figure 4.3. Relative to isolated molecules, change in the intermolecular interaction energy between molecular-pairs involving proline and acetone **1**,**2**, proline and DMSO **1**,**3**, and acetone and DMSO **2**,**3** in the indicated 3-MCs.

Surprisingly, the transition from **4A_inp** → **4A_GMS** showed a large increase in the ${}_{\text{inter}}E_{\text{int}}^{\mathbf{1a,2}}$ energy term, from –34.0 to –15.3 kcal/mol; hence, significant weakening of interactions between **1a** and **2** took place. A very different picture is observed for the trend in the ${}_{\text{inter}}E_{\text{int}}^{\mathbf{1b,2}}$ values. Interactions between **1b** and **2** are not only stronger, relative to the 3-MCs with **1a**, but also strengthened from –52.6 (in **4B_inp**) to –84.5 (in **4B_GMS**) kcal/mol. Clearly, **1b** must be a better catalyst as the latter value is over 5 times more significant than that obtained for the LEC of proline.

Furthermore, we noted that interactions between acetone **2** and a DMSO **3** are much stronger and, relative to the input complex, even strengthened further by –31.1 kcal/mol in the case of 3-MCs with **1a** whereas they hardly changed in complexes with **1b**. Intuitively, one might speculate that the strong interactions between acetone **2** and DMSO **3** need to be weakened before a reaction between **1a** and **2** can proceed and this, potentially, might result in an increase in the associated energy barrier at a TS.

Finally, intermolecular interactions between proline **1** and DMSO **3** are strong in both systems and, relative to **4A_GMS**, they are about –20 kcal/mol stronger in **4B_GMS**. This suggests that the solvent molecule must play a significant role at this stage of the process. As we consider 3-MCs, it was important to analyse interactions between a single molecule and remaining two molecules of molecular systems. From Figure B8, Part B3 of the Appendix B we noted that:

1) Relative to input structures, the $_{\text{inter}}E_{\text{int}}^{\mathbf{1a,(2,3)}}$ = $_{\text{inter}}E_{\text{int}}^{\mathbf{1a,2}}$ + $_{\text{inter}}E_{\text{int}}^{\mathbf{1a,3}}$ term increased (interactions weakened) by about 19 kcal/mol in **4a_GMS** whereas $_{\text{inter}}\Delta E_{\text{int}}^{\mathbf{1b,(2,3)}}$ decreased (interactions strengthened) by about –47 kcal/mol when in **4B_GMS**.
2) The combined intermolecular interactions between **1b** and {**2**+**3**} of –139.6 kcal/mol in **4B_GMS** are 2.7 times stronger than the interactions between **1a** and {**2**+**3**} in **4A_GMS**.

Molecule-specific intramolecular interactions

From the fact that the trend in $_{\text{inter}}E_{\text{int}}^{\text{MS}}$ follows but, at the same time, is below the trend in $\Delta E_{\text{int}}^{\text{MS}}$ (Figure B7, Part B3 of Appendix B) one can conclude that the intramolecular interactions in both MSs must have weakened during the **4_inp** → **4_GMS** transition. It was then important to find out whether all the molecules experienced an increase in the $_{\text{intra}}E_{\text{int}}^{\text{mol}}$ term equally (in other words, whether a comparable weakening of their intramolecular interactions took place) and what the contribution was to $_{\text{intra}}E_{\text{int}}^{\text{mol}}$ coming from covalent bonds and intramolecular L-D interactions in each molecule. From trends shown in Figure 4.4 it follows that, relative to separate molecules, on the 3-MCs formation the intramolecular interactions in both **4_inp** complexes:

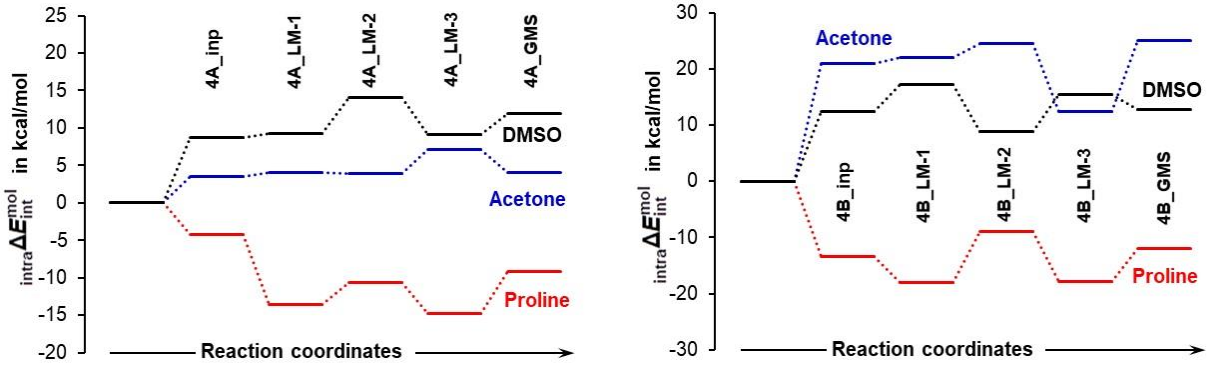

Figure 4.4. Relative to separate molecules, intramolecular interaction energy changes computed for each molecule (proline, acetone, and DMSO) in the indicated 3-MCs.

(i) Strengthened only in proline as the $_{\text{intra}}\Delta E_{\text{int}}^{\mathbf{1a}}$ and $_{\text{intra}}\Delta E_{\text{int}}^{\mathbf{1b}}$ terms are negative, –9.2 and –12.0 kcal/mol, respectively, whereas these interactions

(ii) Became weaker in acetone **2** and DMSO **3** as the $_{\text{intra}}\Delta E_{\text{int}}^{\mathbf{2}}$ of 4.0 and 25.1 kcal/mol and $_{\text{intra}}\Delta E_{\text{int}}^{\mathbf{3}}$ of 11.9 and 12.8 kcal/mol were obtained for **4A_inp** and **4B_inp**, respectively.

A change in the $_{\text{intra}}\Delta E_{\text{int}}^{\text{mol}}$ term must be a consequence of molecules being involved in strong intermolecular interactions and they strengthened in **1** and weakened in **2** more in **4B_GMS** than in **4A_GMS**. Does this carry any significance in terms of molecules' preparation for new bonds formation? Clearly, to answer such a question more systems must be studied to establish if this is a trend of a general nature.

Part A

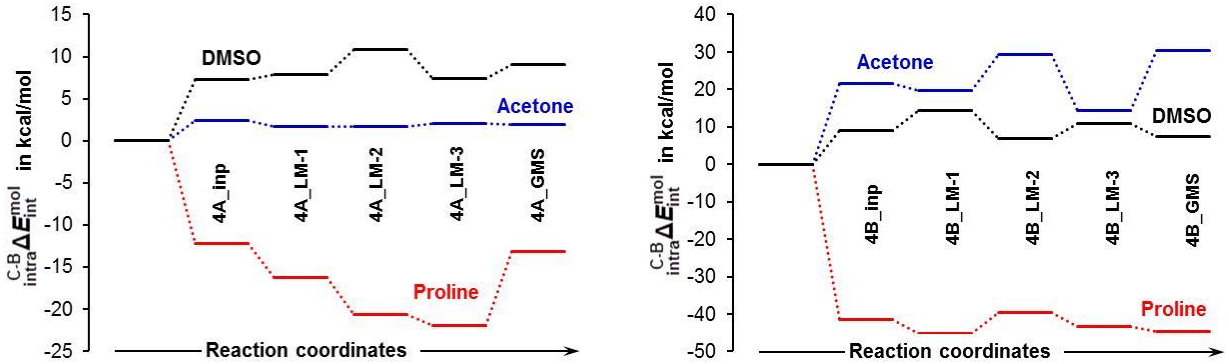

Part B

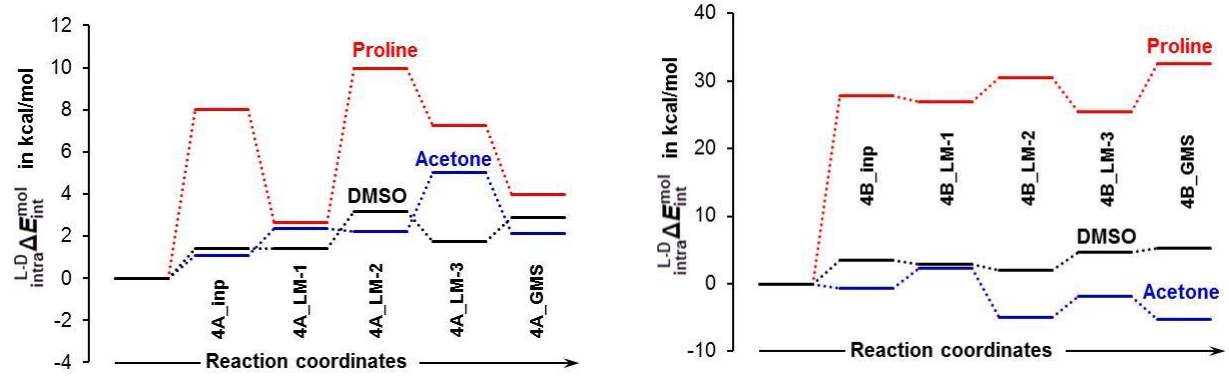

Figure 4.5. Variation of covalent bond strength (Part A) and non-covalent bond (NCB) or long-distance interactions (Part B) in the three unique molecules (proline, acetone, and DMSO) that constitute the 3-MCs of indicated molecules.

One must also note a dramatic difference between trends in covalent bonds' strength in acetone **2** that is destined to merge with proline **1** through the CN-bond formation. Strength of these bonds hardly changed throughout the entire **4A_inp** → **4A_GMS** rearrangement. However, they became much weaker, relative to **4B_inp**, by $_{\text{intra}}^{\text{C-B}}\Delta E_{\text{int}}^{\mathbf{2}}$ of +30.4 kcal/mol in **4B_GMS** (Figure 4.5, Part A). We also found a large variation in the strength of L-D intramolecular interactions – see the trends in the $_{\text{intra}}^{\text{L-D}}\Delta E_{\text{int}}^{\text{mol}}$ values in Figure 4.5 Part B. They became weaker, by 32.5 kcal/mol, in **4B_GMS** that is nearly an order of magnitude more than in **4A_GMS**.

All the above observations, when combined, clearly point at selecting **4B_GMS** for further modelling as it is much better prepared for new bonds formation. Furthermore, a preference for the involvement of **1b** over the **1a** conformer of proline can also be deduced at this stage of the catalytic process. Consequently, one would also predict a lower energy barrier at a transition state during the subsequent HO- and CN-bond formation for the **4B_GMS** as well. Nonetheless, we chose to continue modelling with both 3-MC's but in the case of the LEC we opted to use **4A_LM-3** due to, among others, (i) the $E_{\text{int}}^{\mathbf{1a}}$ term (total intra and intermolecular interactions), (ii) the ${}_{\text{inter}}E_{\text{int}}^{\mathbf{1a,2}}$ term (interaction between proline **1a** and acetone **2**) and (iii) the ${}_{\text{intra}}^{\text{C-B}}E_{\text{int}}^{\mathbf{1a}}$ term (strength of covalent bonds in **1a**) interaction energy terms are all significantly more negative (interactions are stronger) than in the global minimum structure **4A_GMS**. Our interaction energy-based selection is fully supported by a visual inspection of the **4A** 3-MC structures included in Table 4.1 and a classical organic chemist would most likely also select **4A_LM-3** due to much better pre-organisation of molecules, i.e., atom-pairs that are to make new bonds (N13,C18 and H17,O19) are directly facing each other.

Molecular fragments driving a chemical change

The above shows that <u>all molecules</u> interact strongly with each other and this, in turn, impacts on their intramolecular interactions, also including covalent bonds. This implies that the molecule of DMSO is not a 'neutral' observer of chemical changes, but it must have a significant impact. In general, the trends discussed above illustrate the importance of interactions in modelling reaction mechanisms. It is obvious, however, that not all atoms of molecules forming a MS play significant and comparable roles. Hence, to identify atoms driving a chemical change, we change the focus from the molecular to atomic level.

Atoms with largest positive and negative net atomic charges (Tables B1-B2, Part B2 of Appendix B) are also involved in the strongest intermolecular interactions (Tables B4-B5, Part B4 of Appendix B; they must drive the arrangement of molecules that subsequently leads to bonds formation. It became obvious that (i) this is not a single atom-pair that drives a process as typically adopted in a classical approach and (ii) a best way forward is to group selected atoms into molecular fragments. These fragments were named such that it instantly places them in a relevant molecule: $\mathcal{P}$ = {C1,C4,H5,N13,C14,O15,O16,H17} in proline **1**, $\mathcal{A}$ = {C18,O19} in acetone **2** and $\mathcal{D}$ = {S28,O37} in DMSO **3**.

A full set of trends generated for interaction energies between entire molecular fragments $\mathcal{A}$, $\mathcal{D}$ and $\mathcal{P}$ is shown in Figure B9, Part B5 of Appendix B. There are large differences in interfragment

interaction energies computed for **4A** and **4B** molecular systems and they are clearly in favour of the latter – Figure 4.6.

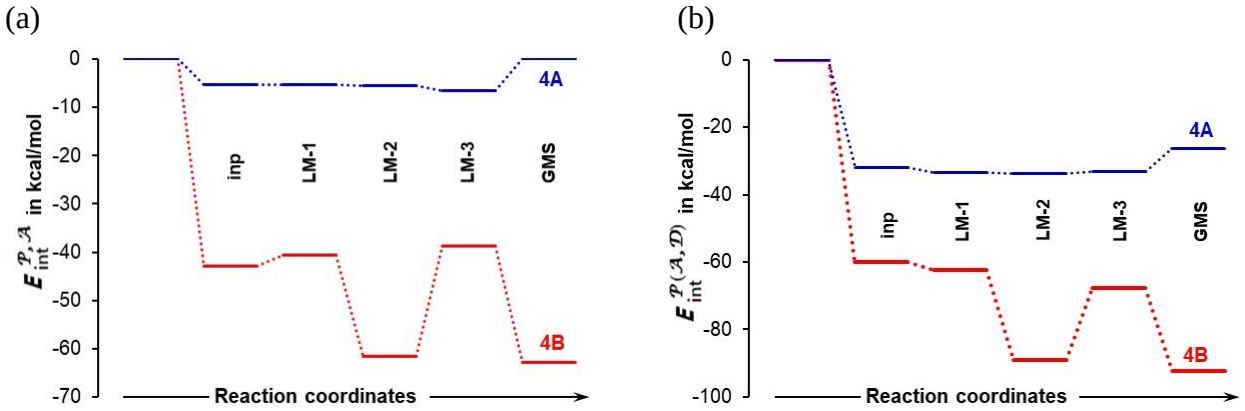

Figure 4.6. Trends in the interaction energies computed for the $\mathcal{P}$ and $\mathcal{A}$ (a) and $\mathcal{P}$ and ($\mathcal{A}$ plus $\mathcal{D}$) (b) fragments in indicated **4A** and **4B** 3-MCs.

Looking at the interfragment interaction involving $\mathcal{P}$ and $\mathcal{A}$ (they are from molecules that are to be involved in bonds formation) the $E_{\text{int}}^{\mathcal{P},\mathcal{A}}$ energy term in **4A_GMS** is zero whereas these fragments strongly attract each other in **4B_GMS** (with $E_{\text{int}}^{\mathcal{P},\mathcal{A}}$ = –62.8 kcal/mol) – see Figure 4.6(a). This finding can also be used to predict a lower energy barrier on bond formation in the case of **4B_GMS** and this is further supported by the interaction between $\mathcal{P}$ and $\mathcal{A}$ being stronger than that between $\mathcal{P}$ and $\mathcal{D}$ by over –30 kcal/mol. In contrast, the strongest interfragment interaction of –26.3 kcal/mol in **4A_GMS** is between $\mathcal{P}$ and $\mathcal{D}$. Notably, $E_{\text{int}}^{\mathcal{P},\mathcal{A}}$ of 0.0 and –6.6 kcal/mol is observed in **4A_GMS** and **4A_LM-3**, respectively, and this is in full support of selecting the latter 3-MC for further studies. Furthermore, the trends in the interfragment interaction energies correlate very well with trends obtained for the intermolecular interactions (Figure 4.3).

Combined intermolecular interactions between $\mathcal{P}$ and ($\mathcal{A}$ plus $\mathcal{D}$), the $E_{\text{int}}^{\mathcal{P},(\mathcal{A},\mathcal{D})} = E_{\text{int}}^{\mathcal{P},\mathcal{A}} + E_{\text{int}}^{\mathcal{P},\mathcal{D}}$ term (Figure 4.6(b)), shows an important role played by the DMSO solvent molecule. Note that $E_{\text{int}}^{\mathcal{P},(\mathcal{A},\mathcal{D})}$ is more negative than $E_{\text{int}}^{\mathcal{P},\mathcal{A}}$ (in Figure 4.6a) for both 3-MCs throughout the entire process of **4_inp** → **4_GMS** transformation. This reveals strong attraction between atoms of $\mathcal{P}$ in proline (**1a** and **1b**) and atoms of $\mathcal{D}$ in the solvent molecule. This is of particular importance in the case of the **4A** 3-MCs showing that the DMSO solvent molecule **3** assists in attaining the most desired 3D placement of **1a** and **2** for subsequent bonds formation. We have also discovered that interactions between the $\mathcal{A}$ and $\mathcal{D}$ fragments are very weak (0.0 and +1.4 kcal/mol in **4A_LM-3**

and **4B_GMS**, respectively) and this is exactly what a synthetic chemist would like to see as the process of bonding between proline and acetone will not require additional energy for breaking interactions between acetone **2** and DMSO **3**. Remarkably, relative to **4A_LM-3**, interactions between the three fragments in Figure 4.6(b) are three times stronger in **4B_GMS** and this must have a facilitating impact on the bond formation between N13 and C18 as well as O19 and H17. In general, the trends observed for the **4A** 3-MCs correlate well with relative placements of molecules (Table 4.1) as exemplified by $E_{\text{int}}^{\mathcal{P},\mathcal{A}}$ of 0.0 kcal/mol obtained for **4A_GMS** that is not well pre-organised for the forthcoming chemical change.

Impact of smaller molecular fragments

To gain additional understanding of the impact made by atoms of $\mathcal{P}$, we grouped them into smaller and meaningful fragments containing: (i) N13 and its neighbours because N13 is destined to form the CN-bond with C18 of acetone **2**: $\mathcal{P}1$ = {H5,N13}, $\mathcal{P}2$ = {C1,C4,H5,N13}, $\mathcal{P}3$ = {C1,C4,H5,N13,H17}, and (ii) H17 and its neighbours because H17 is destined to be transferred from proline **1** to acetone **2** due to the H17–O19 bond formation: $\mathcal{P}4$ = {O16,H17}, $\mathcal{P}5$ = {C14,O16,H17} and $\mathcal{P}6$ = {C14,O15,O16,H17}.

A full set of trends in interaction energies between molecular fragments $\mathcal{P}$n and either $\mathcal{A}$ or $\mathcal{D}$ is presented in Figure B10, Part B5 of Appendix B. For brevity, just a few observations follow:

a) The interactions between $\mathcal{A}$ and either $\mathcal{P}1$, $\mathcal{P}2$, or $\mathcal{P}3$ molecular fragments containing N13 are stronger in **4B_GMS** than in **4A_LM-3** by –15.2, –18.4 and –57.7 kcal/mol, respectively. The large difference in the $E_{\text{int}}^{\mathcal{P}3,\mathcal{A}}$ and $E_{\text{int}}^{\mathcal{P}2,\mathcal{A}}$ values (about –40 kcal/mol in favour of $E_{\text{int}}^{\mathcal{P}3,\mathcal{A}}$) is clearly due to the large and attractive contribution made by H17.

b) Also, interactions between $\mathcal{A}$ and either $\mathcal{P}4$, $\mathcal{P}5$, or $\mathcal{P}6$ fragments containing H17 are stronger in **4B_GMS** by –29.9 –44.9 and –37.8 kcal/mol, respectively. Notably, all fragments containing H17 (from $\mathcal{P}3$ to $\mathcal{P}6$) interact, on average, twice as strong with $\mathcal{A}$ than fragments without H17, i.e., $\mathcal{P}1$ and $\mathcal{P}2$.

There are two atom-pairs, N13,C18 and H17,O19, that must be involved in new bonds formation; their diatomic interactions can be interpreted as navigating to a chemical change even though they are not the strongest (selected diatomic interaction energies are presented in Tables B6-B8, Part B5 of Appendix B). Trends in $E_{\text{int}}^{\text{N13,C18}}$ and $E_{\text{int}}^{\text{H17,O19}}$ shown in Figure 4.7 constitute

yet additional and critical support for (i) selecting **4A_LM-3** and (ii) predicting a lower energy barrier for **4B_GMS**.

Interestingly, $E_{int}^{H17,O19}$ of –150.6 kcal/mol is larger than $E_{int}^{N13,C18}$ by –20.2 kcal/mol in **4B_GMS**; the opposite trend is observed for **4A_LM**-3 where a difference of –22 kcal/mol in favour of $E_{int}^{N13,C18}$ was found. This reveals that the H17,O19 atom-pair plays a leading role in **4B_GMS**, when a 3D arrangement of molecules is considered, whereas the N13,C18 atom-pair does the same in **4A_LM-3**.

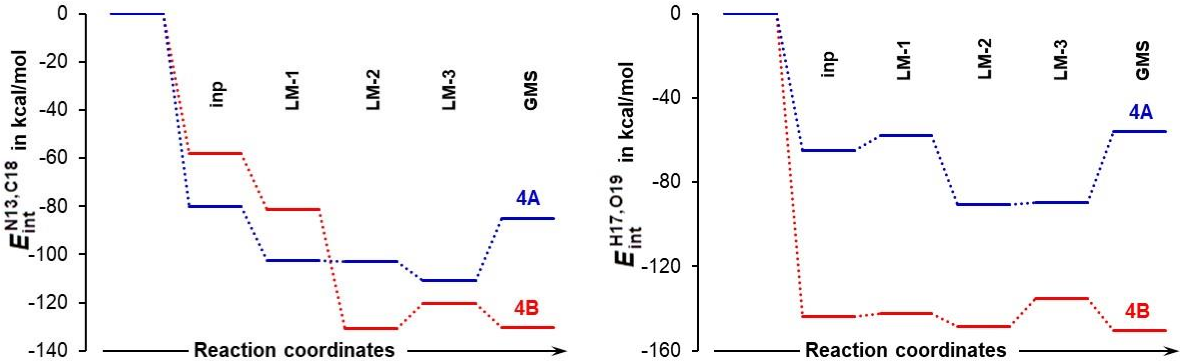

Figure 4.7. Intermolecular interaction energies computed for the N13,C18 and H17,O19 atom-pairs in the indicated 3-MCs

A full set of interaction energies between either N13 or H17 of proline **1** and atoms of either $\mathcal{A}$ or $\mathcal{D}$ is shown in Figure B11 (see also Table B9), Part B5 of Appendix B. Let us follow a classical approach where interactions between two atoms are commonly considered, in this case between N13 and C18.[15,19,23] This interaction is highly attractive: –111.0 kcal/mol in **4A_LM-3** and, even more so, –130.4 kcal/mol in **4B_GMS**. To follow such an approach, however, one must provide scientifically sound answers to the following two questions:

(1) The attractive interaction between N13 and C18 is far from being the strongest between atoms of proline **1** and acetone **2**; so, why is just this interaction considered?

(2) There are also very strong repulsive interactions between atoms of proline **1** and acetone **2**; why are they not considered at all?

Clearly, there is no justification for such a simplistic and orthodox approach. So let us do some simple mathematics related to the main actors, i.e., interactions between either N13 or H17 of proline **1** and C18 and O19 of acetone **2** (atoms of $\mathcal{A}$), as well as S28 and O37 of DMSO **3** (atoms of $\mathcal{D}$) which play major roles in the 1st act of a chemical change in the catalytic process under consideration.

Summing up the interaction energies between N13 and the remaining major players (atoms) in $\mathcal{A}$ and $\mathcal{D}$ specified above we obtained +24.4 (in **4B_GMS**) and +36.7 (in **4A_LM-3**) kcal/mol; in both cases, a large repulsive interaction was computed that would prevent a CN-bond formation.

This is rather an unexpected finding, but one must realise, however, that for example, the attractive interaction between N13 and C18 in **4A_LM-3** (–111 kcal/mol) is counteracted by more significant repulsive interactions, $E_{\text{int}}^{\text{N13,O19}}$ = +123.9 kcal/mol, between N13 and O19 (the atom C18 is bonded to). Considering **4B_GMS**, we obtained the attractive interaction between N13 and C18 (of –130.4 kcal/mol) that counteracts, but only barely, the repulsive interaction between N13 and O19 (of +129.4 kcal/mol).

Following the above approach, we summed up interaction energies between H17 and the remaining major players. This gave us –68.4 (in **4B_GMS**) and –30.8 (in **4A_LM-3**) kcal/mol; in both cases, overall large attractive interaction energies were obtained that promote a proton transfer from proline **1** to acetone **2**. Importantly, only in the case of **4B_GMS**, the attractive interactions involving H17 (of –68.4 kcal/mol) compensated repulsive interactions involving N13 (of +24.4 kcal/mol). Hence, using major players as a predictive tool, the reaction should not proceed via the LEC of proline **1** at all from the very first step.

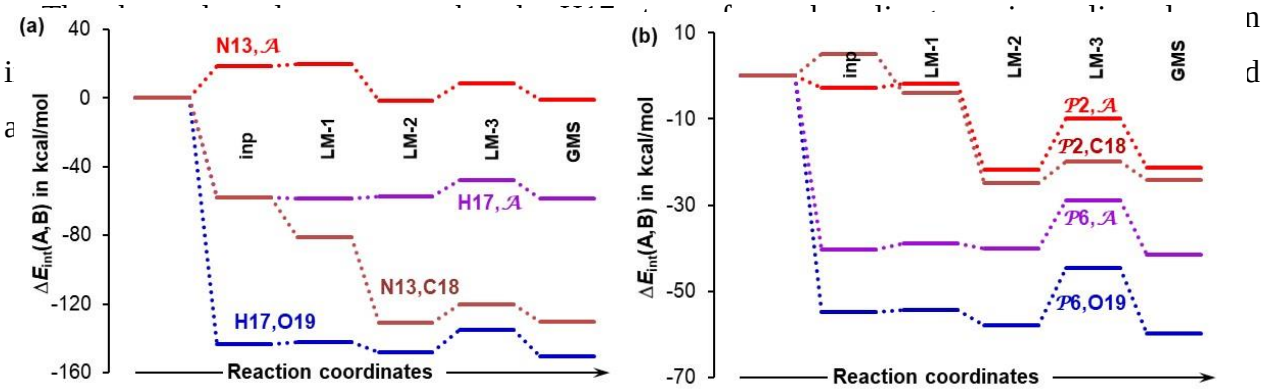

Figure 4.8. Trends (from an input to the global minimum structure, GMS) in the interaction energy between indicated either atoms or molecular fragments $\mathcal{P}2$ = {C1,C4,H5,N13} of the HEC of proline (**1b**), $\mathcal{P}6$ = {C14,O15,O16,H17} of **1b** and $\mathcal{A}$ = {C18,O19} of acetone (**2**), all in **4B** 3-MCs.

Starting from a classical, 2-atom approach, the H17···O19 interaction is highly attractive from the very beginning (starting already from the **4B-inp** structure – Figure 4.8a) and persists to dominate the N13···C18 interaction throughout the entire process of structural rearrangement, from **4B_inp** to **4B_GMS**. Clearly, H17 attracts the in-coming acetone molecule much more than N13. As mentioned already, it is imperative to account for the obstructive (repulsive) interactions which N13 and O19 as well as H17 and C18 are involved in when **2** is approaching **1b**.

To achieve that we computed interaction energies between either N13 or H17 and the molecular fragment $\mathcal{A}$ = {C18,O19} of acetone; trends obtained (Figure 4.8a) strongly point at H17 as a driver of a chemical change. This is because N13 is opposing approaching acetone, starting already from the input structure **4B_inp**, whereas very strong attractive force acts between H17 and $\mathcal{A}$ throughout the **4B_inp** → **4B_GMS** rearrangement. The picture does not change much when 4-atom fragments $\mathcal{P}$2 (with N13) and $\mathcal{P}$6 (with H17) instead of individual atoms N13 and H17 are considered (Figure 4.8b). Regardless whether interactions with a single or both atoms of $\mathcal{A}$ are considered, it is the $\mathcal{P}$6 fragment that attracts **2** much more than $\mathcal{P}$2.

Undoubtedly, the CN-bond formation is the most important chemical change for a classical organic chemist. Hence, we decided to monitor interaction energies between atoms and fragments shown in Figure 4.8 throughout the process of a simulated CN-bond formation. Data obtained from scanning reaction coordinates, starting from d(N13,C18) = 2.6573 Å in **4B_GMS**, through a transition state TS at d(N13,C18) = 1.9527 Å and up to 0.2 Å beyond the TS is shown in Figure 4.9.

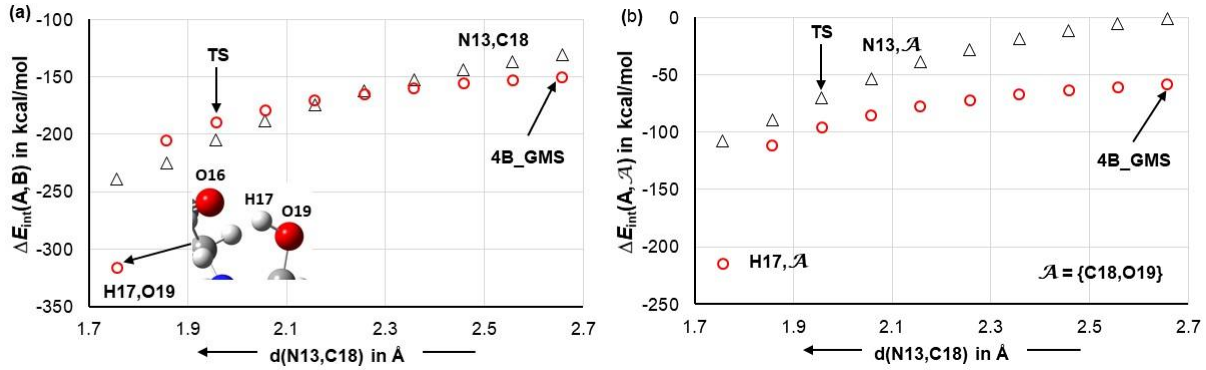

Figure 4.9. Trends in the interaction energy between indicated atoms and a molecular fragment $\mathcal{A}$ obtained on simulated a CN-bond formation by scanning d(C18,13) from the value observed in the **4B_GMS** 3-MC.

Focusing on just diatomic interactions (Figure 4.9a), the H17,O19 atom-pair continues to be in a driving seat up to d(N13,C18) = 2.257 Å where the two atom-pairs experience similar attraction of about –165 kcal/mol. Beyond this point, the interaction energy between N13 and C18 starts to dominate and at the transition state it is –16 kcal/mol stronger than the interaction between H17 and O19. Interestingly, well before the CN-bond is formed, i.e., at d(N13,C18) = 1.7573 Å, H17 permanently leaves proline and forms a new bond with O19 of acetone – see the insert in Figure 4.9a. It is reasonable to assume that H17 would move to acetone even earlier if not for being restrained by a strong interaction with O16. The trends obtained for the interaction energies between either N13 or H17 and the molecular fragment $\mathcal{A}$ (Figure 4.9b) show dominance of H17 over N13, in terms of attracting acetone, in the entire region of the reaction coordinates scan.

Trends obtained for the interactions between molecular fragments $\mathcal{P}2$ and $\mathcal{P}6$ and either atoms of a molecular fragment $\mathcal{A}$ or entire $\mathcal{A}$ are presented in Figure B12, Part B5 of Appendix B and they fully support what we observe on Figure 4.9.

From this it follows that the first step's name as a CN-bond formation, or as it was coined many years ago 'the nucleophilic attack of the amino group', is somewhat misleading. In our opinion and based on evidence provided in this work, a better description of the first step could be 'a first proton transfer/CN-bond formation' as this correctly reflects the sequence of chemical changes taking place during this step. Furthermore, the first step is the result of the attraction between two atom-pairs that guide **2** in approaching **1** and there is no way to separate, either experimentally or theoretically, these chemical events taking place nearly simultaneously. Due to the leading role played by H17 (it is involved in largely dominating attractive interaction with O19 of acetone) and for brevity we will refer to this step as the first proton transfer also because it is a part of a multi-step proton transfer catalytic process involving proline. This is the dominating catalytic activity of a proton of a carboxylic group that not only facilitates the CN-bond formation but makes 'the nucleophilic attack of the amino group' possible. Moreover, as it will be demonstrated in the sections that follow, during the second H-transfer stage, H5 rebuilds the carboxylic COOH group of proline through an intramolecular mechanism, moving across from N13 to O16. The presence of the COOH functionality is a pre-requisite for the third consecutive H-transfer step during which water is eliminated by H5 extracting the O19H17 group from the acetone back-bone.

4.3.2 First H-transfer

The reaction energy profiles obtained for the 2- and 3-MCs (up to the second proton transfer) are presented in Figure 4.10. To facilitate comparative analysis and clearly present the impact of a DMSO solvent molecule, the energy trends are presented relative to the combined energy of isolated reactants of the 2- and 3-MCs. Furthermore, small/capital letters **a/A** and **b/B** represent data obtained for 2-MCs and 3-MCs at each consecutive step along the reaction coordinates; letters **a/A** and **b/B** refer to the MSs containing the LEC and HEC, respectively.

Looking at the relevant free energy data for the first H-transfer (Figures 4.10 b,d), it is clear that DMSO had no significant impact on the free energy barrier $\Delta G^{\ddagger}$ at the **5-TS** stage; relative to isolated molecules, data obtained for the 2- and 3-MCs, is highly comparable. A very different picture is seen for trends in the E_{ZPVE} values (Figures 4.10 a,c); the presence of a DMSO molecule decreased the electronic energies of both MSs such that the values at **5A/B_TS** that were computed for the 3-MCs are below the energies of isolated reactants. Note that the values at **5a/b_TS** for

2MCs, hence without the DMSO explicit solvent molecule, are positive – a full set of energy terms and relevant structures are included in Tables B10-B12, Part B6 of Appendix B.

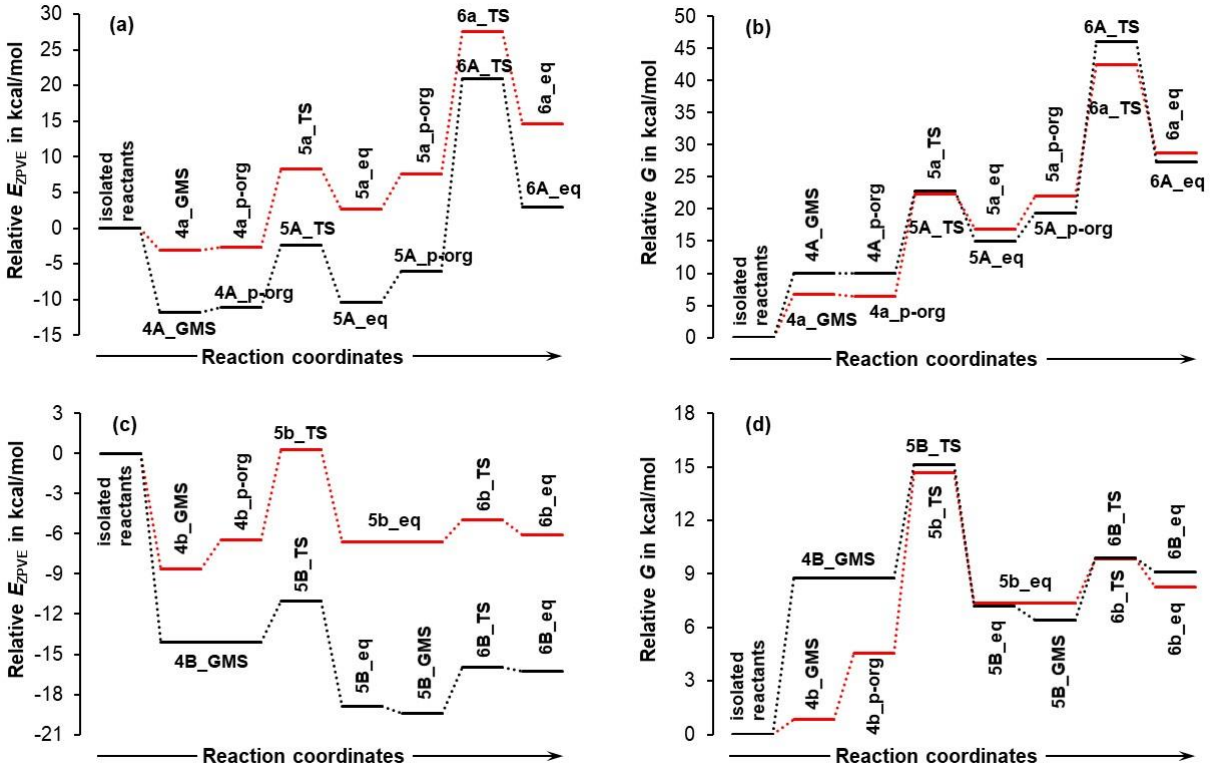

Figure 4.10. Relative to isolated reactants either (**1**+**2**) for the implicit solvent model or (**1**+**2**+**3**) in the presence of an explicit solvent molecule of DMSO, E_{ZPVE} and Gibbs free energy (G) profiles for the formation of the product of 2nd proton transfer **6a/b** and **6A/B** (structures are shown in Table 4.1 and Tables B11–B12 in appendix B). The suffix **p-org**, **TS**, and **eq** represent pre-organised, transition state, and equilibrium structures, respectively.

Moreover, the difference in the electronic energy between the TS and the GMS, hence the energy barriers $\Delta E^{\ddagger}_{ZPVE}$ in the presence of DMSO decreased by nearly 6 (for HEC) and 2 (for LEC) kcal/mol – these values are about 3.1 and 9.4 kcal/mol in the case of HEC- and LEC-containing MSs, respectively.

Relative energy levels in Figure 4.10 that were computed for the products **5** of the first H-proton transfer deserve special attention. For both, E_{ZPVE} and G trends shown in Figure 4.10, the **5a/b_eq** products are a few kcal/mol higher in energy than **4a/b_GMSs** of 2-MCs. A reversal of this trend is observed in the presence of a DMSO molecule but only in the case of the HEC. Notably and specifically for the trend in E_{ZPVE} and relative to **4_GMS**, the energy of **5B_GMS** is lower by –6.2 kcal/mol whereas **5A_eq** is higher in energy than **4A_GMS** by +1.4 kcal/mol. One must add that the **5B_GMS** structure was discovered from the scan of DA(C4,N13,C18,O19), a dihedral angle in the **5B_eq** structure – for details, see commented Figure B13, Part B6 of Appendix B.

It has been established previously[20,21] that structural interconversion from **1a** to **1b** does not require a large energy barrier meaning that the two conformers are always present in a reaction vessel. Combining this knowledge with the data shown in Figures 4.10 a,c implies that the LEC of proline is not catalytically active at all as it will not become involved even in the first H-transfer stage. This is because, when both GMSs, **4A_GMS** and **4B_GMS** are present in a solution, the system will always follow a downwards change in its energy that leads to the most stable a **5B_GMS** state. Note that a system with the LEC must climb the hill of E_{ZPVE} to reach the **5A_eq** state that is not only higher in energy than the starting point, i.e., the **4A_GMS** structure, but also higher in energy, by +3.3 kcal/mol, than the **5B_GMS** structure with the HEC of proline.

This clearly shows that the mechanism through the higher energy conformer **1b** becomes even more favourable in the presence of the explicit DMSO solvent molecule. This conclusion is further and strongly supported by the free energies of products **5** of the first H-transfer/CN-bond formation step (Figures 4.10 b,d). Relative to the **4A/4B_GMS** structures, the change ΔG of +4.9/–1.6 kcal/mol was obtained for **5A_eq/5B_GMS** and even more importantly, the values of G computed for **5B_GMS** is lower, by –2.7 kcal/mol, than that obtained for the **5A_eq** structure.

Two important observations that one can make are:

a) In accordance with our predictions made from the analysis of numerous interaction energy trends, the LEC-containing MS needs to overcome a larger energy barrier at the transition state, i.e., relative to **4A_GMS**, an increase in the E_{ZPVE} and G values of 9.4 and 12.7 kcal/mol, respectively, was obtained at **5A_TS**. For comparison purposes, much smaller values of 3.1 and 6.3 kcal/mol apply, respectively, for E_{ZPVE} and G, in the case of transition from **4B_GMS** to **5B_TS**.

b) Looking at the trends shown in Figures 4.10 a,c, it is obvious that the interaction between the DMSO molecule **3** with either proline **1** or acetone **2** (or both) must have caused a decrease in the E_{ZPVE} values that resulted in significantly smaller energy barriers for the first H-transfer.

It was then of great interest and importance to investigate these interactions at the two transition states, **5A_TS** and **5B_TS**. The ${}_{\mathrm{inter}}E_{\mathrm{int}}^{\mathbf{3,(1,2)}} = {}_{\mathrm{inter}}E_{\mathrm{int}}^{\mathbf{3,1}} + {}_{\mathrm{inter}}E_{\mathrm{int}}^{\mathbf{3,2}}$ energy term was calculated; it quantifies intermolecular interactions between atoms of the DMSO molecule (**3**) and atoms of proline **1** and acetone **2**. We found that at the relevant transition states the intermolecular interactions:

1) Between **3** and **1** as well as **3** and **2** strengthened significantly; ${}_{\mathrm{inter}}E_{\mathrm{int}}^{\mathbf{3,(1,2)}}$ changed favourably (became more negative) by –55.3 and –75.7 kcal/mol, for **5A_TS** and **5B_TS**, respectively. Hence,

the same set of diatomic intermolecular interactions became stronger, by – 20.4 kcal/mol, in the case of the **1b** containing MS.

2) Between DMSO and acetone strengthened more in the case of the LEC-containing MS; ${}_{\text{inter}}E_{\text{int}}^{\mathbf{3,2}}$ of –14.7 (for **5A**) and –7.6 (for **5B**) kcal/mol was obtained.

3) Involving DMSO and proline molecules strengthened a lot; we obtained ${}_{\text{inter}}E_{\text{int}}^{\mathbf{3,1}}$ of –40.6 (**5A**) and –68.1 (**5B**) kcal/mol.

Trends shown in Figure B14, Part B6 of Appendix B, reveal that the total interaction energies, $E_{\text{int}}^{\text{MS}}$, at two transition states, **5A_TS** and **5B_TS**, strengthened (became more negative relative to **4A_LM-3** and **4B_GMS**, respectively, by –13.1 and –17.9 kcal/mol) as was also found for the intermolecular interactions. However, a change in the $E_{\text{int}}^{\text{MS}}$ term is significantly smaller when compared with the change obtained for the ${}_{\text{inter}}E_{\text{int}}^{\mathbf{3,(1,2)}}$ term. From this observation and since interactions between acetone and DMSO molecules strengthened marginally and much less in the case of a **1b**-containing MS, it is clear that stronger (by –27.5 kcal/mol) interactions between the DMSO and proline molecules must have led to a more significant decrease in the energy barrier discovered for the **1b**-containing MS.

4.3.3 Second H-transfer

Although we have shown that the LEC cannot be catalytically active beyond the first proton transfer, we will for illustrative purposes analyse the impact of a DMSO explicit molecule for the two conformers. The energy barriers when going from **5_eq** to **6_TS** - see Figures 4.10 a,b, became even larger in the presence of DMSO; the barriers increased by +6.4 and +5.3 kcal/mol for E_{ZPVE} and G, respectively. As a consequence, and relative to energy of the reactants, the free energy barrier at the **6A_TS** reached an unsurmountable $\Delta G^{\ddagger}$ value of 46 kcal/mol. Moreover, the product of the second proton transfer is much higher in energy than that of the first proton transfer, regardless of whether E_{ZPVE} or G is considered. It is then absolutely clear that the reaction energy profile obtained for the LEC prohibits any reaction progress when starting from reactants but it also shows that the reverse process, from **6_eq** toward reactants would be, if permitted, a highly spontaneous process.

Opposite to the LEC, the presence of a DMSO molecule had largely positive (facilitating) impact on the reaction progress involving the HEC. Figures 4.10 (c,d) show that the energy barriers (from **5B_GMS** to **6B_TS**) are very low, just a few kcal/mol for both energy terms. The fact that (i) these barriers are somewhat larger or (ii) that the energy difference between a transition state **6B_TS** and

the product of the second proton transfer **6B_eq** decreased slightly in the presence of DMSO does not matter at all. What really matters is the energy difference between **6B_eq** and **4B_GMS**. Starting from most abundant complex of the reactants, the **4B_GMS**, and overcoming two negligible energy barriers the product of the second proton transfer finds itself at E_{ZPVE} of –2 kcal/mol below the energy of **4B_GMS**, hence in energetically favourable position. Notably, the energy difference obtained for 2-MCs (without DMSO) was found to be +2.6 kcal/mol; hence, the E_{ZPVE} energy term for **6b_eq** is slightly less favourable when compared with the starting materials, i.e., **4b_GMS**. A very interesting picture is observed in Figure 4.10d where **4B_GMS** is significantly higher in energy than **4b_GMS**. However and importantly, the increase in energy caused by a DMSO molecule must have a beneficial effect because the energy difference between the product of the second proton transfer **6-eq** and **4_GMS** was nearly nullified, from +7.4 (for 2-MC) to +0.3 kcal/mol (for 3-MC). This means that there is essentially no backward driving force in the presence of DMSO, from **6B_eq** to the starting material **4B_GMS** and hence the reaction can proceed forward 'unopposed'.

The changes in the reaction energy profiles due to the presence of a DMSO molecule (Figure 4.10) are very significant and when the HEC is considered, very beneficial. DMSO is not directly involved in the bond breaking/formation (is not a catalyst in a classical sense) but it can hardly be considered as just a neutral solvent. However, as our results reveal, the intermolecular interactions between DMSO and proline as well as acetone (all polar compounds) have a profound impact on the reaction progress and directionality. Importantly, our results corroborate very well with List's finding reported in his first paper[12] '*After screening several solvents, we found anhydrous DMSO at room temperature to be the most suitable condition regarding reaction times and enantioselectivity*.'

4.4 Conclusions

Considering a solvent just as a solubilizing medium for reactants and products might be, as this work demonstrates, far from the full picture. The role of DMSO is revealed to extend well beyond that of a simple spectator through the use of the REP-FAMSEC approach. It reveals that DMSO, although not involved in bond forming/breaking or as a classical catalyst, is a major player in the aldol reaction. Modelling of the proline (**1**) catalysed aldol reaction with acetone (**2**) in the presence of an explicit molecule of DMSO (**3**) has revealed that, due to strong intermolecular interactions, stable 3-molecular complexes (3-MCs) are instantly formed. Importantly, it is the HN-C-COOH (of **1**), CO (of **2**) and SO (of **3**) fragments that lead 3-MCs to the global minimum structures (GMSs)

and, as a matter of fact, they must be seen as driving a chemical change throughout the catalytic reaction. Essentially, a DMSO molecule plays a double role as it (1) leads to the elimination of the lowest energy conformer **1a** (LEC) as a catalyst already at the very beginning of the process, namely at the first H-transfer/CN-bond formation and (2) acts a facilitator by promoting the catalytic ability of the higher energy conformer (HEC) of proline **1b**.

We found that exploring (in detail) the process of structural rearrangement leading to the global minimum structures (GMS) of 3-MCs provides an initial but invaluable insight on either a success or failure of a potential catalytic process/mechanism. At the same time, molecular fragments of each molecule that drive the process can be identified and their role can be quantified. We found that the failure of **1a** as a catalyst was in the making from the very beginning as the total interactions, intra and intermolecular in GMS of 3-MCs, weakened for **1a** but significantly strengthened for **1b** and, importantly, became 2.5 times stronger when compared with exactly the same set of interactions computed for **1a**-containing GMS of the 3-MC. Moreover and opposite to what one expects from a potential catalyst, the interaction between **1a** and acetone **2** became weaker whereas we found the opposite, i.e., strengthening, for the **1b**···**2** interactions that became over 5 times stronger than **1a**···**2** in the GMS of 3-MCs. We discovered a similar trend for the interactions between **1** and {**2**+**3**}, as the combined intermolecular interactions between the higher energy conformer **1b** and acetone **2** plus **1b** and a DMSO molecule **3**, i.e., **1b**·{**2**+**3**}, are 2.7 times stronger than **1a**···{**2**+**3**} in the global minimum structures of the 3-MCs.

Mechanistically, although the N-atom of **1** clearly acts as a harbour for the acetone molecule **2** in the aldol reaction, the actual CN-bond formation is shown to be preceded by a proton transfer from the carboxylic acid group to the oxygen of **2**. Thereafter, a second proton transfer takes place, from the resulting quaternised nitrogen, to rebuild the carboxylic acid group that is necessary for the next proton involvement that leads to water elimination. Once again, DMSO is shown to play key and diverse roles in shaping reaction energy profiles by influencing the energies for the transformation of the LEC and HEC-based molecular systems (MS). Importantly, this effect is by far more favourable for the **1b**-containing MS as the product of the first H-transfer is lower in energy than the proceeding GMS but only in the case of **1b**-containing 3-MC. This energetic observation and above-mentioned interaction-based preferences for **1b** when coupled with the fact that **1a** and **1b** can readily interconvert with minimal energy in solution shows that the 3MC derived from the LEC can be considered catalytically inactive and essentially "cut-off" at the first proton transfer with the reaction preferring to proceed via **1b**. Furthermore, although unlikely, if the mechanism involving **1a** is able to proceed beyond the first proton transfer it is for all intents and

purposes completely cut off at the second H-transfer due to an insurmountably energy barrier. Once again, the dynamics of the DMSO molecule feature prominently facilitating stronger interactions between H5 of proline **1** and O37 of DMSO **3** hindering (but only for **1a**) the required intramolecular transfer of H5 to O16 within proline **1**.

Interestingly, List previously reported that not only the CN-bond formation but most likely entire catalytic process is to be mediated through a series of proton transfers involving the CO_2H group of proline **1**.[12] It is notable that the findings reported herein are in a manner pre-meditated by List[12] who suggested that a) 'clearly both the pyrrolidine ring *and* the carboxylate are essential for efficient catalysis to occur' and, based on experimental data, noted that 1) 'After screening several solvents, we found anhydrous DMSO at room temperature to be the most suitable condition regarding reaction times and enantioselectivity.'

Although our focus is on the proline catalysed aldol reaction, the general approach incorporated in the REP-FAMSEC method will be applicable to many synthetic processes. This is because the interaction energies vary much more, typically by an order of magnitude, than commonly computed energy terms (*E*, *H* or *G*) used in drawing reaction energy profiles. Importantly, the REP-FAMSEC based approach allows one to uncover subtle underlying relationships between atoms/fragments/molecules and how they influence each other; these are not easily predictable, if at all, using only classical approaches and chemical intuition. By investigating any and on purpose selected modes of interactions one can fully explore and explain not only the role played by a solvent molecule(s) but also complex mechanistic processes can be rationalised in terms of molecular fragments driving the chemical change. From that one can also identify catalytically (in)active conformers as well as suggest possible additional functionalities needed to improve a synthetic/catalytic process.

4. 5 References

(1) List, B. Emil Knoevenagel and the roots of aminocatalysis. *Angew. Chem., Int. Ed.* **2010**, *49*, 1730–1734.

(2) MacMillan, D. W. C. The advent and development of organocatalysis. *Nature.* **2008**, *455*, 304–308.

(3) Hajos, Z. G.; Parrish, D. R. Asymmetric synthesis of bicyclic intermediates of natural product chemistry. *J. Org. Chem.* **1974**, *39*, 1615–1621.

(4) Eder, U.; Sauer, G.; Wiechert, R. New type of asymmetric cyclisation to optically active steroid CD partial structures. *Angew. Chem., Int. Ed.* **1971**, *10*, 496–497.

(5) Guillena, G.; Nájera, C.; Ramón, D. J. Enantioselective direct aldol reaction: the blossoming of modern organocatalysis. *Tetrahedron: Asymmetry* **2007**, *18*, 2249–2293.

(6) Pellissier, H. Asymmetric organocatalysis. *Tetrahedron* **2007**, *63*, 9267–9331.

(7) Guillena, G.; Ramón, D. J. Enantioselective α-heterofunctionalisation of carbonyl compounds: organocatalysis is the simplest approach. *Tetrahedron: Asymmetry* **2006**, *17*, 1465–1492.

(8) Sunoj, R. B. Proline-derived organocatalysis and synergism between theory and experiments. *Wiley Interdiscip. Rev.: Comput. Mol. Sci.* **2011**, *1*, 920–931.

(9) Gruttadauria, M.; Giacalone, F.; Noto, R. Supported proline and proline-derivatives as recyclable organocatalysts. *Chem. Soc. Rev.* **2008**, *37*, 1666–1688.

(10) Cobb, A. J.; Shaw, D. M.; Longbottom, D. A.; Gold, J. B.; Ley, S. V. Organocatalysis with proline derivatives: improved catalysts for the asymmetric Mannich, nitro-Michael and aldol reactions. *Org. Biom. Chem.* **2005**, *3*, 84–96.

(11) Notz, W.; Tanaka, F.; Barbas, C. F. Enamine-based organocatalysis with proline and diamines: the development of direct catalytic asymmetric aldol, Mannich, Michael, and Diels− Alder reactions. *Acc. Chem. Res.* **2004**, *37*, 580–591.

(12) List, B.; Lerner, R. A.; Barbas, C. F. Proline-catalysed direct asymmetric aldol reactions. *J. Am. Chem Soc.* **2000**, *122*, 2395–2396.

(13) List, B. Proline-catalysed asymmetric reactions. *Tetrahedron.* **2002**, *28*, 5573–5590.

(14) Córdova, A.; Notz, W.; Barbas III, C. F. Direct organocatalytic aldol reactions in buffered aqueous media. *Chem. Commun.* **2002**, *24*, 3024–3025.

(15) Sakthivel, K.; Notz, W.; Bui, T.; Barbas, C. F. Amino acid catalysed direct asymmetric aldol reactions: a bioorganic approach to catalytic asymmetric carbon-carbon bond-forming reactions. *J. Am. Chem. Soc.* **2001**, *123*, 5260–5267.

(16) Rankin, K. N.; Gauld, J. W.; Boyd, R. J. Density functional study of the proline-catalysed direct aldol reaction. *J. Phys. Chem. A* **2002**, *106*, 5155–5159.
(17) Clemente, F. R.; Houk, K. Computational evidence for the enamine mechanism of intramolecular aldol reactions catalysed by proline. *Angew. Chem.* **2004**, *116*, 5890–5892.
(18) Sharma, A. K.; Sunoj, R. B.; Enamine versus Oxazolidinone: What Controls Stereoselectivity in Proline-Catalysed Asymmetric Aldol Reactions? *Angew. Chem. Int. Ed.* **2010**, *49*, 6373–6377.
(19) Yang, G.; Zhou, L. Mechanisms and reactivity differences of proline-mediated catalysis in water and organic solvents. *Catal. Scie. Technol.* **2016**, *6*, 3378–3385.
(20) Ajitha, M. J.; Suresh, C. H. A higher energy conformer of (S)-proline is the active catalyst in intermolecular aldol reaction: evidence from DFT calculations. *J Mol. Catal. A: Chem.* **2011**, *345*, 37–43.
(21) Cukrowski, I.; Dhimba, G.; Riley, D. L. A reaction energy profile and fragment attributed molecular system energy change (FAMSEC)-based protocol designed to uncover reaction mechanisms: a case study of the proline-catalysed aldol reaction. *Phys. Chem. Chem. Phys.* **2019**, *21*, 16694–16705.
(22) Arnó, M.; Domingo, L. R. Density functional theory study of the mechanism of the proline-catalysed intermolecular aldol reaction. *Theor. Chem. Acc.* **2002**, *108*, 232–239.
(23) Arnó, M.; Zaragozá, R. J.; Domingo, L. R. Density functional theory study of the 5-pyrrolidin-2-yltetrazole-catalysed aldol reaction. *Tetrahedron: Asymmetry* **2005**, *16*, 2764–2770.
(24) Yang, G.; Yang, Z.; Zhou, L.; Zhu, R.; Liu, C. A revisit to proline-catalysed aldol reaction: interactions with acetone and catalytic mechanisms. *J. Mol. Catal. A: Chem.* **2010**, *316*, 112–117.
(25) List, B.; Hoang, L.; Martin, H. J. New mechanistic studies on the proline-catalysed aldol reaction. *Proc. Nat. Acad. Sci. U.S.A.* **2004**, *101*, 5839–5842.
(26) Zhao, L.; Li, S. J.; Fang, D. C. A Theoretical Study of Ene Reactions in Solution: A Solution-Phase Translational Entropy Model. *ChemPhysChem* **2015**, *16*, 3711–3718.
(27) Han, L.-L.; Li, S.-J.; Fang, D.-C. Theoretical estimation of kinetic parameters for nucleophilic substitution reactions in solution: an application of a solution translational entropy model. *Phys. Chem. Chem. Phys.* **2016**, *18*, 6182–6190.
(28) Varghese, J. J.; Mushrif, S. H. Origins of complex solvent effects on chemical reactivity and computational tools to investigate them: a review. *Reac. Chem. Eng.* **2019**, *4*, 165–206.
(29) Wang, H.; Wang, Y.; Han, K.-L.; Peng, X.-J. A DFT study of Diels− Alder reactions of o-quinone methides and various substituted ethenes: selectivity and reaction mechanism. *J. Org. Chem.* **2005**, *70*, 4910–4917.

(30) Zeifman, A. A.; Novikov, F. N.; Stroylov, V. S.; Stroganov, O. V.; Svitanko, I. V.; Chilov, G. G. An explicit account of solvation is essential for modeling Suzuki–Miyaura coupling in protic solvents. *Dalton Trans.* **2015**, *44*, 17795–17799.

(31) Blanco, M.; Pendás, A. M.; Francisco, E. Interacting quantum atoms: a correlated energy decomposition scheme based on the quantum theory of atoms in molecules. *J. Chem. Theory Comput.* **2005**, *1*, 1096–1109.

(32) Francisco, E.; Pendás. A.. M.; Blanco, M. A molecular energy decomposition scheme for atoms in molecules. *J. Chem. Theory Comput.* **2006**, *2*, 90–102.

(33) Bachrach, S. M. Challenges in computational organic chemistry. *Wiley Interdiscip. Rev.: Comput. Mol. Sci.* **2014**, *4*, 482–487.

Chapter 5

Puckering of proline pyrrolidine ring leading to a change from the lowest energy conformer **1a** to the active and higher energy conformer **1b** in proline catalysis.

Abstract

The structural change of proline from the lowest energy conformer **1a** to the active and higher energy conformer **1b** is investigated using DFT calculation with an implicit solvation model and discrete solvent molecules of acetone, DMSO and a combination of the two molecules. All solvent systems show that the structural change from the most abundant and inactive conformer **1a** involves the puckering of the pyrrolidine ring coupled by the rotation of the carboxylic moiety. The largest energy barrier for the structural change was observed in the implicit solvation model (11 kcal/mol), but the energy barrier was decreased by the presence of explicit solvent molecules either of acetone or DMSO. The small energy barrier of 11 kcal/mol observed in the implicit solvation is consistent with shorter reaction times and lower temperatures used in proline catalysis. When modelling of the structural change was done in the presence of an explicit solvent molecule of acetone, the energy barrier decreased by 1 kcal/mol, while replacing the molecule of acetone with DMSO decreased the energy barrier by 3 kcal/mol. The current result gives more insights into the mechanistic details of most proline catalysed organic transformations which are thought to proceed via either enamine or imine intermediates. Since the most abundant proline conformer **1a** cannot result in the formation of the active enamine/imine, its conversion to the catalytically active conformer **1b** is undeniable as large reaction yields are observed in most proline catalysed organic transformations.

5.0 Introduction

The obvious advantages offered by metal-free asymmetric organocatalysis in academic research and their potential use in the chemical industry has resulted in a rapid shift from the traditional metal-mediated catalysis. Their notable advantages, among others, are: (i) they are economically more viable than organometallic catalysts, (ii) they usually involve simple workup, (iii) they are air-stable and can tolerate water hence easy to handle, (iv) they are safe to use and generally less toxic.[1–3] Proline is an archetypical example of organocatalysts, and one of the twenty naturally occurring amino acids.[4] It has attracted much attention recently due to its effectiveness in catalysing a range of organic reactions namely aldol reactions,[5,6] Robinson annulations,[7] Mannich reactions,[8] and α-aminoxylations,[9] among others.

Due to the importance of proline catalysed organic reactions, the mechanism through which it catalyses organic reactions has been studied both theoretically[10,11] and experimentally.[12–15] The large catalytic effect observed in proline catalysed organic reactions can be attributed to the proximity of the amino and carboxylic groups and the rigid pyrrolidine ring.[16] The pyrrolidine ring of proline is not planar and is capable of adopting two distinct and stable pucker conformational modes, i.e., up (endo) and down (exo) which are equally preferential (Figure 5.1). The conformational modes depend on the position of the C^{γ}-atom (C2 according to our naming) relative to the plane of atoms N13–C4–C3.[17–19] The conformer in which C2 is below this plane is referred to as the down or (exo) while the up or (endo) is when C2 is above the plane. Hence, in **1a** the pyrrolidine ring exhibits the endo conformation, while it has the exo conformation in **1b**.

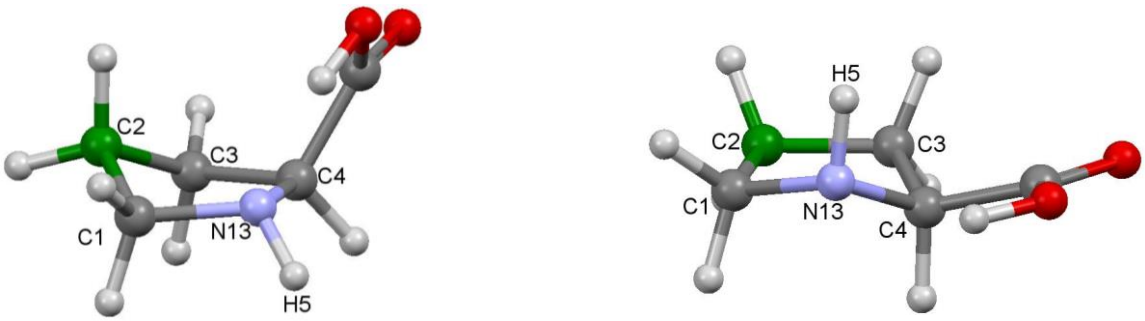

C2 up (endo) **1a** C2 down (exo) **1b**

Figure 5.1. Ball and stick representation of endo (**1a**) and exo (**1b**) conformations of the pyrrolidine ring of proline showing the N13–C4–C3 plane and C2 (in green).

The proximity of the N-lone pair of electrons and the acidic proton in both conformers (**1a** and **1b**) can be anticipated to bring a bi-functionality towards the ketone donor during proline catalysed reactions. However, the mechanism through the endo conformer (**1a**), which is also the lowest in

energy, cannot proceed to form the active enamine catalyst.[20,21] On the other hand, the mechanism through the higher energy conformer **1b** (exo) was reported to be the most preferred and can result in the active enamine catalyst after a bimolecular reaction with the donor ketone. The inactivity of the lowest energy conformer which can be regarded as the most abundant provides more questions than answers. Among them: (i) what happens when the solution population of the higher energy conformer becomes exhausted and (ii) can a puckering of the pyrrolidine ring from an endo in **1a** result in the formation of the exo conformer **1b**? This is the apparent missing link regarding the mechanistic details of proline catalysis. Moreover, elemental steps of most proline catalysed organic reactions are similar as they proceed either via enamine or iminium intermediates.[9,22,23] The lowest energy conformer **1a** cannot result in the formation of either of the two key intermediates mentioned above. This clearly shows that the mechanistic details at the early stages of proline catalysis and the role of conformers have been overlooked and is not fully understood.

Apart from the differences in puckering of the pyrrolidine ring, another notable difference between conformers **1a** and **1b** is the relative orientation of H5 with respect to the COOH moiety, in **1a** it is in the opposite side or *anti*, while in **1b** it is in the same side or *syn* orientation. It is fundamentally important and mechanistically relevant to study if a conformational change from **1a** to **1b** is possible during the progress of the catalytic reaction. Such a study is important for chemists to understand the state of proline catalysis since most proline catalysed organic reaction proceed through the formation of an active enamine or iminium catalyst.

This chapter focuses on achieving the following aims, among others: (i) to investigate, using an implicit solvent model, if the puckering of the pyrrolidine ring in **1a** can result in the reorientation of H5 to the *syn* position (**1b**), (ii) to study the effect of the ketone donor (which is used in large excess and sometimes as the only solvent in proline catalysis) on the ring puckering of proline, (iii) to study solvent effects (DMSO) and DMSO-acetone solvent system on the ring puckering of proline; to the best of our knowledge, no such report is available in the literature.

5.1 Results and discussion

5.1.1 Structural change in the implicit solvent.

The mechanism through the most predominant or lowest energy conformer (LEC) of proline **1a** is known to be cut off and does not proceed to form the active enamine catalyst. Therefore, it is apparent that a conformational change from **1a** to the active higher energy conformer (HEC) **1b** must occur as the reaction progresses; otherwise, the reaction would be terminated when the

solution population of **1b** becomes exhausted. Since this is not the case, it is obvious that a conversion or structural change of proline from **1a** to **1b** occurs at some stage during the course of the reaction. Such a structural change should involve the puckering of the pyrrolidine ring and the re-orientation of H5 from *anti* (in **1a**) to the *syn* orientation in **1b**. It can be hypothesised that to study this conformational change by reaction modelling, one can select and scan any dihedral angle (DA) in **1a** that can result in the puckering of the pyrrolidine ring and re-orientation of H5. Such DA should consist of H5 as one of its atoms while increasing or decreasing the value of the DA should result in the formation of **1b**.

We identified two such dihedral angles in **I-1a** (Table 5.1) namely, DA(H12,C4,N13,H5), and DA(H5,N13,C1,H6) with vales of 3.3°, and 89.4°, respectively (the prefix **I** indicate that modelling was done in the implicit solvation model). In **I-1b**, the two DAs have values of 172.6°, and –45.8°, respectively. When the first DA(H12,C4,N13,H5) was selected and scanned in steps of +6° (Figure C1 in Appendix C), there was a re-orientation of H5 by ~180° to the *syn* orientation resulting in the formation of conformer **1b** as we had predicted. However, when the second DA(H5,N13,C1,H6) was scanned in steps of –6° it yielded intermediate **I-3** (Table 5.1).

Table 5.1. Ball and stick representation of intermediate conformers obtained from a scan of DA(H12,C4,N13,H5) using conformer **1a** leading to its conversion to **1b** in the implicit solvation model.

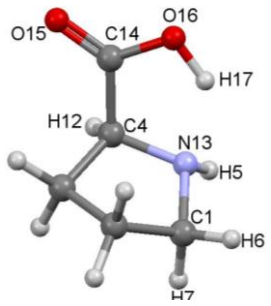 **I-1a**	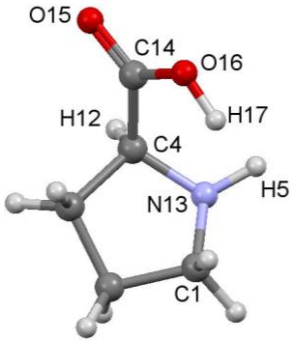 **I-1**	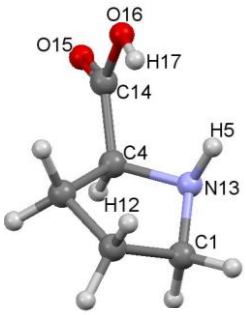 **I-2**
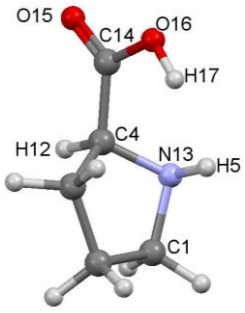 **I-3**	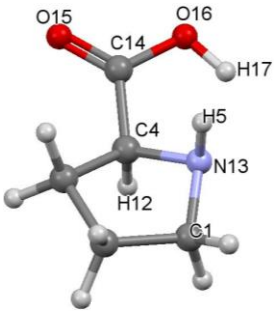 **I-1b**	

Intermediate structures **I-1**, **I-2** and **I-1b** obtained in the implicit solvent model (Table 5.1) shows that the carboxylic moiety plays an important and key role during the structural change from **1-1a** to **I-1b**. It rotates slightly about the C4–C14 single bond, notably, the DA(H12,C4,C14,O15) rotated by – 53.3° from 56.9° in **I-1a** to 3.6° in **I-3**. This allows the puckering of the pyrrolidine ring and the associated turning of H5 from an *anti* to the *syn* orientation. Interestingly, when the ring puckering is completed, the carboxylic moiety rotated by +84.6° in the opposite direction. Notably, the intermediate structure with the highest energy (**I-3**) is not a typical transition state, i.e., a first-order saddle point characterised by a negative frequency in the Hessian matrix. It is simply the most strained conformer, as a full energy optimisation of intermediate conformers along the conformational change show that **I-2** is the only stationary point, whereas **I-1** and **I-3** yielded **I-1a** (the input structure) upon full energy optimisation.

Variation in total intramolecular interaction energies (covalent bonding plus long-distance interaction)

On the change from **I-1a** to **I-1b**, total zero-point vibrational energy-corrected electronic energy (E_{ZPVE}) for molecular system increased by ~ 7 kcal/mol (Figure 5.2) while the energy barrier is ~ 11 kcal/mol. Since there are no intermolecular interactions involved, the change in the energy can be attributed to the weakening of intramolecular interactions which is the sum of total covalent bonds ${}^{\text{C-B}}E_{\text{int}}^{\text{mol}}$ and long distance or non-covalent interactions ${}^{\text{L-D}}E_{\text{int}}^{\text{mol}}$ i.e., ${}_{\text{intra}}E_{\text{int}}^{\text{mol}} = {}^{\text{C-B}}E_{\text{int}}^{\text{mol}} + {}^{\text{L-D}}E_{\text{int}}^{\text{mol}}$.

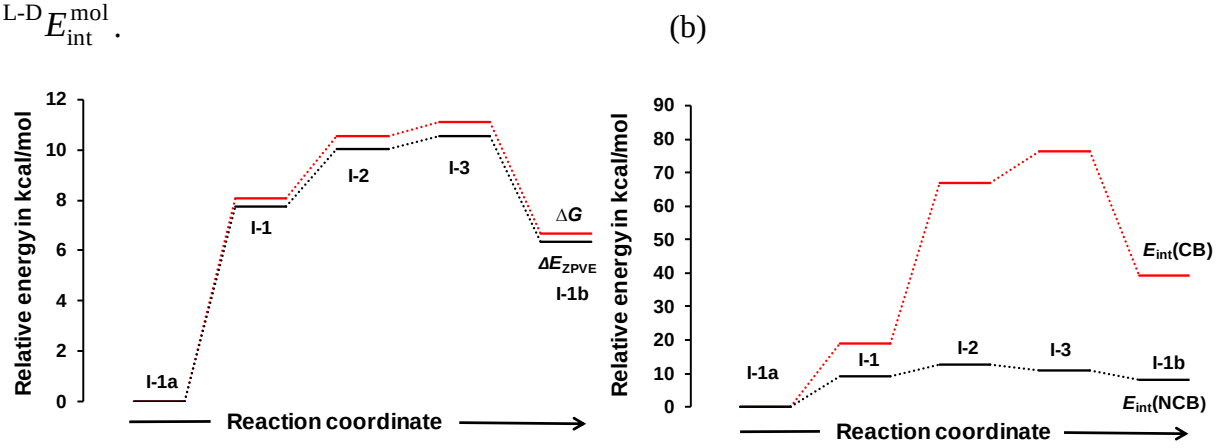

Figure 5.2. Variation in zero-point vibrational energy corrected electronic energy (E_{ZPVE}), Gibbs free energy (G), covalent bonds ${}^{\text{C-B}}E_{\text{int}}^{\text{mol}}$, and long-distance (non-covalent) interactions ${}^{\text{L-D}}E_{\text{int}}^{\text{mol}}$ on moving from **I-1a** to **I-1b** in the implicit solvation model.

Figure 5.2b shows the trend for changes in ${}^{\text{C-B}}E_{\text{int}}^{\text{mol}}$ and ${}^{\text{L-D}}E_{\text{int}}^{\text{mol}}$ on the structural change from **I-1a** to **I-1b** and the data shows that:

(1) Upon moving from **I-1a** to **I-1b** covalent bonds significantly weakened while long-distance interactions weakened marginally.

(2) In the highest energy intermediate conformer **(I-3)**, covalent bonds became weaker by a staggering +76.5 kcal/mol while long-distance interactions became weaker by just +11 kcal/mol.

(3) In the resulting HEC **I-1b** covalent bonds are weaker by +39.2 while long-distance interactions weakened by +8.1 kcal/mol. Thus, covalent bonds weakened by a larger magnitude when compared to long-distance interactions and can be regarded as the major component of the observed energy barrier of 11 kcal/mol and the difference in energy between conformers **1a** and **1b**.

Since the HEC of proline **1b** and acetone **2**, – the ketone coupling partner, form an initial adduct that facilitates the first step of the catalytic reaction,[20,24] it becomes imperative to investigate if interactions between acetone **2** and the most predominant conformer (**1a**) will also facilitate (or inhibit) the formation of the active conformer **1b**. This is the focus of the next section.

5.1.2 Structural change in the presence of an explicit solvent molecule of acetone

Proline (**1a**) and acetone (**2**) can readily form stable adducts or two molecular complexes (2-MCs) which initiate the first step of the catalytic reaction. However, the mechanism cannot proceed further and is cut off before the formation of the active enamine catalyst. On the other hand, 2-MCs involving **1b**, the higher energy conformer, and acetone **2** can result in the formation of the active enamine catalyst.[20] The key question then will be whether acetone will facilitate or inhibit the structural change of **1a** to **1b** by decreasing/increasing the energy barrier from 11 kcal/mol obtained in the implicit solvation model. Acetone is used in large excess as a co-solvent and sometimes as the only solvent under neat conditions,[25] hence its catalytic role at the early stages of the synthetic reaction is fundamental for rationalising the mechanistic details of proline catalysis.

A-1a, the lowest energy 2-MC of **1a** and **2** (Table 5.2) was used as the input structure for running DA(H12,C4,N13,H5) scan, the value for this dihedral angle is 9.5° in **A-1a**, (the prefix **A** represents the acetone complex of proline **1**) while the same DA is 172.6° in **1b**. Hence, one can hypothesise that increasing this dihedral angle by ~ 160° should result in the structural change of **A-1a** to **A-1b**.

Like in the implicit solvation model, in which a puckering of the pyrrolidine ring was observed when the DA was increased, the same phenomenon was also observed in the presence of an explicit solvent molecule of acetone. The plane defined by atoms C1–N13–C4 decreased by ~ 6° from

109.2° in **I-1a** to 103.3° in **I-1b**, the same plane decreased by ~7° from 109.2° in **A-1a** to 102.6° in **A-3**. We observed that the formation of **A-3** was not accompanied by a corresponding rotation of the carboxylic group in the opposite direction as observed in the implicit solvation model. This can be attributed to the presence of strong intermolecular interaction between the carboxylic moiety of proline **1** and the molecule of acetone **2**.

Table 5.2. Ball and stick representation of intermediate 2-MCs along the change from **1a** to **1b** in the presence of an explicit solvent molecule of acetone (**2**).

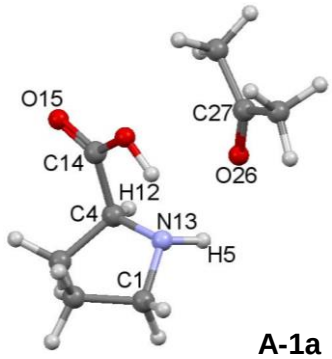 **A-1a**	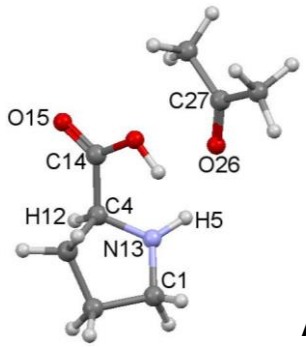 **A-1**	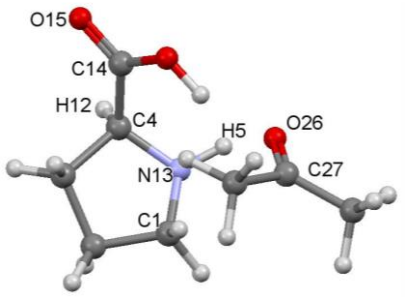 **A-2**
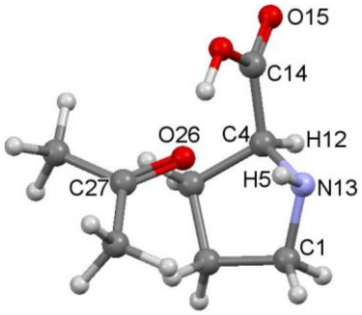 **A-3**	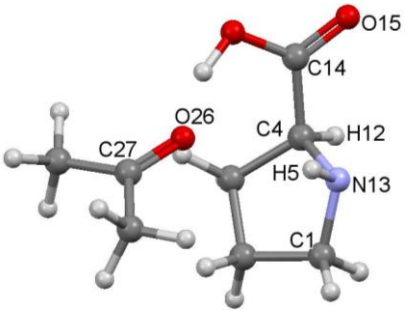 **A-4**	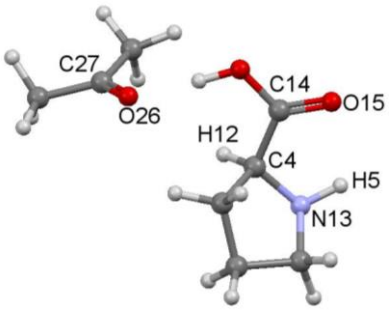 **A-5**
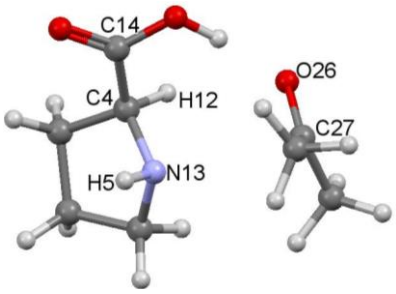 **A-1b**		

Due to the unrestricted rotation of the C4–C14 single bond, one can postulate that the active complex (**A-1b**) can be formed from **A-3** by a rotation of the carboxylic moiety along the C4–C14 single bond. Hence, another DA(H12,C4,C14,O15) was selected in **A-3** and scanned in steps of –10°. This resulted in the rotation of the carboxylic moiety and formation of **A-1b** (Figure C2 in

Appendix C) as we had predicted. Inspection of structures **A-2** and **I-3** shows that the principle proline conformer in the two structures is the same. Hence one can understand the effect of the explicit solvent molecule of acetone by analysing the two structures. Figure 5.3 shows a comparison of trends of changes in zero-point vibrational energy corrected electronic energy (E_{ZPVE}) and Gibbs free energy (G), as the structure of proline changes from **1a** to **1b** in the presence of a molecule of acetone and in the implicit solvation model.

Inspection of the intermediate structures in Tables 1 and 2 shows that the intermediate complexes from the two solvation models are not directly comparable. However, the general trend in Figure 5.3 shows that the graph obtained when an explicit solvent molecule of acetone is present is below the graph of the implicit solvation model. This indicates that acetone facilitates the change from **1a** to **1b** by lowering the energies of key intermediates.

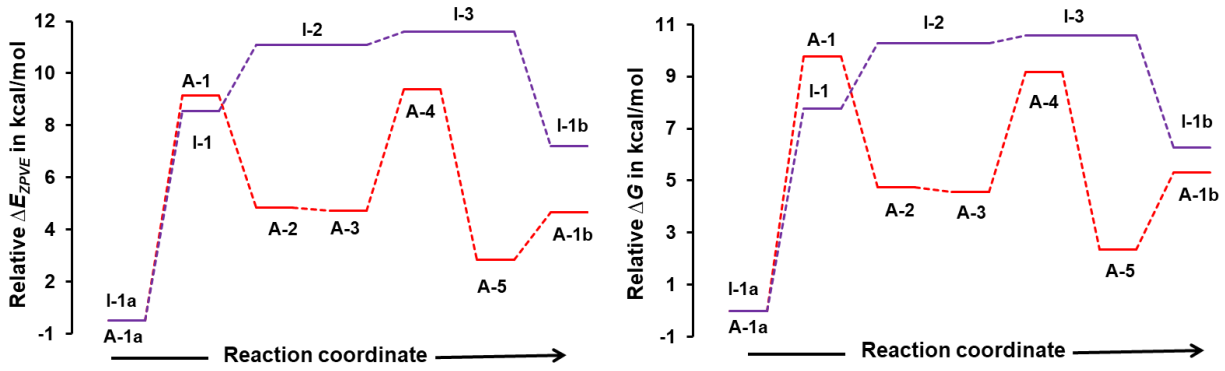

Figure 5.3 Changes in zero-point vibrational energy corrected electronic energy (E_{ZPVE}) and Gibbs free energy (G), along with the transformation from **1a** to **1b** in the implicit (trend in purple) and the presence of an explicit solvent molecule of acetone (the trend in red).

It can also be noticed that the structure of proline conformer in **I-2** is comparable to the one in **A-3** (see Tables 1 and 2), the two structures are also stationary points in their respective potential energy surfaces. However, the relative energy of **A-3** is lower than that of **I-2** by ~ 6 kcal/mol. Moreover, data in Figure 5.3 shows that the presence of an explicit solvent molecule of acetone marginally decreases the E_{ZPVE} barrier by 2.2 kcal/mol and the Gibbs free energy barrier G by ~ 1 kcal/mol. This clearly shows that the presence of an explicit solvent molecule of acetone lowers the energies of key intermediates during the structural change from **1a** to **1b**. To get additional insights into the role of acetone on the change from **1a** to **1b**, one can calculate the variation in intramolecular interactions (sum of covalent bonds and long-distance interactions) across all 2-MCs from **A-1a** to **A-1b** and compare with data obtained in the implicit solvation model (Figure 5.4). Data in Figure 5.4 shows that in the presence of an explicit solvent molecule of acetone:

(1) Covalent bonds in intermediate conformers of proline weakened to a lesser extent in 2-MCs when compared to the same set of covalent bonds in the implicit solvation model. Notably for **A-3** and **A-1b**, covalent bonds became weaker by +21.1 kcal/mol and +20.1 kcal/mol, while in their corresponding structures: **I-2** and **I-1b** they weakened by +66.9 kcal/mol and +39.2 kcal/mol, respectively.

(2) On moving from **A-1a** to **A-1b**, long-distance interaction energies weakened significantly in all 2-MCs, compared to structures obtained in the implicit solvation model. They became weaker by +34.6 kcal/mol (in **A-3**) and +28.2 kcal/mol (in **A-1b**), respectively. This is two times higher than in the implicit solvation model.

(3) For acetone, covalent bonds weakened across all intermediate 2-MCs. They became weaker in **A-3** and **A-1b** by +21.7 and +19.1 kcal/mol respectively, while non-covalent interactions barely change.

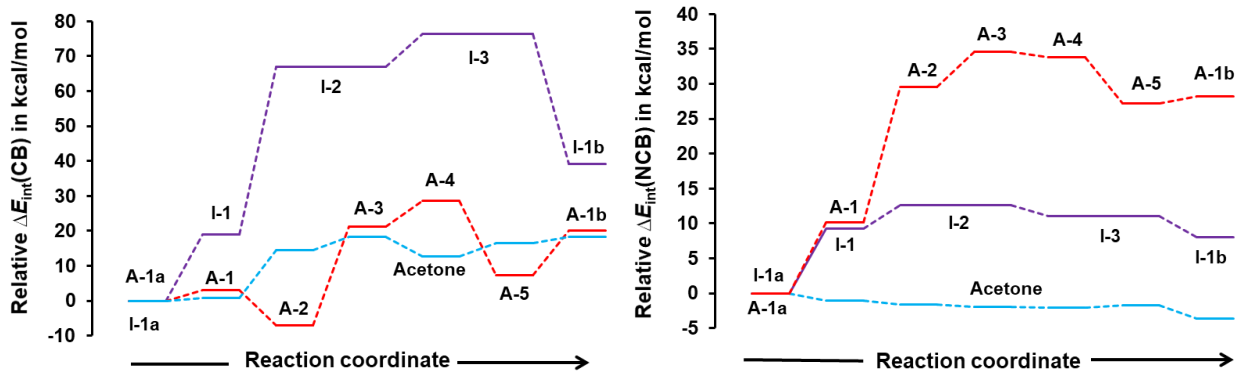

Figure 5.4. Variation in covalent and non-covalent interaction energies in proline conformers along the change from **1a** to **1b** in implicit solvent (the trend in purple) and in an explicit solvent molecule of acetone (trend in red), the trend for changes in intramolecular interaction in the acetone molecule is shown in blue

The weakening of covalent bonding interactions in the molecule of acetone across all 2-MCs must be a result of formation of strong intermolecular interactions with proline. In the following paragraph, we will analyse the variation in intermolecular interaction energies across individual 2-MCs from **A-1a** to **A-1b** (Figure 5.5). Atoms of proline **1** and acetone **2** with the most positive and most negative interaction energies $E_{\text{int}}^{\text{A,B}}$ (Table C4 in Appendix C) are placed as unique atomic fragments $\mathcal{A}$ and $\mathcal{P}$, respectively, where $\mathcal{A}$ is made of {O26,C27) and $\mathcal{P}$ consist of atoms {C1,C4,H5,N13,14,O15.O16,H17}.

Data in Figure 5.5 reveals that:

(1) Molecules of proline **1** and acetone **2** form strong intermolecular interactions and the interaction energies are more than two times stronger in **A-1b** (–71.0 kcal/mol) than in **A-1a**

(–32.9 kcal/mol) hence, strong interactions in **A-1b** can be regarded as the driving force which facilitates the change from **1a** to **1b**.

(2) Since intermolecular interaction between proline **1** and acetone **2** are stronger in the catalytically active conformer **1b** they can be regarded as the driving force leading to the reactivity of **1b** with acetone **2**. Moreover, one can also speculate that interaction between **1a** and **2** can only facilitate the conversion of the former to **1b** rather than its bimolecular reaction.

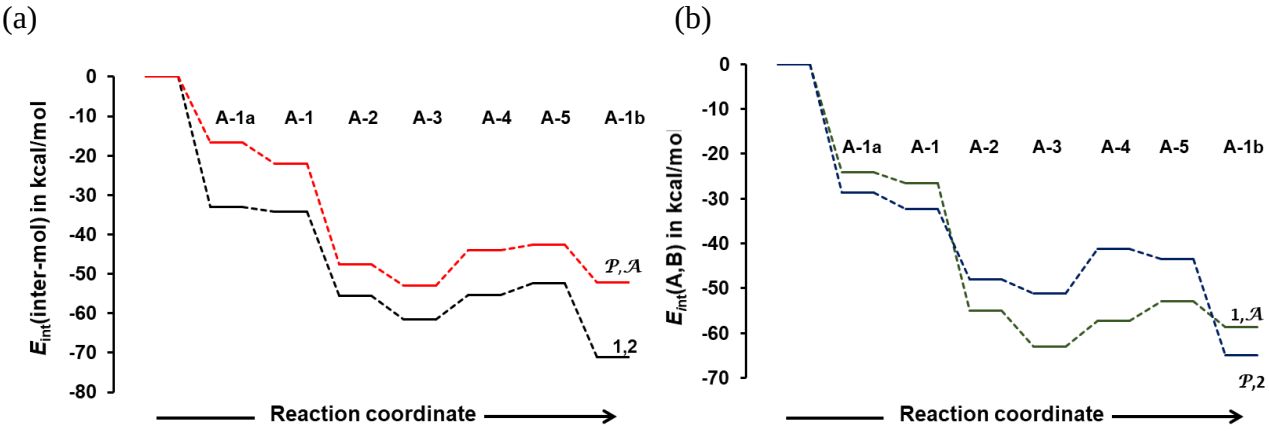

Figure 5.5. Variation in intermolecular interaction between molecules of proline **1** and acetone **2**, and between molecular fragments **P** and **A** of proline and acetone, and intermolecular interaction between entire molecules of proline (**1**) the acetone (**2**) with molecular fragments **A** and **P** respectively.

Inspection of the output complex (**A-1b**) of proline (**1b**) and acetone (**2**) shows that the two molecules are well pre-organised to initiate the first step of the catalytic reaction as we have previously reported.[21] Thus, the C–N bond formation/1st H transfer can be imagined to occur immediately after the formation of **1b**.

It can be concluded that the molecule of acetone facilitates the transformation of proline from **1a** to **1b** through the formation of strong intermolecular interactions which lowers the energies of key intermediates. The current finding provides important insights into the role of acetone or any other ketone coupling partner which are normally used as co-solvents during proline catalysed aldol reaction. Since DMSO has established itself as the solvent of choice in proline catalysed aldol reactions,[25–27] we elected to study if it possesses the same facilitating effect on the structural change from **1a** to **1b** as observed with acetone, this is the focus of the following section.

5.1.3. Structural change in the presence of an explicit solvent molecule of DMSO

To study the effect of an explicit solvent molecule of DMSO **3** on the structural change from **1a** to **1b**, the molecule of acetone in **A-1a** was replaced by a molecule of DMSO **3**, and the resulting complex **D-1a** was energy-optimised, (the prefix **D** stands for the DMSO complex of proline **1a**). The same DA(H12,C4,N13,H5) which was selected in the presence of acetone was scanned in steps

of 6°, this resulted in complex **D-3** which is analogous to **A-3**. Notably, the relative energy of **D-3** is lower than its equivalent **A-3** with respect to both E_{ZPVE} and G by –2.4 kcal/mol and –2.9 kcal/mol, respectively. As observed in the presence of a molecule of acetone **2**, an additional scan of DA(H12,C4,C14,O15) was required to rotate the carboxylic moiety about the C4–C14 single bond before the formation of **D-1b**. The conformers of proline obtained from the scan of DA(H12,C4,C14,O15) are also comparable, but have lower relative energies than those obtained in the presence of a molecule of acetone. Notably, **D-4** and **D-5** are lower in relative energy than their equivalent **A-4** and **A-5** with respect to both E_{ZPVE} and Gibbs free energy G by ~ – 2 kcal/mol. The relative energy of the resulting complex of DMSO **3** and **1b** (**D-1b**) is lower than **A-1b** with respect to E_{ZPVE} and G by – 3.3 kcal/mol and – 4.2 kcal/mol, respectively (Figure 5.6). On moving from **D-1a** to **D-1b** the energy of molecular system marginally increased with respect to E_{ZPVE} and G by 0.8 kcal/mol and 1.1 kcal/mol, respectively, while it increased by 4.2 kcal/mol, and 5.3 kcal/mol, respectively, for the **A-1a** to **A-1b** structural change. Hence, considering both E_{ZPVE} and Gibbs free energy G, the transformation from **1a** to **1b** is more favoured in the presence of DMSO than in acetone. Ball and stick representation of 2-MCs of proline and the solvent molecule of DMSO are shown in Table 5.3.

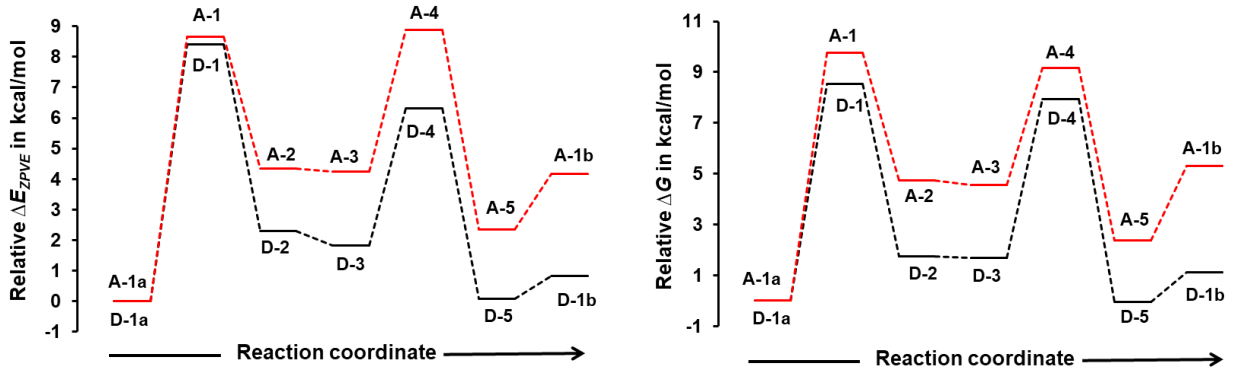

Figure 5.6. Variation in zero-point vibrational energy corrected electronic energy (E_{ZPVE}) and Gibbs free energy (G), along with the transformation from **1a** to **1b** in the presence of explicit solvent molecules of: (i) acetone (the trend in red) and (ii) DMSO (the trend in black).

Since the energy trend for 2-MCs obtained in the presence of a solvent molecule of DMSO is below that of acetone in Figure 5.6, it implies that the molecule of DMSO is more effective and possesses a better-facilitating effect than acetone. To get additional insights into the influence of the two explicit solvent molecules, we compared the variation in intramolecular interaction energy in proline conformers along the structural change from **1a** to **1b** in the presence of solvent molecules of acetone, DMSO and in the implicit solvent model (Figure 5.7).

Table 5.3. Ball and stick representation of intermediate 2-MCs along with the change from **1a** to **1b** in the presence of an explicit solvent molecule of DMSO (**3**).

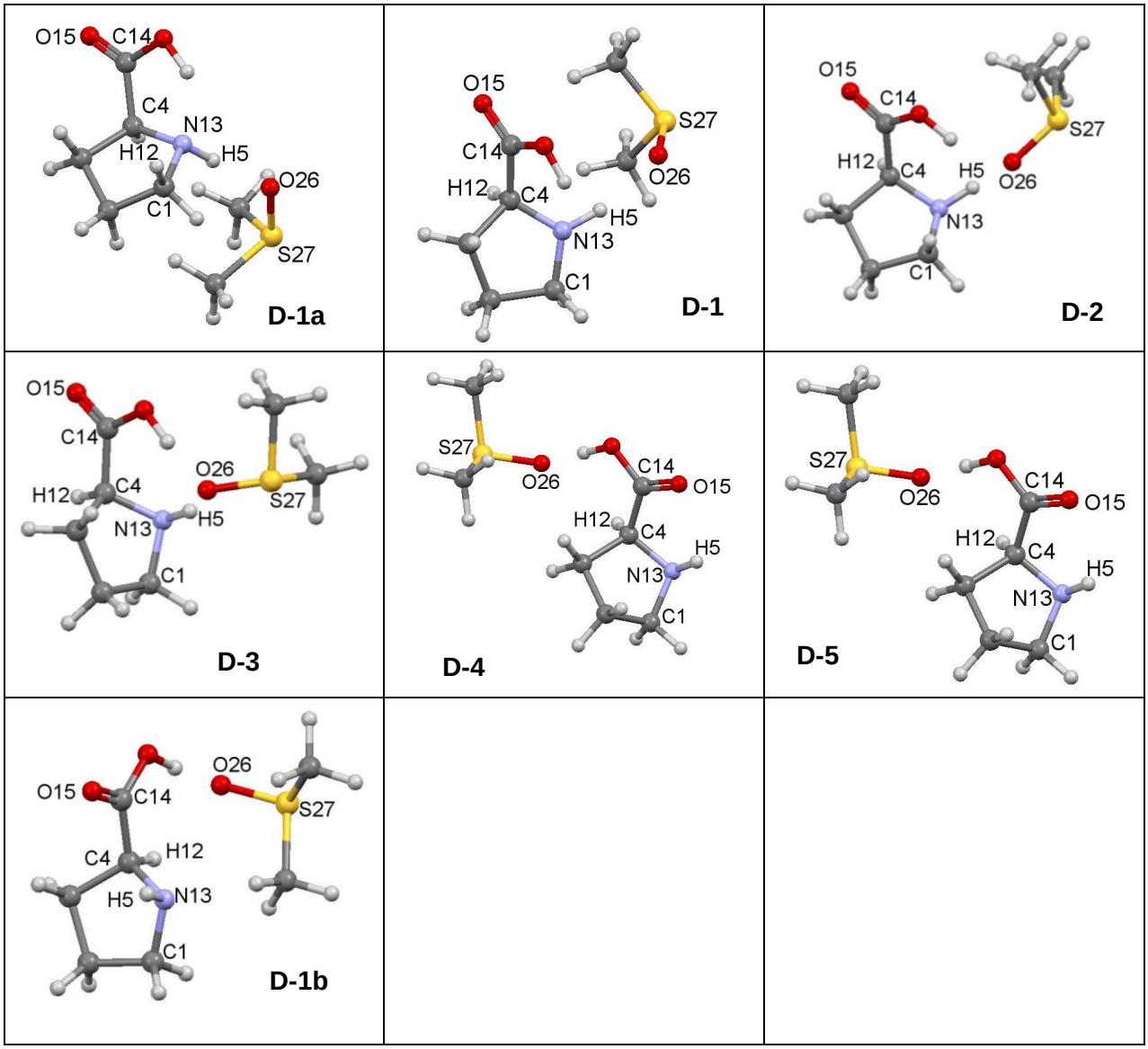

Data in Figure 5.7 shows that in the presence of a solvent molecule of DMSO:

(1) Covalent bonds weakened to a lesser extent in all proline intermediate conformers when compared to the implicit solvent model, in **D-3** and **D-1b** covalent bonds weakened by +22.4 kcal/mol and +17.0 kcal/mol, respectively. In the explicit solvent molecule of DMSO itself, covalent bonds also weakened across all 2-MCs. Notably, in **D-3** and **D-1b** covalent bonds became weaker in DMSO by +31.0 kcal/mol and +28.9 kcal/mol, respectively.

(2) A comparative assessment of the effect of the two solvent molecules on both the covalent bonds and long-distance interaction energy in individual proline conformers shows that there is no significant difference between the effects of the two solvents. Notably, in proline, long-distance interaction energy weakened by ~ +35.6 kcal/mol in both **A-3** and **D-3**, while in **A-**

1b and **D-1b** they became weaker by + 28.2 kcal/mol and + 25.8 kcal/mol, respectively. The change in long-distance interaction energy in the individual solvent molecules of acetone and DMSO are opposite, while they weakened in **D-1b** by + 5.8 kcal/mol, they marginally strengthened in **A-1b** by – 3.6 kcal/mol.

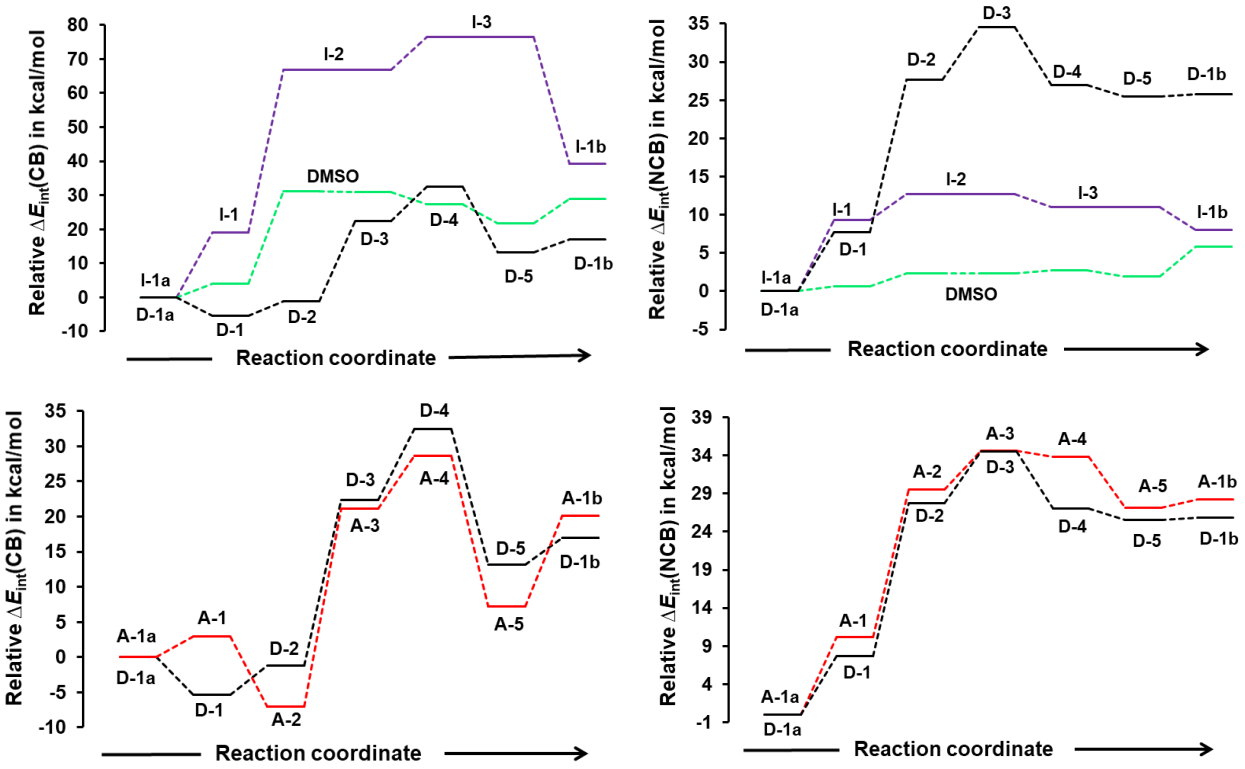

Figure 5.7. Variation in covalent and non-covalent interaction energy along the change from **1a** to **1b**: for the implicit solvation model (trend in purple) and in the presence of explicit solvent molecules of (i) acetone (trend in red), and (ii) DMSO (trend in black). The trend for changes in interaction energies in the solvent molecule of DMSO is shown in green.

We have shown in the previous section that the weakening of covalent bonds in the molecule of acetone in 2-MCs along the change from **A-1a** to **A-1b** is a result of formation of strong intermolecular interaction with proline. It therefore becomes apparent that the weakening of covalent bonds in the solvent molecule of DMSO is a result of formation of strong intermolecular interaction with proline. As a result, we compared the variation in intermolecular interaction energies in 2-MCs of proline and molecules of acetone and DMSO (Figure 5.8a). Alongside is the variation in the inter-fragment interaction energy between the $\mathcal{P}$ fragment made of proline atoms {C1,C4,H5,N13,C14,O15,O16,H17} and fragments $\mathcal{A}$ and $\mathcal{D}$ made of atom pairs {O26,C27} and {O26,S27) in acetone and DMSO, respectively.

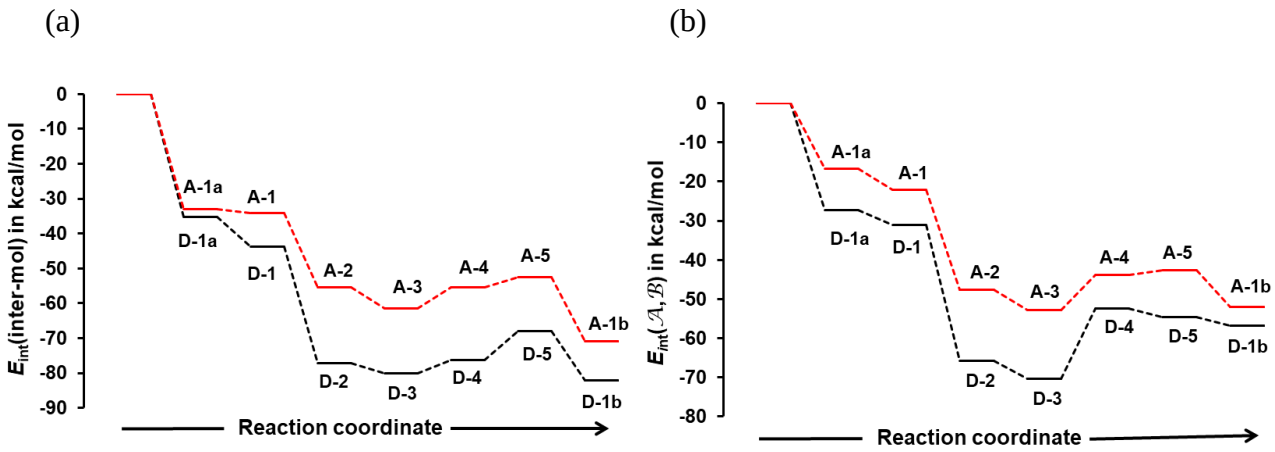

Figure 5.8. (a) Variation in intermolecular interaction energy between a molecule of proline **1** and an explicit solvent molecule of: (i) acetone (trend in red) and (ii) DMSO (trend in black), and (b) between molecular fragments $\mathcal{P}$ and $\mathcal{A}$, and $\mathcal{P}$ and $\mathcal{D}$ of proline and acetone, and proline and DMSO, in the indicated 2-MCs.

Data in Figure 5.8 show that the trend for intermolecular interaction energies between the molecules of proline **1** and DMSO **3** is below that of proline **1** and acetone **2** across all 2-MCs. In addition, the trends for inter-fragment interaction energy between the $\mathcal{P}$ fragments of proline and the $\mathcal{D}$ fragment of DMSO is also below that of the $\mathcal{P}$ and $\mathcal{A}$ fragments. This indicates that proline **1** forms stronger interaction with DMSO **3** than with acetone **2**.

The above, together with data obtained in the previous sections show that the structural change from **1a** to **1b** is more favourable in the presence of an explicit solvent molecule of DMSO, though it is also feasible in acetone. Given the experimental conditions often used in which a 4:1 ratio of DMSO and acetone is used, the above result provides more questions than answers. Among them, if proline forms stronger interaction with DMSO than with acetone why does it eventually reacts with acetone? Based on the calculated intermolecular interaction energies, one is likely to predict that the reaction between proline and DMSO will have more precedence over that of proline and acetone. Moreover, the concentration of DMSO used is in a typical experimental setup is more than 4 times larger than that of acetone so why does proline react with acetone rather than with DMSO? As result of the current observation, there is a need to investigate the variation in interaction energies between proline and explicit solvent molecules of acetone and DMSO in a mixture of the two solvent molecules during the structural change from **1a** to **1b**, this is the focus of the next section.

5.1.4. Exploring structural change in the presence of explicit solvent molecules of acetone and DMSO

Since solvent effects play integral role on the structural change from **1a** to **1b**, a mixture of acetone and DMSO should result in a new solvent system with entirely different solvent effects from the individual solvents. In a typical experimental setup, a 1 ml mixture of DMSO and acetone in a 4:1 ratio (this translates to 11.3:2.7 mmol ratio) is used.[25,27] For simplicity sake, we will use as the input structure, a single molecule of each solvent in a three molecular complex (3-MC) of proline **1a**, acetone **2** and the DMSO molecule **3** (**AD-1a**) (Table 5.4).

Table 5.4. Ball and stick representation of three molecular complexes (3-MCs) of proline (**1**) and solvent molecules of acetone (**2**) and DMSO (**3**) along the change from **1a** to **1b**.

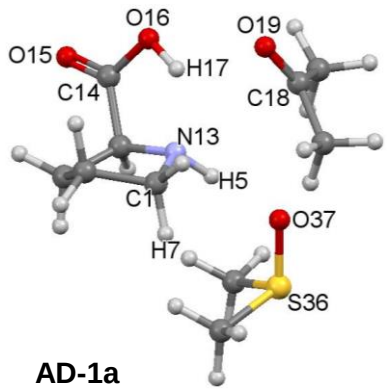 **AD-1a**	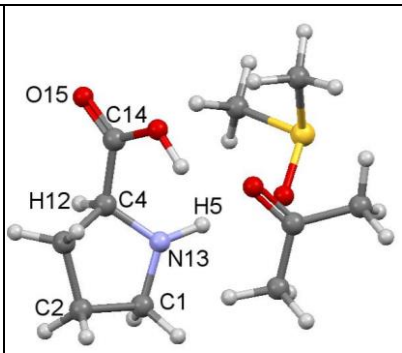 **AD-1**	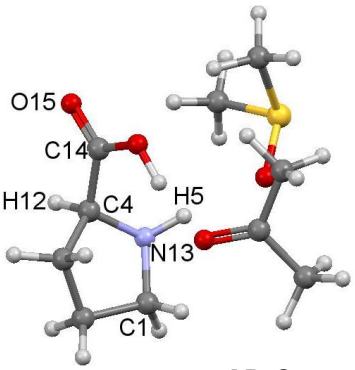 **AD-2**
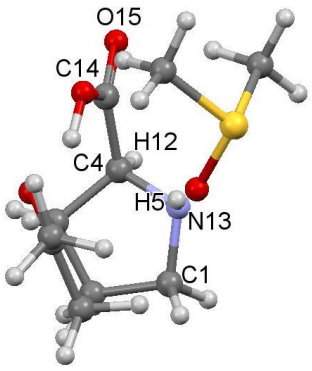 **AD-3**	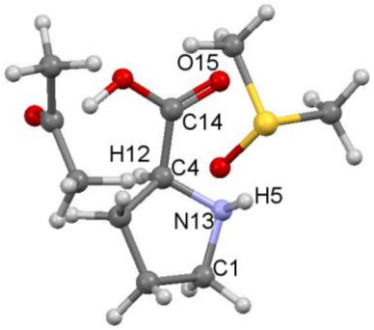 **AD-4**	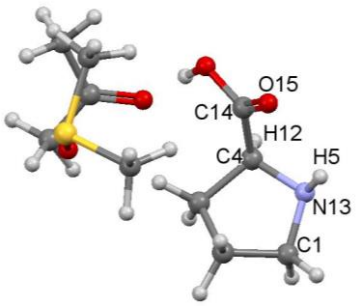 **AD-5**
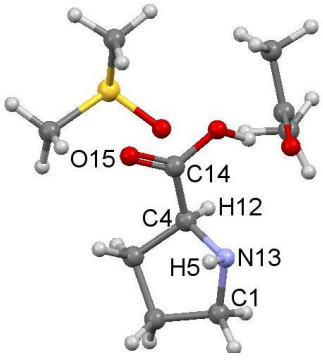 **AD-1b**		

The DA(H12,C4,N13,H5) which was selected in the implicit solvent model and in the presence of solvent molecules of acetone and DMSO was also selected in complex **AD-1a** and scanned in steps of +6° as in previous cases. The resulting data shows complex **AD-1** which is analogous to **A-1** and **D-1** obtained in the presence of solvent molecules of acetone and DMSO, respectively. Notably, in **AD-1** there is evidence of rotation of the carboxylic moiety along the C4–C14 single bond, the DA(H12,C4,C14,O15) changed by –37.7° from 57.3° in **AD-1a** to 19.6° in **AD**-1. The rotation of the carboxylic moiety about the C4–C14 single bond was also observed in structures **A-1** and **D-1** wherein the DA(H12,C4,C14,O15) decreased by –30.6° and –36.5°, respectively. There was also notable evidence of turning of the proton (H5) in complexes **AD-1**, **A-1** and **D-1** to the *syn* orientation relative to the carboxylic moiety. When the DA(H12,C4,N13,H5) was increased further, complex **AD-2** was formed, and the calculation was terminated. Complex **AD-2** was energy-optimised and submitted for DA(H12,C4,C14,O15) scan, this resulted in complex **AD-3**, a further scan of DA resulted in a termination of the calculation. After energy optimisation, complex **AD-3** was further submitted for DA(H12,C4,C14,O15) scan and the resulting data shows the rotation of the carboxylic moiety and formation of complex **AD-1b** (see Table 5.4 and Figure C4 in Appendix C). To compare the effects of acetone, DMSO and a combination of the two solvent molecules on the change from **1a** to **1b**, the zero-point vibrational energy corrected electronic energy (E_{ZPVE}) and Gibbs free energy (G) were plotted for the three solvent systems (Figure 5.9).

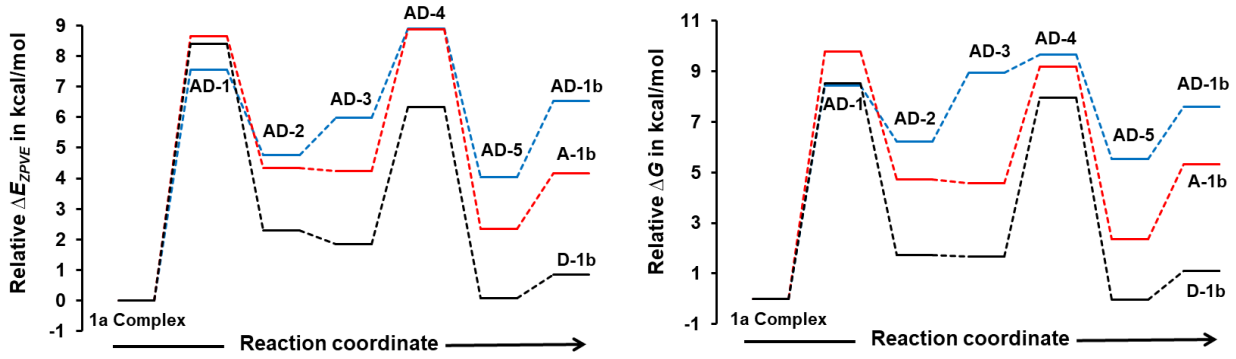

Figure 5.9. Variation in zero-point vibrational energy corrected electronic energy (E_{ZPVE}) and Gibbs free energy (G), along the transformation of proline from conformer **1a** to conformer **1b** in the presence of explicit solvent molecules of: (1) acetone (trend in red), (2) DMSO (trend in black) and (3) a combination of acetone and DMSO (trend in blue), only labels of structures in a mixture of acetone and DMSO (**AD**) are shown.

The trends in Figure 5.9 show that the transformation of **1a** to **1b** is energetically preferable in the presence of a solvent molecule of DMSO and the resulting active conformer (**1b**) is more stabilised in DMSO. The presence of a combination of solvent molecules of acetone and DMSO (**AD**) increases both the free energy G and E_{ZPVE} of the resulting complex (**AD-1b**). The general trend shows two energy maxima, the first one is at (**A-1**, **D-1** and **AD-1**) which can be seen as the

energy barrier for the puckering of pyrrolidine ring resulting in the re-orientation of H5 to the *syn* orientation. The other maximum at (**A-4**, **D-4** and **AD-4**) corresponds to the barrier for the rotation of the carboxylic moiety about the C4–C14 single bond which results in the eventual formation of **1b**.

To get further insights into the roles played by individual solvent molecules in a mixture of acetone and DMSO (**AD**), we calculated the interaction energies of the molecular system $E_{\text{int}}^{\text{MS}}$ for all the 3-MCs from **AD-1a** to **AD-1b**. The interaction energy term $E_{\text{int}}^{\text{MS}}$ is the sum intramolecular interaction ${}_{\text{intra}}E_{\text{int}}^{\text{MS}}$ (sum all covalent bonds and non-covalent bonding interactions), and all intermolecular interaction energies between molecules constituting the MS ${}_{\text{inter}}E_{\text{int}}^{\text{MS}}$, i.e., $E_{\text{int}}^{\text{MS}} = {}_{\text{intra}}E_{\text{int}}^{\text{MS}} + {}_{\text{inter}}E_{\text{int}}^{\text{MS}}$.

Intra and intermolecular interaction energies computed for separate molecules in 3-MCs of proline, acetone and DMSO.

Upon moving from **AD-1a** to **AD-1b** both total interaction energy $E_{\text{int}}^{\text{MS}}$ and total intramolecular interaction energy ${}_{\text{intra}}E_{\text{int}}^{\text{MS}}$ for molecular system weakened, while the latter energy term weakened by a larger magnitude than the former (Figure 5.10a). Markedly, the $E_{\text{int}}^{\text{MS}}$ and ${}_{\text{intra}}E_{\text{int}}^{\text{MS}}$ energy terms changed by +24.8 kcal/mol and +64.2 kcal/mol, respectively. The difference between the two energy terms ($E_{\text{int}}^{\text{MS}} - {}_{\text{intra}}E_{\text{int}}^{\text{MS}}$) is –39.4 kcal/mol and is contribution to $E_{\text{int}}^{\text{MS}}$ due to intermolecular interaction. Thus the ${}_{\text{inter}}E_{\text{int}}^{\text{MS}}$ energy term strengthened on moving from **AD-1a** to **AD-1b**.

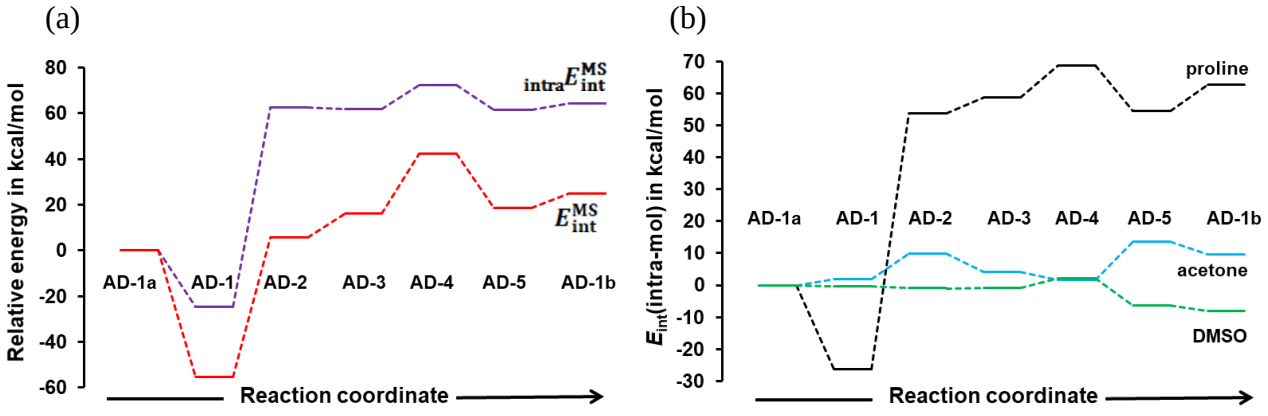

Figure 5.10. Variation in: (a) (1) total interaction energies, $E_{\text{int}}^{\text{MS}}$, (trend in red), (2) total intramolecular interaction energy for molecular system, ${}_{\text{intra}}E_{\text{int}}^{\text{MS}}$ (trend in purple) and (b) (3) total intramolecular interaction energies for individual molecules constituting the MS, proline **1** (trend in black), acetone **2** (trend in blue) and DMSO **3** (trend in green).

To understand in detail the different roles played by the solvent molecules of acetone **2** and DMSO **3**, we decomposed the intramolecular interactions energy term $_{\text{intra}}E_{\text{int}}^{\text{MS}}$ into contributions made by individual molecules constituting the MS, i.e., proline **1**, acetone **2**, and DMSO **3**, (Figure 5.10b). This allows us to uncover which molecule among the three molecules, contributed the most to $_{\text{intra}}E_{\text{int}}^{\text{MS}}$. As one would have expected the $_{\text{intra}}E_{\text{int}}^{\text{mol}}$ term weakened the most in proline **1**, because it is undergoing a structural change (from the most preferred or global minimum **1a** to a local minimum structure **1b**). The $_{\text{intra}}E_{\text{int}}^{\text{mol}}$ term weakened in acetone **2** and strengthened in DMSO **3**.

Notably, on the formation of **AD-1b**, the changes in $_{\text{intra}}E_{\text{int}}^{\text{mol}}$ for proline **1**, acetone **2** and DMSO **3** are +62.6 kcal/mol, +9.7 kcal/mol, and –8.1 kcal/mol, respectively. This clearly shows that the two explicit solvent molecules of acetone and DMSO play different roles during the structural change from **1a** to **1b**. The weakening of the $_{\text{intra}}E_{\text{int}}^{\text{mol}}$ energy term occurs when molecules are involved in strong intermolecular interactions. Therefore, from Figure 5.10b, one can infer that among the three molecules, intermolecular interaction energy involving the molecule of proline **1** is the strongest. Similarly, intermolecular interactions involving the molecule of acetone **2** are expected to be stronger than those involving the molecule of DMSO **3**. This will be subject to further study in the next section. In the interim, to get a detailed understanding of the roles played by the two solvent molecules, it is important to decompose the intramolecular interaction energy $_{\text{intra}}E_{\text{int}}^{\text{mol}}$ into its components, i.e., covalent bonds $^{\text{C-B}}E_{\text{int}}^{\text{mol}}$ and non-covalent or long-distance interactions $^{\text{L-D}}E_{\text{int}}^{\text{mol}}$ (Figure 5.11).

Variation in covalent bonding and long-distance interaction energies in 3-MCs

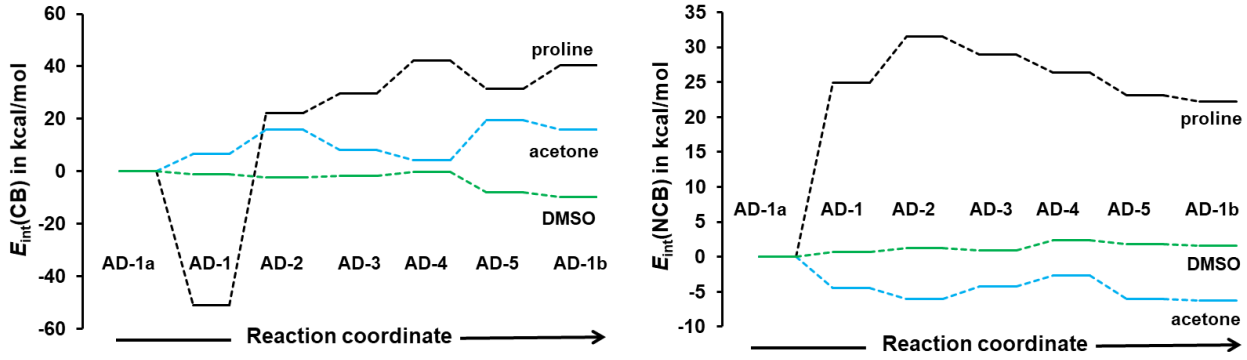

Figure 5.11. Variation in covalent and non-covalent interaction energies of the individual molecules of proline **1**, acetone **2** and DMSO **3**, constituting the indicated 3-MC along the change from **1a** to **1b**.

On moving from **AD-1a** to **AD-1b**, the trends in Figure 5.11 reveal the following:

(1) Both covalent and non-covalent interaction weakened significantly in proline **1**, the ${}^{\text{C-B}}_{\text{intra}}E^{1}_{\text{int}}$ and ${}^{\text{L-D}}_{\text{intra}}E^{1}_{\text{int}}$ energy terms became weaker by +40.4 kcal/mol, and +22.2 kcal/mol, respectively.

(2) In acetone **2**, covalent bonds weakened while long-distance interaction energies strengthened marginally, the ${}^{\text{C-B}}_{\text{intra}}E^{2}_{\text{int}}$ and ${}^{\text{L-D}}_{\text{intra}}E^{2}_{\text{int}}$ energy terms are +16.0 kcal/mol, and –6.3 kcal/mol, respectively.

(3) In the molecule of DMSO, covalent bonds strengthened while long distance interactions marginally weakened, the ${}^{\text{C-B}}_{\text{intra}}E^{3}_{\text{int}}$ and ${}^{\text{L-D}}_{\text{intra}}E^{3}_{\text{int}}$ energy terms are –9.7 kcal/mol, and +1.6 kcal/mol, respectively.

Clearly, one can predict that in a mixture of acetone and DMSO solvent system, acetone forms stronger interaction with proline and therefore plays a major role during the structural change of proline and also in the bimolecular reaction with the resulting proline conformer **1b**. This is mainly because intramolecular interactions barely change in DMSO across individual 3-MCs which predict weaker intermolecular interaction with the other two molecules. On the other hand, a major role is expected from acetone since its covalent bonds became weaker which usually occurs when molecules are involved in stronger intermolecular interactions. In the following section we calculated the variation in intermolecular interactions energies between unique molecular pairs across individual complexes along the structural change from **1a** to **1b**.

Variation in intermolecular interaction energies in 3-MCs

Considering a change from **AD-1a** to **AD-1b**, the intermolecular interaction energy for molecular system ${}_{\text{inter}}E^{\text{MS}}_{\text{int}}$ strengthened by –39.4 kcal/mol. The interaction energy between a single molecule and the remaining two molecules provides information of the contribution to intermolecular interaction energy from individual molecules. Hence, the ${}_{\text{inter}}E^{\mathbf{1,(2,3)}}_{\text{int}}$ = ${}_{\text{inter}}E^{\mathbf{(1,2)}}_{\text{int}}$ + ${}_{\text{inter}}E^{\mathbf{(1,3)}}_{\text{int}}$ term was calculated for the structural change from **1a** to **1b**. Notably the ${}_{\text{inter}}E^{\mathbf{1,(2,3)}}_{\text{int}}$ term strengthened by –38.1 kcal/mol, while the ${}_{\text{inter}}E^{\mathbf{2,(1,3)}}_{\text{int}}$ term calculated for acetone **2** also strengthened by –29.3 kcal/mol (Figure 5.12). Surprisingly for DMSO, the ${}_{\text{inter}}E^{\mathbf{3,(1,2)}}_{\text{int}}$ term strengthened marginally by –11.3 kcal/mol, which is more than two times weaker when compared to acetone. This indicates that in the presence of acetone, the solvent molecule of DMSO becomes less involved in interaction and also in the subsequent reaction (C–N bond formation/H transfer).

Inter-fragment interaction energy between a unique fragment and remaining two other fragments provide further insights into the interaction energies at atomic level.

(a) (b)

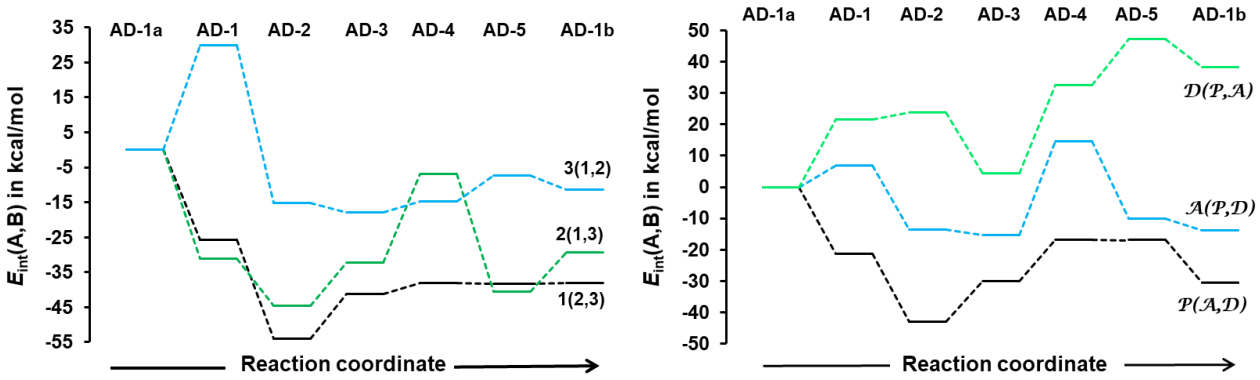

Figure 5.12. Variation in: (a) interaction energy between a single molecule and the remaining two molecules, i.e., ${}_{\text{inter}}E_{\text{int}}^{\mathbf{1,(2,3)}}$, ${}_{\text{inter}}E_{\text{int}}^{\mathbf{2,(1,3)}}$, and ${}_{\text{inter}}E_{\text{int}}^{\mathbf{3,(1,2)}}$ energy terms, respectively, and (b) interaction between an atomic fragment and the remaining two atomic fragments.

On moving from **AD-1a** to **AD-1b** the interaction energy between the $\mathcal{D}$ fragment and the $\mathcal{P}$ and $\mathcal{A}$ fragments of proline and acetone weakened, i.e., the ${}_{\text{inter}}E_{\text{int}}^{\mathbf{D,(P,A)}}$ term is +38.1 kcal/mol, while the ${}_{\text{inter}}E_{\text{int}}^{\mathbf{A,(P,D)}}$ and ${}_{\text{inter}}E_{\text{int}}^{\mathbf{P,(A,D)}}$ terms strengthened by –13.7 kcal/mol and –30.5 kcal/mol respectively. This indicates that when only main players are considered, the molecule of DMSO **3** is involved in repulsive interaction with the remaining main player of proline **1** and acetone **2**. Although complex **AD-1b** is not pre-organised for the subsequent bond formation/breaking, the current results provide a clear picture why acetone rather than DMSO will eventually reacts with proline to form the active enamine catalyst.

Intermolecular interactions between each unique molecular pair provide further insights into the mechanism of the conformational change and the subsequent reaction between proline **1** and acetone **2** as well as roles played by individual solvent molecules (Figure 5.13). Relative to the input 3-MC (**AD-1a**), the trend for change in intermolecular interaction energy between the molecules of proline **1** and acetone **2**, i.e., the ${}_{\text{inter}}E_{\text{int}}^{\mathbf{(1,2)}}$ term strengthened the most in **AD-1b** by –28.1 kcal/mol. On the other hand, the ${}_{\text{inter}}E_{\text{int}}^{\mathbf{(1,3)}}$ term, strengthened by a smaller magnitude (–10.0 kcal/mol) while ${}_{\text{inter}}E_{\text{int}}^{\mathbf{(2,3)}}$ term barely change across all 3-MCs, it strengthened marginally in **AD-1b** by –1.3 kcal/mol (Figure 5.13).

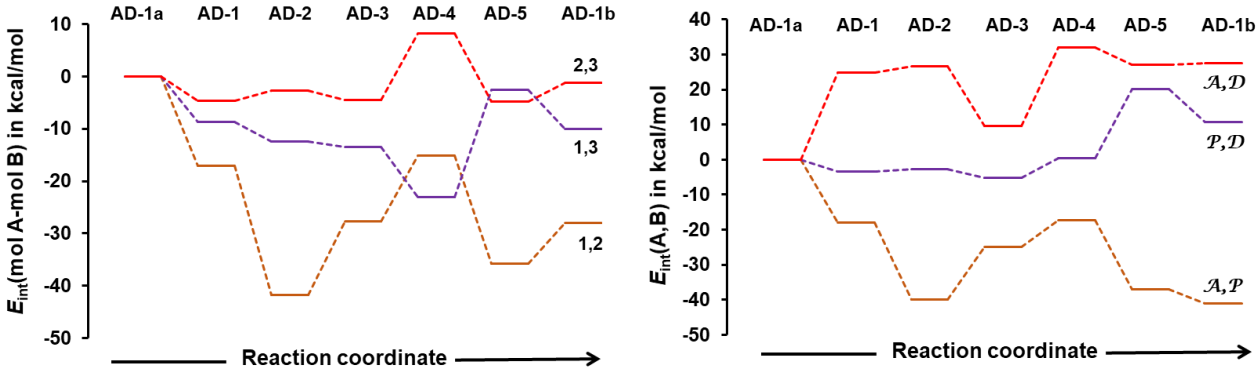

Figure 5.13. Variation in intermolecular interaction energy between unique molecular pairs of proline **1** and acetone **2** (trend in orange), proline **1** and DMSO **3** (trend in purple) and acetone **2** and DMSO **3** (trend in red) and the indicated associated atomic fragments.

Inter-fragment interaction energy between two unique pairs of fragments show that on the formation of **AD-1b**, interaction energy between fragments {$\mathcal{A}$ and $\mathcal{D}$} and {$\mathcal{P}$ and $\mathcal{D}$} weakened, i.e., the ${}_{\text{inter}}E_{\text{int}}^{(\mathbf{A,D})}$ and ${}_{\text{inter}}E_{\text{int}}^{(\mathbf{P,D})}$ terms are +27.5 kcal/mol, and +10.7 kcal/mol, respectively. On the other hand, interaction energy between the $\mathcal{A}$ and $\mathcal{P}$ fragments strengthened by – 41.2 kcal/mol. This predicts that a reaction between proline **1b** and acetone **2** is more likely while a reaction between proline **1b** and DMSO is totally impossible. One can also get additional insights by comparing the interaction energies between key atoms in proline ($\mathcal{P}$ fragment) and key atoms in both acetone and DMSO molecule $\mathcal{A}$ (C18,O19) and $\mathcal{D}$ (S36,O37) fragments, respectively.

In proline, atoms N13 and H17 will be considered while the $\mathcal{A}$ fragment of acetone, i.e., atoms C18 and O19, are of interest since they are directly involved in bond formation in the first step of the mechanism. In the molecule of DMSO, atoms S36 and O37 which are analogous to C18 and O19 will be considered in the analysis. By calculating interaction energies between atoms N13 and H17 in proline **1** and the atomic fragments $\mathcal{A}$ and $\mathcal{D}$ of acetone and DMSO that are expected to be involved in the subsequent bond formation one can establish which molecule will eventually react with proline **1b** (Figure 5.14). Data in Figure 5.14 shows that there is no affinity at all between N13 and the atomic fragments $\mathcal{A}$ and $\mathcal{D}$ of acetone **2** and DMSO **3**, respectively. This correlates well with the finding in chapters 3 and 4 which shows that the C–N bond formation/1st H transfer is not driven by interaction involving N13 but rather H17. Interaction energy between N13 of proline and C18, and S36 of acetone and DMSO is marginally stronger for proline, i.e., the $E_{\text{int}}^{\text{N13,C18}}$ term is stronger that the $E_{\text{int}}^{\text{N13,S36}}$ term by –3.7 kcal/mol.

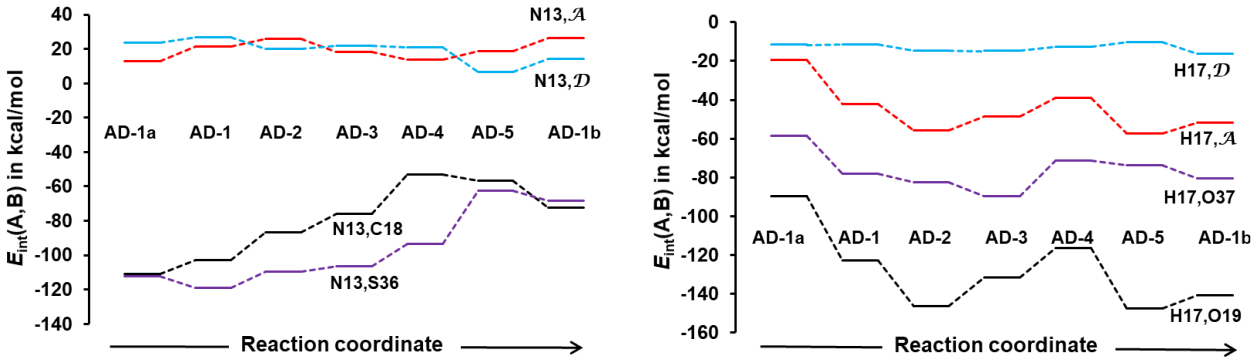

Figure 5.14. Interaction energies of atoms N13 and H17 of proline **1** with atoms C18 and O19 of **2** and and O37 of **3** and the atomic fragments $\mathcal{A}$ and $\mathcal{D}$, respectively.

The interaction energy between H17 and the $\mathcal{D}$ fragment, i.e., the $E_{\text{int}}^{\text{H17, D}}$ term barely change on moving from **AD-1a** to **AD-1b**, while the $E_{\text{int}}^{\text{H17, A}}$ term strengthened by –32.6 kcal/mol. Interaction energy between H17 and atoms O19 and O37 of acetone **2** and DMSO **3** strengthened on the formation of **AD-1b**. However, the $E_{\text{int}}^{\text{H17,O19}}$ term is stronger than the $E_{\text{int}}^{\text{H17,O37}}$ term by –60.5 kcal/mol. Thus, the molecule of proline is expected to react with acetone rather than with the molecule of DMSO due to the stronger interaction energies between key atom pairs and atomic fragments among other reasons.

5.2 Conclusions

In neutral form, proline exists as two main conformers in a chemical equilibrium, i.e., the most dominant conformer **1a**, and the catalytically active **1b**. The most dominant conformer is inactive, and its reaction path is cut off as the reaction progresses. The solution population of the active higher energy conformer **1b** is replenished by the conversion of **1a** into **1b** through the puckering of the pyrrolidine ring from endo to exo ring conformation. The structural change can be considered as a fast reaction due to its small energy barrier of 11 kcal/mol in the implicit solvation model. The presence of the ketone donor (acetone) facilitates the structural change through the formation of strong intermolecular interaction which stabilises covalent bonds of key intermediates along the conformational change. Due to the presence of a molecule of acetone **2**, the energy barrier for the structural change from **1a** to **1b** is reduced with respect to both E_{ZPVE} and G by 2.2 kcal/mol and 1 kcal/mol, respectively. In the presence of an explicit solvent molecule of DMSO, the structural change of proline from **1a** to **1b** is further enhanced. Compared to the implicit solvation model, the energy barrier decreases by 2.5 kcal/mol and 2.1 kcal/mol with respect to E_{ZPVE} and G, respectively. In addition, the solvent molecule of DMSO stabilizes the resulting HEC **1b** by –6

kcal/mol and – 5 kcal/mol, with respect to E_{ZPVE} and G, respectively. In the presence of explicit solvent molecules of acetone and DMSO in 3-MCs, it is acetone that plays a more leading role than DMSO by forming stronger intermolecular interaction with proline. While the energy barrier for the structural change is decreased by 2.2 kcal/mol (E_{ZPVE}) and 1 kcal/mol, (G) respectively. This shows that whether proline is first added to acetone, DMSO or a mixture of the two solvent the structural change from **1a** to **1b** will still occur and the order of addition is not necessary. The current result provides important insights into the nature of any organocatalytic reactions in proline which proceeds by formation of iminium or enamine intermediates. The LEC is transformed into the active HEC through the facilitation of either the solvent (DMSO), the ketone donor used, or both.

5.3 References

1. J. Aleman and S. Cabrera, *Chem. Soc. Rev.*, 2013, **42**, 774-793.
2. V. D. G. Oliveira, M. F. D. C. Cardoso and L. D. S. M. Forezi, *Catal.*, 2018, **8**, 605.
3. M. J. Gaunt, C. C. C. Johansson, A. McNally and N. T. Vo, *Drug Discov., Today.*, 2007, **12**, 8-27.
4. D. W. C. MacMillan, *Nat.*, 2008, **455**, 304.
5. S. Mukherjee, J. W. Yang, S. Hoffmann and B. List, *Chem. Rev.*, 2007, **107**, 5471-5569.
6. Y. Yamashita, T. Yasukawa, W.J. Yoo, T. Kitanosono and S. Kobayashi, *Chem. Soc Rev.*, 2018, **47**, 4388-4480.
7. F. Gallier, A. Martel and G. Dujardin, *Angew. Chem. Int. Ed.*, 2017, **56**, 12424-12458.
8. B. List, P. Pojarliev, W. T. Biller and H. J. Martin, *J. Am. Chem. Soc.*, 2002, **124**, 827-833.
9. P. H.-Y. Cheong and K. N. Houk, *J. Am. Chem. Soc.*, 2004, **126**, 13912-13913.
10. D. Balcells and F. Maseras, *New J. Chem.*, 2007, **31**, 333-343.
11. P. H.-Y. Cheong, C. Y. Legault, J. M. Um, N. Çelebi-Ölçüm and K. Houk, *Chem. Rev.*, 2011, **111**, 5042-5137.
12. M. B. Schmid, K. Zeitler and R. M. Gschwind, *Angew. Chem. Int. Ed.*, 2010, **49**, 4997-5003.
13. M. B. Schmid, K. Zeitler and R. M. Gschwind, *The J. Org. Chem.*, 2011, **76**, 3005-3015.
14. M. B. Schmid, K. Zeitler and R. M. Gschwind, *Chem. Scie.*, 2011, **2**, 1793-1803.
15. L. Hoang, S. Bahmanyar, K. Houk and B. List, *J. Am. Chem. Soc.*, 2003, **125**, 16-17.
16. A. F. L. O. M. Santos, R. Notario and M. A. V. Ribeiro da Silva, *J. Phys. Chem., B*, 2014, **118**, 10130-10141.
17. R. E. London, *J. Am. Chem. Soc.*, 1978, **100**, 2678-2685.
18. C. Allemann, J. M. Um and K. Houk, *J. Mol. Catal., A: Chem.*, 2010, **324**, 31-38.
19. A. M. P. Koskinen, J. Helaja, E. T. T. Kumpulainen, J. Koivisto, H. Mansikkamäki and K. Rissanen, *J. Org. Chem.*, 2005, **70**, 6447-6453.
20. M. J. Ajitha and C. H. Suresh, *J Mol. Catal. A: Chem.*, 2011, **345**, 37-43.
21. I. Cukrowski, G. Dhimba and D. L. Riley, *Phys. Chem. Cheml. Phys.*, 2019, **21**, 16694-16705.
22. F. R. Clemente and K. Houk, *Angew. Chem.*, 2004, **116**, 5890-5892.
23. Q. Chang, J. Zhou and L. H. Gan, *J. Phys. Org. Chem.*, 2012, **25**, 667-673.
24. K. N. Rankin, J. W. Gauld and R. J. Boyd, *J. Phys. Chem. A*, 2002, **106**, 5155-5159.
25. K. Sakthivel, W. Notz, T. Bui and C. F. Barbas, *J. Am. Chem. Soc.*, 2001, **123**, 5260-5267.

26. W. Notz and B. List, *J Am. Chem. Soc.*, 2000, **122**, 7386-7387.
27. B. List, R. A. Lerner and C. F. Barbas, *J. Am. Chem. Soc.*, 2000, **122**, 2395-2396.

Chapter 6

Origin of the relative stability of proline zwitterion complexes with DMSO and water and its reaction energy profile in proline catalysed aldol reactions.

Abstract

We present the origin of the relative stability of proline zwitterion **1c** with respect to the lowest energy non-ionic conformer **1a** using an implicit solvation model and a hybrid of implicit and explicit solvent models. The computed energies show that in the implicit solvation model, the zwitterion is marginally lower in energy than the non-ionic form; the relative stability of the zwitterion originates from its covalent bonds which are stronger than those of the non-ionic conformer. The addition of one, two and three discrete molecules of water increased the intermolecular interaction energy in the zwitterion by –17.0 kcal/mol, –22.8 kcal/mol, and –37.4 kcal/mol, respectively. Furthermore, the molecules of water are in a better chemical environment when they form molecular complexes (MCs) with the zwitterion as their total intramolecular interactions energy (sum of covalent bonding and long-distance interactions) are stronger than when they are in the non-ionic conformer. Relative to MCs of water and the non-ionic conformer **1a**, total intramolecular interaction energies are stronger for water molecules in **1c** MCs by –4.0 kcal/mol, –7.4 kcal/mol, and –11.9 kcal/mol, respectively. The zwitterion is also more stabilised in the presence of an explicit solvent molecule of DMSO. Total intermolecular interactions are stronger between the zwitterion and DMSO by –19.1 kcal/mol. Although the zwitterion becomes more stabilised in DMSO and in the presence of moisture, its reaction pathway is not feasible. It forms very weak intermolecular interaction with acetone the ketone coupling partner resulting in a very high activation energy. Moreover, its reaction profile for the first step of the mechanism becomes identical to that of the lower energy conformer **1a** which is cut-off before the formation of the active enamine catalyst, hence it is not the active catalyst in proline catalysis.

.

6.1. Introduction

The proline catalysed aldol reaction was reported to proceed facially under the solvent dimethyl sulfoxide (DMSO) upon its rejuvenation in the early 2000s.[1] Owing to the hydroscopic nature of DMSO,[2] it can be imagined that the reaction is essentially conducted under "wet" conditions. Under these conditions, proline and most amino acids exist predominantly as zwitterions,[3–6] while the non-ionic form (non-zwitterion) exists in traces. The zwitterion is formed from the non-ionic conformer following protonation of its basic nitrogen atom. However, in the gas phase, theoretical calculations have revealed that amino acids exist mainly in non-ionic form, while the zwitterion does not exist entirely.[5,7,8] For this reason, studies on zwitterion stabilisation of amino acids relative to non-ionic forms are conducted in the gas phase in which several solvent molecules (often water) are required to render it stable.[9] For proline, and in the gas phase, the zwitterion (**1c**) was reported to be marginally lower in energy than the non-ionic conformer (**1a**) by 0.6 kcal/mol at B3LYP/6-31G** (Figure 6.1). However, when a DMSO implicit solvation model was used ($\varepsilon = 46.7$), the zwitterion becomes lower in energy by 2.6 kcal/mol.[10] In our preliminary studies, we found the zwitterion **1c** to be non-existent in the gas phase at room temperature as it was converted to the non-ionic conformer **1a** during energy minimisation.

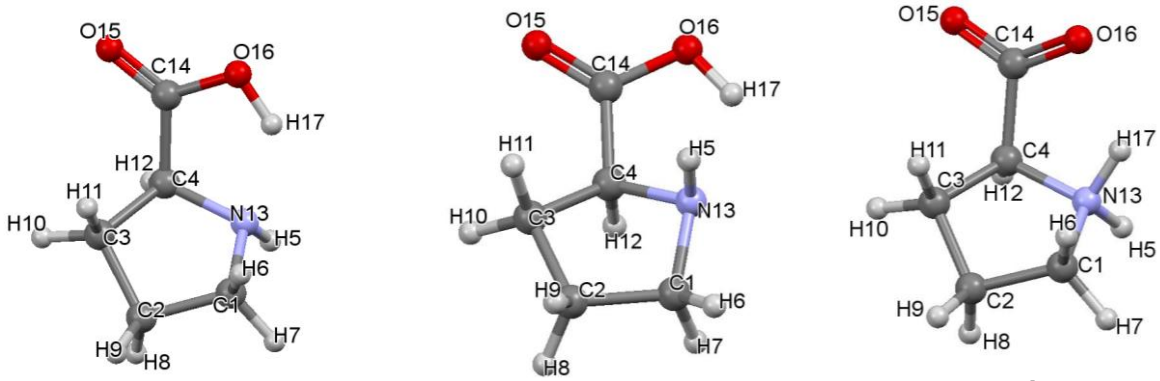

Figure 6.1. Ball and stick representation of *S*-proline conformers, i.e., the lower **1a**, higher **1b** energy conformers and the zwitterion **1c.**

The effects of water molecules on the general stability of the zwitterionic form of amino acids relative to their non-ionic conformers has been studied extensively.[9,11–13] Interest in such studies is triggered by the influence of solvation on the physicochemical properties and general reactivity of biomolecules which is altered significantly by interaction with solvent molecules.[8,11,14] While five to seven molecules of water are required to stabilize the zwitterionic form in amino acids having a hydrophobic side chain (glycine, alanine, and valine, etc.), a few water molecules are deemed enough for those with basic side chain (arginine, lysine, and proline, etc.).[8-9,14–16]

The effects of an explicit solvent molecule of DMSO on the stability of the zwitterionic form of proline relative to its non-ionic conformer have been studied.[3] In this regard, one, two and three solvent molecules of DMSO were reported to be enough to render the zwitterion energetically more stable and conformationally more dominant. As a result of this observation, Yang and Zhou suggested that the zwitterion should be considered for mechanistic modelling in proline catalysed aldol reactions.[3,17] The consideration of the zwitterion as a possible conformer that initiates the catalytic reaction appears justifiable because zwitterions are significantly stabilised by interactions with solvent molecules.

Despite the widely available evidence that solvent effect increases the solution population of the zwitterion, most calculations on zwitterion stabilisation were conducted mainly in the gas phase.[3,9,16,18,19] It is known however, that for chemical reactions involving non-volatile reactants at room temperature, reactants will be populated in solution rather than the gas phase. Hence, such studies should be conducted using at least an implicit solvation model. It is therefore worthwhile to study the extent of zwitterion dominance using both an implicit and a hybrid of implicit and explicit solvation models. In addition, there is no fundamental insight into the effect of solvent molecules, of either water or DMSO, on the amino acid molecules. Moreover, there is no information available on the influence of these solvent molecules on the resulting interaction energies with either the zwitterion or the non-ionic conformers. As a result, we aim to provide: (i) the origins of the relative stability of the zwitterion when an implicit solvation model is considered, (ii) the effect of discrete solvent molecules of water and DMSO on the stability established in (i), (iii) the reaction energy profiles when the zwitterion is considered as the catalyst.

There is a single report suggesting that proline zwitterion (**1c**) is the active catalyst in proline catalysis. However, the reported activation energy of (88.8 kJ/mol ≈ 21 kcal/mol) is unusually high when compared to other proposed mechanisms.[20,21] For this reason, we felt that modelling of the catalytic role of the zwitterion warranted a revisit.

6.2. Results and discussion

6.2.1. Origin of the relative stability of the zwitterion.

We have shown in a previous paper that though the lower energy conformer **1a** is more predominant relative to the higher energy conformer **1b**, the latter is the catalytically active species in proline catalysis.[22] We further highlighted in Chapter 5 that the solvent molecules of DMSO and the ketone coupling partner (which is normally used as a co-solvent) drives the conversion of **1a** to **1b**. Although this partially solves the puzzle regarding the catalytic activities of proline conformers, the zwitterion **1c** was recently proposed to be the active conformer owing to its predominance in both DMSO solvent and in the presence of moisture.[17] Due to the importance of understanding the active forms of conformers in rationalising and predicting reaction outcomes we find it pressing to reconsider the catalytic activity of the zwitterion **1c**. We calculated the origin of the relative stability of the zwitterion using an implicit solvation model with DMSO as the solvent ($\varepsilon = 46.7$) at room temperature. An implicit solvation model was chosen rather than the traditional gas phase at low temperature because most proline catalysed organic reactions are conducted at room temperature in which reactants occupies the solution phase rather than the gas phase.

Using an implicit solvation model, we found the zwitterion **1c** to be marginally lower in energy than **1a** with respect to both E_{ZPVE} and G by 0.2 kcal/mol and 0.5 kcal/mol, respectively, while it is significantly lower in energy than **1b** by $\sim$ 7 kcal/mol with respect to both E_{ZPVE} and G. This shows that when an implicit solvation model is considered, the zwitterion will have approximately the same solution population as the lower energy conformer **1a**. Since the relative stability of **1a** with respect to **1b** is known,[20,22] we will only compare the stability of conformers **1a** with respect to **1c**. First, we calculated the variation in intramolecular interaction energies (sum of covalent and non-covalent interactions) in the two conformers. Thereafter, we explored how molecules of water and DMSO affect these interactions and the resulting intermolecular interaction energies of the associated complexes.

Insight from covalent and non-covalent interactions

When a classical approach is used to rationalize the difference in the stability of the zwitterion **1c**, relative to the lower energy conformer **1a** one would likely consider the strength of the interactions (covalent bonding and hydrogen bonding) that are broken and formed during the change from **1a** to **1c**. Since **1c** is lower in energy than **1a**, this approach will likely predict that

the combined interaction energies of N13–H17 (covalent bond) and N13–H17···O16 (hydrogen bonding interaction) in **1c** would be stronger than their equivalents in **1a**, i.e., interaction energy of O16–H17 (covalent bond) and O16–H17···N13 (hydrogen bonding interaction). Using this classical two-atom approach, $E_{\text{int}}^{\text{N13,H17}}$of –258.4 kcal/mol in **1c** and –132.8 kcal/mol in **1a**, and $E_{\text{int}}^{\text{O16,H17}}$ of –111.8 kcal in **1c** and –312.1 kcal/mol in **1a** were calculated. Hence, the combined interaction energies considered are stronger in **1a** by a staggering –74.7 kcal/mol indicating a clear failure of the classical approach when interpreting and predicting chemical processes.

Strikingly, the acidic proton H17 forms stronger covalent bonding interaction with O16 in **1a** than with N13 in **1c**, the $E_{\text{int}}^{\text{O16,H17}}$ term in **1a** is stronger than the $E_{\text{int}}^{\text{N13,H17}}$ term in **1c** by –53.7 kcal/mol. Classically, this is attributed to atomic charges on N13, O16, and H17 – net atomic charges are shown in Table D1 in Appendix D. The charges on H17 are +0.602*e* and +0.472*e* in **1a** and **1c**, respectively, while that of O16 and N13 are –1.137*e* and –0.990*e*, in **1a** and –1.232*e* and –0.944*e* for **1c**, respectively. Thus, the electrostatic or coulombic component of the diatomic interaction of H17 is stronger with O16 in **1a** than with N13 in **1c**, this approach predicts the dominance of the H17–O16 interaction in **1a** over the H17–N13 interaction in the zwitterion **1c**. In simple terms the classical two atom approach predicts conformer **1a** to be predominant over the zwitterion **1c**.

Since the above classical two atom approach fails to account for the relative stability of the zwitterion, it follows that interpretation should be done by studying the entire molecules rather than only two atom pairs. There are 136 distinct atom pairs of which 17 are covalent bonding interaction and 119 are non-covalent interaction. Total covalent bonds (Tables D2-D3 in Appendix D), are stronger in **1c** by $\Delta E_{\text{int}}^{Cov\text{-bonds}}$ = –64.0 kcal/mol, the decomposed components of the covalent bonds namely the $\Delta V_{\text{XC}}^{Cov\text{-bonds}}$ is –0.3 kcal/mol while the $\Delta V_{\text{cl}}^{Cov\text{-bonds}}$ is –63.7 kcal/mol . This shows that the classical term or the electrostatic component contributes nearly entirely towards stabilisation of covalent bonds in **1c**. Quite surprisingly, the computed non-covalent interaction energies ($E_{\text{int}}^{\text{Tot}}$) are weaker in **1c**, by $\Delta E_{\text{int}}^{\text{Tot}}$ = +45.0 kcal/mol, (ΔV_{XC}^{Tot} = + 6.5 kcal/mol and ΔV_{cl}^{Tot} = +38.5 kcal/mol). The net effect of the two energy components is that the total intramolecular interaction (combined covalent bonds and non-covalent interactions) is stronger in the zwitterion **1c** by –18.9 kcal/mol. Thus, the zwitterion is lower in energy than **1a** owing to its relatively stronger covalent bonding interaction.

Insight from interaction between a single atom (A) and the remaining atoms of a molecular system (R), the $E_{\text{int}}^{\text{A},\mathcal{R}}$ ***term.*** This energy term is a measure of the stabilizing (attractiveness) of a given molecular environment towards an atom of interest within a molecule. The $E_{\text{int}}^{\text{A},\mathcal{R}}$ term can be interpreted as a measure of "friendliness" of a molecular environment towards a specific atom, increase in "friendliness" will result in a more negative $E_{\text{int}}^{\text{A},\mathcal{R}}$ term. We observed that all atoms interact attractively with the remaining atoms in R but the more negative the $E_{\text{int}}^{\text{A},\mathcal{R}}$ term, the more stabilizing is the molecular environment R. Hence, one can compare which molecule between **1c** and **1a** has a more stabilizing chemical environment. The difference between the sums of all $E_{\text{int}}^{\text{A},\mathcal{R}}$ terms of atoms in the two molecules will qualitatively show the molecule with an overall stabilizing chemical environment. The $E_{\text{int}}^{\text{A},\mathcal{R}}$ data in Table D4 in Appendix D shows that when a change from **1a** to **1c** is considered 12 out 17 atoms became destabilised, i.e., they are involved in weaker interactions with R. The most destabilizing change was observed in atoms C1, C4, H5, H7,O15, O16, and H17 with $E_{\text{int}}^{\text{A},\mathcal{R}}$ terms of +23.7, +17.3, +16.4, +7.8, +68.4, +60.4 and +62.3 kcal/mol, respectively. On the other hand, two atoms in **1c**, are in a favourable chemical environment, i.e., N13 and C14 with $E_{\text{int}}^{\text{A},\mathcal{R}}$ terms of –132.4 and –177.5 kcal/mol, respectively. This means that the large negative $E_{\text{int}}^{\text{A},\mathcal{R}}$ terms for the two atoms, among other terms is the reason for the observed relative stability of **1c**.

6.2.2. Effect of water molecules on the relative stability of conformers 1a and 1c.

The effect of explicit solvent molecules on the relative stability of the zwitterion **1c** with respect to the non-ionic conformer **1a** can be established by calculating how the solvent molecules alter the barrier for the **1c** to **1a** structural change and the relative stabilities of the resulting complexes. Molecular complexes of the zwitterion **1c** with water molecules (**1w**–**3w**) and with an explicit solvent molecule of DMSO (**1D**) are shown in Table 6.1. The energy barriers for the H17 to O16 proton transfer and the relative energy of the resulting complex of **1a** and the respective solvent molecule/s were then calculated and compared with complexes of the input zwitterion **1c**.

In the implicit solvation model, the energy barrier for the H17→O16 proton transfer from **1c** to **1a** is 1.4 kcal/mol (E_{ZPVE}) and 2.1 kcal/mol (G), respectively (Table D7 in Appendix D). In the presence of a molecule of water (see complexes in Table 1), the energy barrier increased to ∼4 kcal/mol (E_{ZPVE} and G) and **1c** becomes more stabilised than **1a** by 4 kcal/mol (E_{ZPVE}) and 2 kcal/mol (G), respectively. In the presence of two water molecules the energy barrier increases to

~5 kcal/mol with respect to both E_{ZPVE} and G while **1c** became more stabilised by 5 kcal/mol. The presence of three water molecules further increases the energy barrier to 8 kcal/mol (E_{ZPVE}) and 7 kcal/mol (G) respectively, while the zwitterion becomes more stabilised by 8 kcal/mol (E_{ZPVE}) and 7 kcal/mol (G) respectively. Thus, the barrier for H17 to O16 transfer and the relative stability of the zwitterion increases as the number of water molecules increases, thereby making the zwitterion the most predominant conformer when moisture is present. Importantly, these energy barriers must be seen as insignificant and hence do not prevent the formation of **1a** and subsequently **1b** as we have shown in Chapter 5.

Effects of explicit solvent molecule/s of water on intra and intermolecular interactions of complexes of the zwitterion 1c and non-ionic conformer 1a

Initially we investigated how the presence of a single solvent molecule of water changes the variation in intramolecular interactions in **1a** and **1c**. The results indicate that when compared to the implicit solvation model, covalent bonds weakened in both **1a** and **1c** by +7.4 kcal/mol and +10.1 kcal/mol, respectively, while non-covalent interaction marginally weakened in both molecules by +2 kcal/mol. The combined intramolecular interaction $_{\text{intra}}E_{\text{int}}^{\text{mol}}$ which is sum of covalent and long distance interaction are stronger in **1c**. Markedly, the $_{\text{intra}}E_{\text{int}}^{\mathbf{1c}}$ term is stronger than the $_{\text{intra}}E_{\text{int}}^{\mathbf{1a}}$ term by –15.9 kcal/mol while the $_{\text{intra}}E_{\text{int}}^{\mathbf{4}}$ term which is intramolecular interaction in the molecule of water is also stronger in **1c** two-molecular complex (2-MC) by – 4 kcal/mol. Hence total intramolecular interactions are negative in **1c** 2-MC by –20.0 kcal/mol.

Importantly, intermolecular interactions involving the water molecule **4** and **1c** are negative i.e., *the* $_{\text{inter}}E_{\text{int}}^{\mathbf{1c,4}}$ term is negative than the $_{\text{inter}}E_{\text{int}}^{\mathbf{1a,4}}$ term by –17.0 kcal/mol. The major component of this intermolecular interaction energy originates from interactions between atoms forming the proline carboxylic moiety, i.e., atoms of the {C14,O15,O16,H17} group. Interactions between these atoms and the three atoms of the water molecule {O18,H19,H20} contribute –16.6 kcal/mol to $_{\text{inter}}E_{\text{int}}^{\mathbf{1,4}}$, while contribution from the rest of the atoms forming the pyrrolidine ring is negligible, i.e., –0.4 kcal/mol. In the presence of two molecules of water, intramolecular interactions in proline $_{\text{intra}}E_{\text{int}}^{\mathbf{1}}$ are negative in **1c** by –7.1 kcal/mol, while they are also negative in the two water molecules of **1c** 3-MC by –7.4 kcal/mol.

Table 6.1. Ball and stick representation of complexes of the zwitterion **1c**, the lowest energy conformer **1a** and their respective transition state **TS** in the presence of one (**1w**), two (**2w**) and three water molecules (**3w**), and in the presence of a solvent molecule of DMSO (**1D**).

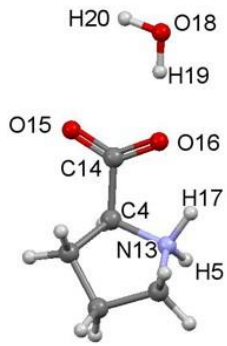 **1c_1w**	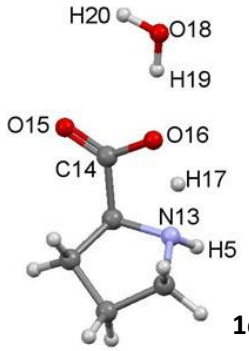 **1c_1w-TS**	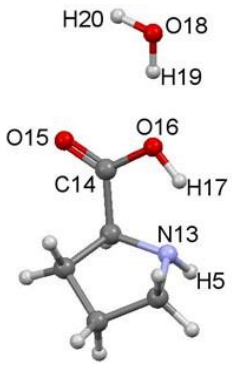 **1a_1w**
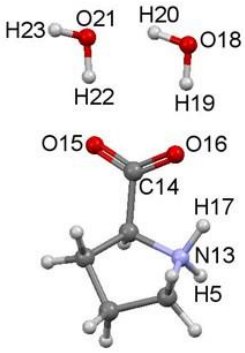 **1c_2w**	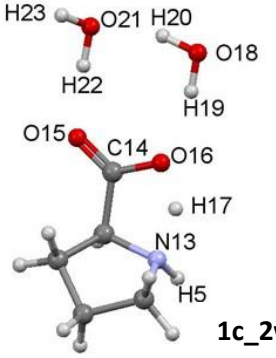 **1c_2w-TS**	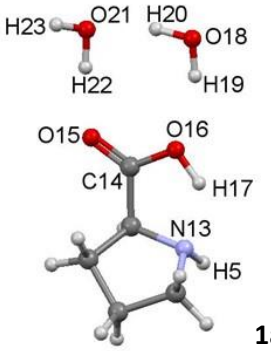 **1a_2w**
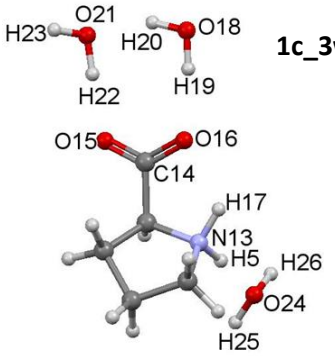 **1c_3w**	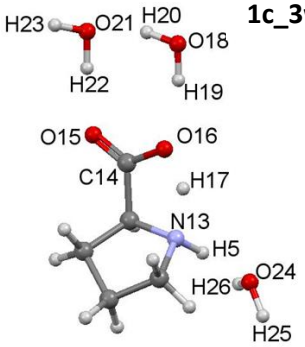 **1c_3w-TS**	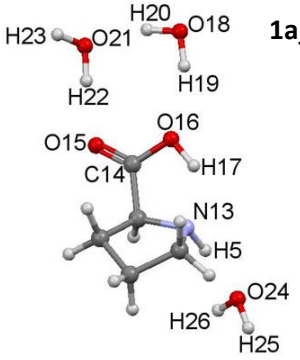 **1a_3w**
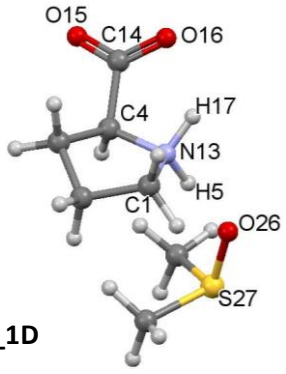 **1c_1D**	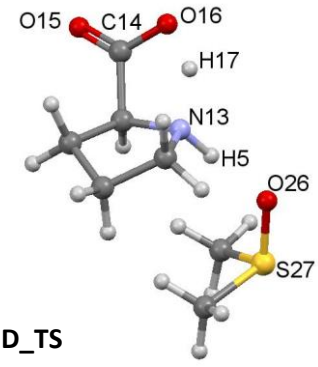 **1D_TS**	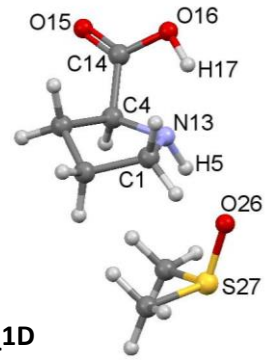 **1a_1D**

Thus, total intramolecular interactions are stronger in **1c** 3-MC by –14.5 kcal/mol. On the other hand, intermolecular interaction between the proline conformers and the two water molecules are stronger in **1c** 3-MC by –22.8 kcal/mol. Interactions between the carboxylic group {C14,O15,O16,H17} and atoms of the two water molecules contribute –22.1 kcal/mol to total intermolecular interactions while interactions between atoms of the pyrrolidine ring and the water molecules contribute only –0.7 kcal/mol. The decomposed components of intermolecular interaction energy reveal that the two molecules of water do not contribute equally to interaction energy. The water molecule forming the O18–H19⋯O16 classical hydrogen bond (see Table 6.1) contributes – 14.9 kcal/mol while the other water molecule contributes –9.3 kcal/mol.

A third molecule of water was added in order to form a four molecular complex 4-MC (Table 6.1). The placement of the three water molecules was chosen such that they could form classical hydrogen bonds with the two carboxyl oxygen atoms (O15 and O16) and H5 of the pyrrolidine ring. By classical thinking the three water molecules were deemed enough to fill the inner solvation shell of the zwitterion through hydrogen bonding interactions. Notably, intramolecular interactions are negative in **1c** 4-MC by –5 kcal/mol, while total intramolecular interactions in the three water molecules are negative in **1c** 4-MC by –11.9 kcal/mol. Hence, the combined intramolecular interactions are negative in **1c** 4-MC by –16.9 kcal/mol. Notably, total intermolecular interactions are negative in **1c** 4-MC by –37.4 kcal/mol. This indicates that the strength of intermolecular interaction energy significantly increases in **1c** molecular complexes as the number of water molecules increases. This result, together with data obtained in the presence of one and two water molecules indicates that the molecules of water are in a better chemical environment when they form complexes with the zwitterion.

6.2.3. Effect of an explicit solvent molecule of DMSO in the relative stability of 1c.

In the presence of one solvent molecule of DMSO the energy barrier for the change from **1c** to **1a** is ~ 5 kcal/mol (E_{ZPVE}) and 6 kcal/mol (G), respectively, while **1c** is more stabilised than **1a** by ~ 5 kcal/mol with respect to both E_{ZPVE} and G. Covalent bonds are stronger in **1c** by –69.8 kcal/mol, while non-covalent interactions became weaker in **1c** by +50.4 kcal/mol. Thus, total intramolecular interactions (combined strength of covalent bonds and non-covalent interactions) are stronger in **1c** by –19.4 kcal/mol. Interestingly, both covalent bonds and non-covalent interactions are weaker in the DMSO solvent molecule itself in **1c** 2-MC by +13.9 kcal/mol and +1.2 kcal/mol, respectively. As a result, the combined strength of intramolecular interactions (in both DMSO and proline conformers) are stronger in **1c** 2-MC by –4.3 kcal/mol. On the other hand, intermolecular interactions are stronger between the molecule of DMSO and **1c** by –19.1 kcal/mol.

Thus, when both inter and intramolecular interactions are combined, the zwitterion 2-MC is more favoured by –23.4 kcal/mol.

Hence, in the presence of molecules of water and DMSO, intra and intermolecular interaction energy are negative in **1c** MCs, this is the origin of the observed higher stability of the zwitterion under "wet" conditions and in DMSO. The trend for intermolecular interactions between **1c** and molecules of water and the solvent molecule of DMSO is below that of **1a** (Figure 6.2) indicating that interaction energies are stronger in the zwitterion **1c**.

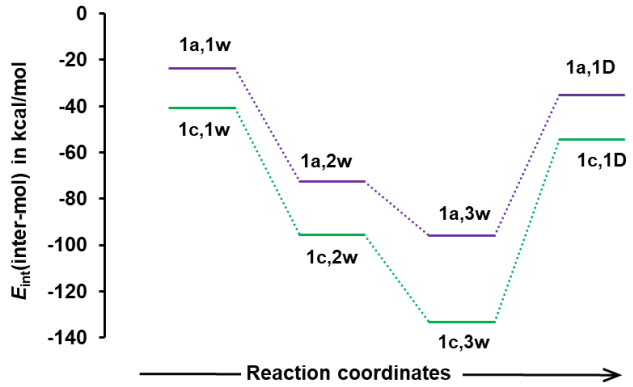

Figure 6.2. Variation in intermolecular interactions between proline complexes, **1a** or **1c** and the indicated number of water molecules and with a solvent molecule of DMSO.

6.2.3. Exploration of the adduct formation between the zwitterion 1c and acetone 2

The dominance of the zwitterion as the principal proline conformer in "wet" solvents and in DMSO prompted us to model its reaction pathway as a possible initiator of the catalytic reaction in proline catalysis. As a result, we explored the formation of adducts between the zwitterion **1c** and acetone **2**, this is usually the practice before modelling of any reaction mechanism. This would allow global minimum energy structures (GMS) and best preorganised structures (pre-org) for the reaction to be determined. However, due to the unlimited number of degrees of freedom, it is practically impossible to exhaust all possible molecular complexes between **1c** and acetone **2**. As a result, we only concentrated in complexes in which O19 of **2** forms hydrogen bonding interaction with either H5 or H17 of **1c** because these protons are very crucial and drive the first few steps of the catalytic reaction.[22]

The input complex, **2c_inp** was hand generated by placing the carbonyl oxygen O19 at an approximately equidistance from the two protons attached to the ring nitrogen (H5 and H17). This allowed the two protons to freely compete for (O19) during energy optimisation. The energy

optimised complex **2c_1** shows a classical intermolecular hydrogen bonding interaction between H5 of **1c** and O19 of **2** while H17 retained its intramolecular hydrogen bond with O16 (Table 6.2).

Table 6.2. Ball and stick representation of molecular complexes between the zwitterion of proline **1c** and acetone **2**.

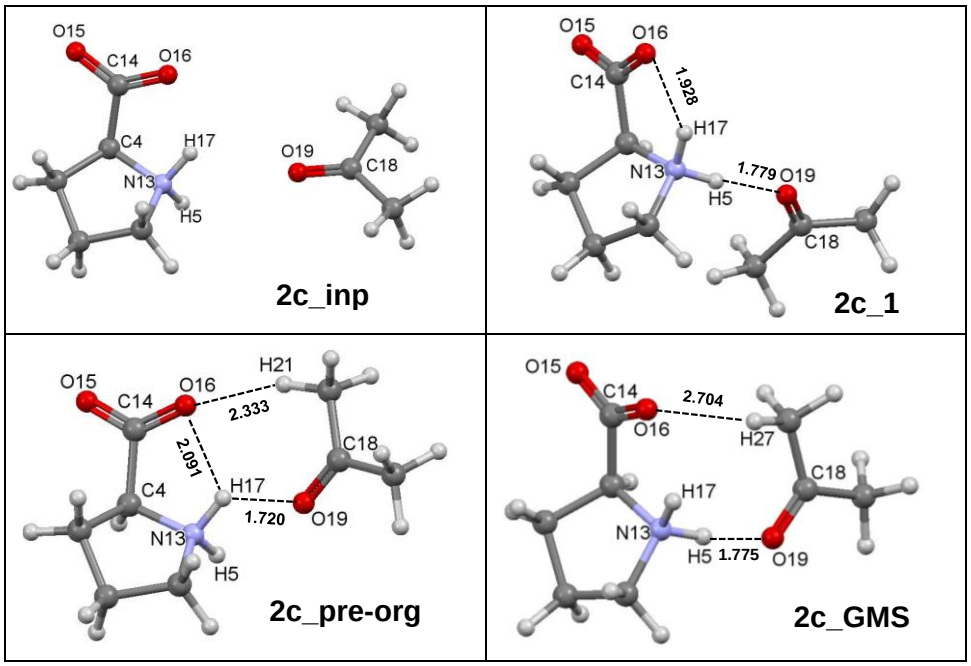

Due to the absence of the prerequisite N13–H17···O19 hydrogen bonding interaction in **2c_1**, which drives the first step of the catalytic reaction between proline and acetone, a second complex was generated by deliberately constructing this crucial hydrogen bond. Importantly, the hand generated N13–H17···O19 intermolecular hydrogen bond was strong enough to be preserved during the energy optimisation process. Notably, the resulting energy optimised complex (**2c_pre-org)** in Table 6.2) is higher in energy than **2c_1** by ~ 3 kcal/mol (E_{ZPVE}) and 2 kcal/mol (G), respectively. In the search for the GMS, DA(N13,C4,C18,C20) in **2c_1** and DA(N13,C4,C18,C24) in **2c_pre-org** were scanned (Figure 6.3) resulting in complex **2c_GMS** which is marginally lower in energy than **2c_1** by less than 0.5 kcal/mol with respect to both E_{ZPVE} and G. The data in Figure 6.3 shows negligible rotational energy which indicates free rotation and possible several other molecular complexes between the two molecules. However, for the purposes of the current study, the obtained three complexes will suffice.

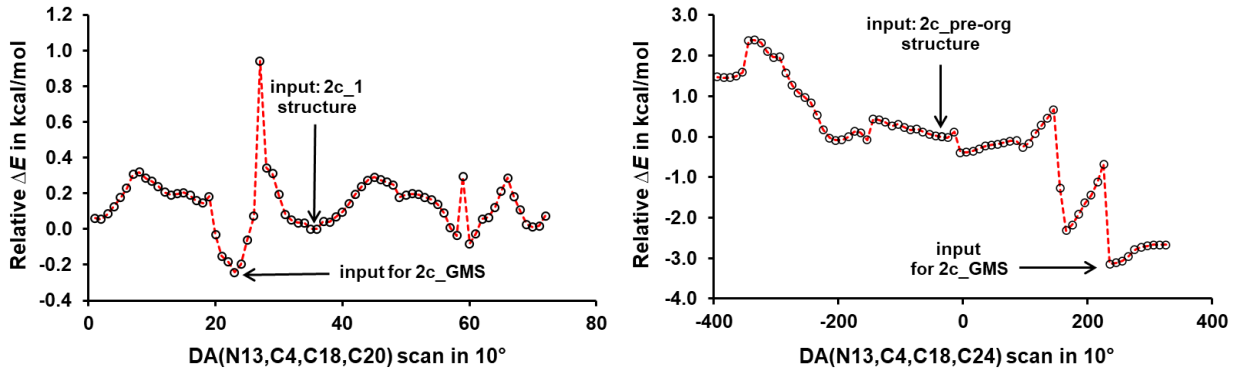

Figure 6.3. Data for scan of DA(N13,C4,C18,C20) and DA(C4,N13,C24,C18) using complexes **2c_1** and **2c_pre-org** of **1c** and **2** in the search of the global minimum structure resulting in GMS **2c_GMS**.

6.2.4. Mechanism through 2-MCs of the zwitterion 1c and acetone 2

Since the difference between the energy optimised complexes (shown in Table 6.2) is marginal, i.e., within 3 kcal/mol, it makes sense to model the three complexes as possible adducts to initiate the catalytic reaction. The data obtained from complexes **2c_1**, and **2c_GMS** is identical, they show an initial proton transfer of H17 to O16 as the d(N13,C18) distance is decreased (see Figure 6.4a). The proton transfer resulted in the conversion of the zwitterion **1c** into canonical conformer **1a**, however, due to the lack of the crucial O16–H17···O19 classical H-bonding interaction (see **2a_1** in Table 6.3) required for bond formation the reaction path could not proceed further. Strikingly, the energy barrier for the H17 to O16 proton transfer is above 32 kcal/mol with respect to both E_{ZPVE} and G. This is too large a barrier given that it only result in the formation of **1a**, (recall that the barrier for **1c** to **1a** structural change is ~ 2 and 4 kcal/mol in implicit and in the presence of one molecule of water, respectively). This clearly indicates that this reaction pathway is forbidden, and the reaction will unlikely progress via this pathway at room temperature.

When the d(N13,C18) reaction coordinate was decreased using complex **2c_pre-org**, (Figure 6.4b), the obtained data shows an initial transfer of H17 to O16 before it is finally transferred to O19 (see ball and stick representation of structures in Table 6.3). The extremely high energy barrier for H17 to O16 proton transfer (~ 40 kcal/mol with respect to both E_{ZPVE} and G) makes this reaction pathway unfeasible. Moreover, the resulting transition state (**2a_ts**) is identical to the transition state obtained from a complex of **1a** and **2** indicating that as acetone **2** approaches the zwitterion **1c**, the latter initially converts into **1a** before bonds are formed/broken.

Table 6.3. Ball and stick representation of intermediate structures along the d(N13,C18) reaction coordinate scan using complexes **2c_Pre-org** and **2c_GMS**.

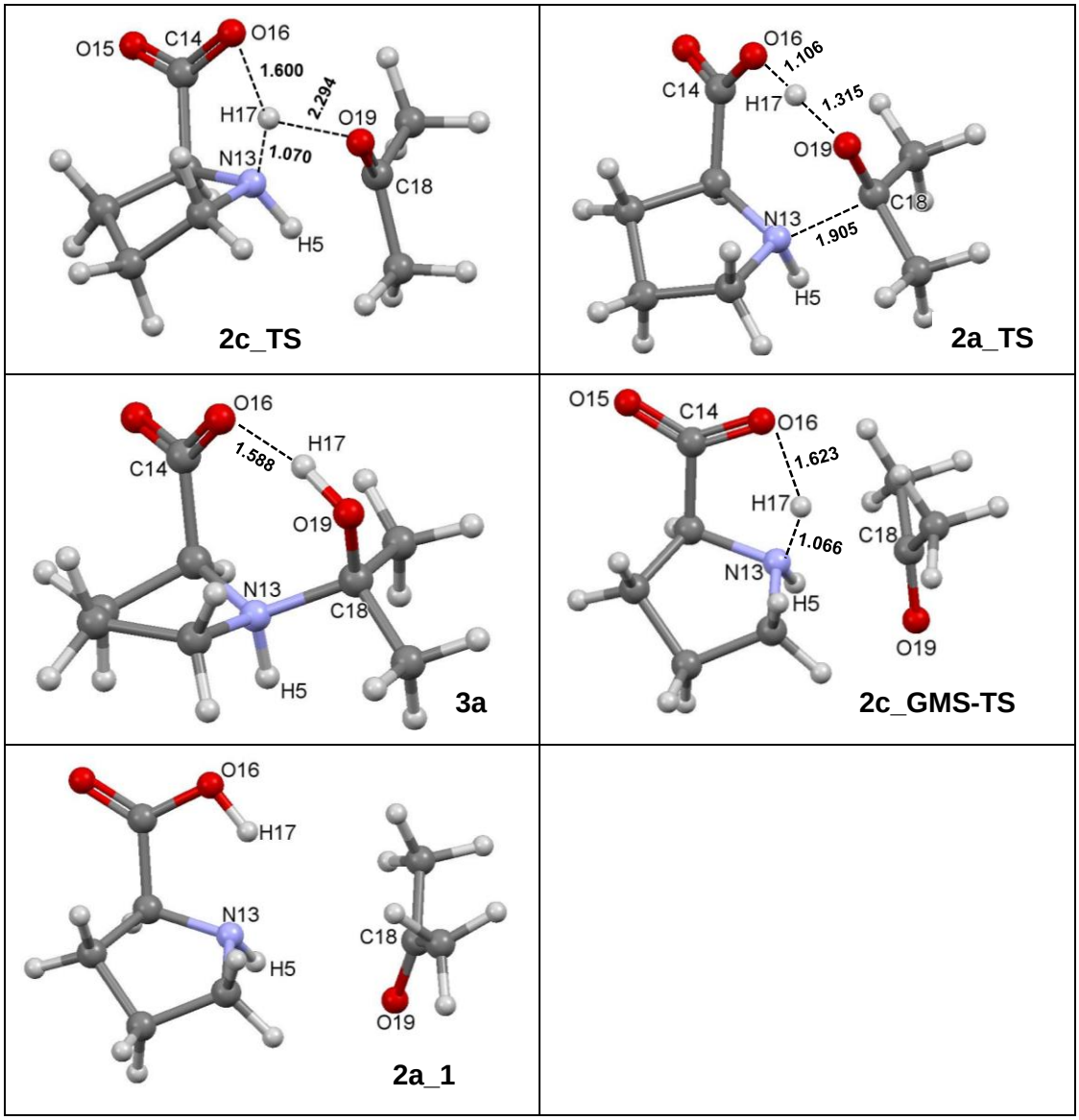

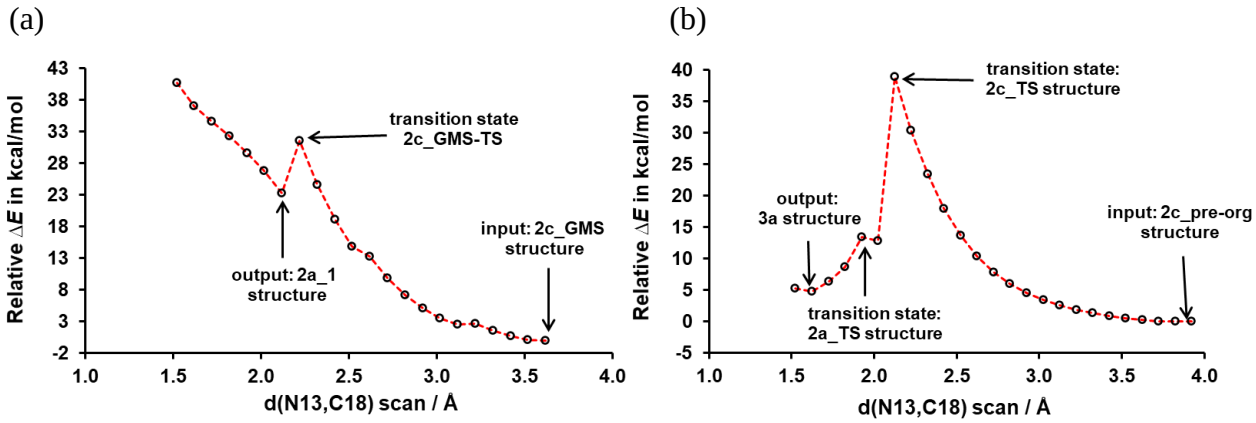

Figure 6.4. Data for scan of d(N13,C18) reaction coordinate using input complexes **2c_pre-org** and **2c_GMS** in an effort to construct the N13–C18 bond between proline **1c** and acetone **2**.

Since it has been demonstrated in previously studies that the reaction path through the resulting intermediate **3a** cannot result in the active enamine catalyst,[20,22] it implies that the zwitterion is not an active catalyst when an implicit solvation model is used. In the following section we will study the effect of a solvent molecule of DMSO on the catalytic activity of the zwitterion **1c**. In Chapter 4 we found that the presence of an explicit solvent molecule of DMSO facilitates the reaction energy profile of the higher energy conformer **1b**.

6.2.5. Effect of a solvent molecule of DMSO on the catalytic activity of the zwitterion 1c

A single solvent molecule of DMSO was placed in complex **2c_pre-org** such that the oxygen atom of DMSO (O37) interacted with H5 of proline. We aimed at establishing if the solvent molecule of DMSO would improve the reactivity of the zwitterion by either decreasing the energy barriers for the first step or providing an alternative mechanism. The energy optimised complex of DMSO and **2c_pre-org** was renamed **2C_pre-org** (when a molecule of DMSO is present) and its d(N13,C18) reaction coordinate was decreased as in previous cases. The data obtained showed that the molecule of DMSO does not provide an alternative mechanism neither does it lower the energy barrier for the H17 to O16 proton transfer. The energy barrier for the H17 to O16 transfer is higher than in the implicit solvation model, it is higher than 40 kcal/mol with respect to both E_{ZPVE} and G. Moreover, the resulting complex **3A** (see Table 6.4) cannot result in the active enamine catalyst as its reaction path is cut off as in the case of **3a**. This clearly shows that even in the presence of a molecule of DMSO the zwitterion **1c** is not an active conformer in proline catalysis.

6.2.6. Interaction of proline conformers (1a, 1b and 1c) with acetone 2

To get additional insights into the catalytic activity of the zwitterion **1c** we compared its intermolecular interaction energies with acetone **2** and the interaction energies of acetone and the non-ionic conformers (**1a**, and **1b**). Thus, we calculated intermolecular interaction energies between proline **1** and acetone **2**, i.e., the $E_{\text{int}}^{(1,2)}$ energy terms for **1a**, **1b** and **1c**. The conformer with the most negative $E_{\text{int}}^{(1,2)}$ term for GMS, pre-org and TS structures has a high affinity to acetone and will result in a relatively lower energy barrier for the bond formation/breaking. Table 6.5 shows molecular structures involving the GMS, pre-org and TS formed by the respective proline conformers and acetone **2**, complexes of proline (**1a** and **1b**) have been reported in a previous study.[22]

Table 6.4. Ball and stick models for intermediate complexes along the d(N13,C18) reaction coordinate scan using 2C_pre-org in the presence of a molecule of DMSO.

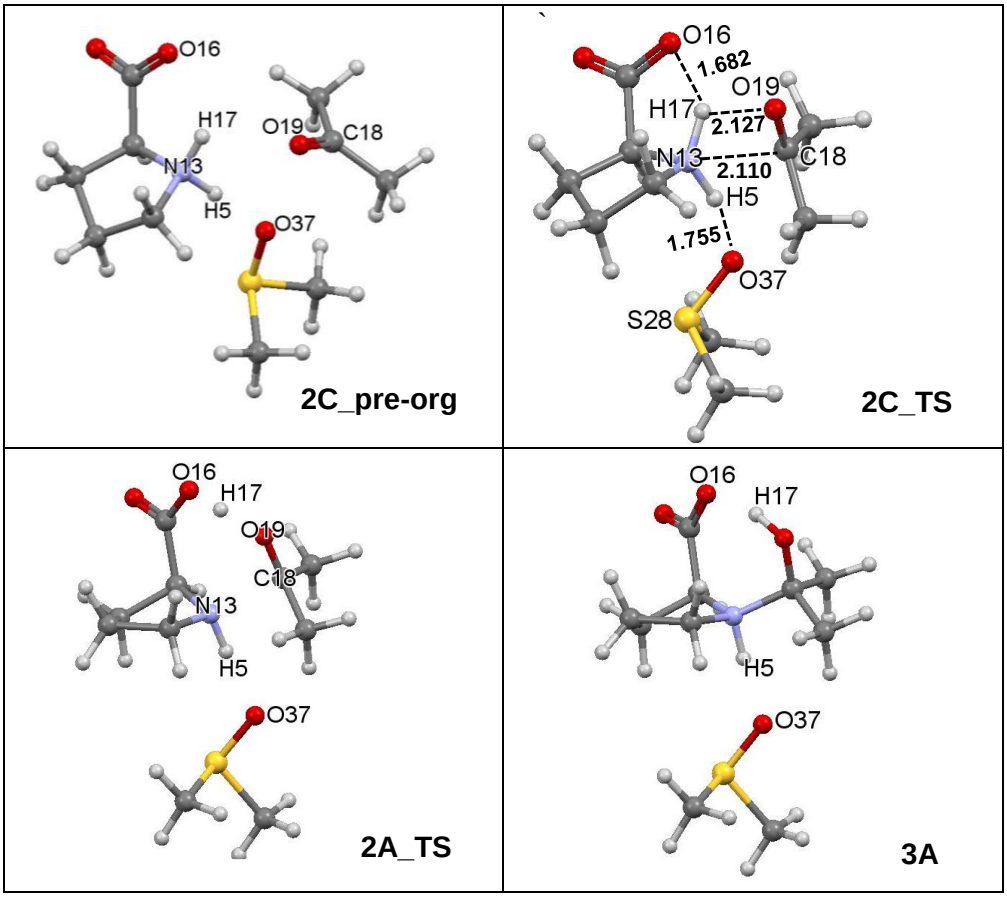

Atoms with $\left|\Delta E_{\text{int}}^{\mathbf{A,B}}\right| > 10$ in **1** and **2** are considered as the drivers of a chemical event in the REP-FAMSEC approach and are clustered as unique atomic fragments. As such, atoms {C18,O19} in **2** and atoms {C1,C4,H5,N13,C14,O15,O16,H17} in **1** where identified and placed in atomic fragments $\mathcal{A}$ and $\mathcal{P}$, respectively. The trends in Figure 6.5a show that in the respective GMSs, the $E_{\text{int}}^{(1,2)}$ energy term is comparable for conformers **1b** and **1c**, notably the $E_{\text{int}}^{(1b,2)}$ and $E_{\text{int}}^{(1c,2)}$ terms are –53.6 kcal/mol, and –50.9 kcal/mol respectively, while the $E_{\text{int}}^{(1a,2)}$ term is the weakest among the three, i.e., –34 kcal/mol. Interestingly, on moving from the GMS to pre-org, the $E_{\text{int}}^{(1,2)}$ term strengthened in **1b** 2-MC, and it weakened in the other two complexes, notably the $E_{\text{int}}^{(1,2)}$ terms changed by +10.4 kcal/mol, –16.7 kcal/mol and +6.2 kcal/mol for complexes of **1a**, **1b** and **1c**, respectively.

Table 6.5. Ball and stick representation of intermediate complexes along the reaction coordinate from the indicated GMSs to the respective transition states.

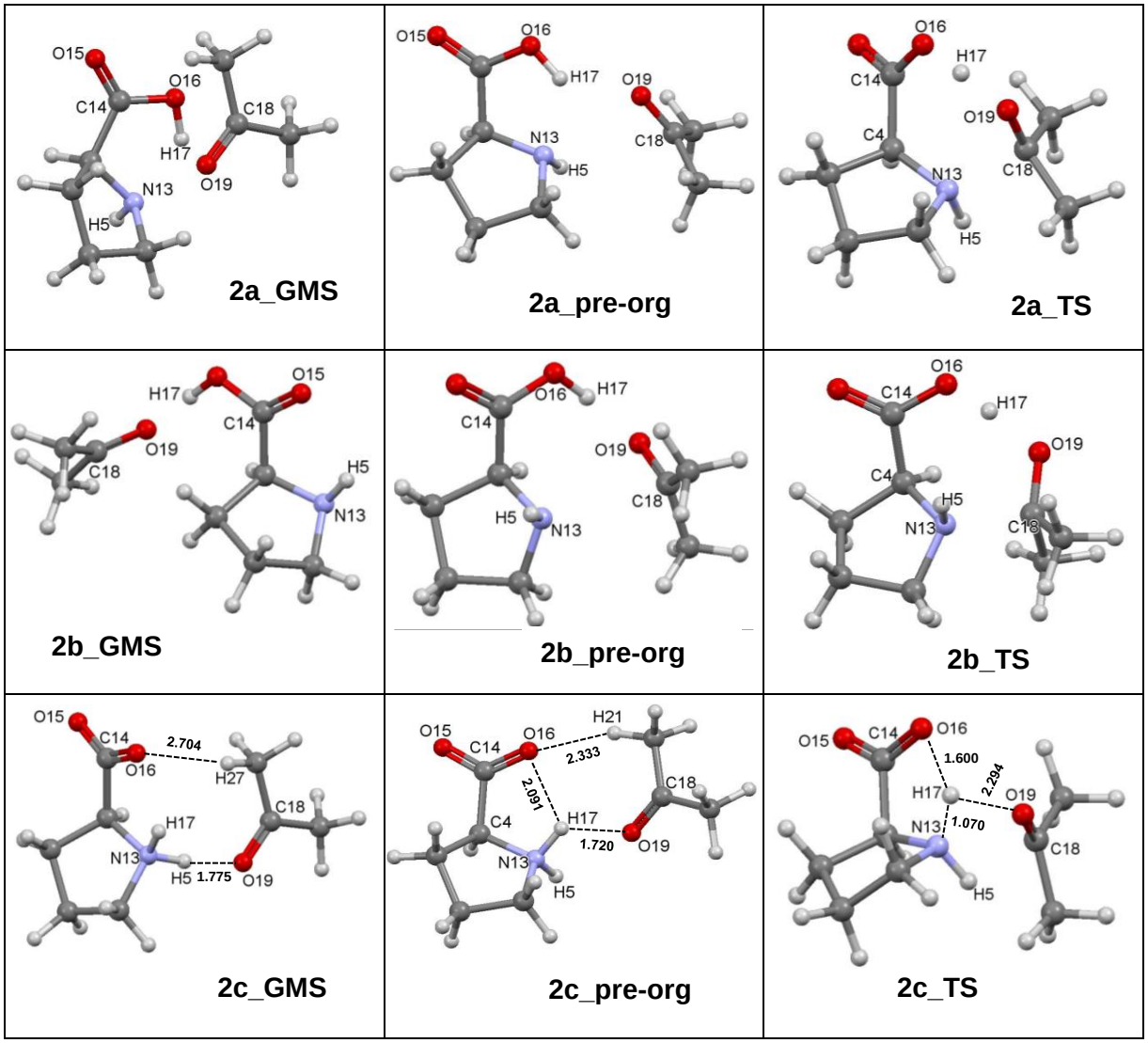

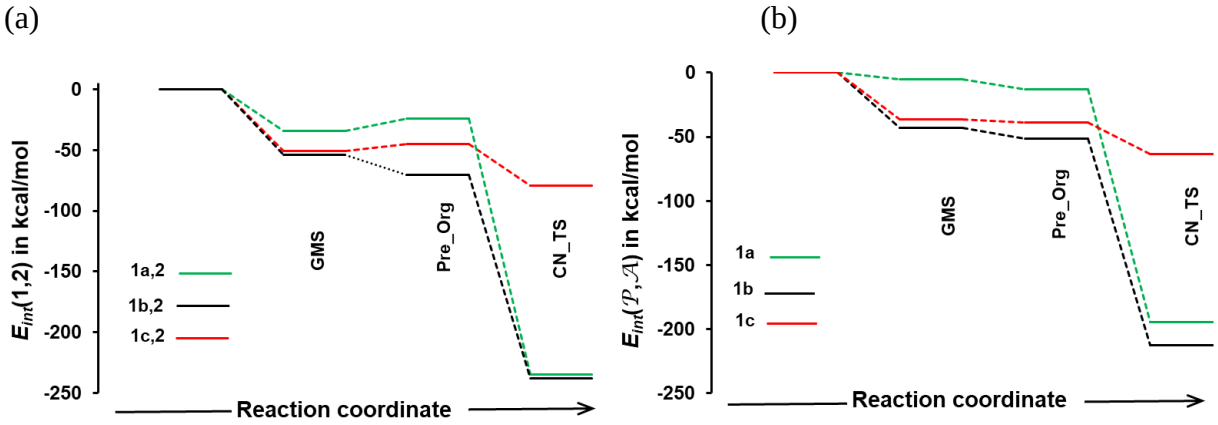

Figure 6.5. Relative to isolated proline conformers (**1a**, **1b** and **1c**) and acetone **2**, interaction energies between (a) molecules of acetone **2** and proline (either **1a**, **1b** or **1c**) and (b) interaction between the $\mathcal{P}$ and $\mathcal{A}$ fragments of proline **1** and acetone **2** at the indicated stages along the reaction coordinate.

At the transition state, the $E_{\text{int}}^{(1,2)}$ energy term is comparable for both **1a** and **1b** with values of –235.0 and –238.1 kcal/mol, respectively, while the calculated $E_{\text{int}}^{(1,2)}$ term for **1c** of –79.3 kcal/mol is three times weaker than that of **1a** and **1b** . This could be the reason why **1c** has a significantly high energy barrier for the first step of the catalytic reaction. The trends for the leading fragments $\mathcal{P}$ and $\mathcal{A}$ of proline and acetone resemble that for the molecular system (Figure 6.5b).

Intermolecular interaction energies from a classical two atom perspective

We also considered a classical two atom approach which utilises the electrophilicity (δ^+) and nucleophilicity (δ^-) of atoms involved in bond formation and breaking. As a result, we calculated interaction energies between atoms (N13 and H17) in **1** and their corresponding pairs (C18 and O19) in **2**, i.e., the $E_{\text{int}}^{\text{N13,C18}}$ and $E_{\text{int}}^{\text{H17,O19}}$ energy terms. These atoms are directly involved in the formation of covalent bonds (N13–C18 and H17–O19) during the first step of the catalytic reaction (Figure 6.6).

The general trends in Figure 6.6 shows that intermolecular interaction energies between atom pairs N13,C18 and H17,O19 are weakest in the zwitterion **1c**. Notably, when pre-org and TS structures are considered, the $E_{\text{int}}^{\text{N13,C18}}$ energy term is weaker in **1c** than in **1b** by +26.0 kcal/mol and +60.2 kcal/mol, respectively. Interestingly, the $E_{\text{int}}^{\text{H17,O19}}$ term, which has been described as the leading interaction driving the formation of the C–N bond/H-transfer, is weaker in both pre-org and TS structures of **1c** relative to **1b** by +57.3 kcal/mol and +108.4 kcal/mol, respectively. These are large differences and they clearly shows that the zwitterion cannot be the active catalyst in proline catalysed organic transformations.

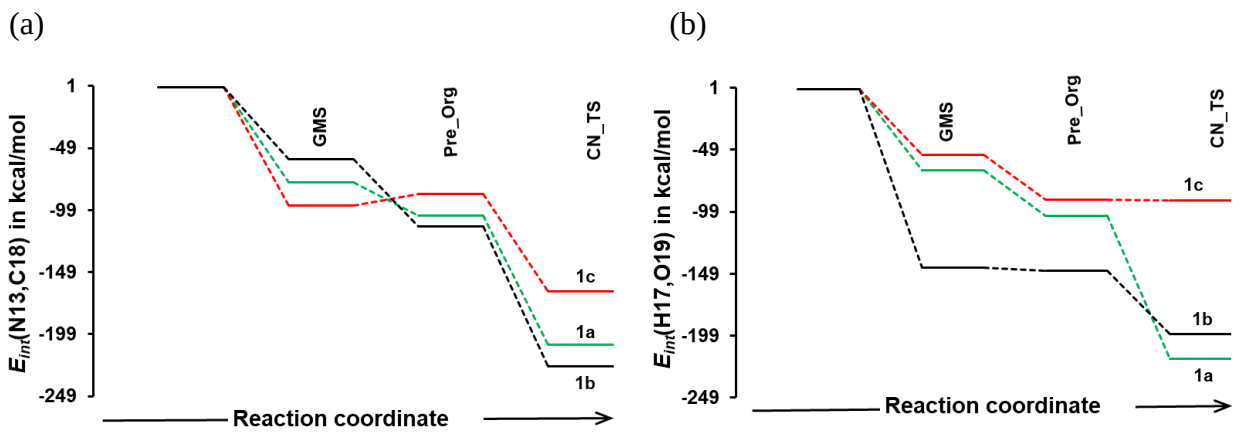

Figure 6.6. Intermolecular interaction energies between atom pairs: (a) N13,C18 and (b) H17,O19 of **1** and **2**, respectively, at the indicated stages of along the reaction coordinate.

Intermolecular interaction energies between individual atoms (N13,H17,C18 and O19) and entire molecule, the $E_{\mathrm{int}}^{\mathrm{A,1}}$, and $E_{\mathrm{int}}^{\mathrm{A,2}}$ energy terms.

The $E_{\mathrm{int}}^{(\mathrm{A,2})}$ and $E_{\mathrm{int}}^{(\mathrm{B,1})}$ energy terms calculate mutual attraction between an atom of interest A or B and all the atoms of the other molecule. In other words, how "friendly" is a molecular environment **1** and **2** towards the atom of interest A or B (Figures 6.7–6.8). The more negative the $E_{\mathrm{int}}^{(\mathrm{A,mol})}$ term, the more "friendly" is the chemical environment in attracting an atom of interest. On the contrary, a positive $E_{\mathrm{int}}^{(\mathrm{A,mol})}$ term indicates unfavourable (repulsive), hence destabilising chemical environment. The trends in Figure 6.7 reveal that intermolecular interaction energy between the atom N13 of **1** and the acetone molecule **2** is weak in the case of conformer **1c**. Compared to **1b**, the $E_{\mathrm{int}}^{(\mathrm{N13,2})}$ term is more positive in **1c**, for pre-org and TS structures, by +37 kcal/mol and +148.9 kcal/mol, respectively. Interestingly, the $E_{\mathrm{int}}^{(\mathrm{H17,2})}$ term for TS is not only weak in **1c** compared to **1a** and **1b** but it is positive and unfavourable with $E_{\mathrm{int}}^{(\mathrm{H17,2})}$ term of +1.1 kcal/mol. This indicates that H17 of the zwitterion **1c** is entirely not attracted at all to the molecule of acetone **2**. This is one of the reasons for the significantly high activation energy observed in **1c_TS**. As a result, H17 is first transferred to O16 to form **1a_TS** before bonds are formed/broken between atom pairs N13–C18 and H17–O19.

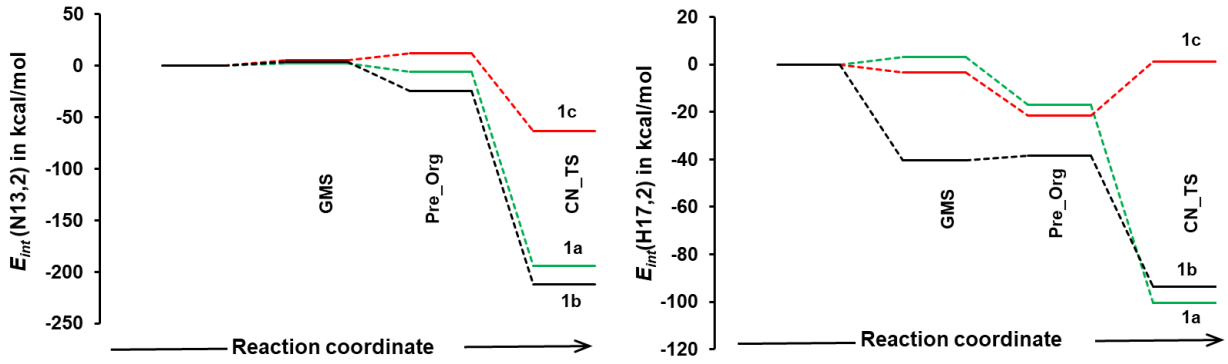

Figure 6.7. Intermolecular interaction energy between atoms N13 and H17 of **1** with the entire molecule of acetone **2.**

Finally, we calculated intermolecular interaction energies between atoms C18 and O19 of **2** and the entire molecule of **1** (Figure 6.8). The trend for $E_{\mathrm{int}}^{(\mathrm{C18,1})}$ shows that there is no affinity between C18 of acetone **2** and the molecule of the zwitterion **1c** at the three major stages along the reaction path, i.e., GMS, pre-org and TS.

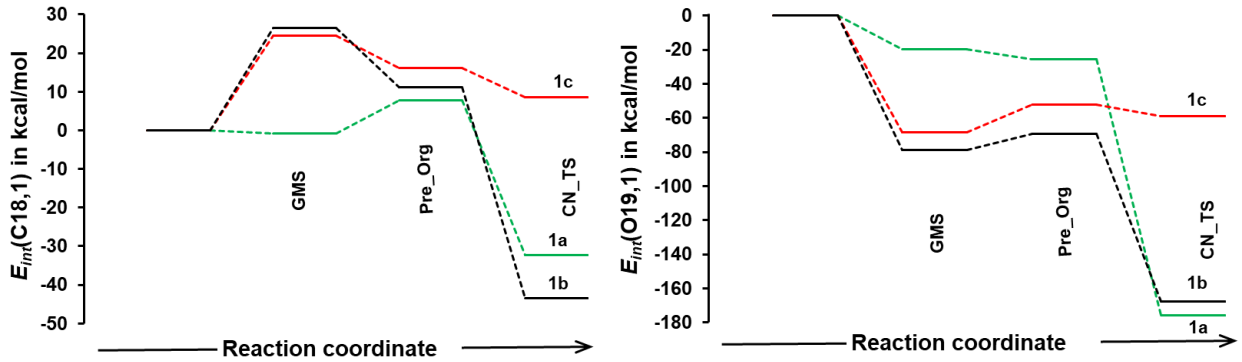

Figure 6.8. Intermolecular interaction energy between atoms C18 and O19 of **2** with the entire molecule of proline **1**.

Notably, the $E_{\text{int}}^{(\text{C18,1c})}$ energy terms are +24.5 kcal/mol, +16.1 kcal/mol and +8.5 kcal/mol for structures at GMS, pre-org and TS respectively. It can also be observed that the $E_{\text{int}}^{(\text{C18,1})}$ terms for both **1a** and **1b** are positive for pre-org structures at +7.8 kcal/mol and +11.2 kcal/mol, respectively. However, at the transition states the $E_{\text{int}}^{(\text{C18,1})}$ terms became attractive for both **1a** and **1b** with values of –32.4 kcal/mol and –43.4 kcal/mol, respectively. We therefore attribute the high transition state energy for **1c_TS** also to the lack of attraction between C18 and the zwitterion **1c** among other things. The trend for $E_{\text{int}}^{(\text{O19,1})}$ shows weak intermolecular interaction between O19 of acetone **2** and the zwitterion molecule **1c** at the three major steps considered when compared to **1b**. As a result, the zwitterion is an inactive conformer and not the active catalyst in proline catalysis.

6.3. Conclusions

We have demonstrated that though the zwitterion **1c** and the non-ionic conformer of proline **1a** are nearly isoenergetic when an implicit solvation model is used, the presence of discrete molecules of water increases the relative stability of **1c** with stability increasing with each additional water molecule. The relative stability of **1c** is further enhanced by the presence of an explicit solvent molecule of DMSO. This confirms that the zwitterionic of proline becomes the most dominant in solution. Intermolecular interaction energy between explicit solvent molecules (either water or DMSO) and proline are more attractive in the zwitterion **1c** and the solvent molecules of water are in a better environment in the zwitterion. However, the dominance of the zwitterion in solution does not make it the active catalyst in proline catalysis. It forms weak intermolecular interaction with the molecule of acetone when compared to non-ionic conformers.

This results in a very high energy barrier (~ 40 kcal/mol) for bond formation, as the proton H17, which is the driver of the first step in proline catalysis is not attracted to the molecule of acetone even at the transition state. The energy barrier for the first step in the catalytic reaction reported herein is higher than 21 kcal/mol reported by Yang and Zhou.[17] However, one must realize that even 21 kcal/mol is still too large a barrier. When considering either an implicit solvation model or in the presence of moisture, it requires less than 5 kcal/mol to transform the zwitterion to conformer **1a**. Once formed, conformer **1a** undergoes a structural change to **1b** as demonstrated in Chapter 5. The overall barrier for this conversion is less than 10 kcal/mol, hence the zwitterion is not an active form in proline catalysis, it only acts as a source of the catalytically active conformer **1b**.

6.4. References

1. List, B.; Lerner, R. A.; Barbas, C. F. *J. Am Chem. Soc.*, **2000**, *122* (10), 2395-2396.
2. LeBel, R.; Goring, D. *J. Chem. Eng.*,**1962**, *7* (1), 100-101.
3. Yang, G.; Zhu, C.; Zhou, L. *Int. J. Quantum. Chem.*, **2015**, *115* (24), 1746-1752.
4. Julian, R. R.; Jarrold, M. F. *J. Phys. Chem. A*, **2004**, *108* (49), 10861-10864.
5. Jensen, J. H.; Gordon, M. S. *J. Am. Chem. Soc.*, **1995**, *117* (31), 8159-8170.
6. Ding, Y.; Krogh-Jespersen, K. *Chem. Phys. Lett.*, **1992**, *199* (3), 261-266.
7. Snoek, L. C.; Kroemer, R. T.; Simons, J. P. *Phys. Chem. Chem. Phys.*, **2002**, *4* (11), 2130-2139.
8. Park, S. W.; Im, S.; Lee, S.; Desfrancois, C. *Int. J. Quantum. Chem.*, **2007**, *107* (6), 1316-1327.
9. Yang, G.; Zhou, L.; Chen, Y. *SpringerPlus* **2016**, *5* (1), 19.
10. Arnó, M.; Domingo, L. R. *Theor Chem. Acc.*, **2002**, *108* (4), 232-239.
11. Blom, M. N.; Compagnon, I.; Polfer, N. C.; von Helden, G.; Meijer, G.; Suhai, S.; Paizs, B.; Oomens, J. *J. Phys. Chem. A,* **2007**, *111* (31), 7309-7316.
12. Xu, S.; Nilles, J. M.; Bowen Jr, K. H. *J. Chem. Phys.* ,**2003**, *119* (20), 10696-10701.
13. Liu, L.; Liu, Z.-T.; Liu, Z.-W.; Xue, D. *Sci. China Chem.*, **2010**, *53* (7), 1586-1591.
14. Aikens, C. M.; Gordon, M. S. *J. Am. Chem. Soc.*, **2006**, *128* (39), 12835-12850.
15. Im, S.; Jang, S.-W.; Lee, S.; Lee, Y.; Kim, B. *J. Phys. Chem. A,* **2008**, *112* (40), 9767-9770.
16. Hwang, T.-K.; Eom, G.-Y.; Choi, M.-S.; Jang, S.-W.; Kim, J.-Y.; Lee, S.; Lee, Y.; Kim, B. *J. Phys. Chem. B,* **2011**, *115* (33), 10147-10153.
17. Yang, G.; Zhou, L. *Catal. Sci. Technol.*, **2016**, *6* (10), 3378-3385.
18. Kim, J.-Y.; Ahn, D.-S.; Park, S.-W.; Lee, S. *RSC Adv.*, **2014**, *4* (31), 16352-16361.
19. Wu, R.; McMahon, T. B. *Angew. Chem. Int. Ed.*, **2007**, *46* (20), 3668-3671.
20. Ajitha, M. J.; Suresh, C. H. *J. Mol. Catal., A: Chem.*, **2011**, *345* (1), 37-43.
21. Rankin, K. N.; Gauld, J. W.; Boyd, R. J. *J. Phys. Chem, A,* **2002**, *106* (20), 5155-5159.
22. Cukrowski, I.; Dhimba, G.; Riley, D. L. *Phys. Chem. Chem. Phys.***2019**, *21* (30), 16694-16705.

Chapter 7

Formation of the active enamine catalyst from the product of C–N bond formation/1st proton transfer in proline catalysed aldol reactions

---

Abstract

This chapter is a description of two consecutive steps which take place after the first and second proton transfers, namely the elimination of a water molecule and the subsequent formation of the active enamine catalyst. The two steps were modelled in the implicit solvation model and in the presence of an explicit solvent molecule of DMSO. The energy barrier $\Delta G^{\ddagger}$ for water elimination is comparable and very small ($\sim$ 2 kcal/mol) for the two solvation models, while the resulting imine complex is lower in relative free energy G by $\sim$ 3 kcal/mol in the implicit solvent model. Dehydration of the imine complex was found to be unfavourable, hence modelling of the enamine formation step should be done with the inclusion of a water molecule. The presence of an explicit solvent molecule of DMSO facilitates the formation of the active enamine catalyst, by decreasing the energy barrier and stabilizing the resulting active enamine catalyst.

7.1. Introduction

It is now widely accepted that the proline catalysed aldol reaction proceeds via the formation of an active enamine. Through computational modelling, it was confirmed that the carboxylic acid assisted enamine mechanism is the most preferred channel through which the reaction proceeds.[1] The enamine mechanism was reaffirmed when enamines were detected *in situ* during experimental studies.[2–4] Although the field of organocatalysis has rapidly flourished, especially with new catalytic applications being proposed there is little progress made in rationalising the mechanistic details. The identification, and characterisation of reaction intermediates is very important for detailed understanding of reaction profiles, control and optimisation of catalytic conditions. Though the enamine formed from proline and acetone is known,[5,6] there are several reactive channels proposed for its formation from isolated reactants.[5–8] This clearly shows that rationalising mechanistic details is still at its exploratory stage and more studies are required for a detailed understanding of the mechanism. We have shown in Chapter 4 that the solvent molecule of DMSO plays a subtle and critical role during the first few steps of the reaction. The catalytic role of the solvent molecule of DMSO in the subsequent water elimination is unknown. Moreover, the catalytic role of the eliminated water molecule in the next stages of the reaction is also unreported. To get a fuller mechanistic understanding of the mechanism of this reaction, these little details need to be fully understood. In this chapter, we will explore the catalytic role of the solvent molecule of DMSO during the elimination of a water molecule and the formation of the active enamine. We will also explore the catalytic role of the eliminated molecule of water in the formation of the active enamine catalyst.

7.2. Result and discussion

7.2.1. Water elimination in implicit solvent model

Water elimination is one of the key mechanistic steps in proline catalysed aldol reactions;[5,6,9] it results in the formation of imines which are intermediates for the formation of the active enamine catalyst. The water molecule is formed by the condensation reaction between the hydroxyl group {H17,O19) and H5. At first, we assumed that the product from the C–N bond formation/1st H-transfer (**6b)** would initiate the water elimination reaction. To this effect, the d(H5,O19) reaction coordinate was decreased in steps of 0.1 Å using **6b**, (Figure 7.1).

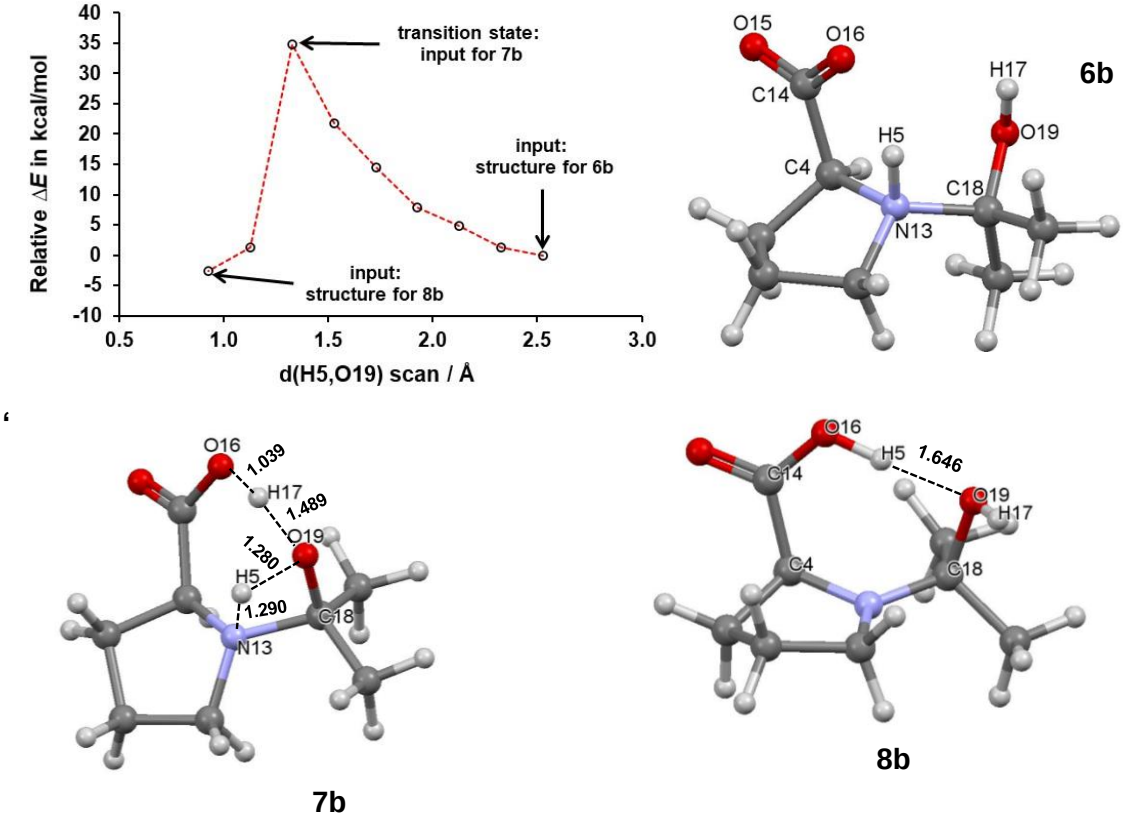

Figure 7.1. Data for d(H5,O19) reaction coordinate scan using **6b** as input in an attempt to eliminate a water molecule and ball and stick representation of structures of **6b**, **7b** and **8b**.

The obtained scan data shows a significant increase in electronic energy as the d(H5,O19) reaction coordinate is decreased while the energy of the associated transition state **7b** is higher (with respect to both Gibbs free energy *G* and E_{ZPVE}) than the input **6b** by ~31 kcal/mol. Notably, the transition state corresponds to a double proton transfer of H5→O19 and H17→O16. Evidently, the selected reaction coordinate does not result in the elimination of a water molecule, but it results in intermediate **8b** which is higher in energy than input **6b** (with respect to both E_{ZPVE} and free energy *G*) by 6.4 kcal/mol. Moreover, the unsurmountable energy of **7b** indicates that the selected reaction coordinate is unfavourable and will not result in water elimination. It can also be observed in intermediate **8b** that the acidic proton H17 of proline was transferred back to O16 while it is replaced by H5, this is clear evidence that the elimination of a water molecule from **6b** is preceded by an initial proton transfer as we have demonstrated in chapters 3 and 4. In the following section, we will explore water elimination from intermediate **10b**.

7.2.2. Water elimination using the proton transfer product 10b

A detailed account of the H5→O16 proton transfer from **6b** to **10b** is given in Chapter 3 using an implicit solvation model, and in Chapter 4 by the use of an explicit solvation model. In this

section, we assumed **10b** to be the intermediate structure from which the water molecule is eliminated. Two experiments were conducted, in the first, the d(H5,O19) reaction coordinate was decreased (Figure 7.2a).

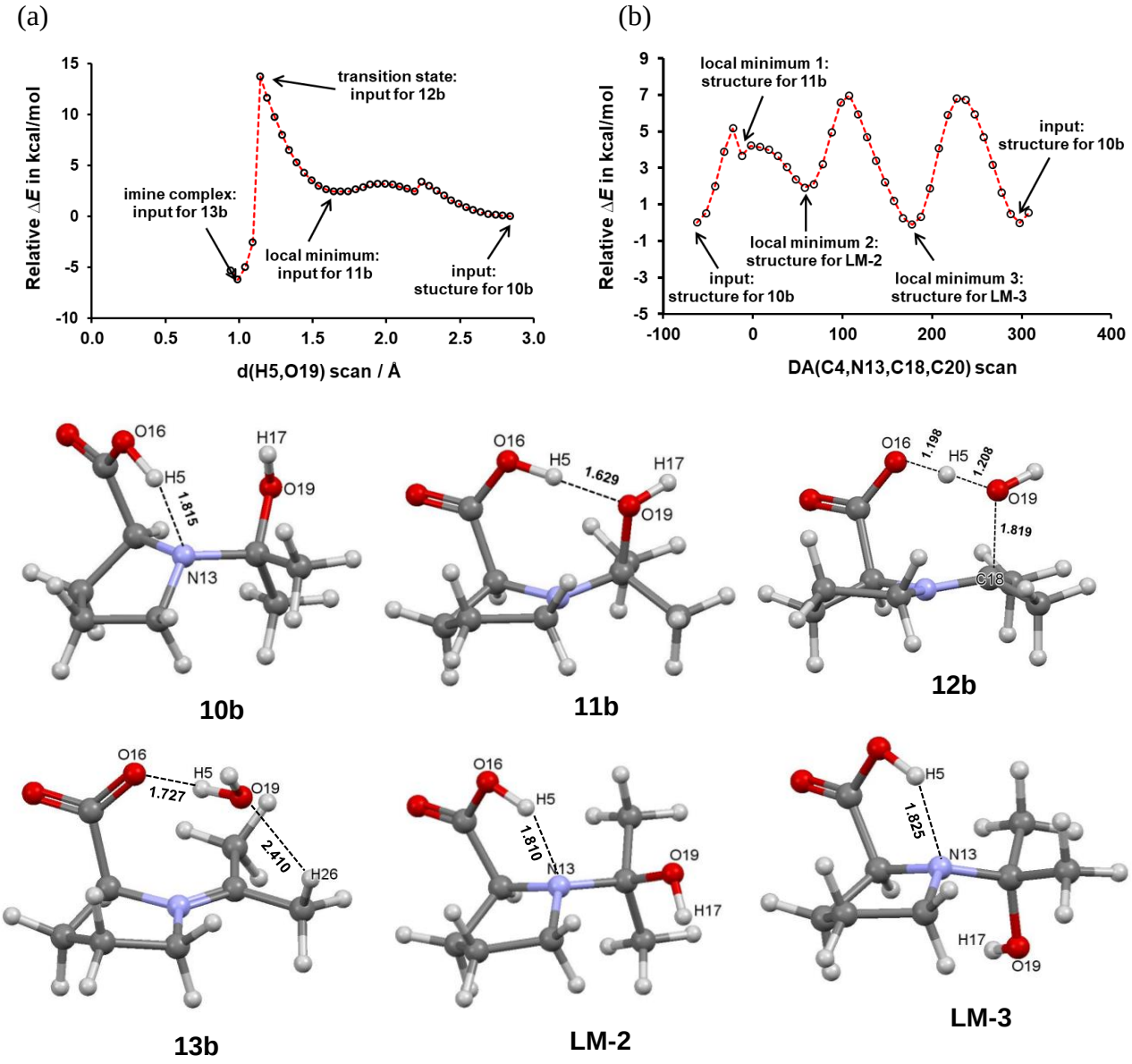

Figure 7.2. Data for scan of: (a) d(H5,O19) reaction coordinate resulting in the elimination of a water molecule and (b) DA(C4,N13,C18,C20) in the search of a global minimum structure, and ball and stick representation of structures **10b**, **11b**, **12b**, **13b**, **LM**-2 and **LM-3**.

In the second experiment, it was assumed that the molecule **10b** can freely rotate about the N13–C18 single bond, hence the dihedral angle DA(C4,N13,C18,C20) in **10b** was scanned in steps of 10° (Figure 7.2b). In the first experiment, a local minimum structure **11b** which is ~ 2 kcal/mol higher in energy than **10b** with respect to both the free energy (*G*) and (E_{ZPVE}) was identified at d(H5,O19) = 1.629 Å. Interestingly, the same local minimum structure **11b** was also identified (at

DA = –12.3°) in the second experiment. When the d(H5,O19) reaction coordinate scan was done using the first local minimum structure obtained from the DA(C4,N13,C18,C20) scan, the data obtained is identical to the one in Figure 7.2a. It shows transition state **12b** and an imine complex of water **13b**. Two other local minimum structures were obtained from the DA(C4,N13,C18,C20) scan, i.e., (**LM-2** and **LM-3** at dihedral angles 57.7° and 117.7°, respectively), however, the two minima are unsuitable for water elimination due to their lack of proper pre-organisation. Surprisingly, there was a major drop in electronic energy by ~ 5 kcal/mol when **12b**, the input from the scan was energy minimised, this normally occurs when there exists a lower energy reaction pathway than the one being assumed. But since we arrived at the same local minimum structure **11b** using two different approaches, we can conclude that **12b** is indeed the transition state for water elimination in the implicit solvent model. Complete transfer of H5 to O19 results in the cleavage of the C18–O19 single bond and the elimination of the {H5–O19–H17} water molecule.

7.2.3. Water elimination in the presence of an explicit solvent molecule of DMSO

Water elimination through 10B

For the sake of simplicity, structures are represented by a capital letter when an explicit solvent molecule of DMSO is present, for instance, **6b** in implicit solvent becomes **6B** in the presence of DMSO explicit solvent molecule. The elimination of a molecule of water through intermediate **10B** was studied by decreasing the d(H5,O19) reaction coordinate as was the case in **10b** (Figure 7.3). The scan data resembles the one obtained in the implicit solvation model: It consists of local minimum structure **11B** which is pre-organised for water elimination, the associated transition state **12B**, and the product from water elimination **13B**. Structure **12B** obtained from the scan is 8.5 kcal/mol higher in electronic energy than the input **10B** and this is 5.2 kcal/mol lower when compared to the same process in an implicit solvent model. The drop in electronic energy when transition state **12B** from the scan was energy minimised is ~ 3 kcal/mol this is 2 kcal/mol lower when compared to the implicit solvent model. This difference can be attributed to the presence of an explicit solvent molecule of DMSO which stabilizes the intermediate structures. Interestingly, the relative change in energy for the **10b→13b** transition is more negative than the **10B→13B** change by ~ – 2 kcal/mol, with respect to both E_{ZPVE}, and free energy G.

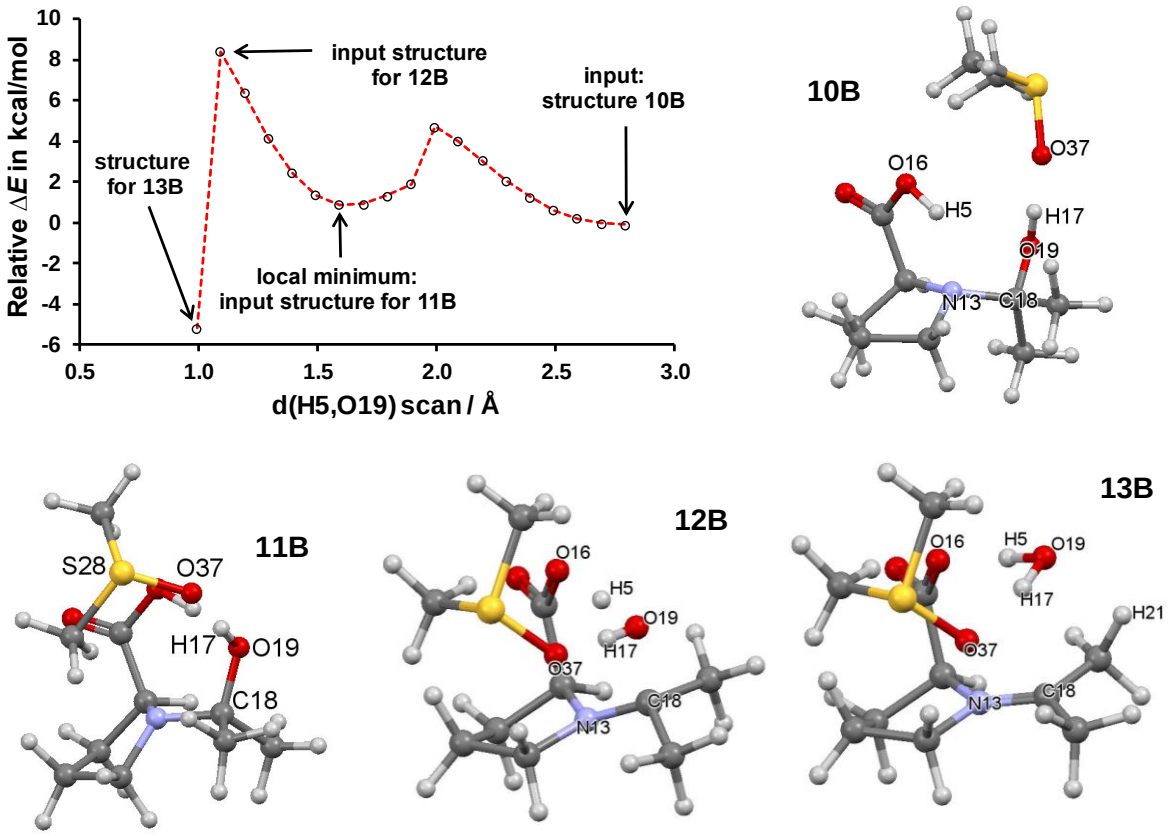

Figure 7.3. Data for d(H5,O19) reaction coordinate scan using complex **10B** resulting in the elimination of a water molecule and ball and stick representation of structures **10B, 11B**, **12B** and **13B**.

7.2.4. Water elimination through 11B'

In this experiment, it was assumed that the unrestricted rotation of the C18–O19 single bond in **11B** and the dynamics of the DMSO explicit solvent molecule allows free rotation of this bond and unobstructed movement of the solvent molecule of DMSO. This would allow the existence of a complementary structure (**11B'**) in which the orientation of the {O19,H17} hydroxyl group is 180° in relation to the original structure **11B**. The explicit solvent molecule of DMSO is also expected to move freely, hence the dihedral angle DA(C18,O19,C29,S28) made of atoms of the DMSO molecule and the hydroxyl group were scanned in –10º steps. The resulting data (Figure 7.4a) shows that the rotational energy required for the transformation from **11B** to **11B'** is marginal (less than 3 kcal/mol), and it occurs when the DA is rotated by exactly –180° as we had predicted. Two other stationary points were also located, i.e., the global minimum structure **14B** and a local minimum at DA, –149.7°, and –269.9° respectively. However, these two are not pre-organised for water elimination. Ball and stick representation of structures **14B** and **11B'** shows that the main difference between the two complexes is intramolecular hydrogen bonding interaction formed by H5, in **14B**, there exist the O16–H5···N13 H-bond (1.778 Å) while in **11B'**, there is the O16–

H5···O19 H-bond (1.717Å). The presence of the O16–H5···O19 H-bonding interaction in **11B'** makes it pre-organised for the elimination of a water molecule since a molecule of water is formed following a condensation reaction between H5 and the (O19–H17) hydroxyl group. Notably, the global minimum structure **14B** is lower in E_{ZPVE} and Gibbs free energy G than the pre-organised structure **11B'** by ~ 2 kcal/mol and 1 kcal/mol, respectively. Due to the small energy difference it is sensible to consider complex **14B** in modelling the water elimination reaction. Figure 7.4b shows the data obtained from d(H5,O19) reaction coordinate scan using the global minimum structure **14B**, it shows the formation of the best pre-organised structure **11B'** before the water molecule is eliminated in **13B'**.

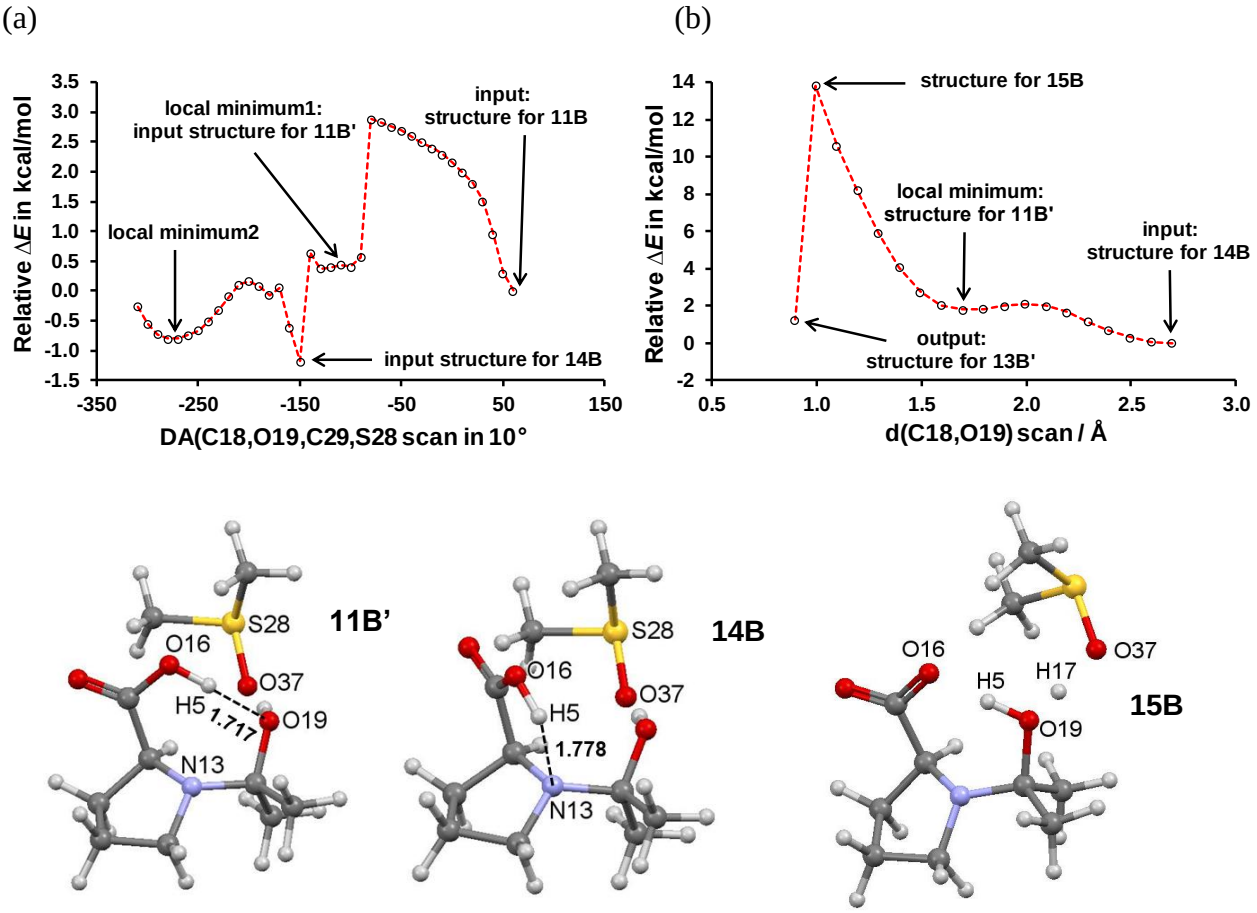

Figure 7.4. Data for scan of: (a) DA(C18,O19,C29,S28) using complex **11B** as the input (resulting to local minimum structure **11B'** and global minimum structure **14B**) and (b) reaction coordinate d(H5,O19) using global minimum structure **14B**, and ball and stick representation of complexes **11B'**, **14B** and **15B.**

Although decreasing the d(H5,O19) reaction coordinate using the global minimum structure (**14B**) resulted in the elimination of a water molecule (Figure 7.4b), the associated transition state structure **15B** is not a typical first-order saddle point, it shows replacement of H17 by H5 rather than cleavage of the C18–O19 bond. Moreover, the complex **15B** is higher in both E_{ZPVE} and free energy G than transition state **12B** G by ~ 8 kcal/mol. Clearly, this is not the correct reactive channel through

which the water molecule is eliminated. Hence the d(C18,O19) reaction coordinate was increased using **11B'** as the input (Figure 7.5). The data obtained shows a simultaneous decrease in the d(H5,O19) distance as the d(C18,O19) reaction coordinate is increased, resulting in transition state **12B'** and elimination of a molecule of water. A comparative assessment of the mechanisms through structures **11B** and **11B'** indicate that the two mechanisms compete: the associated transition states **12B**, and **12B'** have identical energies. The resulting imine complexes (**13B** and **13B'**) are also isoenergetic, however, they are pre-organised for the formation of different enamine conformers, a detailed account of the enamine formation through **13B** and **13B'** is given in the following section.

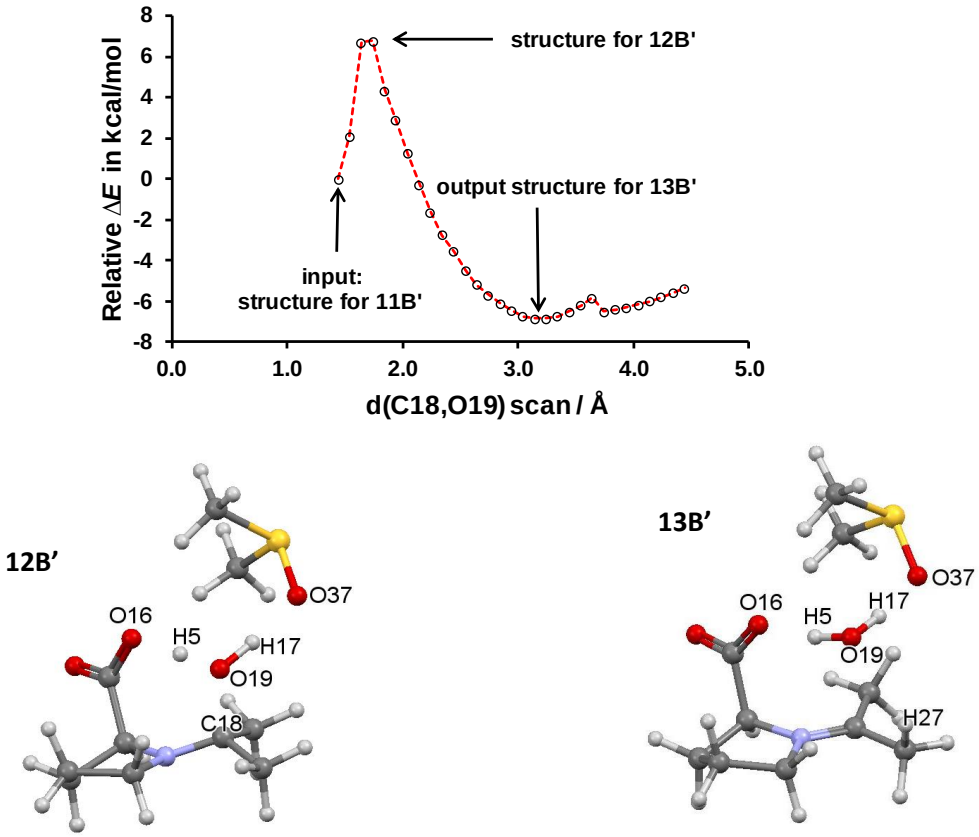

Figure 7.5. Data for d(C18,O19) reaction coordinate scan using structure **11B'** resulting in the elimination of a water molecule and ball and stick representation for structures of transition state **12B'** and imine **13B'**.

7.3. Enamine formation

The formation of the active enamine catalyst is a sequel to water elimination in the multi-step mechanism. Enamines are regarded as key intermediates and active catalysts in proline catalysis, they possess two conformational preferences due to unrestricted rotation about the C–N single bond

(Figure 7.6).[6,10] The conformer nomenclature depends on the relative orientation of the active methylene group with respect to the carboxylic moiety, it can either be in a *syn* or *anti* orientation.

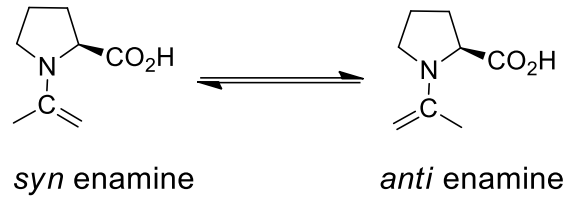

Figure 7.6. Structures of *syn* and *anti*-enamine conformers

In previous studies, it was proposed that the *syn*–enamine is preferentially formed followed by a rotation about the C–N single bond resulting in the catalytically active *anti*–enamine.[6,10] The involvement of a molecule of water in the formation of the active enamine catalyst was found to increase the activation energy for the enamine formation. However, reaction modelling was done in the absence of an explicit solvent molecule of DMSO. The presence of water molecules in the reaction mixture at the stage of enamine formation is indisputable since it is eliminated in the previous water elimination step. It is known that in reactions that produce water, the molecule of water can be involved in the subsequent step of the mechanism either actively in proton transfer relays or passively as additives that provide additional key hydrogen bonding interactions.[11,12] The catalytic role of a combination of solvent molecules of water and DMSO in the formation of the active enamine catalyst should be re-investigated. This is the focus of the next section.

7.3.1 Enamine formation mechanism in the implicit solvation model

The role of explicit solvent molecules in enamine formation has been previously reported in a reaction between dimethylamine and propanal.[13] It was found that the presence of two molecules of methanol stabilised the transition state and decreased the activation free energy $\Delta G^{\ddagger}$ by 16.7 kcal/mol. In the present study, we aimed to understand the role of the eliminated water molecule in the enamine formation step. The imine complex **13b** was used as the input structure for studying the role of water as a medium for proton transfer relay and as an additive for providing additional hydrogen bonds to the transition state. Ball and stick representation of transition state structures obtained when the imine complex **13b** was used as the input structure are shown in (Table 7.1).

The free energy barriers $\Delta G^{\ddagger}$ for enamine formation through the three transition states **15b**, **16b**, and **17b**, were found to be 22.1 kcal/mol, 22.8 kcal/mol, and 20.5 kcal/mol, respectively. The data shows that the formation of the inactive *syn*-enamine (**17b-*syn***) through transition state **17b** is the most favourable due to its relatively lower energy. This correlates well with findings previously

reported by Ajitha and Suresh.[6] As a result of the high energy barrier observed when modelling is done in water, they proposed an enamine formation mechanism in which the water molecule is completely dissociated from the parent imine adduct. However, such a mechanism must be supported by dissociation studies in which the energy barrier for dehydration to form isolated imine and water molecules is established. In the following section we will investigate the energy barriers for the dehydration of the parent imine complex to form isolated molecules.

Table 7.1. Ball and stick representation of transition states and associated enamine intermediates formed from imine complex **13b**.

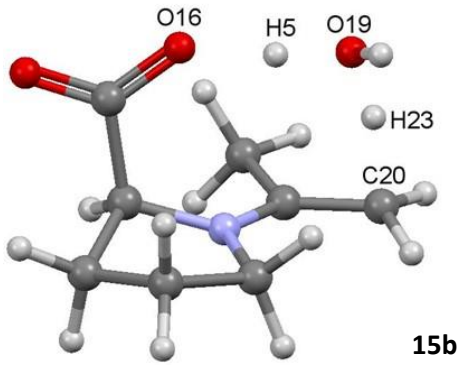 **15b**	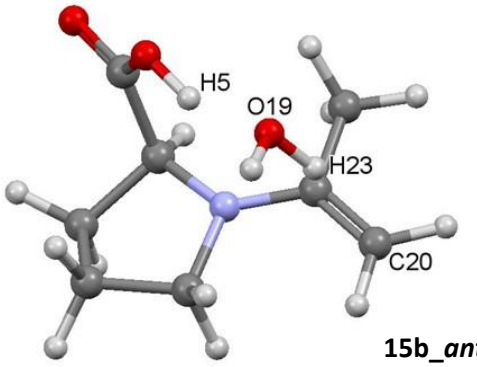 **15b_*anti***
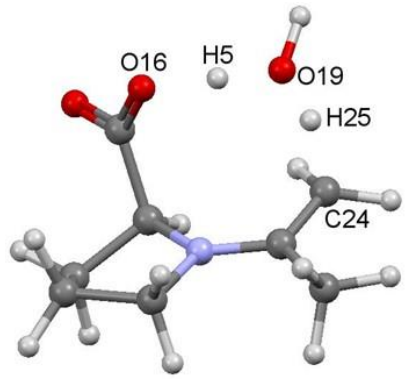 **16b**	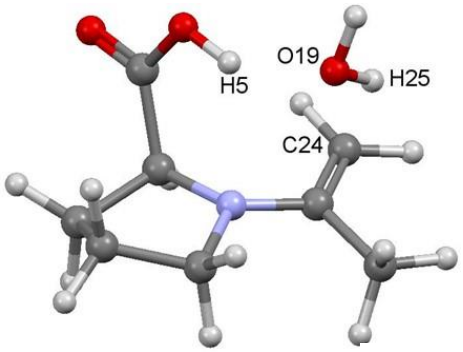 **16b_*syn***
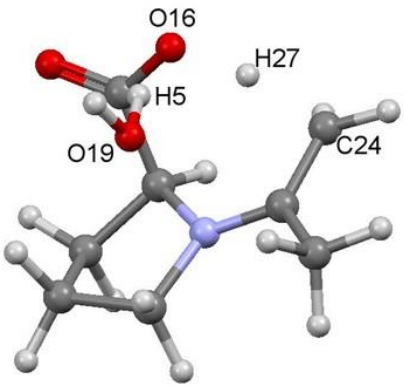 **17b**	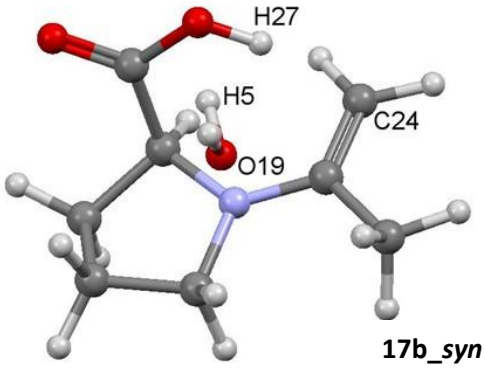 **17b_*syn***

7.3.2 Dissociation of the water molecule from the parent imine

In this experiment, we aimed to determine the energy barrier for the dissociation of the water molecule from the imine complex **13b** using an implicit solvation model. The d(N13,O19) reaction coordinate was selected and increased in steps of 0.2 Å (Figure 7.7). The data obtained shows a local minimum complex **14b** at d(N13,O19) = 5.429 Å which is marginally higher in E_{ZPVE} by ~ 1.3 kcal/mol but comparable in Gibbs free energy *G* to **13b**. The change in E_{ZPVE} when the water molecule is completely dissociated to form an isolated imine adduct (**13** in Figure 7.8) is +8 kcal/mol while Gibbs free energy *G* increased by +3.4 kcal/mol.

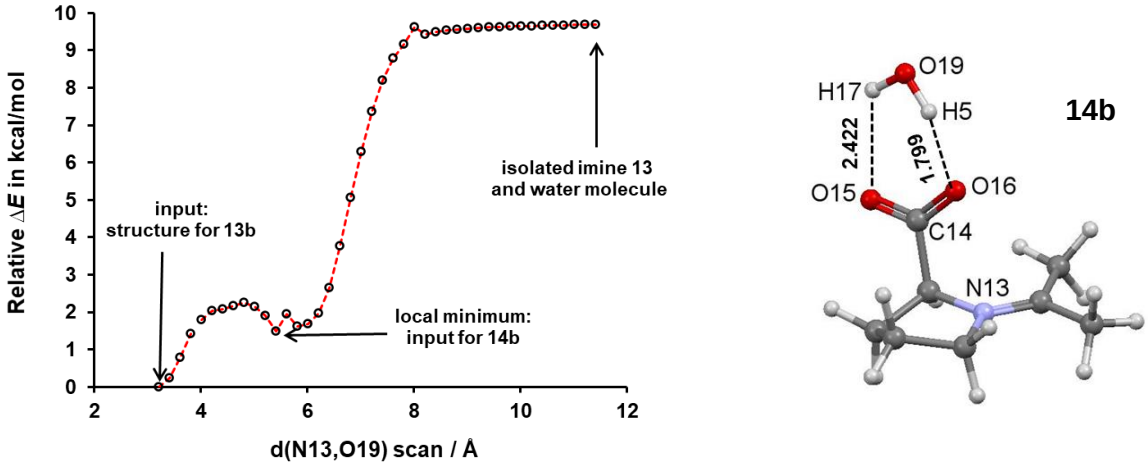

Figure 7.7. Data for d(N13,O19) reaction coordinate scan using the complex of water and imine adduct **13b**, resulting to a local minimum complex **14b** and complete separation/dehydration of the imine adduct at infinite separation.

The interaction of the water molecule with the parent imine in structures **13b** and **14b** is different, yet there is no difference in Gibbs free energy *G* in the two complexes. This implies that the molecule of water can easily float around the imine molecule. However, complete dissociation of the water molecule from the parent imine resulted to an increase in the energy of the molecular system as discussed above. To understand if the formation of the active enamine is feasible under dry conditions, there is a need to model this step using the imine **13** obtained from the dehydration of **13b** (Figure 6.8). The free energy barrier through **13-*syn*-ts** is 17.7 kcal/mol, which is lower than the three transition states obtained in the presence of a molecule of water. The barrier for the rotation of the C–N single bond in **13-*syn*** to form the catalytically active **13-*anti*** was found to be 6.4 kcal/mol (Part B in Figure 7.8). Since the imine adduct **13** is 3.4 kcal/mol higher in free energy than complex **13b**, the total free energy barrier for the formation of **13-*syn*** from **13b** is 21.1 kcal/mol. This reaction channel is unfavourable when compared to the mechanism through transition state **17b** obtained in the presence of water. Hence the complete dehydration of the imine

resulted in an unfeasible reactive channel. In the following section we investigated the influence of explicit solvent molecules water and DMSO in the enamine formation step.

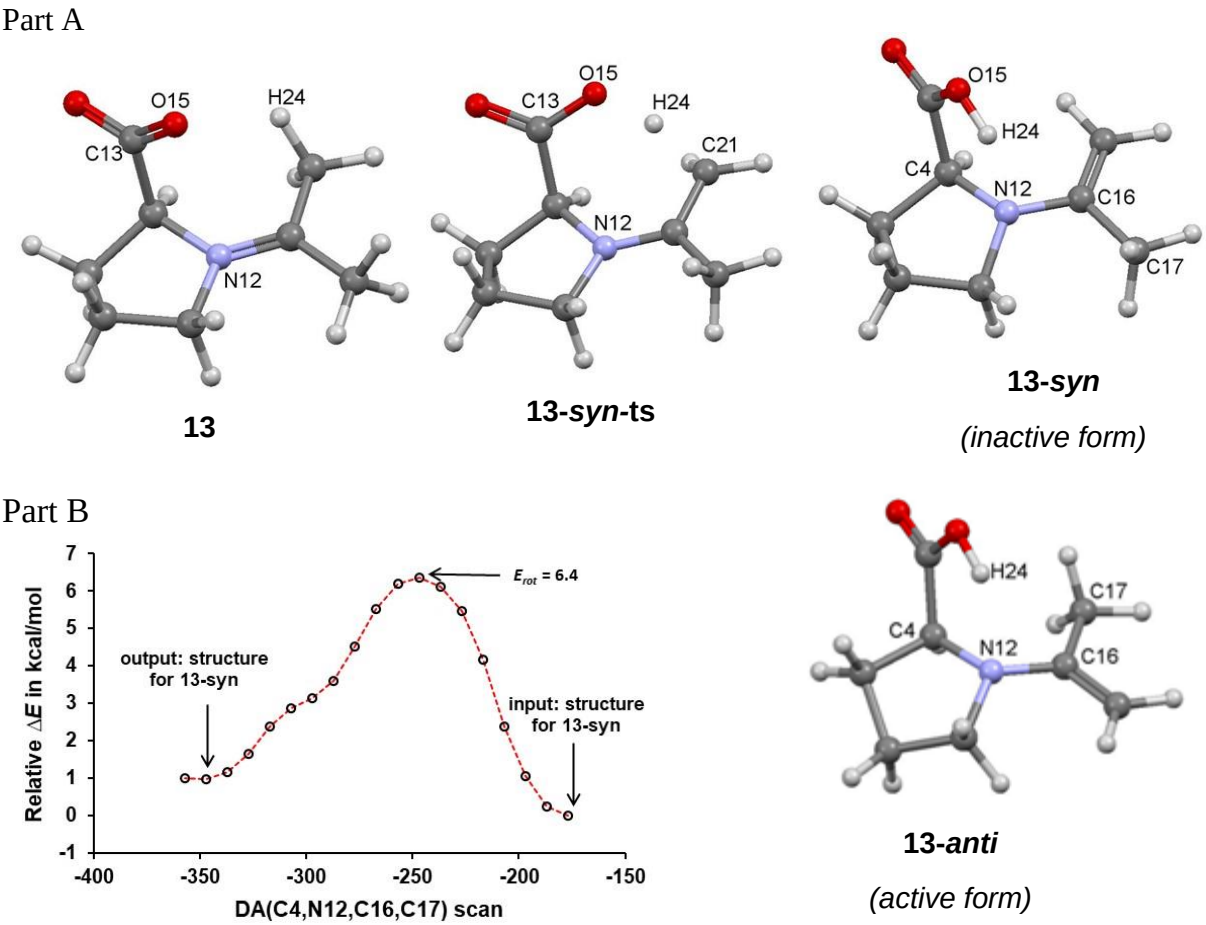

Figure 7. 8. Part A: Intermediate structures in *syn*-enamine formation (**13-*syn*)** from imine **13** through transition state **13-*syn*-ts**. Part B: rotation of the N12–C16 single bond of *syn*-enamine **13-*syn*** to *anti*–enamine **13-*anti***.

7.3.3 Enamine formation in the presence of an explicit solvent molecule of DMSO

The formation of the active enamine catalyst from the imine complexes **13B/B'** in the presence of explicit solvent molecules of water and DMSO was investigated. For the sake of simplicity, in place of **13B** and **13B'**, structures were renamed **13B-*syn*** and **13B-*anti*** respectively, (where the suffix indicates the identity of enamine conformer that will be eventually formed). In **13B-*syn***, the distance between O16 and H5 is 1.777 Å (not shown) while the d(O19,H23) distance is 2.610Å (Table 7.2). This suggests that the water molecule can act as a proton relay medium in the transfer of H5 to O19 while it is replaced by H23 resulting in the *syn* enamine. To this effect, the d(O19,H23) reaction coordinate of complex **13B-*syn*** was decreased in steps of –0.1 Å resulting in transition state **13B-*syn*-ts** and the *syn* enamine **13B-*syn*** (Figure 7.9). In **13B-*anti***, H27 is adjacent to O19 and the d(O19,H27) distance is 2.430 Å while the O19–H5···O16 hydrogen bonding

interaction is 1.786 Å (not shown). As in the case of the *syn* enamine formation, the active *anti*-enamine is formed by a proton relay mechanism mediated by the molecule of water. The proton, H27 in **13B-*anti*** is transferred to O19 of water, this pushes H5 to the oxygen atom (O16) of the carboxylic moiety resulting in the catalytically active *anti*-enamine.

Table 7.2. Ball and stick representation of structures leading to the formation of the enamine catalyst from imine complexes **13B-*syn*** and **13B-*anti***.

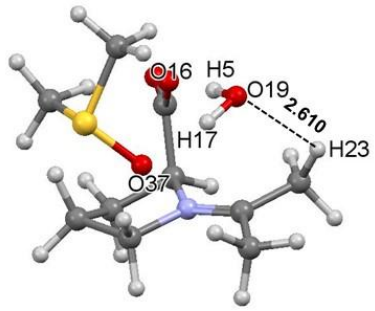 **13B-*syn***	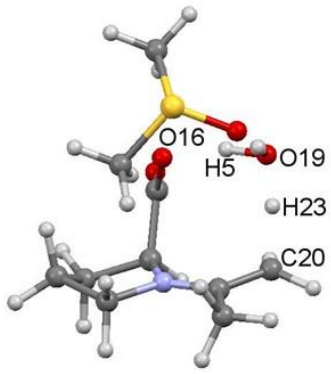 **13B-*syn*-ts**	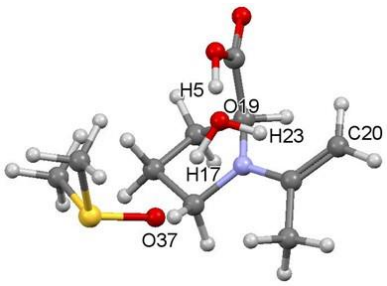 **14B-*syn***
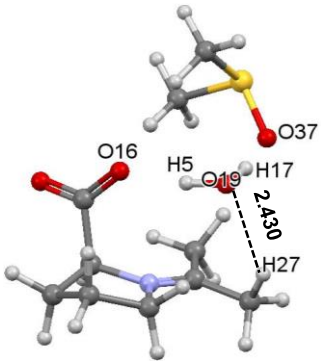 **13B-*anti***	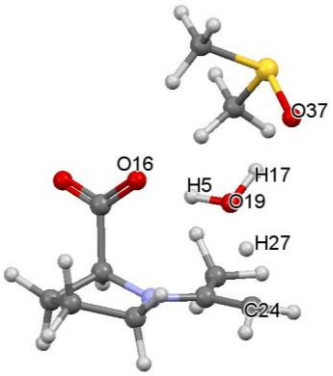 **13B-*anti*-ts**	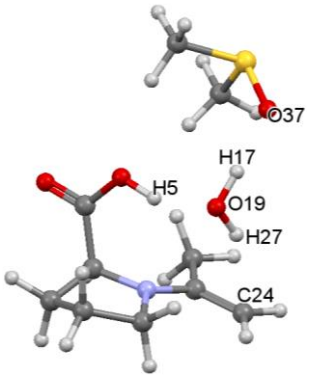 **14B-*anti***

Animation of the two transition states **13B-*syn*/*anti*-ts** show a concerted mechanism of the transfer of H5 from the water molecule to O16 while it is replaced by either H23 or H27. The free energy barrier for the formation of the enamine complexes **14-*anti*/14-*syn*** from imine complexes **13B-*anti*/13B-*syn*** is 17.1/18.9 kcal/mol, respectively. The relative energies of the two enamine conformers show that the catalytically active *anti*-enamine **14B-*anti*** is lower in energy than the inactive *syn* enamine **14B-*syn*** by ~ – 2 kcal/mol with respect to both E_{ZPVE} and Gibbs free energy *G*. In addition, on moving from **10B** to **14B-*anti*/*syn***, the data obtained shows that the formation of the **14B-*anti*** is also both free energy *G* and E_{ZPVE} favoured over the formation of **14B-*syn*** by – 2 kcal/mol. Although the difference between

the two mechanisms is marginal when modelled in the presence of solvent molecules of water and DMSO, the equilibrium of formation of **14B-*anti*** is expected to be pushed to the right due to its favourable reaction with the aldol acceptor substrate.[6, 10,14,15]

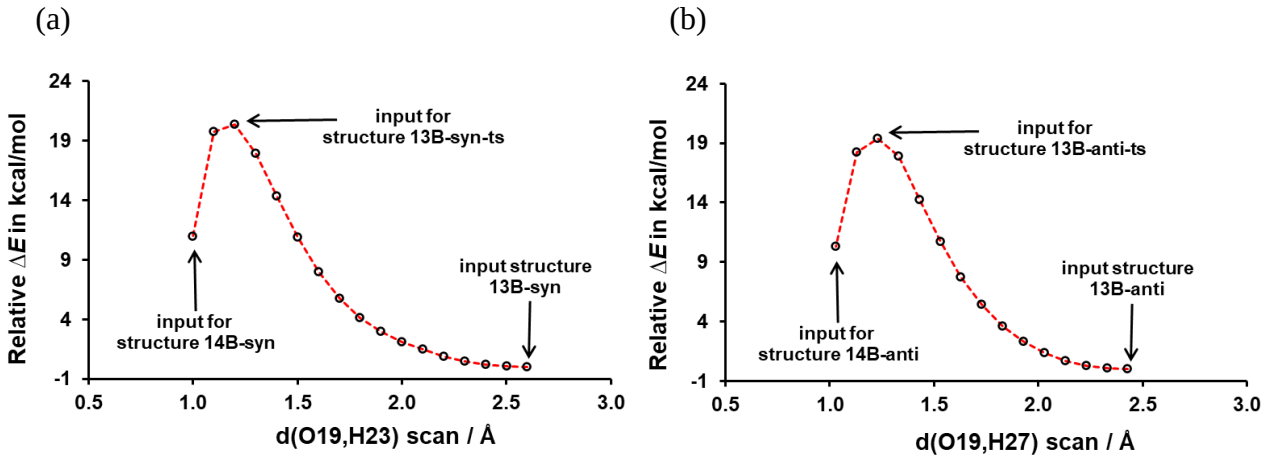

Figure 7.9. Data for scan of: (a) d(O19,H23) reaction coordinate using complex **13B-*syn*** and (b) d(O19,H27) reaction coordinate using complex **13B-*anti***, resulting in the formation of enamine complexes **14B-*syn*** and **14B-*anti***, respectively.

The overall mechanism of formation of the enamine catalyst through **10b/10B** using the two solvation models is shown in Figure 7.10. The energy barriers for the elimination of a water molecule is comparable under the two solvation models.

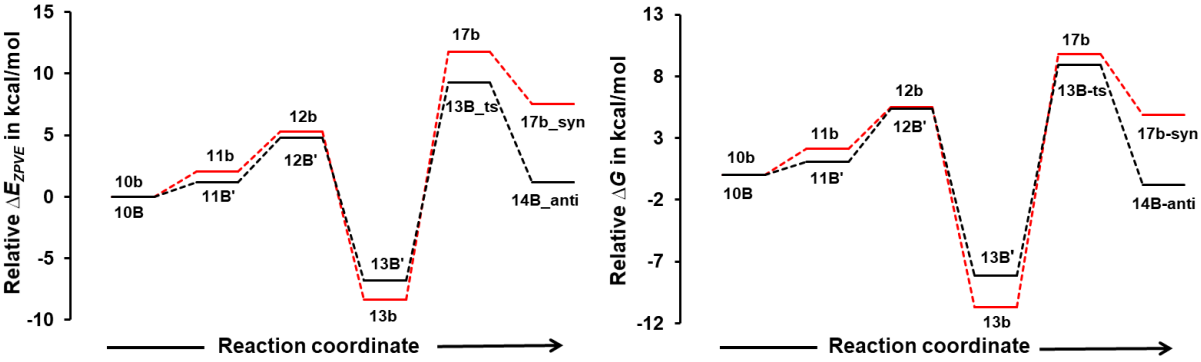

Figure 7.10. Reaction energy profiles for the formation of the active *anti*-enamine catalyst from complexes **10b** and **10B** obtained in the implicit solvation model and in the presence of a solvent molecule of DMSO, respectively.

The relative energy of **13b**, the water complex of imine **13** is lower than that of **13B'** by ~ – 2 kcal/mol. However, in the implicit solvation model, the transition state for enamine formation **17b** and the resulting *syn* enamine **17b-*syn*** are higher in energy than their equivalent structures obtained in the presence of an explicit solvent molecule of DMSO. Moreover, the change in free energy on moving from **10B** to **14B-*anti*** is negative ~ – 1 kcal/mol, this represent favourable and downhill energy change when an explicit solvent molecule of DMSO is used. On the other hand, the free

energy change on moving from **10b** to **17b-*syn*** is ~ 5 kcal/mol which represents an uphill and unfavourable pathway. Our results show that the water molecule directly participates in the formation of the active enamine catalyst while the solvent molecule of DMSO plays an important role of formation of key stabilizing hydrogen bonding interaction with both the imine and the molecule of water.

7.4. Conclusions

We have explained the mechanism of formation of the active enamine catalyst from the product of 2nd proton transfer. Contrary to the previous proposed enamine mechanism in the absence of a water molecule, we have shown that the dehydration or complete removal of the water molecule results in unfavourable change in Gibbs free energy. The dehydration of the imine adduct is Gibbs free energy unfavourable and reaction modelling can only be done with the inclusion of a water molecule. When the mechanism of enamine formation was modelled in the presence of an explicit solvent molecule of water, the change in free energy from **10b** to enamine **17b-*syn*** is ~ +5 kcal/mol. This clearly shows that the formation of an active enamine will not occur via this reaction pathway. When modelled in the presence of explicit solvent molecules of both water and DMSO, the formation of the active *anti* enamine **14B-*anti*** from **10B** represents a downhill change in free energy by – 1 kcal/mol. This shows that the solvent molecule of DMSO plays yet another critical and subtle role as already shown in Chapter 4.

7.5. References

1. Clemente, F. R.; Houk, K., *Angew, Chem.,* **2004**, *116* (43), 5890-5892.
2. Schmid, M. B.; Zeitler, K.; Gschwind, R. M., *Angew, Chem, Int, Ed.,* **2010**, *49* (29), 4997-5003.
3. Schmid, M. B.; Zeitler, K.; Gschwind, R. M., *J. Org, Chem.,* **2011**, *76* (9), 3005-3015.
4. Schmid, M. B.; Zeitler, K.; Gschwind, R. M., *Chem, Sci.,* **2011**, *2* (9), 1793-1803.
5. Rankin, K. N.; Gauld, J. W.; Boyd, R. J., *J. Phys, Chem., A:* **2002**, *106* (20), 5155-5159.
6. Ajitha, M. J.; Suresh, C. H., *J. Mol. Catal. A: Chem.,* **2011**, *345* (1), 37-43.
7. Yang, G.; Yang, Z.; Zhou, L.; Zhu, R.; Liu, C., *J. Mol. Catal. A: Chem.,* **2010**, *316* (1), 112-117.
8. Yang, G.; Zhou, L., *Catal, Sci, Technol.,* **2016**, *6* (10), 3378-3385.
9. List, B.; Lerner, R. A.; Barbas, C. F., *J. Am Chem, Soc.,* **2000**, *122* (10), 2395-2396.
10. Arnó, M.; Domingo, L. R., *Theor. Chem, Acc.,* **2002**, *108* (4), 232-239.
11. Armstrong, A.; Boto, R. A.; C*hem, Sci.,* **2014**, *5* (5), 2057-2071.
12. Pomès, R., Proton Relay in Membrane Proteins. ACS Publications: 2004.
13. Patil, M. P.; Sunoj, R. B., *J. Org, Chem.,* **2007**, *72* (22), 8202-8215.
14. Arnó, M.; Zaragozá, R. J.; Domingo, L. R., *Tetrahedron: Asymmetry* **2005**, *16* (16), 2764-2770.
15. Cheong, P. H.-Y.; Legault, C. Y.; Um, J. M.; Çelebi-Ölçüm, N.; Houk, K., *Chem, Rev.,* **2011,** *111* (8), 5042-5137.

Chapter 8

Conclusions and outlook

8.1. Conclusions

In this thesis, I have investigated and explained the mechanism of the formation of the active enamine which is the key intermediate in proline catalysed aldol reactions and proline catalysis in general. Enamines are known to be key intermediates and active catalysts in proline catalysis, hence their formation in proline catalysed organic transformations is fundamental. Beyond the classical use of changes in electronic energies as a means of explaining and predicting catalytic processes we have developed a protocol that provides an in-depth understanding of why perceived reactions are sometimes (un)successful. With this approach, every synthetic step is considered essential and the roles played by conformers, which are often ignored in classical studies are fully articulated and outlined using the REP-FAMSEC approach. Also, the subtle and critical role played by the explicit solvent molecule/s, in this case DMSO, is clearly highlighted.

This novel method explores the reaction pathway or reaction energy profile from conformers, to adduct formation, (global minimum adducts and best pre-organised adducts) through transition states to intermediates and products. The roles played by different conformers of *S*-proline (lowest energy conformer **1a**, higher energy conformer **1b** and the zwitterion **1c**) and the origins of their relative stability are fully explored. The relative increased stability of **1a** when compared to **1b** originates from the strength of covalent bonds and non-covalent bonding interactions which are stronger in **1a** by –39.2 kcal/mol, and – 8 kcal/mol, respectively. On the other hand, the increased stability of the zwitterion **1c** relative to **1a** is due to the strength of its covalent bonds which causes its total intramolecular interactions energy to be stronger by –18.9 kcal/mol compared to **1a**.

However, it is conformer **1b** rather than the lowest energy conformer **1a** or the zwitterion **1c** which leads to the formation of the active enamine catalyst after a reaction with acetone. The first step in the mechanism is commonly referred to as the C–N bond formation/1st H-transfer and is caused by an initial interaction between the molecules of proline and acetone. The interactions between the molecules of acetone and conformer **1b** are the strongest and this results in the smallest activation energy for the C–N bond formation/1st H-transfer. Intermolecular interaction between molecules of acetone and the zwitterion are the weakest and the reaction energy profile through the zwitterion is unfeasible, hence, this reaction pathway is cut-off before the initial proton transfer. The reaction energy profile through conformer **1a** cannot proceed beyond the initial H-transfer as it involves an extremely high energy barrier for the 2nd H-transfer step. The solvent molecule of DMSO plays a subtle yet critical role through its interactions with the molecules of proline and acetone. For **1a**, the solvent molecule of DMSO results in weak interactions between 1**a** and

acetone. On the contrary, **1b** and acetone intermolecular interactions are enhanced by the solvent molecule of DMSO. The energy barrier for the C–N bond formation/1st H-transfer is generally reduced when modelled in the presence of an explicit solvent molecule of DMSO but is more significantly decreased in the case of **1b**.

The zwitterion which is dominant in the presence of moisture and in DMSO can easily be converted to **1a** by an intramolecular H-transfer in which one of the protons attached to the ring nitrogen is transferred to the carboxylic group to form **1a**. Once conformer **1a** is formed it undergoes a ring puckering resulting in a structural change to form the catalytic active conformer **1b**. The structural change to **1b** is further enhanced by the presence of a solvent molecule of DMSO which lowers the energy barrier and relative energies of key intermediates by forming stabilizing intermolecular interactions.

At the point of formation of the active enamine catalyst from the imine, molecules of water will be undeniably present in the reaction vessel because the preceding step involves the elimination of a water molecule. I have demonstrated that the water molecule together with the explicit solvent molecule of DMSO forms a 3-MC with the parent imine which results in water acting as a medium for a proton relay and the formation of the active *anti*-enamine.

The mechanistic details discussed in this thesis are difficult and impossible to obtain using experimental tools alone. Moreover, large amounts of time, effort, ingenuity, and expensive instrumentation are required to probe the mechanism using experimental techniques. The use of theoretical calculations has proven to be very powerful and has great potential in the development of this area. The identification of key intermediates using theoretical tools allows important properties like NMR, absorption, or Raman spectra among others, to be obtained. These properties can easily be determined experimentally resulting in a comprehensive probing of the mechanism. It is important to stress that reaction mechanisms obtained using theoretical calculation must be supported by experimental observation or must have comparatively small energy barriers for them to be acceptable. This is mainly because theoretical chemists can model anything that is appealing to their imagination. Moreover, every proposed theoretical mechanism will look appealing to someone regardless of the calculated energy barriers.

8.2. Outlook

This case study on the mechanism of proline catalysed aldol reactions was incited by our interest in understanding reaction mechanisms at atomic and molecular fragment level. Proline and its analogues have been successfully used as organocatalysts for a range of both racemic and chiral organic transformations including closely related aldol condensations, Mannich reactions and Michael reactions. The role of the proline and the 5-membered pyrrolidine ring is also reasonably well understood and reported. However, there is no evidence to rationalise why structural changes to the amino acid result in large changes in its ability to catalyse reactions in terms of yield and enantioselectivity. For example, the six membered ring (pipecolic acid) and the four membered azetidine ring are unreactive towards the direct aldol reactions of aldehydes and ketones. This lack of fundamental understanding makes the development of new organocatalysts both difficult and time consuming as most endeavours rely on the synthesis and subsequent testing of libraries of these catalysts. The approaches reported in this thesis have the potential to open avenues for rationalizing why the above-mentioned amino acids and other naturally occurring amino acids are unreactive, towards the aldol reaction

On the other hand, subtle substitution on the pyrrolidine ring of proline dramatically affects the reaction yields and the stereoselectivity of the aldol product. There is no fundamental understanding of why such phenomena are observed. As result, efforts to improve the catalytic performance of proline is a monotonous process based on trial and error. The REP-FAMSEC approach has the potential to provide explanation or even predict such phenomenon before the derivatisation is done in the laboratory. As such, methods and procedures for the derivatising proline with key functional groups aimed at improving its efficiency and catalytic performance can be developed.

It was also observed that branched substrates like isobutyraldehyde gave high yields and selectivity of the aldol product compared to straight chain substrates like 1-pentanal, and this could not be explained using classical approaches. The REP-FAMSEC methodology described in this thesis has the potential of providing explanations for such observations.

There is another and long-term potential benefit of the REP-FAMSEC approach. There are many well-established protocols in synthetic organic chemistry, often named by the researchers who developed them. Unfortunately, there is little information available in terms of the fundamental origin of their (un)successful performance in many instances. It would be of utmost interest and

importance to embark on exploration of well-established reactions using the REP-FAMSEC approach with the aim of discovering common and differentiating fundamental properties.

Appendix A

Supporting Information for Chapter 3

PART A1

Computational details and coordinates for all structures

All calculations were performed in Gaussian 09 Rev. D01 at the RB3LYP/6–311++G(d,p) with Grimme's empirical correction for dispersion (GD3) and RMP2/6–311++G(d,p) levels of theory in solvent (DMSO) using the implicit default solvation model. The B3LYP-optimised local, global and transition state (TS) structures were also optimised at the RMP2 level and frequency calculations were performed on these structures at both levels of theory. None and one imaginary frequency was obtained for minimum energy (local and global) and TS structures, respectively. Topological calculations were performed in AIMAll (ver. 17.11.14) using B3LYP-generated wavefunctions.

RB3LYP Coordinates

2

Atom	X	Y	Z
C1	-0.00462863	0.178140532	0.6151523
O2	-0.0134421	0.517341082	1.7864747
C3	-1.28134278	-0.124580786	-0.1338366
H4	-2.13578709	-0.108943756	0.5416987
H5	-1.42267733	0.624186195	-0.9201481
H6	-1.21074387	-1.096426665	-0.6304427
C7	1.28356795	0.038941613	-0.1618913
H8	1.43279417	-1.013549159	-0.4243945
H9	1.22377847	0.594769111	-1.1018739
C10	2.12848123	0.39012183	0.4292614

Zero-point correction =	0.083228 (Hartree/Particle)
Thermal correction to Energy =	0.088510
Thermal correction to Enthalpy =	0.089454
Thermal correction to Gibbs Free Energy =	0.056063
Sum of electronic and zero-point Energies =	–193.146706
Sum of electronic and thermal Energies =	–193.141424
Sum of electronic and thermal Enthalpies=	–193.140480
Sum of electronic and thermal Free Energies=	–193.173871

1a

Atom	X	Y	Z
C1	-0.0945820881	-1.3616508300	-0.8365335880
C2	-0.5190690347	-1.2573374716	0.6302290991
C3	-1.0788227389	0.1706950832	0.7151583197
C4	-0.1246813852	0.9722544295	-0.1992426764
H5	0.3281244270	0.2480799094	-2.1025552561
H6	0.6591109463	-2.1308210435	-1.0132112033
H7	-0.9632543973	-1.5761338223	-1.4696052990
H8	-1.2490175462	-2.0185574329	0.9075498900
H9	0.3511233168	-1.3671245973	1.2850414934
H10	-2.0880936170	0.2049830909	0.2983008665
H11	-1.1155132690	0.5735847011	1.7271909176
H12	-0.6469204573	1.7777075250	-0.7198264624
N13	0.4628012476	-0.0166263775	-1.1345153508
C14	1.0098594764	1.6334091005	0.6007483932
O15	0.8307496198	2.4944067393	1.4355402361
O16	2.2188399062	1.1665470996	0.2925674012
H17	2.0193456037	0.4865838968	-0.4168367709

Zero-point correction =	0.144439 (Hartree/Particle)
Thermal correction to Energy =	0.151574
Thermal correction to Enthalpy =	0.152518
Thermal correction to Gibbs Free Energy =	0.112465
Sum of electronic and zero-point Energies =	–401.167135
Sum of electronic and thermal Energies =	–401.160000
Sum of electronic and thermal Enthalpies =	–401.159056
Sum of electronic and thermal Free Energies =	–401.199110

1b

Atom	X	Y	Z
C1	-0.4090342829	-1.2417777602	-1.0365123470
C2	-0.6679877535	-1.5447881579	0.4695639391
C3	-0.3162309883	-0.2234293381	1.2092014177
C4	-0.0898466893	0.7677367134	0.0537820277
H5	1.3839410276	-0.3040841776	-0.8583830776
H6	0.0865113893	-2.0562345172	-1.5651403464
H7	-1.3492538419	-1.0266239834	-1.5514139257
H8	-1.7054929740	-1.8402176315	0.6362186313
H9	-0.0336802727	-2.3620827660	0.8174100463
H10	-1.1028450646	0.1090238381	1.8868095774
H11	0.6032172475	-0.3273668019	1.7897031322
H12	-1.0601281261	1.1753315470	-0.2628674836
N13	0.4290475018	-0.0221423670	-1.0821181369
C14	0.7733566709	1.9810686690	0.3373918600
O15	0.9007085432	2.5009165302	1.4196362013
O16	1.3832903879	2.4938242140	-0.7505225570
H17	1.1744272251	1.9208459692	-1.5127589589

Zero-point correction =	0.144477 (Hartree/Particle)
Thermal correction to Energy =	0.151947
Thermal correction to Enthalpy =	0.152891
Thermal correction to Gibbs Free Energy =	0.111845
Sum of electronic and zero-point Energies =	–401.156469
Sum of electronic and thermal Energies =	–401.149000
Sum of electronic and thermal Enthalpies =	–401.148056
Sum of electronic and thermal Free Energies =	–401.189101

3a

Atom	X	Y	Z
C1	-0.6916850048	-1.9375015508	-1.2185793238
C2	-1.6069619830	-2.3973912377	-0.0787230580
C3	-1.6756783939	-1.1474146077	0.8128553526
C4	-1.6270080967	0.0247043311	-0.2081486431
H5	-1.7704851814	-0.4732417091	-2.2069861297
H6	0.3512071852	-1.9667144146	-0.8932061339
H7	-0.7883639362	-2.5209893400	-2.1346306448
H8	-2.5984753746	-2.6468021265	-0.4697230819
H9	-1.2178388612	-3.2685219087	0.4522526545
H10	-2.5713304507	-1.1019025535	1.4316952680
H11	-0.8035236500	-1.1094406505	1.4685078165
H12	-2.6229400284	0.4422444921	-0.3716703728
N13	-1.0753773719	-0.5240601710	-1.4719324254
C14	-0.7413908516	1.1752989962	0.2726118365
O15	-0.9240760916	1.7908845175	1.3008615327
O16	0.2768470597	1.4393638881	-0.5494302064
H17	0.1495733464	0.7766572727	-1.2886132891
C18	2.3804416706	-0.3210758444	1.0129221934
O19	1.7233567346	-1.3294925621	1.2145379515
C20	3.1570755963	-0.1243680716	-0.2663318614
H21	2.8825172843	-0.8796087298	-1.0021978211
H22	2.9830106501	0.8770626844	-0.6662276427
H23	4.2268303159	-0.2050568301	-0.0454639043
C24	2.4480348022	0.7957037052	2.0249368385
H25	3.4689521540	1.1722585878	2.1262586158
H26	1.8279292207	1.6204998632	1.6594133813
H27	2.0658592563	0.4631039696	2.9895110972

Zero-point correction =	0.228970 (Hartree/Particle)
Thermal correction to Energy =	0.243408
Thermal correction to Enthalpy =	0.244352
Thermal correction to Gibbs Free Energy =	0.184586
Sum of electronic and zero-point Energies =	–594.318801
Sum of electronic and thermal Energies =	–594.304363
Sum of electronic and thermal Enthalpies =	–594.303419
Sum of electronic and thermal Free Energies =	–594.363185

3b

Atom	X	Y	Z
C1	-2.2641727131	0.5704324091	-2.2935412506
C2	-2.0183714657	1.5842351092	-1.1681108589
C3	-0.8059885576	0.9801408678	-0.4439682103
C4	-0.9740779599	-0.5687808272	-0.6636731390
H5	-2.8582022975	-1.0642012062	-1.2137865744
H6	-3.2712514758	0.6079634282	-2.7124366242
H7	-1.5537592881	0.7355269124	-3.1115116773
H8	-1.8282619419	2.5974992927	-1.5286952714
H9	-2.8862263879	1.6138216175	-0.5022746603
H10	0.1252672965	1.3075405241	-0.9106044184
H11	-0.7610090224	1.2544835081	0.6109148953
H12	-0.0230654376	-0.9870289409	-1.0036226683
N13	-2.0144019294	-0.7549819190	-1.6896299842
C14	-1.3453822750	-1.2676302056	0.6389173393
O15	-2.4684636724	-1.6472373097	0.9006609884
O16	-0.3565017639	-1.4231858963	1.5223523830
H17	0.5146478782	-1.0923819410	1.1767835190
C18	2.5928144812	0.4425407195	0.8724470209
O19	1.9985879889	-0.5861617150	0.5635727742
C20	2.0666762043	1.3731017646	1.9301715900
H21	1.7603282723	2.3101156938	1.4538636000
H22	1.2171640502	0.9375330099	2.4539337205
H23	2.8588761693	1.6234335351	2.6401492003
C24	3.8783079403	0.8204182318	0.1938785126
H25	3.8232290415	1.8504326052	-0.1691391111
H26	4.6912234572	0.7862626391	0.9265267231
H27	4.0954134082	0.1396080928	-0.6274778183

Zero-point correction =	0.228937 (Hartree/Particle)
Thermal correction to Energy =	0.243389
Thermal correction to Enthalpy =	0.244334
Thermal correction to Gibbs Free Energy =	0.183671
Sum of electronic and zero-point Energies =	–594.317076
Sum of electronic and thermal Energies =	–594.302624
Sum of electronic and thermal Enthalpies =	–594.301680
Sum of electronic and thermal Free Energies =	–594.362342

4a

Atom	X	Y	Z
C1	-0.2142578068	-1.3418801271	-0.6664473997
C2	-1.5993364941	-1.9535653225	-0.9065553140
C3	-2.4317407846	-1.3178920232	0.2147961561
C4	-1.8537336948	0.1227623131	0.3059517752
H5	-0.3465398083	0.7035998494	-0.9764160675
H6	0.3093019067	-1.8825469812	0.1290069959
H7	0.4270260249	-1.3405016675	-1.5488502351
H8	-1.9812426733	-1.6456154512	-1.8848729234
H9	-1.5982367073	-3.0445856784	-0.8650357576
H10	-3.5037840457	-1.3096521626	0.0208739079
H11	-2.2644169649	-1.8526202978	1.1544787088
H12	-2.4658115594	0.8145605046	-0.2778743371
N13	-0.4747751384	0.0473074059	-0.2171946258
C14	-1.8626370569	0.6309580569	1.7456262804
O15	-2.8816372374	0.8780779951	2.3574583669
O16	-0.6586507062	0.7624525769	2.3025529247
H17	0.0073932101	0.5297890487	1.6066048547
C18	2.7366003409	-0.0651676578	0.6869122870
O19	2.1165168599	-0.1564435759	1.7337352907
C20	3.5475739128	-1.2165586342	0.1448892824
H21	3.5698117180	-2.0404322372	0.8570093945
H22	3.1006535318	-1.5566501065	-0.7950054992
H23	4.5651123049	-0.8903302141	-0.0880145211
C24	2.7316702357	1.2037349710	-0.1295742178
H25	3.7288412825	1.6549083488	-0.0870051502
H26	2.5269593588	0.9845679163	-1.1807225829
H27	1.9962399911	1.9063231507	0.2584724064

Zero-point correction =	0.228542 (Hartree/Particle)
Thermal correction to Energy =	0.243192
Thermal correction to Enthalpy =	0.244136
Thermal correction to Gibbs Free Energy =	0.183038
Sum of electronic and zero-point Energies =	–594.318198
Sum of electronic and thermal Energies =	–594.303549
Sum of electronic and thermal Enthalpies =	–594.302604
Sum of electronic and thermal Free Energies =	–594.363702

4b

Atom	X	Y	Z
C1	-0.1705743733	2.2625588835	-0.2296233115
C2	-1.6761737669	2.5380035918	0.0194944711
C3	-2.2901023528	1.1345282590	0.2746682983
C4	-1.0790489148	0.1804647631	0.2294733497
H5	-0.3068646154	0.7383195994	-1.5847054566
H6	0.2691896879	2.8933345220	-1.0034665566
H7	0.3989802266	2.4155604209	0.6925745741
H8	-1.8230059502	3.2141048018	0.8641064264
H9	-2.1328889599	3.0030084112	-0.8568177672
H10	-2.8138662671	1.0674281728	1.2299900201
H11	-2.9954616580	0.8632950354	-0.5118461906
H12	-0.6485011465	0.0793254136	1.2320526387
N13	-0.0488869504	0.8401142533	-0.6048232405
C14	-1.3742978437	-1.2264964519	-0.2913608127
O15	-2.3747288993	-1.5187670048	-0.9110364716
O16	-0.4444313465	-2.1536309177	-0.0417117532
H17	0.3372161545	-1.7845212918	0.4494772794
C18	2.3797330493	-0.3848354803	0.4472006969
O19	1.6399069737	-1.0241979952	1.1921448964
C20	2.6822270222	-0.8422165771	-0.9536016125
H21	1.9475290966	-1.5684235454	-1.2967404908
H22	2.7247829471	0.0044841248	-1.6392909278
H23	3.6721920945	-1.3134559482	-0.9451927161
C24	3.0858460230	0.8480144796	0.9339154646
H25	4.1672709971	0.7269121054	0.8181619936
H26	2.7906698696	1.6961909234	0.3104755157
H27	2.8403909027	1.0490004512	1.9756416826

Zero-point correction =	0.229360 (Hartree/Particle)
Thermal correction to Energy =	0.243496
Thermal correction to Enthalpy =	0.244441
Thermal correction to Gibbs Free Energy =	0.186547
Sum of electronic and zero-point Energies =	–594.313547
Sum of electronic and thermal Energies =	–594.299411
Sum of electronic and thermal Enthalpies =	–594.298466
Sum of electronic and thermal Free Energies =	–594.356360

5a

Atom	X	Y	Z
C1	-0.0171571315	-1.9617347208	-0.4179515031
C2	-1.5104260512	-2.1161066394	-0.6847728431
C3	-2.1145567745	-1.0140397845	0.1894788547
C4	-1.0800479450	0.1488501252	0.1230439600
H5	0.3431549380	-0.1531409416	-1.3248784554
H6	0.2598532175	-2.3563482371	0.5630904862
H7	0.6209771353	-2.4107147098	-1.1757246461
H8	-1.7246885314	-1.9372197639	-1.7423963487
H9	-1.8774877917	-3.1095480543	-0.4237611380
H10	-3.0968917020	-0.6779127909	-0.1387118297
H11	-2.2054524682	-1.3678063925	1.2198196968
H12	-1.3776079701	0.8826085825	-0.6228925990
N13	0.2084380865	-0.4874363814	-0.3744340564
C14	-1.1222967116	0.8851515543	1.4752560128
O15	-2.0335630020	1.6895119170	1.6199679096
O16	-0.3030363747	0.5738758265	2.4421832989
H17	0.6192000107	0.0398139417	2.1519041614
C18	1.8651856094	-0.1017953435	0.4842933168
O19	1.7094576568	-0.5393201226	1.6910288907
C20	2.8380475301	-0.8893770490	-0.3759160618
H21	2.7271615466	-1.9591519660	-0.2043707467
H22	2.7394021364	-0.6660248145	-1.4397873798
H23	3.8453066734	-0.5990076149	-0.0632659391
C24	1.9416025032	1.4052948871	0.2627397574
H25	2.9179841381	1.7318104600	0.6322268536
H26	1.8744880872	1.6693386528	-0.7941016133
H27	1.1798531848	1.9452293796	0.8226319615

Zero-point correction =	0.229618 (Hartree/Particle)
Thermal correction to Energy =	0.241264
Thermal correction to Enthalpy =	0.242208
Thermal correction to Gibbs Free Energy =	0.192049
Sum of electronic and zero-point Energies =	–594.300687
Sum of electronic and thermal Energies =	–594.289042
Sum of electronic and thermal Enthalpies =	–594.288098
Sum of electronic and thermal Free Energies =	–594.338256

5b

Atom	X	Y	Z
C1	-0.4029099281	1.3024110333	-1.3257489985
C2	-1.9174399546	1.1114922786	-1.2901921809
C3	-2.1834922370	0.8312475511	0.1981415825
C4	-0.9399721225	0.0612790829	0.6793408962
H5	0.1943058859	-0.6154258908	-0.9217070965
H6	0.0561870105	1.1769755716	-2.3047158504
H7	-0.1273985150	2.2768937074	-0.9233666977
H8	-2.4507093678	1.9873852726	-1.6609547142
H9	-2.2025856696	0.2523472733	-1.9039702688
H10	-2.2678017114	1.7688597043	0.7506649607
H11	-3.0878022452	0.2499351600	0.3684762229
H12	-0.5325898950	0.4806547448	1.6016662342
N13	0.1122124629	0.2513814606	-0.3926802541
C14	-1.1493198352	-1.4420429328	0.9512781460
O15	-2.2523012523	-1.9540080953	0.9621994976
O16	-0.0446733842	-2.1218056864	1.1794168958
H17	0.8046998199	-1.4830678168	1.2384240659
C18	1.7889211545	0.3746539540	0.3300891472
O19	1.7806308693	-0.4765103396	1.3163419522
C20	1.9013903880	1.8343898516	0.7458282002
H21	1.9060922502	2.5253085689	-0.0977119907
H22	1.1037110631	2.1040017957	1.4408652989
H23	2.8521357775	1.9371285989	1.2747447019
C24	2.6385386973	0.0005673327	-0.8805560437
H25	2.4516086592	0.6421630568	-1.7440071915
H26	3.6876550476	0.1113665282	-0.5934985386
H27	2.4739070320	-1.0445817657	-1.1523679766

Zero-point correction =	0.230689 (Hartree/Particle)
Thermal correction to Energy =	0.242251
Thermal correction to Enthalpy =	0.243195
Thermal correction to Gibbs Free Energy =	0.193182
Sum of electronic and zero-point Energies =	–594.302870
Sum of electronic and thermal Energies =	–594.291308
Sum of electronic and thermal Enthalpies =	–594.290364
Sum of electronic and thermal Free Energies =	–594.340377

6a

Atom	X	Y	Z
C1	-0.1603524393	-1.5611266845	0.9399083284
C2	-1.6587996187	-1.7059470406	0.6222442348
C3	-1.7869742887	-1.2988729275	-0.8548002985
C4	-0.7551554935	-0.1738990383	-1.0005381376
H5	0.7958921265	-1.4796061116	-0.8835772537
H6	0.0371684123	-0.9891542427	1.8409757273
H7	0.3593910856	-2.5145947462	0.9964298973
H8	-2.0088865609	-2.7212415294	0.8055698201
H9	-2.2398111414	-1.0291770444	1.2509376054
H10	-1.5259016630	-2.1327896799	-1.5128308850
H11	-2.7813104438	-0.9496536568	-1.1249600856
H12	-0.4340085535	-0.0265851489	-2.0295651408
N13	0.4305112578	-0.7822587489	-0.2340376859
C14	-1.3269921850	1.1783591290	-0.4810370308
O15	-2.2443068597	1.6205342628	-1.1914411544
O16	-0.8618964088	1.6943083531	0.5751585493
H17	0.5754507787	1.3025383786	1.1139162385
C18	1.7006089781	0.0987347134	0.1254193602
O19	1.4371168523	0.8172042996	1.2746771558
C20	1.9993966296	0.9840846083	-1.0835998143
H21	1.2171637880	1.7273717131	-1.2355518816
H22	2.9334213687	1.5112627790	-0.8852576306
H23	2.1232021099	0.3965009921	-1.9960270247
C24	2.8361320230	-0.8757807549	0.4182230516
H25	3.0706191044	-1.4981672330	-0.4477161235
H26	3.7220174294	-0.2921002793	0.6704665720
H27	2.5930037120	-1.5108443624	1.2704136064

Zero-point correction =	0.234574 (Hartree/Particle)
Thermal correction to Energy =	0.246325
Thermal correction to Enthalpy =	0.247270
Thermal correction to Gibbs Free Energy =	0.197264
Sum of electronic and zero-point Energies =	–594.309671
Sum of electronic and thermal Energies =	–594.297919
Sum of electronic and thermal Enthalpies =	–594.296975
Sum of electronic and thermal Free Energies =	–594.346980

6b

Atom	X	Y	Z
C1	-0.3093767288	1.0397269453	-1.4207433194
C2	-1.8304584926	0.9978867458	-1.2953874471
C3	-2.0460736433	1.0078190952	0.2237853641
C4	-0.9464056075	0.0785582145	0.7513967534
H5	0.1604945402	-0.8367186830	-0.6044614963
H6	0.0830306840	0.6544180127	-2.3589974143
H7	0.0677758136	2.0475499194	-1.2583573451
H8	-2.2940884610	1.8436074136	-1.8030670647
H9	-2.2223914799	0.0775699166	-1.7361995974
H10	-1.9090971057	2.0178113930	0.6182649102
H11	-3.0299790730	0.6532052101	0.5271947259
H12	-0.5645824023	0.3675162666	1.7258979511
N13	0.1696130890	0.1627216567	-0.2845289097
C14	-1.3653211282	-1.4238718667	0.8260269206
O15	-2.2686926995	-1.6975288939	1.6340280314
O16	-0.7322979609	-2.1991396262	0.0530376434
H17	1.8432089004	-1.4054178552	0.9529364658
C18	1.5881531700	0.4171985520	0.2664039693
O19	1.7746888382	-0.5094075679	1.3097579027
C20	1.6989050150	1.8018486852	0.8858444600
H21	1.5830808106	2.5890799146	0.1424441601
H22	0.9629832456	1.9436232260	1.6775949174
H23	2.6932337290	1.8914971152	1.3238205334
C24	2.5791611458	0.1974166469	-0.8724772391
H25	2.4522935387	0.9365720409	-1.6640801261
H26	3.5887621219	0.2909511223	-0.4714316655
H27	2.4664801407	-0.8013935996	-1.3030030842

Zero-point correction =	0.234061 (Hartree/Particle)
Thermal correction to Energy =	0.246190
Thermal correction to Enthalpy =	0.247135
Thermal correction to Gibbs Free Energy =	0.195918
Sum of electronic and zero-point Energies =	–594.313838
Sum of electronic and thermal Energies =	–594.301708
Sum of electronic and thermal Enthalpies =	–594.300764
Sum of electronic and thermal Free Energies =	–94.3519810

7

Atom	X	Y	Z
C1	0.2982293938	-2.0957021832	-0.4912330199
C2	-0.7260973320	-2.1544267976	0.6378051803
C3	-1.7174141961	-1.0072549374	0.3240957042
C4	-1.1035792293	-0.2288594418	-0.8555576085
H5	0.7575080752	-0.5246842948	-1.7763055902
H6	1.2771671522	-2.4982136219	-0.2562184256
H7	-0.0689391928	-2.5887120491	-1.3921868467
H8	-1.2041425600	-3.1331476852	0.6687251897
H9	-0.2382779542	-1.9803862466	1.5968523904
H10	-2.6997084266	-1.3780026380	0.0303667777
H11	-1.8446451550	-0.3545890537	1.1854061615
H12	-1.4481751480	-0.6472632872	-1.7994757675
N13	0.3910404865	-0.6205093904	-0.8293921071
C14	-1.4619194341	1.2920571162	-0.8883873446
O15	-2.0250069703	1.6865806774	-1.9234707462
O16	-1.2035886527	1.9725327664	0.1477687642
H17	-0.0545122369	1.2328756540	0.9891994773
C18	1.3660682428	0.2619859602	0.0940490550
O19	0.6850505314	0.6038257707	1.2434451571
C20	1.7831044493	1.4575064467	-0.7706280475
H21	0.9308208164	2.0302444661	-1.1299317228
H22	2.3956177425	2.1145931395	-0.1521203414
H23	2.3836824854	1.1309619727	-1.6226875648
C24	2.5818585135	-0.5641720622	0.4890840280
H25	3.0832105609	-1.0018263430	-0.3753236552
H26	3.2822953772	0.1110438584	0.9823836404
H27	2.3139526606	-1.3443577962	1.2008372624

Zero-point correction =	0.235153 (Hartree/Particle)
Thermal correction to Energy =	0.246784
Thermal correction to Enthalpy =	0.247728
Thermal correction to Gibbs Free Energy =	0.198108
Sum of electronic and zero-point Energies =	–594.301751
Sum of electronic and thermal Energies =	–594.290120
Sum of electronic and thermal Enthalpies =	–594.289176
Sum of electronic and thermal Free Energies =	–594.338796

8

Atom	X	Y	Z
C1	0.4722714307	-1.7931193190	-0.9699678577
C2	-0.4084548344	-2.3899837540	0.1522703504
C3	-1.3985562225	-1.2621027291	0.5513734610
C4	-1.2529491073	-0.2406661687	-0.5694321616
H5	0.3577413833	0.1187470566	-1.8156092944
H6	1.5325036959	-2.0135683130	-0.8949277460
H7	0.1315259609	-2.1063362616	-1.9558229237
H8	-0.9349600091	-3.2640493246	-0.2303796979
H9	0.1938721403	-2.7147355704	0.9995090589
H10	-2.4267311843	-1.6108980450	0.6183435781
H11	-1.1386506982	-0.8106335601	1.5099483000
H12	-1.7114743236	-0.6581651505	-1.4734605802
N13	0.2396286985	-0.2982596936	-0.8925697359
C14	-1.8843429405	1.1669184142	-0.4665066339
O15	-2.9801121548	1.2193441845	0.1120313904
O16	-1.2627192158	2.1007540316	-1.0592171982
H17	0.1199172494	2.0588027397	-0.0518459130
C18	1.2892098462	0.5044542251	0.0353783839
O19	0.6424706199	1.5721016590	0.6303783040
C20	2.3781341306	0.9466297365	-0.9418450452
H21	1.9705523324	1.6400320807	-1.6823297266
H22	3.1557102360	1.4642788739	-0.3796567208
H23	2.8303524838	0.0966710353	-1.4575571574
C24	1.8405738948	-0.3529445445	1.1673319674
H25	2.4034459947	-1.2162659385	0.8185750861
H26	2.5241135899	0.2856382542	1.7283907884
H27	1.0507270033	-0.6705439186	1.8445977239

Zero-point correction =	0.234647 (Hartree/Particle)
Thermal correction to Energy =	0.246415
Thermal correction to Enthalpy =	0.247359
Thermal correction to Gibbs Free Energy =	0.197330
Sum of electronic and zero-point Energies =	–594.296720
Sum of electronic and thermal Energies =	–594.284952
Sum of electronic and thermal Enthalpies =	–594.284008
Sum of electronic and thermal Free Energies =	–594.334037

9a

Atom	X	Y	Z
C1	0.3840649949	-1.6807530894	-1.1254104814
C2	-0.4296596300	-2.4017196034	0.0076021589
C3	-1.3647230266	-1.3097792510	0.6350233223
C4	-1.2628190561	-0.2419604123	-0.4347763148
H5	-0.1615703227	0.7968619808	-1.5892177371
H6	1.4410339258	-1.9318985223	-1.1383940911
H7	-0.0245704768	-1.9060248712	-2.1105153911
H8	-1.0179709031	-3.2118135273	-0.4248388703
H9	0.2296125906	-2.8396732140	0.7562331855
H10	-2.3865417351	-1.6666041934	0.7588184012
H11	-1.0074045981	-0.9576618061	1.6019462897
H12	-1.7738342961	-0.6641265278	-1.3130267784
N13	0.1733214716	-0.2243149459	-0.8690517737
C14	-1.7122547391	1.2167690212	-0.5345692081
O15	-2.6427349748	1.7256654320	0.0663782109
O16	-0.9778565964	1.7694267751	-1.4763114182
H17	0.5018658321	2.2154649446	0.2179058519
C18	1.2362249533	0.4017566503	0.0863071479
O19	0.6469257400	1.4632234373	0.8069227220
C20	2.3456705639	0.9025168979	-0.8406478492
H21	1.9586718254	1.6555060344	-1.5319281176
H22	3.1430460117	1.3489083176	-0.2449282725
H23	2.7652465233	0.0832161630	-1.4273067950
C24	1.7991649574	-0.5359313787	1.1545645389
H25	2.2807273640	-1.4141821813	0.7291181010
H26	2.5551333010	0.0263715307	1.7041954333
H27	1.0349302998	-0.8467436608	1.8628077349

Zero-point correction =	0.229737 (Hartree/Particle)
Thermal correction to Energy =	0.241029
Thermal correction to Enthalpy =	0.241973
Thermal correction to Gibbs Free Energy =	0.193718
Sum of electronic and zero-point Energies =	–594.270035
Sum of electronic and thermal Energies =	–594.258743
Sum of electronic and thermal Enthalpies =	–594.257799
Sum of electronic and thermal Free Energies =	–594.306054

9b

Atom	X	Y	Z
C1	-0.2904715225	0.9838139059	-1.4196713284
C2	-1.8149650931	0.9955604922	-1.2892345895
C3	-2.0271383548	1.0514628972	0.2303058807
C4	-0.9324878909	0.1212379562	0.7653786955
H5	-0.0109712243	-1.1168594758	-0.4546821646
H6	0.0677018400	0.5381292459	-2.3465734295
H7	0.1062718851	1.9979639595	-1.3418893946
H8	-2.2592749475	1.8394684401	-1.8172032231
H9	-2.2394421723	0.0762273606	-1.7022450837
H10	-1.8596541476	2.0657550685	0.6011262606
H11	-3.0192103283	0.7306738217	0.5477791686
H12	-0.5809358965	0.3870550280	1.7591518630
N13	0.1726818060	0.1630038622	-0.2544570093
C14	-1.3561552668	-1.3721986990	0.7848170475
O15	-2.2383952230	-1.7874553696	1.5233606451
O16	-0.6623498087	-2.0625163538	-0.0724158385
H17	1.8882642924	-1.3925524188	0.9393538602
C18	1.5611563603	0.4286486574	0.2696050840
O19	1.7905308224	-0.5077057816	1.3141350033
C20	1.6930762776	1.8076477177	0.9088348054
H21	1.5026324334	2.6012281807	0.1865603497
H22	1.0042721313	1.9185633631	1.7472645407
H23	2.7103859126	1.9237487666	1.2846685743
C24	2.5560984931	0.2267600654	-0.8721019139
H25	2.4343044337	0.9820082839	-1.6496665547
H26	3.5681719695	0.3040784385	-0.4729123532
H27	2.4291032190	-0.7606474124	-1.3238888956

Zero-point correction =	0.229342 (Hartree/Particle)
Thermal correction to Energy =	0.241006
Thermal correction to Enthalpy =	0.241950
Thermal correction to Gibbs Free Energy =	0.192443
Sum of electronic and zero-point Energies =	–594.311156
Sum of electronic and thermal Energies =	–594.299492
Sum of electronic and thermal Enthalpies =	–594.298548
Sum of electronic and thermal Free Energies =	–594.348055

10a

Atom	X	Y	Z
C1	0.5114657874	-1.6413051547	-1.2748653443
C2	-0.2645314974	-2.4937815007	-0.2316325121
C3	-1.3103889259	-1.5206633124	0.3650321054
C4	-1.1237636008	-0.2422774071	-0.4783541488
H5	-1.5991368613	1.8429498781	-1.5802733636
H6	1.5711868715	-1.8772173809	-1.3168667209
H7	0.0987974020	-1.8179231343	-2.2727226806
H8	-0.7322100510	-3.3558393303	-0.7105899673
H9	0.4020632976	-2.8752267807	0.5435264316
H10	-2.3328322826	-1.8928056827	0.2802955050
H11	-1.1216331218	-1.3157208973	1.4176800683
H12	-1.7169223291	-0.3713051422	-1.3933000808
N13	0.2872060490	-0.2139892093	-0.9461491176
C14	-1.6515939214	1.0394671019	0.1622730874
O15	-1.9376436977	1.1562182589	1.3282816661
O16	-1.9108389746	2.0572860657	-0.6898630358
H17	0.9690079951	2.1961151620	-0.8810532573
C18	1.3049899153	0.4423071152	-0.0816281577
O19	0.9351360334	1.8232834294	0.0092655666
C20	2.6802562945	0.3389612605	-0.7536415676
H21	2.6082448845	0.6028825337	-1.8116348515
H22	3.3552586729	1.0383176514	-0.2578501897
H23	3.1119764304	-0.6589992474	-0.6695668673
C24	1.3794211188	-0.0379761750	1.3726442635
H25	1.5838010310	-1.1081096210	1.4131826178
H26	2.1879560050	0.4858697471	1.8866438888
H27	0.4481274751	0.1714817722	1.897566662

Zero-point correction =	0.232583 (Hartree/Particle)
Thermal correction to Energy =	0.244807
Thermal correction to Enthalpy =	0.245751
Thermal correction to Gibbs Free Energy =	0.195193
Sum of electronic and zero-point Energies =	–594.290553
Sum of electronic and thermal Energies =	–594.278329
Sum of electronic and thermal Enthalpies =	–594.277385
Sum of electronic and thermal Free Energies =	–594.327943

10b

Atom	X	Y	Z
C1	-0.2608052919	1.0213456904	-1.4225500310
C2	-1.7871631051	0.9962275516	-1.3276666580
C3	-2.0242453754	1.0351967108	0.1872570910
C4	-0.8996048405	0.1326060263	0.7337562740
H5	-0.1836369914	-1.5768179484	-0.4857147364
H6	0.1177070659	0.6106558699	-2.3589359143
H7	0.1018105229	2.0518904404	-1.3290859007
H8	-2.2461009247	1.8332597776	-1.8549923090
H9	-2.1817087136	0.0696657724	-1.7555725005
H10	-1.8785725983	2.0500107754	0.5653743982
H11	-3.0143198036	0.6970051912	0.4931125567
H12	-0.5692875304	0.4490818048	1.7225826512
N13	0.1865414414	0.1875833991	-0.2756571013
C14	-1.3705642127	-1.3209043281	0.8906618703
O15	-2.1903171150	-1.6753473824	1.7100464395
O16	-0.8061247925	-2.1664887088	0.0269190724
H17	1.8898329401	-1.4018251731	0.8501400974
C18	1.5520402004	0.4415116402	0.2520323040
O19	1.8022327142	-0.5354952959	1.2670314038
C20	1.6997271603	1.7958614273	0.9513163871
H21	1.4908551140	2.6149754372	0.2620491100
H22	1.0246693457	1.8742545758	1.8051341596
H23	2.7222942507	1.9061662842	1.3157724709
C24	2.5623679489	0.2927459223	-0.8866791455
H25	2.4505037151	1.0833548720	-1.6304138273
H26	3.5715586671	0.3487023032	-0.4757541811
H27	2.4335102083	-0.6720226354	-1.3847639811

Zero-point correction =	0.232629 (Hartree/Particle)
Thermal correction to Energy =	0.244708
Thermal correction to Enthalpy =	0.245652
Thermal correction to Gibbs Free Energy =	0.195050
Sum of electronic and zero-point Energies =	–594.313014
Sum of electronic and thermal Energies =	–594.300935
Sum of electronic and thermal Enthalpies =	–594.299990
Sum of electronic and thermal Free Energies =	–594.350592

RMP2 structures

2

Atom	X	Y	Z
C1	0.0000002401	0.0000000016	-0.1823577806
O2	-0.0000000282	-0.0000000042	-1.4070023784
C3	0.0059732125	-1.2828331316	0.6152245810
H4	-0.1416589027	-2.1416048267	-0.0400419070
H5	0.9678073510	-1.3749155602	1.1307415356
H6	-0.7725471034	-1.2527026549	1.3829058667
C7	-0.0059731895	1.2828331346	0.6152245820
H8	-0.9678073665	1.3749152644	1.1307415216
H9	0.7725471204	1.2527029009	1.3829058816
H10	0.1416586663	2.1416048761	-0.0400419027

Zero-point correction =	0.084443 (Hartree/Particle)
Thermal correction to Energy =	0.089745
Thermal correction to Enthalpy =	0.090690
Thermal correction to Gibbs Free Energy =	0.056565
Sum of electronic and zero-point Energies =	–192.577358
Sum of electronic and thermal Energies =	–192.572056
Sum of electronic and thermal Enthalpies =	–192.571111
Sum of electronic and thermal Free Energies =	–192.605236

1a

Atom	X	Y	Z
C1	-0.0930450355	-1.3525486764	-0.8294345799
C2	-0.4933360795	-1.2349863656	0.6399189512
C3	-1.0852610950	0.1772179399	0.6965711676
C4	-0.1260162716	0.9756594110	-0.2052119551
H5	0.2993832548	0.2504353650	-2.1062773624
H6	0.6603940790	-2.1215823350	-1.0147473898
H7	-0.9759486265	-1.5637056966	-1.4451117267
H8	-1.2025683360	-2.0094040441	0.9400448430
H9	0.3933538838	-1.3055967138	1.2799499658
H10	-2.0845533442	0.1798018560	0.2503335022
H11	-1.1494572102	0.5969938990	1.7025981479
H12	-0.6341555336	1.7911044461	-0.7279251993
N13	0.4627631679	-0.0106441180	-1.1389138639
C14	1.0104448310	1.6014758021	0.6134482664
O15	0.8336039203	2.4519870011	1.4650880665
O16	2.2114663311	1.1116161764	0.3039269229
H17	1.9729320640	0.4621760528	-0.4242577566

Zero-point correction =	0.146422 (Hartree/Particle)
Thermal correction to Energy =	0.153475
Thermal correction to Enthalpy =	0.154420
Thermal correction to Gibbs Free Energy =	0.114528
Sum of electronic and zero-point Energies =	–400.050286
Sum of electronic and thermal Energies =	–400.043233
Sum of electronic and thermal Enthalpies =	–400.042289
Sum of electronic and thermal Free Energies =	–400.082180

1b

Atom	X	Y	Z
C1	1.9908283126	-0.8840891838	0.0728809425
C2	2.2108924055	0.6505878302	-0.0762849780
C3	0.7833220463	1.2519092515	-0.0998089025
C4	-0.0702920017	0.0781134971	0.3874849106
H5	0.4196984994	-1.1001098358	-1.1854360616
H6	2.5930362845	-1.4757111915	-0.6192837656
H7	2.2196129921	-1.2049711527	1.0934932825
H8	2.7904396949	1.0403838814	0.7646018485
H9	2.7506300454	0.8880252463	-0.9961776488
H10	0.6789002677	2.1383957011	0.5292651270
H11	0.4832516879	1.5138651954	-1.1194419761
H12	0.0096136273	-0.0005251072	1.4821453456
N13	0.5535547484	-1.1347528549	-0.1717448156
C14	-1.5511372777	0.1306409581	0.0791330605
O15	-2.1958141065	1.1495292204	-0.0377072227
O16	-2.1350556815	-1.0822835363	-0.0175455489
H17	-1.4211815446	-1.7401079194	0.0780264025

Zero-point correction =	0.146368 (Hartree/Particle)
Thermal correction to Energy =	0.153795
Thermal correction to Enthalpy =	0.154739
Thermal correction to Gibbs Free Energy =	0.113870
Sum of electronic and zero-point Energies =	–400.039435
Sum of electronic and thermal Energies =	–400.032008
Sum of electronic and thermal Enthalpies =	–400.031064
Sum of electronic and thermal Free Energies =	–400.071933

3a

Atom	X	Y	Z
C1	-0.6729361151	-1.9319506865	-1.2282175341
C2	-1.6630400586	-2.4396035610	-0.1782814686
C3	-1.7590092337	-1.2358194314	0.7674120007
C4	-1.6607238856	-0.0249137099	-0.1945386097
H5	-1.7434817258	-0.4656658028	-2.2020945144
H6	0.3431197802	-1.9590411008	-0.8225183998
H7	-0.6937165312	-2.4778032337	-2.1740467666
H8	-2.6334065751	-2.6376791956	-0.6475733238
H9	-1.3222292321	-3.3469000399	0.3283541617
H10	-2.6821328818	-1.2081448076	1.3497243801
H11	-0.9100835121	-1.2343877249	1.4569920755
H12	-2.6479882437	0.4076902290	-0.3848512750
N13	-1.0562440556	-0.5166781356	-1.4555007983
C14	-0.7885648137	1.0909446083	0.3748225010
O15	-1.0024980537	1.6385679443	1.4393766403
O16	0.2438914905	1.4066804462	-0.4134697134
H17	0.1116188946	0.7775803903	-1.1801224302
C18	2.3738754420	-0.1949190219	1.0577048382
O19	1.6177723128	-1.1144393047	1.3516419061
C20	3.1184548147	-0.1677369189	-0.2559337520
H21	2.7228342364	-0.9240548760	-0.9353930540
H22	3.0505007333	0.8248725934	-0.7086180954
H23	4.1779542362	-0.3716145851	-0.0635457695
C24	2.6261704422	0.9621834148	1.9925898667
H25	3.7027381063	1.0945462160	2.1399039437
H26	2.2415885151	1.8765996337	1.5304264086
H27	2.1319359135	0.7959866604	2.9504567820

Zero-point correction =	0.231870 (Hartree/Particle)
Thermal correction to Energy =	0.246282
Thermal correction to Enthalpy =	0.247226
Thermal correction to Gibbs Free Energy =	0.187797
Sum of electronic and zero-point Energies =	–592.633705
Sum of electronic and thermal Energies =	–592.619293
Sum of electronic and thermal Enthalpies =	–592.618349
Sum of electronic and thermal Free Energies =	–592.677777

3b

Atom	X	Y	Z
C1	-2.1985833244	0.5602395425	-2.3077718592
C2	-2.0314286486	1.5675205861	-1.1676954048
C3	-0.8196106734	0.9949957466	-0.4228504998
C4	-0.9538140629	-0.5514787472	-0.6440698472
H5	-2.8251351989	-1.0287779632	-1.2020543668
H6	-3.1823482567	0.5823380082	-2.7832473445
H7	-1.4366087451	0.7330323413	-3.0770297188
H8	-1.8667181826	2.5936102902	-1.5085288885
H9	-2.9203364955	1.5446190792	-0.5276406818
H10	0.1101872425	1.3448822706	-0.8822625043
H11	-0.8022092643	1.2693868264	0.6359062698
H12	0.0091700362	-0.9617300085	-0.9629159850
N13	-1.9700325992	-0.7600418148	-1.6884445466
C14	-1.3652451460	-1.2352722447	0.6492831330
O15	-2.5092164113	-1.5727035545	0.8912239183
O16	-0.3929175560	-1.4168295624	1.5515264012
H17	0.4726850206	-1.0970172864	1.2000408724
C18	2.5806644698	0.4246659074	0.8641904378
O19	1.9880441443	-0.6144454315	0.5711328125
C20	2.0907416796	1.3440973386	1.9512941169
H21	1.7343908741	2.2717556014	1.4898401054
H22	1.2844205688	0.8856374838	2.5245949853
H23	2.9198762331	1.6098844613	2.6129992748
C24	3.8338052836	0.8314526646	0.1400302519
H25	3.7523436416	1.8721715084	-0.1867362679
H26	4.6768126381	0.7749890002	0.8369684741
H27	4.0141627325	0.1762179566	-0.7119831383

Zero-point correction =	0.232246 (Hartree/Particle)
Thermal correction to Energy =	0.246582
Thermal correction to Enthalpy =	0.247526
Thermal correction to Gibbs Free Energy =	0.187705
Sum of electronic and zero-point Energies =	–592.629674
Sum of electronic and thermal Energies =	–592.615338
Sum of electronic and thermal Enthalpies =	–592.614394
Sum of electronic and thermal Free Energies =	–592.674215

4a

Atom	X	Y	Z
C1	-0.2316316844	-1.3623380847	-0.6141142402
C2	-1.6180772759	-1.9314004293	-0.9202550070
C3	-2.4571894909	-1.3042986940	0.1968291638
C4	-1.8639709632	0.1229120007	0.3104470782
H5	-0.3564199577	0.6659015936	-0.9742606557
H6	0.2257045247	-1.9137091711	0.2163648025
H7	0.4575828688	-1.3800002554	-1.4619025568
H8	-1.9601730005	-1.5742049737	-1.8979769450
H9	-1.6456340298	-3.0244144139	-0.9102082899
H10	-3.5289940315	-1.2782949802	-0.0090402843
H11	-2.2985560757	-1.8531885059	1.1321952480
H12	-2.4560388199	0.8330039161	-0.2752532088
N13	-0.4755954640	0.0360568086	-0.1870992324
C14	-1.8765744649	0.5980324116	1.7573835288
O15	-2.9008448265	0.8259840788	2.3742745349
O16	-0.6663801453	0.7077421096	2.3099839583
H17	-0.0357494243	0.5012813901	1.5729981181
C18	2.7679813694	-0.0443300717	0.6793362814
O19	2.1560949945	-0.1196161341	1.7387694562
C20	3.5872771199	-1.1972739868	0.1506290419
H21	3.5683704119	-2.0326870064	0.8511684690
H22	3.1872054497	-1.5138457715	-0.8182609890
H23	4.6184418900	-0.8705803041	-0.0171590076
C24	2.7493161243	1.2068521743	-0.1649213126
H25	3.7631140609	1.6187395172	-0.2178312172
H26	2.4470659357	0.9620261527	-1.1878053416
H27	2.0707749048	1.9463506295	0.2606086071

Zero-point correction =	0.231822 (Hartree/Particle)
Thermal correction to Energy =	0.246308
Thermal correction to Enthalpy =	0.247252
Thermal correction to Gibbs Free Energy =	0.187177
Sum of electronic and zero-point Energies =	–592.632613
Sum of electronic and thermal Energies =	–592.618127
Sum of electronic and thermal Enthalpies =	–592.617183
Sum of electronic and thermal Free Energies =	–592.677257

4b

Atom	X	Y	Z
C1	-0.7881216404	1.5672720187	-1.1912572882
C2	-2.3202246126	1.5465250623	-0.9315364042
C3	-2.5495829801	0.2731863897	-0.0835734652
C4	-1.1327759017	-0.1143017016	0.3502770063
H5	-0.4292524052	-0.4080435999	-1.5304390700
H6	-0.5272626414	1.7579972690	-2.2351300739
H7	-0.3134794057	2.3361889343	-0.5723225337
H8	-2.6335400779	2.4462533236	-0.3952343431
H9	-2.8829785644	1.5000192052	-1.8673907830
H10	-3.2153905943	0.4382173153	0.7679709397
H11	-2.9620156196	-0.5351292467	-0.6935207379
H12	-0.8230135439	0.4957719107	1.2087499415
N13	-0.2490186993	0.2554202501	-0.7744891982
C14	-0.9426685875	-1.5827329864	0.7035847581
O15	-1.7093002094	-2.4608355091	0.3576663491
O16	0.1544763073	-1.8787458415	1.4150666396
H17	0.7034958823	-1.0704960792	1.5583323953
C18	2.3056196502	0.6183150423	0.6678339392
O19	1.6377551648	0.3552624831	1.6691647294
C20	2.6228379907	2.0400652072	0.2958122575
H21	2.2193288452	2.2421472759	-0.7011698302
H22	2.1965548744	2.7334012965	1.0213503244
H23	3.7085671195	2.1705505326	0.2402767893
C24	2.9042602565	-0.4556953117	-0.2005285952
H25	2.7832302525	-0.2005315566	-1.2552187986
H26	3.9790806883	-0.4996743125	0.0130880414
H27	2.4563184517	-1.4271073714	0.0081370105

Zero-point correction =	0.232156 (Hartree/Particle)
Thermal correction to Energy =	0.246439
Thermal correction to Enthalpy =	0.247383
Thermal correction to Gibbs Free Energy =	0.188899
Sum of electronic and zero-point Energies =	–592.627022
Sum of electronic and thermal Energies =	–592.612739
Sum of electronic and thermal Enthalpies =	–592.611794
Sum of electronic and thermal Free Energies =	–592.670279

5a

Atom	X	Y	Z
C1	-0.0325483717	-1.9637505485	-0.3452700522
C2	-1.5145781302	-2.1214369424	-0.6670383306
C3	-2.1378941223	-0.9871932452	0.1477077728
C4	-1.0762219712	0.1529684625	0.0869714884
H5	0.3380739245	-0.2095616549	-1.3352703532
H6	0.1973164002	-2.3169164304	0.6671391990
H7	0.6324333943	-2.4541004081	-1.0570749339
H8	-1.6794155898	-1.9665064470	-1.7385575957
H9	-1.9049963917	-3.1030875775	-0.3872333306
H10	-3.1010926184	-0.6415745101	-0.2322579028
H11	-2.2724851276	-1.3107800949	1.1855182222
H12	-1.3568773511	0.9025938544	-0.6550189356
N13	0.1980440374	-0.4981297975	-0.3668985349
C14	-1.1181682986	0.8606278074	1.4418043944
O15	-1.9988584278	1.6900492112	1.6159693384
O16	-0.3308155346	0.4710881086	2.4321190736
H17	0.5415127835	0.0069390296	2.1359435568
C18	1.9537424010	-0.0984650280	0.5233050832
O19	1.8097773294	-0.5628771884	1.6960932799
C20	2.8593074513	-0.8606275535	-0.4226975188
H21	2.7615743132	-1.9355925883	-0.2649945854
H22	2.6811201843	-0.6090680598	-1.4712260816
H23	3.8877783727	-0.5693344760	-0.1777193298
C24	1.9497135304	1.4055832216	0.3038361872
H25	2.9420282344	1.7715219554	0.5940886770
H26	1.7858928364	1.6631529373	-0.7453926453
H27	1.2126367418	1.9095779626	0.9306538575

Zero-point correction =	0.232998 (Hartree/Particle)
Thermal correction to Energy =	0.244918
Thermal correction to Enthalpy =	0.245863
Thermal correction to Gibbs Free Energy =	0.194664
Sum of electronic and zero-point Energies =	–592.615564
Sum of electronic and thermal Energies =	–592.603643
Sum of electronic and thermal Enthalpies =	–592.602699
Sum of electronic and thermal Free Energies =	–592.653898

5b

Atom	X	Y	Z
C1	-0.4931520269	1.4573344709	-1.2217818524
C2	-1.9920280957	1.1677583604	-1.2342526966
C3	-2.2384966239	0.7440519968	0.2211066828
C4	-0.9427638160	0.0214508839	0.6321460143
H5	0.1724249962	-0.4649615830	-1.0450751722
H6	-0.0150683936	1.4845912554	-2.2033515203
H7	-0.2920769939	2.3932973161	-0.6926675384
H8	-2.5869943715	2.0341296359	-1.5341191055
H9	-2.2033262434	0.3397116257	-1.9196004231
H10	-2.3771189389	1.6276264476	0.8504742399
H11	-3.1038415465	0.0902405269	0.3380375457
H12	-0.5436864473	0.3974131291	1.5817963738
N13	0.0753446700	0.3405329555	-0.4216440016
C14	-1.0600266915	-1.4990879786	0.7609996522
O15	-2.0909586260	-2.1113695925	0.5508092349
O16	0.0691267003	-2.1145259239	1.1036359309
H17	0.8012885942	-1.4285200583	1.2913849098
C18	1.8654727652	0.4269670417	0.4388704554
O19	1.7130847833	-0.2370928495	1.5148674552
C20	2.0209128400	1.9266771127	0.5715785990
H21	2.0143971664	2.4355662128	-0.3944781232
H22	1.2397178543	2.3341524008	1.2193666859
H23	2.9894187158	2.1086960411	1.0515795281
C24	2.6338367473	-0.2132324237	-0.7032683078
H25	2.4635520498	0.2989227630	-1.6538974851
H26	3.7012752030	-0.1458406058	-0.4617852056
H27	2.3725857296	-1.2712891610	-0.7949318761

Zero-point correction =	0.233729 (Hartree/Particle)
Thermal correction to Energy =	0.245487
Thermal correction to Enthalpy =	0.246431
Thermal correction to Gibbs Free Energy =	0.195828
Sum of electronic and zero-point Energies =	–592.619637
Sum of electronic and thermal Energies =	–592.607878
Sum of electronic and thermal Enthalpies =	–592.606934
Sum of electronic and thermal Free Energies =	–592.657537

6a

Atom	X	Y	Z
C1	-0.1587304226	-1.5501116033	0.9441872032
C2	-1.6587834289	-1.6533633291	0.6280703560
C3	-1.7555997457	-1.3044659504	-0.8626254362
C4	-0.7258865193	-0.1816944187	-1.0074479727
H5	0.8122382482	-1.4899951641	-0.8698523036
H6	0.0612917559	-0.9872369830	1.8487929634
H7	0.3344638079	-2.5215560705	0.9836390963
H8	-2.0414429511	-2.6504473421	0.8533268527
H9	-2.2137258022	-0.9234932280	1.2217874301
H10	-1.4637074868	-2.1606449899	-1.4815413384
H11	-2.7471509759	-0.9703037594	-1.1696818201
H12	-0.3951818201	-0.0364595726	-2.0369450409
N13	0.4388059679	-0.7824543405	-0.2279879980
C14	-1.3067881229	1.1510698259	-0.4711117251
O15	-2.1752639993	1.6368292109	-1.2205310399
O16	-0.9069633090	1.5937370701	0.6490669196
H17	0.5533935350	1.2533422898	1.1291755628
C18	1.6814733612	0.0923886041	0.1223550770
O19	1.4328429098	0.8051252616	1.2812157179
C20	1.9623542358	0.9864469624	-1.0789168757
H21	1.1715592796	1.7271331769	-1.2162605250
H22	2.8982308908	1.5155406470	-0.8827967851
H23	2.0803911608	0.4026001185	-1.9970139733
C24	2.8234414310	-0.8737654423	0.3961835317
H25	3.0526842126	-1.4808029788	-0.4843634268
H26	3.7074368970	-0.2849632190	0.6512575489
H27	2.5852168904	-1.5234547756	1.2414180009

Zero-point correction =	0.237459 (Hartree/Particle)
Thermal correction to Energy =	0.249096
Thermal correction to Enthalpy =	0.250040
Thermal correction to Gibbs Free Energy =	0.200283
Sum of electronic and zero-point Energies =	–592.633272
Sum of electronic and thermal Energies =	–592.621635
Sum of electronic and thermal Enthalpies =	–592.620691
Sum of electronic and thermal Free Energies =	–592.670448

6b

Atom	X	Y	Z
C1	-0.2947971507	0.9667429939	-1.4289354612
C2	-1.8126522317	0.9731916689	-1.2710534732
C3	-1.9825457500	1.0572281445	0.2488420897
C4	-0.9273797036	0.0770409613	0.7596620032
H5	0.1523536763	-0.8907171017	-0.5528939587
H6	0.0680251107	0.5229542390	-2.3562496825
H7	0.1110209093	1.9734786115	-1.3187930173
H8	-2.2622128427	1.8114011559	-1.8074163359
H9	-2.2375048100	0.0401995620	-1.6546851547
H10	-1.7617266514	2.0715446384	0.5986135049
H11	-2.9771659166	0.7735582285	0.5974178287
H12	-0.5335780486	0.3164011823	1.7467126221
N13	0.1810875674	0.1323998138	-0.2677058831
C14	-1.4115692923	-1.4036659940	0.7626891533
O15	-2.3436935621	-1.6739091547	1.5424018609
O16	-0.7895089744	-2.1661910813	-0.0424724585
H17	1.9280636572	-1.3839303018	0.9173017672
C18	1.5738841259	0.4204927688	0.2707274754
O19	1.7936087095	-0.5083831156	1.3053163348
C20	1.6453024995	1.7992127724	0.9006347620
H21	1.4728749615	2.5887636046	0.1676601637
H22	0.9277042390	1.8985143365	1.7180751205
H23	2.6509762088	1.9252488120	1.3082255802
C24	2.5638991782	0.2398846156	-0.8697093645
H25	2.4153764799	0.9875974946	-1.6521311980
H26	3.5732473505	0.3532096369	-0.4673335705
H27	2.4700102602	-0.7590684924	-1.3094007088

Zero-point correction =	0.236235 (Hartree/Particle)
Thermal correction to Energy =	0.248267
Thermal correction to Enthalpy =	0.249211
Thermal correction to Gibbs Free Energy =	0.198480
Sum of electronic and zero-point Energies =	–592.639677
Sum of electronic and thermal Energies =	–592.627646
Sum of electronic and thermal Enthalpies =	–592.626702
Sum of electronic and thermal Free Energies =	–592.677432

7

Atom	X	Y	Z
C1	0.2987398617	-2.0879109216	-0.4996657570
C2	-0.6971932152	-2.1418293263	0.6534579935
C3	-1.6937708661	-0.9987844987	0.3489608870
C4	-1.0947319332	-0.2296613092	-0.8396021560
H5	0.7502773158	-0.5134894282	-1.7842208710
H6	1.2848377734	-2.4962260517	-0.2939249965
H7	-0.1046410924	-2.5674113129	-1.3951301260
H8	-1.1758277320	-3.1222468563	0.6937660124
H9	-0.1878861455	-1.9615104850	1.6017505772
H10	-2.6764958671	-1.3790289944	0.0595461163
H11	-1.8172232368	-0.3414969202	1.2095660770
H12	-1.4510799802	-0.6598057724	-1.7779930921
N13	0.3889959100	-0.6181379593	-0.8304016139
C14	-1.4040147330	1.2947961949	-0.8979477646
O15	-1.8112428289	1.7168971133	-1.9989793822
O16	-1.2417619836	1.9526472929	0.1761418896
H17	-0.0929393129	1.1958346768	0.9779197648
C18	1.3303377288	0.2466114720	0.0827471121
O19	0.6487410917	0.5761290611	1.2400232576
C20	1.7444637654	1.4510382504	-0.7629233918
H21	0.8907591433	2.0199025979	-1.1317119235
H22	2.3461256890	2.1066624261	-0.1288896187
H23	2.3586909918	1.1287437012	-1.6095370203
C24	2.5519296468	-0.5670433375	0.4751757108
H25	3.0508577586	-1.0035095658	-0.3937747642
H26	3.2488036667	0.1193574077	0.9622602537
H27	2.2890485838	-1.3485274547	1.1904868260

Zero-point correction =	0.238064 (Hartree/Particle)
Thermal correction to Energy =	0.249538
Thermal correction to Enthalpy =	0.250483
Thermal correction to Gibbs Free Energy =	0.201319
Sum of electronic and zero-point Energies =	–592.625458
Sum of electronic and thermal Energies =	–592.613983
Sum of electronic and thermal Enthalpies =	–592.613039
Sum of electronic and thermal Free Energies =	–592.662202

8

Atom	X	Y	Z
C1	0.4707044690	-1.7964709736	-0.9629932964
C2	-0.4063219850	-2.3700585879	0.1733404314
C3	-1.3706408213	-1.2229070719	0.5711467345
C4	-1.2333817309	-0.2410862266	-0.5811918380
H5	0.3748174995	0.1118659067	-1.8222426830
H6	1.5326721793	-2.0232418073	-0.8963116290
H7	0.1083460476	-2.1108669773	-1.9432907750
H8	-0.9579072436	-3.2335527581	-0.2041272949
H9	0.2008156051	-2.7033288690	1.0160212041
H10	-2.4026100514	-1.5611607137	0.6671305489
H11	-1.0793564447	-0.7457556081	1.5102987335
H12	-1.6882755857	-0.6958379159	-1.4727656700
N13	0.2493247592	-0.3057624561	-0.8946200615
C14	-1.8463110971	1.1720135846	-0.5182672905
O15	-2.9519654460	1.2466077549	0.0466170645
O16	-1.1931642891	2.0834562472	-1.1212688192
H17	0.0938426464	2.0047546629	-0.0202303601
C18	1.2591754979	0.4740464603	0.0376527944
O19	0.5890662347	1.5088629744	0.6732181318
C20	2.3328730366	0.9767872645	-0.9205000123
H21	1.8988349173	1.6821515711	-1.6372754795
H22	3.0998143097	1.4951367249	-0.3410359962
H23	2.8017100254	0.1513614504	-1.4653828310
C24	1.8418772091	-0.3954529435	1.1409792298
H25	2.4294503769	-1.2324294391	0.7636474955
H26	2.5123301187	0.2552160093	1.7082047293
H27	1.0679797625	-0.7522482631	1.8202469389

Zero-point correction =	0.237697 (Hartree/Particle)
Thermal correction to Energy =	0.249323
Thermal correction to Enthalpy =	0.250267
Thermal correction to Gibbs Free Energy =	0.200337
Sum of electronic and zero-point Energies =	–592.620415
Sum of electronic and thermal Energies =	–592.608789
Sum of electronic and thermal Enthalpies =	–592.607845
Sum of electronic and thermal Free Energies =	–592.657775

9a

Atom	X	Y	Z
C1	-1.077507	1.275562	-1.111182
C2	-0.858728	2.312844	0.044262
C3	0.363104	1.792919	0.875418
C4	0.921841	0.802030	-0.123400
H5	0.571315	-0.605621	-1.325369
H6	-2.115598	0.993261	-1.279036
H7	-0.662798	1.641501	-2.053385
H8	-0.633628	3.291509	-0.387085
H9	-1.751484	2.418077	0.663046
H10	1.074270	2.591988	1.094015
H11	0.066792	1.329117	1.818042
H12	1.252141	1.425469	-0.970834
N13	-0.267306	0.096905	-0.698956
C14	2.029449	-0.259242	-0.129733
O15	2.999609	-0.279624	0.618578
O16	1.777783	-1.041590	-1.148899
H17	-1.168481	-2.225095	-1.262060
C18	-1.064122	-0.894620	0.155915
O19	-1.792851	-1.659958	-0.788226
C20	-2.131295	-0.275532	1.054978
H21	-2.847296	0.327147	0.496277
H22	-2.677056	-1.107882	1.506069
H23	-1.695093	0.318101	1.857414
C24	-0.151508	-1.781959	0.996456
H25	0.445928	-1.193144	1.697926
H26	-0.792991	-2.450860	1.575328
H27	0.515509	-2.384502	0.378440

Zero-point correction =	0.232632 (Hartree/Particle)
Thermal correction to Energy =	0.243900
Thermal correction to Enthalpy =	0.244844
Thermal correction to Gibbs Free Energy =	0.196511
Sum of electronic and zero-point Energies =	–592.595620
Sum of electronic and thermal Energies =	–592.584353
Sum of electronic and thermal Enthalpies =	–592.583409
Sum of electronic and thermal Free Energies =	–592.631742

9b

Atom	X	Y	Z
C1	-0.279253	0.956384	-1.419055
C2	-1.800988	0.969247	-1.279547
C3	-1.990485	1.073191	0.237517
C4	-0.917702	0.121378	0.768408
H5	-0.013783	-1.102123	-0.449641
H6	0.078115	0.498359	-2.343134
H7	0.118850	1.972728	-1.342541
H8	-2.248867	1.798846	-1.830844
H9	-2.223679	0.031329	-1.654939
H10	-1.780534	2.093247	0.576361
H11	-2.987439	0.786895	0.579904
H12	-0.551599	0.370158	1.764798
N13	0.180237	0.144914	-0.250453
C14	-1.377628	-1.358328	0.762960
O15	-2.282712	-1.748330	1.496203
O16	-0.697203	-2.058360	-0.099564
H17	1.903641	-1.386072	0.901942
C18	1.555504	0.425362	0.271257
O19	1.797882	-0.513663	1.304465
C20	1.662339	1.797753	0.918290
H21	1.444679	2.593199	0.202736
H22	0.982140	1.882965	1.769161
H23	2.685048	1.931210	1.279933
C24	2.544740	0.249700	-0.872797
H25	2.404997	1.012028	-1.643020
H26	3.558023	0.340401	-0.473726
H27	2.428978	-0.739315	-1.329175

Zero-point correction =	0.231918 (Hartree/Particle)
Thermal correction to Energy =	0.243596
Thermal correction to Enthalpy =	0.244540
Thermal correction to Gibbs Free Energy =	0.194908
Sum of electronic and zero-point Energies =	–592.640210
Sum of electronic and thermal Energies =	–592.628532
Sum of electronic and thermal Enthalpies =	–592.627588
Sum of electronic and thermal Free Energies =	–592.677220

10a

Atom	X	Y	Z
C1	0.4947346475	-1.6086895308	-1.3086157010
C2	-0.2248074604	-2.4694914275	-0.2362158966
C3	-1.2700624906	-1.5146086263	0.3865663064
C4	-1.1229381824	-0.2429479982	-0.4678039644
H5	-1.5494674091	1.8023635864	-1.5798433357
H6	1.5565643468	-1.8323117953	-1.4023887731
H7	0.0285279620	-1.7810043322	-2.2853753602
H8	-0.6932028968	-3.3423296809	-0.6987964271
H9	0.4779369682	-2.8314922831	0.5180311234
H10	-2.2894440106	-1.9045329254	0.3183167649
H11	-1.0601188410	-1.3063336882	1.4362016225
H12	-1.7293183818	-0.3984089382	-1.3730681606
N13	0.2721255763	-0.1864524901	-0.9672629642
C14	-1.6516271741	1.0397142951	0.1581361326
O15	-1.9420708947	1.1668197446	1.3264340601
O16	-1.9000038053	2.0470045631	-0.7121208565
H17	1.0148009980	2.1755548563	-0.8879075307
C18	1.2829377779	0.4385306758	-0.0814686907
O19	0.9356808241	1.8206074896	0.0075302837
C20	2.6606640005	0.3092229352	-0.7309894248
H21	2.6036348937	0.5618052474	-1.7946747357
H22	3.3343585837	1.0107500452	-0.2319520564
H23	3.0788514445	-0.6939204696	-0.6236225199
C24	1.3363400802	-0.0404503378	1.3695084937
H25	1.5187807887	-1.1162084015	1.4166429153
H26	2.1607583568	0.4704755462	1.8762659504
H27	0.4100642978	0.1985339401	1.8947727446

Zero-point correction =	0.235564 (Hartree/Particle)
Thermal correction to Energy =	0.247650
Thermal correction to Enthalpy =	0.248594
Thermal correction to Gibbs Free Energy =	0.198381
Sum of electronic and zero-point Energies =	–592.618379
Sum of electronic and thermal Energies =	–592.606293
Sum of electronic and thermal Enthalpies =	–592.605349
Sum of electronic and thermal Free Energies =	–592.655562

10b

Atom	X	Y	Z
C1	-0.2469283623	0.9734388674	-1.4249744494
C2	-1.7699572043	0.9715402275	-1.3079515033
C3	-1.9703428630	1.0675857929	0.2070318057
C4	-0.8832106785	0.1204855673	0.7376995217
H5	-0.1958941985	-1.5492104575	-0.4719433383
H6	0.1171945255	0.5449015647	-2.3616139036
H7	0.1296376327	2.0016499650	-1.3390544878
H8	-2.2248208108	1.7987118191	-1.8578724818
H9	-2.1801116860	0.0303454521	-1.6908742152
H10	-1.7563727301	2.0857273679	0.5490852207
H11	-2.9689704089	0.7852643976	0.5484906900
H12	-0.5275181136	0.4037046895	1.7307664218
N13	0.1984836370	0.1426558226	-0.2757552793
C14	-1.4115271633	-1.3139772488	0.8546443855
O15	-2.2710860643	-1.6468412782	1.6480458592
O16	-0.8485136923	-2.1585513084	-0.0127484228
H17	1.9169131560	-1.3876809690	0.8219738930
C18	1.5484773542	0.4371839336	0.2539703316
O19	1.8257296317	-0.5320485067	1.2612721132
C20	1.6544290212	1.7890997450	0.9543379771
H21	1.4036245100	2.6037520687	0.2707311089
H22	0.9924124097	1.8357686378	1.8227111924
H23	2.6818816328	1.9334338406	1.2992256279
C24	2.5540349747	0.3244636435	-0.8861787781
H25	2.4112832114	1.1167662340	-1.6253667704
H26	3.5635270123	0.4106950854	-0.4758176024
H27	2.4508252666	-0.6453649538	-1.3847349162

Zero-point correction =	0.235218 (Hartree/Particle)
Thermal correction to Energy =	0.247268
Thermal correction to Enthalpy =	0.248212
Thermal correction to Gibbs Free Energy =	0.197632
Sum of electronic and zero-point Energies =	–592.641242
Sum of electronic and thermal Energies =	–592.629192
Sum of electronic and thermal Enthalpies =	–592.628248
Sum of electronic and thermal Free Energies =	–592.678828

End of PART A1

PART A2

Examples of strategies one might consider in the study of reaction mechanisms and relative stability of molecular systems: potential advantages and insights they can provide.

IQA, in our opinion, is perfectly suited for the purpose of studying reaction mechanisms as it allows computing atomic and interaction energies at any stage of a chemical process. Unfortunately, just by looking at the large energy terms of self-atomic energies or much smaller in value diatomic interaction energies it is difficult, or even impossible, to gain a direct and meaningful insight on their significance when reaction mechanism is of interest. However, the general concept of the FAMSEC method, where changes in energy terms are monitored, provides convenient means of their mathematical and chemical significance by purposely grouping of the IQA-defined terms. To this effect, using intuition and experience, a chemist can identify molecular fragments in order to analyse specific energy changes and interpret them in terms of bringing molecules together, most reactive sites of molecules, bond formation and breaking, etc. with an aim of understanding reaction mechanism.

Examples of strategies and approaches one can take are provided below with pointing on some (not exhaustive) insights one can gain at each consecutive step leading to a final product:

a) A **molecular system** approach – examining of $\Delta E_{\text{self}}^{\text{Tot}}$ and $\Delta E_{\text{int}}^{\text{Tot}}$ values. This will indicate whether self or interaction energies can be seen as responsible for the computed ΔE. It should be highly informative to monitor these three global energy terms throughout a multi-step process as this might reveal some important/interesting trends.

b) An **intermolecular** approach. In this case two (or more) molecules are treated as separate fragments ($\mathcal{M}$ and $\mathcal{N}$) of the molecular system. Computed inter-fragment $\Delta E_{\text{self}}^{\mathcal{M},\mathcal{N}}$ and $\Delta E_{\text{int}}^{\mathcal{M},\mathcal{N}}$ energy values might be useful in interpreting the formation of (i) global energy minimum adducts, (ii) or local energy minimum structures that are better pre-organised for a chemical bond formation, or (iii) a transitional state (TS) structure, etc.

c) An **inter-fragment** approach where selected two fragments, namely an *m*-atom fragment $\mathcal{G}$ of a molecule $\mathcal{M}$ and another *n*-atom fragment $\mathcal{H}$ of a molecule $\mathcal{N}$, are investigated. One can use either (i) on purpose selected molecular fragments that might play a leading role or be seen as a driving force throughout the process, or (ii) analyse all possible 2-, 3-, 4- (etc.) atom fragments $\mathcal{G}$ and treating remaining atoms of a molecular system as another molecular fragment $\mathcal{H}$. From this approach one can identify $\mathcal{G}$ fragments that experienced,

at each step of a chemical process, most (un)favourable change in inter-fragment interactions $\Delta E_{\text{int}}^{\mathcal{G},\mathcal{H}}$. Fragments for which most significant $\Delta E_{\text{int}}^{\mathcal{G},\mathcal{H}} < 0$ is obtained can be seen as driving a process toward a product (or TS) and fragments for which $\Delta E_{\text{int}}^{\mathcal{G},\mathcal{H}} >> 0$ can be seen as opposing a chemical change most.

d) Accounting for all interactions in a **(atom A)-(molecular system)** approach. By computing the $\Delta E_{\text{int}}^{\text{A},\mathcal{R}}$ term, where $\mathcal{R}$ is made of all atoms of a molecular system but an atom A, one can identify atoms that drive (or oppose) a chemical change most.

e) Accounting for all non-bonding interactions in a (**atom A)-(molecular system)** approach. Here, only changes in the long-distance interaction energies are considered in computing the $\Delta E_{\text{int}}^{\text{A},\mathcal{R}}$ term. By doing this (by eliminating interaction energies between the selected atom A and atoms to which A is covalently bonded to) might provide better insight on the role played by A in terms of facilitating/opposing a change.

f) Accounting for all non-bonding interactions in a (**atom A of $\mathcal{M}$)-(atoms of $\mathcal{N}$)** approach. The computed the $\Delta E_{\text{int}}^{\text{A},\mathcal{N}}$ term is possibly a best descriptor one can use in identifying most prominent atoms of $\mathcal{M}$ in driving/opposing the chemical change in terms of interactions (either attractive or repulsive) with all atoms of an oncoming molecule $\mathcal{N}$. Exactly the same approach can be used for atoms of $\mathcal{N}$ and their interactions with entire molecule $\mathcal{M}$. By grouping most prominent atoms of either $\mathcal{M}$ or $\mathcal{N}$ one can identify molecular fragments of $\mathcal{M}$ and $\mathcal{N}$ that play most significant roles.

g) An (**atom A in $\mathcal{M}$)-(molecular fragment $\mathcal{G}$ in $\mathcal{N}$)** approach. Having identified fragments under f) above one can calculate $\Delta E_{\text{int}}^{\text{A},\mathcal{G}}$ to identify individual atoms interacting with the fragment $\mathcal{G}$ of an on-coming molecule most significantly, hence one can understand the role played by the atom A better at any stage of the process.

h) A selected ***n*-atom fragment** $\mathcal{G}$ approach. A fragment, selected by chemical intuition or using the above points as guiding rules, can be investigated in order to establish whether this fragment (i) experienced most (un)favourable change in the intrafragment interactions, $\Delta E_{\text{int}}^{\mathcal{G}}$, or (ii) became most stabilised or strained in the molecular system after a particular transformation by examining *loc*-FAMSEC energy term, or (iii) experienced most/least favourable change in inter-fragment interactions, $\Delta E_{\text{int}}^{\mathcal{G},\mathcal{H}}$; a chemist is free to select any *n*-

atom $\mathcal{H}$ fragment, or (iv) (de)stabilised an entire molecular system most on a change from an initial to a final state by computing the *mol*-FAMSEC term, e.g., from monomers to adduct, or form pre-organised molecule to TS, etc.

i) A **2-atom A–B** approach involving atoms between which covalent bonds are being broken and/or formed. By monitoring $\Delta E_{\text{int}}^{\text{A,B}}$ and delocalisation index ΔDI(A,B) (and most likely also $\Delta E_{\text{self}}^{\text{A,B}}$ as well as changes in these atoms net charges) along the reaction coordinates one can gain an invaluable insight on the process of covalent bonds formation/braking.

All the above provides lots of descriptive (qualitative) as well energetic (quantitative) information from which one should be able to propose fully-supported mechanism of a chemical process and pin-point the origin, on a fundamental atomic and molecular fragment levels, of structural and chemical events.

End of PART A2

PART A3

Data pertaining to lowest and higher energy (**1a** and **1b**, respectively) conformers of *S*-proline, **1**, and their relative stability.

Part a

Table A1. Energies computed for **1a** (lowest energy) and **1b** (higher energy) conformers of **1** (part a) and acetone **2** (part b) at the B3LYP/6-311++G(d,p)/GD3 and MP2/6-311++G(d.p) (italic) levels.

Proline	***E***	**Δ**	E_{ZPVE}	**Δ**	***H***	**Δ**	***G***	**Δ**	**d(N13,H17)**
1a	-401.3116		-401.1671		-401.1591		-401.1991		1.7864
	-400.1967		*-400.0503*		*-400.0394*		*-400.0822*		*1.7363*
1b	-401.3009	-6.7	-401.1565	-6.7	-401.1481	-6.9	-401.1891	-6.3	2.1251
	-400.1858	*-6.8*	*-400.0503*	*-6.8*	*-400.0311*	*-7.0*	*-400.0719*	*-6.4*	*2.0805*

Part b

	E	E_{ZPVE}	***H***	***G***
Acetone	-193.2299	-193.1467	-193.1405	-193.1739
	-192.6618	*-192.5774*	*-192.5711*	*-192.6052*

Note that differences in all energy terms computed for both conformers of proline at both levels of theory are only about 0.1 kcal mol^{-1}.

Classically, the higher stability of **1a** would be attributed to the presence of the significantly shorter H-bond (~ 0.339 Å shorter than in **3b**) between {N13,H17}. This might be the case, but would have to be proven, and this is not an easy (if at all possible) task. Hence, instead of focusing on a single interaction, we decided to analyse the entire molecules.

Inspection of net atomic charges, *Q*(A), in both conformers (Table A2) instantly reveals that there are significant differences observed for a number of atoms. Unexpectedly, the largest change in *Q*(A) is observed for H5 and its electron population, *N*(H5), is smaller in **1a**; hence, H5 in **1a** is more positively charged by 33 m*e*. Comparable $|\Delta Q(A)|$ values are also observed for N13, O15 and O16, but their electron populations increased, relative to **1b**; hence they became more negatively charged.

Table A2. Net atomic charges Q(A) and electron populations N(A) in **1a** and **1b.** ΔQ(A) ΔN(A) stand for a difference between values in **1a** and **1b**, e.g., ΔQ(A) = {Q(A) in **1a**} – {Q(A) in **1b**}. All values are in *e*.

	***Q*(A)**			***N*(A)**		
Atom A	**1a**	**1b**	**ΔQ(A)**	**1a**	**1b**	**ΔN(A)**
C1	0.3219	0.3195	0.0024	5.6781	5.6805	-0.0024
C2	0.0441	0.0291	0.0150	5.9559	5.9709	-0.0150
C3	0.0437	0.0379	0.0058	5.9563	5.9621	-0.0058
C4	0.3016	0.3056	-0.0039	5.6984	5.6944	0.0039
H5	0.3698	0.3369	0.0329	0.6302	0.6631	-0.0329
H6	0.0153	0.0206	-0.0053	0.9847	0.9794	0.0053
H7	0.0025	0.0077	-0.0052	0.9975	0.9923	0.0052
H8	0.0136	0.0012	0.0124	0.9864	0.9988	-0.0124
H9	-0.0015	0.0000	-0.0015	1.0015	1.0000	0.0015
H10	0.0098	0.0121	-0.0023	0.9902	0.9879	0.0023
H11	0.0221	0.0055	0.0166	0.9779	0.9945	-0.0166
H12	0.0505	0.0441	0.0064	0.9495	0.9559	-0.0064
N13	-0.9898	-0.9631	-0.0267	7.9898	7.9631	0.0267
C14	1.5252	1.5184	0.0068	4.4748	4.4816	-0.0068
O15	-1.1940	-1.1726	-0.0214	9.1940	9.1726	0.0214
O16	-1.1375	-1.1096	-0.0279	9.1375	9.1096	0.0279
H17	0.6024	0.6058	-0.0034	0.3976	0.3942	0.0034

Table A3. Full set of intramolecular non-covalent diatomic interaction energies $E_{\mathrm{int}}^{\mathrm{A,B}}$ and their components ($V_{\mathrm{XC}}^{\mathrm{A,B}}$ and $V_{\mathrm{cl}}^{\mathrm{A,B}}$) in the lowest (**1a**) and higher (**1b**) energy conformers of *S*-proline also showing changes in these energy components on structural transformation from **1a** to **1b**. All values in kcal mol^{-1}.

Atom		$E_{\mathrm{int}}^{\mathrm{A,B}}$		$V_{\mathrm{XC}}^{\mathrm{A,B}}$		$V_{\mathrm{cl}}^{\mathrm{A,B}}$		**1a** *minus* **1b**		
A	**B**	**1a**	**1b**	**1a**	**1b**	**1a**	**1b**	$\Delta E_{\mathrm{int}}^{\mathrm{A,B}}$	$\Delta V_{\mathrm{XC}}^{\mathrm{A,B}}$	$\Delta V_{\mathrm{cl}}^{\mathrm{A,B}}$
C3	C1	-1.7	-0.8	-5.5	-4.1	3.9	3.3	-0.9	-1.4	0.6
C4	C1	21.8	21.3	-2.8	-4.3	24.6	25.6	0.6	1.6	-1.0
C4	C2	-1.8	-2.4	-5.1	-4.9	3.3	2.6	0.6	-0.2	0.7
H5	C1	28.3	26.5	-1.7	-2.0	29.9	28.5	1.8	0.3	1.5
H5	C2	2.3	1.5	-0.4	-0.2	2.7	1.8	0.8	-0.1	0.9
H5	C3	2.6	2.0	-0.2	-0.4	2.8	2.4	0.6	0.2	0.4
H5	C4	26.0	24.3	-1.8	-2.0	27.8	26.4	1.7	0.3	1.4
H6	C2	-2.1	-2.2	-3.3	-3.2	1.2	0.9	0.1	-0.1	0.2
H6	C3	-0.2	0.0	-0.5	-0.3	0.3	0.3	-0.2	-0.2	0.0
H6	C4	1.1	1.3	-0.4	-0.5	1.6	1.8	-0.2	0.1	-0.2
H6	H5	1.9	1.8	-0.1	-0.3	1.9	2.1	0.1	0.2	-0.2
H7	C2	-2.5	-2.7	-3.5	-3.5	1.0	0.9	0.2	0.0	0.2
H7	C3	-0.2	0.1	-0.5	-0.1	0.2	0.2	-0.3	-0.3	0.0
H7	C4	1.0	0.8	-0.1	-0.5	1.1	1.4	0.2	0.4	-0.2
H7	H5	0.9	1.1	-0.3	-0.5	1.2	1.5	-0.2	0.1	-0.3
H7	H6	-1.9	-1.7	-3.1	-3.1	1.2	1.3	-0.1	0.0	-0.1
H8	C1	-1.2	-1.8	-3.6	-3.6	2.4	1.8	0.6	0.0	0.6
H8	C3	-2.5	-2.8	-3.5	-3.6	1.0	0.8	0.3	0.1	0.2
H8	C4	0.7	0.7	-0.5	-0.2	1.2	0.8	0.1	-0.3	0.4
H8	H5	1.0	0.8	-0.1	0.0	1.0	0.8	0.2	0.0	0.3
H8	H6	0.2	0.1	-0.1	-0.1	0.3	0.2	0.1	0.0	0.1
H8	H7	-0.2	-0.4	-0.4	-0.7	0.3	0.3	0.2	0.2	0.0
H9	C1	-2.1	-1.9	-3.7	-3.6	1.7	1.7	-0.1	-0.1	0.0
H9	C3	-2.9	-2.9	-3.7	-3.7	0.8	0.8	0.0	0.0	0.0
H9	C4	0.2	0.5	-0.3	-0.3	0.6	0.8	-0.2	0.0	-0.2
H9	H5	0.4	0.5	0.0	0.0	0.4	0.5	-0.1	0.0	-0.1
H9	H6	-0.2	-0.3	-0.4	-0.6	0.3	0.3	0.1	0.1	0.0
H9	H7	-0.4	-0.2	-0.5	-0.4	0.1	0.2	-0.2	-0.1	0.0
H9	H8	-2.0	-2.2	-3.2	-3.4	1.2	1.2	0.2	0.2	0.0
H10	C1	0.7	1.0	-0.5	-0.3	1.2	1.3	-0.3	-0.3	-0.1
H10	C2	-2.6	-2.4	-3.6	-3.3	1.0	0.9	-0.2	-0.3	0.1
H10	C4	-2.0	-1.6	-3.9	-3.6	1.8	1.9	-0.4	-0.3	-0.1
H10	H5	0.7	1.1	0.0	0.0	0.8	1.1	-0.4	0.0	-0.4
H10	H6	0.1	0.1	0.0	0.0	0.1	0.1	0.0	0.0	0.0
H10	H7	-0.2	0.1	-0.3	0.0	0.1	0.1	-0.3	-0.3	0.0
H10	H8	-0.1	-0.3	-0.4	-0.6	0.3	0.3	0.2	0.2	0.0
H10	H9	-0.4	0.0	-0.5	-0.2	0.2	0.2	-0.4	-0.4	0.0
H11	C1	1.2	0.9	-0.5	-0.2	1.6	1.0	0.3	-0.3	0.6
H11	C2	-2.1	-2.6	-3.2	-3.5	1.1	0.9	0.5	0.3	0.2
H11	C4	-1.1	-2.1	-3.3	-3.8	2.2	1.6	1.0	0.5	0.6

Table A3 continues

Atom		$E_{int}^{A,B}$		$V_{XC}^{A,B}$		$V_{cl}^{A,B}$		**1a** *minus* **1b**		
A	**B**	**1a**	**1b**	**1a**	**1b**	**1a**	**1b**	$\Delta E_{int}^{A,B}$	$\Delta V_{XC}^{A,B}$	$\Delta V_{cl}^{A,B}$
H11	H5	1.3	0.5	0.0	-0.2	1.3	0.6	0.8	0.1	0.7
H11	H6	0.1	0.1	-0.1	0.0	0.1	0.1	0.0	0.0	0.0
H11	H7	0.1	0.0	0.0	0.0	0.1	0.1	0.0	0.0	0.0
H11	H8	0.2	-0.1	-0.1	-0.3	0.3	0.2	0.3	0.2	0.1
H11	H9	-0.1	-0.5	-0.4	-0.8	0.3	0.3	0.3	0.4	0.0
H11	H10	-1.7	-1.9	-3.1	-3.2	1.4	1.3	0.2	0.1	0.1
H12	C1	2.9	2.4	-0.2	-0.8	3.1	3.1	0.5	0.6	-0.1
H12	C2	0.1	0.1	-0.4	-0.3	0.5	0.4	0.0	-0.1	0.1
H12	C3	-1.3	-1.8	-3.0	-3.3	1.6	1.5	0.5	0.3	0.2
H12	H5	3.4	2.5	-0.4	-0.5	3.8	3.0	1.0	0.1	0.8
H12	H6	0.2	0.2	-0.1	0.0	0.2	0.2	0.0	0.0	0.0
H12	H7	0.1	-0.4	0.0	-0.6	0.1	0.2	0.5	0.6	-0.1
H12	H8	0.2	0.1	0.0	0.0	0.2	0.1	0.0	0.0	0.1
H12	H9	0.1	0.1	0.0	0.0	0.1	0.1	0.0	0.0	0.0
H12	H10	-0.2	-0.1	-0.6	-0.5	0.4	0.4	-0.1	-0.1	0.0
H12	H11	0.4	-0.2	-0.1	-0.5	0.5	0.3	0.6	0.4	0.2
N13	C2	-16.4	-13.0	-7.8	-7.3	-8.6	-5.8	-3.3	-0.5	-2.8
N13	C3	-15.6	-15.1	-6.4	-7.4	-9.2	-7.7	-0.5	1.0	-1.5
N13	H6	-11.6	-11.9	-5.4	-5.2	-6.2	-6.6	0.3	-0.2	0.4
N13	H7	-10.2	-10.6	-5.6	-5.7	-4.6	-4.9	0.4	0.1	0.3
N13	H8	-4.1	-2.7	-0.6	-0.5	-3.5	-2.2	-1.4	-0.1	-1.3
N13	H9	-1.9	-2.2	-0.5	-0.3	-1.3	-1.9	0.3	-0.3	0.6
N13	H10	-3.0	-3.9	-0.2	-0.7	-2.8	-3.2	0.8	0.4	0.4
N13	H11	-4.7	-2.7	-0.5	-0.5	-4.2	-2.2	-2.0	0.0	-2.0
N13	H12	-15.8	-15.0	-4.8	-5.4	-11.0	-9.7	-0.8	0.6	-1.4
C14	C1	50.7	47.1	-0.2	-0.5	50.9	47.6	3.5	0.3	3.3
C14	C2	6.9	4.7	-0.4	-0.4	7.3	5.1	2.2	0.0	2.2
C14	C3	6.0	5.8	-4.4	-3.3	10.4	9.1	0.2	-1.1	1.3
C14	H5	58.6	60.2	-0.2	-0.3	58.8	60.5	-1.6	0.2	-1.8
C14	H6	3.2	3.5	0.0	-0.1	3.2	3.6	-0.3	0.1	-0.4
C14	H7	2.0	1.9	0.0	0.0	2.0	1.9	0.1	0.0	0.1
C14	H8	3.5	1.5	0.0	0.0	3.6	1.5	2.0	0.0	2.0
C14	H9	-0.8	1.2	-0.2	0.0	-0.6	1.3	-2.0	-0.2	-1.8
C14	H10	3.7	3.7	-0.4	-0.1	4.1	3.8	0.1	-0.3	0.4
C14	H11	4.1	1.4	-0.7	-0.6	4.8	1.9	2.7	-0.2	2.9
C14	H12	11.4	9.4	-4.1	-4.9	15.5	14.3	2.0	0.8	1.2
C14	N13	-188.2	-176.9	-6.0	-5.7	-182.2	-171.1	-11.3	-0.3	-11.1
O15	C1	-32.4	-31.2	-0.1	-0.1	-32.4	-31.1	-1.2	0.0	-1.2
O15	C2	-5.1	-3.7	-0.1	-0.2	-5.0	-3.6	-1.4	0.0	-1.4
O15	C3	-8.3	-7.7	-2.1	-2.7	-6.3	-5.0	-0.7	0.6	-1.2

Table A3 continues

Atom		$E_{int}^{A,B}$		$V_{XC}^{A,B}$		$V_{cl}^{A,B}$		**1a** *minus* **1b**		
A	**B**	**1a**	**1b**	**1a**	**1b**	**1a**	**1b**	$\Delta E_{int}^{A,B}$	$\Delta V_{XC}^{A,B}$	$\Delta V_{cl}^{A,B}$
O15	C4	-57.6	-58.2	-9.7	-9.5	-47.9	-48.7	0.6	-0.1	0.8
O15	H5	-37.2	-37.7	-0.1	0.0	-37.2	-37.7	0.5	0.0	0.5
O15	H6	-2.1	-2.4	0.0	0.0	-2.1	-2.4	0.4	0.0	0.3
O15	H7	-1.1	-1.3	0.0	0.0	-1.1	-1.2	0.1	0.0	0.1
O15	H8	-2.4	-1.0	0.0	0.0	-2.3	-1.0	-1.3	0.0	-1.3
O15	H9	0.3	-0.8	0.0	0.0	0.3	-0.8	1.1	0.0	1.2
O15	H10	-3.0	-2.9	-0.1	-0.5	-2.9	-2.4	-0.1	0.4	-0.5
O15	H11	-4.9	-2.3	-2.1	-1.4	-2.8	-0.9	-2.7	-0.8	-1.9
O15	H12	-10.8	-9.4	-1.4	-1.0	-9.4	-8.3	-1.4	-0.3	-1.1
O15	N13	109.0	104.0	-0.9	-0.9	109.8	104.9	4.9	0.0	4.9
O16	C1	-40.5	-34.7	-0.2	-0.2	-40.3	-34.5	-5.8	0.0	-5.8
O16	C2	-5.3	-3.2	-0.3	-0.1	-5.0	-3.1	-2.1	-0.2	-1.9
O16	C3	-7.0	-5.9	-0.5	-0.5	-6.4	-5.3	-1.1	0.0	-1.1
O16	C4	-63.6	-61.1	-8.2	-8.4	-55.4	-52.7	-2.5	0.2	-2.7
O16	H5	-47.4	-47.3	-0.1	-0.5	-47.3	-46.8	-0.1	0.4	-0.5
O16	H6	-2.4	-2.5	0.0	0.0	-2.3	-2.5	0.1	0.0	0.2
O16	H7	-1.8	-1.3	-0.1	0.0	-1.7	-1.3	-0.5	-0.1	-0.4
O16	H8	-2.6	-1.0	0.0	0.0	-2.6	-0.9	-1.6	0.0	-1.6
O16	H9	0.4	-0.7	-0.6	0.0	0.9	-0.7	1.1	-0.6	1.7
O16	H10	-2.5	-2.1	-0.1	0.0	-2.4	-2.1	-0.4	-0.1	-0.3
O16	H11	-3.2	-1.1	-0.1	0.0	-3.1	-1.0	-2.1	0.0	-2.1
O16	H12	-9.2	-8.5	-0.5	-0.7	-8.7	-7.8	-0.7	0.2	-0.9
O16	N13	140.9	128.0	-11.9	-7.0	152.8	134.9	12.9	-5.0	17.9
O16	O15	178.9	170.1	-28.4	-28.7	207.3	198.8	8.8	0.3	8.5
H17	C1	27.1	21.6	-0.2	-0.1	27.3	21.7	5.5	-0.1	5.6
H17	C2	3.0	1.7	0.0	-0.1	3.0	1.8	1.2	0.0	1.2
H17	C3	3.8	3.0	0.0	0.0	3.8	3.0	0.8	0.0	0.8
H17	C4	33.6	30.3	-0.5	-0.4	34.1	30.7	3.3	-0.1	3.4
H17	H5	32.2	30.0	-0.1	-0.1	32.4	30.1	2.2	0.0	2.3
H17	H6	1.5	1.5	-0.1	0.0	1.6	1.5	0.0	0.0	0.0
H17	H7	1.2	0.8	-0.1	0.0	1.2	0.8	0.3	-0.1	0.4
H17	H8	1.5	0.6	0.0	0.0	1.5	0.6	1.0	0.0	1.0
H17	H9	-0.4	0.4	0.0	0.0	-0.4	0.4	-0.8	0.0	-0.8
H17	H10	1.3	1.1	0.0	0.0	1.3	1.1	0.2	0.0	0.2
H17	H11	1.8	0.6	0.0	0.0	1.8	0.6	1.2	0.0	1.2
H17	H12	4.8	4.3	0.0	0.0	4.9	4.4	0.5	0.0	0.5
H17	N13	-132.8	-99.4	-19.1	-6.9	-113.8	-92.5	-33.5	-12.2	-21.3
H17	C14	175.6	171.5	-1.0	-0.9	176.6	172.4	4.2	-0.1	4.3
H17	O15	-86.3	-85.3	-0.5	-0.7	-85.8	-84.7	-1.0	0.2	-1.1

Table A4. Diatomic interaction energies $E_{\text{int}}^{\text{A,B}}$ and their components ($V_{\text{XC}}^{\text{A,B}}$ and $V_{\text{cl}}^{\text{A,B}}$) between covalently bonded atoms in the lowest (**1a**) and higher (**1b**) energy conformers of *S*-proline also showing changes in these energy components on structural transformation from **1a** to **1b**.. All values in kcal mol^{-1}.

Atom		$E_{\text{int}}^{\text{A,B}}$		$V_{\text{XC}}^{\text{A,B}}$		$V_{\text{cl}}^{\text{A,B}}$		**1a** *minus* **1b**		
A	**B**	**1a**	**1b**	**1a**	**1b**	**1a**	**1b**	$\Delta E_{\text{int}}^{\text{A,B}}$	$\Delta V_{\text{XC}}^{\text{A,B}}$	$\Delta V_{\text{cl}}^{\text{A,B}}$
C2	C1	-166.9	-164.4	-182.9	-177.4	15.9	12.9	-2.50	-5.51	3.01
C3	C2	-171.5	-169.0	-182.9	-179.4	11.5	10.5	-2.50	-3.52	1.02
C4	C3	-162.9	-165.3	-177.3	-179.4	14.3	14.1	2.37	2.19	0.18
H6	C1	-148.4	-148.1	-173.9	-174.2	25.5	26.1	-0.34	0.25	-0.59
H7	C1	-149.4	-148.7	-173.1	-173.2	23.7	24.5	-0.69	0.08	-0.77
H8	C2	-153.3	-154.4	-175.2	-175.7	21.9	21.3	1.11	0.52	0.59
H9	C2	-153.6	-154.5	-174.3	-175.7	20.7	21.2	0.91	1.41	-0.49
H10	C3	-153.3	-153.7	-174.4	-175.4	21.1	21.7	0.39	1.01	-0.62
H11	C3	-152.7	-153.3	-174.6	-174.4	21.9	21.1	0.62	-0.19	0.81
H12	C4	-144.0	-141.8	-170.8	-167.1	26.8	25.3	-2.18	-3.66	1.48
N13	C1	-274.8	-273.3	-177.7	-180.7	-97.0	-92.7	-1.45	2.94	-4.39
N13	C4	-269.3	-265.6	-182.0	-184.7	-87.3	-81.0	-3.67	2.64	-6.30
N13	H5	-247.1	-238.2	-161.8	-163.6	-85.3	-74.5	-8.91	1.88	-10.79
C14	C4	-80.3	-82.9	-174.2	-179.9	93.9	97.0	2.66	5.74	-3.08
O15	C14	-862.3	-865.2	-244.1	-247.7	-618.3	-617.5	2.82	3.64	-0.82
O16	C14	-665.4	-632.4	-180.1	-173.5	-485.4	-459.0	-33.00	-6.63	-26.38
H17	O16	-312.1	-317.3	-100.5	-112.7	-211.6	-204.6	5.19	12.23	-7.04
	Total:	-4267	-4228	-2980	-2995	-1288	-1234	-39.2	15.0	-54.2

Table A5. Interaction energies ($E_{\text{int}}^{\text{A},\mathcal{R}}$ in kcal mol^{-1}) between atom A and a molecular fragment $\mathcal{R}$ (made of remaining atoms of *S*-proline) computed for **1a** and **1b**. $\Delta E_{\text{int}}^{\text{A},\mathcal{R}}$ = { $E_{\text{int}}^{\text{A},\mathcal{R}}$ in **1a**} – { $E_{\text{int}}^{\text{A},\mathcal{R}}$ in **1b**}.

	$E_{\text{int}}^{\text{A},\mathcal{R}}$		$\Delta V_{\text{XC}}^{\text{A},\mathcal{R}}$		$\Delta V_{\text{cl}}^{\text{A},\mathcal{R}}$		**1a** *minus* **1b**		
Atom A	**1a**	**1b**	**1a**	**1b**	**1a**	**1b**	$\Delta E_{\text{int}}^{\text{A},\mathcal{R}}$	$\Delta V_{\text{XC}}^{\text{A},\mathcal{R}}$	$\Delta V_{\text{cl}}^{\text{A},\mathcal{R}}$
C1	-684.7	-683.0	-726.9	-725.3	42.2	42.3	-1.7	-1.6	-0.1
C2	-670.3	-665.7	-743.5	-735.2	73.2	69.5	-4.6	-8.3	3.7
C3	-668.2	-666.2	-739.7	-738.4	71.5	72.3	-2.0	-1.3	-0.8
C4	-697.7	-700.9	-740.9	-749.7	43.3	48.7	3.3	8.7	-5.5
H5	-171.9	-170.4	-167.1	-170.8	-4.9	0.4	-1.5	3.7	-5.2
H6	-160.7	-160.6	-187.5	-187.7	26.9	27.1	-0.1	0.1	-0.2
H7	-162.6	-162.4	-187.8	-188.3	25.2	25.9	-0.2	0.5	-0.7
H8	-161.1	-163.0	-187.7	-188.7	26.6	25.7	2.0	1.0	1.0
H9	-163.3	-163.5	-188.6	-189.0	25.3	25.5	0.2	0.4	-0.2
H10	-162.5	-161.8	-188.2	-188.4	25.7	26.6	-0.7	0.1	-0.8
H11	-161.5	-163.3	-188.8	-189.2	27.3	25.8	1.8	0.4	1.4
H12	-157.9	-158.0	-186.3	-185.6	28.5	27.5	0.2	-0.8	1.0
N13	-945.6	-899.9	-591.4	-582.3	-354.2	-317.5	-45.8	-9.1	-36.7
C14	-1470.3	-1443.1	-616.3	-618.2	-854.1	-824.9	-27.2	1.9	-29.2
O15	-826.2	-835.2	-289.5	-293.5	-536.7	-541.7	9.1	4.1	5.0
O16	-842.7	-820.8	-331.7	-332.5	-511.1	-488.4	-21.9	0.8	-22.7
H17	-244.2	-234.3	-122.2	-122.0	-121.9	-112.4	-9.8	-0.3	-9.6

Insight from a single atom perspective considering the $E_{\text{int}}^{\text{A},\mathcal{R}}$ ***term*.** The total interaction energy between an atom A and all remaining atoms in a molecule (they constitute a molecular fragment $\mathcal{R}$) can also be interpreted as how 'friendly' a molecular environment is toward a particular atom and with increase in 'friendliness' atoms are involved in overall stronger (more negative) $E_{\text{int}}^{\text{A},\mathcal{R}}$ intramolecular interactions. A full set of $E_{\text{int}}^{\text{A},\mathcal{R}}$ data provided in Table A5 reveals that, on **1b** to **1a** structural change, 11 out of 17 atoms became involved in stronger interactions with $\mathcal{R}$. Most favourable change in $E_{\text{int}}^{\text{A},\mathcal{R}}$ by –45.8, –27.2, –21.9, and –9.8 kcal mol^{-1} was found for N13, C14, O16 and H17, respectively, whereas O15 experienced most 'unfriendly' change when in **1a**, but only by +9.1 kcal mol^{-1}. Interestingly, C14 and N13 are

involved in most attractive interactions with $\mathcal{R}$ in both conformers with, e.g., $E_{\text{int}}^{\text{A},\mathcal{R}}$ of –1470.3 and –945.6 kcal mol^{-1}, respectively, in **1a**.

Insight from a molecular fragment perspective. Treating all 136 unique 2-atom pairs as molecular fragments of **1** on equal footing we found that, on the **1b** → **1a** structural change the {H17,N13} molecular fragment became most stabilised with *loc*-FAMSEC of –18.3 kcal mol^{-1} and also contributed –7.0 kcal mol^{-1} to **1a** stability, as defined by *mol*-FAMSEC. However, the {O16,N13} fragment stabilised **1a** most (*mol*-FAMSEC = –49.7 kcal mol^{-1}) as its interactions with remaining atoms became stronger by –93.5 kcal mol^{-1}.

Often, H-bonds are analysed using a 3-atom molecular fragment involving PD–H···PA (or X–H···Y) where PD = X stands for a proton donor and PA = Y represents a proton acceptor. As expected, significantly stronger O16–H17···N13 H-bond in **1a** contributed –29.7 kcal mol^{-1} (as a molecular fragment {O16,H17,N16}) toward stability of **1a**. However, among all 680 unique 3-atom fragments in **1**, {N13,O15,O16} stabilised **1a** most with *mol*-FAMSEC = –56 kcal mol^{-1} and this is due to most significant change (in stabilising manner) in the interaction energy between this fragment and the remaining atoms of **1** (–111.9 kcal mol^{-1}).

End of PART A3

PART A4

Data pertaining to global minimum adducts of **1a** and **1b** with acetone **2**. *S*-proline (**1a** and **1b**) and acetone (**2**) molecules were placed relative to each other in such a way as to facilitate the consecutive C–N bond formation and were energy optimised without any constrain – resultant adducts are shown in Figure A1.

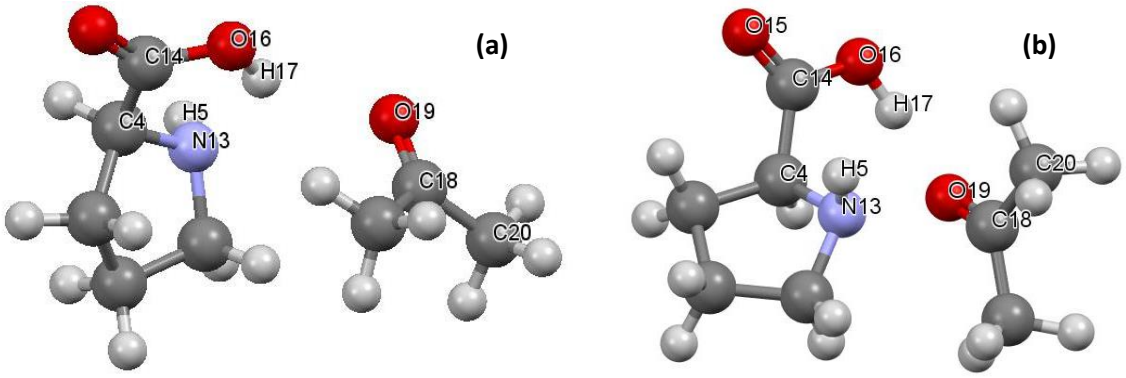

Figure A1. Initial optimised adduct structures used as inputs for search of global minimum structures of adducts: (a) – **1a** plus **2**; (b) – **1b** plus **2**.

In search for a global minimum structure (GMS) of adducts, structures shown in Figure A1 were used as inputs for a dihedral scan, DA(C4,N13,C18,C20) that resulted in rotating **2** relative to **1** – results obtained are shown in Figure A2.

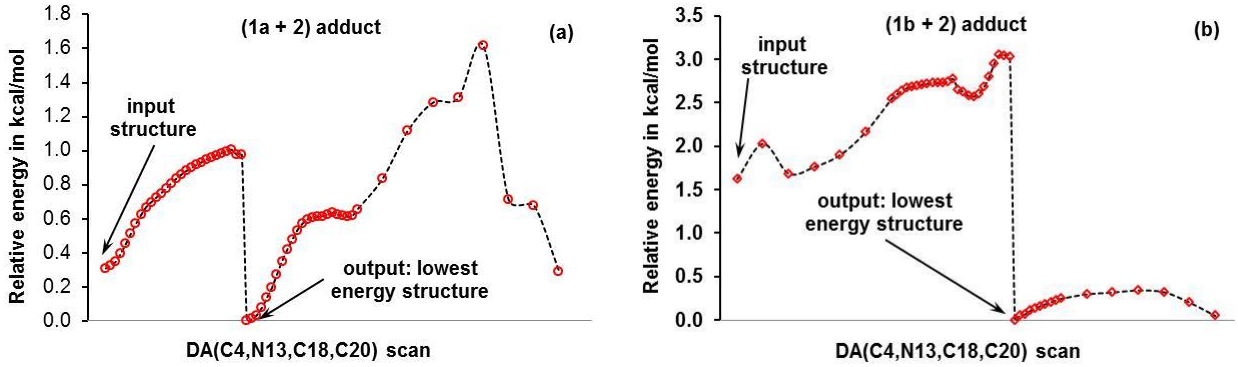

Figure A2. Data obtained from DA(C4,N13,C18,C20) scans in search for GMS of adducts between **1** and **2**. Part (a) – data for **1a** and **2**. Part (b) – data for **1b** and **2**. Energy change was computed relative to energies of GMS of adducts, either **3a** or **3b**.

Data shown in Figure A2 makes it clear that molecules are free to move relative to each other with rotational energy barrier of about 1.6 kcal mol^{-1} found for **1a** being lower, relative to the **1b**, by about 1.4 kcal mol^{-1}. The lowest energy adducts obtained from the scans shown in Figure A2 were energy optimised and the resultant GMS of **3a** and **3b**, as molecular graphs, are shown in Figure A3.

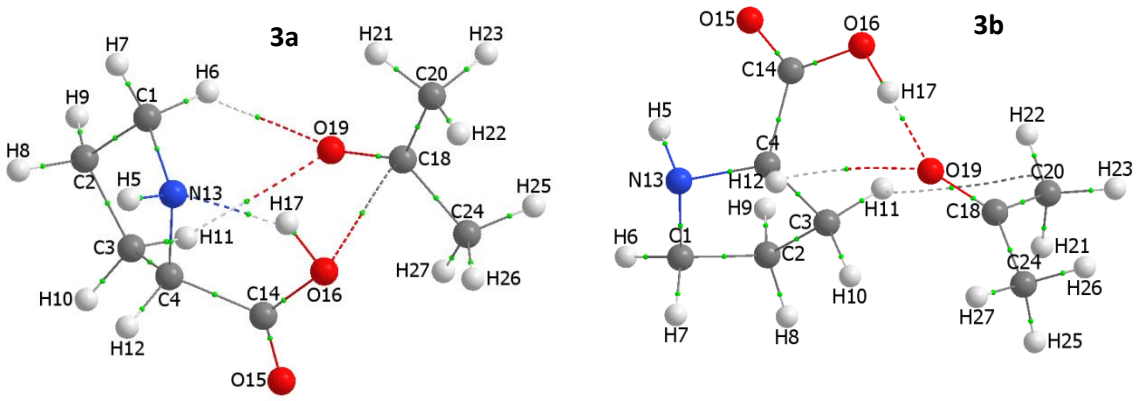

Figure A3. Molecular graphs of the global minimum energy structures **3a** (containing **1a**) and **3b** (containing **1b**) obtained for adducts between **1** and **2**.

Molecular graphs in Figure A3 show that the intramolecular O16H17···N13 H-bond in **1b** has been broken and intermolecular O16H17···O19 H-bond has been formed in **3b**; this makes **3b** well pre-organised for the subsequent proton transfer. None of the GMS of adducts shows suitable placement of C18 of **2** relative to N13 of **1**. This already suggests that adducts must be pre-organised prior the N13–C18 bond formation.

Table A6. Energies (in au) and changes in energies as E(**3**) – E(**1**+**2**) (in kcal mol^{-1}) computed for the indicated structures at the B3LYP/6-311++G(d,p)/GD3 and MP2/6-311++G(d.p) (italic) levels.

Structure	***E***	**Δ**	E_{ZPVE}	**Δ**	***H***	**Δ**	***G***	**Δ**
1a + 2	-594.5415		-594.3138		-594.2995		-594.3730	
	-592.8585		*-592.6276*		*-592.6134*		*-592.6874*	
3a	-594.5478	-3.9	-594.3188	-3.1	-594.3034	-2.4	-594.3632	6.1
	-592.8656	*-4.4*	*-592.6337*	*-3.8*	*-592.6183*	*-3.1*	*-592.6778*	*6.0*
1b + 2	-594.5309	–	-594.3032		-594.2885		-594.3630	
	-592.8476		*-592.6168*		*-592.6022*		*-592.6772*	
3b	-594.5460	-9.5	-594.3171	-8.7	-594.3017	-8.2	-594.3623	0.4
	-592.8619	*-9.0*	*-592.6297*	*-8.1*	*-592.6144*	*-7.7*	*-592.6742*	*1.9*
		Energy difference for 3a relative to 3b						
		-1.1		-1.1		-1.1		-0.5
		-2.3		*-2.5*		*-2.5*		*-2.2*

The origin of 3b adduct larger, relative to 3a, gain in stability

Our focus throughout this work is mainly on changes in the interaction energies, $\Delta E_{\text{int}}^{\text{A,B}}$, rather than self-atomic energy changes, $\Delta E_{\text{self}}^{\text{A}}$. This is because $\Delta E_{\text{int}}^{\text{A,B}}$ (i) can be seen as a driving force facilitating (or otherwise) a chemical change, (ii) there are many more diatomic interactions than atoms in a molecule. To this effect, the number of unique atom-pairs in any molecule (or molecular system) is (n×(n-1))/2 where n is the number of atoms (e.g., n = 27 in **3a** and **3b**) whereas the number of unique diatomic pairs is 351 and interaction energies can vary extensively, and (iii) the $\Delta E_{\text{int}}^{\text{A,B}}$ values are often well over an order in magnitude larger when compared with $\Delta E_{\text{self}}^{\text{A}}$. For instance, 22 atoms (out of 27) experienced $\left| \Delta E_{\text{self}}^{\text{A}} \right| < 2$ kcal mol^{-1} and the largest change found on the **3a** formation is +8.3 kcal mol^{-1}. At the same time, the most significant changes $\Delta E_{\text{int}}^{\text{A,B}}$ were found to be –161.3 and +138.3 kcal mol^{-1} for {O19,C14} and {O18,14} atom pairs, respectively.

Relative to monomers **1** and **2**:

A) The total interaction energy change on the formation of adducts **3a** and **3b** (this includes all intra and intermolecular diatomic interactions) was computed to be –21.3 (in **3a**) and –46.1 (in **3b**) kcal mol^{-1}; hence, interactions have changed in more stabilizing manner, by –24.8 kcal mol^{-1}, in **3b**.

B) On adducts formation, the total intermolecular interaction energy between atoms of **1** and atoms of **2**, i.e., the intermolecular interaction energy, was found to be –34.3 (in **3a**) and –53.6 (in **3b**) kcal mol^{-1}; hence entire molecules, **1** and **2**, interact stronger when in **3b**, by –19.3 kcal mol^{-1}.

C) From data under A) and B) it follows that intramolecular interactions in **1** and **2** also became stronger on the **3a** and **3b** formation but, at the same time, interactions between molecules played a dominant role in stabilizing the adducts.

D) The intramolecular O16H17···N13 in **1a** was preserved in **3a** but its strength slightly weakened, from $E_{\text{int}}^{\text{N13,H17}}$ of –132.8 kcal mol^{-1} in **1a** to –131.0 kcal mol^{-1} in the adduct **3a**. Totally opposite applies to **3b** as the intramolecular O16H17···N13 bond in **1b** is no longer present in **3b**. Importantly, however, a new intermolecular O16H17···O19 H-bond was formed in **3b** with $E_{\text{int}}^{\text{H17,O19}}$ of –143.9 kcal mol^{-1}. This is –44.5 kcal mol^{-1} stronger relative to the initial

intramolecular O16H17···N13 H-bond in **1b** and also –11.1 kcal mol^{-1} stronger than the intramolecular O16H17···N13 H-bond in the **3a** adduct.

Inspection of all unique 351 diatomic interactions and their energy changes on both adducts formation showed that two molecular fragments, $\mathcal{G}$ = {C1,C4,H5,N13,C14,O15,O16,H17} containing atoms of **1** and $\mathcal{H}$ = {C18,O19} made of atoms of **2**, should be considered. This is because their diatomic intermolecular interaction energies, $E_{\text{int}}^{\text{A,B}}$, in **3a** and **3b** are strongest among all intermolecular interactions (in absolute value, they all are well above 10 kcal mol^{-1} - see Table A7); full set of data, i.e., interaction energies and their components are provided in Tables S8 and S9. Furthermore, it is important to add that nearly all intramolecular interactions in **1a**, **1b** and **2** changed on the **3a** and **3b** formation but much less than 10 kcal mol^{-1}. Clearly, these two fragments, $\mathcal{G}$ and $\mathcal{H}$, that contain 10 atoms in total, can be seen as a driving force towards adducts formation.

Analysis of data in Table A7 leads to several important observations:

1. There are many atom pairs that became involved in strong diatomic interactions with $\left|E_{\text{int}}^{\text{A,B}}\right|$ > 50 kcal mol^{-1}. This demonstrates that formation of adducts **3a** and **3b** is an intermolecular event that cannot be ascribed just to a single 'obvious' classical interaction(s).
2. Considering the degree of preparedness for the C–N bond formation, the atoms in question (N13 and C18) are already involved in strong attractive interaction in both adducts with that in **3a** being stronger by about –19 kcal mol^{-1}. Focusing on the proton transfer, H17 and O19 are also involved in highly attractive interaction in **3a** and **3b** but by far more, by about –78.3 kcal mol^{-1} in **3b**. Hence, the two atom pairs, through their interactions, will facilitate the two chemical events but one must note that they are not the strongest among those shown in Table A7.
3. C14 of **1** is involved in the strongest intermolecular diatomic interactions, namely: (i) repulsive with C18 of **2** with $E_{\text{int}}^{\text{C14,C18}}$ = +138.3 kcal mol^{-1} (note that $E_{\text{int}}^{\text{C14,C18}}$ is more repulsive, by +20.5 kcal mol^{-1}, in **3a**) and (ii) attractive with O19 of **2** in both adducts, **3a** and **3b**. Remarkably, $E_{\text{int}}^{\text{C14,O19}}$ of –159.8 kcal mol^{-1} that was computed for the interaction in **3b**, shows that C14 and O19 interact stronger than H17 and O19 of the intermolecular O16H17···O19 H-bond in **3b**.

4. Molecular fragment $\mathcal{G}$ in **3a** shows (i) affinity to C18 of **2,** as it is involved in the overall attractive interactions of $E_{\text{int}}^{\mathcal{G},\text{C18}}$ = –19.5 kcal mol^{-1} and (ii) repulsive character toward O19 of **2**, $E_{\text{int}}^{\mathcal{G},\text{O19}}$ = +14.1 kcal mol^{-1}. As a result, fragment $\mathcal{G}$ (formally in **1a**) slightly attracts oncoming **2** through interactions with $\mathcal{H}$ with $E_{\text{int}}^{\mathcal{G},\mathcal{H}}$ of –5.3 kcal mol^{-1}.
5. Exactly opposite trends are observed for the molecular fragment $\mathcal{G}$ in **1b**: (i) $\mathcal{G}$ is involved in the overall repulsive interaction with C18 $E_{\text{int}}^{\mathcal{G},\text{C18}}$ = +18.8 kcal mol^{-1}) but (ii) it shows large affinity to O19 with $E_{\text{int}}^{\mathcal{G},\text{O19}}$ of –62.0 kcal mol^{-1}. Due to the latter (it compensates over the repulsive interaction with C18) the two fragments, $\mathcal{G}$ and $\mathcal{H}$, are involved in highly attractive interaction of $E_{\text{int}}^{\mathcal{G},\mathcal{H}}$ = –43.2 kcal mol^{-1}.

Additional insight one can gain from two FAMSEC-defined terms that also indicate the importance of a molecular environment (placement of atoms relative to each other):

(a) Among 351 unique 2-atom fragments in each adduct, we found that the {O16,O19} fragment is involved in the strongest attractive interactions with remaining atoms of **3** (–287.4 and –396.6 kcal mol^{-1} in **3a** and **3b**, respectively) and this fragment contributed most to adducts stability, –148.3 (in **3a**) and –217.7 (in **3b**) kcal mol^{-1}. Note that both contributions are significantly larger in **3b**.

(b) Among 2925 unique 3-atom fragments in adducts, the {O15,O16,O19} fragment's interactions with remaining atoms of adducts improved most and became stronger by –525.0 (in **3a**) and –604.1 (in **3b**) kcal mol^{-1} and this fragment contribution to adducts stability was most significant, –268.4 (in **3a**) –314.8 (in **3b**) kcal mol^{-1}, in both cases, highly in favour of **3b**.

Table A7. Interaction energies (in kcal mol^{-1}) between atoms of molecular fragments $\mathcal{G}$ made of C1, C4, H5, N13, C14, O15, O16, and H17 (in **1**) and $\mathcal{H}$ = {C18,O19} (in **2**) computed for global minimum energy structures of **3a** and **3b** adducts.

PART A. Data for C18 of $\mathcal{H}$

Atom		**3a**			**3b**		
A	**B**	$E_{\text{int}}^{\text{A,B}}$	$V_{\text{XC}}^{\text{A,B}}$	$V_{\text{cl}}^{\text{A,B}}$	$E_{\text{int}}^{\text{A,B}}$	$V_{\text{XC}}^{\text{A,B}}$	$V_{\text{cl}}^{\text{A,B}}$
C18	C1	26.23	-0.04	26.27	19.66	0.00	19.66
C18	C4	24.04	-0.01	24.05	21.87	-0.06	21.93
C18	H5	24.01	0.00	24.01	20.08	0.00	20.08
C18	N13	-76.94	-0.01	-76.92	-58.03	-0.01	-58.02
C18	C14	138.29	-0.13	138.42	117.75	-0.01	117.76
C18	O15	-98.63	-0.11	-98.52	-73.85	-0.01	-73.84
C18	O16	-113.43	-1.72	-111.72	-114.24	-0.18	-114.07
C18	H17	56.95	-0.01	56.96	85.59	-0.25	85.84
		$E_{\text{int}}^{\mathcal{G},\text{C18}}$	$V_{\text{XC}}^{\mathcal{G},\text{C18}}$	$V_{\text{cl}}^{\mathcal{G},\text{C18}}$	$E_{\text{int}}^{\mathcal{G},\text{C18}}$	$V_{\text{XC}}^{\mathcal{G},\text{C18}}$	$V_{\text{cl}}^{\mathcal{G},\text{C18}}$
		-19.5	-2.0	-17.4	18.8	-0.51	19.33

PART B. Data for O19 of $\mathcal{H}$

Atom		**3a**			**3b**		
A	**B**	$E_{\text{int}}^{\text{A,B}}$	$V_{\text{XC}}^{\text{A,B}}$	$V_{\text{cl}}^{\text{A,B}}$	$E_{\text{int}}^{\text{A,B}}$	$V_{\text{XC}}^{\text{A,B}}$	$V_{\text{cl}}^{\text{A,B}}$
O19	C1	-34.37	-1.05	-33.32	-25.50	-0.01	-25.49
O19	C4	-29.66	-0.10	-29.56	-30.70	-1.38	-29.32
O19	H5	-29.51	-0.01	-29.50	-26.41	-0.01	-26.39
O19	N13	94.34	-0.11	94.45	76.41	-0.11	76.52
O19	C14	-161.33	-0.30	-161.03	-159.84	-0.18	-159.66
O19	O15	115.09	-0.16	115.25	97.83	-0.17	98.00
O19	O16	125.14	-0.94	126.08	150.04	-8.19	158.23
O19	H17	-65.55	-0.01	-65.54	-143.88	-18.25	-125.62
		$E_{\text{int}}^{\mathcal{G},\text{O19}}$	$V_{\text{XC}}^{\mathcal{G},\text{O19}}$	$V_{\text{cl}}^{\mathcal{G},\text{O19}}$	$E_{\text{int}}^{\mathcal{G},\text{O19}}$	$V_{\text{XC}}^{\mathcal{G},\text{O19}}$	$V_{\text{cl}}^{\mathcal{G},\text{O19}}$
		14.1	-2.7	16.8	-62.0	-28.3	-33.7

PART C. Inter-fragment interaction energies.

Inter-fragment interaction energies					
3a			**3b**		
$E_{\text{int}}^{\mathcal{G},\mathcal{H}}$	$V_{\text{XC}}^{\mathcal{G},\mathcal{H}}$	$V_{\text{cl}}^{\mathcal{G},\mathcal{H}}$	$E_{\text{int}}^{\mathcal{G},\mathcal{H}}$	$V_{\text{XC}}^{\mathcal{G},\mathcal{H}}$	$V_{\text{cl}}^{\mathcal{G},\mathcal{H}}$
-5.3	-4.7	-0.6	-43.2	-28.8	-14.4

Table A8. Full set of intra and intermolecular diatomic interaction energies $E_{\mathrm{int}}^{\mathrm{A,B}}$ and their components, $V_{\mathrm{XC}}^{\mathrm{A,B}}$ and $V_{\mathrm{cl}}^{\mathrm{A,B}}$, obtained for the global minimum energy adduct **3a** and changes in these energies on (**1a**+**2**) → **3a**. All values in kcal mol^{-1}.

Atom		**3a**			**3a *minus* (1a+2)**		
A	**B**	$E_{\mathrm{int}}^{\mathrm{A,B}}$	$V_{\mathrm{XC}}^{\mathrm{A,B}}$	$V_{\mathrm{cl}}^{\mathrm{A,B}}$	$\Delta E_{\mathrm{int}}^{\mathrm{A,B}}$	$\Delta V_{\mathrm{XC}}^{\mathrm{A,B}}$	$\Delta V_{\mathrm{cl}}^{\mathrm{A,B}}$
C2	C1	-167.0	-182.4	15.5	-0.05	0.42	-0.46
C3	C1	-2.1	-5.6	3.5	-0.39	-0.02	-0.36
C3	C2	-171.2	-182.7	11.4	0.24	0.28	-0.04
C4	C1	21.2	-3.0	24.2	-0.68	-0.21	-0.46
C4	C2	-1.8	-4.9	3.2	0.04	0.16	-0.12
C4	C3	-161.8	-175.0	13.2	1.12	2.24	-1.12
H5	C1	27.7	-1.8	29.5	-0.56	-0.12	-0.44
H5	C2	2.4	-0.1	2.6	0.07	0.21	-0.14
H5	C3	2.5	-0.1	2.6	-0.17	0.05	-0.22
H5	C4	25.3	-1.9	27.2	-0.70	-0.09	-0.60
H6	C1	-147.1	-172.1	25.0	1.35	1.86	-0.51
H6	C2	-2.4	-3.5	1.1	-0.23	-0.18	-0.05
H6	C3	-0.1	-0.4	0.3	0.09	0.05	0.04
H6	C4	1.6	-0.1	1.8	0.50	0.29	0.21
H6	H5	1.8	-0.3	2.1	-0.09	-0.29	0.21
H7	C1	-148.3	-174.2	25.8	1.03	-1.09	2.12
H7	C2	-2.1	-3.2	1.1	0.36	0.35	0.01
H7	C3	-0.2	-0.5	0.3	0.04	0.00	0.03
H7	C4	1.2	-0.4	1.6	0.20	-0.30	0.49
H7	H5	1.7	-0.3	2.0	0.76	-0.04	0.79
H7	H6	-1.5	-2.9	1.4	0.35	0.18	0.17
H8	C1	-2.3	-3.8	1.5	-1.09	-0.18	-0.92
H8	C2	-153.8	-174.5	20.7	-0.54	0.67	-1.20
H8	C3	-3.0	-3.8	0.8	-0.56	-0.33	-0.23
H8	C4	0.2	-0.3	0.5	-0.56	0.19	-0.76
H8	H5	0.0	-0.1	0.0	-1.00	0.00	-0.99
H8	H6	-0.3	-0.5	0.2	-0.52	-0.41	-0.11
H8	H7	-0.2	-0.4	0.2	-0.01	0.02	-0.03
H9	C1	-1.4	-3.5	2.0	0.62	0.25	0.37
H9	C2	-153.3	-174.9	21.7	0.34	-0.64	0.98
H9	C3	-2.7	-3.5	0.8	0.20	0.20	0.00
H9	C4	0.5	-0.5	1.0	0.26	-0.16	0.41
H9	H5	0.9	0.0	1.0	0.53	0.00	0.53
H9	H6	-0.1	-0.4	0.3	0.12	0.07	0.05
H9	H7	0.2	-0.1	0.3	0.54	0.43	0.11
H9	H8	-2.1	-3.2	1.1	-0.11	-0.03	-0.08
H10	C1	0.9	-0.5	1.4	0.19	0.02	0.17
H10	C2	-2.3	-3.3	1.0	0.30	0.28	0.02
H10	C3	-153.8	-175.6	21.8	-0.50	-1.22	0.72
H10	C4	-1.8	-3.6	1.8	0.22	0.23	-0.02

Table A8 continues

Atom		3a			3a *minus* (1a+2)		
A	**B**	$E_{\text{int}}^{\text{A,B}}$	$V_{\text{XC}}^{\text{A,B}}$	$V_{\text{cl}}^{\text{A,B}}$	$\Delta E_{\text{int}}^{\text{A,B}}$	$\Delta V_{\text{XC}}^{\text{A,B}}$	$\Delta V_{\text{cl}}^{\text{A,B}}$
H10	H5	1.0	0.0	1.0	0.28	-0.01	0.29
H10	H6	0.1	0.0	0.1	0.04	0.01	0.04
H10	H7	0.1	-0.1	0.1	0.23	0.25	-0.02
H10	H8	-0.2	-0.5	0.2	-0.10	-0.04	-0.05
H10	H9	0.2	-0.1	0.2	0.54	0.45	0.08
H11	C1	1.4	-0.3	1.7	0.22	0.15	0.07
H11	C2	-2.3	-3.5	1.1	-0.24	-0.25	0.02
H11	C3	-152.2	-173.2	21.0	0.56	1.43	-0.87
H11	C4	-1.4	-3.5	2.1	-0.25	-0.19	-0.06
H11	H5	1.4	0.0	1.4	0.05	0.01	0.04
H11	H6	0.0	-0.1	0.2	-0.03	-0.08	0.05
H11	H7	0.1	0.0	0.1	0.08	0.01	0.07
H11	H8	-0.3	-0.5	0.2	-0.53	-0.40	-0.13
H11	H9	-0.1	-0.4	0.3	0.00	-0.06	0.06
H11	H10	-1.6	-3.0	1.4	0.08	0.05	0.02
H12	C1	2.8	-0.2	3.0	-0.07	-0.03	-0.04
H12	C2	0.3	-0.2	0.5	0.19	0.19	-0.01
H12	C3	-1.5	-3.0	1.5	-0.17	-0.03	-0.14
H12	C4	-144.2	-170.6	26.5	-0.14	0.15	-0.29
H12	H5	3.3	-0.4	3.7	-0.15	-0.10	-0.05
H12	H6	0.2	0.0	0.2	0.05	0.02	0.03
H12	H7	0.2	0.0	0.2	0.07	-0.02	0.09
H12	H8	0.0	-0.1	0.1	-0.13	-0.01	-0.12
H12	H9	0.1	0.0	0.2	0.08	0.00	0.08
H12	H10	-0.2	-0.6	0.4	0.05	0.02	0.03
H12	H11	0.1	-0.3	0.4	-0.28	-0.25	-0.03
N13	C1	-273.4	-177.7	-95.7	1.39	0.05	1.34
N13	C2	-16.3	-8.0	-8.2	0.10	-0.23	0.33
N13	C3	-14.0	-5.9	-8.1	1.53	0.48	1.05
N13	C4	-266.6	-182.2	-84.4	2.69	-0.16	2.85
N13	H5	-245.9	-162.3	-83.7	1.16	-0.49	1.65
N13	H6	-12.5	-5.6	-6.9	-0.83	-0.15	-0.68
N13	H7	-11.8	-5.3	-6.5	-1.63	0.35	-1.98
N13	H8	-1.6	-0.7	-0.9	2.53	-0.09	2.62
N13	H9	-3.6	-0.7	-2.9	-1.69	-0.16	-1.53
N13	H10	-3.8	-0.4	-3.4	-0.73	-0.18	-0.55
N13	H11	-4.4	-0.2	-4.2	0.31	0.33	-0.02
N13	H12	-15.7	-5.0	-10.8	0.11	-0.15	0.26
C14	C1	50.2	-0.2	50.4	-0.47	0.00	-0.48
C14	C2	7.2	-0.3	7.5	0.30	0.04	0.26

Table A8 continues

Atom		3a			3a *minus* (1a+2)		
A	**B**	$E_{\text{int}}^{\text{A,B}}$	$V_{\text{XC}}^{\text{A,B}}$	$V_{\text{cl}}^{\text{A,B}}$	$\Delta E_{\text{int}}^{\text{A,B}}$	$\Delta V_{\text{XC}}^{\text{A,B}}$	$\Delta V_{\text{cl}}^{\text{A,B}}$
C14	C3	4.9	-4.4	9.3	-1.10	0.02	-1.12
C14	C4	-82.7	-176.4	93.8	-2.39	-2.23	-0.16
C14	H5	57.1	-0.2	57.3	-1.54	-0.04	-1.50
C14	H6	3.5	0.0	3.5	0.27	-0.01	0.28
C14	H7	3.7	0.0	3.8	1.75	0.00	1.75
C14	H8	0.6	0.0	0.6	-2.90	0.02	-2.91
C14	H9	2.1	0.0	2.2	2.94	0.18	2.77
C14	H10	4.1	-0.1	4.2	0.37	0.26	0.11
C14	H11	3.7	-1.1	4.8	-0.39	-0.34	-0.06
C14	H12	11.0	-4.3	15.3	-0.35	-0.13	-0.22
C14	N13	-186.4	-5.8	-180.5	1.78	0.16	1.62
O15	C1	-32.1	-0.1	-32.0	0.32	0.01	0.32
O15	C2	-5.3	-0.2	-5.2	-0.23	-0.06	-0.17
O15	C3	-7.5	-2.3	-5.2	0.87	-0.18	1.05
O15	C4	-56.9	-9.6	-47.3	0.70	0.07	0.63
O15	H5	-36.4	-0.1	-36.3	0.83	-0.01	0.84
O15	H6	-2.3	0.0	-2.3	-0.22	0.01	-0.23
O15	H7	-2.4	0.0	-2.4	-1.28	-0.01	-1.27
O15	H8	-0.4	0.0	-0.3	2.00	0.00	2.01
O15	H9	-1.4	0.0	-1.4	-1.75	0.03	-1.78
O15	H10	-2.9	-0.3	-2.7	0.02	-0.18	0.20
O15	H11	-4.2	-1.1	-3.1	0.73	1.01	-0.28
O15	H12	-10.5	-1.2	-9.3	0.31	0.14	0.18
O15	N13	108.0	-0.9	108.9	-0.96	-0.01	-0.95
O15	C14	-862.2	-244.1	-618.1	0.19	-0.03	0.22
O16	C1	-40.3	-0.2	-40.0	0.25	-0.03	0.28
O16	C2	-5.3	-0.1	-5.2	0.03	0.18	-0.14
O16	C3	-6.2	-0.5	-5.7	0.75	0.00	0.76
O16	C4	-63.0	-8.2	-54.8	0.53	-0.04	0.58
O16	H5	-46.1	-0.2	-45.9	1.34	-0.02	1.35
O16	H6	-2.6	-0.1	-2.5	-0.26	-0.09	-0.17
O16	H7	-2.9	0.0	-2.9	-1.15	0.06	-1.22
O16	H8	-0.5	0.0	-0.5	2.14	0.01	2.13
O16	H9	-1.5	0.0	-1.5	-1.89	0.53	-2.43
O16	H10	-2.6	0.0	-2.6	-0.14	0.05	-0.19
O16	H11	-3.0	-0.1	-2.9	0.21	-0.02	0.23
O16	H12	-9.1	-0.5	-8.6	0.09	-0.01	0.10
O16	N13	140.4	-11.6	152.0	-0.50	0.32	-0.81
O16	C14	-662.8	-178.7	-484.1	2.66	1.44	1.22
O16	O15	179.7	-28.0	207.7	0.82	0.43	0.39

Table A8 continues

Atom		**3a**			**3a *minus* (1a+2)**		
A	**B**	$E_{\text{int}}^{\text{A,B}}$	$V_{\text{XC}}^{\text{A,B}}$	$V_{\text{cl}}^{\text{A,B}}$	$\Delta E_{\text{int}}^{\text{A,B}}$	$\Delta V_{\text{XC}}^{\text{A,B}}$	$\Delta V_{\text{cl}}^{\text{A,B}}$
H17	C1	26.8	-0.2	27.0	-0.32	0.00	-0.32
H17	C2	3.0	-0.1	3.1	0.06	-0.03	0.08
H17	C3	3.3	0.0	3.3	-0.53	-0.01	-0.53
H17	C4	33.0	-0.5	33.6	-0.53	0.01	-0.54
H17	H5	31.2	-0.1	31.3	-1.08	0.00	-1.08
H17	H6	1.6	-0.1	1.7	0.11	-0.02	0.13
H17	H7	1.9	0.0	1.9	0.77	0.06	0.71
H17	H8	0.3	0.0	0.3	-1.25	0.00	-1.25
H17	H9	0.9	0.0	0.9	1.29	0.02	1.27
H17	H10	1.5	0.0	1.5	0.14	0.00	0.14
H17	H11	1.7	0.0	1.7	-0.12	0.00	-0.12
H17	H12	4.8	0.0	4.8	-0.04	0.01	-0.05
H17	N13	-131.0	-18.2	-112.7	1.88	0.84	1.04
H17	C14	175.6	-1.0	176.6	0.01	0.04	-0.03
H17	O15	-86.5	-0.5	-86.0	-0.25	0.00	-0.25
H17	O16	-314.4	-100.7	-213.7	-2.26	-0.23	-2.03
C18	C1	26.2	0.0	26.3	26.23	-0.04	26.27
C18	C2	3.6	0.0	3.6	3.58	-0.01	3.59
C18	C3	3.1	-0.1	3.2	3.11	-0.06	3.16
C18	C4	24.0	0.0	24.1	24.04	-0.01	24.05
C18	H5	24.0	0.0	24.0	24.01	0.00	24.01
C18	H6	1.2	-0.1	1.3	1.17	-0.14	1.31
C18	H7	2.2	0.0	2.2	2.21	0.00	2.21
C18	H8	0.6	0.0	0.6	0.60	0.00	0.60
C18	H9	0.6	0.0	0.6	0.64	-0.01	0.65
C18	H10	1.9	0.0	1.9	1.92	-0.01	1.93
C18	H11	1.4	-0.1	1.6	1.42	-0.15	1.56
C18	H12	4.1	0.0	4.1	4.08	0.00	4.09
C18	N13	-76.9	0.0	-76.9	-76.94	-0.01	-76.92
C18	C14	138.3	-0.1	138.4	138.29	-0.13	138.42
C18	O15	-98.6	-0.1	-98.5	-98.63	-0.11	-98.52
C18	O16	-113.4	-1.7	-111.7	-113.43	-1.72	-111.72
C18	H17	56.9	0.0	57.0	56.95	-0.01	56.96
O19	C1	-34.4	-1.1	-33.3	-34.37	-1.05	-33.32
O19	C2	-4.8	-0.2	-4.6	-4.77	-0.21	-4.56
O19	C3	-5.2	-1.2	-4.0	-5.23	-1.18	-4.05
O19	C4	-29.7	-0.1	-29.6	-29.66	-0.10	-29.56
O19	H5	-29.5	0.0	-29.5	-29.51	-0.01	-29.50
O19	H6	-5.4	-3.7	-1.7	-5.37	-3.66	-1.71
O19	H7	-3.0	-0.1	-2.9	-2.98	-0.06	-2.93

Table A8 continues

Atom		3a			3a *minus* (1a+2)		
A	**B**	$E_{\text{int}}^{\text{A,B}}$	$V_{\text{XC}}^{\text{A,B}}$	$V_{\text{cl}}^{\text{A,B}}$	$\Delta E_{\text{int}}^{\text{A,B}}$	$\Delta V_{\text{XC}}^{\text{A,B}}$	$\Delta V_{\text{cl}}^{\text{A,B}}$
O19	H8	-0.9	0.0	-0.9	-0.93	-0.03	-0.90
O19	H9	-0.9	-0.1	-0.7	-0.86	-0.15	-0.72
O19	H10	-2.6	-0.1	-2.6	-2.64	-0.06	-2.58
O19	H11	-5.9	-3.9	-2.0	-5.89	-3.85	-2.04
O19	H12	-5.1	0.0	-5.1	-5.07	-0.01	-5.06
O19	N13	94.3	-0.1	94.4	94.34	-0.11	94.45
O19	C14	-161.3	-0.3	-161.0	-161.33	-0.30	-161.03
O19	O15	115.1	-0.2	115.2	115.09	-0.16	115.25
O19	O16	125.1	-0.9	126.1	125.14	-0.94	126.08
O19	H17	-65.6	0.0	-65.5	-65.55	-0.01	-65.54
O19	C18	-723.5	-257.3	-466.3	0.82	1.47	-0.64
C20	C1	-0.4	0.0	-0.4	-0.40	-0.04	-0.36
C20	C2	0.0	0.0	0.0	-0.04	0.00	-0.04
C20	C3	0.0	0.0	0.0	-0.03	-0.01	-0.03
C20	C4	-0.3	0.0	-0.3	-0.35	0.00	-0.34
C20	H5	-0.4	0.0	-0.4	-0.40	0.00	-0.40
C20	H6	-0.3	-0.2	0.0	-0.26	-0.25	-0.01
C20	H7	0.0	0.0	0.0	-0.02	0.00	-0.02
C20	H8	0.0	0.0	0.0	0.00	0.00	0.00
C20	H9	0.0	0.0	0.0	-0.01	0.00	-0.01
C20	H10	0.0	0.0	0.0	-0.01	0.00	-0.01
C20	H11	0.0	0.0	0.0	-0.04	-0.02	-0.02
C20	H12	0.0	0.0	0.0	-0.05	0.00	-0.05
C20	N13	1.3	0.0	1.3	1.29	-0.04	1.33
C20	C14	-1.6	0.0	-1.6	-1.61	-0.03	-1.58
C20	O15	0.8	0.0	0.8	0.79	-0.03	0.82
C20	O16	0.5	-1.7	2.2	0.48	-1.68	2.16
C20	H17	-1.5	-0.1	-1.5	-1.52	-0.06	-1.46
C20	C18	-167.3	-187.5	20.2	0.18	-0.08	0.26
C20	O19	-15.5	-11.8	-3.8	-0.08	0.16	-0.24
H21	C1	0.5	-0.2	0.6	0.48	-0.17	0.65
H21	C2	0.1	0.0	0.1	0.07	-0.02	0.09
H21	C3	0.1	0.0	0.1	0.08	0.00	0.08
H21	C4	0.7	0.0	0.7	0.66	0.00	0.66
H21	H5	0.6	0.0	0.6	0.65	0.00	0.65
H21	H6	-0.5	-0.5	0.0	-0.49	-0.53	0.04
H21	H7	0.0	0.0	0.1	0.05	-0.01	0.05
H21	H8	0.0	0.0	0.0	0.00	-0.01	0.01
H21	H9	0.0	0.0	0.0	0.02	0.00	0.02
H21	H10	0.0	0.0	0.0	0.04	0.00	0.05

Table A8 continues

Atom		**3a**			**3a *minus* (1a+2)**		
A	**B**	$E_{\text{int}}^{\text{A,B}}$	$V_{\text{XC}}^{\text{A,B}}$	$V_{\text{cl}}^{\text{A,B}}$	$\Delta E_{\text{int}}^{\text{A,B}}$	$\Delta V_{\text{XC}}^{\text{A,B}}$	$\Delta V_{\text{cl}}^{\text{A,B}}$
H21	H11	0.00	0.0	0.0	0.04	0.00	0.04
H21	H12	0.00	0.1	0.0	0.11	0.00	0.11
H21	N13	0.00	-2.1	-0.1	-2.12	-0.07	-2.06
H21	C14	0.01	4.3	0.0	4.28	0.00	4.28
H21	O15	0.00	-2.9	0.0	-2.94	0.00	-2.93
H21	O16	-0.01	-4.1	-0.1	-4.06	-0.10	-3.96
H21	H17	0.00	1.9	0.0	1.90	-0.03	1.93
H21	C18	0.01	5.1	-3.3	-0.54	-0.03	-0.50
H21	O19	-0.01	-8.8	-2.0	0.62	0.17	0.45
H21	C20	0.03	-153.0	-174.6	0.22	0.27	-0.04
H22	C1	0.00	1.1	0.0	1.06	0.00	1.06
H22	C2	0.00	0.1	0.0	0.14	0.00	0.14
H22	C3	0.00	0.1	0.0	0.11	-0.01	0.11
H22	C4	0.00	0.9	0.0	0.93	-0.01	0.94
H22	H5	0.00	1.0	0.0	0.99	0.00	0.99
H22	H6	0.00	0.0	0.0	0.03	-0.01	0.04
H22	H7	0.00	0.1	0.0	0.08	0.00	0.08
H22	H8	0.00	0.0	0.0	0.02	0.00	0.02
H22	H9	0.00	0.0	0.0	0.03	0.00	0.03
H22	H10	0.00	0.1	0.0	0.06	0.00	0.06
H22	H11	0.00	0.1	0.0	0.05	-0.01	0.06
H22	H12	0.00	0.2	0.0	0.15	0.00	0.15
H22	N13	-0.01	-3.2	0.0	-3.20	-0.01	-3.19
H22	C14	0.01	5.1	0.0	5.13	-0.04	5.17
H22	O15	-0.01	-3.6	0.0	-3.55	-0.03	-3.52
H22	O16	-0.01	-6.6	-2.0	-6.58	-1.99	-4.59
H22	H17	0.00	2.4	0.0	2.42	-0.02	2.45
H22	C18	0.01	5.2	-4.0	0.38	0.61	-0.23
H22	O19	-0.01	-8.9	-1.1	0.26	0.20	0.06
H22	C20	0.03	-151.0	-172.4	-0.66	-0.72	0.06
H22	H21	0.00	-1.1	-2.9	-0.03	0.07	-0.09
H23	C1	0.00	1.1	0.0	1.08	0.00	1.08
H23	C2	0.00	0.1	0.0	0.14	0.00	0.14
H23	C3	0.00	0.1	0.0	0.12	0.00	0.12
H23	C4	0.00	1.0	0.0	0.97	0.00	0.97
H23	H5	0.00	1.0	0.0	1.05	0.00	1.05
H23	H6	0.00	0.0	0.0	0.03	-0.02	0.04
H23	H7	0.00	0.1	0.0	0.08	0.00	0.08
H23	H8	0.00	0.0	0.0	0.02	0.00	0.02
H23	H9	0.00	0.0	0.0	0.03	0.00	0.03

Table A8 continues

Atom		3a			3a *minus* (1a+2)		
A	**B**	$E_{\mathrm{int}}^{\mathrm{A,B}}$	$V_{\mathrm{XC}}^{\mathrm{A,B}}$	$V_{\mathrm{cl}}^{\mathrm{A,B}}$	$\Delta E_{\mathrm{int}}^{\mathrm{A,B}}$	$\Delta V_{\mathrm{XC}}^{\mathrm{A,B}}$	$\Delta V_{\mathrm{cl}}^{\mathrm{A,B}}$
H23	H10	0.1	0.0	0.1	0.06	0.00	0.06
H23	H11	0.1	0.0	0.1	0.06	0.00	0.06
H23	H12	0.2	0.0	0.2	0.16	0.00	0.16
H23	N13	-3.3	0.0	-3.3	-3.35	0.00	-3.35
H23	C14	5.5	0.0	5.5	5.51	0.00	5.51
H23	O15	-3.7	0.0	-3.7	-3.73	-0.01	-3.73
H23	O16	-5.2	-0.1	-5.1	-5.22	-0.11	-5.11
H23	H17	2.7	0.0	2.7	2.73	0.00	2.73
H23	C18	4.6	-4.7	9.3	0.08	-0.53	0.61
H23	O19	-9.1	-1.3	-7.9	-0.71	-0.13	-0.58
H23	C20	-150.2	-171.5	21.3	1.23	1.27	-0.04
H23	H21	-1.2	-3.0	1.8	-0.03	-0.04	0.01
H23	H22	-1.1	-3.1	2.0	0.12	0.10	0.01
C24	C1	-0.2	0.0	-0.2	-0.24	-0.01	-0.23
C24	C2	0.0	0.0	0.0	-0.04	0.00	-0.04
C24	C3	-0.1	0.0	-0.1	-0.06	-0.01	-0.05
C24	C4	-0.3	0.0	-0.3	-0.33	-0.01	-0.32
C24	H5	-0.3	0.0	-0.3	-0.30	0.00	-0.30
C24	H6	-0.1	0.0	0.0	-0.05	-0.03	-0.02
C24	H7	0.0	0.0	0.0	-0.01	0.00	-0.01
C24	H8	0.0	0.0	0.0	0.00	0.00	0.00
C24	H9	0.0	0.0	0.0	-0.01	0.00	-0.01
C24	H10	0.0	0.0	0.0	-0.02	0.00	-0.02
C24	H11	-0.1	0.0	0.0	-0.05	-0.04	-0.01
C24	H12	-0.1	0.0	-0.1	-0.06	0.00	-0.06
C24	N13	0.8	0.0	0.8	0.83	0.00	0.83
C24	C14	-2.9	-0.1	-2.8	-2.93	-0.12	-2.81
C24	O15	1.6	-1.0	2.5	1.57	-0.96	2.53
C24	O16	0.8	-1.0	1.7	0.76	-0.97	1.74
C24	H17	-0.7	0.0	-0.7	-0.71	-0.01	-0.70
C24	C18	-168.0	-187.8	19.8	-0.53	-0.43	-0.10
C24	O19	-15.1	-11.8	-3.3	0.29	0.15	0.14
C24	C20	-4.1	-5.0	0.9	0.04	0.05	-0.01
C24	H21	-0.4	-0.5	0.1	0.00	0.01	-0.01
C24	H22	-0.7	-0.8	0.1	-0.25	-0.28	0.03
C24	H23	-0.3	-0.4	0.1	0.27	0.31	-0.04
H25	C1	0.7	0.0	0.7	0.72	0.00	0.72
H25	C2	0.1	0.0	0.1	0.10	0.00	0.10
H25	C3	0.1	0.0	0.1	0.09	0.00	0.10
H25	C4	0.7	0.0	0.7	0.74	0.00	0.74

Table A8 continues

Atom		3a			3a *minus* (1a+2)		
A	**B**	$E_{\text{int}}^{\text{A,B}}$	$V_{\text{XC}}^{\text{A,B}}$	$V_{\text{cl}}^{\text{A,B}}$	$\Delta E_{\text{int}}^{\text{A,B}}$	$\Delta V_{\text{XC}}^{\text{A,B}}$	$\Delta V_{\text{cl}}^{\text{A,B}}$
H25	H5	0.7	0.0	0.7	0.71	0.00	0.71
H25	H6	0.0	0.0	0.0	0.04	0.00	0.04
H25	H7	0.1	0.0	0.1	0.06	0.00	0.06
H25	H8	0.0	0.0	0.0	0.01	0.00	0.01
H25	H9	0.0	0.0	0.0	0.02	0.00	0.02
H25	H10	0.1	0.0	0.1	0.05	0.00	0.05
H25	H11	0.0	0.0	0.0	0.04	0.00	0.04
H25	H12	0.1	0.0	0.1	0.13	0.00	0.13
H25	N13	-2.2	0.0	-2.2	-2.24	0.00	-2.24
H25	C14	5.3	0.0	5.3	5.25	-0.01	5.26
H25	O15	-4.1	-0.1	-4.0	-4.11	-0.06	-4.05
H25	O16	-4.0	0.0	-4.0	-4.04	-0.04	-4.00
H25	H17	1.8	0.0	1.8	1.82	0.00	1.82
H25	C18	3.7	-4.0	7.8	-1.11	0.55	-1.66
H25	O19	-7.5	-1.1	-6.5	1.66	0.20	1.46
H25	C20	-0.7	-0.9	0.2	-0.32	-0.38	0.06
H25	H21	0.1	-0.1	0.2	-0.11	-0.04	-0.07
H25	H22	0.1	-0.1	0.2	-0.16	-0.10	-0.06
H25	H23	-0.1	-0.4	0.3	0.01	0.05	-0.04
H25	C24	-152.2	-173.6	21.4	-1.84	-1.85	0.01
H26	C1	1.3	0.0	1.3	1.25	0.00	1.25
H26	C2	0.2	0.0	0.2	0.18	0.00	0.18
H26	C3	0.2	0.0	0.2	0.16	0.00	0.17
H26	C4	1.3	0.0	1.3	1.26	-0.03	1.29
H26	H5	1.3	0.0	1.3	1.26	0.00	1.26
H26	H6	0.1	0.0	0.1	0.06	-0.01	0.07
H26	H7	0.1	0.0	0.1	0.10	0.00	0.10
H26	H8	0.0	0.0	0.0	0.02	0.00	0.02
H26	H9	0.0	0.0	0.0	0.03	0.00	0.03
H26	H10	0.1	0.0	0.1	0.09	0.00	0.09
H26	H11	0.1	0.0	0.1	0.07	-0.01	0.08
H26	H12	0.2	0.0	0.2	0.22	0.00	0.22
H26	N13	-3.9	0.0	-3.9	-3.92	-0.01	-3.91
H26	C14	8.9	-0.2	9.1	8.86	-0.20	9.06
H26	O15	-9.2	-2.2	-6.9	-9.16	-2.24	-6.92
H26	O16	-8.9	-2.0	-6.9	-8.92	-2.02	-6.90
H26	H17	3.1	0.0	3.2	3.14	-0.01	3.16
H26	C18	7.0	-4.6	11.7	2.55	-0.43	2.98
H26	O19	-11.6	-1.3	-10.3	-3.13	-0.12	-3.01
H26	C20	-0.3	-0.3	0.1	0.35	0.39	-0.04

Table A8 continues

Atom		**3a**			**3a *minus* (1a+2)**		
A	**B**	$E_{\text{int}}^{\text{A,B}}$	$V_{\text{XC}}^{\text{A,B}}$	$V_{\text{cl}}^{\text{A,B}}$	$\Delta E_{\text{int}}^{\text{A,B}}$	$\Delta V_{\text{XC}}^{\text{A,B}}$	$\Delta V_{\text{cl}}^{\text{A,B}}$
H26	H21	0.3	0.0	0.3	0.12	0.03	0.08
H26	H22	0.1	-0.3	0.4	0.26	0.17	0.09
H26	H23	0.3	0.0	0.4	0.15	0.02	0.13
H26	C24	-148.4	-169.5	21.1	2.97	3.23	-0.27
H26	H25	-1.0	-3.1	2.0	0.23	0.17	0.06
H27	C1	0.7	0.0	0.7	0.70	0.00	0.70
H27	C2	0.1	0.0	0.1	0.10	0.00	0.10
H27	C3	0.1	0.0	0.1	0.08	-0.01	0.09
H27	C4	0.7	0.0	0.7	0.71	0.00	0.72
H27	H5	0.7	0.0	0.7	0.70	0.00	0.70
H27	H6	0.0	0.0	0.0	0.04	0.00	0.04
H27	H7	0.1	0.0	0.1	0.05	0.00	0.05
H27	H8	0.0	0.0	0.0	0.01	0.00	0.01
H27	H9	0.0	0.0	0.0	0.02	0.00	0.02
H27	H10	0.0	0.0	0.0	0.05	0.00	0.05
H27	H11	0.0	0.0	0.0	0.01	-0.03	0.05
H27	H12	0.1	0.0	0.1	0.12	0.00	0.12
H27	N13	-2.2	0.0	-2.2	-2.21	0.00	-2.21
H27	C14	5.0	0.0	5.0	5.04	-0.01	5.05
H27	O15	-3.8	-0.1	-3.7	-3.80	-0.13	-3.67
H27	O16	-4.1	0.0	-4.1	-4.10	-0.04	-4.07
H27	H17	1.9	0.0	1.9	1.86	0.00	1.86
H27	C18	5.1	-3.4	8.4	-0.59	-0.10	-0.49
H27	O19	-8.9	-2.1	-6.8	0.49	0.06	0.44
H27	C20	-0.4	-0.5	0.1	0.02	0.01	0.01
H27	H21	0.1	-0.1	0.2	-0.02	0.01	-0.02
H27	H22	0.2	-0.1	0.2	-0.05	-0.03	-0.02
H27	H23	0.2	0.0	0.2	0.04	0.03	0.01
H27	C24	-153.2	-174.8	21.6	0.01	0.09	-0.08
H27	H25	-1.3	-2.9	1.7	-0.18	0.02	-0.20
H27	H26	-0.9	-2.9	2.0	0.24	0.03	0.21
				Total:	**-21.3**	**-15.9**	**-5.4**

Table A9. Full set of intra and intermolecular diatomic interaction energies $E_{\text{int}}^{\text{A,B}}$ and their components, $V_{\text{XC}}^{\text{A,B}}$ and $V_{\text{cl}}^{\text{A,B}}$, obtained for the global minimum energy adduct **3b** and changes in these energies on (**1b**+**2**) → **3b**. All values in kcal mol^{-1}.

Atom		**3b**			**3b *minus* (1b + 2)**		
A	**B**	$E_{\text{int}}^{\text{A,B}}$	$V_{\text{XC}}^{\text{A,B}}$	$V_{\text{cl}}^{\text{A,B}}$	$\Delta E_{\text{int}}^{\text{A,B}}$	$\Delta V_{\text{XC}}^{\text{A,B}}$	$\Delta V_{\text{cl}}^{\text{A,B}}$
C2	C1	-166.7	-181.8	15.1	-2.27	-4.40	2.13
C3	C1	-2.8	-5.6	2.8	-1.98	-1.50	-0.48
C3	C2	-171.8	-183.1	11.3	-2.84	-3.72	0.88
C4	C1	22.4	-3.4	25.8	1.12	0.97	0.16
C4	C2	-1.4	-4.5	3.1	1.00	0.47	0.53
C4	C3	-158.6	-170.2	11.6	6.67	9.21	-2.54
H5	C1	27.9	-1.8	29.7	1.37	0.13	1.24
H5	C2	2.1	-0.2	2.3	0.54	0.01	0.52
H5	C3	1.8	-0.1	1.9	-0.25	0.28	-0.52
H5	C4	26.9	-1.8	28.7	2.61	0.25	2.36
H6	C1	-148.4	-173.8	25.5	-0.29	0.35	-0.65
H6	C2	-2.4	-3.3	0.9	-0.12	-0.10	-0.03
H6	C3	-0.3	-0.5	0.2	-0.28	-0.18	-0.10
H6	C4	1.0	-0.5	1.5	-0.31	0.01	-0.32
H6	H5	1.4	-0.3	1.7	-0.42	-0.02	-0.40
H7	C1	-149.7	-172.9	23.2	-1.02	0.29	-1.31
H7	C2	-2.9	-3.7	0.8	-0.27	-0.19	-0.07
H7	C3	-0.4	-0.5	0.2	-0.45	-0.38	-0.07
H7	C4	0.6	-0.2	0.8	-0.26	0.30	-0.56
H7	H5	0.6	-0.4	1.0	-0.49	0.07	-0.55
H7	H6	-2.0	-3.2	1.1	-0.30	-0.10	-0.20
H8	C1	-1.4	-3.4	2.0	0.36	0.19	0.18
H8	C2	-153.5	-175.0	21.5	0.89	0.64	0.25
H8	C3	-2.9	-3.6	0.8	-0.10	-0.04	-0.05
H8	C4	0.5	-0.5	0.9	-0.22	-0.29	0.07
H8	H5	0.8	0.0	0.8	0.07	0.00	0.07
H8	H6	0.1	-0.1	0.2	0.03	0.03	0.01
H8	H7	-0.2	-0.4	0.2	0.22	0.26	-0.05
H9	C1	-2.3	-3.7	1.5	-0.37	-0.12	-0.25
H9	C2	-153.8	-174.5	20.6	0.70	1.23	-0.53
H9	C3	-3.1	-3.8	0.7	-0.21	-0.12	-0.10
H9	C4	0.2	-0.2	0.4	-0.29	0.10	-0.39
H9	H5	-0.1	-0.1	0.0	-0.62	-0.08	-0.54
H9	H6	-0.2	-0.4	0.2	0.10	0.15	-0.05
H9	H7	-0.4	-0.5	0.1	-0.22	-0.16	-0.05
H9	H8	-2.1	-3.2	1.1	0.06	0.12	-0.06
H10	C1	0.7	-0.3	1.0	-0.34	-0.09	-0.25
H10	C2	-2.5	-3.5	1.0	-0.13	-0.19	0.07
H10	C3	-153.5	-174.5	20.9	0.15	0.95	-0.79
H10	C4	-2.1	-3.6	1.6	-0.44	-0.09	-0.35

Table A9 continues

Atom		3b			3b *minus* (1b+2)		
A	**B**	$E_{\mathrm{int}}^{\mathrm{A,B}}$	$V_{\mathrm{XC}}^{\mathrm{A,B}}$	$V_{\mathrm{cl}}^{\mathrm{A,B}}$	$\Delta E_{\mathrm{int}}^{\mathrm{A,B}}$	$\Delta V_{\mathrm{XC}}^{\mathrm{A,B}}$	$\Delta V_{\mathrm{cl}}^{\mathrm{A,B}}$
H10	H5	0.8	0.0	0.8	-0.33	0.01	-0.34
H10	H6	0.1	0.0	0.1	-0.03	0.01	-0.04
H10	H7	-0.1	-0.2	0.1	-0.21	-0.24	0.03
H10	H8	-0.2	-0.5	0.3	0.11	0.14	-0.02
H10	H9	-0.4	-0.5	0.1	-0.40	-0.34	-0.06
H11	C1	0.6	-0.5	1.1	-0.23	-0.31	0.07
H11	C2	-2.3	-3.3	1.0	0.24	0.14	0.10
H11	C3	-153.4	-174.7	21.3	-0.07	-0.27	0.20
H11	C4	-1.8	-3.2	1.5	0.37	0.54	-0.17
H11	H5	0.7	0.0	0.7	0.27	0.15	0.12
H11	H6	0.0	-0.1	0.1	-0.07	-0.05	-0.01
H11	H7	0.0	0.0	0.0	-0.04	-0.01	-0.03
H11	H8	0.1	-0.1	0.2	0.24	0.20	0.04
H11	H9	-0.3	-0.5	0.2	0.21	0.26	-0.05
H11	H10	-2.0	-3.2	1.2	-0.11	0.00	-0.10
H12	C1	2.3	-0.2	2.5	-0.02	0.60	-0.62
H12	C2	0.2	-0.2	0.4	0.03	0.02	0.01
H12	C3	-2.1	-3.2	1.1	-0.33	0.08	-0.41
H12	C4	-145.0	-170.1	25.1	-3.15	-3.01	-0.14
H12	H5	2.4	-0.3	2.6	-0.10	0.21	-0.31
H12	H6	0.1	0.0	0.2	-0.06	0.02	-0.08
H12	H7	0.0	0.0	0.1	0.40	0.53	-0.13
H12	H8	0.1	0.0	0.1	-0.04	-0.01	-0.03
H12	H9	0.0	0.0	0.1	-0.07	0.00	-0.08
H12	H10	-0.4	-0.7	0.3	-0.33	-0.25	-0.08
H12	H11	0.1	-0.1	0.2	0.27	0.32	-0.05
N13	C1	-275.2	-183.2	-92.0	-1.88	-2.50	0.62
N13	C2	-15.5	-8.3	-7.2	-2.50	-1.03	-1.47
N13	C3	-11.8	-6.1	-5.7	3.33	1.32	2.01
N13	C4	-268.5	-188.2	-80.4	-2.90	-3.50	0.60
N13	H5	-239.8	-159.4	-80.4	-1.67	4.22	-5.89
N13	H6	-10.7	-5.3	-5.4	1.19	-0.06	1.25
N13	H7	-8.6	-5.8	-2.8	1.98	-0.05	2.03
N13	H8	-3.2	-0.8	-2.4	-0.44	-0.23	-0.21
N13	H9	-1.5	-0.8	-0.7	0.67	-0.48	1.15
N13	H10	-2.5	-0.2	-2.2	1.41	0.46	0.95
N13	H11	-2.8	-0.4	-2.4	-0.06	0.10	-0.16
N13	H12	-13.1	-5.2	-7.9	1.92	0.16	1.76
C14	C1	50.7	-0.3	51.0	3.57	0.16	3.41
C14	C2	6.6	-0.2	6.9	1.93	0.13	1.80

Table A9 continues

Atom		3b			3b *minus* (1b+2)		
A	**B**	$E_{\text{int}}^{\text{A,B}}$	$V_{\text{XC}}^{\text{A,B}}$	$V_{\text{cl}}^{\text{A,B}}$	$\Delta E_{\text{int}}^{\text{A,B}}$	$\Delta V_{\text{XC}}^{\text{A,B}}$	$\Delta V_{\text{cl}}^{\text{A,B}}$
C14	C3	1.1	-5.1	6.2	-4.68	-1.79	-2.89
C14	C4	-81.0	-178.3	97.3	1.98	1.64	0.34
C14	H5	71.2	-0.6	71.8	10.96	-0.26	11.21
C14	H6	2.7	0.0	2.7	-0.82	0.03	-0.85
C14	H7	0.8	0.0	0.8	-1.14	0.01	-1.15
C14	H8	2.1	0.0	2.2	0.63	-0.02	0.66
C14	H9	-1.0	0.0	-1.0	-2.22	-0.01	-2.21
C14	H10	3.1	-0.3	3.4	-0.60	-0.22	-0.38
C14	H11	0.3	-1.1	1.4	-1.09	-0.53	-0.56
C14	H12	7.6	-4.0	11.6	-1.77	0.94	-2.71
C14	N13	-178.1	-5.6	-172.4	-1.20	0.10	-1.29
O15	C1	-39.3	-0.1	-39.2	-8.08	-0.03	-8.05
O15	C2	-5.0	-0.2	-4.8	-1.20	-0.03	-1.18
O15	C3	-4.9	-1.1	-3.8	2.82	1.58	1.24
O15	C4	-66.0	-8.9	-57.2	-7.85	0.64	-8.49
O15	H5	-66.7	-5.9	-60.9	-29.00	-5.82	-23.17
O15	H6	-2.0	0.0	-2.0	0.45	0.03	0.43
O15	H7	-0.8	-0.1	-0.7	0.48	-0.04	0.52
O15	H8	-1.7	0.0	-1.6	-0.65	-0.02	-0.63
O15	H9	1.0	-0.3	1.3	1.82	-0.28	2.10
O15	H10	-2.3	-0.1	-2.2	0.59	0.38	0.21
O15	H11	-1.1	-0.2	-0.9	1.19	1.18	0.02
O15	H12	-7.5	-0.8	-6.8	1.88	0.30	1.58
O15	N13	129.5	-5.3	134.7	25.45	-4.37	29.82
O15	C14	-858.1	-243.0	-615.2	7.02	4.70	2.32
O16	C1	-30.9	-0.1	-30.8	3.81	0.17	3.65
O16	C2	-4.6	-0.1	-4.5	-1.43	0.01	-1.44
O16	C3	-4.7	-1.4	-3.3	1.14	-0.89	2.03
O16	C4	-54.2	-8.9	-45.3	6.85	-0.57	7.42
O16	H5	-37.7	-0.1	-37.6	9.58	0.40	9.18
O16	H6	-1.7	0.0	-1.7	0.79	-0.02	0.81
O16	H7	-0.2	0.0	-0.2	1.15	0.02	1.13
O16	H8	-1.3	0.0	-1.2	-0.29	0.00	-0.29
O16	H9	0.4	0.0	0.4	1.13	0.01	1.13
O16	H10	-2.1	0.0	-2.0	0.02	-0.02	0.04
O16	H11	-1.3	-1.2	-0.1	-0.27	-1.15	0.88
O16	H12	-7.6	-1.3	-6.3	0.84	-0.63	1.48
O16	N13	98.4	-0.7	99.1	-29.57	6.25	-35.82
O16	C14	-665.1	-176.7	-488.4	-32.64	-3.27	-29.38
O16	O15	180.6	-29.3	209.9	10.49	-0.62	11.11

Table A9 continues

Atom		3b			3b *minus* (1b+2)		
A	**B**	$E_{\text{int}}^{\text{A,B}}$	$V_{\text{XC}}^{\text{A,B}}$	$V_{\text{cl}}^{\text{A,B}}$	$\Delta E_{\text{int}}^{\text{A,B}}$	$\Delta V_{\text{XC}}^{\text{A,B}}$	$\Delta V_{\text{cl}}^{\text{A,B}}$
H17	C1	16.3	0.0	16.3	-5.32	0.13	-5.45
H17	C2	2.5	0.0	2.5	0.74	0.05	0.70
H17	C3	1.4	-0.1	1.5	-1.56	-0.06	-1.50
H17	C4	21.5	-0.4	22.0	-8.72	-0.04	-8.68
H17	H5	18.7	0.0	18.7	-11.35	0.11	-11.46
H17	H6	0.9	0.0	0.9	-0.63	0.00	-0.63
H17	H7	0.0	0.0	0.0	-0.81	0.01	-0.82
H17	H8	0.6	0.0	0.6	0.07	0.01	0.06
H17	H9	-0.1	0.0	-0.1	-0.52	0.00	-0.52
H17	H10	0.9	0.0	0.9	-0.21	0.00	-0.21
H17	H11	0.1	-0.1	0.1	-0.55	-0.05	-0.49
H17	H12	2.8	-0.3	3.1	-1.55	-0.27	-1.28
H17	N13	-51.3	0.0	-51.2	48.11	6.86	41.25
H17	C14	174.1	-0.7	174.8	2.65	0.17	2.48
H17	O15	-87.0	-0.5	-86.5	-1.70	0.16	-1.86
H17	O16	-320.5	-97.2	-223.3	-3.15	15.54	-18.69
C18	C1	19.7	0.0	19.7	19.66	0.00	19.66
C18	C2	3.0	0.0	3.0	2.99	-0.02	3.00
C18	C3	1.3	-0.2	1.5	1.28	-0.22	1.49
C18	C4	21.9	-0.1	21.9	21.87	-0.06	21.93
C18	H5	20.1	0.0	20.1	20.08	0.00	20.08
C18	H6	1.1	0.0	1.1	1.13	0.00	1.13
C18	H7	-0.3	0.0	-0.3	-0.34	0.00	-0.34
C18	H8	0.5	0.0	0.5	0.52	0.00	0.52
C18	H9	0.1	0.0	0.1	0.07	0.00	0.08
C18	H10	-0.7	-0.3	-0.3	-0.66	-0.34	-0.32
C18	H11	0.2	-0.1	0.2	0.18	-0.07	0.25
C18	H12	2.5	-0.1	2.6	2.54	-0.10	2.64
C18	N13	-58.0	0.0	-58.0	-58.03	-0.01	-58.02
C18	C14	117.8	0.0	117.8	117.75	-0.01	117.76
C18	O15	-73.9	0.0	-73.8	-73.85	-0.01	-73.84
C18	O16	-114.2	-0.2	-114.1	-114.24	-0.18	-114.07
C18	H17	85.6	-0.2	85.8	85.59	-0.25	85.84
O19	C1	-25.5	0.0	-25.5	-25.50	-0.01	-25.49
O19	C2	-4.0	-0.1	-3.9	-3.96	-0.08	-3.88
O19	C3	-3.1	-1.2	-1.9	-3.09	-1.20	-1.89
O19	C4	-30.7	-1.4	-29.3	-30.70	-1.38	-29.32
O19	H5	-26.4	0.0	-26.4	-26.41	-0.01	-26.39
O19	H6	-1.5	0.0	-1.5	-1.48	0.00	-1.47
O19	H7	0.4	0.0	0.4	0.40	0.00	0.40

Table A9 continues

Atom		3b			3b *minus* (1b+2)		
A	**B**	$E_{\text{int}}^{\text{A,B}}$	$V_{\text{XC}}^{\text{A,B}}$	$V_{\text{cl}}^{\text{A,B}}$	$\Delta E_{\text{int}}^{\text{A,B}}$	$\Delta V_{\text{XC}}^{\text{A,B}}$	$\Delta V_{\text{cl}}^{\text{A,B}}$
O19	H8	-0.7	0.0	-0.7	-0.75	0.00	-0.74
O19	H9	-0.1	0.0	-0.1	-0.12	-0.01	-0.11
O19	H10	-0.8	-1.0	0.2	-0.81	-0.96	0.15
O19	H11	-0.7	-0.2	-0.5	-0.75	-0.22	-0.53
O19	H12	-6.3	-2.9	-3.4	-6.34	-2.90	-3.44
O19	N13	76.4	-0.1	76.5	76.41	-0.11	76.52
O19	C14	-159.8	-0.2	-159.7	-159.84	-0.18	-159.66
O19	O15	97.8	-0.2	98.0	97.83	-0.17	98.00
O19	O16	150.0	-8.2	158.2	150.04	-8.19	158.23
O19	H17	-143.9	-18.3	-125.6	-143.88	-18.25	-125.62
O19	C18	-706.3	-249.9	-456.4	18.04	8.83	9.22
C20	C1	-0.3	0.0	-0.3	-0.27	-0.01	-0.27
C20	C2	-0.1	0.0	-0.1	-0.08	-0.03	-0.05
C20	C3	-0.4	-0.4	0.0	-0.44	-0.41	-0.03
C20	C4	-0.3	0.0	-0.3	-0.28	-0.02	-0.27
C20	H5	-0.3	0.0	-0.3	-0.26	0.00	-0.26
C20	H6	0.0	0.0	0.0	-0.02	0.00	-0.02
C20	H7	0.0	0.0	0.0	0.00	0.00	0.00
C20	H8	0.0	0.0	0.0	-0.01	0.00	-0.01
C20	H9	0.0	0.0	0.0	0.00	0.00	0.00
C20	H10	-0.2	-0.2	0.0	-0.24	-0.22	-0.02
C20	H11	-0.8	-0.8	0.1	-0.75	-0.82	0.07
C20	H12	-0.1	0.0	0.0	-0.06	-0.01	-0.04
C20	N13	0.7	0.0	0.7	0.67	-0.01	0.68
C20	C14	-1.3	0.0	-1.3	-1.34	-0.01	-1.33
C20	O15	1.0	0.0	1.0	0.97	-0.01	0.98
C20	O16	0.6	-0.4	1.0	0.57	-0.40	0.97
C20	H17	-0.5	-0.1	-0.4	-0.52	-0.15	-0.37
C20	C18	-168.6	-190.0	21.3	-1.16	-2.58	1.42
C20	O19	-15.9	-11.3	-4.6	-0.49	0.63	-1.12
H21	C1	1.0	0.0	1.0	1.04	0.00	1.04
H21	C2	0.1	0.0	0.2	0.15	-0.02	0.16
H21	C3	-0.2	-0.3	0.1	-0.22	-0.30	0.09
H21	C4	1.1	0.0	1.1	1.10	-0.02	1.13
H21	H5	1.1	0.0	1.1	1.07	0.00	1.07
H21	H6	0.1	0.0	0.1	0.06	0.00	0.06
H21	H7	0.0	0.0	0.0	-0.01	0.00	-0.01
H21	H8	0.0	0.0	0.0	0.02	0.00	0.02
H21	H9	0.0	0.0	0.0	-0.01	0.00	-0.01
H21	H10	-0.2	-0.2	0.0	-0.22	-0.22	0.01

Table A9 continues

Atom		3b			3b *minus* (1b+2)		
A	**B**	$E_{\text{int}}^{\text{A,B}}$	$V_{\text{XC}}^{\text{A,B}}$	$V_{\text{cl}}^{\text{A,B}}$	$\Delta E_{\text{int}}^{\text{A,B}}$	$\Delta V_{\text{XC}}^{\text{A,B}}$	$\Delta V_{\text{cl}}^{\text{A,B}}$
H21	H11	-0.4	-0.4	0.0	-0.41	-0.37	-0.04
H21	H12	0.1	0.0	0.1	0.14	-0.01	0.15
H21	N13	-3.0	0.0	-3.0	-3.01	-0.01	-2.99
H21	C14	6.3	0.0	6.3	6.32	0.00	6.32
H21	O15	-4.1	0.0	-4.1	-4.10	0.00	-4.10
H21	O16	-6.0	0.0	-6.0	-6.00	-0.01	-5.99
H21	H17	3.9	0.0	3.9	3.94	0.00	3.95
H21	C18	6.0	-4.9	10.9	0.34	-1.60	1.94
H21	O19	-11.0	-1.2	-9.8	-1.64	0.96	-2.60
H21	C20	-149.1	-170.4	21.3	4.13	4.48	-0.35
H22	C1	0.7	0.0	0.7	0.74	0.00	0.74
H22	C2	0.1	0.0	0.1	0.10	-0.01	0.11
H22	C3	-0.1	-0.2	0.0	-0.15	-0.19	0.04
H22	C4	0.8	0.0	0.8	0.77	-0.01	0.79
H22	H5	0.7	0.0	0.7	0.74	0.00	0.74
H22	H6	0.0	0.0	0.0	0.04	0.00	0.04
H22	H7	0.0	0.0	0.0	-0.01	0.00	-0.01
H22	H8	0.0	0.0	0.0	0.01	0.00	0.01
H22	H9	0.0	0.0	0.0	0.00	0.00	0.00
H22	H10	0.0	0.0	0.0	-0.03	-0.01	-0.02
H22	H11	-0.6	-0.6	0.0	-0.59	-0.58	-0.01
H22	H12	0.1	0.0	0.1	0.10	0.00	0.10
H22	N13	-2.1	0.0	-2.1	-2.12	0.00	-2.12
H22	C14	4.1	0.0	4.1	4.08	-0.02	4.10
H22	O15	-2.7	0.0	-2.7	-2.70	-0.02	-2.68
H22	O16	-4.9	-1.1	-3.8	-4.92	-1.12	-3.80
H22	H17	2.4	-0.2	2.6	2.43	-0.18	2.61
H22	C18	5.8	-3.3	9.2	0.99	1.26	-0.27
H22	O19	-9.7	-1.7	-8.0	-0.45	-0.42	-0.03
H22	C20	-152.8	-174.4	21.6	-2.45	-2.69	0.24
H22	H21	-0.7	-2.8	2.1	0.36	0.12	0.24
H23	C1	1.0	0.0	1.0	0.98	0.00	0.98
H23	C2	0.1	0.0	0.2	0.15	0.00	0.15
H23	C3	0.1	0.0	0.1	0.06	-0.02	0.08
H23	C4	1.1	0.0	1.1	1.05	0.00	1.05
H23	H5	1.0	0.0	1.0	1.00	0.00	1.00
H23	H6	0.1	0.0	0.1	0.06	0.00	0.06
H23	H7	0.0	0.0	0.0	-0.01	0.00	-0.01
H23	H8	0.0	0.0	0.0	0.02	0.00	0.02
H23	H9	0.0	0.0	0.0	0.00	0.00	0.00

Table A9 continues

Atom		3b			3b *minus* (1b+2)		
A	**B**	$E_{\text{int}}^{\text{A,B}}$	$V_{\text{XC}}^{\text{A,B}}$	$V_{\text{cl}}^{\text{A,B}}$	$\Delta E_{\text{int}}^{\text{A,B}}$	$\Delta V_{\text{XC}}^{\text{A,B}}$	$\Delta V_{\text{cl}}^{\text{A,B}}$
H23	H10	0.0	0.0	0.0	-0.02	-0.01	0.00
H23	H11	-0.1	-0.1	0.0	-0.09	-0.05	-0.03
H23	H12	0.1	0.0	0.1	0.14	0.00	0.14
H23	N13	-2.8	0.0	-2.8	-2.81	0.00	-2.81
H23	C14	5.9	0.0	5.9	5.85	0.00	5.85
H23	O15	-3.8	0.0	-3.8	-3.81	0.00	-3.81
H23	O16	-5.5	0.0	-5.5	-5.54	-0.02	-5.52
H23	H17	3.6	0.0	3.6	3.63	-0.01	3.64
H23	C18	5.7	-4.4	10.1	1.24	-0.18	1.42
H23	O19	-10.2	-1.1	-9.1	-1.72	0.06	-1.79
H23	C20	-150.7	-172.2	21.4	0.66	0.61	0.05
H23	H21	-0.7	-3.1	2.4	0.44	-0.14	0.58
H23	H22	-0.7	-2.8	2.1	0.51	0.43	0.09
C24	C1	-0.1	0.0	-0.1	-0.07	0.00	-0.07
C24	C2	0.0	0.0	0.0	0.00	0.00	0.00
C24	C3	0.0	0.0	0.0	-0.03	-0.01	-0.01
C24	C4	0.0	0.0	0.0	-0.03	-0.01	-0.02
C24	H5	-0.1	0.0	-0.1	-0.05	0.00	-0.05
C24	H6	0.0	0.0	0.0	0.00	0.00	0.00
C24	H7	0.0	0.0	0.0	0.01	0.00	0.01
C24	H8	0.0	0.0	0.0	0.01	0.00	0.01
C24	H9	0.0	0.0	0.0	0.00	0.00	0.00
C24	H10	0.0	0.0	0.0	-0.02	-0.04	0.02
C24	H11	0.0	0.0	0.0	-0.02	-0.01	-0.01
C24	H12	0.0	0.0	0.0	0.00	-0.01	0.01
C24	N13	0.2	0.0	0.2	0.18	0.00	0.18
C24	C14	0.2	0.0	0.2	0.22	0.00	0.22
C24	O15	0.0	0.0	0.0	-0.01	0.00	-0.01
C24	O16	-0.6	-0.1	-0.5	-0.58	-0.09	-0.49
C24	H17	0.5	-0.1	0.6	0.48	-0.11	0.58
C24	C18	-167.4	-190.2	22.8	0.15	-2.80	2.95
C24	O19	-17.3	-11.4	-5.9	-1.95	0.50	-2.45
C24	C20	-3.6	-4.7	1.1	0.48	0.28	0.20
C24	H21	-0.3	-0.5	0.2	0.11	-0.01	0.11
C24	H22	-0.3	-0.4	0.2	0.13	0.07	0.06
C24	H23	-0.5	-0.8	0.2	0.08	-0.01	0.09
H25	C1	0.8	0.0	0.8	0.83	0.00	0.84
H25	C2	0.1	0.0	0.1	0.12	0.00	0.12
H25	C3	0.1	0.0	0.1	0.06	-0.01	0.08
H25	C4	0.9	0.0	0.9	0.88	0.00	0.88

Table A9 continues

Atom		3b			3b *minus* (1b+2)		
A	**B**	$E_{\mathrm{int}}^{\mathrm{A,B}}$	$V_{\mathrm{XC}}^{\mathrm{A,B}}$	$V_{\mathrm{cl}}^{\mathrm{A,B}}$	$\Delta E_{\mathrm{int}}^{\mathrm{A,B}}$	$\Delta V_{\mathrm{XC}}^{\mathrm{A,B}}$	$\Delta V_{\mathrm{cl}}^{\mathrm{A,B}}$
H25	H5	0.8	0.0	0.8	0.84	0.00	0.84
H25	H6	0.0	0.0	0.0	0.05	0.00	0.05
H25	H7	0.0	0.0	0.0	-0.02	0.00	-0.02
H25	H8	0.0	0.0	0.0	0.02	0.00	0.02
H25	H9	0.0	0.0	0.0	0.00	0.00	0.00
H25	H10	0.0	0.0	0.0	-0.05	-0.02	-0.02
H25	H11	0.0	0.0	0.0	0.01	0.00	0.02
H25	H12	0.1	0.0	0.1	0.10	0.00	0.10
H25	N13	-2.4	0.0	-2.4	-2.44	0.00	-2.44
H25	C14	4.4	0.0	4.4	4.39	0.00	4.39
H25	O15	-2.9	0.0	-2.9	-2.92	0.00	-2.91
H25	O16	-4.0	0.0	-4.0	-3.96	-0.01	-3.95
H25	H17	2.6	0.0	2.6	2.62	-0.01	2.63
H25	C18	5.4	-4.5	9.8	0.52	0.11	0.41
H25	O19	-9.9	-1.1	-8.8	-0.65	0.18	-0.83
H25	C20	-0.6	-0.7	0.2	-0.15	-0.22	0.07
H25	H21	0.0	-0.4	0.4	-0.22	-0.40	0.18
H25	H22	0.3	0.0	0.3	0.01	-0.01	0.02
H25	H23	0.3	-0.1	0.4	0.49	0.39	0.09
H25	C24	-150.5	-172.0	21.5	-0.15	-0.31	0.16
H26	C1	0.9	0.0	0.9	0.94	0.00	0.94
H26	C2	0.1	0.0	0.1	0.13	0.00	0.13
H26	C3	0.1	0.0	0.1	0.08	0.00	0.09
H26	C4	1.0	0.0	1.0	0.98	0.00	0.98
H26	H5	0.9	0.0	0.9	0.94	0.00	0.94
H26	H6	0.1	0.0	0.1	0.05	0.00	0.05
H26	H7	0.0	0.0	0.0	-0.03	0.00	-0.03
H26	H8	0.0	0.0	0.0	0.01	0.00	0.01
H26	H9	0.0	0.0	0.0	0.00	0.00	0.00
H26	H10	0.0	0.0	0.0	-0.03	0.00	-0.03
H26	H11	0.0	0.0	0.0	0.02	0.00	0.02
H26	H12	0.1	0.0	0.1	0.11	0.00	0.11
H26	N13	-2.7	0.0	-2.7	-2.73	0.00	-2.73
H26	C14	4.8	0.0	4.8	4.83	0.00	4.83
H26	O15	-3.2	0.0	-3.2	-3.22	0.00	-3.22
H26	O16	-4.3	0.0	-4.3	-4.33	-0.01	-4.32
H26	H17	2.9	0.0	2.9	2.86	-0.01	2.87
H26	C18	5.8	-4.9	10.6	1.27	-0.68	1.94
H26	O19	-10.8	-1.2	-9.5	-2.33	-0.09	-2.25
H26	C20	-0.4	-0.5	0.1	0.26	0.25	0.02

Table A9 continues

Atom		3b			3b *minus* (1b+2)		
A	**B**	$E_{\mathrm{int}}^{\mathrm{A,B}}$	$V_{\mathrm{XC}}^{\mathrm{A,B}}$	$V_{\mathrm{cl}}^{\mathrm{A,B}}$	$\Delta E_{\mathrm{int}}^{\mathrm{A,B}}$	$\Delta V_{\mathrm{XC}}^{\mathrm{A,B}}$	$\Delta V_{\mathrm{cl}}^{\mathrm{A,B}}$
H26	H21	0.4	0.0	0.5	0.23	0.01	0.22
H26	H22	0.3	0.0	0.3	0.48	0.44	0.04
H26	H23	0.0	-0.4	0.4	-0.19	-0.39	0.20
H26	C24	-149.4	-170.9	21.5	1.97	1.89	0.08
H26	H25	-0.8	-3.1	2.3	0.46	0.11	0.35
H27	C1	0.8	0.0	0.8	0.77	0.00	0.77
H27	C2	0.1	0.0	0.1	0.11	0.00	0.11
H27	C3	0.1	0.0	0.1	0.07	0.00	0.07
H27	C4	0.8	0.0	0.8	0.81	0.00	0.81
H27	H5	0.8	0.0	0.8	0.77	0.00	0.77
H27	H6	0.0	0.0	0.0	0.04	0.00	0.04
H27	H7	0.0	0.0	0.0	-0.02	0.00	-0.02
H27	H8	0.0	0.0	0.0	0.01	0.00	0.01
H27	H9	0.0	0.0	0.0	0.00	0.00	0.00
H27	H10	0.0	0.0	0.0	-0.03	0.00	-0.03
H27	H11	0.0	0.0	0.0	0.01	0.00	0.01
H27	H12	0.1	0.0	0.1	0.09	0.00	0.09
H27	N13	-2.2	0.0	-2.2	-2.22	0.00	-2.22
H27	C14	4.1	0.0	4.1	4.06	0.00	4.06
H27	O15	-2.7	0.0	-2.7	-2.69	0.00	-2.69
H27	O16	-3.7	0.0	-3.7	-3.68	-0.01	-3.68
H27	H17	2.5	0.0	2.5	2.47	0.00	2.47
H27	C18	6.7	-3.3	10.1	1.08	-0.07	1.15
H27	O19	-11.0	-2.1	-8.8	-1.59	0.04	-1.63
H27	C20	-0.3	-0.5	0.1	0.06	0.01	0.05
H27	H21	0.4	0.0	0.4	0.22	0.07	0.15
H27	H22	0.2	-0.1	0.3	-0.03	-0.06	0.03
H27	H23	0.3	0.0	0.4	0.12	0.00	0.12
H27	C24	-152.9	-174.7	21.8	0.38	0.25	0.13
H27	H25	-0.7	-2.8	2.1	0.36	0.14	0.22
H27	H26	-0.7	-2.8	2.2	0.47	0.08	0.39
				Total:	**-46.1**	**-9.1**	**-37.0**

End of PART A4

PART A5

Data pertaining to multi-step processes leading to the CN-bond formation.

A structural re-arrangement from 3a and 3b to pre-organised for the C–N bond formation and H-transfer structures, 4a and 4b.

Data obtained from d(N13,C18) scans performed on GMS of **3a** and **3b** adducts is shown in Figure A4. Structures at the local minima and those pertaining to products after CN-bond formation were energy optimised without any constrain. Transitional state structures (**5a** and **5b**) and their energies were obtained by applying Berny protocol.

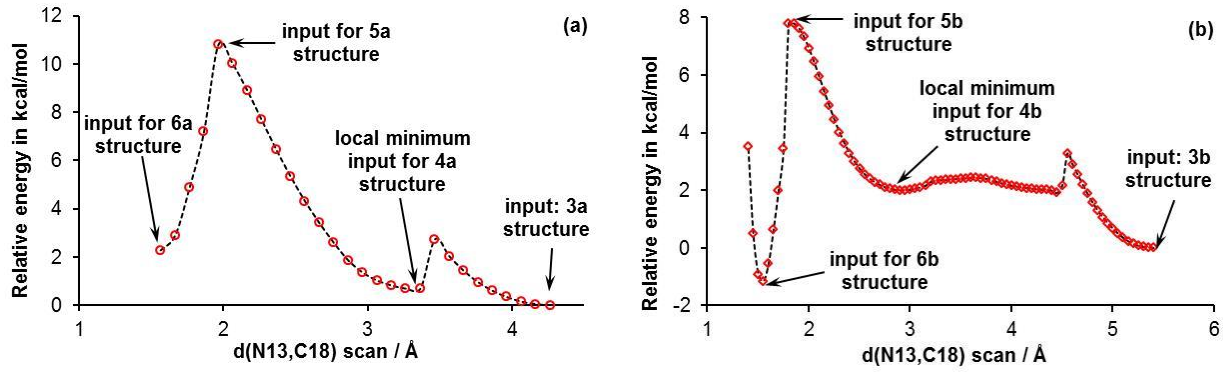

Figure A4. B3LYP data obtained from the d(N13,C18) scans performed on GMS of **3a** and **3b** adducts.

To facilitate interpretation of energies included in Table A10, analysis for selected structures (based on the MP2 data as it is a higher level of theory relative to B3LYP) follows:

1) ***Local minimum structures*** **4a** ***and*** **4b**. Both GMS adducts (**3a** and **3b**) had to overcome a small energy barrier (of about 3 kcal mol^{-1}, see Figure A4) to attained local minimum structures **4a** and **4b** that are much better pre-organised for the C18N13-bond formation accompanied by the H17 transfer from O16 to O19 (Figure A5). **4a** is higher in energy then **3a** by +0.7, +0.7 and +0.3 kcal mol^{-1} obtained for ΔE_{ZPVE}, ΔH and ΔG, respectively. Note that these energy changes (shown as Δ in Table A10) represent differences between consecutive structures, e.g., ΔH = H(**4a**) – H(**3a**) = 0.7 kcal mol^{-1}. For **4b** we obtained +1.7, +1.5 and +2.5 kcal mol^{-1} for ΔE_{ZPVE}, ΔH and ΔG, respectively. The energy of **4a** is lower than that of **4b** by –2.9, –2.6 and –4.6 kcal mol^{-1} obtained for ΔE_{ZPVE}, ΔH and ΔG, respectively.

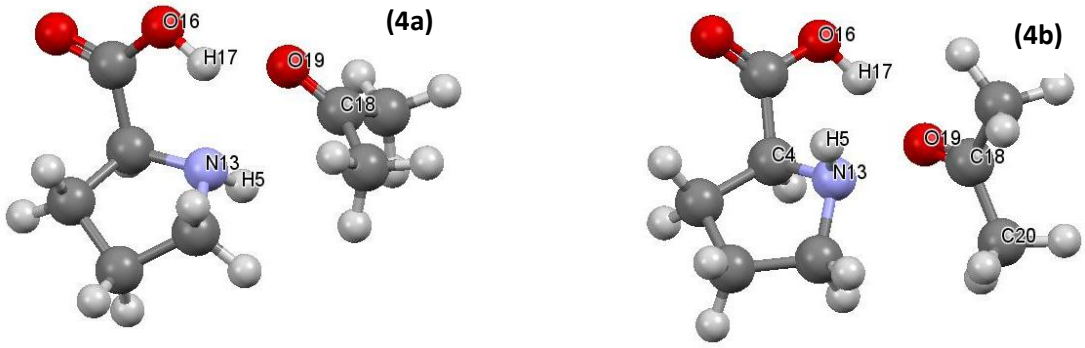

Figure A5. Ball-and-stick representation of energy optimised local minimum B3LYP structures **4a** (d(N13,C18) =3.338 Å. d(N17,O19) =2.222 Å) and **4b** (d(N13,C18) =2.9278 Å. d(H17,O19) =1.6806 Å).

2) ***Transitional state (TS) structures*** **5a** ***and*** **5b**. To attain the TS structure (Figure A6), the pre-organised (local minimum) **4a** and **4b** structures had to climb an energy barrier of 10.7 (ΔE_{ZPVE}), 9.1 (ΔH) and 14.7 (ΔG) kcal mol^{-1} in the case of **4a** and significantly smaller energy barriers of 4.6 (ΔE_{ZPVE}), 3.1 (ΔH) and 8.0 (ΔG) kcal mol^{-1} in the case of **4b**. As a result, on an absolute scale, the energy of TS(**5a**) structure is higher than that of TS(**5b**) (computed as, e.g., (ΔH) =H(**5a**) – H(**5b**)) by 2.6 (ΔE_{ZPVE}), 2.7 (ΔH) and 2.3 (ΔG) kcal mol^{-1}.

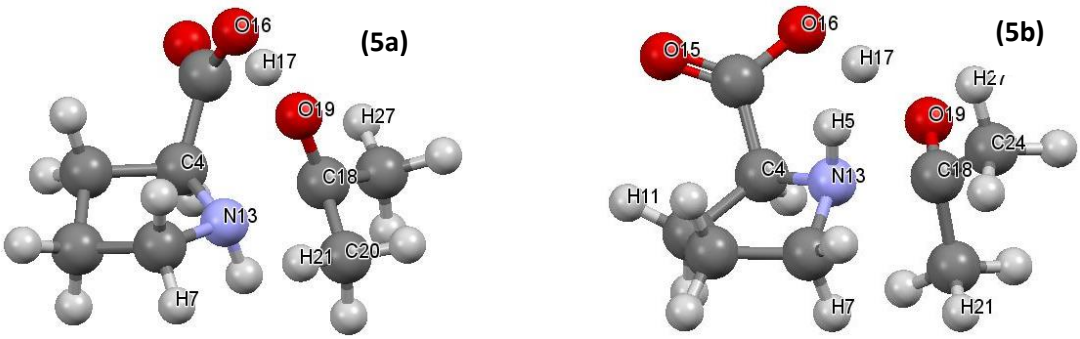

Figure A6. Ball-and-stick representation of B3LYP TS structures **5a** (d(N13,C18) = 1.9055 Å, d(O16,O19) = 2.4194 Å, d(O16,H17) = 1.1045 Å, d(H17,O19) = 1.3178 Å) and **5b** (d(N13,C18) = 1.8300 Å, d(O16,O19) = 2.4612 Å, d(O16,H17) = 1.0644 Å, d(H17,O19) = 1.4042 Å,.

Table A10. B3LYP/6-311++G(d,p)/GD3 energies (in au) and associated energy changes (in kcal mol^{-1}) between consecutive steps from **3a** and **3b**, followed by **4a** and **4b** (local minimum structures), **5a** and **5b** (TS structures) to **6a** and **6b** (products on CN-bond formation). Δ stands for an energy difference (in kcal mol^{-1}) between consecutive structures, e.g., *E*(**5a**) – *E*(**4a**) or *G*(**6b**) – *G*(**5b**). Energy differences between structures containing **1a** and **1b** as, e.g., Δ*E*(**4**) = *E*(**4a**) – *E*(**4b**), are also provided (values in kcal mol^{-1}). Data obtained at the MP2/6-311++G(d,p) level is printed in italic.

Structure	***E***	**Δ**	E_{ZPVE}	**Δ**	***H***	**Δ**	***G***	**Δ**
	Structures containing **1a**							
3a	-594.5478		-594.3188		-594.3034		-594.3632	
	-592.8656		*-592.6337*		*-592.6183*		*-592.6778*	
4a	-594.5467	0.6	-594.3182	0.4	-594.3026	0.5	-594.3637	-0.3
	-592.8644	*0.7*	*-592.6326*	*0.7*	*-592.6172*	*0.7*	*-592.6773*	*0.3*
5a	-594.5303	11.0	-594.3007	11.4	-594.2881	9.6	-594.3383	15.6
	-592.8486	*10.0*	*-592.6156*	*10.7*	*-592.6027*	*9.1*	*-592.6539*	*14.7*
6a	-594.5442	2.2	-594.3097	5.7	-594.2970	4.0	-594.3470	10.2
	-592.8707	*-13.9*	*-592.6333*	*-11.1*	*-592.6207*	*-11.3*	*-592.6704*	*-10.4*
	Structures containing **1b**							
3b	-594.5460		-594.3171		-594.3017		-594.3623	
	-592.8619		*-592.6297*		*-592.6144*		*-592.6742*	
4b	-594.5428	3.1	-594.3136	3.3	-594.2985	3.1	-594.3564	4.2
	-592.8592	*1.7*	*-592.6270*	*1.7*	*-592.6118*	*1.6*	*-592.6703*	*2.5*
5b	-594.5336	7.8	-594.3029	8.9	-594.2904	7.1	-594.3404	13.8
	-592.8534	*3.6*	*-592.6196*	*4.6*	*-592.6069*	*3.1*	*-592.6575*	*8.0*
6b	-594.5479	-1.2	-594.3138	2.0	-594.3008	0.6	-594.3520	6.5
	-592.8759	*-14.1*	*-592.6397*	*-12.6*	*-592.6267*	*-12.4*	*-592.6774*	*-12.5*
		Energy difference for 4a relative to 4b						
		-2.5		-2.9		-2.6		-4.6
		-3.3		*-3.5*		*-3.4*		*-4.4*
		Energy difference for 5a relative to 5b						
		2.0		1.4		1.4		1.3
		3.0		*2.6*		*2.7*		*2.3*
		Energy difference for 6a relative to 6b						
		2.3		2.6		2.4		3.1
		3.3		*4.0*		*3.8*		*4.4*

Table A11. Net atomic charges, Q(A) and differences, ΔQ(A), computed for the indicated structures - values in *e*.

	Q(A)		ΔQ(A)	Q(A)		ΔQ(A)		
Atom	**3a**	**4a**	**4a – 3a**	**3b**	**4b**	**4b – 3b**	**3a – 3b**	**4a – 4b**
C1	0.3162	0.3241	0.0080	0.3313	0.3252	-0.0061	-0.0151	-0.0011
C2	0.0437	0.0450	0.0014	0.0388	0.0306	-0.0082	0.0049	0.0144
C3	0.0375	0.0414	0.0039	0.0265	0.0298	0.0033	0.0110	0.0116
C4	0.2955	0.3112	0.0157	0.3101	0.3071	-0.0030	-0.0146	0.0041
H5	0.3643	0.3604	-0.0039	0.3547	0.3342	-0.0205	0.0096	0.0262
H6	0.0224	0.0014	-0.0210	0.0115	0.0150	0.0035	0.0109	-0.0136
H7	0.0181	0.0162	-0.0019	-0.0069	-0.0018	0.0050	0.0250	0.0181
H8	-0.0064	-0.0036	0.0028	0.0024	-0.0032	-0.0056	-0.0088	-0.0005
H9	0.0065	0.0072	0.0006	-0.0076	-0.0069	0.0008	0.0141	0.0140
H10	0.0135	0.0185	0.0050	0.0051	0.0003	-0.0048	0.0083	0.0182
H11	0.0245	0.0031	-0.0214	0.0054	0.0150	0.0096	0.0191	-0.0119
H12	0.0494	0.0426	-0.0068	0.0339	0.0309	-0.0030	0.0155	0.0117
N13	-0.9855	-0.9831	0.0025	-0.9705	-0.9332	0.0373	-0.0150	-0.0499
C14	1.5236	1.5242	0.0005	1.5233	1.5278	0.0045	0.0003	-0.0037
O15	-1.1914	-1.1960	-0.0045	-1.1828	-1.1778	0.0050	-0.0086	-0.0182
O16	-1.1387	-1.1419	-0.0032	-1.1612	-1.1566	0.0046	0.0225	0.0147
H17	0.6051	0.6213	0.0162	0.6302	0.6298	-0.0004	-0.0251	-0.0085
C18	0.9662	0.9685	0.0023	0.9400	0.9547	0.0146	0.0261	0.0138
O19	-1.1579	-1.1537	0.0042	-1.1516	-1.1619	-0.0103	-0.0063	0.0082
C20	-0.0158	-0.0170	-0.0013	-0.0158	-0.0091	0.0067	0.0000	-0.0080
H21	0.0303	0.0343	0.0040	0.0557	0.0502	-0.0055	-0.0253	-0.0159
H22	0.0407	0.0405	-0.0001	0.0400	0.0369	-0.0031	0.0007	0.0036
H23	0.0399	0.0382	-0.0017	0.0509	0.0426	-0.0083	-0.0110	-0.0044
C24	-0.0200	-0.0147	0.0053	-0.0103	-0.0017	0.0086	-0.0096	-0.0130
H25	0.0295	0.0420	0.0125	0.0484	0.0408	-0.0075	-0.0189	0.0012
H26	0.0585	0.0352	-0.0233	0.0537	0.0440	-0.0098	0.0048	-0.0088
H27	0.0302	0.0355	0.0053	0.0442	0.0375	-0.0067	-0.0140	-0.0020

Note that (i) N13 is not the most negatively charged atom in all structures and its charge decreased on **3a** → **4a** by 25m*e* and **3b** → **4b** by 373m*e*, (ii) C18 is most positively charged in all structures and became more positively charged due to a loss of electrons on **3a** → **4a** by 23m*e* and **3b** → **4b** by 146m*e*, and (iii) many atoms experienced significant change in net atomic charges on both structural changes, **3a** → **4a** and **3b** → **4b**.

Table A12. Top 30 atom-pairs for which most significant increase/decrease in the net 2-atom fragment charge (in e) took place on the pre-organisation from: **3a** to **4a** – part a, **3b** to **4b** – part b. $\Delta\Delta Q(A,B)$ = {$\Delta Q(A,B)$ in **4**} – {$\Delta Q(A,B)$ in **3**} where $\Delta Q(A,B)$ is a difference in net atomic charges between atoms A and B.

Part A: change from **3a** to **4a**.

Charge difference increased			**Charge difference decreased**		
Atom A	**Atom B**	**$\Delta\Delta Q(A,B)$**	**Atom A**	**Atom B**	**$\Delta\Delta Q(A,B)$**
H26	H17	0.0395	H25	H5	-0.0164
H26	C4	0.0391	O15	H6	-0.0165
H17	H11	0.0376	O15	H11	-0.0169
H17	H6	0.0372	O16	H6	-0.0178
H11	C4	0.0372	O16	H11	-0.0182
H6	C4	0.0367	H26	O15	-0.0188
H25	H11	0.0340	H25	H12	-0.0193
H25	H6	0.0335	H5	C4	-0.0196
H26	C1	0.0313	C20	H6	-0.0197
H11	C1	0.0294	H26	O16	-0.0201
H6	C1	0.0290	C20	H11	-0.0202
H27	H11	0.0268	H26	H7	-0.0214
H27	H6	0.0263	H26	C20	-0.0221
H26	C18	0.0257	H26	H25	-0.0222
H21	H11	0.0254	N13	H6	-0.0235
H11	C3	0.0253	H8	H6	-0.0238
H21	H6	0.0250	N13	H11	-0.0239
H6	C3	0.0249	H26	H9	-0.0239
H26	C14	0.0238	H11	H8	-0.0242
C18	H11	0.0238	O19	H6	-0.0252
C18	H6	0.0233	O19	H11	-0.0256
H17	H12	0.0230	H26	N13	-0.0258
H11	C2	0.0228	H26	H8	-0.0261
H12	C4	0.0225	C24	H6	-0.0263
H6	C2	0.0224	C24	H11	-0.0267
C14	H11	0.0220	H26	H21	-0.0273
C14	H6	0.0215	H26	O19	-0.0275
H22	H11	0.0213	H27	H26	-0.0280
H22	H6	0.0209	H26	H10	-0.0283
H17	O15	0.0207	H26	C24	-0.0286
Atom-pairs of special interest					
O19	H17	0.0120	C18	N13	-0.0001

Part B: change from **3b** to **4b**.

Charge difference increased			**Charge difference decreased**		
Atom A	**Atom B**	**ΔΔ*Q*(A,B)**	**Atom A**	**Atom B**	**ΔΔ*Q*(A,B)**
O19	N13	0.0476	H5	C3	-0.0238
C18	H5	0.0351	H6	H5	-0.0240
O16	N13	0.0327	O16	H5	-0.0251
O15	N13	0.0323	O15	H5	-0.0255
C14	H5	0.0250	H7	H5	-0.0255
O19	C18	0.0249	C20	H5	-0.0272
H26	C18	0.0244	N13	H11	-0.0277
H23	C18	0.0229	C24	N13	-0.0287
C18	C2	0.0228	C24	H5	-0.0291
H25	C18	0.0222	H11	H5	-0.0301
H27	C18	0.0213	C20	N13	-0.0306
C18	C1	0.0207	N13	H7	-0.0323
C18	H8	0.0202	C14	N13	-0.0328
H21	C18	0.0201	N13	H6	-0.0339
H17	H5	0.0201	N13	C3	-0.0340
O19	H11	0.0199	N13	H9	-0.0366
C18	H10	0.0194	H17	N13	-0.0377
C24	O19	0.0189	N13	C4	-0.0404
H22	C18	0.0177	N13	H12	-0.0404
C18	H12	0.0177	H22	N13	-0.0404
C18	C4	0.0177	N13	H10	-0.0421
C20	O19	0.0170	H21	N13	-0.0428
O19	H7	0.0154	N13	H8	-0.0429
H11	H8	0.0152	N13	C1	-0.0434
C18	H17	0.0150	H27	N13	-0.0440
O19	C14	0.0148	H25	N13	-0.0449
H11	H10	0.0144	N13	C2	-0.0455
H26	C14	0.0143	H23	N13	-0.0456
C18	H9	0.0139	H26	N13	-0.0471
O19	H6	0.0138	N13	H5	-0.0578
Atom-pairs of special interest					
O19	H17	0.0099	C18	N13	-0.0227

Table A13. Top 10 atom-pairs with strongest attractive/repulsive diatomic intermolecular interactions in: **3a** – part A, **3b** – part B. Interaction energies are in kcal mol^{-1}.

Part A: data for **3a**.

Strongest attractive interactions					**Strongest repulsive interactions**				
Atom A	**Atom B**	$E_{\text{int}}^{\text{A,B}}$	$V_{\text{XC}}^{\text{A,B}}$	$V_{\text{cl}}^{\text{A,B}}$	**Atom A**	**Atom B**	$E_{\text{int}}^{\text{A,B}}$	$V_{\text{XC}}^{\text{A,B}}$	$V_{\text{cl}}^{\text{A,B}}$
O19	C14	-161.3	-0.3	-161.0	H23	C14	5.5	0.0	5.5
C18	O16	-113.4	-1.7	-111.7	H26	C14	8.9	-0.2	9.1
C18	O15	-98.6	-0.1	-98.5	C18	H5	24.0	0.0	24.0
C18	N13	-76.9	0.0	-76.9	C18	C4	24.0	0.0	24.0
O19	H17	-65.6	0.0	-65.6	C18	C1	26.2	0.0	26.2
O19	C1	-34.4	-1.1	-33.3	C18	H17	56.9	0.0	56.9
O19	C4	-29.7	-0.1	-29.6	O19	N13	94.3	-0.1	94.4
O19	H5	-29.5	0.0	-29.5	O19	O15	115.1	-0.2	115.3
H26	O15	-9.2	-2.2	-7.0	O19	O16	125.1	-0.9	126.0
H26	O16	-8.9	-2.0	-6.9	C18	C14	138.3	-0.1	138.4

All interactions and components			
	$E_{\text{int}}^{\text{A,B}}$	$V_{\text{XC}}^{\text{A,B}}$	$V_{\text{cl}}^{\text{A,B}}$
Total:	-34.3	-26.7	-7.6

Part B: data for **3b**.

Strongest attractive interactions					**Strongest repulsive interactions**				
Atom A	**Atom B**	$E_{\text{int}}^{\text{A,B}}$	$V_{\text{XC}}^{\text{A,B}}$	$V_{\text{cl}}^{\text{A,B}}$	**Atom A**	**Atom B**	$E_{\text{int}}^{\text{A,B}}$	$V_{\text{XC}}^{\text{A,B}}$	$V_{\text{cl}}^{\text{A,B}}$
O19	C14	-159.8	-0.2	-159.6	H23	C14	5.9	0.0	5.9
O19	H17	-143.9	-18.3	-125.6	H21	C14	6.3	0.0	6.3
C18	O16	-114.2	-0.2	-114.0	C18	C1	19.7	0.0	19.7
C18	O15	-73.9	0.0	-73.9	C18	H5	20.1	0.0	20.1
C18	N13	-58.0	0.0	-58.0	C18	C4	21.9	-0.1	22.0
O19	C4	-30.7	-1.4	-29.3	O19	N13	76.4	-0.1	76.5
O19	H5	-26.4	0.0	-26.4	C18	H17	85.6	-0.2	85.8
O19	C1	-25.5	0.0	-25.5	O19	O15	97.8	-0.2	98.0
O19	H12	-6.3	-2.9	-3.4	C18	C14	117.8	0.0	117.8
H21	O16	-6.0	0.0	-6.0	O19	O16	150.0	-8.2	158.2

All interactions and components			
	$E_{\text{int}}^{\text{A,B}}$	$V_{\text{XC}}^{\text{A,B}}$	$V_{\text{cl}}^{\text{A,B}}$
Total:	-53.6	-40.7	-12.9

Table A14. Top 10 atom-pairs with strongest attractive/repulsive diatomic intermolecular interactions in: **4a** – part A, **4b** – part B. Interaction energies are in kcal mol^{-1}.

Part A: data for **4a**.

Strongest attractive interactions					**Strongest repulsive interactions**				
Atom A	**Atom B**	$E_{int}^{A,B}$	$V_{XC}^{A,B}$	$V_{cl}^{A,B}$	**Atom A**	**Atom B**	$E_{int}^{A,B}$	$V_{XC}^{A,B}$	$V_{cl}^{A,B}$
O19	C14	-139.6	-0.1	-139.5	H26	C14	3.8	0.0	3.8
C18	O16	-104.5	-0.1	-104.4	H25	C14	4.5	0.0	4.5
C18	N13	-103.4	-0.9	-102.5	C18	C4	26.0	0.0	26.0
O19	H17	-102.7	-3.8	-98.9	C18	C1	31.0	-0.4	31.4
C18	O15	-69.9	0.0	-69.9	C18	H5	33.2	0.0	33.2
O19	H5	-38.7	0.0	-38.7	C18	H17	73.4	-0.1	73.5
O19	C1	-37.9	-0.6	-37.3	O19	O15	88.9	-0.1	89.0
O19	C4	-32.0	0.0	-32.0	C18	C14	108.1	0.0	108.1
H25	N13	-4.7	-0.1	-4.6	O19	N13	119.8	-3.0	122.8
H27	N13	-4.7	-1.1	-3.6	O19	O16	135.0	-4.3	139.3

All interactions and components			
	$E_{int}^{A,B}$	$V_{XC}^{A,B}$	$V_{cl}^{A,B}$
Total:	-23.9	-23.0	-0.9

Sum of all intermolecular interactions

Part B: data for **4b**.

Strongest attractive interactions					**Strongest repulsive interactions**				
Atom A	**Atom B**	$E_{int}^{A,B}$	$V_{XC}^{A,B}$	$V_{cl}^{A,B}$	**Atom A**	**Atom B**	$E_{int}^{A,B}$	$V_{XC}^{A,B}$	$V_{cl}^{A,B}$
O19	C14	-165.3	-0.2	-165.1	H25	C14	5.3	0.0	5.3
O19	H17	-146.5	-18.3	-128.2	H26	C14	5.7	0.0	5.7
C18	O16	-120.5	-0.3	-120.2	C18	C1	30.6	-0.1	30.7
C18	N13	-112.2	-4.7	-107.4	C18	H5	31.2	0.0	31.2
C18	O15	-78.8	0.0	-78.8	C18	C4	31.4	-0.2	31.6
O19	C4	-40.4	-1.4	-38.9	C18	H17	90.3	-0.3	90.6
O19	H5	-36.5	-0.1	-36.4	O19	O15	100.2	-0.2	100.4
O19	C1	-35.9	-0.1	-35.8	O19	N13	120.1	-4.0	124.1
O19	H12	-6.7	-3.1	-3.5	C18	C14	127.2	0.0	127.2
H27	O16	-5.9	-2.0	-3.9	O19	O16	153.1	-8.1	161.2

All interactions and components			
	$E_{int}^{A,B}$	$V_{XC}^{A,B}$	$V_{cl}^{A,B}$
Total:	-70.3	-55.4	-14.9

Table A15. Top 10 atom-pairs for which most significant increase/decrease in the intermolecular diatomic interaction energy (in kcal mol^{-1}) that took place on the pre-organisation from: **3a** to **4a** – part A, **3b** to **4b** – part B. $\Delta E_{\text{int}}^{\text{A,B}}$ = { $E_{\text{int}}^{\text{A,B}}$ in **4**} – { $E_{\text{int}}^{\text{A,B}}$ in **3**}.

Part A: from **3a** to **4a**.

Strongest attractive interactions					**Strongest repulsive interactions**				
Atom A	**Atom B**	$\Delta E_{\text{int}}^{\text{A,B}}$	$\Delta V_{\text{XC}}^{\text{A,B}}$	$\Delta V_{\text{cl}}^{\text{A,B}}$	**Atom A**	**Atom B**	$\Delta E_{\text{int}}^{\text{A,B}}$	$\Delta V_{\text{XC}}^{\text{A,B}}$	$\Delta V_{\text{cl}}^{\text{A,B}}$
O19	H17	-37.1	-3.8	-33.3	H26	O16	5.4	2.0	3.4
C18	C14	-30.2	0.1	-30.3	O19	H11	5.8	3.8	2.0
C18	N13	-26.4	-0.9	-25.5	H26	O15	6.7	2.2	4.5
O19	O15	-26.1	0.1	-26.2	C18	O16	8.9	1.6	7.3
O19	H5	-9.2	0.0	-9.2	C18	H5	9.2	0.0	9.2
H26	C14	-5.1	0.2	-5.3	O19	O16	9.9	-3.3	13.2
O19	C1	-3.6	0.4	-4.0	C18	H17	16.5	-0.1	16.6
H25	N13	-2.5	-0.1	-2.4	O19	C14	21.8	0.2	21.6
H27	N13	-2.4	-1.1	-1.3	O19	N13	25.4	-2.9	28.3
O19	C4	-2.3	0.1	2.4	C18	O15	28.8	0.1	28.7

All interactions and components			
	$\Delta E_{\text{int}}^{\text{A,B}}$	$\Delta V_{\text{XC}}^{\text{A,B}}$	$\Delta V_{\text{cl}}^{\text{A,B}}$
Total:	10.4	3.8	6.6

Part B: from **3b** to **4b**.

Strongest attractive interactions					**Strongest repulsive interactions**				
Atom A	**Atom B**	$\Delta E_{\text{int}}^{\text{A,B}}$	$\Delta V_{\text{XC}}^{\text{A,B}}$	$\Delta V_{\text{cl}}^{\text{A,B}}$	**Atom A**	**Atom B**	$\Delta E_{\text{int}}^{\text{A,B}}$	$\Delta V_{\text{XC}}^{\text{A,B}}$	$\Delta V_{\text{cl}}^{\text{A,B}}$
C18	N13	-54.1	-4.7	-49.4	H21	O16	1.7	0.0	1.7
O19	C1	-10.4	0.0	-10.4	H23	O16	1.8	0.0	1.8
O19	H5	-10.0	0.0	-10.0	O19	O15	2.4	0.0	2.4
O19	C4	-9.7	-0.1	-9.6	O19	O16	3.1	0.1	3.0
C18	O16	-6.3	-0.2	-6.1	C18	H17	4.7	-0.1	4.8
O19	C14	-5.5	0.0	-5.5	C18	C14	9.4	0.0	9.4
C18	O15	-4.9	0.0	-4.9	C18	C4	9.5	-0.1	9.6
H25	N13	-3.1	-1.0	-2.0	C18	C1	11.0	-0.1	11.1
O19	H17	-2.6	0.0	-2.6	C18	H5	11.2	0.0	11.2
C24	N13	-2.6	-2.9	0.3	O19	N13	43.7	-3.9	47.6

All interactions and components			
	$\Delta E_{\text{int}}^{\text{A,B}}$	$\Delta V_{\text{XC}}^{\text{A,B}}$	$\Delta V_{\text{cl}}^{\text{A,B}}$
Total:	-16.7	-14.7	-2.0

Data in Table A16 can be used to pin-point individual atoms that played most important role in the **3** to **4** pre-organisation process. There are just few atoms interactions of which changed most significantly. It is clear that this is not the C18 atom of **2** that attracts entire **1** (even though it is to form a bond with N13 at the later stage of a process) as we found $E_{\text{int}}^{\text{C18,}\mathbf{1}}$ of +7.8 (in **4a**) and +11.2 kcal mol^{-1} (in **4b**). Importantly, note that C18 is involved in strongest repulsive interactions with **1** in both pre-organised adducts, **4a** and **4b**. There is however a significant difference when the trend in $E_{\text{int}}^{\text{C18,}\mathbf{1}}$ is considered on the **3** $\rightarrow$ **4** change, namely the interaction between C18 and all atoms of **1** (i) became repulsive as it changed from very weak attractive in **3a** (–0.7 kcal mol^{-1}) to repulsive in **4a** (+7.8 kcal mol^{-1}) whereas (ii) opposite trend is seen for **3b** $\rightarrow$ **4b** as it became less repulsive by –15.3 kcal mol^{-1} in the latter.

Focusing on atoms of **1** we found that:

a) O16 in **3a** attracts **2** by far the most with $E_{\text{int}}^{\text{O16,}\mathbf{2}}$ of –20 kcal mol^{-1} whereas H17 and C14 of **3b** interact most favourably with **2** with $E_{\text{int}}^{\text{H17,}\mathbf{2}}$ and $E_{\text{int}}^{\text{C14,}\mathbf{2}}$ of –40.4 and –13.7 kcal mol^{-1}, respectively.

b) After the pre-organisation process, H17, C14 and N13 in **4a** can be seen as keeping **1** and **2** in close proximity as their interactions with **2** of –17.0, –11.8 and –5.8 kcal mol^{-1}, respectively, are dominating. Interestingly, these atoms place the same role in **4b** but their interactions with **1** are stronger in **4b** (we obtained –38.4, –24.6 and –9.1 kcal mol^{-1}, respectively, for H17, N13 and C14). Furthermore, there is no atom of **1b** in **4b** that is repelling **2** by more than 2.9 kcal mol^{-1} whereas there are two atoms of **1a** in **4a** (O15 and O16) that are involved in repulsive interactions (with **2**) larger than +6 kcal mol^{-1}.

Considering atoms of **2**, it is very clear that this is the O19 that attracts **1** most (and by far) in both structures of **3** and **4**. Moreover, $E_{\text{int}}^{\text{O19,}\mathbf{2}}$ of –78.9 and –69.3 kcal mol^{-1} in **3b** and **4b**, respectively, are about three times stronger when compared with the same interactions in **3a** and **3b**.

All the above nicely indicates the origin of much higher affinity between **1** and **2** observed for structures containing **1b** (the higher energy conformer of *S*-proline). It is clear that just few atoms are responsible for intermolecular interaction energy $E_{\text{int}}^{\mathbf{1,2}}$ of (i) –53.6 kcal mol^{-1} in **3b** being stronger, relative to **3a**, by nearly –30 kcal mol^{-1} and (ii) –70.3 kcal mol^{-1} in **4b** being stronger, relative to **4a**, by as much as –46 kcal mol^{-1}. It is reasonable to suggest that such large difference in affinity between **1** and **2** (in favour of **4b**) can be linked with significantly lower energy barrier at a TS computed for **5b**.

Table A16. Interaction energy and its components (in kcal mol^{-1}) between atoms of **1** (*S*-proline) and entire molecule **2** (acetone) as well as atoms of **2** and entire molecule **1** in adducts **3** and pre-organised structures **4**.

Part A. Interaction energies.

Atom A of 1	$E_{\text{int}}^{\text{A,2}}$					
	3a	**4a**	$\Delta_{\textbf{4a – 3a}}$	**3b**	**4b**	$\Delta_{\textbf{4b – 3b}}$
C1	-3.5	-2.1	1.4	-0.9	1.2	2.1
C2	-0.5	-0.2	0.3	-0.3	0.0	0.3
C3	-1.6	-0.2	1.4	-2.4	-0.2	2.1
C4	-1.0	-1.3	-0.2	-3.5	-1.8	1.7
H5	-0.8	0.4	1.2	-1.3	2.4	3.7
H6	-4.8	-2.1	2.7	-0.1	-0.2	-0.1
H7	-0.4	-1.6	-1.2	0.0	-2.1	-2.1
H8	-0.2	-0.1	0.1	-0.1	0.0	0.1
H9	-0.1	0.0	0.1	0.0	-0.1	0.0
H10	-0.4	-0.1	0.3	-2.1	0.1	2.2
H11	-4.3	0.1	4.4	-2.4	-0.1	2.3
H12	-0.2	-0.2	0.0	-3.2	-3.3	-0.1
N13	2.5	-5.8	-8.3	3.9	-24.6	-28.5
C14	6.5	-11.8	-18.3	-13.7	-9.1	4.5
O15	-8.5	6.1	14.6	5.5	2.9	-2.6
O16	-20.0	11.9	31.8	7.3	2.9	-4.4
H17	3.1	-17.0	-20.0	-40.4	-38.4	2.0
	$E_{\text{int}}^{\textbf{1,2}}$					
	-34.3	-23.9	10.4	-53.6	-70.3	-16.7

Atom A of 2	$E_{\text{int}}^{\text{A,1}}$					
	3a	**4a**	$\Delta_{\textbf{4a – 3a}}$	**3b**	**4b**	$\Delta_{\textbf{4b – 3b}}$
C18	-0.7	7.8	8.5	26.5	11.2	-15.3
O19	-19.6	-25.8	-6.2	-78.9	-69.3	9.6
C20	-2.2	-1.2	1.0	-2.0	-1.9	0.1
H21	-1.2	0.2	1.4	-0.1	-2.6	-2.4
H22	-2.1	-1.1	1.0	-1.5	-0.1	1.4
H23	-0.3	0.3	0.6	0.7	0.1	-0.6
C24	-1.7	-2.4	-0.7	0.1	-3.4	-3.5
H25	-0.6	0.3	0.8	0.5	-1.3	-1.8
H26	-5.3	-0.7	4.6	0.6	-0.2	-0.8
H27	-0.6	-1.2	-0.6	0.6	-2.9	-3.4
	$E_{\text{int}}^{\textbf{1,2}}$					
	-34.3	-23.9	10.4	-53.6	-70.3	-16.7

Table A16 continues

Part B. Exchange-correlation component of the interaction energies.

Atom A of 1	$V_{XC}^{A,2}$					
	3a	**4a**	$\Delta_{\mathbf{4a-3a}}$	**3b**	**4b**	$\Delta_{\mathbf{4b-3b}}$
C1	-1.3	-1.9	-0.6	0.0	-1.3	-1.2
C2	-0.2	-0.1	0.1	-0.2	-0.2	0.0
C3	-1.3	0.0	1.2	-2.4	-0.2	2.2
C4	-0.2	-0.1	0.0	-1.5	-1.7	-0.2
H5	0.0	-0.6	-0.5	0.0	-0.2	-0.2
H6	-4.6	-2.4	2.3	0.0	-0.2	-0.2
H7	-0.1	-1.3	-1.2	0.0	-2.1	-2.1
H8	0.0	0.0	0.0	0.0	0.0	0.0
H9	-0.2	0.0	0.1	0.0	0.0	0.0
H10	-0.1	0.0	0.1	-1.8	0.0	1.8
H11	-4.1	0.0	4.1	-2.1	0.0	2.1
H12	0.0	0.0	0.0	-3.0	-3.4	-0.3
N13	-0.3	-7.3	-7.1	-0.1	-15.2	-15.0
C14	-0.8	-0.1	0.7	-0.2	-0.3	0.0
O15	-3.7	-0.1	3.6	-0.2	-0.2	0.0
O16	-9.6	-4.7	4.9	-10.0	-11.3	-1.3
H17	-0.2	-4.2	-4.0	-19.0	-19.2	-0.2
	$V_{XC}^{1,2}$					
	-26.7	-23.0	3.8	-40.7	-55.4	-14.7

Atom A of 2	$V_{XC}^{A,1}$					
	3a	**4a**	$\Delta_{\mathbf{4a-3a}}$	**3b**	**4b**	$\Delta_{\mathbf{4b-3b}}$
C18	-2.4	-2.0	0.4	-1.3	-6.0	-4.8
O19	-11.9	-13.3	-1.4	-33.7	-35.6	-1.9
C20	-2.2	-1.1	1.1	-2.1	-2.1	0.0
H21	-0.9	-0.1	0.8	-1.0	-2.8	-1.8
H22	-2.1	-1.4	0.7	-2.2	-0.2	1.9
H23	-0.2	-0.1	0.1	-0.1	-0.2	0.0
C24	-2.2	-2.3	-0.2	-0.3	-4.0	-3.7
H25	-0.1	-0.2	0.0	-0.1	-1.3	-1.3
H26	-4.5	-0.9	3.6	0.0	-0.3	-0.3
H27	-0.2	-1.6	-1.4	0.0	-2.9	-2.9
	$V_{XC}^{1,2}$					
	-26.7	-23.0	3.8	-40.7	-55.4	-14.7

Table A16 continues

Part C. Classical component of the interaction energies.

Atom A of 1	$V_{cl}^{A,2}$					
	3a	**4a**	$\Delta_{\mathbf{4a-3a}}$	**3b**	**4b**	$\Delta_{\mathbf{4b-3b}}$
C1	-2.2	-0.1	2.1	-0.8	2.5	3.4
C2	-0.3	-0.1	0.3	-0.1	0.1	0.3
C3	-0.3	-0.1	0.2	0.0	0.0	0.0
C4	-0.8	-1.1	-0.3	-2.0	-0.1	1.9
H5	-0.8	0.9	1.8	-1.3	2.7	3.9
H6	-0.2	0.3	0.4	-0.1	0.0	0.1
H7	-0.3	-0.3	0.0	0.0	0.0	0.0
H8	-0.2	-0.1	0.1	-0.1	0.0	0.2
H9	0.1	0.0	-0.1	0.0	0.0	0.0
H10	-0.3	-0.1	0.2	-0.3	0.1	0.3
H11	-0.2	0.1	0.3	-0.3	-0.1	0.2
H12	-0.2	-0.2	0.0	-0.2	0.1	0.2
N13	2.7	1.5	-1.2	4.1	-9.4	-13.5
C14	7.3	-11.7	-19.0	-13.4	-8.9	4.6
O15	-4.7	6.2	11.0	5.7	3.1	-2.6
O16	-10.4	16.6	26.9	17.4	14.2	-3.1
H17	3.2	-12.8	-16.0	-21.4	-19.2	2.2
	$V_{cl}^{1,2}$					
	-7.6	-0.9	6.7	-12.9	-14.9	-2.0

Atom A of 2	$V_{cl}^{A,1}$					
	3a	**4a**	$\Delta_{\mathbf{4a-3a}}$	**3b**	**4b**	$\Delta_{\mathbf{4b-3b}}$
C18	1.7	9.8	8.1	27.8	17.2	-10.5
O19	-7.7	-12.5	-4.8	-45.2	-33.8	11.5
C20	0.0	-0.1	-0.1	0.0	0.2	0.1
H21	-0.3	0.3	0.6	0.8	0.2	-0.6
H22	0.0	0.3	0.3	0.7	0.1	-0.5
H23	-0.1	0.4	0.5	0.8	0.2	-0.5
C24	0.5	0.0	-0.6	0.3	0.6	0.3
H25	-0.5	0.4	0.9	0.6	0.1	-0.5
H26	-0.8	0.2	0.9	0.7	0.1	-0.5
H27	-0.4	0.3	0.7	0.6	0.1	-0.5
	$V_{cl}^{1,2}$					
	-7.6	-0.9	6.7	-12.9	-14.9	-2.0

From the pre-organised for the C–N bond formation and H-transfer structures, 4a and 4b, to transition state structures 5a and 5b.

In search for the origin of the small difference in the $E_{\text{int}}^{\text{Tot}}$ values computed for **5a** and **5b**, we decomposed the total interaction energy to contributions made by all covalent and non-covalent interactions in **4** and **5**. This approach revealed that on the **4** to **5** change:

1. Covalent interactions (bonds) became largely weakened in **5** relative to **4**, by about 162.7 and 136.8 kcal mol^{-1} in **5a** and **5b**, respectively. The most affected C18–O19 bond experienced the energy decrease by about 128 kcal mol^{-1} in both **5a** and **5b** structures.
2. Non-covalent intra and intermolecular interactions became much stronger in **5**, by about –171 and –148 kcal mol^{-1} in **5a** and **5b**, respectively.
3. The largest and of stabilizing nature change is observed for intermolecular interactions. They became stronger by –211 and –168 kcal mol^{-1} in **5a** and **5b**, respectively, and the main contribution came from interactions between atoms of the $\mathcal{G}$ and $\mathcal{H}$ molecular fragments (we obtained $\Delta E_{\text{int}}^{\mathcal{G},\mathcal{H}}$ of –181.2 and –146.4 kcal mol^{-1} for changes from **4a** to **5a** and **4b** to **5b**, respectively.

It is important to stress that {H17,O19} and {N13,C18} atom-pairs experienced most significant strengthening in their di-atomic interactions among all possible 351 2-atom fragments and, as a consequence, these fragments of molecular system became most stabilised in **5a** and **5b**.

Clearly, there is not a single cause that can be linked with the small observed difference in energy barriers computed for transitional states **5a** and **5b**. In this instance, it is a result of combined large increases and decreases in interaction energies between all atoms.

Table A17. Net atomic charges, Q(A) and differences, ΔQ(A), computed for the indicated structures – values in *e*.

	Q(A)		ΔQ(A)	Q(A)		ΔQ(A)		
Atom	**4a**	**5a**	**5a – 4a**	**4b**	**5b**	**5b – 4b**	**4a – 4b**	**5a – 5b**
C1	0.3241	0.2933	-0.0309	0.3252	0.2887	-0.0365	-0.0011	0.0046
C2	0.0450	0.0496	0.0046	0.0306	0.0490	0.0184	0.0144	0.0007
C3	0.0414	0.0443	0.0029	0.0298	0.0423	0.0125	0.0116	0.0020
C4	0.3112	0.2501	-0.0612	0.3071	0.2493	-0.0578	0.0041	0.0008
H5	0.3604	0.3865	0.0260	0.3342	0.3865	0.0523	0.0262	-0.0001
H6	0.0014	0.0435	0.0421	0.0150	0.0468	0.0318	-0.0136	-0.0033
H7	0.0162	0.0400	0.0237	-0.0018	0.0382	0.0400	0.0181	0.0018
H8	-0.0036	0.0072	0.0109	-0.0032	0.0239	0.0271	-0.0005	-0.0167
H9	0.0072	0.0228	0.0157	-0.0069	0.0091	0.0159	0.0140	0.0138
H10	0.0185	0.0299	0.0114	0.0003	0.0134	0.0131	0.0182	0.0164
H11	0.0031	0.0129	0.0098	0.0150	0.0442	0.0291	-0.0119	-0.0313
H12	0.0426	0.0591	0.0165	0.0309	0.0696	0.0387	0.0117	-0.0105
N13	-0.9831	-0.8774	0.1056	-0.9332	-0.8693	0.0639	-0.0499	-0.0081
C14	1.5242	1.5779	0.0538	1.5278	1.5704	0.0426	-0.0037	0.0076
O15	-1.1960	-1.1976	-0.0016	-1.1778	-1.1814	-0.0037	-0.0182	-0.0162
O16	-1.1419	-1.1872	-0.0453	-1.1566	-1.1712	-0.0146	0.0147	-0.0161
H17	0.6213	0.6252	0.0039	0.6298	0.6287	-0.0012	-0.0085	-0.0034
C18	0.9685	0.8658	-0.1027	0.9547	0.8701	-0.0846	0.0138	-0.0043
O19	-1.1537	-1.2064	-0.0527	-1.1619	-1.2280	-0.0662	0.0082	0.0216
C20	-0.0170	0.0128	0.0298	-0.0091	0.0122	0.0213	-0.0080	0.0006
H21	0.0343	0.0255	-0.0089	0.0502	0.0078	-0.0424	-0.0159	0.0177
H22	0.0405	0.0148	-0.0257	0.0369	0.0142	-0.0227	0.0036	0.0006
H23	0.0382	0.0321	-0.0061	0.0426	0.0300	-0.0126	-0.0044	0.0021
C24	-0.0147	0.0101	0.0248	-0.0017	0.0090	0.0108	-0.0130	0.0011
H25	0.0420	0.0309	-0.0111	0.0408	0.0090	-0.0318	0.0012	0.0219
H26	0.0352	0.0156	-0.0196	0.0440	0.0261	-0.0178	-0.0088	-0.0105
H27	0.0355	0.0199	-0.0156	0.0375	0.0135	-0.0240	-0.0020	0.0064

Table A18. Top 30 atom-pairs for which most significant increase/decrease in the net 2-atom fragment charge (in e) took place on reaching the transitional state (TS) from: **4a** to **5a** – part a, **4b** to **5b** – part b. $\Delta\Delta Q(A,B) = \{\Delta Q(A,B)$ in **5**$\} - \{\Delta Q(A,B)$ in **4**$\}$ where $\Delta Q(A,B)$ is a difference in net atomic charges between atoms A and B.

Part A: change from **4a** to **5a**.

Charge difference increased			**Charge difference decreased**		
Atom A	**Atom B**	**$\Delta\Delta Q(A,B)$**	**Atom A**	**Atom B**	**$\Delta\Delta Q(A,B)$**
O19	N13	0.1584	N13	H8	-0.0948
C18	C14	0.1565	N13	H11	-0.0959
O16	N13	0.1510	H23	C18	-0.0966
C14	C4	0.1149	N13	C2	-0.1010
O15	N13	0.1073	C18	O15	-0.1011
O19	C14	0.1065	H17	N13	-0.1018
O16	C14	0.0991	N13	C3	-0.1027
O19	H6	0.0948	H6	C4	-0.1032
O16	H6	0.0874	C18	C3	-0.1056
H5	C4	0.0872	C18	H17	-0.1066
C14	C1	0.0847	C18	C2	-0.1073
C20	O19	0.0825	H23	N13	-0.1117
H22	C14	0.0795	C18	H11	-0.1125
O19	H5	0.0788	C18	H8	-0.1136
C24	O19	0.0776	C18	H10	-0.1141
O19	H7	0.0764	H21	N13	-0.1145
C20	O16	0.0751	H25	N13	-0.1168
H26	C14	0.0734	C18	H9	-0.1184
O16	H5	0.0714	C18	H12	-0.1192
C24	O16	0.0702	H27	N13	-0.1212
H27	C14	0.0694	H26	N13	-0.1252
O19	H12	0.0693	C18	H7	-0.1264
O16	H7	0.0691	C24	C18	-0.1275
O19	H9	0.0684	C18	H5	-0.1287
H17	C4	0.0650	H22	N13	-0.1313
H25	C14	0.0649	C20	C18	-0.1325
O19	H10	0.0641	N13	C1	-0.1365
O19	H8	0.0636	C18	H6	-0.1448
H21	C14	0.0627	N13	C4	-0.1668
O19	H11	0.0625	C18	N13	-0.2083
Atom-pairs of special interest					
O19	H17	0.0566	C18	N13	-0.2083

Part B: change from **4b** to **5b**.

Charge difference increased			**Charge difference decreased**		
Atom A	**Atom B**	**ΔΔ*Q*(A,B)**	**Atom A**	**Atom B**	**ΔΔ*Q*(A,B)**
O19	N13	0.1300	H23	N13	-0.0765
C18	C14	0.1272	H7	C1	-0.0765
O19	H5	0.1185	C20	C4	-0.0791
H5	C4	0.1102	C18	O15	-0.0810
O19	C14	0.1087	H26	N13	-0.0817
O19	H7	0.1062	C18	H17	-0.0834
O19	H12	0.1048	H8	C4	-0.0849
C14	C4	0.1004	H22	N13	-0.0865
O19	H6	0.0979	H11	C4	-0.0869
O19	H11	0.0953	H27	N13	-0.0879
H21	H5	0.0947	H6	C4	-0.0896
O19	H8	0.0932	C24	C18	-0.0954
H5	C1	0.0889	H25	N13	-0.0956
C20	O19	0.0874	H12	C4	-0.0965
H21	C14	0.0850	C18	C3	-0.0971
O19	C2	0.0845	C18	H10	-0.0977
H25	H5	0.0841	H7	C4	-0.0978
O19	H9	0.0821	N13	C1	-0.1004
O19	H10	0.0793	C18	H9	-0.1005
C14	C1	0.0791	C18	C2	-0.1030
O19	C3	0.0786	C20	C18	-0.1059
O16	N13	0.0785	H21	N13	-0.1063
C24	O19	0.0769	C18	H8	-0.1117
H27	H5	0.0764	C18	H11	-0.1137
H22	H5	0.0750	C18	H6	-0.1164
H25	C14	0.0743	N13	C4	-0.1217
H26	H5	0.0701	C18	H12	-0.1233
O15	N13	0.0675	C18	H7	-0.1246
O16	H5	0.0669	C18	H5	-0.1369
H27	C14	0.0666	C18	N13	-0.1485
Atom-pairs of special interest					
O19	H17	0.0516	C18	N13	-0.1483

Table A19. Top 10 atom-pairs with strongest attractive/repulsive diatomic intermolecular interactions in: **5a** – part A, **5b** – part B. Interaction energies are in kcal mol^{-1}.

Part A: data for **5a**.

Strongest attractive interactions					**Strongest repulsive interactions**				
Atom A	**Atom B**	$E_{\text{int}}^{\text{A,B}}$	$V_{\text{XC}}^{\text{A,B}}$	$V_{\text{cl}}^{\text{A,B}}$	**Atom A**	**Atom B**	$E_{\text{int}}^{\text{A,B}}$	$V_{\text{XC}}^{\text{A,B}}$	$V_{\text{cl}}^{\text{A,B}}$
O19	H17	-217.0	-44.9	-172.1	H25	C14	5.7	0.0	5.7
C18	N13	-207.6	-74.2	-133.4	C18	H12	5.8	-0.1	5.9
O19	C14	-193.9	-0.4	-193.5	C18	C4	30.0	-0.9	30.9
C18	O16	-125.6	-0.8	-124.8	C18	C1	36.9	-1.2	38.1
C18	O15	-81.4	-0.1	-81.3	C18	H5	45.7	-0.7	46.4
O19	H5	-50.0	-0.3	-49.7	C18	H17	101.6	-0.8	102.4
O19	C1	-45.7	-1.5	-44.2	O19	O15	111.9	-0.3	112.2
O19	C4	-36.5	-0.3	-36.2	O19	N13	127.9	-13.1	141.1
O19	H6	-9.4	-3.6	-5.8	C18	C14	137.4	-0.3	137.7
C24	N13	-8.1	-6.1	-2.0	O19	O16	171.9	-16.9	188.8

All interactions and components			
	$E_{\text{int}}^{\text{A,B}}$	$V_{\text{XC}}^{\text{A,B}}$	$V_{\text{cl}}^{\text{A,B}}$
Total:	-235.0	-196.2	-38.8

Part B: data for **5b**.

Strongest attractive interactions					**Strongest repulsive interactions**				
Atom A	**Atom B**	$E_{\text{int}}^{\text{A,B}}$	$V_{\text{XC}}^{\text{A,B}}$	$V_{\text{cl}}^{\text{A,B}}$	**Atom A**	**Atom B**	$E_{\text{int}}^{\text{A,B}}$	$V_{\text{XC}}^{\text{A,B}}$	$V_{\text{cl}}^{\text{A,B}}$
C18	N13	-224.8	-85.8	-139.0	C18	H6	4.7	0.0	4.7
O19	H17	-198.0	-36.2	-161.8	C18	H12	7.7	-0.6	8.3
O19	C14	-197.4	-0.5	-196.9	C18	C4	33.6	-1.2	34.8
C18	O16	-119.0	-0.7	-118.3	C18	C1	34.3	-0.9	35.2
C18	O15	-78.7	0.0	-78.7	C18	H5	52.4	-0.9	53.3
O19	H5	-60.1	-0.3	-59.8	C18	H17	92.6	-0.5	93.1
O19	C4	-43.3	-2.8	-40.5	O19	O15	113.4	-0.3	113.7
O19	C1	-38.2	-0.5	-37.7	O19	N13	129.7	-13.5	143.2
O19	H12	-14.3	-3.6	-10.7	C18	C14	133.4	-0.1	133.5
C24	N13	-8.4	-6.7	-1.7	O19	O16	172.0	-15.1	187.1

All interactions and components			
	$\Delta E_{\text{int}}^{\text{A,B}}$	$\Delta V_{\text{XC}}^{\text{A,B}}$	$\Delta V_{\text{cl}}^{\text{A,B}}$
Total:	-238.1	-197.5	-40.6

Table A20. Top 10 atom-pairs for which most significant increase/decrease in the intermolecular diatomic interaction energy (in kcal mol^{-1}) took place on reaching the transitional state from: **4a** to **5a** – part A, **4b** to **5b** – part B. $\Delta E_{\text{int}}^{\text{A,B}}$ = { $E_{\text{int}}^{\text{A,B}}$ in **5**} – { $E_{\text{int}}^{\text{A,B}}$ in **4**}.

Part A: from **4a** to **5a**.

Strongest attractive interactions					**Strongest repulsive interactions**				
Atom A	**Atom B**	$\Delta E_{\text{int}}^{\text{A,B}}$	$\Delta V_{\text{XC}}^{\text{A,B}}$	$\Delta V_{\text{cl}}^{\text{A,B}}$	**Atom A**	**Atom B**	$\Delta E_{\text{int}}^{\text{A,B}}$	$\Delta V_{\text{XC}}^{\text{A,B}}$	$\Delta V_{\text{cl}}^{\text{A,B}}$
O19	H17	-114.3	-41.1	-73.2	C20	C14	3.6	0.0	3.6
C18	N13	-104.2	-73.2	-31.0	C18	C4	4.0	-0.9	4.9
O19	C14	-54.3	-0.3	-54.0	C18	H6	5.6	-0.1	5.7
C18	O16	-21.1	-0.7	-20.4	C18	C1	5.9	-1.0	6.9
C18	O15	-11.5	0.0	-11.5	O19	N13	8.2	-10.1	18.3
O19	H5	-11.3	-0.3	-11.0	C18	H5	12.5	-0.7	13.2
O19	H6	-9.1	-2.3	-6.8	O19	O15	22.9	-0.3	23.2
C24	N13	-8.5	-4.3	-4.2	C18	H17	28.2	-0.6	28.8
C20	N13	-8.2	-5.1	-3.1	C18	C14	29.3	-0.2	29.5
O19	C1	-7.8	-1.0	-6.8	O19	O16	36.8	-12.6	49.4

All interactions and components			
	$\Delta E_{\text{int}}^{\text{A,B}}$	$\Delta V_{\text{XC}}^{\text{A,B}}$	$\Delta V_{\text{cl}}^{\text{A,B}}$
Total:	–211.1	-173.3	-37.8

Part B: from **4b** to **5b**.

Strongest attractive interactions					**Strongest repulsive interactions**				
Atom A	**Atom B**	$\Delta E_{\text{int}}^{\text{A,B}}$	$\Delta V_{\text{XC}}^{\text{A,B}}$	$\Delta V_{\text{cl}}^{\text{A,B}}$	**Atom A**	**Atom B**	$\Delta E_{\text{int}}^{\text{A,B}}$	$\Delta V_{\text{XC}}^{\text{A,B}}$	$\Delta V_{\text{cl}}^{\text{A,B}}$
C18	N13	-112.6	-81.1	-31.5	H21	N13	3.4	0.5	2.9
O19	H17	-51.5	-18.0	-33.5	C18	C1	3.6	-0.8	4.4
O19	C14	-32.1	-0.3	-31.8	C18	H7	4.2	-0.2	4.4
O19	H5	-23.6	-0.2	-23.4	H27	O16	4.8	1.8	3.0
O19	H12	-7.6	-0.4	-7.2	C18	H12	5.0	-0.4	5.4
C20	N13	-6.9	-4.3	-2.6	C18	C14	6.2	-0.1	6.3
C24	N13	-6.0	-3.8	-2.2	O19	N13	9.6	-9.5	19.1
O19	H7	-4.9	0.0	-4.9	O19	O15	13.2	-0.1	13.3
H25	C14	-3.5	0.0	-3.5	O19	O16	18.9	-7.0	25.9
H21	C14	-3.3	0.0	-3.3	C18	H5	21.2	-0.8	22.0

All interactions and components			
	$\Delta E_{\text{int}}^{\text{A,B}}$	$\Delta V_{\text{XC}}^{\text{A,B}}$	$\Delta V_{\text{cl}}^{\text{A,B}}$
Total:	-167.8	-142.1	-25.7

Table A21. Interaction energy and its components (in kcal mol^{-1}) between atoms of **1** (*S*-proline) and entire molecule **2** (acetone) as well as atoms of **2** and entire molecule **1** in pre-organised structures **4** and transition state structures **5**.

Part A. Interaction energies

Atom A of 1	$E_{\text{int}}^{\text{A,2}}$					
	4a	**5a**	$\Delta_{\mathbf{5a-4a}}$	**4b**	**5b**	$\Delta_{\mathbf{5b-4b}}$
C1	-2.1	-5.2	-3.1	1.2	-1.8	-3.1
C2	-0.2	-1.2	-1.0	0.0	-0.9	-0.8
C3	-0.2	-0.7	-0.6	-0.2	-1.0	-0.8
C4	-1.3	-2.3	-1.0	-1.8	-6.1	-4.3
H5	0.4	3.2	2.8	2.4	-1.9	-4.4
H6	-2.1	-4.7	-2.6	-0.2	-1.5	-1.3
H7	-1.6	-3.4	-1.8	-2.1	-4.8	-2.7
H8	-0.1	-0.3	-0.2	0.0	-0.3	-0.3
H9	0.0	-0.3	-0.3	-0.1	0.0	0.0
H10	-0.1	-0.5	-0.4	0.1	-0.3	-0.3
H11	0.1	0.1	0.0	-0.1	-0.6	-0.5
H12	-0.2	-0.8	-0.6	-3.3	-7.8	-4.6
N13	-5.8	-120.0	-114.1	-24.6	-131.9	-107.3
C14	-11.8	-33.3	-21.5	-9.1	-45.9	-36.7
O15	6.1	14.8	8.7	2.9	23.8	20.9
O16	11.9	19.4	7.5	2.9	36.6	33.7
H17	-17.0	-100.0	-83.0	-38.4	-93.8	-55.4
	$E_{\text{int}}^{\mathbf{1,2}}$					
	-23.9	-235.0	-211.1	-70.3	-238.1	-167.8

Atom A of 2	$E_{\text{int}}^{\text{A,1}}$					
	4a	**5a**	$\Delta_{\mathbf{5a-4a}}$	**4b**	**5b**	$\Delta_{\mathbf{5b-4b}}$
C18	7.8	-32.3	-40.1	11.2	-43.4	-54.6
O19	-25.8	-174.9	-149.1	-69.3	-167.6	-98.3
C20	-1.2	-8.6	-7.4	-1.9	-9.1	-7.2
H21	0.2	-2.7	-2.9	-2.6	-3.2	-0.6
H22	-1.1	-1.6	-0.5	-0.1	-3.2	-3.1
H23	0.3	0.4	0.1	0.1	0.4	0.3
C24	-2.4	-9.2	-6.8	-3.4	-8.8	-5.4
H25	0.3	0.3	0.0	-1.3	-2.3	-1.1
H26	-0.7	-1.3	-0.6	-0.2	0.4	0.6
H27	-1.2	-5.2	-3.9	-2.9	-1.3	1.6
	$E_{\text{int}}^{\mathbf{1,2}}$					
	-23.9	-235.0	-211.1	-70.3	-238.1	-167.8

Table A21 continues

Part B. Exchange-correlation component of the interaction energies.

Atom A of 1	$V_{XC}^{A,2}$					
	4a	**5a**	$\Delta_{\mathbf{5a-4a}}$	**4b**	**5b**	$\Delta_{\mathbf{5b-4b}}$
C1	-1.9	-6.0	-4.1	-1.3	-4.8	-3.5
C2	-0.1	-0.7	-0.6	-0.2	-0.7	-0.6
C3	0.0	-0.4	-0.4	-0.2	-0.5	-0.3
C4	-0.1	-2.7	-2.6	-1.7	-5.4	-3.7
H5	-0.6	-2.7	-2.2	-0.2	-3.2	-3.0
H6	-2.4	-4.8	-2.4	-0.2	-1.7	-1.5
H7	-1.3	-3.1	-1.9	-2.1	-5.0	-3.0
H8	0.0	-0.1	0.0	0.0	-0.1	-0.1
H9	0.0	-0.1	-0.1	0.0	-0.1	0.0
H10	0.0	-0.1	0.0	0.0	-0.1	-0.1
H11	0.0	0.0	0.0	0.0	-0.1	0.0
H12	0.0	-0.4	-0.4	-3.4	-6.6	-3.2
N13	-7.3	-102.8	-95.4	-15.2	-115.0	-99.8
C14	-0.1	-2.8	-2.7	-0.3	-0.7	-0.4
O15	-0.1	-0.8	-0.7	-0.2	-0.4	-0.2
O16	-4.7	-22.5	-17.8	-11.3	-16.2	-4.9
H17	-4.2	-46.2	-42.0	-19.2	-37.0	-17.9
	$V_{XC}^{1,2}$					
	-23.0	-196.2	-173.3	-55.4	-14.9	-238.1

Atom A of 2	$V_{XC}^{A,1}$					
	4a	**5a**	$\Delta_{\mathbf{5a-4a}}$	**4b**	**5b**	$\Delta_{\mathbf{5b-4b}}$
C18	-2.0	-80.1	-78.1	-6.0	-91.7	-85.7
O19	-13.3	-81.8	-68.5	-35.6	-73.1	-37.5
C20	-1.1	-9.1	-8.0	-2.1	-9.8	-7.7
H21	-0.1	-3.6	-3.5	-2.8	-3.6	-0.8
H22	-1.4	-2.1	-0.7	-0.2	-3.7	-3.4
H23	-0.1	-1.0	-0.9	-0.2	-1.0	-0.9
C24	-2.3	-9.7	-7.4	-4.0	-9.1	-5.0
H25	-0.2	-1.0	-0.8	-1.3	-2.8	-1.5
H26	-0.9	-1.8	-0.9	-0.3	-1.0	-0.7
H27	-1.6	-6.1	-4.5	-2.9	-1.8	1.1
	$V_{XC}^{1,2}$					
	-23.0	-196.2	-173.3	-55.4	-14.9	-238.1

Table A21 continues

Part C. Classical component of the interaction energies.

Atom A of 1	$V_{cl}^{A,2}$					
	4a	**5a**	$\Delta_{\mathbf{5a-4a}}$	**4b**	**5b**	$\Delta_{\mathbf{5b-4b}}$
C1	-0.1	0.8	1.0	2.5	2.9	0.4
C2	-0.1	-0.4	-0.4	0.1	-0.1	-0.2
C3	-0.1	-0.3	-0.2	0.0	-0.5	-0.5
C4	-1.1	0.4	1.5	-0.1	-0.7	-0.6
H5	0.9	5.9	5.0	2.7	1.3	-1.4
H6	0.3	0.1	-0.2	0.0	0.2	0.2
H7	-0.3	-0.3	0.0	0.0	0.2	0.3
H8	-0.1	-0.2	-0.1	0.0	-0.2	-0.2
H9	0.0	-0.2	-0.2	0.0	0.0	0.1
H10	-0.1	-0.4	-0.3	0.1	-0.1	-0.2
H11	0.1	0.1	0.0	-0.1	-0.5	-0.5
H12	-0.2	-0.4	-0.2	0.1	-1.2	-1.3
N13	1.5	-17.2	-18.7	-9.4	-16.9	-7.5
C14	-11.7	-30.5	-18.8	-8.9	-45.2	-36.4
O15	6.2	15.7	9.4	3.1	24.2	21.0
O16	16.6	41.9	25.3	14.2	52.8	38.6
H17	-12.8	-53.8	-41.0	-19.2	-56.8	-37.5
	$V_{cl}^{1,2}$					
	-0.9	-38.7	-37.8	-14.9	-40.6	-25.7

Atom A of 2	$V_{cl}^{A,1}$					
	4a	**5a**	$\Delta_{\mathbf{5a-4a}}$	**4b**	**5b**	$\Delta_{\mathbf{5b-4b}}$
C18	9.8	47.8	38.0	17.2	48.3	31.1
O19	-12.5	-93.1	-80.7	-33.8	-94.5	-60.7
C20	-0.1	0.5	0.6	0.2	0.6	0.4
H21	0.3	0.9	0.6	0.2	0.4	0.1
H22	0.3	0.5	0.2	0.1	0.5	0.3
H23	0.4	1.4	1.0	0.2	1.4	1.2
C24	0.0	0.5	0.6	0.6	0.3	-0.3
H25	0.4	1.3	0.9	0.1	0.5	0.4
H26	0.2	0.5	0.3	0.1	1.3	1.2
H27	0.3	1.0	0.6	0.1	0.6	0.5
	$V_{cl}^{1,2}$					
	-0.9	-38.7	-37.8	-14.9	-40.6	-25.7

End of PART A5

PART A6

Data pertaining to multi-step processes leading from **6a** and **6b** to the first proton transfer.

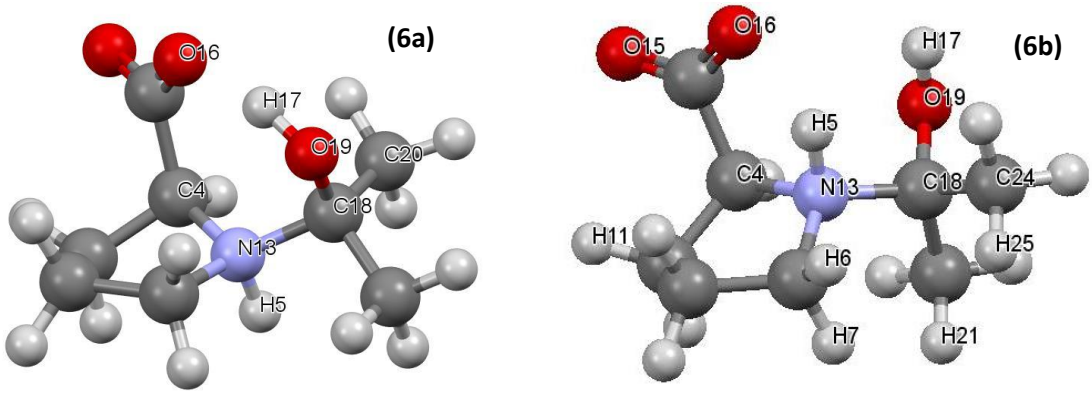

Figure A7. Ball-and-stick representation of **6a (**d(N13,C18) = 1.58697 Å, d(H17,O19) of 1.00186 Å, d(H5,O16) = 3.86653 Å, d(O16,H17) = 1.58424 Å) and **6b** (d(N13,C18) = 1.54295 Å, d(H17,O19) = 0.96689, Å d(H5,O16) = 1.75657 Å) structures.

In search for the GMS of **6a** and **6b**, a dihedral scan DA(C4,N13,C18,O19) was performed - data obtained are shown in Figure A8.

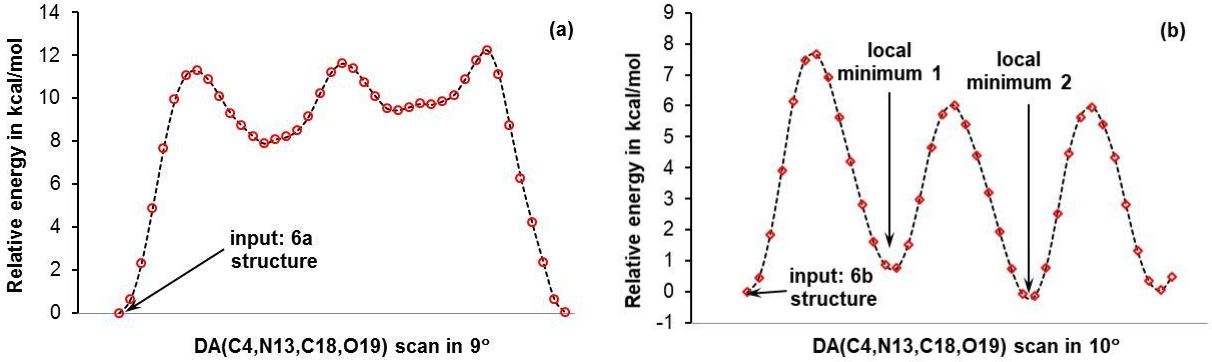

Figure A8. B3LYP data obtained from the DA(C4,N13,C18,O19) scan performed on **6a** (part a) and **6b** (part b).

From Figure A8(a) it is clear that **6a** is indeed the GMS. There are two local minima of comparable to **6b** energies seen in Figure A8(b). Energy of local minimum 1 structure is about 1 kcal mol^{-1} higher relative to **6b**. Due to being slightly higher in energy and not ideally pre-organised for the proton transfer (Figure A9(a)), it was no longer considered. Energies of the local minimum 2 structure (Figure A8(b)) and **6b** are the same. Comparing these two structures makes it clear that **6b** is not only best pre-organised for the H-transfer but also for the subsequent water elimination step. Moreover, the interatomic distance d(H5,O16) = 1.79507 Å in the local

minimum 2 structure is longer, by 0.0385 Å, relative to that observed in **6b**; hence, **6b** was selected for further studies.

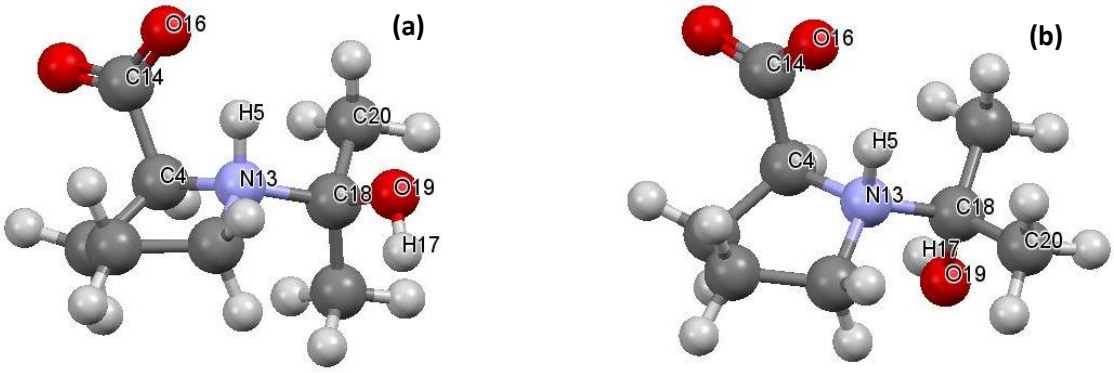

Figure A9. Ball-and-stick representation of energy optimised local minimum 1 (part a) and local minimum 2 (part b) structures obtained from the DA(C4,N13,C18,O19) scan shown in Figure A8(b).

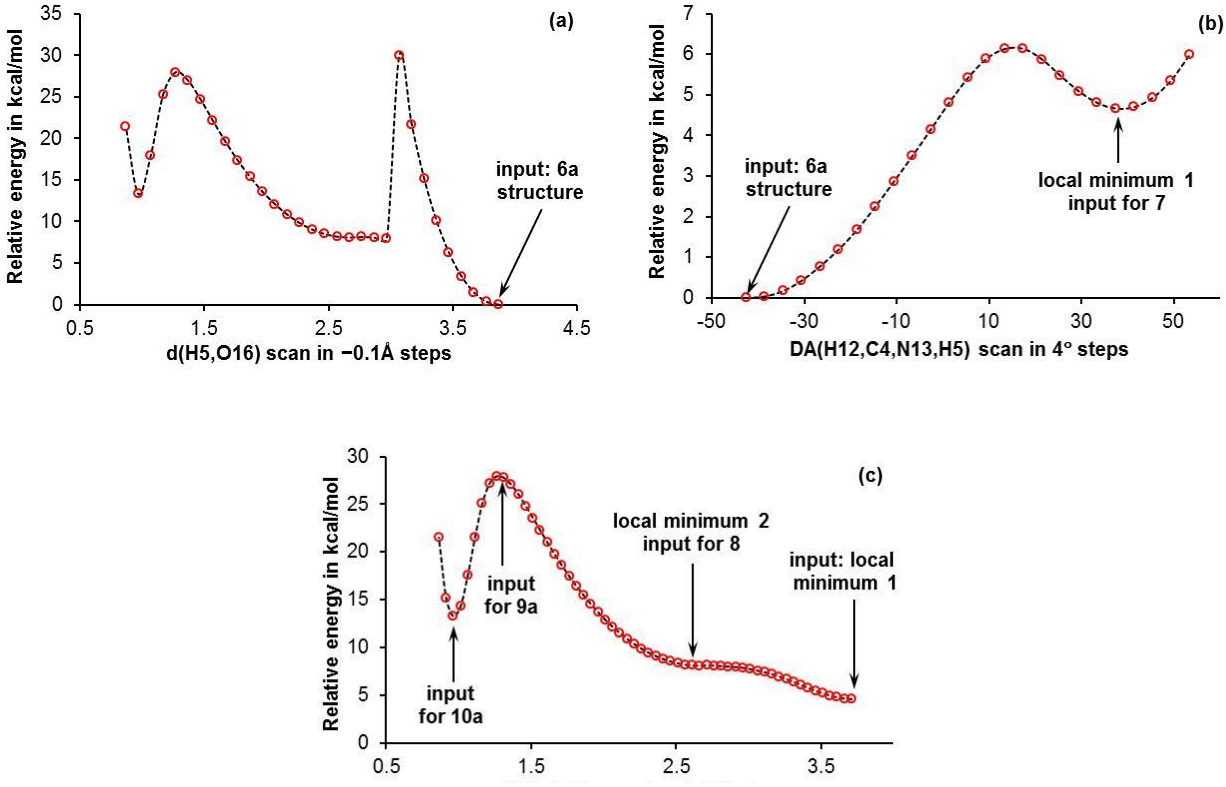

Figure A10. B3LYP data obtained from the indicated scans performed on **6a**.

Scan along the reaction coordinates performed on **6a** (by decreasing the interatomic distance between H5 and O16) shows (Figure A10(a)) a sharp initial rise in energy with a barrier of 30 kcal mol^{-1}. Because a large structural change took place after overcoming this energy barrier, we concluded that **6a** must undergo an initial pre-organisation first.

Indeed a smooth increase in energy is observed in Figure A10(b) where, after overcoming an energy barrier of only about 6 kcal mol^{-1}, a local minimum 1 is observed – this structure was energy optimised without any constrain to give structure **7** (shown in Figure A11) that was subjected to the d(H5,O16) scan. Data obtained (Figure A10(c)) shows (i) an additional local minimum 2 (it was energy optimised to give structure **8** shown in Figure A11), (ii) data point corresponding to the structure that was subjected to the Berny optimisation (to obtain a transitional state structure **9a**) and (iii) data point corresponding to the structure that was subjected to full energy optimisation without any constrain in order to obtain product of the proton transfer **10a**.

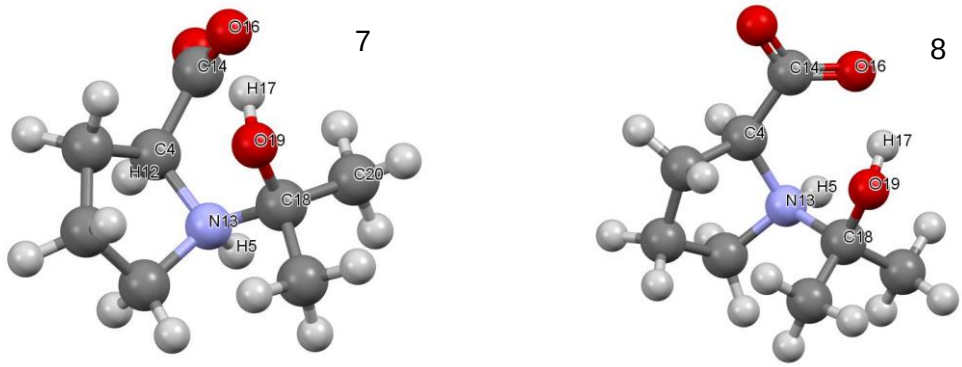

Figure A11. Ball-and-stick representation of structures **7** and **8** obtained from energy optimised local minimum structures 1 and 2, respectively; these minima are shown in Figs. S10(b) and (c).

Scan along the reaction coordinates performed on **6b** is shown in Figure A12 and transitional state structures of **9a** and **9b** are shown in Figure A13.

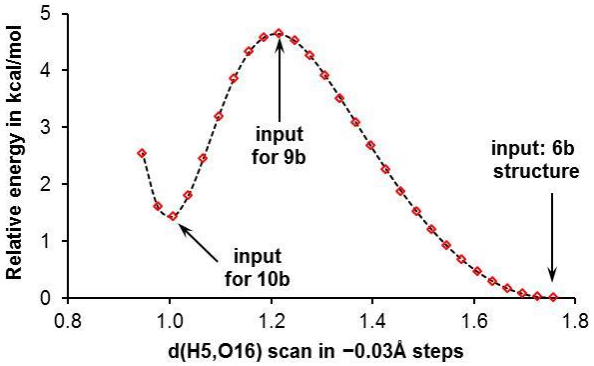

Figure A12. B3LYP data obtained from the d(H5,O16) scan performed on **6b**.

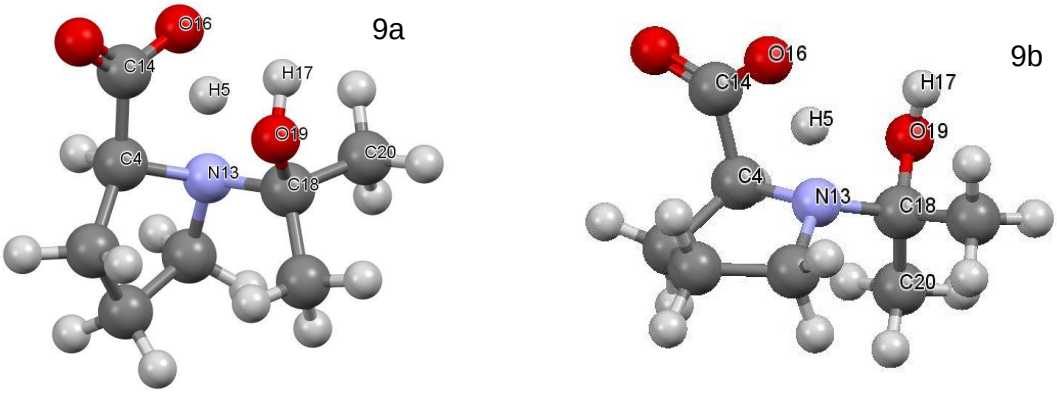

Figure A13. Ball-and-stick representation of transitional state structures **9a (**d(H5,O16) = 1.27470 Å, d(H5,N13) = 1.29366 Å) and **9b** (d(H5,O16) = 0.99901 Å, d(H5,N13) = 1.81499 Å).

Table A22. B3LYP/6-311++G(d,p)/GD3 energies (in au) and associated energy changes (in kcal mol^{-1}) between consecutive steps from **6a** and **6b**, followed by **7** and **8** (local minima structures with **1a**), **9a** and **9b** (TS structures) to **10a** and **10b** (products on H-transfer). Energy differences between structures that originated from **1a** and **1b** as, e.g. ΔE(**9**) = E(**9a**) – E(**9b**), are also provided (values in kcal mol^{-1}). Data obtained at the MP2/6-311++G(d,p) level is printed in italic.

Structure	***E***	**Δ**	E_{ZPVE}	**Δ**	***H***	**Δ**	***G***	**Δ**
	Structures that originated from **1a**							
6a	-594.5442		-594.3097		-594.2970		-594.3470	
	-592.8707		*-592.6333*		*-592.6207*		*-592.6704*	
7	-594.5369	4.6	-594.3018	5.0	-594.2892	4.9	-594.3388	5.1
	-592.8635	*4.5*	*-592.6255*	*4.9*	*-592.6130*	*4.8*	*-592.6622*	*5.2*
8	-594.5314	3.5	-594.2967	3.2	-594.2840	3.2	-594.3340	3.0
	-592.8581	*3.4*	*-592.6204*	*3.2*	*-592.6078*	*3.3*	*-592.6578*	*2.8*
9a	-594.4958	22.3	-594.2659	19.3	-594.2536	19.1	-594.3022	20.0
	-592.8283	*18.7*	*-592.5956*	*15.6*	*-592.5834*	*15.3*	*-592.6317*	*16.3*
10a	-594.5231	–17.2	-594.2906	-15.5	-594.2774	-14.9	-594.3279	-16.2
	-592.8539	*–16.1*	*-592.6184*	*–14.3*	*-592.6053*	*–13.8*	*-592.6556*	*–14.9*
	Structures that originated from **1b**							
6b	-594.5479		-594.3138		-594.3008		-594.3520	
	-592.8759		*-592.6397*		*-592.6267*		*-592.6774*	
9b	-594.5405	4.6	-594.3112	1.7	-594.2985	1.4	-594.3481	2.5
	-592.8721	*2.4*	*-592.6402*	*–0.3*	*-592.6276*	*–0.6*	*-592.6772*	*0.1*
10b	-594.5456	–3.2	-594.3130	–1.2	-594.3000	–0.9	-594.3506	–1.6
	-592.8765	*–2.7*	*-592.6412*	*–0.6*	*-592.6282*	*–0.4*	*-592.6788*	*–1.0*
		Energy difference for 6a relative to 6b						
		2.3		2.6		2.4		3.1
		3.3		*4.0*		*3.8*		*4.4*
		Energy difference for 9a relative to 9b						
		25.8		25.8		25.8		25.6
		24.3		*24.0*		*24.0*		*24.2*
		Energy difference for 10a relative to 10b						
		11.8		11.5		11.8		11.1
		10.9		*10.3*		*10.6*		*10.2*

Comments related to consecutive structural changes from 6a, via 7 and 8, to 9a.

From 6a to 7

The total energy of all (bonded and non-bonded) 371 intramolecular interactions weakened in **7**, hence decreased, by 14.1 kcal mol^{-1}. Selected data for covalent bonds is included in Table A23.

Table A23. Top 6 atom-pairs for which most significant increase/decrease in covalent bond strength (as measured by the interatomic interaction energy change in kcal mol^{-1}) took place on the pre-organisation from **6a** to **7**. $\Delta E_{\text{int}}^{\text{A,B}}$ = { $E_{\text{int}}^{\text{A,B}}$ in **7**} – { $E_{\text{int}}^{\text{A,B}}$ in **6a**}.

Strengthened bonds			**Weakened bonds**		
Atom A	**Atom B**	$\Delta E_{\text{int}}^{\text{A,B}}$	**Atom A**	**Atom B**	$\Delta E_{\text{int}}^{\text{A,B}}$
N13	C1	-6.8	O19	H17	2.3
C2	C1	-1.4	C3	C2	2.4
H11	C3	-1.0	N13	C4	3.3
H6	C1	-1.0	O15	C14	6.1
H12	C4	-0.8	O16	C14	6.7
C14	C4	-0.7	C18	N13	8.8
Sum of all changes in the intermolecular interactions					
Attractive:		-13.4	Repulsive:		+34.2
	Total:	+20.8			

Note that covalent bonds weakened in total by 20.8 kcal mol^{-1}. This is a result of some bonds that became either weaker (in total by 34.2 kcal mol^{-1}) or stronger (in total by –13.4 kcal mol^{-1}) The link N13–C18 became strained (hence weakened) most in terms of interatomic interaction energy, by 8.8 kcal mol^{-1}.

The molecular systems **6a** and **6b** were considered in discussions that follow as made of two molecular fragments, $\mathcal{K}$ and $\mathcal{L}$, that are shown in Figure A14.

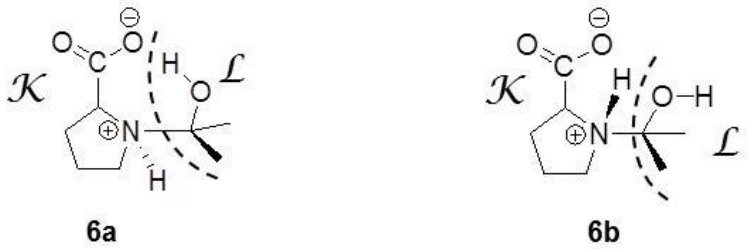

6a **6b**

Figure A14. Schematic partitioning of entire **6** to two molecular fragments $\mathcal{K}$ and $\mathcal{L}$.

The same fragments apply to the **7** and **8** structures. Atom-pairs for which most significant increase/decrease in the interfragment diatomic interaction energy (in kcal mol^{-1}) took place on the pre-organisation from **6a** to **7** are shown in Table A24.

Table A24. Top 10 atom-pairs for which most significant increase/decrease in the inter-fragment diatomic interaction energy (in kcal mol^{-1}) took place on the pre-organisation from **6a** to **7.** $\Delta E_{\text{int}}^{\text{A,B}}$ = { $E_{\text{int}}^{\text{A,B}}$ in **7**} – { $E_{\text{int}}^{\text{A,B}}$ in **6a**}. Atom A belongs to the fragment K (**1a** minus H17) and atom B belongs to the fragment L (**2** + H17).

Strengthened interactions			**Weakened interactions**		
Atom A	**Atom B**	$\Delta E_{\text{int}}^{\text{A,B}}$	**Atom A**	**Atom B**	$\Delta E_{\text{int}}^{\text{A,B}}$
O19	C14	-7.8	C18	H10	1.3
H21	O16	-4.0	C24	H5	1.5
O19	C4	-3.5	H21	C14	1.6
C24	H6	-3.2	O19	C1	3.2
O19	H9	-2.8	H17	C14	3.7
C18	H6	-2.5	O19	O15	4.3
H17	H6	-2.5	C18	O16	4.6
O19	H10	-2.4	H17	N13	5.1
C18	O15	-2.4	C18	N13	8.8
O19	N13	-2.3	O19	H6	9.9
Sum of all changes in the intermolecular interactions					
Attractive:		-65.4	Repulsive:		+64.8
	Total:	–0.6			

The inter-fragment interaction energy, i.e., between all atoms of the molecular fragment $\mathcal{K}$ = {atoms of **1a** minus H17} and all atoms of the molecular fragment $\mathcal{L}$ = {atoms of **2** plus H17}, $E_{\text{int}}^{\mathcal{K},\mathcal{L}}$, essentially remained the same in **7** as $\Delta E_{\text{int}}^{\mathcal{K},\mathcal{L}}$ = –0.6 kcal mol^{-1}. Note that this also includes the interaction energy between N13 and all atoms of $\mathcal{L}$; hence this also includes the N13–C18-covalent bond interaction energy. When only non-bonded interactions between $\mathcal{K}$ and $\mathcal{L}$ are considered (excluding interaction energy between N13 and C18), they became stronger in **7** by –13.1 kcal mol^{-1}.

Considering interaction energies between (i) individual atoms of $\mathcal{K}$ and entire molecular fragment $\mathcal{L}$ as well as(ii) individual atoms of $\mathcal{L}$ and entire molecular fragment $\mathcal{K}$ (see data in Table A25) we note that:

Table A25. Interaction energies (in kcal mol^{-1}) between atoms of a molecular fragment $\mathcal{K}$ and entire molecular fragment $\mathcal{L}$ and atoms of $\mathcal{L}$ and entire molecular fragment $\mathcal{K}$ in **6a** and **7**.

Atom A of $\mathcal{K}$	$E_{\text{int}}^{\text{A},\mathcal{L}}$			**Atom A od $\mathcal{L}$**	$E_{\text{int}}^{\text{A},\mathcal{K}}$		
	6a	**7**	$\Delta_{\mathbf{7-6a}}$		**6a**	**7**	$\Delta_{\mathbf{7-6a}}$
C1	18.2	18.6	0.4	H17	-82.5	-77.9	4.7
C2	2.5	0.8	-1.7	C18	-190.3	-181.6	8.7
C3	2.8	0.6	-2.2	O19	30.7	22.6	-8.1
C4	17.8	17.0	-0.9	C20	-12.7	-12.6	0.1
H5	38.3	37.1	-1.1	H21	-6.3	-9.0	-2.8
H6	-1.4	-3.0	-1.6	H22	-2.5	-2.6	-0.1
H7	1.7	2.7	1.0	H23	-3.6	-3.1	0.5
H8	1.6	1.3	-0.3	C24	-11.7	-13.5	-1.8
H9	1.1	-1.5	-2.6	H25	-2.5	-3.1	-0.6
H10	1.0	1.3	0.4	H26	-1.7	-1.7	0.0
H11	2.2	-0.3	-2.5	H27	-4.1	-5.3	-1.2
H12	2.2	3.4	1.2		$E_{\text{int}}^{\mathcal{K},\mathcal{L}}$		
N13	-285.0	-272.5	12.5		-287.2	-287.8	-0.6
C14	101.9	100.6	-1.3				
O15	-55.2	-57.6	-2.4				
O16	-136.8	-136.4	0.4				
	$E_{\text{int}}^{\mathcal{K},\mathcal{L}}$						
	-287.2	-287.8	-0.6				

-

- In the case of atoms of $\mathcal{K}$, their interaction energies with $\mathcal{L}$, on average, changed slightly ($\Delta E_{\text{int}}^{\text{A},\mathcal{L}}$ = –0.6±1.3 kcal mol^{-1}) except for N13 that experienced the largest unfavourable change with $\Delta E_{\text{int}}^{\text{N13},\mathcal{L}}$ = 12.5 kcal mol^{-1}.
- In the case of atoms of $\mathcal{L}$, largest changes in the $E_{\text{int}}^{\text{A},\mathcal{K}}$ energy term were found for C18, O19 and H17 (the C18–OH fragment of $\mathcal{L}$) of +8.7, –8.1 and +4.7 kcal mol^{-1}, respectively.

From 7 to 8

We noted that the energy of all (bonded and non-bonded) 371 intramolecular interactions marginally improved (by –1.3 kcal mol^{-1}); covalent bonds strengthened by –11.6 kcal mol^{-1} (this is a result of some bonds that became either weaker (in total by 22.8 kcal mol^{-1}) or stronger (in total by –34.3 kcal mol^{-1}) whereas non-bonded weakened by +18.0 kcal mol^{-1}. The link N13–C18 became somewhat more strained (hence weakened) by 2.6 kcal mol^{-1}. The C18–O19 covalent bond became strained the most, its energy decreased by 8.7 kcal mol^{-1}.

Table A26. Interaction energies (in kcal mol^{-1}) between atoms of a molecular fragment $\mathcal{K}$ and entire molecular fragment $\mathcal{L}$ and atoms of $\mathcal{L}$ and entire molecular fragment $\mathcal{K}$ in **7** and **8**.

Atom A of $\mathcal{K}$	$E_{\text{int}}^{\text{A},\mathcal{L}}$			**Atom A of $\mathcal{L}$**	$E_{\text{int}}^{\text{A},\mathcal{K}}$		
	7	**8**	$\Delta_{\mathbf{8}-\mathbf{7}}$		**7**	**8**	$\Delta_{\mathbf{8}-\mathbf{7}}$
C1	18.6	19.6	0.9	H17	-77.9	-67.3	10.6
C2	0.8	-0.1	-0.9	C18	-181.6	-181.0	0.6
C3	0.6	0.9	0.3	O19	22.6	30.0	7.4
C4	17.0	18.9	2.0	C20	-12.6	-12.1	0.5
H5	37.1	39.0	1.9	H21	-9.0	-2.8	6.2
H6	-3.0	-2.2	0.8	H22	-2.6	-2.1	0.5
H7	2.7	3.2	0.6	H23	-3.1	-3.6	-0.5
H8	1.3	1.5	0.2	C24	-13.5	-13.5	0.0
H9	-1.5	-1.6	0.0	H25	-3.1	-6.1	-3.0
H10	1.3	1.8	0.5	H26	-1.7	-1.9	-0.3
H11	-0.3	-2.6	-2.3	H27	-5.3	-6.8	-1.4
H12	3.4	3.0	-0.4		$E_{\text{int}}^{\mathcal{K},\mathcal{L}}$		
N13	-272.5	-273.6	-1.1		-287.8	-267.1	20.6
C14	100.6	88.0	-12.6				
O15	-57.6	-47.1	10.5				
O16	-136.4	-116.0	20.4				
	$E_{\text{int}}^{\mathcal{K},\mathcal{L}}$						
	-287.8	-267.1	20.6				

Looking at data in Table A26 one can note that:

- Inter-fragment interaction energy between molecular fragments $\mathcal{K}$ and $\mathcal{L}$, $E_{\text{int}}^{\mathcal{K},\mathcal{L}}$, weakened by 20.6 kcal mol^{-1}. Note that this also includes the interaction energy between N13 and all atoms of $\mathcal{L}$; hence this also includes the N13C18-covalent bond interaction energy. When only non-bonded interactions between $\mathcal{K}$ and $\mathcal{L}$ are considered (excluding interaction energy between N13 and C18), they became weaker in **8** by +21.7 kcal mol^{-1}.
- N13 of $\mathcal{K}$ are involved in strongest (by far) interactions with $\mathcal{L}$ in **7** and **8**, namely –272.5 and –273.6 kcal mol^{-1}, respectively; these interactions became slightly more attractive in **8**, by –1.1 kcal mol^{-1}.
- Considering atoms of $\mathcal{K}$, C14, O15 and O16 (functional COO^- group) experienced largest change in their interaction energies with $\mathcal{L}$ by –12.6, 10.5 and 20.4 kcal mol^{-1}, respectively.

- Considering atoms of $\mathcal{L}$, largest unfavourable changes in the $E_{\text{int}}^{\text{A},\mathcal{K}}$ energy term was found for H17 of +10.6 kcal mol^{-1}.
- Notably, interactions between C18 and $\mathcal{K}$ remained nearly the same, $\Delta E_{\text{int}}^{\text{C18},\mathcal{K}}$ = 0.6 kcal mol^{-1}. C18 of $\mathcal{L}$ is involved in strongest (by far) interactions with $\mathcal{K}$ in **7** and **8**, namely –181.6 and –180.0 kcal mol^{-1}, respectively.

From 8 to 9a

It is important to note that:

- Energy of all (bonded and non-bonded) 371 intramolecular interactions weakened drastically (by +32.0 kcal mol^{-1}). Covalent bonds were influenced most by the **8** to **9a** change and became weaker by +145.1 kcal mol^{-1}. This has been partly compensated by very significant strengthening of all non-bonded interactions (–111.3 kcal mol^{-1}).
- To illustrate an extent of changes in $E_{\text{int}}^{\text{A,B}}$ among covalent bonds, we obtained the total energy of –74.3/+219.4 kcal mol^{-1} for all bonds that strengthened/weakened. Most strengthened/weakened covalent bonds are N13–C18 (the link) and C14–O16 followed by C18–O19 with the change in their interaction energy of –28.4, +93.7 and +50.9 kcal mol^{-1}, respectively.
- Focusing on non-bonded interactions, the most strengthened was between O16 and on-coming H5, $\Delta E_{\text{int}}^{\text{O16,H17}}$ of –144.4 kcal mol^{-1}.

Looking at data in Table A27 one can note that:

- Inter-fragment interaction between molecular fragments $\mathcal{K}$ and $\mathcal{L}$ hardly changed (less than 1 kcal mol^{-1} but numerous atoms' interactions, either with $\mathcal{K}$ or $\mathcal{L}$, changed a lot (inter-fragment interactions between non-bonded atoms weakened by 22.7 kcal mol^{-1}).
- Considering atoms of $\mathcal{K}$, N13, C14 and O16 experienced largest change in their interaction energies with $\mathcal{L}$ by –22.9, –12.3 and +42.0 kcal mol^{-1}, respectively.
- Considering atoms of $\mathcal{L}$, H17, C18 and O19 (the C–OH fragment) experienced largest changes in the $E_{\text{int}}^{\text{A},\mathcal{K}}$ energy term of +46.2, –18.4 and –16.4 kcal mol^{-1}, respectively.

From the data discussed it follows that due to structural re-arrangement from **6a** to **8** (a better suited structure for the intramolecular proton transfer) a small increase in *E* is observed at each step. However, a wide spread and of moderate changes in interaction energies took place involving nearly entirely the atoms of the $\mathcal{G}$ and $\mathcal{H}$ fragments.

On the **8** to **9a** change with large change in *E*, extremely large changes took place and they were mainly located on covalent bonds. This means that the skeleton of a molecule became highly strained on reaching the TS (**9a**).

Table A27. Interaction energies (in kcal mol^{-1}) between atoms of a molecular fragment $\mathcal{K}$ and entire molecular fragment $\mathcal{L}$ and atoms of $\mathcal{L}$ and entire molecular fragment $\mathcal{K}$ in **8** and **9a**.

Atom A of $\mathcal{K}$	$E_{\text{int}}^{\text{A},\mathcal{L}}$			**Atom A of $\mathcal{L}$**	$E_{\text{int}}^{\text{A},\mathcal{K}}$		
	8	**9a**	$\Delta_{\mathbf{9a-8}}$		**8**	**9a**	$\Delta_{\mathbf{9a-8}}$
C1	19.6	19.7	0.1	H17	-67.3	-21.0	46.2
C2	-0.1	-1.5	-1.4	C18	-181.0	-199.4	-18.4
C3	0.9	0.1	-0.8	O19	30.0	13.6	-16.4
C4	18.9	18.3	-0.6	C20	-12.1	-14.3	-2.2
H5	39.0	43.1	4.1	H21	-2.8	-7.7	-4.8
H6	-2.2	-3.1	-0.9	H22	-2.1	-1.8	0.3
H7	3.2	1.9	-1.3	H23	-3.6	-6.9	-3.3
H8	1.5	1.1	-0.4	C24	-13.5	-13.9	-0.4
H9	-1.6	-2.2	-0.7	H25	-6.1	-6.1	0.0
H10	1.8	1.6	-0.2	H26	-1.9	-2.5	-0.6
H11	-2.6	-4.7	-2.1	H27	-6.8	-7.9	-1.2
H12	3.0	2.7	-0.3		$E_{\text{int}}^{\mathcal{K},\mathcal{L}}$		
N13	-273.6	-296.5	-22.9		-267.1	-267.9	-0.7
C14	88.0	75.7	-12.3				
O15	-47.1	-50.1	-3.0				
O16	-116.0	-74.0	42.0				
	$E_{\text{int}}^{\mathcal{K},\mathcal{L}}$						
	-267.1	-267.9	-0.7				

An overall change from 6a to 9a and from 6b to 9b

In search for the origin of such large energy differences observed at TSs (**9a** and **9b**) we noted the following:

- Total interaction energy changed highly unfavourably in **9a** (by +47.5 kcal mol^{-1}) but opposite trend applies to **9b** (–8.6 kcal mol^{-1}). This illustrates how interactions are working against the change from **6a** to **9a**. On the other hand, one might suggest that interactions drive the change from **6b** to **9b**. This is strongly supported by an 'absence' of a TS at the higher MP2 level as on the **6b** to **9b** we obtained –0.3, –0.6 and +0.1 kcal mol^{-1} for ΔE_{corr}, ΔH and ΔG, respectively.

- The $E_{\text{int}}^{\text{O16,H5}}$ term is –211.1 (in **9a**) and –227.4 (in **9b**) kcal mol^{-1}. In both cases they are strongest among all non-covalent interactions and largely assist (facilitate) reaching the TS. To this effect, interaction between O16 and H5 became stronger, relative to **6**, by –165.1 (in **9a**) and –108.3 (in **9b**) kcal mol^{-1}. This shows how extensive structural change had to take place on **6a** to **9a** to bring these atoms so much closer, hence make the interaction so much stronger.
- Overall, covalent bonds' strength weakened by +154.3 (in **9a**) and +92.7 (in **9b**) kcal mol^{-1}. N13–C1, N13–C18 and N13–C4 as well as C14–O15 strengthened in **9a** and **9b** by between –10 and –22 kcal mol^{-1}. Next, C14–O16 and N15–H5 became weaker in **9a** and **9b** by between 97 and 43 kcal mol^{-1}. Moreover C18–C19 and O19–H17 became weaker in **9a** by 59 and 10 kcal mol^{-1}, respectively, but much smaller effect is observed in **9b** with 9 and 2 kcal mol^{-1}, respectively. It is clear that due H5 being in a process of departing from N15, some density shared between them was utilised to increase density between N13 and all three neighbouring atoms it is covalently bonded to (these interactions (bonds) became stronger). What is somewhat surprising is that the network of covalent bonds effected is reaching as far as O15 in $\mathcal{K}$ and H17 in $\mathcal{L}$. Clearly, a molecular skeleton (a framework of all covalently bonded atoms) in **9a** became by far more strained than in **9b**.
- Inter-fragment (between $\mathcal{K}$ and $\mathcal{L}$) interactions changed by 36.3 (in **9a**) and 3.6 (in **9b**) kcal mol^{-1}. This indicates that $\mathcal{L}$ had to re-position itself relative to $\mathcal{K}$ significantly on **6a** to **9a** and to achieve that a significant energy barrier (working against strong inter-fragment interactions) had to be overcome.

However, one can wonder what would be a classic organic chemist explanation of such small (at B3LYP) or none (at MP2) energy required for the intramolecular H5-transfer, hence the step from **6b** to **10b**. We decided to make use of our approach to gain an insight on a fundamental level. Firstly, we note that H5 is involved in attractive interactions only with 4 atoms, namely: N13 to which it is bonded to in **6b**, O15 and O16 of the COO functional group of $\mathcal{K}$ and O19 in $\mathcal{L}$. Due to the fact that on a proton transfer process H5 is heading not only towards O16 but rather in the direction of the entire COO group, it makes sense to partition $\mathcal{K}$ to two fragments, one containing COO atoms (we will call it $\mathcal{C}$) and remaining atoms of $\mathcal{K}$ with exclusion of N13 (let us call it $\mathcal{D}$). We considered specifically selected for the purpose interactions:

e) $E_{\text{int}}^{\text{H5,N13}} / E_{\text{int}}^{\text{H5,O16}}$ is –127.1/–59.6 (in **6b**) and –101.9/–113.7 (in **9b**) kcal mol^{-1}. Clearly, the attraction to O16 in **6b** is not sufficient to easily overcome attraction to N13.

f) H5 is being attracted by atoms of C with $E_{\text{int}}^{\text{H5},C}$ of –32.7 (in **6b**) and –74.0 (in **9b**) kcal mol^{-1} and this is not sufficient for the proton transfer either.

g) H5 is being repelled by atoms of $\mathcal{L}$ with $E_{\text{int}}^{\text{H5},\mathcal{L}}$ of +46.2 (in **6b**) and +43.5 (in **9b**) kcal mol^{-1}. By repelling H5, atoms of $\mathcal{L}$ facilitate its transfer to O16.

h) H5 is also being repelled by atoms of $\mathcal{D}$ with $E_{\text{int}}^{\text{H5},\mathcal{D}}$ of +42.8 (in **6b**) and +43.3 (in **9b**) kcal mol^{-1}. Also in this case atoms of $\mathcal{D}$ assist in the transfer process of H5.

Latter two terms, by repelling H5 can be seen as counteracting the H5 attraction to N13 by pushing H5 towards O16 (or C in general). As a result, nearly perfect balance in interaction energies is obtained, i.e., resulting in weakening (energy-wise) the overall bonding strength between N13 and H5. Hence, an estimate of the effective (or corrected) interaction energy between H5 and N13 can be obtained by summing up $E_{\text{int}}^{\text{H5,N13}}$, $E_{\text{int}}^{\text{H5},\mathcal{L}}$ and $E_{\text{int}}^{\text{H5},\mathcal{D}}$ giving a product of –38.3 (in **6b**) and –15.1 (in **9b**) kcal mol^{-1}. From this it follows that the attractive interaction between H5 and C in **6b** is nearly as strong as the corrected (effective) attraction between N13 and H5. In case of **9b**, the $E_{\text{int}}^{\text{H5},C}$ term of –74.0 kcal mol^{-1} represents much larger attraction than effective interaction (of –15.1 kcal mol^{-1}) between N13 and H5.

End of PART A6

Appendix B

Supporting Information for Chapter 4

Part B1

Computational details

All calculations were performed in Gaussian 09 Rev. D01 at the RB3LYP/6–311++G(d,p) level of theory with Grimme's empirical correction for dispersion (GD3) in solvent (DMSO) using the implicit default solvation model. Frequency calculations were performed for the B3LYP-optimised local, global and transition state (TS) structures. None and one imaginary frequency were obtained for minimum energy (local and global) and TS structures, respectively. The lowest energy pathway connecting a given transition state with the two associated energy minima (intrinsic reaction coordinate – IRC) was calculated to verify each transition state. Topological calculations were performed in AIMAll (ver. 17.11.14) using B3LYP-generated wavefunctions.

Coordinates for all structures discussed in the main body

1a – the lowest energy conformer (LEC) of proline

Atom	X	Y	Z
C1	-0.0945820881	-1.3616508300	-0.8365335880
C2	-0.5190690347	-1.2573374716	0.6302290991
C3	-1.0788227389	0.1706950832	0.7151583197
C4	-0.1246813852	0.9722544295	-0.1992426764
H5	0.3281244270	0.2480799094	-2.1025552561
H6	0.6591109463	-2.1308210435	-1.0132112033
H7	-0.9632543973	-1.5761338223	-1.4696052990
H8	-1.2490175462	-2.0185574329	0.9075498900
H9	0.3511233168	-1.3671245973	1.2850414934
H10	-2.0880936170	0.2049830909	0.2983008665
H11	-1.1155132690	0.5735847011	1.7271909176
H12	-0.6469204573	1.7777075250	-0.7198264624
N13	0.4628012476	-0.0166263775	-1.1345153508
C14	1.0098594764	1.6334091005	0.6007483932
O15	0.8307496198	2.4944067393	1.4355402361
O16	2.2188399062	1.1665470996	0.2925674012
H17	2.0193456037	0.4865838968	-0.4168367709

Zero-point correction =	0.144439 (Hartree/Particle)
Thermal correction to Energy =	0.151574
Thermal correction to Enthalpy =	0.152518
Thermal correction to Gibbs Free Energy =	0.112465
Sum of electronic and zero-point Energies =	–401.167135
Sum of electronic and thermal Energies =	–401.160000
Sum of electronic and thermal Enthalpies =	–401.159056
Sum of electronic and thermal Free Energies =	–401.199110

2 - Acetone

Atom	X	Y	Z
C1	-0.00462863	0.178140532	0.6151523
O2	-0.0134421	0.517341082	1.7864747
C3	-1.28134278	-0.124580786	-0.1338366
H4	-2.13578709	-0.108943756	0.5416987
H5	-1.42267733	0.624186195	-0.9201481
H6	-1.21074387	-1.096426665	-0.6304427
C7	1.28356795	0.038941613	-0.1618913
H8	1.43279417	-1.013549159	-0.4243945
H9	1.22377847	0.594769111	-1.1018739
C10	2.12848123	0.39012183	0.4292614

Zero-point correction =	0.083228 (Hartree/Particle)
Thermal correction to Energy =	0.088510
Thermal correction to Enthalpy =	0.089454
Thermal correction to Gibbs Free Energy =	0.056063
Sum of electronic and zero-point Energies =	–193.146706
Sum of electronic and thermal Energies =	–193.141424
Sum of electronic and thermal Enthalpies=	–193.140480
Sum of electronic and thermal Free Energies=	–193.173871

1b – The higher energy conformer (HEC) of proline

Atom	**X**	**Y**	**Z**
C1	-0.4090342829	-1.2417777602	-1.0365123470
C2	-0.6679877535	-1.5447881579	0.4695639391
C3	-0.3162309883	-0.2234293381	1.2092014177
C4	-0.0898466893	0.7677367134	0.0537820277
H5	1.3839410276	-0.3040841776	-0.8583830776
H6	0.0865113893	-2.0562345172	-1.5651403464
H7	-1.3492538419	-1.0266239834	-1.5514139257
H8	-1.7054929740	-1.8402176315	0.6362186313
H9	-0.0336802727	-2.3620827660	0.8174100463
H10	-1.1028450646	0.1090238381	1.8868095774
H11	0.6032172475	-0.3273668019	1.7897031322
H12	-1.0601281261	1.1753315470	-0.2628674836
N13	0.4290475018	-0.0221423670	-1.0821181369
C14	0.7733566709	1.9810686690	0.3373918600
O15	0.9007085432	2.5009165302	1.4196362013
O16	1.3832903879	2.4938242140	-0.7505225570
H17	1.1744272251	1.9208459692	-1.5127589589

Zero-point correction =	0.144477 (Hartree/Particle)
Thermal correction to Energy =	0.151947
Thermal correction to Enthalpy =	0.152891
Thermal correction to Gibbs Free Energy =	0.111845
Sum of electronic and zero-point Energies =	–401.156469
Sum of electronic and thermal Energies =	–401.149000
Sum of electronic and thermal Enthalpies =	–401.148056
Sum of electronic and thermal Free Energies =	–401.189101

3 – The DMSO solvent molecule

Atom	X	Y	Z
C1	0.1390831286	1.3738971442	0.1548933110
H2	-0.3718709417	1.4568834113	1.1151183087
H3	1.1968515605	1.1433203786	0.2883211020
H4	0.0148603640	2.2937622891	-0.4153420520
C5	-0.1941417441	-1.3453122695	0.2887444938
H6	-0.6986171498	-1.2094582639	1.2463671140
H7	-0.5430439196	-2.2588948032	-0.1912406887
H8	0.8895271679	-1.3645337763	0.4117684699
O9	0.2089180421	-0.1281355626	-2.0829901667
S10	-0.6415665170	0.0384712824	-0.8156401979

Zero-point correction=	0.078866 (Hartree/Particle)
Thermal correction to Energy=	0.084550
Thermal correction to Enthalpy=	0.085494
Thermal correction to Gibbs Free Energy=	0.050476
Sum of electronic and zero-point Energies=	–553.208027
Sum of electronic and thermal Energies=	–553.202343
Sum of electronic and thermal Enthalpies=	–553.201399
Sum of electronic and thermal Free Energies=	–553.236418

4a_GMS

Atom	X	Y	Z
C1	-0.6916850048	-1.9375015508	-1.2185793238
C2	-1.6069619830	-2.3973912377	-0.0787230580
C3	-1.6756783939	-1.1474146077	0.8128553526
C4	-1.6270080967	0.0247043311	-0.2081486431
H5	-1.7704851814	-0.4732417091	-2.2069861297
H6	0.3512071852	-1.9667144146	-0.8932061339
H7	-0.7883639362	-2.5209893400	-2.1346306448
H8	-2.5984753746	-2.6468021265	-0.4697230819
H9	-1.2178388612	-3.2685219087	0.4522526545
H10	-2.5713304507	-1.1019025535	1.4316952680
H11	-0.8035236500	-1.1094406505	1.4685078165
H12	-2.6229400284	0.4422444921	-0.3716703728
N13	-1.0753773719	-0.5240601710	-1.4719324254
C14	-0.7413908516	1.1752989962	0.2726118365
O15	-0.9240760916	1.7908845175	1.3008615327
O16	0.2768470597	1.4393638881	-0.5494302064
H17	0.1495733464	0.7766572727	-1.2886132891
C18	2.3804416706	-0.3210758444	1.0129221934
O19	1.7233567346	-1.3294925621	1.2145379515
C20	3.1570755963	-0.1243680716	-0.2663318614
H21	2.8825172843	-0.8796087298	-1.0021978211
H22	2.9830106501	0.8770626844	-0.6662276427
H23	4.2268303159	-0.2050568301	-0.0454639043
C24	2.4480348022	0.7957037052	2.0249368385
H25	3.4689521540	1.1722585878	2.1262586158
H26	1.8279292207	1.6204998632	1.6594133813
H27	2.0658592563	0.4631039696	2.9895110972

Zero-point correction =	0.228970 (Hartree/Particle)
Thermal correction to Energy =	0.243408
Thermal correction to Enthalpy =	0.244352
Thermal correction to Gibbs Free Energy =	0.184586
Sum of electronic and zero-point Energies =	–594.318801
Sum of electronic and thermal Energies =	–594.304363
Sum of electronic and thermal Enthalpies =	–594.303419
Sum of electronic and thermal Free Energies =	–594.363185

4a_p-org

Atom	X	Y	Z
C1	-0.2142578068	-1.3418801271	-0.6664473997
C2	-1.5993364941	-1.9535653225	-0.9065553140
C3	-2.4317407846	-1.3178920232	0.2147961561
C4	-1.8537336948	0.1227623131	0.3059517752
H5	-0.3465398083	0.7035998494	-0.9764160675
H6	0.3093019067	-1.8825469812	0.1290069959
H7	0.4270260249	-1.3405016675	-1.5488502351
H8	-1.9812426733	-1.6456154512	-1.8848729234
H9	-1.5982367073	-3.0445856784	-0.8650357576
H10	-3.5037840457	-1.3096521626	0.0208739079
H11	-2.2644169649	-1.8526202978	1.1544787088
H12	-2.4658115594	0.8145605046	-0.2778743371
N13	-0.4747751384	0.0473074059	-0.2171946258
C14	-1.8626370569	0.6309580569	1.7456262804
O15	-2.8816372374	0.8780779951	2.3574583669
O16	-0.6586507062	0.7624525769	2.3025529247
H17	0.0073932101	0.5297890487	1.6066048547
C18	2.7366003409	-0.0651676578	0.6869122870
O19	2.1165168599	-0.1564435759	1.7337352907
C20	3.5475739128	-1.2165586342	0.1448892824
H21	3.5698117180	-2.0404322372	0.8570093945
H22	3.1006535318	-1.5566501065	-0.7950054992
H23	4.5651123049	-0.8903302141	-0.0880145211
C24	2.7316702357	1.2037349710	-0.1295742178
H25	3.7288412825	1.6549083488	-0.0870051502
H26	2.5269593588	0.9845679163	-1.1807225829
H27	1.9962399911	1.9063231507	0.2584724064

Zero-point correction =	0.228542 (Hartree/Particle)
Thermal correction to Energy =	0.243192
Thermal correction to Enthalpy =	0.244136
Thermal correction to Gibbs Free Energy =	0.183038
Sum of electronic and zero-point Energies =	–594.318198
Sum of electronic and thermal Energies =	–594.303549
Sum of electronic and thermal Enthalpies =	–594.302604
Sum of electronic and thermal Free Energies =	–594.363702

5a_TS

Atom	X	Y	Z
C1	-0.0171571315	-1.9617347208	-0.4179515031
C2	-1.5104260512	-2.1161066394	-0.6847728431
C3	-2.1145567745	-1.0140397845	0.1894788547
C4	-1.0800479450	0.1488501252	0.1230439600
H5	0.3431549380	-0.1531409416	-1.3248784554
H6	0.2598532175	-2.3563482371	0.5630904862
H7	0.6209771353	-2.4107147098	-1.1757246461
H8	-1.7246885314	-1.9372197639	-1.7423963487
H9	-1.8774877917	-3.1095480543	-0.4237611380
H10	-3.0968917020	-0.6779127909	-0.1387118297
H11	-2.2054524682	-1.3678063925	1.2198196968
H12	-1.3776079701	0.8826085825	-0.6228925990
N13	0.2084380865	-0.4874363814	-0.3744340564
C14	-1.1222967116	0.8851515543	1.4752560128
O15	-2.0335630020	1.6895119170	1.6199679096
O16	-0.3030363747	0.5738758265	2.4421832989
H17	0.6192000107	0.0398139417	2.1519041614
C18	1.8651856094	-0.1017953435	0.4842933168
O19	1.7094576568	-0.5393201226	1.6910288907
C20	2.8380475301	-0.8893770490	-0.3759160618
H21	2.7271615466	-1.9591519660	-0.2043707467
H22	2.7394021364	-0.6660248145	-1.4397873798
H23	3.8453066734	-0.5990076149	-0.0632659391
C24	1.9416025032	1.4052948871	0.2627397574
H25	2.9179841381	1.7318104600	0.6322268536
H26	1.8744880872	1.6693386528	-0.7941016133
H27	1.1798531848	1.9452293796	0.8226319615

Zero-point correction =	0.229618 (Hartree/Particle)
Thermal correction to Energy =	0.241264
Thermal correction to Enthalpy =	0.242208
Thermal correction to Gibbs Free Energy =	0.192049
Sum of electronic and zero-point Energies =	–594.300687
Sum of electronic and thermal Energies =	–594.289042
Sum of electronic and thermal Enthalpies =	–594.288098
Sum of electronic and thermal Free Energies =	–594.338256

5a_eq

Atom	X	Y	Z
C1	-0.1603524393	-1.5611266845	0.9399083284
C2	-1.6587996187	-1.7059470406	0.6222442348
C3	-1.7869742887	-1.2988729275	-0.8548002985
C4	-0.7551554935	-0.1738990383	-1.0005381376
H5	0.7958921265	-1.4796061116	-0.8835772537
H6	0.0371684123	-0.9891542427	1.8409757273
H7	0.3593910856	-2.5145947462	0.9964298973
H8	-2.0088865609	-2.7212415294	0.8055698201
H9	-2.2398111414	-1.0291770444	1.2509376054
H10	-1.5259016630	-2.1327896799	-1.5128308850
H11	-2.7813104438	-0.9496536568	-1.1249600856
H12	-0.4340085535	-0.0265851489	-2.0295651408
N13	0.4305112578	-0.7822587489	-0.2340376859
C14	-1.3269921850	1.1783591290	-0.4810370308
O15	-2.2443068597	1.6205342628	-1.1914411544
O16	-0.8618964088	1.6943083531	0.5751585493
H17	0.5754507787	1.3025383786	1.1139162385
C18	1.7006089781	0.0987347134	0.1254193602
O19	1.4371168523	0.8172042996	1.2746771558
C20	1.9993966296	0.9840846083	-1.0835998143
H21	1.2171637880	1.7273717131	-1.2355518816
H22	2.9334213687	1.5112627790	-0.8852576306
H23	2.1232021099	0.3965009921	-1.9960270247
C24	2.8361320230	-0.8757807549	0.4182230516
H25	3.0706191044	-1.4981672330	-0.4477161235
H26	3.7220174294	-0.2921002793	0.6704665720
H27	2.5930037120	-1.5108443624	1.2704136064

Zero-point correction =	0.234574 (Hartree/Particle)
Thermal correction to Energy =	0.246325
Thermal correction to Enthalpy =	0.247270
Thermal correction to Gibbs Free Energy =	0.197264
Sum of electronic and zero-point Energies =	–594.309671
Sum of electronic and thermal Energies =	–594.297919
Sum of electronic and thermal Enthalpies =	–594.296975
Sum of electronic and thermal Free Energies =	–594.346980

5a_p-org

Atom	X	Y	Z
C1	0.4722714307	-1.7931193190	-0.9699678577
C2	-0.4084548344	-2.3899837540	0.1522703504
C3	-1.3985562225	-1.2621027291	0.5513734610
C4	-1.2529491073	-0.2406661687	-0.5694321616
H5	0.3577413833	0.1187470566	-1.8156092944
H6	1.5325036959	-2.0135683130	-0.8949277460
H7	0.1315259609	-2.1063362616	-1.9558229237
H8	-0.9349600091	-3.2640493246	-0.2303796979
H9	0.1938721403	-2.7147355704	0.9995090589
H10	-2.4267311843	-1.6108980450	0.6183435781
H11	-1.1386506982	-0.8106335601	1.5099483000
H12	-1.7114743236	-0.6581651505	-1.4734605802
N13	0.2396286985	-0.2982596936	-0.8925697359
C14	-1.8843429405	1.1669184142	-0.4665066339
O15	-2.9801121548	1.2193441845	0.1120313904
O16	-1.2627192158	2.1007540316	-1.0592171982
H17	0.1199172494	2.0588027397	-0.0518459130
C18	1.2892098462	0.5044542251	0.0353783839
O19	0.6424706199	1.5721016590	0.6303783040
C20	2.3781341306	0.9466297365	-0.9418450452
H21	1.9705523324	1.6400320807	-1.6823297266
H22	3.1557102360	1.4642788739	-0.3796567208
H23	2.8303524838	0.0966710353	-1.4575571574
C24	1.8405738948	-0.3529445445	1.1673319674
H25	2.4034459947	-1.2162659385	0.8185750861
H26	2.5241135899	0.2856382542	1.7283907884
H27	1.0507270033	-0.6705439186	1.8445977239

Zero-point correction =	0.234647 (Hartree/Particle)
Thermal correction to Energy =	0.246415
Thermal correction to Enthalpy =	0.247359
Thermal correction to Gibbs Free Energy =	0.197330
Sum of electronic and zero-point Energies =	–594.296720
Sum of electronic and thermal Energies =	–594.284952
Sum of electronic and thermal Enthalpies =	–594.284008
Sum of electronic and thermal Free Energies =	–594.334037

6a_TS

Atom	X	Y	Z
C1	0.3840649949	-1.6807530894	-1.1254104814
C2	-0.4296596300	-2.4017196034	0.0076021589
C3	-1.3647230266	-1.3097792510	0.6350233223
C4	-1.2628190561	-0.2419604123	-0.4347763148
H5	-0.1615703227	0.7968619808	-1.5892177371
H6	1.4410339258	-1.9318985223	-1.1383940911
H7	-0.0245704768	-1.9060248712	-2.1105153911
H8	-1.0179709031	-3.2118135273	-0.4248388703
H9	0.2296125906	-2.8396732140	0.7562331855
H10	-2.3865417351	-1.6666041934	0.7588184012
H11	-1.0074045981	-0.9576618061	1.6019462897
H12	-1.7738342961	-0.6641265278	-1.3130267784
N13	0.1733214716	-0.2243149459	-0.8690517737
C14	-1.7122547391	1.2167690212	-0.5345692081
O15	-2.6427349748	1.7256654320	0.0663782109
O16	-0.9778565964	1.7694267751	-1.4763114182
H17	0.5018658321	2.2154649446	0.2179058519
C18	1.2362249533	0.4017566503	0.0863071479
O19	0.6469257400	1.4632234373	0.8069227220
C20	2.3456705639	0.9025168979	-0.8406478492
H21	1.9586718254	1.6555060344	-1.5319281176
H22	3.1430460117	1.3489083176	-0.2449282725
H23	2.7652465233	0.0832161630	-1.4273067950
C24	1.7991649574	-0.5359313787	1.1545645389
H25	2.2807273640	-1.4141821813	0.7291181010
H26	2.5551333010	0.0263715307	1.7041954333
H27	1.0349302998	-0.8467436608	1.8628077349

Zero-point correction =	0.229737 (Hartree/Particle)
Thermal correction to Energy =	0.241029
Thermal correction to Enthalpy =	0.241973
Thermal correction to Gibbs Free Energy =	0.193718
Sum of electronic and zero-point Energies =	–594.270035
Sum of electronic and thermal Energies =	–594.258743
Sum of electronic and thermal Enthalpies =	–594.257799
Sum of electronic and thermal Free Energies =	–594.306054

6a_eq

Atom	X	Y	Z
C1	0.5114657874	-1.6413051547	-1.2748653443
C2	-0.2645314974	-2.4937815007	-0.2316325121
C3	-1.3103889259	-1.5206633124	0.3650321054
C4	-1.1237636008	-0.2422774071	-0.4783541488
H5	-1.5991368613	1.8429498781	-1.5802733636
H6	1.5711868715	-1.8772173809	-1.3168667209
H7	0.0987974020	-1.8179231343	-2.2727226806
H8	-0.7322100510	-3.3558393303	-0.7105899673
H9	0.4020632976	-2.8752267807	0.5435264316
H10	-2.3328322826	-1.8928056827	0.2802955050
H11	-1.1216331218	-1.3157208973	1.4176800683
H12	-1.7169223291	-0.3713051422	-1.3933000808
N13	0.2872060490	-0.2139892093	-0.9461491176
C14	-1.6515939214	1.0394671019	0.1622730874
O15	-1.9376436977	1.1562182589	1.3282816661
O16	-1.9108389746	2.0572860657	-0.6898630358
H17	0.9690079951	2.1961151620	-0.8810532573
C18	1.3049899153	0.4423071152	-0.0816281577
O19	0.9351360334	1.8232834294	0.0092655666
C20	2.6802562945	0.3389612605	-0.7536415676
H21	2.6082448845	0.6028825337	-1.8116348515
H22	3.3552586729	1.0383176514	-0.2578501897
H23	3.1119764304	-0.6589992474	-0.6695668673
C24	1.3794211188	-0.0379761750	1.3726442635
H25	1.5838010310	-1.1081096210	1.4131826178
H26	2.1879560050	0.4858697471	1.8866438888
H27	0.4481274751	0.1714817722	1.897566662

Zero-point correction =	0.232583 (Hartree/Particle)
Thermal correction to Energy =	0.244807
Thermal correction to Enthalpy =	0.245751
Thermal correction to Gibbs Free Energy =	0.195193
Sum of electronic and zero-point Energies =	–594.290553
Sum of electronic and thermal Energies =	–594.278329
Sum of electronic and thermal Enthalpies =	–594.277385
Sum of electronic and thermal Free Energies =	–594.327943

4b_GMS

Atom	X	Y	Z
C1	-2.2641727131	0.5704324091	-2.2935412506
C2	-2.0183714657	1.5842351092	-1.1681108589
C3	-0.8059885576	0.9801408678	-0.4439682103
C4	-0.9740779599	-0.5687808272	-0.6636731390
H5	-2.8582022975	-1.0642012062	-1.2137865744
H6	-3.2712514758	0.6079634282	-2.7124366242
H7	-1.5537592881	0.7355269124	-3.1115116773
H8	-1.8282619419	2.5974992927	-1.5286952714
H9	-2.8862263879	1.6138216175	-0.5022746603
H10	0.1252672965	1.3075405241	-0.9106044184
H11	-0.7610090224	1.2544835081	0.6109148953
H12	-0.0230654376	-0.9870289409	-1.0036226683
N13	-2.0144019294	-0.7549819190	-1.6896299842
C14	-1.3453822750	-1.2676302056	0.6389173393
O15	-2.4684636724	-1.6472373097	0.9006609884
O16	-0.3565017639	-1.4231858963	1.5223523830
H17	0.5146478782	-1.0923819410	1.1767835190
C18	2.5928144812	0.4425407195	0.8724470209
O19	1.9985879889	-0.5861617150	0.5635727742
C20	2.0666762043	1.3731017646	1.9301715900
H21	1.7603282723	2.3101156938	1.4538636000
H22	1.2171640502	0.9375330099	2.4539337205
H23	2.8588761693	1.6234335351	2.6401492003
C24	3.8783079403	0.8204182318	0.1938785126
H25	3.8232290415	1.8504326052	-0.1691391111
H26	4.6912234572	0.7862626391	0.9265267231
H27	4.0954134082	0.1396080928	-0.6274778183

Zero-point correction =	0.228937 (Hartree/Particle)
Thermal correction to Energy =	0.243389
Thermal correction to Enthalpy =	0.244334
Thermal correction to Gibbs Free Energy =	0.183671
Sum of electronic and zero-point Energies =	–594.317076
Sum of electronic and thermal Energies =	–594.302624
Sum of electronic and thermal Enthalpies =	–594.301680
Sum of electronic and thermal Free Energies =	–594.362342

4b_p-org

Atom	X	Y	Z
C1	-0.1705743733	2.2625588835	-0.2296233115
C2	-1.6761737669	2.5380035918	0.0194944711
C3	-2.2901023528	1.1345282590	0.2746682983
C4	-1.0790489148	0.1804647631	0.2294733497
H5	-0.3068646154	0.7383195994	-1.5847054566
H6	0.2691896879	2.8933345220	-1.0034665566
H7	0.3989802266	2.4155604209	0.6925745741
H8	-1.8230059502	3.2141048018	0.8641064264
H9	-2.1328889599	3.0030084112	-0.8568177672
H10	-2.8138662671	1.0674281728	1.2299900201
H11	-2.9954616580	0.8632950354	-0.5118461906
H12	-0.6485011465	0.0793254136	1.2320526387
N13	-0.0488869504	0.8401142533	-0.6048232405
C14	-1.3742978437	-1.2264964519	-0.2913608127
O15	-2.3747288993	-1.5187670048	-0.9110364716
O16	-0.4444313465	-2.1536309177	-0.0417117532
H17	0.3372161545	-1.7845212918	0.4494772794
C18	2.3797330493	-0.3848354803	0.4472006969
O19	1.6399069737	-1.0241979952	1.1921448964
C20	2.6822270222	-0.8422165771	-0.9536016125
H21	1.9475290966	-1.5684235454	-1.2967404908
H22	2.7247829471	0.0044841248	-1.6392909278
H23	3.6721920945	-1.3134559482	-0.9451927161
C24	3.0858460230	0.8480144796	0.9339154646
H25	4.1672709971	0.7269121054	0.8181619936
H26	2.7906698696	1.6961909234	0.3104755157
H27	2.8403909027	1.0490004512	1.9756416826

Zero-point correction =	0.229360 (Hartree/Particle)
Thermal correction to Energy =	0.243496
Thermal correction to Enthalpy =	0.244441
Thermal correction to Gibbs Free Energy =	0.186547
Sum of electronic and zero-point Energies =	–594.313547
Sum of electronic and thermal Energies =	–594.299411
Sum of electronic and thermal Enthalpies =	–594.298466
Sum of electronic and thermal Free Energies =	–594.356360

5b_TS

Atom	X	Y	Z
C1	-0.4029099281	1.3024110333	-1.3257489985
C2	-1.9174399546	1.1114922786	-1.2901921809
C3	-2.1834922370	0.8312475511	0.1981415825
C4	-0.9399721225	0.0612790829	0.6793408962
H5	0.1943058859	-0.6154258908	-0.9217070965
H6	0.0561870105	1.1769755716	-2.3047158504
H7	-0.1273985150	2.2768937074	-0.9233666977
H8	-2.4507093678	1.9873852726	-1.6609547142
H9	-2.2025856696	0.2523472733	-1.9039702688
H10	-2.2678017114	1.7688597043	0.7506649607
H11	-3.0878022452	0.2499351600	0.3684762229
H12	-0.5325898950	0.4806547448	1.6016662342
N13	0.1122124629	0.2513814606	-0.3926802541
C14	-1.1493198352	-1.4420429328	0.9512781460
O15	-2.2523012523	-1.9540080953	0.9621994976
O16	-0.0446733842	-2.1218056864	1.1794168958
H17	0.8046998199	-1.4830678168	1.2384240659
C18	1.7889211545	0.3746539540	0.3300891472
O19	1.7806308693	-0.4765103396	1.3163419522
C20	1.9013903880	1.8343898516	0.7458282002
H21	1.9060922502	2.5253085689	-0.0977119907
H22	1.1037110631	2.1040017957	1.4408652989
H23	2.8521357775	1.9371285989	1.2747447019
C24	2.6385386973	0.0005673327	-0.8805560437
H25	2.4516086592	0.6421630568	-1.7440071915
H26	3.6876550476	0.1113665282	-0.5934985386
H27	2.4739070320	-1.0445817657	-1.1523679766

Zero-point correction =	0.230689 (Hartree/Particle)
Thermal correction to Energy =	0.242251
Thermal correction to Enthalpy =	0.243195
Thermal correction to Gibbs Free Energy =	0.193182
Sum of electronic and zero-point Energies =	–594.302870
Sum of electronic and thermal Energies =	–594.291308
Sum of electronic and thermal Enthalpies =	–594.290364
Sum of electronic and thermal Free Energies =	–594.340377

5b_eq

Atom	X	Y	Z
C1	-0.3093767288	1.0397269453	-1.4207433194
C2	-1.8304584926	0.9978867458	-1.2953874471
C3	-2.0460736433	1.0078190952	0.2237853641
C4	-0.9464056075	0.0785582145	0.7513967534
H5	0.1604945402	-0.8367186830	-0.6044614963
H6	0.0830306840	0.6544180127	-2.3589974143
H7	0.0677758136	2.0475499194	-1.2583573451
H8	-2.2940884610	1.8436074136	-1.8030670647
H9	-2.2223914799	0.0775699166	-1.7361995974
H10	-1.9090971057	2.0178113930	0.6182649102
H11	-3.0299790730	0.6532052101	0.5271947259
H12	-0.5645824023	0.3675162666	1.7258979511
N13	0.1696130890	0.1627216567	-0.2845289097
C14	-1.3653211282	-1.4238718667	0.8260269206
O15	-2.2686926995	-1.6975288939	1.6340280314
O16	-0.7322979609	-2.1991396262	0.0530376434
H17	1.8432089004	-1.4054178552	0.9529364658
C18	1.5881531700	0.4171985520	0.2664039693
O19	1.7746888382	-0.5094075679	1.3097579027
C20	1.6989050150	1.8018486852	0.8858444600
H21	1.5830808106	2.5890799146	0.1424441601
H22	0.9629832456	1.9436232260	1.6775949174
H23	2.6932337290	1.8914971152	1.3238205334
C24	2.5791611458	0.1974166469	-0.8724772391
H25	2.4522935387	0.9365720409	-1.6640801261
H26	3.5887621219	0.2909511223	-0.4714316655
H27	2.4664801407	-0.8013935996	-1.3030030842

Zero-point correction =	0.234061 (Hartree/Particle)
Thermal correction to Energy =	0.246190
Thermal correction to Enthalpy =	0.247135
Thermal correction to Gibbs Free Energy =	0.195918
Sum of electronic and zero-point Energies =	–594.313838
Sum of electronic and thermal Energies =	–594.301708
Sum of electronic and thermal Enthalpies =	–594.300764
Sum of electronic and thermal Free Energies =	–94.3519810

6b_TS

Atom	X	Y	Z
C1	-0.2904715225	0.9838139059	-1.4196713284
C2	-1.8149650931	0.9955604922	-1.2892345895
C3	-2.0271383548	1.0514628972	0.2303058807
C4	-0.9324878909	0.1212379562	0.7653786955
H5	-0.0109712243	-1.1168594758	-0.4546821646
H6	0.0677018400	0.5381292459	-2.3465734295
H7	0.1062718851	1.9979639595	-1.3418893946
H8	-2.2592749475	1.8394684401	-1.8172032231
H9	-2.2394421723	0.0762273606	-1.7022450837
H10	-1.8596541476	2.0657550685	0.6011262606
H11	-3.0192103283	0.7306738217	0.5477791686
H12	-0.5809358965	0.3870550280	1.7591518630
N13	0.1726818060	0.1630038622	-0.2544570093
C14	-1.3561552668	-1.3721986990	0.7848170475
O15	-2.2383952230	-1.7874553696	1.5233606451
O16	-0.6623498087	-2.0625163538	-0.0724158385
H17	1.8882642924	-1.3925524188	0.9393538602
C18	1.5611563603	0.4286486574	0.2696050840
O19	1.7905308224	-0.5077057816	1.3141350033
C20	1.6930762776	1.8076477177	0.9088348054
H21	1.5026324334	2.6012281807	0.1865603497
H22	1.0042721313	1.9185633631	1.7472645407
H23	2.7103859126	1.9237487666	1.2846685743
C24	2.5560984931	0.2267600654	-0.8721019139
H25	2.4343044337	0.9820082839	-1.6496665547
H26	3.5681719695	0.3040784385	-0.4729123532
H27	2.4291032190	-0.7606474124	-1.3238888956

Zero-point correction =	0.229342 (Hartree/Particle)
Thermal correction to Energy =	0.241006
Thermal correction to Enthalpy =	0.241950
Thermal correction to Gibbs Free Energy =	0.192443
Sum of electronic and zero-point Energies =	–594.311156
Sum of electronic and thermal Energies =	–594.299492
Sum of electronic and thermal Enthalpies =	–594.298548
Sum of electronic and thermal Free Energies =	–594.348055

6b_eq

Atom	X	Y	Z
C1	-0.2608052919	1.0213456904	-1.4225500310
C2	-1.7871631051	0.9962275516	-1.3276666580
C3	-2.0242453754	1.0351967108	0.1872570910
C4	-0.8996048405	0.1326060263	0.7337562740
H5	-0.1836369914	-1.5768179484	-0.4857147364
H6	0.1177070659	0.6106558699	-2.3589359143
H7	0.1018105229	2.0518904404	-1.3290859007
H8	-2.2461009247	1.8332597776	-1.8549923090
H9	-2.1817087136	0.0696657724	-1.7555725005
H10	-1.8785725983	2.0500107754	0.5653743982
H11	-3.0143198036	0.6970051912	0.4931125567
H12	-0.5692875304	0.4490818048	1.7225826512
N13	0.1865414414	0.1875833991	-0.2756571013
C14	-1.3705642127	-1.3209043281	0.8906618703
O15	-2.1903171150	-1.6753473824	1.7100464395
O16	-0.8061247925	-2.1664887088	0.0269190724
H17	1.8898329401	-1.4018251731	0.8501400974
C18	1.5520402004	0.4415116402	0.2520323040
O19	1.8022327142	-0.5354952959	1.2670314038
C20	1.6997271603	1.7958614273	0.9513163871
H21	1.4908551140	2.6149754372	0.2620491100
H22	1.0246693457	1.8742545758	1.8051341596
H23	2.7222942507	1.9061662842	1.3157724709
C24	2.5623679489	0.2927459223	-0.8866791455
H25	2.4505037151	1.0833548720	-1.6304138273
H26	3.5715586671	0.3487023032	-0.4757541811
H27	2.4335102083	-0.6720226354	-1.3847639811

Zero-point correction =	0.232629 (Hartree/Particle)
Thermal correction to Energy =	0.244708
Thermal correction to Enthalpy =	0.245652
Thermal correction to Gibbs Free Energy =	0.195050
Sum of electronic and zero-point Energies =	–594.313014
Sum of electronic and thermal Energies =	–594.300935
Sum of electronic and thermal Enthalpies =	–594.299990
Sum of electronic and thermal Free Energies =	–594.350592

Data pertaining to 3-MCs

4A_inp-1

Atom	X	Y	Z
C1	-0.27077	-1.78594	-1.73105
C2	-1.34838	-2.41046	-0.83594
C3	-1.67841	-1.26699	0.13731
C4	-1.50108	0.00752	-0.73527
H5	-1.23821	-0.2698	-2.76472
H6	0.69742	-1.81919	-1.22405
H7	-0.1701	-2.26856	-2.7044
H8	-2.22687	-2.67275	-1.43281
H9	-1.00475	-3.31066	-0.32196
H10	-2.68227	-1.33022	0.5572
H11	-0.96279	-1.25922	0.96166
H12	-2.46979	0.40375	-1.05174
N13	-0.68709	-0.37367	-1.90997
C14	-0.79861	1.14059	0.01603
O15	-1.20633	1.63822	1.04489
O16	0.32965	1.53167	-0.57739
H17	0.36638	0.92566	-1.73105
C18	2.22388	-0.31814	1.15325
O19	1.5818	-1.35439	1.20736
C20	3.17096	-0.0324	0.01293
H21	3.03964	-0.76076	-0.78669
H22	3.01404	0.97998	-0.36614
H23	4.19958	-0.08441	0.38552
C24	2.10221	0.74596	2.21581
H25	3.08369	1.14076	2.49018
H26	1.51963	1.5734	1.79867
	1.58916	0.35464	3.09372
S28	-3.7352	-0.35368	-4.65722
C29	-4.36649	-1.40493	-3.30614
H30	-4.16543	-0.92569	-2.34776
H31	-5.43754	-1.54942	-3.45335
H32	-3.84691	-2.35934	-3.37818
C33	-4.63693	1.16965	-4.21975
H34	-4.33199	1.93466	-4.9327
H35	-5.70749	0.97996	-4.30828
H36	-4.37039	1.4617	-3.20347
O37	-2.25435	-0.07826	-4.33818

Zero-point correction=	0.309247 (Hartree/Particle)
Thermal correction to Energy=	0.331115
Thermal correction to Enthalpy=	0.332059
Thermal correction to Gibbs Free Energy=	0.253265
Sum of electronic and zero-point Energies=	–1147.536703
Sum of electronic and thermal Energies=	–1147.514835
Sum of electronic and thermal Enthalpies=	–1147.513891
Sum of electronic and thermal Free Energies=	–1147.592685

4A_LM-1

Atom	X	Y	Z
C1	1.84745	0.38565	1.60019
C2	2.69765	1.60966	1.25826
C3	1.63510	2.66761	0.92111
C4	0.51912	1.84654	0.22680
H5	-0.09611	-0.03338	0.88515
H6	2.38993	-0.55719	1.53015
H7	1.44483	0.47263	2.61762
H8	3.35116	1.91202	2.07763
H9	3.32190	1.39878	0.38421
H10	1.23759	3.10597	1.83921
H11	2.00144	3.47989	0.29298
H12	-0.47028	2.19376	0.53489
N13	0.76514	0.43455	0.59242
C14	0.56737	1.96828	-1.30389
O15	0.34734	2.99391	-1.91370
O16	0.87661	0.81753	-1.89825
H17	0.98653	0.20828	-1.09584
C18	1.58371	-2.71561	-0.14921
O19	1.62110	-3.01012	1.03374
C20	0.27525	-2.68307	-0.90387
H21	-0.52793	-2.37797	-0.23350
H22	0.31507	-2.02786	-1.77566
H23	0.07106	-3.69763	-1.26472
C24	2.83742	-2.38760	-0.92278
H25	2.86403	-2.94969	-1.86073
H26	2.82558	-1.32603	-1.19176
H27	3.72536	-2.59842	-0.32799
S28	-3.17493	-0.61899	0.50595
C29	-3.58083	1.15234	0.66151
H30	-2.77927	1.74948	0.22666
H31	-4.52599	1.33589	0.14876
H32	-3.68531	1.36077	1.72547
C33	-2.87133	-0.63770	-1.29392
H34	-2.58418	-1.65333	-1.56104
H35	-3.79704	-0.36533	-1.80250
H36	-2.07099	0.06321	-1.53153
O37	-1.80401	-0.81346	1.17967

Zero-point correction=	0.309232 (Hartree/Particle)
Thermal correction to Energy=	0.331000
Thermal correction to Enthalpy=	0.331944
Thermal correction to Gibbs Free Energy=	0.253731
Sum of electronic and zero-point Energies=	–1147.537023
Sum of electronic and thermal Energies=	–1147.515254
Sum of electronic and thermal Enthalpies=	–1147.514310
Sum of electronic and thermal Free Energies=	–1147.592523

4A_LM-2

Atom	X	Y	Z
C1	1.90654	0.80786	-1.67917
C2	3.30525	0.25076	-1.40287
C3	3.01068	-1.20473	-1.01246
C4	1.69347	-1.08705	-0.21081
H5	0.10342	0.01102	-0.95579
H6	1.86046	1.89506	-1.60191
H7	1.57541	0.52284	-2.68597
H8	3.96963	0.33628	-2.26384
H9	3.76427	0.78550	-0.56518
H10	2.83314	-1.80584	-1.90750
H11	3.80488	-1.68105	-0.43730
H12	1.04618	-1.95100	-0.38565
N13	1.06028	0.17584	-0.64029
C14	1.94531	-1.03888	1.30382
O15	2.45141	-1.94696	1.93181
O16	1.54810	0.09411	1.87578
H17	1.16709	0.62431	1.11491
C18	-1.00585	2.69772	0.51744
O19	-0.78751	2.09977	1.55901
C20	0.01778	3.62274	-0.09237
H21	0.99688	3.46645	0.35885
H22	0.06795	3.48850	-1.17534
H23	-0.30152	4.65569	0.08585
C24	-2.30469	2.53858	-0.23017
H25	-2.63064	3.48344	-0.67053
H26	-2.12919	1.82845	-1.04676
H27	-3.07723	2.13386	0.42352
S28	-2.68629	-1.11757	-0.33837
C29	-2.81334	-2.91034	-0.64068
H30	-1.81143	-3.34124	-0.63498
H31	-3.43796	-3.35137	0.13734
H32	-3.28208	-3.03764	-1.61566
C33	-1.82334	-1.19708	1.26606
H34	-1.54124	-0.17667	1.52485
H35	-2.51552	-1.59960	2.00690
H36	-0.94508	-1.83601	1.17272
O37	-1.65667	-0.58878	-1.35683

Zero-point correction=	0.309732 (Hartree/Particle)
Thermal correction to Energy=	0.331197
Thermal correction to Enthalpy=	0.332141
Thermal correction to Gibbs Free Energy=	0.256013
Sum of electronic and zero-point Energies=	–1147.538803
Sum of electronic and thermal Energies=	–1147.517337
Sum of electronic and thermal Enthalpies=	–1147.516393
Sum of electronic and thermal Free Energies=	–1147.592521

4A_LM-3

Atom	X	Y	Z
C1	1.10226	-0.00349	-1.01483
C2	2.46431	-0.70368	-1.03161
C3	2.41761	-1.55980	0.24321
C4	1.66477	-0.64855	1.23970
H5	-0.13475	0.22542	0.65742
H6	1.09310	0.92622	-1.58688
H7	0.32805	-0.66315	-1.42582
H8	2.62135	-1.29328	-1.93583
H9	3.26959	0.03476	-0.96518
H10	1.82854	-2.46365	0.06898
H11	3.39802	-1.86088	0.61290
H12	1.05182	-1.23000	1.93324
N13	0.85780	0.27436	0.41953
C14	2.63596	0.17239	2.10437
O15	3.40865	-0.31602	2.90357
O16	2.55350	1.48299	1.88913
H17	1.83149	1.55115	1.19287
C18	-0.16415	3.26648	0.21313
O19	0.97485	3.60602	-0.06762
C20	-1.16327	2.87193	-0.84574
H21	-0.70258	2.88050	-1.83295
H22	-1.56731	1.88251	-0.61371
H23	-2.00590	3.57115	-0.82670
C24	-0.65336	3.22809	1.64095
H25	-1.44336	3.97575	1.76915
H26	-1.09797	2.25271	1.85407
H27	0.16233	3.43871	2.33186
S28	-2.89707	-1.06982	0.95730
C29	-2.22595	-2.14365	-0.35650
H30	-1.17797	-2.36000	-0.14818
H31	-2.81630	-3.06034	-0.38964
H32	-2.32982	-1.59735	-1.29315
C33	-2.42825	-2.10554	2.38234
H34	-2.73107	-1.56805	3.27999
H35	-2.96028	-3.05538	2.31534
H36	-1.34826	-2.25618	2.36896
O37	-1.97740	0.16504	1.01233

Zero-point correction=	0.309537 (Hartree/Particle)
Thermal correction to Energy=	0.331147
Thermal correction to Enthalpy=	0.332091
Thermal correction to Gibbs Free Energy=	0.254836
Sum of electronic and zero-point Energies=	–1147.539532
Sum of electronic and thermal Energies	–1147.517922
Sum of electronic and thermal Enthalpies=	–1147.516978
Sum of electronic and thermal Free Energies=	–1147.594233

4A_GMS

Atom	X	Y	Z
C1	-1.5730555951	-2.0617530106	1.0844074249
C2	-2.7323730260	-2.2802811089	0.1059728514
C3	-2.3164806578	-1.4302581202	-1.1037891093
C4	-1.6661149450	-0.1976995567	-0.4448948324
H5	-0.1637807932	-0.5259396441	0.9594234732
H6	-1.8558333572	-2.2330990969	2.1249901679
H7	-0.7413167040	-2.7355054766	0.8444319623
H8	-2.8792464753	-3.3329704170	-0.1393404173
H9	-3.6655661460	-1.8999517990	0.5336682649
H10	-1.5684241260	-1.9600854394	-1.6994382920
H11	-3.1421550148	-1.1610515052	-1.7628008742
H12	-0.8638009587	0.2291581207	-1.0492739705
N13	-1.1762819740	-0.6454714362	0.8782011431
C14	-2.6738021053	0.9434113501	-0.2322984001
O15	-3.2719451558	1.4994021787	-1.1304087047
O16	-2.8195801686	1.2733042289	1.0493236647
H17	-2.1956741891	0.6187369928	1.5021290251
C18	1.2280891891	2.4388546489	-0.0957433584
O19	0.6566427911	2.1383023906	-1.1323870103
C20	0.4761623388	2.6663897142	1.1903770226
H21	-0.5933547517	2.7548604854	1.0066075310
H22	0.6644060460	1.8006993091	1.8326562159
H23	0.8492391112	3.5518461492	1.7111250571
C24	2.7270254156	2.6015777411	-0.0354388451
H25	2.9626822979	3.6626673805	0.0991446617
H26	3.1281137152	2.0652455031	0.8270968238
H27	3.1920239628	2.2450527401	-0.9541826025
S28	2.7064576826	-0.9788290882	-0.0299266417
C29	2.7444119928	-2.7687684100	0.3123174289
H30	1.7219947806	-3.1472855999	0.3338677877
H31	3.3317369206	-3.2605570519	-0.4642771678
H32	3.2225476968	-2.8977355312	1.2825116641
C33	1.8268701045	-1.0455717109	-1.6267607235
H34	1.5971423722	-0.0157020399	-1.8971981544
H35	2.4892931394	-1.4975512237	-2.3660661779
H36	0.9137745799	-1.6298966750	-1.5139535127
O37	1.7162380066	-0.3702299921	0.9810116246

Zero-point correction=	0.309634 (Hartree/Particle)
Thermal correction to Energy=	0.331102
Thermal correction to Enthalpy=	0.332046
Thermal correction to Gibbs Free Energy=	0.256055
Sum of electronic and zero-point Energies=	–1147.540681
Sum of electronic and thermal Energies=	–1147.519213
Sum of electronic and thermal Enthalpies=	–1147.518269
Sum of electronic and thermal Free Energies=	–1147.594260

5A_TS

Atom	X	Y	Z
C1	1.07268	0.23314	-0.98043
C2	2.04672	-0.93550	-0.69372
C3	1.81017	-1.26882	0.78917
C4	1.42844	0.10167	1.38810
H5	-0.38592	0.29634	0.50321
H6	1.57374	1.07633	-1.46070
H7	0.23062	-0.06498	-1.60463
H8	1.86419	-1.79020	-1.34582
H9	3.08001	-0.61539	-0.84909
H10	0.96226	-1.94809	0.90188
H11	2.67150	-1.71336	1.28528
H12	0.85463	0.00136	2.31038
N13	0.55338	0.68535	0.33993
C14	2.71046	0.87196	1.77256
O15	3.45474	0.35451	2.58995
O16	3.00434	2.03144	1.22657
H17	2.26322	2.51987	0.65827
C18	0.15875	2.65031	0.30573
O19	1.25546	3.17577	-0.08763
C20	-0.99196	2.63387	-0.68162
H21	-0.63278	2.37271	-1.67726
H22	-1.78659	1.95369	-0.37451
H23	-1.39636	3.65071	-0.72230
C24	-0.25033	2.80180	1.76181
H25	-0.65050	3.81387	1.88305
H26	-1.02550	2.08671	2.03962
H27	0.60738	2.70123	2.42733
S28	-2.91309	-1.39448	0.87631
C29	-2.37075	-2.22573	-0.65382
H30	-1.29499	-2.39690	-0.61640
H31	-2.91342	-3.16767	-0.74490
H32	-2.62832	-1.56351	-1.47934
C33	-2.20943	-2.57868	2.06931
H34	-2.41905	-2.18893	3.06447
H35	-2.69800	-3.54436	1.93304
H36	-1.13445	-2.65395	1.90450
O37	-2.06226	-0.11471	0.99773

Zero-point correction=	0.310786 (Hartree/Particle)
Thermal correction to Energy=	0.329901
Thermal correction to Enthalpy=	0.330846
Thermal correction to Gibbs Free Energy=	0.262461
Sum of electronic and zero-point Energies=	–1147.525664
Sum of electronic and thermal Energies=	–1147.506549
Sum of electronic and thermal Enthalpies=	–1147.505605
Sum of electronic and thermal Free Energies=	–1147.573989

5A_TS-1

Atom	X	Y	Z
C1	1.55009	-0.61757	-1.80702
C2	1.41179	-2.14894	-1.62180
C3	0.76510	-2.32501	-0.22299
C4	0.88552	-0.95108	0.44744
H5	-0.24236	-0.06215	-0.94799
H6	2.58859	-0.30508	-1.69749
H7	1.18040	-0.25102	-2.76384
H8	0.78597	-2.58739	-2.40002
H9	2.39128	-2.62567	-1.67422
H10	-0.29619	-2.55576	-0.32288
H11	1.24225	-3.10331	0.36936
H12	0.06362	-0.74969	1.13227
N13	0.75824	-0.00425	-0.70626
C14	2.19243	-0.76581	1.25233
O15	3.04284	-1.63638	1.30910
O16	2.30281	0.36241	1.92397
H17	1.56269	1.06827	1.63060
C18	0.89989	1.85913	-0.27321
O19	0.61367	1.89970	0.98666
C20	2.33014	2.18183	-0.68817
H21	3.06016	1.61100	-0.11571
H22	2.49697	2.02810	-1.75447
H23	2.48614	3.24247	-0.46951
C24	-0.14246	2.43145	-1.21969
H25	-0.06612	3.52181	-1.17169
H26	0.02398	2.12386	-2.25353
H27	-1.14666	2.14652	-0.91074
S28	-3.12531	0.22077	-0.09914
C29	-4.39273	-1.03301	0.27078
H30	-3.90733	-1.89445	0.73084
H31	-5.13214	-0.59094	0.94010
H32	-4.85761	-1.30943	-0.67454
C33	-2.49274	0.45303	1.59411
H34	-1.60424	1.08284	1.51669
H35	-3.26472	0.94956	2.18367
H36	-2.24432	-0.52022	2.01989
O37	-2.01474	-0.52751	-0.86868

Zero-point correction=	0.310951 (Hartree/Particle)
Thermal correction to Energy=	0.330107
Thermal correction to Enthalpy=	0.331051
Thermal correction to Gibbs Free Energy=	0.262038
Sum of electronic and zero-point Energies=	–1147.522468
Sum of electronic and thermal Energies=	–1147.503312
Sum of electronic and thermal Enthalpies=	–1147.502368
Sum of electronic and thermal Free Energies=	–1147.571381

5A_eq

Atom	X	Y	Z
C1	0.89099	-0.22200	-1.55635
C2	1.79950	-1.36382	-1.06599
C3	1.52664	-1.45515	0.44410
C4	1.28900	0.00552	0.84925
H5	-0.52126	0.02334	-0.05005
H6	1.41389	0.51329	-2.16055
H7	0.02107	-0.57725	-2.10529
H8	1.58650	-2.29803	-1.58534
H9	2.84584	-1.10949	-1.24444
H10	0.62473	-2.03978	0.63981
H11	2.34820	-1.88922	1.00998
H12	0.70302	0.08863	1.76235
N13	0.39388	0.46783	-0.29978
C14	2.63698	0.74708	1.07714
O15	3.26601	0.32862	2.06533
O16	2.99642	1.66157	0.28054
H17	1.91009	2.40289	-0.62498
C18	0.03707	1.97841	-0.47665
O19	1.07617	2.63367	-1.12551
C20	-1.19741	2.04461	-1.37185
H21	-0.98844	1.61913	-2.35415
H22	-2.03882	1.52137	-0.91712
H23	-1.46076	3.09446	-1.50580
C24	-0.24933	2.54799	0.91372
H25	-0.61650	3.56784	0.79190
H26	-1.01152	1.95990	1.42923
H27	0.65527	2.58439	1.52127
S28	-3.01424	-1.56969	0.24840
C29	-2.67441	-2.03303	-1.48077
H30	-1.64719	-2.38871	-1.56523
H31	-3.38105	-2.81078	-1.77288
H32	-2.83125	-1.14071	-2.08519
C33	-2.50143	-3.12870	1.03660
H34	-2.57366	-2.97713	2.11265
H35	-3.18704	-3.91645	0.72146
H36	-1.47664	-3.35842	0.74508
O37	-1.93545	-0.53094	0.63274

Zero-point correction=	0.315316 (Hartree/Particle)
Thermal correction to Energy=	0.334225
Thermal correction to Enthalpy=	0.335170
Thermal correction to Gibbs Free Energy=	0.267392
Sum of electronic and zero-point Energies=	–1147.538477
Sum of electronic and thermal Energies=	–1147.519567
Sum of electronic and thermal Enthalpies=	–1147.518623
Sum of electronic and thermal Free Energies=	–1147.586400

5A_pre-org

Atom	X	Y	Z
C1	1.65157	0.41531	-1.75691
C2	3.07014	0.48379	-1.19813
C3	2.95171	-0.11557	0.22466
C4	1.44323	-0.32131	0.46607
H5	-0.17210	0.15670	-0.77577
H6	1.42066	1.14229	-2.52747
H7	1.42290	-0.57736	-2.14837
H8	3.76297	-0.06618	-1.83522
H9	3.40334	1.52049	-1.14570
H10	3.46307	-1.07469	0.31449
H11	3.36593	0.55995	0.97082
H12	1.14500	-1.31531	0.13596
H13	0.75395	0.59623	-0.55586
C14	0.99750	-0.19905	1.95711
O15	0.35320	-1.16393	2.41095
O16	1.35698	0.83784	2.58612
H17	1.55498	2.04599	1.48622
C18	0.45225	2.07659	-0.11303
O19	1.52224	2.55893	0.63139
C20	0.30295	2.96383	-1.34301
H21	1.26440	3.13281	-1.82772
H22	-0.40607	2.54643	-2.06001
H23	-0.07760	3.92953	-1.00784
C24	-0.87165	2.03383	0.66293
H25	-1.06197	3.03433	1.05327
H26	-1.69152	1.75257	0.00017
H27	-0.84402	1.34165	1.50156
C28	-3.83921	-2.03928	-1.23354
H29	-3.35962	-2.73645	-1.92100
H30	-4.56081	-2.54782	-0.59318
H31	-4.32258	-1.22828	-1.77642
C32	-1.85322	-2.80844	0.52186
H33	-1.01593	-2.49241	1.14630
H34	-2.61813	-3.29729	1.12731
H35	-1.52500	-3.45200	-0.29550
O36	-1.49860	-0.75741	-1.17492
S37	-2.56237	-1.28933	-0.17917

Zero-point correction=	0.315264 (Hartree/Particle)
Thermal correction to Energy=	0.334190
Thermal correction to Enthalpy=	0.335134
Thermal correction to Gibbs Free Energy=	0.267268
Sum of electronic and zero-point Energies=	–1147.531521
Sum of electronic and thermal Energies=	–1147.512595
Sum of electronic and thermal Enthalpies=	–1147.511651
Sum of electronic and thermal Free Energies=	–1147.579517

6A_TS

Atom	X	Y	Z
C1	-0.38104	0.31631	-1.86408
C2	0.83867	-0.29283	-2.64219
C3	1.82895	-0.82918	-1.55058
C4	0.91103	-0.80667	-0.34610
H5	-0.36896	0.11462	0.71704
H6	-0.72662	1.26820	-2.25910
H7	-1.21657	-0.38165	-1.84780
H8	0.49166	-1.10616	-3.28089
H9	1.31682	0.44668	-3.28389
H10	2.17869	-1.83668	-1.77475
H11	2.70013	-0.18665	-1.42612
H12	0.15067	-1.58007	-0.54319
N13	0.10084	0.45103	-0.45593
C14	1.10641	-1.02004	1.14718
O15	1.97702	-1.68517	1.68156
O16	0.06389	-0.46729	1.74421
H17	1.29920	1.46182	1.71324
C18	0.77973	1.81139	-0.14668
O19	1.74389	1.62987	0.87202
C20	1.54669	2.44995	-1.30543
H21	2.40397	1.84930	-1.60042
H22	0.91434	2.63105	-2.17252
H23	1.91719	3.41354	-0.95304
C24	-0.35677	2.72259	0.32199
H25	0.04185	3.70877	0.56426
H26	-1.11481	2.83397	-0.45554
H27	-0.83786	2.30830	1.21171
S28	-2.72084	-2.92981	0.21818
C29	-1.76361	-3.47248	1.67490
H30	-1.05973	-2.68681	1.95095
H31	-2.46164	-3.68052	2.48719
H32	-1.24238	-4.38487	1.38739
C33	-3.32397	-1.35231	0.91119
H34	-3.85534	-0.83645	0.11239
H35	-4.00516	-1.57373	1.73413
H36	-2.47104	-0.76813	1.25531
O37	-1.69042	-2.55862	-0.86301

Zero-point correction=	0.309900 (Hartree/Particle)
Thermal correction to Energy=	0.328863
Thermal correction to Enthalpy=	0.329807
Thermal correction to Gibbs Free Energy=	0.261574
Sum of electronic and zero-point Energies=	–1147.488638
Sum of electronic and thermal Energies=	–1147.469676
Sum of electronic and thermal Enthalpies=	–1147.468731
Sum of electronic and thermal Free Energies=	–1147.536964

6A_eq

Atom	X	Y	Z
C1	0.86269	0.55144	-1.87803
C2	2.35100	0.12516	-1.74814
C3	2.54000	-0.15573	-0.23747
C4	1.12121	0.02542	0.34332
H5	-0.72993	-0.44874	1.87319
H6	0.70311	1.32602	-2.62339
H7	0.25894	-0.31269	-2.17377
H8	2.55743	-0.75402	-2.36164
H9	3.01890	0.92041	-2.08415
H10	2.91374	-1.16185	-0.03678
H11	3.23173	0.54962	0.22096
H12	0.58391	-0.91947	0.21232
N13	0.40341	0.97998	-0.54075
C14	1.07620	0.31003	1.84862
O15	2.02155	0.74885	2.47184
O16	-0.04152	-0.04586	2.48130
H17	-1.03348	2.15317	0.99488
C18	0.45833	2.42677	-0.23103
O19	-0.17380	2.59129	1.04618
C20	1.85508	3.03951	-0.06942
H21	2.38661	2.57123	0.75742
H22	2.43115	2.91438	-0.98731
H23	1.76551	4.10859	0.13644
C24	-0.34858	3.20379	-1.28129
H25	-0.51755	4.21255	-0.90114
H26	0.17496	3.28795	-2.23466
H27	-1.31450	2.72172	-1.45056
S28	-3.97898	-2.60849	0.31000
C29	-4.13632	-1.91966	-0.52045
H30	-4.24009	-3.63065	0.03320
H31	-4.54740	-2.29823	1.18547
H32	-1.51424	-3.00700	-0.84222
C33	-0.43064	-2.99471	-0.73360
H34	-1.85037	-4.00993	-1.10865
H35	-1.83779	-2.27037	-1.57825
H36	-2.22262	-2.56946	0.77696
O37	-1.90193	-1.06635	0.97013

Zero-point correction=	0.312731 (Hartree/Particle)
Thermal correction to Energy=	0.332228
Thermal correction to Enthalpy=	0.333172
Thermal correction to Gibbs Free Energy=	0.263394
Sum of electronic and zero-point Energies=	–1147.517269
Sum of electronic and thermal Energies=	–1147.497771
Sum of electronic and thermal Enthalpies=	–1147.496827
Sum of electronic and thermal Free Energies=	–1147.566605

4B_inp

Atom	X	Y	Z
C1	-2.72417	0.87076	-1.98040
C2	-2.36016	1.72826	-0.75467
C3	-1.19393	0.95218	-0.10520
C4	-1.31449	-0.49503	-0.72413
H5	-3.32179	-0.77840	-0.96782
H6	-3.75065	1.01000	-2.32103
H7	-2.05134	1.09237	-2.81704
H8	-2.08657	2.75421	-1.01122
H9	-3.21565	1.76615	-0.07478
H10	-0.22786	1.38497	-0.36778
H11	-1.26472	0.94219	0.98409
H12	-0.44015	-0.67116	-1.35782
N13	-2.52388	-0.52354	-1.55181
C14	-1.33791	-1.56996	0.34825
O15	-2.34603	-2.14318	0.70497
O16	-0.16501	-1.84508	0.92951
H17	0.58694	-1.33309	0.53078
C18	2.51316	0.39655	0.37816
O19	1.90063	-0.52561	-0.15208
C20	2.13040	0.92512	1.73312
H21	1.70863	1.92817	1.60904
H22	1.39577	0.28303	2.21640
H23	3.01624	1.02958	2.36428
C24	3.67621	1.04633	-0.31544
H25	3.57386	2.13443	-0.29029
H26	4.59309	0.80173	0.23134
H27	3.75908	0.69409	-1.34234
S28	-5.97773	-2.00033	-1.65790
C29	-5.22360	-1.76997	-3.30479
H30	-5.44522	-2.64673	-3.91479
H31	-5.68551	-0.88489	-3.74121
H32	-4.15010	-1.62470	-3.17852
C33	-4.98249	-3.44105	-1.14029
H34	-5.31738	-3.71474	-0.14041
H35	-5.16686	-4.26109	-1.83554
H36	-3.93134	-3.15345	-1.12064
O37	-5.49798	-0.81732	-0.79776

Zero-point correction=	0.309466 (Hartree/Particle)
Thermal correction to Energy=	0.331329
Thermal correction to Enthalpy=	0.332273
Thermal correction to Gibbs Free Energy=	0.253610
Sum of electronic and zero-point Energies=	–1147.531381
Sum of electronic and thermal Energies=	–1147.509518
Sum of electronic and thermal Enthalpies=	–1147.508574
Sum of electronic and thermal Free Energies=	–1147.587237

4B_LM-1

Atom	X	Y	Z
C1	0.05382	1.90358	-1.38113
C2	0.03264	1.71113	-2.92604
C3	-0.26984	0.20228	-3.12702
C4	-0.65127	-0.27984	-1.71634
H5	1.09655	0.24935	-0.77232
H6	0.89293	2.50730	-1.03139
H7	-0.86929	2.38860	-1.04647
H8	-0.72773	2.34330	-3.38954
H9	0.99425	1.97665	-3.36972
H10	-1.06387	0.01749	-3.85330
H11	0.62054	-0.33666	-3.45582
H12	-1.71476	-0.08860	-1.53289
N13	0.12053	0.56021	-0.77756
C14	-0.36877	-1.75025	-1.41979
O15	0.47366	-2.40389	-1.99673
O16	-1.07912	-2.29425	-0.42673
H17	-1.76495	-1.67633	-0.06212
C18	-3.22002	0.04681	1.35944
O19	-3.13120	-0.88467	0.56400
C20	-4.56008	0.49608	1.86735
H21	-4.76108	1.50201	1.48353
H22	-5.34792	-0.18404	1.54717
H23	-4.53998	0.57456	2.95807
C24	-1.99928	0.76246	1.86591
H25	-1.19579	0.71195	1.12706
H26	-2.22192	1.79678	2.13295
H27	-1.67180	0.25124	2.77912
S28	2.87183	-0.28723	1.48011
C29	2.08198	1.25686	2.05234
H30	1.91929	1.18726	3.12867
H31	2.77303	2.06872	1.82890
H32	1.14340	1.38498	1.51372
C33	1.49446	-1.41451	1.88587
H34	1.77988	-2.40478	1.53336
H35	1.36118	-1.42361	2.968502
H36	0.595556	-1.0691	1.377331
O37	2.914287	-0.20071	-0.05824

Zero-point correction=	0.309697 (Hartree/Particle)
Thermal correction to Energy=	0.331437
Thermal correction to Enthalpy=	0.332382
Thermal correction to Gibbs Free Energy=	0.254900
Sum of electronic and zero-point Energies=	–1147.531731
Sum of electronic and thermal Energies=	–1147.509990
Sum of electronic and thermal Enthalpies=	–1147.509046
Sum of electronic and thermal Free Energies=	–1147.586527

4B_LM-2

Atom	X	Y	Z
C1	-0.85602	1.84018	-1.69646
C2	-0.09542	1.44867	-2.97464
C3	-0.39147	-0.06232	-3.11382
C4	-0.86584	-0.49844	-1.69976
H5	0.18058	0.69559	-0.36931
H6	-0.46061	2.72867	-1.20080
H7	-1.91443	2.01894	-1.92024
H8	-0.40470	2.02384	-3.85013
H9	0.97496	1.61214	-2.82259
H10	-1.18263	-0.24814	-3.84319
H11	0.48784	-0.62695	-3.42312
H12	-1.92534	-0.77869	-1.73367
N13	-0.74714	0.67618	-0.80332
C14	-0.11267	-1.68611	-1.09974
O15	0.91381	-2.14564	-1.55253
O16	-0.64423	-2.20886	0.01237
H17	-1.49308	-1.76171	0.27222
C18	-2.63102	0.26121	1.01957
O19	-2.87826	-0.87441	0.60678
C20	-3.47235	1.43071	0.58921
H21	-2.87751	2.34096	0.51431
H22	-3.96085	1.21639	-0.36075
H23	-4.24232	1.59565	1.35211
C24	-1.63186	0.49411	2.12273
H25	-1.04731	1.39525	1.94250
H26	-2.19067	0.63385	3.05595
H27	-0.97502	-0.36701	2.23701
S28	2.90071	0.35619	1.27735
C29	2.39795	0.92617	2.93566
H30	2.97473	0.37775	3.68171
H31	2.62881	1.98926	2.99121
H32	1.32827	0.75800	3.06285
C33	2.34080	-1.37105	1.43400
H34	2.48744	-1.84341	0.46391
H35	2.94759	-1.86136	2.19639
H36	1.28399	-1.38732	1.69787
O37	1.94271	1.03509	0.28147

Zero-point correction=	0.310372 (Hartree/Particle)
Thermal correction to Energy=	0.331455
Thermal correction to Enthalpy=	0.332399
Thermal correction to Gibbs Free Energy=	0.258740
Sum of electronic and zero-point Energies=	–1147.531703
Sum of electronic and thermal Energies=	–1147.510620
Sum of electronic and thermal Enthalpies=	–1147.509676
Sum of electronic and thermal Free Energies=	–1147.583335

4B_LM-3

Atom	X	Y	Z
C1	-0.81228	1.94107	-1.51629
C2	-0.18553	1.68373	-2.91137
C3	-0.16506	0.13785	-3.04559
C4	-0.77044	-0.36058	-1.70986
H5	0.38766	0.70244	-0.42911
H6	-0.38542	2.80340	-1.00111
H7	-1.89076	2.10973	-1.61361
H8	-0.75723	2.16501	-3.70774
H9	0.83073	2.08211	-2.94812
H10	-0.73812	-0.22082	-3.90203
H11	0.85332	-0.23832	-3.15033
H12	-1.85125	-0.51531	-1.84335
N13	-0.59354	0.72009	-0.72502
C14	-0.23098	-1.69940	-1.22897
O15	0.35867	-2.47756	-1.94687
O16	-0.47576	-2.03600	0.04630
H17	-0.95929	-1.35203	0.56352
C18	-2.25853	0.53193	1.66868
O19	-1.62208	-0.47242	1.97105
C20	-3.42002	0.47169	0.71589
H21	-3.40352	1.31868	0.02855
H22	-3.42274	-0.46725	0.16425
H23	-4.34437	0.54376	1.30058
C24	-1.94051	1.87038	2.27435
H25	-1.50966	2.49785	1.48771
H26	-2.85019	2.36574	2.62333
H27	-1.22504	1.76773	3.08874
S28	2.90333	0.00214	1.18893
C29	1.68907	0.45773	2.47157
H30	2.06790	0.12513	3.43919
H31	1.61010	1.54432	2.45597
H32	0.72648	-0.00102	2.24465
C33	2.74364	-1.80875	1.33226
H34	3.40498	-2.24481	0.58432
H35	3.06098	-2.10799	2.33225
H36	1.70753	-2.08670	1.13967
O37	2.25739	0.37984	-0.15928

Zero-point correction=	0.309541 (Hartree/Particle)
Thermal correction to Energy=	0.331144
Thermal correction to Enthalpy=	0.332088
Thermal correction to Gibbs Free Energy=	0.255922
Sum of electronic and zero-point Energies=	–1147.533389
Sum of electronic and thermal Energies=	–1147.511786
Sum of electronic and thermal Enthalpies=	–1147.510842
Sum of electronic and thermal Free Energies=	–1147.587008

4B_GMS

Atom	X	Y	Z
C1	-0.97824	1.13659	-1.82654
C2	0.21969	0.57721	-2.61281
C3	0.28537	-0.89988	-2.16143
C4	-0.55257	-0.94829	-0.85323
H5	-0.26212	0.88010	0.07075
H6	-0.93768	2.21597	-1.66864
H7	-1.91667	0.90507	-2.34447
H8	0.10831	0.68459	-3.69395
H9	1.12894	1.10599	-2.31530
H10	-0.15305	-1.56579	-2.90740
H11	1.30883	-1.22882	-1.98248
H12	-1.46542	-1.53307	-1.01837
N13	-0.96308	0.43878	-0.53216
C14	0.15969	-1.57166	0.34844
O15	1.34547	-1.83325	0.37595
O16	-0.59711	-1.80915	1.42213
H17	-1.55333	-1.57208	1.27620
C18	-3.22825	0.12772	0.82326
O19	-3.09849	-1.09767	0.88629
C20	-2.69536	1.02858	1.90574
H21	-3.52217	1.23935	2.59521
H22	-1.89517	0.53957	2.45928
H23	-2.34487	1.97632	1.49944
C24	-4.10566	0.74959	-0.22707
H25	-4.28207	0.04710	-1.04087
H26	-5.06567	1.00802	0.23497
H27	-3.66456	1.67083	-0.60826
S28	2.45276	1.75860	1.48797
C29	2.66160	0.35976	2.63974
H30	3.72866	0.20768	2.80896
H31	2.17358	0.64541	3.57105
H32	2.19802	-0.52727	2.20790
C33	3.22824	0.99180	0.02499
H34	3.11078	1.69641	-0.79737
H35	4.28776	0.84138	0.23769
H36	2.72909	0.04709	-0.18932
O37	0.94417	1.84081	1.18686

Zero-point correction=	0.310374 (Hartree/Particle)
Thermal correction to Energy=	0.331477
Thermal correction to Enthalpy=	0.332421
Thermal correction to Gibbs Free Energy=	0.258015
Sum of electronic and zero-point Energies=	–1147.533811
Sum of electronic and thermal Energies=	–1147.512707
Sum of electronic and thermal Enthalpies=	–1147.511763
Sum of electronic and thermal Free Energies=	–1147.586170

5B_TS

Atom	X	Y	Z
C1	-1.09395	1.21968	-1.62083
C2	0.10096	0.68837	-2.41269
C3	-0.01601	-0.83354	-2.21420
C4	-0.66495	-0.99889	-0.82305
H5	-0.42894	0.76166	0.24924
H6	-1.01658	2.26619	-1.32739
H7	-2.01942	1.07480	-2.18063
H8	0.07259	0.98510	-3.46221
H9	1.02923	1.06357	-1.97562
H10	-0.66862	-1.26793	-2.97393
H11	0.94551	-1.34244	-2.25922
H12	-1.54746	-1.64291	-0.86649
N13	-1.12500	0.36655	-0.40281
C14	0.24997	-1.58977	0.26502
O15	1.39738	-1.93814	0.04748
O16	-0.28952	-1.68910	1.46280
H17	-1.28782	-1.36459	1.46687
C18	-2.72531	0.23730	0.68444
O19	-2.63431	-0.92243	1.23896
C20	-2.49191	1.45627	1.56328
H21	-3.36846	1.56901	2.20915
H22	-1.61096	1.31119	2.18898
H23	-2.37384	2.37118	0.97962
C24	-3.82551	0.38406	-0.34998
H25	-3.75468	-0.40770	-1.09832
H26	-4.77716	0.26520	0.17627
H27	-3.82577	1.35892	-0.83797
S28	2.30401	1.62103	1.55873
C29	2.49444	0.16687	2.64177
H30	3.55255	0.06218	2.88632
H31	1.92154	0.37296	3.54513
H32	2.11351	-0.71660	2.13072
C33	3.20556	0.97471	0.11085
H34	3.13023	1.72971	-0.67078
H35	4.25030	0.83670	0.39347
H36	2.75303	0.03339	-0.19989
O37	0.81481	1.67086	1.16004

Zero-point correction=	0.311476 (Hartree/Particle)
Thermal correction to Energy=	0.330283
Thermal correction to Enthalpy=	0.331227
Thermal correction to Gibbs Free Energy=	0.264328
Sum of electronic and zero-point Energies=	–1147.528905
Sum of electronic and thermal Energies=	–1147.510098
Sum of electronic and thermal Enthalpies=	–1147.509154
Sum of electronic and thermal Free Energies=	–1147.576053

5B_eq

Atom	X	Y	Z
C1	-1.10418	1.23198	-1.77974
C2	-0.12330	0.74850	-2.83896
C3	-0.39094	-0.76148	-2.87441
C4	-0.62720	-1.14215	-1.40714
H5	-0.15728	0.47251	-0.15223
H6	-0.85960	2.19444	-1.33848
H7	-2.12267	1.24140	-2.16244
H8	-0.29207	1.23908	-3.79774
H9	0.90066	0.95588	-2.51757
H10	-1.28621	-0.96961	-3.46535
H11	0.43601	-1.33901	-3.28233
H12	-1.46863	-1.82388	-1.29184
N13	-0.99572	0.17190	-0.70636
C14	0.57229	-1.81078	-0.66439
O15	1.41867	-2.40684	-1.34607
O16	0.54795	-1.69962	0.60078
H17	-0.95921	-1.26116	1.11553
C18	-2.16272	0.09054	0.30933
O19	-1.92914	-1.02974	1.12127
C20	-2.14270	1.37686	1.13639
H21	-2.91196	1.29045	1.90481
H22	-1.17231	1.50521	1.61693
H23	-2.35836	2.25800	0.52947
C24	-3.49719	-0.11428	-0.39887
H25	-3.45716	-0.95443	-1.09380
H26	-4.23664	-0.34717	0.36831
H27	-3.82822	0.77866	-0.92854
S28	2.34671	1.44982	1.17733
C29	1.85367	0.49898	2.65050
H30	2.74706	0.29990	3.24439
H31	1.16355	1.12641	3.21350
H32	1.37519	-0.42065	2.31601
C33	3.37942	0.17766	0.38185
H34	3.67150	0.57516	-0.58956
H35	4.26324	0.02361	1.00290
H36	2.79973	-0.73802	0.27601
O37	1.07255	1.57740	0.31098

Zero-point correction=	0.314879 (Hartree/Particle)
Thermal correction to Energy=	0.333770
Thermal correction to Enthalpy=	0.334714
Thermal correction to Gibbs Free Energy=	0.267560
Sum of electronic and zero-point Energies=	–1147.541380
Sum of electronic and thermal Energies=	–1147.522489
Sum of electronic and thermal Enthalpies=	–1147.521545
Sum of electronic and thermal Free Energies=	–1147.588699

5B_1

Atom	X	Y	Z
C1	-0.45738	1.58977	-1.62299
C2	0.01940	0.94057	-2.91808
C3	-0.95327	-0.23325	-3.08530
C4	-1.08982	-0.78664	-1.65898
H5	-0.01258	0.15075	-0.21091
H6	0.29439	2.16149	-1.08667
H7	-1.33308	2.21283	-1.78946
H8	-0.00642	1.64386	-3.75071
H9	1.04477	0.57750	-2.80721
H10	-1.92126	0.12609	-3.44515
H11	-0.60081	-1.00515	-3.76766
H12	-2.07387	-1.20736	-1.47254
N13	-0.86095	0.41588	-0.75443
C14	-0.02755	-1.87791	-1.32150
O15	-0.14111	-2.94206	-1.96017
O16	0.82588	-1.56962	-0.44840
H17	-0.65565	1.78710	1.31659
C18	-1.94596	0.72910	0.31005
O19	-1.55590	1.91493	0.94470
C20	-3.29633	0.98275	-0.34338
H21	-4.00551	1.23268	0.44647
H22	-3.25236	1.82316	-1.03594
H23	-3.66826	0.10353	-0.86875
C24	-1.97885	-0.44533	1.28835
H25	-1.00027	-0.58190	1.74802
H26	-2.70460	-0.21587	2.06927
H27	-2.27428	-1.37778	0.80570
S28	2.23953	0.77629	1.97997
C29	1.73692	-0.85502	2.61615
H30	2.61383	-1.32682	3.06162
H31	0.98180	-0.67979	3.38163
H32	1.34254	-1.44011	1.78541
C33	3.38158	0.20039	0.68575
H34	3.73153	1.08719	0.15879
H35	4.21983	-0.30601	1.16658
H36	2.82849	-0.46626	0.02388
O37	1.02038	1.32654	1.19974

Zero-point correction=	0.315352 (Hartree/Particle)
Thermal correction to Energy=	0.334336
Thermal correction to Enthalpy=	0.335280
Thermal correction to Gibbs Free Energy=	0.268286
Sum of electronic and zero-point Energies=	–1147.543657
Sum of electronic and thermal Energies=	–1147.524673
Sum of electronic and thermal Enthalpies=	–1147.523729
Sum of electronic and thermal Free Energies=	–1147.590723

5B_2

Atom	X	Y	Z
C1	-1.06639	0.91108	-2.33231
C2	-0.59583	-0.06417	-3.41068
C3	-0.96864	-1.43054	-2.82146
C4	-0.58408	-1.28520	-1.34762
H5	0.09719	0.44966	-0.65476
H6	-0.52763	1.85551	-2.30633
H7	-2.13057	1.11322	-2.42977
H8	-1.07656	0.14103	-4.36727
H9	0.48571	0.01082	-3.54821
H10	-2.04311	-1.60862	-2.91841
H11	-0.43953	-2.26410	-3.28050
H12	-1.16311	-1.90975	-0.67373
N13	-0.83966	0.17877	-1.02236
C14	0.92587	-1.56391	-1.07362
O15	1.31402	-2.72402	-1.29757
O16	1.59397	-0.58023	-0.64561
H17	-0.69961	0.20979	1.70118
C18	-1.86178	0.44377	0.12331
O19	-1.40986	-0.28809	1.21796
C20	-1.86543	1.94773	0.39209
H21	-2.52892	2.13898	1.23652
H22	-0.86484	2.29166	0.66010
H23	-2.23018	2.51321	-0.46581
C24	-3.23536	-0.08853	-0.26415
H25	-3.20677	-1.16500	-0.43588
H26	-3.91081	0.10342	0.56997
H27	-3.63886	0.40464	-1.14809
S28	1.85899	0.93501	2.92571
C29	2.22493	-0.82403	2.62682
H30	3.29018	-0.98170	2.80266
H31	1.63925	-1.39364	3.34741
H32	1.95292	-1.06700	1.59945
C33	2.77378	1.63052	1.51316
H34	2.57579	2.70178	1.50850
H35	3.83757	1.44831	1.67355
H36	2.42192	1.15043	0.60069
O37	0.36024	1.12471	2.58552

Zero-point correction=	0.315056 (Hartree/Particle)
Thermal correction to Energy=	0.334065
Thermal correction to Enthalpy=	0.335010
Thermal correction to Gibbs Free Energy=	0.267311
Sum of electronic and zero-point Energies=	–1147.542199
Sum of electronic and thermal Energies=	–1147.523189
Sum of electronic and thermal Enthalpies=	–1147.522245
Sum of electronic and thermal Free Energies=	–1147.589943

6B_TS

Atom	X	Y	Z
C1	-0.41123	1.50688	-1.06529
C2	0.27249	0.77192	-2.21964
C3	-0.74692	-0.31481	-2.58983
C4	-1.28804	-0.75873	-1.22424
H5	-0.27642	-0.29332	0.42488
H6	0.28115	1.99718	-0.38459
H7	-1.12933	2.23536	-1.45014
H8	0.50597	1.44213	-3.04739
H9	1.20718	0.31847	-1.87906
H10	-1.55970	0.11251	-3.18280
H11	-0.32007	-1.14892	-3.14710
H12	-2.31468	-1.11492	-1.26081
N13	-1.12594	0.42504	-0.31834
C14	-0.42290	-1.85849	-0.55842
O15	-0.33344	-2.98964	-1.01539
O16	0.17338	-1.39825	0.50376
H17	-2.11366	-0.53901	1.87941
C18	-2.33476	0.82479	0.48009
O19	-2.75860	-0.33635	1.18961
C20	-3.51472	1.22854	-0.40036
H21	-3.25940	2.07795	-1.03428
H22	-3.83766	0.40051	-1.03243
H23	-4.35056	1.51639	0.23881
C24	-1.93774	1.93653	1.44912
H25	-1.71273	2.86295	0.91808
H26	-2.77344	2.12215	2.12563
H27	-1.05233	1.64864	2.01866
S28	2.65273	0.81443	1.97895
C29	2.37191	-0.71214	2.94051
H30	3.32515	-1.22931	3.06074
H31	1.98743	-0.40707	3.91328
H32	1.64645	-1.32460	2.40566
C33	3.22006	0.01756	0.43636
H34	3.33824	0.81081	-0.30101
H35	4.18107	-0.46245	0.62675
H36	2.46755	-0.70428	0.12120
O37	1.26125	1.39492	1.67939

Zero-point correction=	0.309621 (Hartree/Particle)
Thermal correction to Energy=	0.328759
Thermal correction to Enthalpy=	0.329703
Thermal correction to Gibbs Free Energy=	0.262021
Sum of electronic and zero-point Energies	–1147.528246
Sum of electronic and thermal Energies=	–1147.509108
Sum of electronic and thermal Enthalpies=–	–1147.508164
Sum of electronic and thermal Free Energies=–	–1147.575847

6B_TS-1

Atom	X	Y	Z
C1	-0.04769	1.91159	-1.13164
C2	0.26713	1.35181	-2.51987
C3	-1.00233	0.56073	-2.86400
C4	-1.37165	-0.08980	-1.52252
H5	-0.00269	-0.18268	-0.07925
H6	0.83328	2.13240	-0.53307
H7	-0.65670	2.81420	-1.20875
H8	0.48800	2.14162	-3.23840
H9	1.13214	0.68369	-2.47455
H10	-1.80257	1.23948	-3.16991
H11	-0.86430	-0.18156	-3.65039
H12	-2.44162	-0.26176	-1.42260
N13	-0.82386	0.81921	-0.46602
C14	-0.62760	-1.43156	-1.28909
O15	-0.85316	-2.43377	-1.95108
O16	0.24418	-1.31198	-0.32769
H17	-0.15719	1.63587	1.72704
C18	-1.74669	1.25051	0.64845
O19	-0.99847	2.09101	1.50071
C20	-2.22055	0.00679	1.40996
H21	-2.80663	-0.66801	0.78300
H22	-1.36695	-0.54093	1.80945
H23	-2.84742	0.32968	2.24205
C24	-2.92955	2.07192	0.13883
H25	-3.56150	1.48693	-0.53107
H26	-3.53367	2.38440	0.99223
H27	-2.59121	2.96703	-0.38349
S28	2.30590	-0.07539	2.43741
C29	1.22103	-1.47030	2.88935
H30	1.83778	-2.24390	3.34923
H31	0.49994	-1.09013	3.61207
H32	0.72735	-1.83724	1.99006
C33	3.26177	-0.92057	1.13744
H34	3.94616	-0.18305	0.72012
H35	3.82259	-1.73731	1.59399
H36	2.56398	-1.28289	0.38281
O37	1.42054	0.93735	1.67898

Zero-point correction=	0.310072 (Hartree/Particle)
Thermal correction to Energy=	0.328754
Thermal correction to Enthalpy=	0.329699
Thermal correction to Gibbs Free Energy=	0.263446
Sum of electronic and zero-point Energies=	–1147.535622
Sum of electronic and thermal Energies=	–1147.516939
Sum of electronic and thermal Enthalpies=	–1147.515995
Sum of electronic and thermal Free Energies=	–1147.582247

6B_TS-2

Atom	X	Y	Z
C1	-1.25527	0.86650	-2.38637
C2	-0.66289	-0.05746	-3.45308
C3	-0.90762	-1.45516	-2.86679
C4	-0.62858	-1.25073	-1.37259
H5	0.33869	0.35534	-0.73684
H6	-0.82618	1.86786	-2.38932
H7	-2.33633	0.95185	-2.51591
H8	-1.13326	0.09032	-4.42554
H9	0.40930	0.12732	-3.56426
H10	-1.95044	-1.75092	-3.00737
H11	-0.27232	-2.22992	-3.29627
H12	-1.18511	-1.92530	-0.72658
N13	-0.94413	0.18844	-1.08845
C14	0.87404	-1.38137	-1.02027
O15	1.48155	-2.43939	-1.09925
O16	1.36343	-0.23212	-0.64661
H17	-0.62811	0.30037	1.59728
C18	-1.88082	0.44547	0.07243
O19	-1.34784	-0.23483	1.18544
C20	-1.92951	1.95507	0.31608
H21	-2.53181	2.14600	1.20574
H22	-0.92344	2.34236	0.48833
H23	-2.38068	2.48498	-0.52409
C24	-3.27266	-0.13545	-0.17640
H25	-3.22518	-1.21747	-0.30991
H26	-3.89690	0.07222	0.69387
H27	-3.74862	0.30774	-1.05176
S28	1.91302	0.92169	2.94189
C29	2.13009	-0.86225	2.63565
H30	3.14927	-1.13625	2.91183
H31	1.41734	-1.38061	3.27588
H32	1.93573	-1.06263	1.58314
C33	3.04936	1.53871	1.65836
H34	2.97162	2.62536	1.66686
H35	4.06368	1.23526	1.92261
H36	2.74513	1.12562	0.69743
O37	0.49027	1.26888	2.44529

Zero-point correction=	0.309846 (Hartree/Particle)
Thermal correction to Energy=	0.328654
Thermal correction to Enthalpy=	0.329598
Thermal correction to Gibbs Free Energy=	0.262280
Sum of electronic and zero-point Energies=	–1147.536777
Sum of electronic and thermal Energies=	–1147.517970
Sum of electronic and thermal Enthalpies=	–1147.517026
Sum of electronic and thermal Free Energies=	–1147.584344

6B_eq

Atom	X	Y	Z
C1	-1.33708	0.92993	-2.33358
C2	-0.65282	0.09730	-3.41878
C3	-0.85808	-1.33507	-2.91033
C4	-0.65467	-1.18178	-1.38955
H5	0.74018	0.33933	-0.47460
H6	-0.97214	1.95678	-2.28831
H7	-2.41840	0.96198	-2.51751
H8	-1.08390	0.26994	-4.40575
H9	0.41398	0.33639	-3.46856
H10	-1.88382	-1.66058	-3.10139
H11	-0.18045	-2.06745	-3.34921
H12	-1.23870	-1.90925	-0.82572
N13	-1.02721	0.21403	-1.07004
C14	0.80830	-1.43490	-1.00133
O15	1.35775	-2.50950	-1.12790
O16	1.44136	-0.36807	-0.51758
H17	-0.62536	0.33386	1.47552
C18	-1.97866	0.39578	0.06092
O19	-1.39572	-0.21280	1.20553
C20	-2.17680	1.89712	0.29961
H21	-2.76686	2.03150	1.20800
H22	-1.20979	2.38512	0.43317
H23	-2.70797	2.37297	-0.52664
C24	-3.32489	-0.30307	-0.15921
H25	-3.19778	-1.38315	-0.25090
H26	-3.97688	-0.11138	0.69494
H27	-3.81889	0.06930	-1.05838
S28	1.95425	1.11506	2.67443
C29	2.04107	-0.70311	2.79254
H30	2.95995	-0.97015	3.31610
H31	1.17488	-1.02437	3.36981
H32	2.01747	-1.11914	1.78642
C33	3.38543	1.36363	1.57435
H34	3.42847	2.42846	1.34866
H35	4.28541	1.05834	2.10996
H36	3.23796	0.77611	0.66928
O37	0.70521	1.42630	1.81646

Zero-point correction=	0.313339 (Hartree/Particle)
Thermal correction to Energy=	0.332540
Thermal correction to Enthalpy=	0.333484
Thermal correction to Gibbs Free Energy=	0.264890
Sum of electronic and zero-point Energies=	–1147.537170
Sum of electronic and thermal Energies=	–1147.517969
Sum of electronic and thermal Enthalpies=	–1147.517025
Sum of electronic and thermal Free Energies=	–1147.585618

Part B2

Data pertaining to the net atomic charges in the 3-MCs

Table B1. Net atomic charges (Q(A) in e) for: Part A - **4A** 3-MCs involving **1a** (LEC of proline), **2** (acetone) and **3** (DMSO) and Part B – **4B** 3-MCs involving **1b** (HEC of proline), **2** and **3**.

Part A: 4A 3-MCs

Inp-1		LM-1		LM-2		LM-3		GMS	
Atom	Q(A)	Atom	Q(A)	Atom	Q(A)	Atom	Q(A)	Atom	Q(A)
Atoms with largest negative net charges									
O37	-1.244	O37	-1.242	O37	-1.243	O37	-1.244	O37	-1.240
O15	-1.196	O15	-1.197	O15	-1.198	O15	-1.199	O15	-1.199
O19	-1.158	O19	-1.157	O19	-1.158	O19	-1.161	O19	-1.164
O16	-1.143	O16	-1.143	O16	-1.143	O16	-1.144	O16	-1.145
N13	-1.027	N13	-1.033	N13	-1.025	N13	-1.032	N13	-1.030
C29	-0.123	C33	-0.123	C33	-0.136	C29	-0.124	C33	-0.132
Atoms with largest positive net charges									
C1	0.320	C1	0.327	C1	0.328	C1	0.325	C1	0.322
H5	0.428	H5	0.431	H5	0.424	H5	0.427	H5	0.429
H17	0.602	H17	0.590	H17	0.609	H17	0.605	H17	0.599
C18	0.967	C18	0.967	C18	0.967	C18	0.963	C18	0.973
S28	1.133	S28	1.131	S28	1.122	S28	1.132	S28	1.126
C14	1.522	C14	1.522	C14	1.519	C14	1.522	C14	1.521

Part B: 4B 3MCs

Inp-1		LM-1		LM-2		LM-3		GMS	
Atom	Q(A)	Atom	Q(A)	Atom	Q(A)	Atom	Q(A)	Atom	Q(A)
Atoms with largest negative net charges									
O37	-1.243	O37	-1.240	O37	-1.247	O37	-1.244	O37	-1.247
O15	-1.183	O15	-1.180	O15	-1.179	O15	-1.181	O15	-1.184
O16	-1.162	O16	-1.159	O19	-1.178	O19	-1.172	O19	-1.178
O19	-1.151	O19	-1.157	O16	-1.157	O16	-1.153	O16	-1.158
N13	-0.982	N13	-0.981	N13	-0.967	N13	-0.984	N13	-0.969
C29	-0.135	C29	-0.129	C33	-0.128	C29	-0.135	C33	-0.133
Atoms with largest positive net charges									
C1	0.333	C1	0.325	C1	0.332	C1	0.331	C1	0.333
H5	0.380	H5	0.389	H5	0.407	H5	0.400	H5	0.409
H17	0.629	H17	0.633	H17	0.629	H17	0.629	H17	0.631
C18	0.940	C18	0.939	C18	0.955	C18	0.967	C18	0.953
S28	1.117	S28	1.118	S28	1.128	S28	1.117	S28	1.120
C14	1.523	C14	1.527	C14	1.522	C14	1.524	C14	1.524

Table B2. Atoms with the most negative and most positive charges in 3-MCs of LEC **4A** and HEC **4B**.

	Atoms with most negative charge					**Atoms with most positive charge**				
	O37	**O15**	**O19**	**O16**	**N13**	**C14**	**S28**	**C18**	**H17**	**H5**
	LEC									
4A_inp	-1.244	-1.196	-1.158	-1.143	-1.027	1.522	1.133	0.967	0.602	0.428
4A_LM-1	-1.242	-1.197	-1.157	-1.143	-1.033	1.522	1.131	0.967	0.590	0.431
4A_LM-2	-1.243	-1.198	-1.158	-1.143	-1.025	1.519	1.122	0.967	0.609	0.424
4A_LM-3	-1.244	-1.199	-1.161	-1.144	-1.032	1.522	1.132	0.963	0.605	0.427
4A_GMS	-1.240	-1.199	-1.164	-1.145	-1.030	1.521	1.126	0.973	0.599	0.429
Avr:	-1.243	-1.198	-1.160	-1.144	-1.029	1.521	1.129	0.967	0.601	0.428
StDev:	0.002	0.001	0.003	0.001	0.003	0.001	0.005	0.004	0.007	0.003
	HEC									
4B_inp	-1.243	-1.183	-1.151	-1.162	-0.982	1.523	1.117	0.940	0.629	0.380
4B_LM-1	-1.240	-1.180	-1.157	-1.159	-0.981	1.527	1.118	0.939	0.633	0.389
4B_LM-2	-1.247	-1.179	-1.178	-1.157	-0.967	1.522	1.128	0.955	0.629	0.407
4B_LM-3	-1.244	-1.181	-1.172	-1.153	-0.984	1.524	1.117	0.967	0.629	0.400
4B_GMS	-1.247	-1.184	-1.178	-1.158	-0.969	1.524	1.120	0.953	0.631	0.409
Avr:	-1.244	-1.181	-1.167	-1.158	-0.977	1.524	1.120	0.951	0.630	0.397
StDev:	0.003	0.002	0.012	0.003	0.008	0.002	0.005	0.012	0.002	0.012
	Difference: Average (HEC) minus Average (LEC)									
	-0.002	0.016	-0.008	-0.014	0.053	0.003	-0.009	-0.017	0.029	-0.031

Some observations follow:

1) O37 of **3** is most negatively charged whereas C14 of **1** is most positively charged in both systems.
2) In general, net atomic charges do not vary much on going from input to GMSs in both systems.
3) There are only few highly +/– charged atoms in each molecule. Hence, they must be seen, presumably, as leading to relative placement of molecules in 3D space.
4) Notably, neither N13 of **1** nor C18 of **2** (they are destined to form a C–N bond) carry largest negative or positive charge, respectively. The same applies to O19 of **2** and H17 of **1** (a proton transfer is to take place between them).
5) Moreover, H5 has significantly lower positive charge than H17 but the O37 of **3** is always close to H5 in all equilibrium structures; note that the **4A-inp-2** in Table 1 of the main body was prepared in such a way as to facilitate the expected O37⋯H17 interaction but, on

energy optimisation, the DMSO molecule moved away and came close to H5 in the optimised system.

6) All the above clearly shows that the relative placement of molecules is a result of most effective (most energy minimising) set of interactions between all atoms.
7) Notably, it is not the interaction between N13 and C18 that leads to their perfect relative arrangement (the same applies to O19 and H17 atom-pair); their relative and suitable for subsequent bond formation placement is facilitated by numerous interactions. Clearly, an orthodox approach involving assumed most positively and negatively charged atoms is of no use in this case and might, in some cases generate wrong predictions or explanations.

End of Part B2

Part B3

1a-containing 3MCs and their energies

The DMSO molecule was placed such that its oxygen atom (O37) interacted with **1a 2_MC** through H5 - Figure B1; the resulting complex was renamed **4A_inp** after it was energy optimised. Notably, there was no significant change in the structure of **4A_inp** before and after energy optimisation. The d(N13,C18) reaction coordinate of **4A_inp** was then decreased to construct a bond between N13 of **1a** and C18 of **2**. This resulted in a local minimum structure **4A_LM-1** where, after energy optimisation, the d(N13,C18) distance was 3.338 Å. Further decrease in d(N13,C18) distance resulted in a tremendous increase in the electronic energy of the molecular system due to the lack of proper pre-arrangement between the two molecules of proline (**1a**) and acetone (**2**). Although there is a significant structural difference between complexes **4A_inp** and **4A_LM-1**, the energy difference is insignificant (less than 0.5 kcal/mol) Table B3, this shows that there is a free rotation between the molecules.

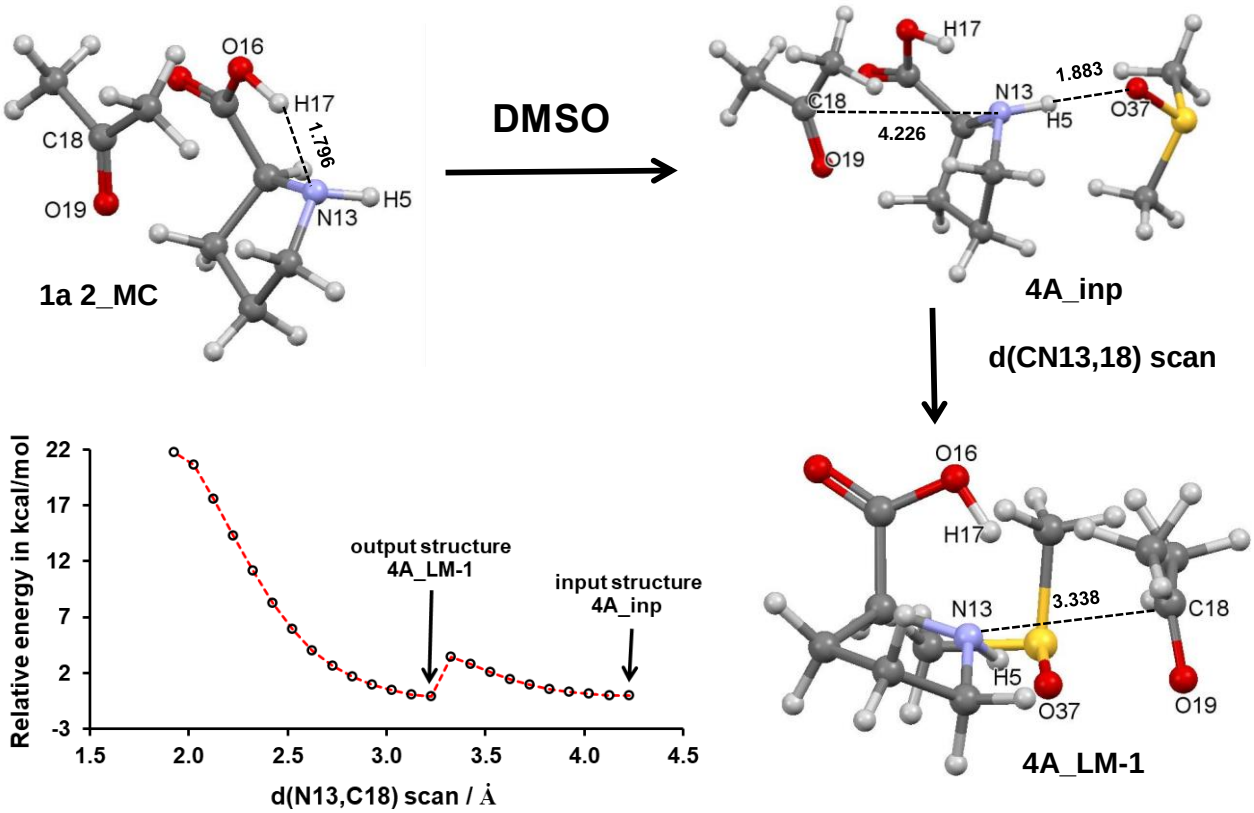

Figure B1. Structure of **2_MC,** made of proline **1a** and acetone **2,** used to generate **4A_inp** and data from the d(N13,C18) scan using **4A_inp** as an input structure that changed to the local minimum structure **4A_LM-1**.

Notably, the O16–H17···O19 classical hydrogen bond which drives the formation of a formal bond between N13 of **1a** and C18 of **2** is absent in **4A_LM-1**. This means that as the molecules approach each other, the desired N13–C18 bond will not be formed as indicated by the data in Figure B1. To form the desired O16–H17···O19 hydrogen bond, either proline **1a** or acetone **2** must rotate, hence dihedral angle DA(H17,N13,C18,O19) made of atoms of proline **1a** and acetone **2** was scanned in steps of 10º resulting in the rotation of the molecule of acetone **2**. The scan data revealed a local minimum structure **4A_LM-2**, after energy optimisation of **4A_LM-2**, the desired O16-H17···O19 hydrogen bond has a value of 2.489 Å (Figure B2). Notably, the orientation of proline relative to acetone in **4A_LM-2** is suitable and pre-organised for the N13–C18 bond formation.

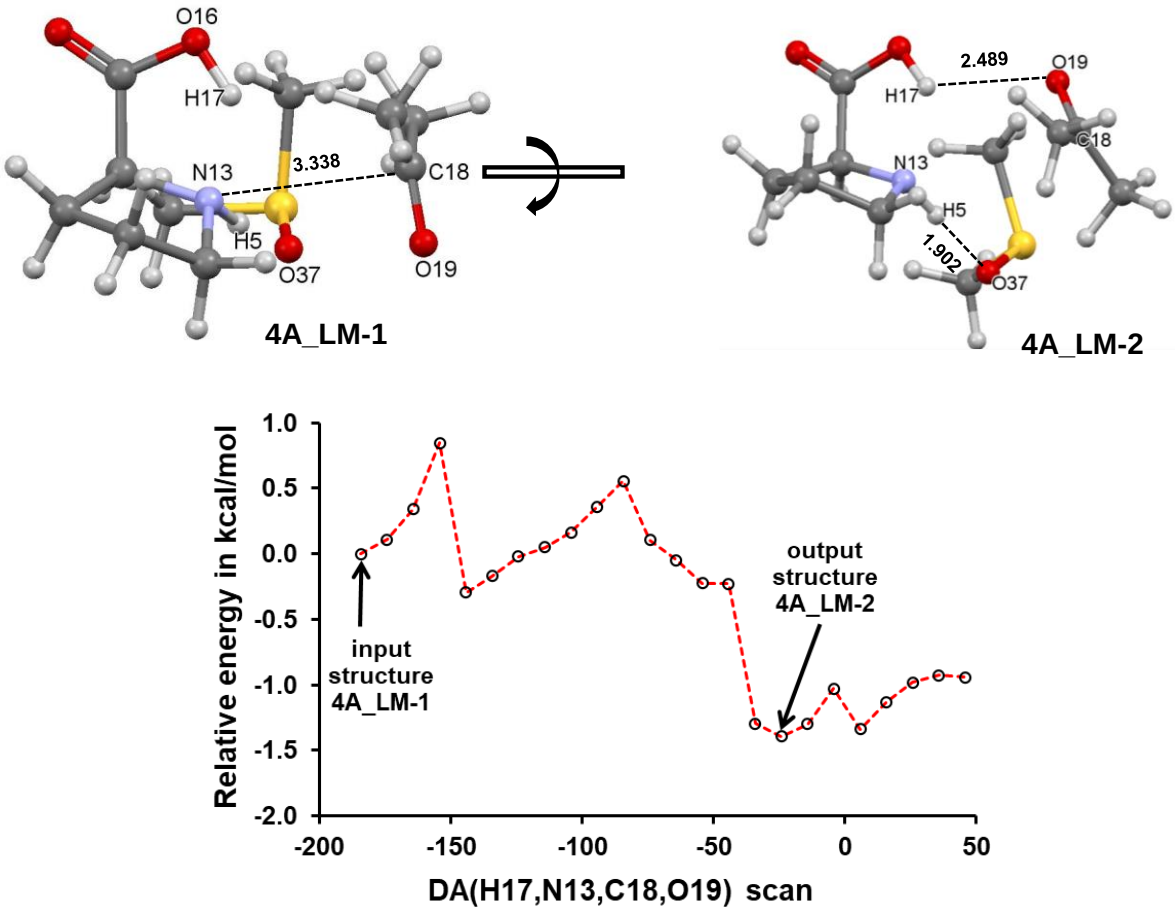

Figure B2. Data for the scan of DA(N13,H17,C18,O19) to construct the O16–H17···O19 hydrogen bond (required for the N13–C18 bond formation) leading to the rotation of acetone (**2**) and formation of **4A_LM-2**.

Interaction mode of the DMSO solvent molecule

The interaction mode of the molecule of DMSO in input structure **4A_inp** was pre-determined by chemical intuition. However, one might want to establish if O37 can still interact with H5 when placed in the vicinity of H17, hence the Cartesian coordinates of DMSO were changed

(while the coordinates of proline and acetone were left unaltered) to **4A-inp*** in which O37 is closer to H17 than H5 followed by a full energy optimisation. The energy-optimised geometry (**4A_LM-3**) shows that the molecule of DMSO moved from top to bottom during energy optimisation, indicating that the N13–H5···O37 H-bond is preferred over the O16–H17···O37 H-bond. (Figure B3).

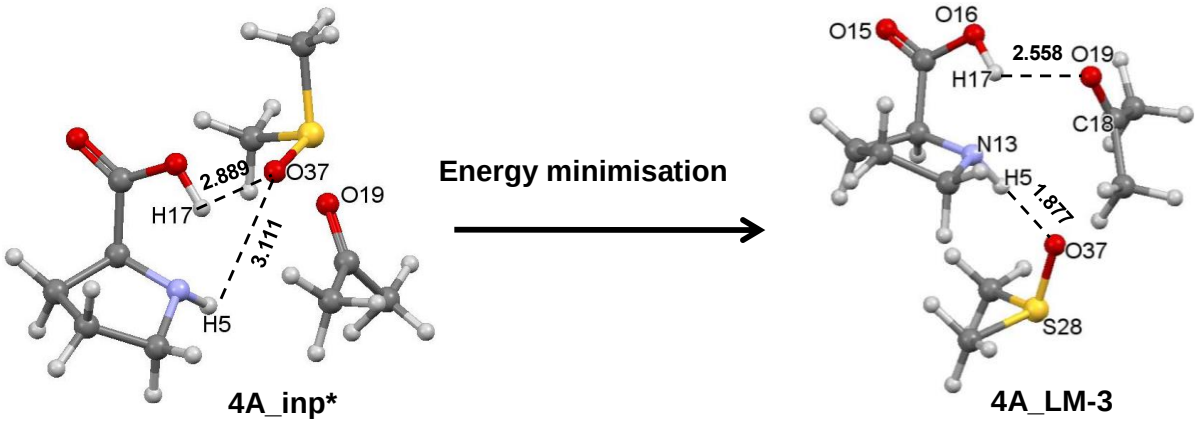

Figure B3. Ball and stick models for input structure **4A-inp*** and the resulting energy-optimised structure **4A_LM-3** used to establish the interaction mode of the DMSO solvent molecule.

Search for the global minimum structure (GMS) of a (3MC) LEC-Ac-DMSO

In the search for the GMS for a 3-MC of proline **1a**, acetone **2** and the DMSO molecule **3**, **4A_LM-3** was submitted for the DA(N13,C1,C18,C20) scan. The resulting data (Figure B4) shows the lowest energy structure **4A_GMS**, which after energy optimisation has the same free energy *G* as **4A_LM-3** but is marginally lower in E_{ZPVE} and *H* by ~ 1 kcal/mol.

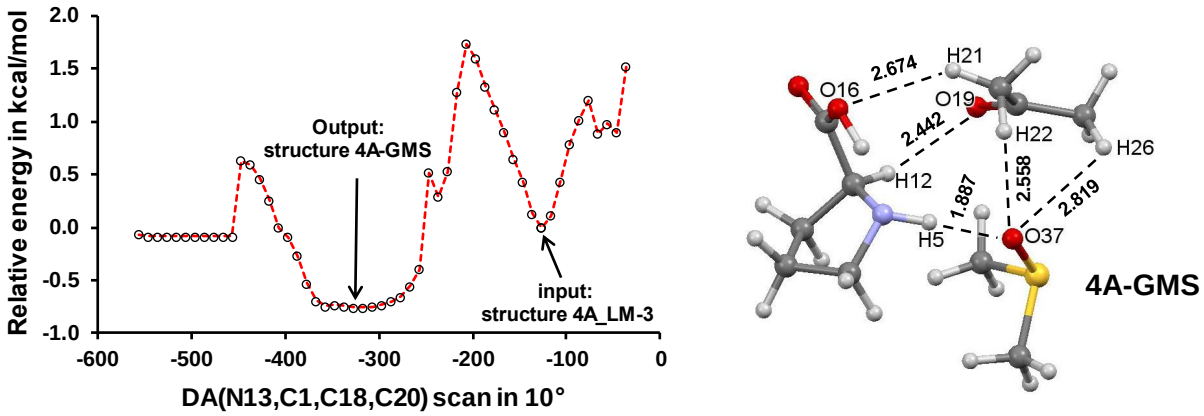

Figure B4. The DA(N13,C1,C18,C20) scan data obtained using **3A-LM3** as input in the search for the **4A-GMS**.

Formation of a three-molecule complex (3MC) HEC-Ac-DMSO

An initial formation of a 3-MC of the HEC (**1b**), acetone (**2**), and DMSO solvent molecule (**3**) was done as in the case of the LEC (**1a**). Unlike in **1a 2_MC** which lacks the O16–H17···O19 hydrogen bond, **1b 2_MC**, consists of this classical hydrogen bond with d(H17,O19) of 1.684 Å (Figure B5). The DMSO solvent molecule was placed such that it interacted with **1b 2_MC** through the N13–H5···O37 hydrogen bond; after energy optimisation, the resulting complex was named **4B_inp** (Figure B5). To construct a covalent bond between N13 of **1b** and C18 of **2**, the d(N13,C18) reaction coordinate of **4B-inp** was decreased resulting in two local minimum structures **4B_LM-1** and **4B_LM-2** which were energy-optimised and are presented in Table 1 in the main body.

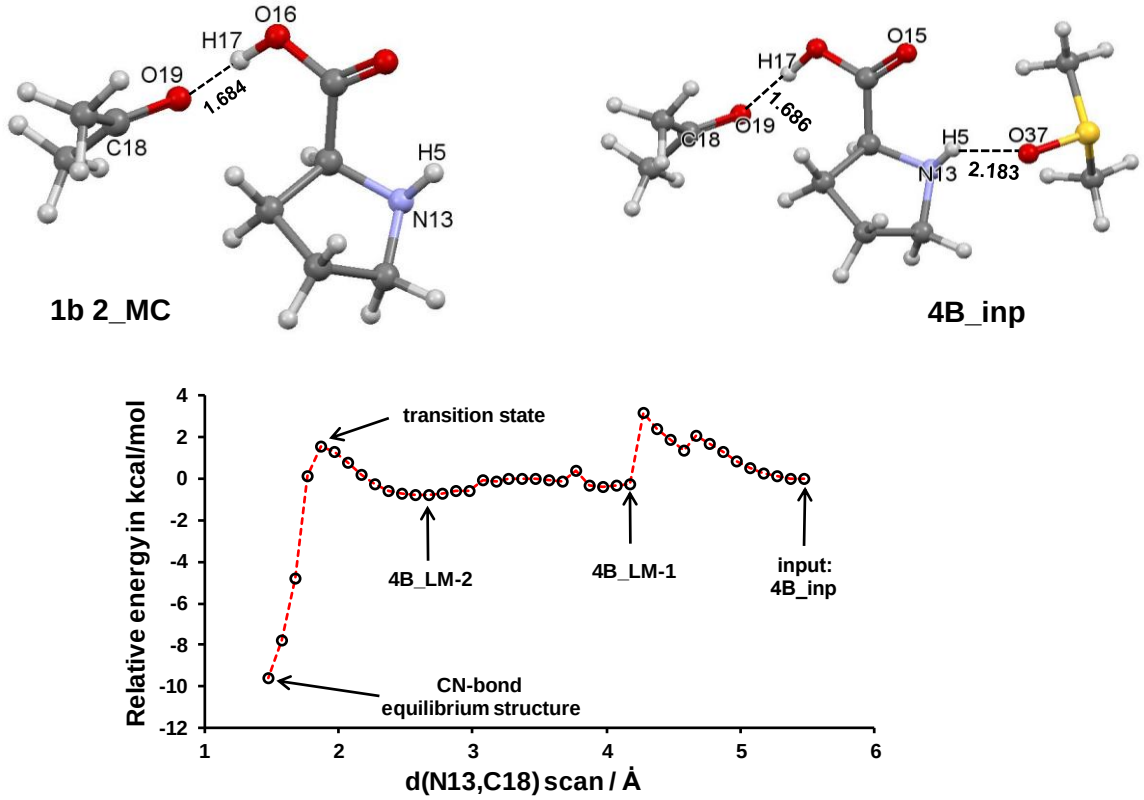

Figure B5. Ball and stick representation of the **2_MC** of proline **1b** and acetone **2**, used to construct the input structure **4B_inp**, and data for d(N13,C18) reaction coordinate scan using **4B_inp** as the input structure resulting in local minima **4B_LM-1** and **4B_LM-2** (shown in Table 1).

Search for the global minimum structure of a 3MC HEC-Ac-DMSO

In the search of a global minimum structure, the energy-optimised complex (**4B_LM-2**) was submitted for DA(N13,C4,C20,C18) and DA(N13,H17,C18,O19) reaction coordinate scans. This resulted in the local minimum structure **4B_LM-3** and the lowest energy structure **4B_GMS**, the energy-optimised structures of the two complexes are shown in Table 1 of the main body. Data obtained from the two scans is shown in Figure B6.

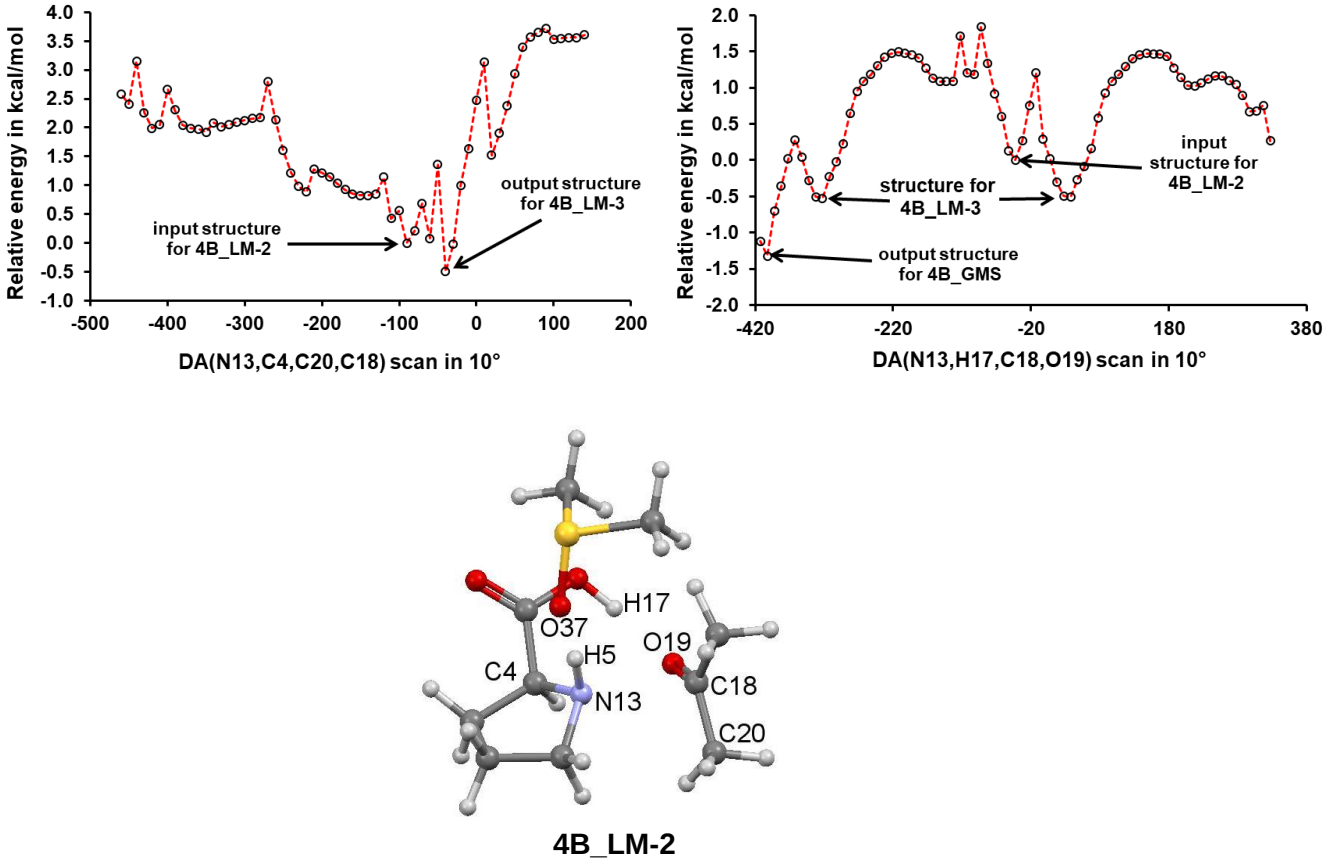

Figure B6. Ball and stick representation of **4B_LM-2** showing atoms selected in scanning dihedral angles DA(N13,C4,C20,C18) and DA(N13,H17,C18,O19) and the associated data showing output structures **4B_LM-3** and **4B_GMS** (shown in Table 1).

Table B3. Energies (in a.u.) and, relative to reactants, differences in energies (in kcal/mol) for 3-MC made of proline (**1**), acetone (**2**) and DMSO solvent molecule (**3**). Data obtained at the 6-311++G(d,p)/GD3 level.

Part A – LEC-containing 3-MCs

	E	**Δ*E***	E_{ZPVE}	ΔE_{ZPVE}	***H***	**Δ*H***	***G***	**Δ*G***
	3-MC							
1a+**2**+**3**	-1147.8284	0.0	-1147.5219	0.0	-1147.501	0.0	-1147.6103	0.0
4A_inp-1	-1147.8459	-11.0	-1147.5367	-9.3	-1147.5139	-8.1	-1147.5927	11.0
4A_LM-1	-1147.8463	-11.2	-1147.5370	-9.5	-1147.5143	-8.4	-1147.5925	11.1
4A_LM-2	-1147.8485	-12.6	-1147.5388	-10.6	-1147.5164	-9.7	-1147.5925	11.1
4A_inp-2	-1147.8252	2.0	-1147.5172	3.0	-1147.4967	2.7	-1147.5709	24.7
4A_LM-3	-1147.8491	-13.0	-1147.5395	-11.0	-1147.5170	-10.0	-1147.5942	10.1
4A_GMS	-1147.8503	-13.8	-1147.5407	-11.8	-1147.5183	-10.9	-1147.5943	10.0

Part B – HEC-containing 3-MCs

	E	**Δ*E***	E_{ZPVE}	ΔE_{ZPVE}	***H***	**Δ*H***	***G***	**Δ*G***
	3-MC							
1b+**2**+**3**	-1147.8178	0.0	-1147.5113	0.0	-1147.4900	0.0	-1147.6001	0.0
4B_inp	-1147.8408	-14.5	-1147.5314	-12.6	-1147.5086	-11.7	-1147.5872	8.1
4B_LM-1	-1147.8414	-14.8	-1147.5317	-12.8	-1147.5090	-12.0	-1147.5865	8.5
4B_LM-2	-1147.8421	-15.3	-1147.5317	-12.8	-1147.5097	-12.3	-1147.5833	10.5
4B_LM-3	-1147.8429	-15.8	-1147.5334	-13.9	-1147.5108	-13.1	-1147.5870	8.2
4B_GMS	-1147.8442	-16.6	-1147.5338	-14.1	-1147.5118	-13.7	-1147.5862	8.8

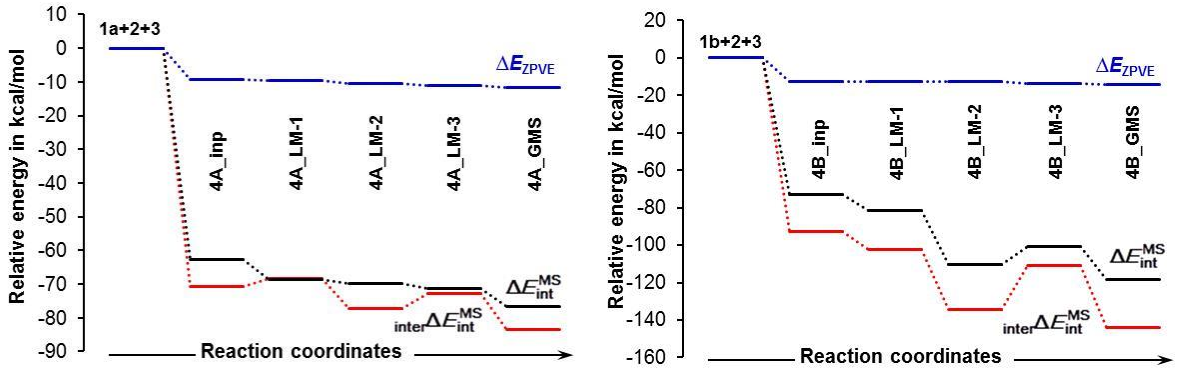

Figure B7. Relative to the energy of isolated molecules **1** (proline, either **1a** or **1b**), **2** (acetone) and **3** (DMSO solvent molecule), energy changes ΔE_{ZPVE}, ${}_{\mathrm{inter}}\Delta E_{\mathrm{int}}^{\mathrm{MS}}$ and $\Delta E_{\mathrm{int}}^{\mathrm{MS}}$ computed for the indicated 3-MCs.

For the purpose of full comparison, changes in E_{ZPVE}, all interaction energies as the $E_{\mathrm{int}}^{\mathrm{MS}}$ term and extracted intermolecular interaction energies ${}_{\mathrm{inter}}E_{\mathrm{int}}^{\mathrm{MS}}$ computed for both molecular systems, from input to GMS complexes, are shown in Figure B7. It is clear that ${}_{\mathrm{inter}}E_{\mathrm{int}}^{\mathrm{MS}}$ changed several times more than E_{ZPVE}. This exemplifies and supports our view that the interaction energies and intermolecular ones in particular carry information most useful in explaining chemical reactivity leading to a chemical change. Furthermore, we note that intermolecular interactions changed more significantly than combined, inter and intramolecular interactions, in both systems and this is due to the contributions made by intramolecular interactions.

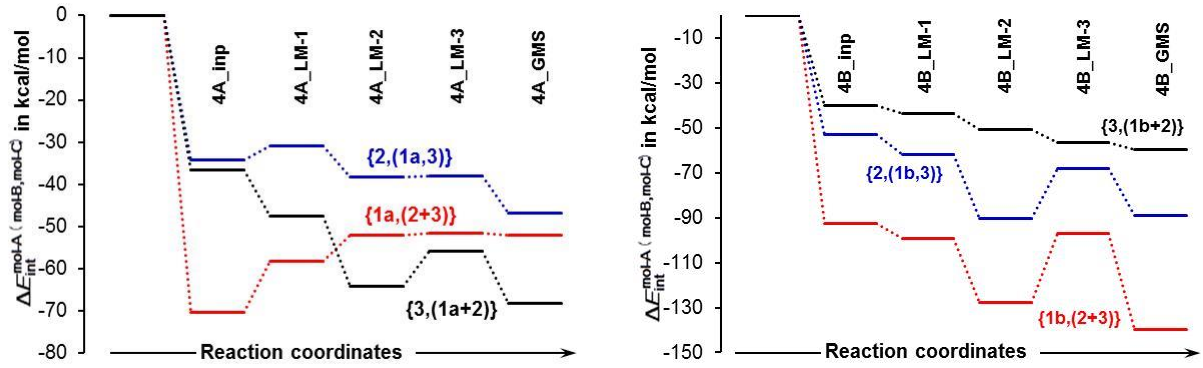

Figure B8. Relative to isolated molecules, unique interactions between a single molecule and remaining two molecules of molecular systems ie {**1**,(**2**+**3**)}, {**2**.(**1**+**3**)} and {**3**(**1**+**2**)}

End of Part B3

Part B4

Most significant attractive and repulsive intermolecular di-atomic interactions in all 3-MCs

Table B4. Top eight strongest attractive and repulsive diatomic intermolecular interactions (in kcal/mol) in the indicated **4A** 3-MCs involving **1a** (LEC of proline), **2** (acetone) and **3** (DMSO solvent molecule). Part A. Molecules **1a** and **2** in **4A_inp-1**

Atom A of **1a**	Atom B of **2**	E_{int}(A,B)
Most attractive interactions		
C14	O19	-160.6
O16	C18	-113.4
O15	C18	-98.8
N13	C18	-80.2
H17	O19	-64.7
C1	O19	-34.7
H5	O19	-33.9
C4	O19	-29.9
Most repulsive interactions		
C4	C18	24.4
C1	C18	26.7
H5	C18	27.8
H17	C18	56.5
N13	O19	97.6
O15	O19	115.4
O16	O19	124.7
C14	C18	137.9

Part B. Molecules **1a** and **3** in **4A_inp-1**

Atom A of **1a**	Atom B of **3**	E_{int}(A,B)
Most significant attractive changes		
C14	O37	-123.7
N13	S28	-109.2
H5	O37	-94.4
O16	S28	-80.0
O15	S28	-76.1
H17	O37	-58.1
C1	O37	-38.9
C4	O37	-36.1
Most significant repulsive		
C4	S28	29.3
C1	S28	31.0
H17	S28	46.8
H5	S28	59.6
O15	O37	86.6
O16	O37	96.6
C14	S28	105.8
N13	O37	134.0

Part C. Molecules **2** and **3** in **4A_inp-1**

Atom A of **2**	Atom B of **3**	E_{int}(A,B)
Most significant attractive changes		
C18	O37	-128.9
O19	S28	-121.7
O19	H34	-16.0
H22	O37	-11.6
C18	C33	-11.6
H26	O37	-7.4
O19	H35	-7.3
C18	C29	-7.3
Most significant repulsive		
C18	H36	5.0
C18	H35	5.8
H22	S28	6.2
O19	C29	8.6
C18	H34	8.8
O19	C33	12.9
C18	S28	105.0
O19	O37	140.2

Part D. Molecules **1a** and **2** in **4A_LM-1**

Atom A of **1a**	Atom B of **2**	E_{int}(A,B)
Most significant attractive changes		
C14	O19	-103.5
N13	C18	-102.7
O16	C18	-84.8
O15	C18	-61.6
H17	O19	-57.7
H5	O19	-48.7
C1	O19	-38.1
C4	O19	-26.8
Most significant repulsive		
C4	C18	23.3
C1	C18	31.1
H5	C18	41.6
H17	C18	53.5
O15	O19	69.6
O16	O19	92.0
C14	C18	92.7
N13	O19	114.9

Part E. Molecules **1a** and **3** in **4A_LM-1**

Atom A of **1a**	Atom B of **3**	E_{int}(A,B)
Most significant attractive changes		
C14	O37	-134.9
N13	S28	-111.3
O16	S28	-96.9
H5	O37	-94.2
O15	S28	-87.8
H17	O37	-63.0
C1	O37	-38.1
C4	O37	-36.8
Most significant repulsive		
C1	S28	30.0
C4	S28	30.3
H17	S28	54.4
H5	S28	60.0
O15	O37	93.7
O16	O37	107.6
C14	S28	123.5
N13	O37	135.2

Part F. Molecules **2** and **3** in **4A_LM-1**

Atom A of **2**	Atom B of **3**	E_{int}(A,B)
Most significant attractive changes		
C18	O37	-96.0
O19	S28	-90.2
H21	O37	-14.2
C18	C33	-7.6
C18	C29	-6.0
H23	O37	-5.4
O19	H35	-4.6
O19	H34	-4.6
Most significant repulsive		
C18	H34	4.0
C18	H35	4.1
H23	S28	4.5
H21	S28	7.1
O19	C29	7.1
O19	C33	8.6
C18	S28	76.7
O19	O37	114.2

Part G. Molecules **1a** and **2** in **4A_LM-2**

Atom A of **1a**	Atom B of **2**	E_{int}(A,B)
Most significant attractive changes		
C14	O19	-136.8
N13	C18	-102.8
O16	C18	-102.5
H17	O19	-90.8
O15	C18	-69.4
H5	O19	-48.9
C1	O19	-32.3
C4	O19	-30.2
Most significant repulsive		
C4	C18	24.7
C1	C18	27.6
H5	C18	41.5
H17	C18	67.7
O15	O19	88.7
C14	C18	106.1
N13	O19	119.5
O16	O19	132.5

Part H. Molecules **1a** and **3** in **4A_LM-2**

Atom A of **1a**	Atom B of **3**	E_{int}(A,B)
Most significant attractive changes		
C14	O37	-131.8
N13	S28	-111.6
O16	S28	-94.1
H5	O37	-93.4
O15	S28	-85.5
H17	O37	-62.1
C1	O37	-38.4
C4	O37	-37.8
Most significant repulsive		
C1	S28	30.1
C4	S28	30.9
H17	S28	54.8
H5	S28	59.7
O15	O37	92.5
O16	O37	103.2
C14	S28	120.2
N13	O37	134.8

Part I. Molecules **2** and **3** in **4A_LM-2**

Atom A of **2**	Atom B of **3**	E_{int}(A,B)
Most significant attractive changes		
O19	C14	-136.8
C18	N13	-102.8
C18	O16	-102.5
O19	H17	-90.8
C18	O15	-69.4
O19	H5	-48.9
O19	C1	-32.3
O19	C4	-30.2
Most significant repulsive		
C18	C4	24.7
C18	C1	27.6
C18	H5	41.5
C18	H17	67.7
O19	O15	88.7
C18	C14	106.1
O19	N13	119.5
O19	O16	132.5

Part J. Molecules **1a** and **2** in **4A_LM-3**

Atom A of **1a**	Atom B of **2**	E_{int}(A,B)
Most significant attractive changes		
C14	O19	-132.6
N13	C18	-111.0
O16	C18	-104.9
H17	O19	-89.5
O15	C18	-69.8
H5	O19	-47.2
C1	O19	-36.6
C4	O19	-30.9
Most significant repulsive		
C4	C18	26.0
C1	C18	30.5
H5	C18	42.2
H17	C18	70.3
O15	O19	85.6
C14	C18	107.7
N13	O19	123.9
O16	O19	129.7

Part K. Molecules **1a** and **3** in **4A_LM-3**

Atom A of **1a**	Atom B of **3**	E_{int}(A,B)
Most significant attractive changes		
C14	O37	-123.9
N13	S28	-112.3
H5	O37	-95.8
O16	S28	-79.5
O15	S28	-75.2
H17	O37	-58.5
C1	O37	-39.7
C4	O37	-37.1
Most significant repulsive		
C4	S28	30.4
C1	S28	32.5
H17	S28	46.9
H5	S28	60.9
O15	O37	86.9
O16	O37	97.0
C14	S28	104.7
N13	O37	136.1

Part L. Molecules **2** and **3** in **4A_LM-3**

Atom A of **2**	Atom B of **3**	E_{int}(A,B)
Most significant attractive changes		
C18	O37	-94.8
O19	S28	-80.1
H22	O37	-15.6
H26	O37	-13.7
C18	C29	-6.6
C18	C33	-6.0
H23	O37	-4.6
H25	O37	-4.6
Most significant repulsive		
C18	H32	3.6
C18	H31	3.6
H26	S28	6.4
O19	C33	6.8
H22	S28	7.3
O19	C29	7.4
C18	S28	73.2
O19	O37	101.7

Part M. Molecules **1a** and **2** in **4A_GMS**

Atom A of **1a**	Atom B of **2**	E_{int}(A,B)
Most significant attractive changes		
C14	O19	-153.5
O15	C18	-89.3
O16	C18	-88.1
N13	C18	-85.0
H17	O19	-55.9
H5	O19	-47.2
C4	O19	-32.9
C1	O19	-26.8
Most significant repulsive		
C1	C18	22.1
C4	C18	25.1
H5	C18	39.9
H17	C18	46.8
N13	O19	101.8
O16	O19	106.9
O15	O19	115.7
C14	C18	120.3

Part N. Molecules **1a** and **3** in **4A_GMS**

Atom A of **1a**	Atom B of **3**	E_{int}(A,B)
Most significant attractive changes		
C14	O37	-123.3
N13	S28	-111.6
H5	O37	-95.5
O16	S28	-79.0
O15	S28	-74.9
H17	O37	-57.7
C1	O37	-39.3
C4	O37	-35.3
Most significant repulsive		
C4	S28	28.9
C1	S28	32.3
H17	S28	46.3
H5	S28	60.9
O15	O37	86.6
O16	O37	96.3
C14	S28	104.2
N13	O37	134.9

Part O. Molecules **2** and **3** in **4A_GMS**

Atom A of **2**	Atom B of **3**	E_{int}(A,B)
Most significant attractive changes		
C18	O37	-128.9
O19	S28	-121.7
O19	H34	-16.0
H22	O37	-11.6
C18	C33	-11.6
H26	O37	-7.4
O19	H35	-7.3
C18	C29	-7.3
Most significant repulsive		
C18	H36	5.0
C18	H35	5.8
H22	S28	6.2
O19	C29	8.6
C18	H34	8.8
O19	C33	12.9
C18	S28	105.0
O19	O37	140.2

Table B5. Top eight strongest attractive and repulsive diatomic intermolecular interactions (in kcal/mol) in the indicated **4B** 3-MCs involving **1b** (HEC of proline), **2** (acetone) and **3** (DMSO solvent molecule).

Part A. Molecules **1b** and **2** in **4B_inp**

Atom A of **1b**	Atom B of **2**	E_{int}(A,B)
Most significant attractive changes		
C14	O19	-158.8
H17	O19	-143.5
O16	C18	-114.5
O15	C18	-73.7
N13	C18	-58.1
C4	O19	-31.2
H5	O19	-27.6
C1	O19	-25.7
Most significant repulsive		
C1	C18	19.8
H5	C18	21.1
C4	C18	22.4
N13	O19	76.7
H17	C18	85.6
O15	O19	97.5
C14	C18	117.1
O16	O19	150.0

Part B. Molecules **1b** and **3** in **4B_inp**

Atom A of **1b**	Atom B of **3**	E_{int}(A,B)
Most significant attractive changes		
C14	O37	-141.1
N13	S28	-112.2
O15	S28	-110.8
O16	S28	-73.6
H5	O37	-73.1
C1	O37	-42.2
H17	O37	-41.5
C4	O37	-35.4
Most significant repulsive		
C4	S28	30.3
C1	S28	34.8
H17	S28	36.6
H5	S28	53.5
O16	O37	83.5
C14	S28	123.0
N13	O37	124.8
O15	O37	126.4

Part C. Molecules **2** and **3** in **4B_inp**

Atom A of **2**	Atom B of **3**	E_{int}(A,B)
Most significant attractive changes		
O19	S28	-55.2
C18	O37	-48.7
C18	C29	-5.0
C18	C33	-4.9
O19	H36	-4.2
O19	H32	-4.2
O19	H34	-2.9
O19	H35	-2.9
Most significant repulsive		
C18	H34	2.2
H21	S28	2.4
C18	H32	3.2
C18	H36	3.2
O19	C33	6.3
O19	C29	6.5
C18	S28	42.9
O19	O37	62.4

Part D. Molecules **1b** and **2** in **4B_LM-1**

Atom A of **1b**	Atom B of **2**	E_{int}(A,B)
Most significant attractive changes		
C14	O19	-157.8
H17	O19	-142.1
O16	C18	-111.6
N13	C18	-81.2
O15	C18	-72.4
C4	O19	-35.2
H5	O19	-33.8
C1	O19	-29.7
Most significant repulsive		
C1	C18	24.0
C4	C18	26.3
H5	C18	26.9
H17	C18	83.9
O15	O19	96.6
N13	O19	101.0
C14	C18	115.5
O16	O19	149.0

Part E. Molecules **1b** and **3** in **4B_LM-1**

Atom A of **1b**	Atom B of **3**	E_{int}(A,B)
Most significant attractive changes		
C14	O37	-158.4
N13	S28	-117.1
O15	S28	-104.9
O16	S28	-97.2
H5	O37	-83.3
H17	O37	-53.4
C1	O37	-38.8
C4	O37	-36.8
Most significant repulsive		
C4	S28	31.4
C1	S28	33.0
H17	S28	50.0
H5	S28	57.5
O16	O37	105.6
O15	O37	125.3
N13	O37	128.8
C14	S28	136.5

Part F. Molecules **2** and **3** in **4B_LM-1**

Atom A of **2**	Atom B of **3**	E_{int}(A,B)
Most significant attractive changes		
O19	S28	-74.2
C18	O37	-62.3
C18	C33	-8.0
H25	O37	-7.7
C18	C29	-7.2
O19	H36	-6.1
O19	H32	-5.2
O19	H34	-5.0
Most significant repulsive		
C18	H34	4.0
C18	H32	4.3
C18	H36	4.8
H25	S28	7.5
O19	C29	8.6
O19	C33	9.8
C18	S28	60.2
O19	O37	77.5

Part G. Molecules **1b** and **2** in **4B_LM-2**

Atom A of **1b**	Atom B of **2**	E_{int}(A,B)
Most significant attractive changes		
C14	O19	-168.4
H17	O19	-148.4
N13	C18	-130.9
O16	C18	-122.5
O15	C18	-80.2
H5	O19	-46.9
C4	O19	-42.0
C1	O19	-37.2
Most significant repulsive		
C1	C18	32.3
C4	C18	32.9
H5	C18	40.9
H17	C18	91.4
O15	O19	102.6
C14	C18	129.2
N13	O19	129.2
O16	O19	156.5

Part H. Molecules **1b** and **3** in **4B_LM-2**

Atom A of **1b**	Atom B of **3**	E_{int}(A,B)
Most significant attractive changes		
C14	O37	-171.7
O15	S28	-123.2
O16	S28	-103.0
N13	S28	-100.8
H5	O37	-89.2
H17	O37	-61.1
C1	O37	-40.5
C4	O37	-36.8
Most significant repulsive		
C4	S28	29.7
C1	S28	31.5
H17	S28	50.9
H5	S28	55.3
O16	O37	120.1
N13	O37	126.2
O15	O37	130.9
C14	S28	152.1

Part I. Molecules **2** and **3** in **4B_LM-2**

Atom A of **2**	Atom B of **3**	E_{int}(A,B)
Most significant attractive changes		
O19	S28	-81.8
C18	O37	-80.5
C18	C33	-7.6
C18	C29	-6.9
O19	H34	-6.0
O19	H36	-4.9
O19	H35	-4.6
H26	O37	-4.4
Most significant repulsive		
C18	H35	3.7
H26	S28	3.9
C18	H36	4.0
C18	H34	4.9
O19	C29	8.0
O19	C33	9.3
C18	S28	69.7
O19	O37	93.6

Part J. Molecules **1b** and **2** in **4B_LM-3**

Atom A of **1b**	Atom B of **2**	E_{int}(A,B)
Most significant attractive changes		
C14	O19	-155.2
H17	O19	-135.4
N13	C18	-120.5
O16	C18	-116.8
O15	C18	-75.6
H5	O19	-47.8
C4	O19	-36.3
C1	O19	-34.9
Most significant repulsive		
C4	C18	30.3
C1	C18	30.6
H5	C18	39.9
H17	C18	87.7
O15	O19	96.0
C14	C18	120.5
N13	O19	129.0
O16	O19	150.0

Part K. Molecules **1b** and **3** in **4B_LM-3**

Atom A of **1b**	Atom B of **3**	E_{int}(A,B)
Most significant attractive changes		
C14	O37	-176.9
O16	S28	-117.1
O15	S28	-105.6
N13	S28	-105.3
H5	O37	-88.1
H17	O37	-69.7
C4	O37	-39.7
C1	O37	-39.6
Most significant repulsive		
C1	S28	30.8
C4	S28	31.2
H5	S28	55.9
H17	S28	62.9
O15	O37	126.3
N13	O37	127.6
O16	O37	130.5
C14	S28	147.8

Part L. Molecules **2** and **3** in **4B_LM-3**

Atom A of **2**	Atom B of **3**	E_{int}(A,B)
Most significant attractive changes		
O19	S28	-100.1
C18	O37	-84.6
O19	H32	-17.3
C18	C29	-11.1
C18	C33	-8.3
O19	H36	-7.6
O19	H30	-6.9
O19	H31	-6.7
Most significant repulsive		
C18	H31	5.1
C18	H30	5.2
C18	H36	5.7
C18	H32	8.8
O19	C33	11.0
O19	C29	12.8
C18	S28	78.2
O19	O37	106.1

Part M. Molecules **1b** and **2** in **4B_GMS**

Atom A of **1b**	Atom B of **2**	E_{int}(A,B)
Most significant attractive changes		
C14	O19	-169.4
H17	O19	-150.6
N13	C18	-130.4
O16	C18	-122.6
O15	C18	-80.5
H5	O19	-47.4
C4	O19	-42.1
C1	O19	-37.2
Most significant repulsive		
C1	C18	32.2
C4	C18	32.9
H5	C18	41.2
H17	C18	92.0
O15	O19	103.3
N13	O19	129.4
C14	C18	129.5
O16	O19	156.9

Part N. Molecules **1b** and **3** in **4B_GMS**

Atom A of **1b**	Atom B of **3**	E_{int}(A,B)
Most significant attractive changes		
C14	O37	-171.7
O15	S28	-123.2
O16	S28	-103.0
N13	S28	-100.8
H5	O37	-89.2
H17	O37	-61.1
C1	O37	-40.5
C4	O37	-36.8
Most significant repulsive		
C4	S28	29.7
C1	S28	31.5
H17	S28	50.9
H5	S28	55.3
O16	O37	120.1
N13	O37	126.2
O15	O37	130.9
C14	S28	152.1

Part O. Molecules **2** and **3** in **4B_GMS**

Atom A of **2**	Atom B of **3**	E_{int}(A,B)
Most significant attractive changes		
C18	O37	-82.2
O19	S28	-78.1
C18	C29	-6.9
C18	C33	-6.5
O19	H32	-5.8
O19	H36	-5.4
H21	O37	-4.4
H23	O37	-4.2
Most significant repulsive		
C18	H30	3.1
H21	S28	3.3
C18	H36	4.4
C18	H32	4.7
O19	C33	7.9
O19	C29	8.4
C18	S28	65.6
O19	O37	96.0

End of Part B4

Part B5

Interaction energies between meaningful molecular fragments $\mathcal{A}$, $\mathcal{P}$n and $\mathcal{D}$ in the 3-MC

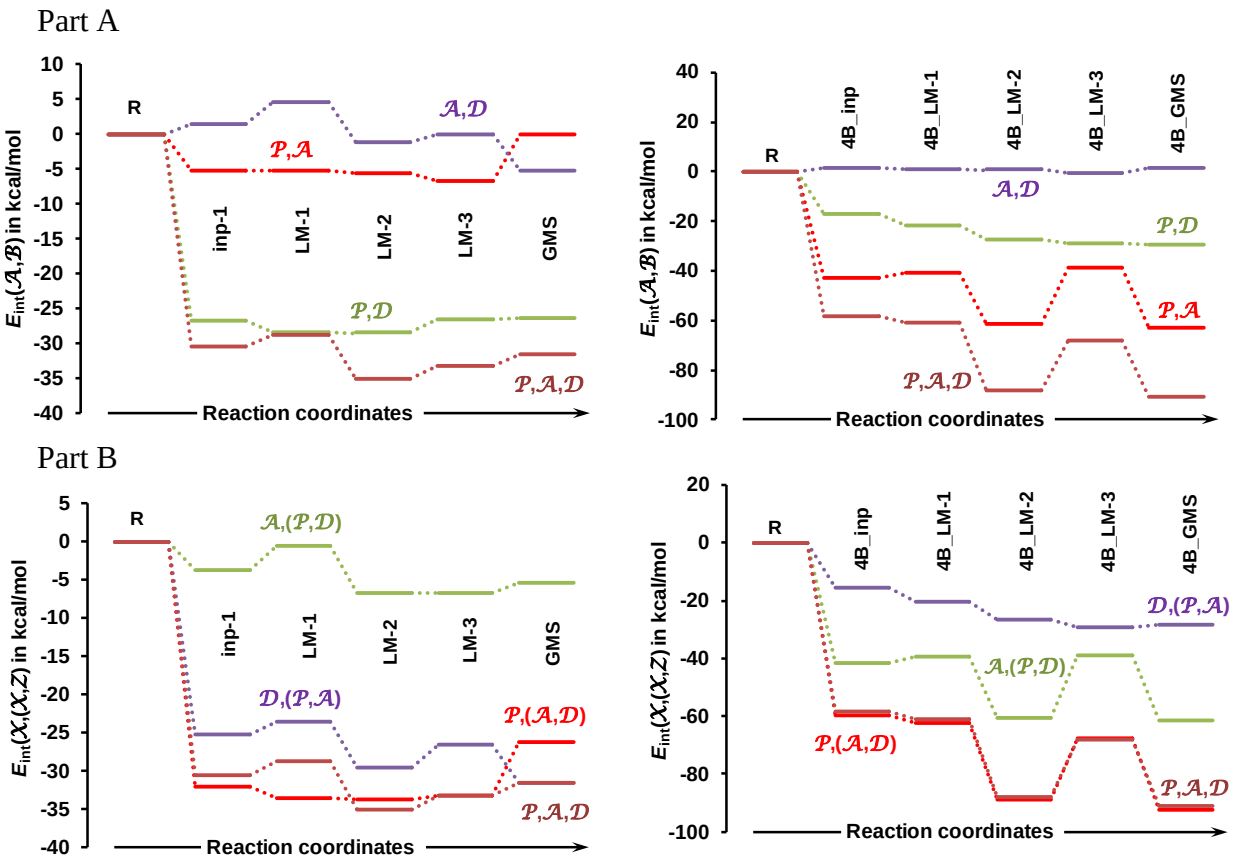

Figure B9. Interaction between atomic fragments {$\mathcal{P}$,$\mathcal{A}$}, {$\mathcal{P}$,$\mathcal{D}$}, {$\mathcal{A}$,$\mathcal{D}$} and {$\mathcal{P}$,$\mathcal{A}$,$\mathcal{D}$} in Part A and an atomic fragment and two remaining atomic fragments in Part B $\mathcal{A}$,($\mathcal{P}$,$\mathcal{D}$), $\mathcal{D}$($\mathcal{P}$,$\mathcal{A}$), $\mathcal{P}$($\mathcal{A}$,$\mathcal{D}$) and $\mathcal{P}$,$\mathcal{A}$,$\mathcal{D}$ in the 3-MCs considered in this work.

Part A

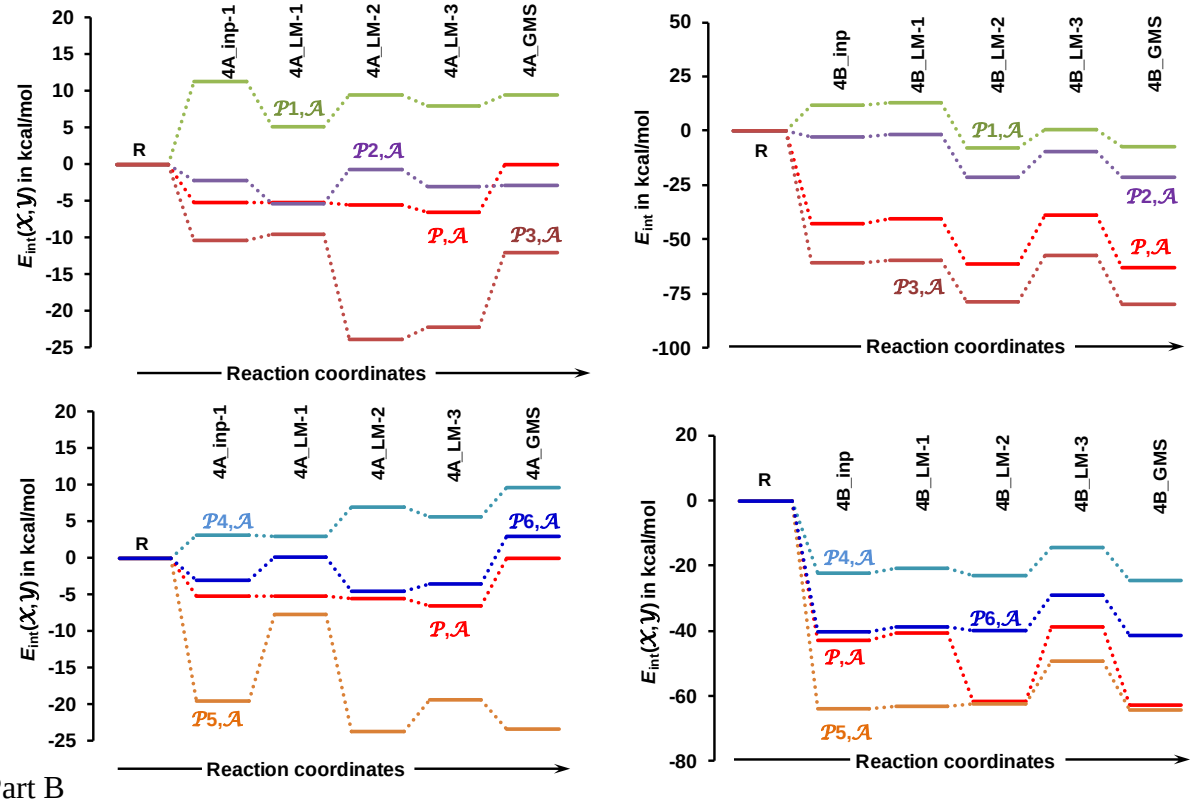

Part B

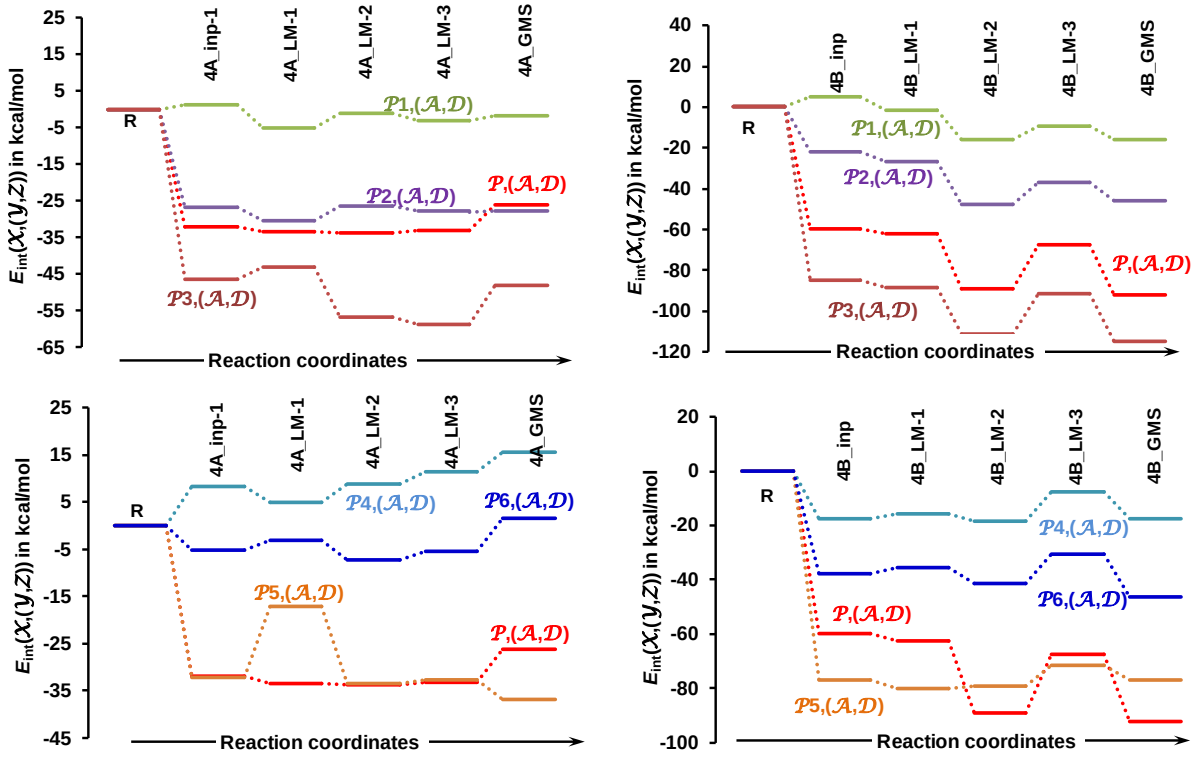

Figure B10. Interaction between the Pn fragment (P, P1, P2, P3, P4, P5 and P6) made of atoms of proline and fragment A of acetone in Part A and interaction between the same fragment of proline with the combined fragments made of atoms A of acetone and D of DMSO (A,D) in Part B.

Table B6. Strongest intermolecular di-atomic interaction energies (in kcal/mol) between selected atoms of **1** and atoms (C18,O19) of **2** and atoms (S28,O37) of **3** in the indicated 3-MC (shown in Table 1) involving **1** (proline), **2** (acetone) and **3** (DMSO solvent molecule).

Part A LEC

	4A_LM-3				4A_GMS			
Atom	C18	O19	S28	O37	C18	O19	S28	O37
C1	30.5	-36.6	32.5	-39.7	22.1	-26.8	32.3	-39.3
C4	26.0	-30.9	30.4	-37.1	25.1	-32.9	28.9	-35.3
H5	42.2	-47.2	60.9	-95.8	39.9	-47.2	60.9	-95.5
N13	-111.0	123.9	-112.3	136.1	-85.0	101.8	-111.6	134.9
C14	107.7	-132.6	104.7	-123.9	120.3	-153.5	104.2	-123.3
O15	-69.8	85.6	-75.2	86.9	-89.3	115.7	-74.9	86.6
O16	-104.9	129.7	-79.5	97.0	-88.1	106.9	-79.0	96.3
H17	70.3	-89.5	46.9	-58.5	46.8	-55.9	46.3	-57.7

Part B HEC

	4B_LM-3				4B_GMS			
Atom	C18	O19	S28	O37	C18	O19	S28	O37
C1	30.6	-34.9	30.8	-39.6	32.2	-37.2	31.5	-40.5
C4	30.3	-36.3	31.2	-39.7	32.9	-42.1	29.7	-36.8
H5	39.9	-47.8	55.9	-88.1	41.2	-47.4	55.3	-89.2
N13	-120.5	129	127.6	-105.3	-130.4	129.4	126.2	-100.8
C14	120.5	-155.2	147.8	-176.9	129.5	-169.4	152.1	-171.7
O15	-75.6	96	126.3	-105.6	-80.5	103.3	130.9	-123.2
O16	-116.8	150	130.5	-117.1	-122.6	156.9	120.1	-103
H17	87.7	-135.4	62.9	-69.7	92	-150.6	50.9	-61.1

Table B7. Strongest intermolecular di-atomic interaction energies (in kcal/mol) between atoms of **2** (C18,O19) and atoms of either **1** or **3** (S28,O37) in the indicated 3-MC (shown in Table 1) involving **1** (proline), **2** (acetone) and **3** (DMSO solvent molecule).

Part A LEC

Atom	C1	C4	H5	N13	C14	O15	O16	H17	S28	O37
	4A_LM-3									
C18	30.5	26.0	42.2	-111.0	107.7	-69.8	-104.9	70.3	73.2	-94.8
O19	-36.6	-30.9	-47.2	123.9	-132.6	85.6	129.7	-89.5	-80.1	101.7
	4A_GMS									
C18	22.1	25.1	39.9	-85.0	120.3	-89.3	-88.1	46.8	105.0	-128.9
O19	-26.8	-32.9	-47.2	101.8	-153.5	115.7	106.9	-55.9	-121.7	140.2

Part B HEC

Atom	C1	C4	H5	N13	C14	O15	O16	H17	S28	O37
	4B_LM-3									
C18	30.6	30.3	39.9	-120.5	120.5	-75.6	-116.8	87.7	78.2	-84.6
O19	-34.9	-36.3	-47.8	129	-155.2	96	150	-135.4	-100.1	106.1
	4B_GMS									
C18	32.2	32.9	41.2	-130.4	129.5	-80.5	-122.6	92	65.6	-82.2
O19	-37.2	-42.1	-47.4	129.4	-169.4	103.3	156.9	-150.6	-78.1	96

Table B8. Strongest intermolecular di-atomic interaction energies (in kcal/mol) between atoms of **3** (S28,O37) and atoms of either **1** (C1,C4, H5, N13, C14, O15, O16, H17) or **2** (C18,O19) in the indicated 3-MCs for both LEC Part A and HEC Part B.

Part A LEC

Atom	C1	C4	H5	N13	C14	O15	O16	H17	C18	O19
	4A_LM-3									
S28	32.5	30.4	60.9	-112.3	104.7	-75.2	-79.5	46.9	73.2	-80.1
O37	-39.7	-37.1	-95.8	136.1	-123.9	86.9	97.0	-58.5	-94.8	101.7
	4A_GMS									
S28	32.3	28.9	60.9	-111.6	104.2	-74.9	-79.0	46.3	105.0	-121.7
O37	-39.3	-35.3	-95.5	134.9	-123.3	86.6	96.3	-57.7	-128.9	140.2

Part B HEC

Atom	C1	C4	H5	N13	C14	O15	O16	H17	C18	O19
	4B_LM-3									
S28	30.8	31.2	55.9	-105.3	147.8	-105.6	-117.1	62.9	78.2	-100.1
O37	-39.6	-39.7	-88.1	127.6	-176.9	126.3	130.5	-69.7	-84.6	106.1
	4B_GMS									
S28	31.5	29.7	55.3	-100.8	152.1	-123.2	-103	50.9	65.6	-78.1
O37	-40.5	-36.8	-89.2	126.2	-171.7	130.9	120.1	-61.1	-82.2	96

Part A

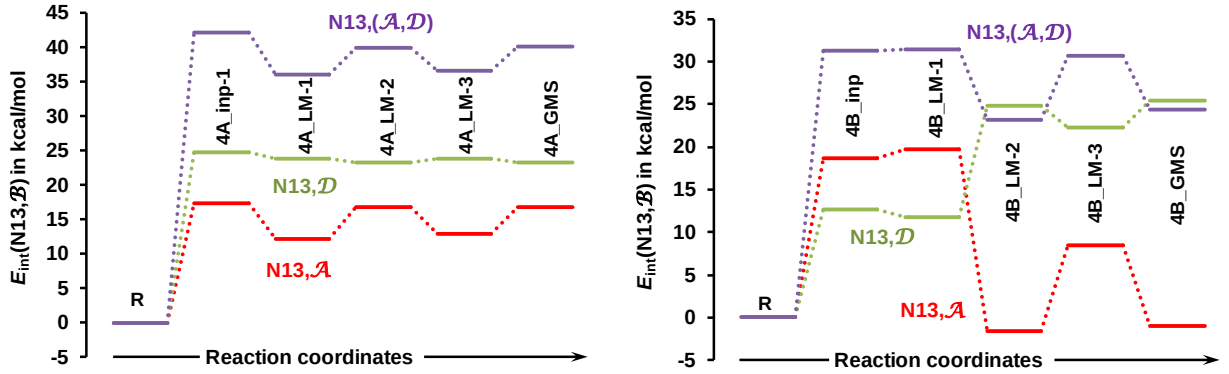

Part B

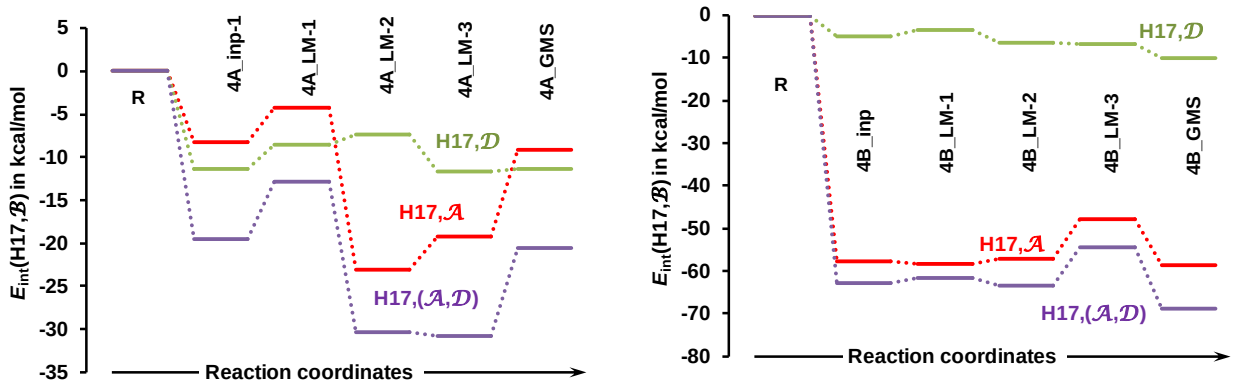

Figure B11. Interaction energies between fragments $\mathcal{A}$ (C18,O19) of acetone, $\mathcal{D}$ (S28,O37) of DMSO and the combined ($\mathcal{A}$,$\mathcal{D}$) fragment of acetone and DMSO with atoms N13 (Part A) and H17 (Part B) of proline (**1**).

Table B9. Intermolecular interactions (in kcal/mol) between the indicated atoms of proline either **1a** or **1b** in Part A and Part B respectively and molecular fragment $\mathcal{A}$ = {C18,O19} of **2** and $\mathcal{D}$ = {S28,O37} of **3** in the indicated 3-MCs (shown in Table 1)

Part A LEC

	4A_LM-3		4A_GMS	
Atom	$\mathcal{A}$	$\mathcal{D}$	$\mathcal{A}$	$\mathcal{D}$
C1	-6.1	-7.2	-4.7	-7.0
C4	-4.9	-6.7	-7.7	-6.4
H5	-5.0	-34.8	-7.3	-34.6
N13	13.0	23.8	13.8	23.3
C14	-25.0	-19.2	-33.2	-19.1
O15	15.8	11.6	26.4	11.7
O16	24.8	17.4	18.7	17.3
H17	-19.3	-11.6	-9.1	-11.4
C18	–	-21.6	–	-23.8
O19	–	21.6	–	18.5
S28	-6.9	–	-16.6	–
O37	6.9	–	11.3	–

Part B HEC

	4B_LM-3		4B_GMS	
Atom	$\mathcal{A}$	$\mathcal{D}$	$\mathcal{A}$	$\mathcal{D}$
C1	-4.3	-8.7	-5.0	-9.0
C4	-6.0	-8.5	-9.2	-7.1
H5	-8.0	-32.3	-6.2	-33.9
N13	8.5	22.2	-260.8	25.4
C14	-34.8	-29.1	-39.9	-19.6
O15	20.4	20.7	22.8	7.7
O16	33.2	13.4	34.3	17.1
H17	-47.7	-6.8	-58.6	-10.1
C18	–	-6.4	–	-16.5
O19	–	6.0	–	17.9
S28	-21.9		-12.4	–
O37	21.5		13.9	–

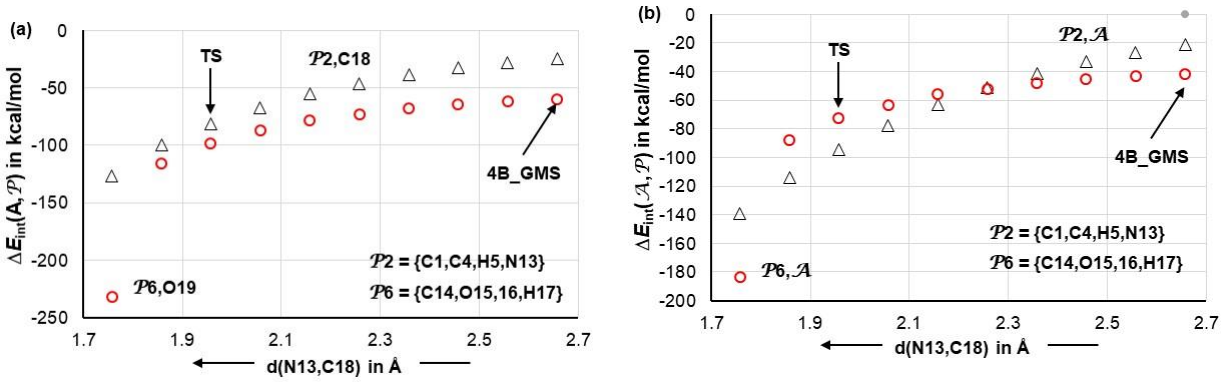

Figure B12. Trends in the interaction energy between indicated (i) atoms and a molecular fragment $\mathcal{P}$ (part a) and (ii) molecular fragment A and indicated molecular fragment P (part b). Data was obtained on simulating a CN-bond formation by scanning d(C18,13) from the value observed in the **4B_GMS** 3-MC.

End of Part B5

Part B6

Data pertaining to the 1st and 2nd proton transfers

Table B10. Energies (in a.u.) and associated changes (in kcal/mol) relative to GMS for 2-MC of proline (**1**) acetone (**2**) and 3-MC of proline (**1**) and acetone (**2**) and DMSO solvent molecule (**3**).

Data for LEC								
	E	ΔE	E_{ZPVE}	ΔE_{ZPVE}	H	ΔH	G	ΔG
	3-MC							
4A_GMS	-1147.8503	0.00	-1147.5407	0.00	-1147.5183	0.00	-1147.5943	0.00
4A_LM-3	-1147.8491	0.78	-1147.5395	0.72	-1147.5170	0.81	-1147.5942	0.02
5A_TS	-1147.8365	8.70	-1147.5257	9.42	-1147.5056	7.95	-1147.5740	12.72
5A_eq	-1147.8538	-2.18	-1147.5385	1.38	-1147.5186	-0.22	-1147.5864	4.93
5A_TS-1	-1147.8334	10.61	-1147.5225	11.43	-1147.5024	9.98	-1147.5714	14.36
5A_eq-1	-1147.8486	1.08	-1147.5334	4.60	-1147.5133	3.10	-1147.5813	8.15
5A_p-org	-1147.8468	2.22	-1147.5315	5.75	-1147.5117	4.15	-1147.5795	9.3
6A_TS	-1147.7985	32.49	-1147.4886	32.66	-1147.4687	31.09	-1147.5370	36.0
6A_eq	-1147.8300	12.75	-1147.5173	14.69	-1147.4968	13.46	-1147.5666	17.3
	2-MC							
4a_GMS	-594.5478	0.00	-594.3188	0.00	-594.3034	0.00	-594.3632	0.00
4a_p-org	-594.5467	0.65	-594.3182	0.38	-594.3026	0.51	-594.3637	-0.32
5a_TS	-594.5303	10.96	-594.3007	11.37	-594.2881	9.61	-594.3383	15.64
5a_eq	-594.5442	2.21	-594.3097	5.73	-594.2970	4.04	-594.3470	10.17
5a_p-org	-594.5368	6.86	-594.3018	10.67	-594.2892	8.92	-594.3388	15.30
6a_TS	-594.4998	30.12	-594.2700	30.60	-594.2578	28.63	-594.3061	35.85
6a_eq	-594.5231	15.46	-594.2906	17.73	-594.2774	16.34	-594.3279	22.11
Data for HEC								
3-MC								
4B_GMS	-1147.8442	0.00	-1147.5338	0.00	-1147.5118	0.00	-1147.5862	0.00
5B_TS	-1147.8404	2.39	-1147.5289	3.08	-1147.5092	1.64	-1147.5761	6.35
5B_eq	-1147.8563	-7.58	-1147.5414	-4.75	-1147.5220	-6.14	-1147.5890	-1.59
5B_LM-1(GMS)	-1147.8590	-9.30	-1147.5437	-6.18	-1147.5237	-7.51	-1147.5907	-2.86
5B_LM-2	-1147.8573	-8.23	-1147.5422	-5.26	-1147.5222	-6.58	-1147.5899	-2.37
6B_TS	-1147.8379	3.96	-1147.5282	3.49	-1147.5082	2.26	-1147.5758	6.48
6B_LM-1-TS	-1147.8457	-0.95	-1147.5356	-1.14	-1147.5160	-2.66	-1147.5822	2.46
6B_LM_2-TS	-1147.8466	-1.52	-1147.5368	-1.86	-1147.5170	-3.30	-1147.5843	1.15
6B_eq	-1147.8505	-3.96	-1147.5372	-2.11	-1147.5170	-3.30	-1147.586	0.35
2-MC								
4b_GMS	-594.5460	0.00	-594.3171	0.00	-594.3017	0.00	-594.3623	0.00
4b_p-org	-594.5428	2.00	-594.3136	2.18	-594.2985	2.00	-594.3564	3.72
5b_TS	-594.5336	7.82	-594.3029	8.91	-594.2904	7.10	-594.3404	13.78
5b_eq	-594.5479	-1.18	-594.3138	2.03	-594.3008	0.57	-594.3520	6.50
6b_TS	-594.5405	3.46	-594.3112	3.71	-594.2985	1.97	-594.3481	8.97
6b_eq	-594.5456	0.23	-594.3130	2.55	-594.3000	1.06	-594.3506	7.37

Table B11. Ball and stick models of 3-MC (Part A) and 2-MC (Part B) involving the LEC of proline. (For relevant energies – see Table B10).

Part A

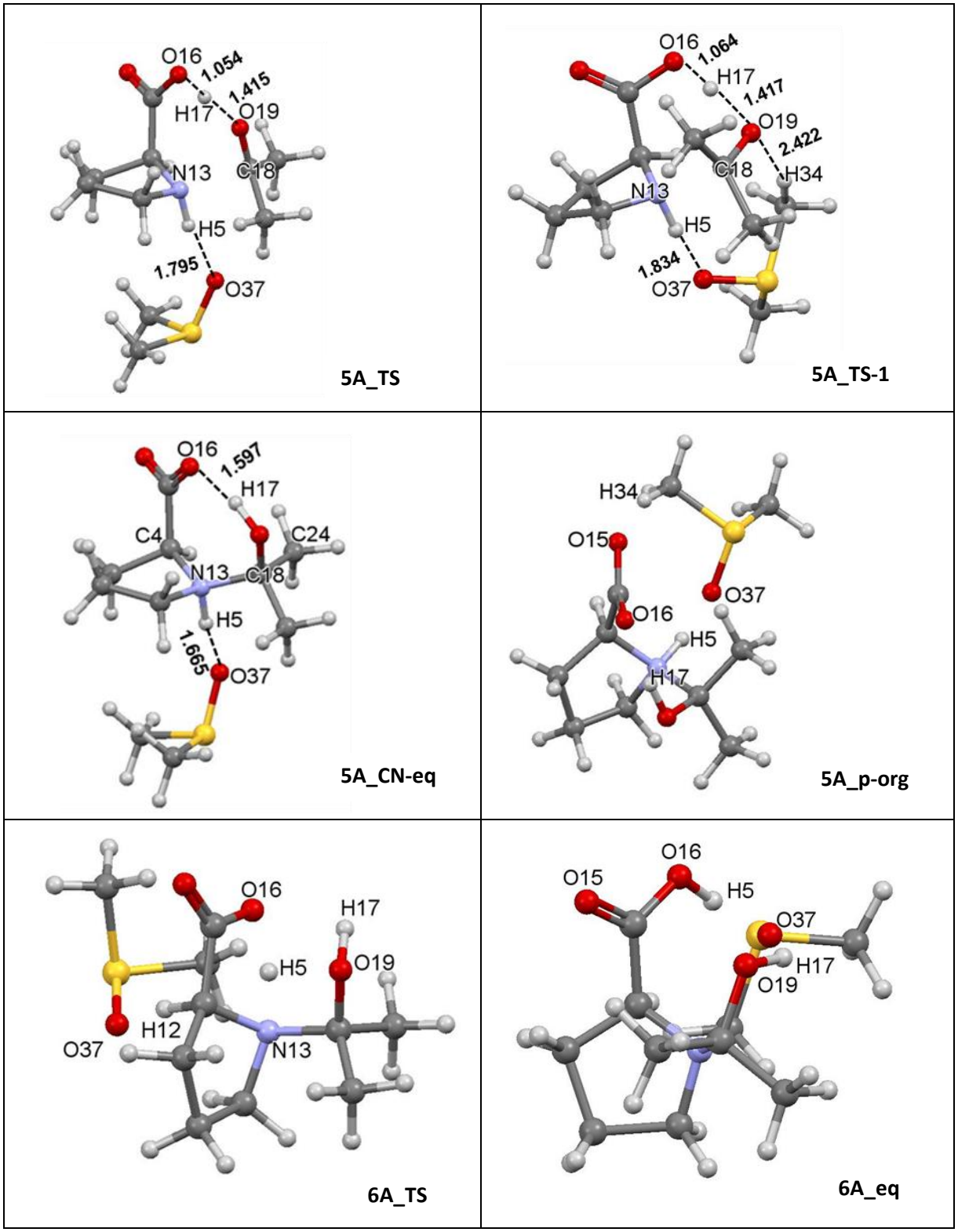

Part B

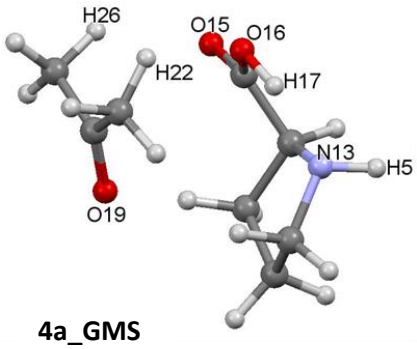

4a_GMS

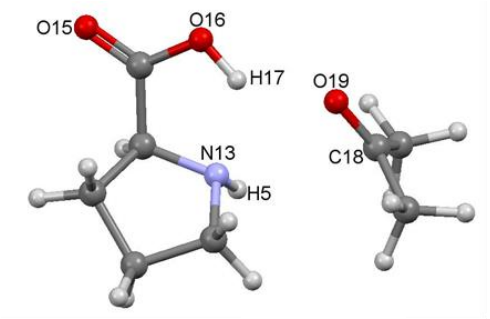

4a_p-org

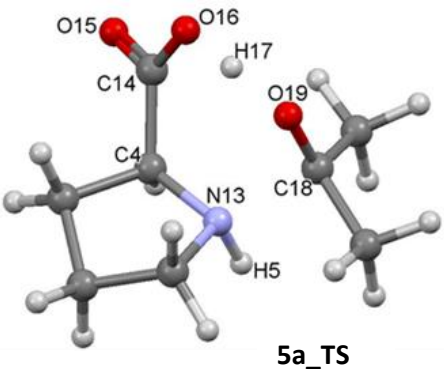

5a_TS

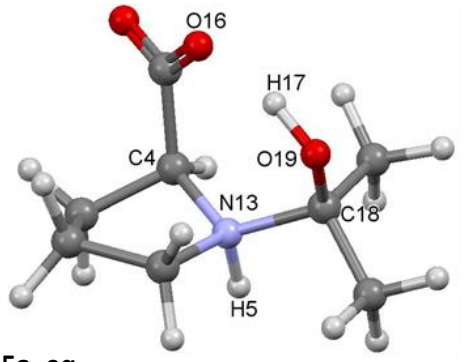

5a_eq

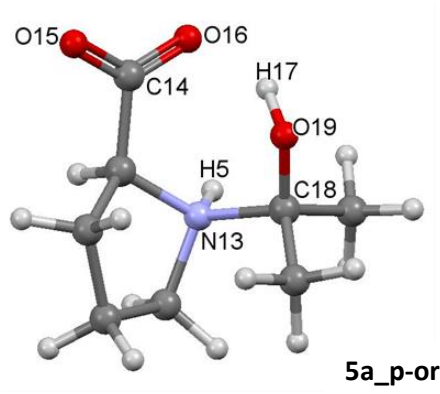

5a_p-org

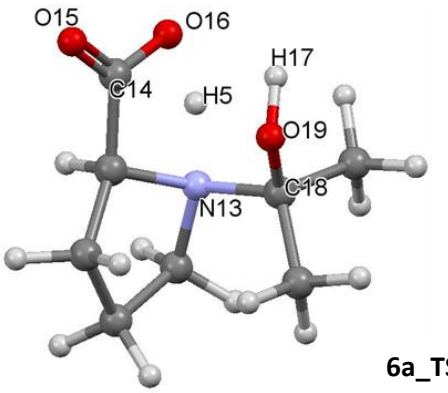

6a_TS

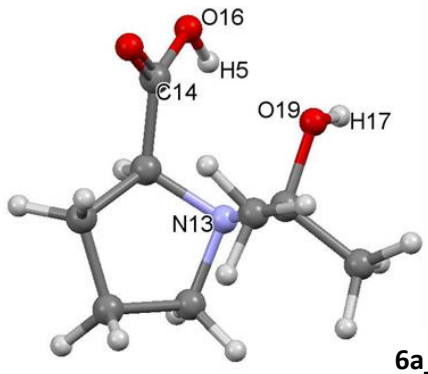

6a_eq

Table B 12. Ball and stick models of 3-MC (Part A) and 2-MC (Part B) involving the HEC of proline. (For relevant energies – see Table B10).

Part A

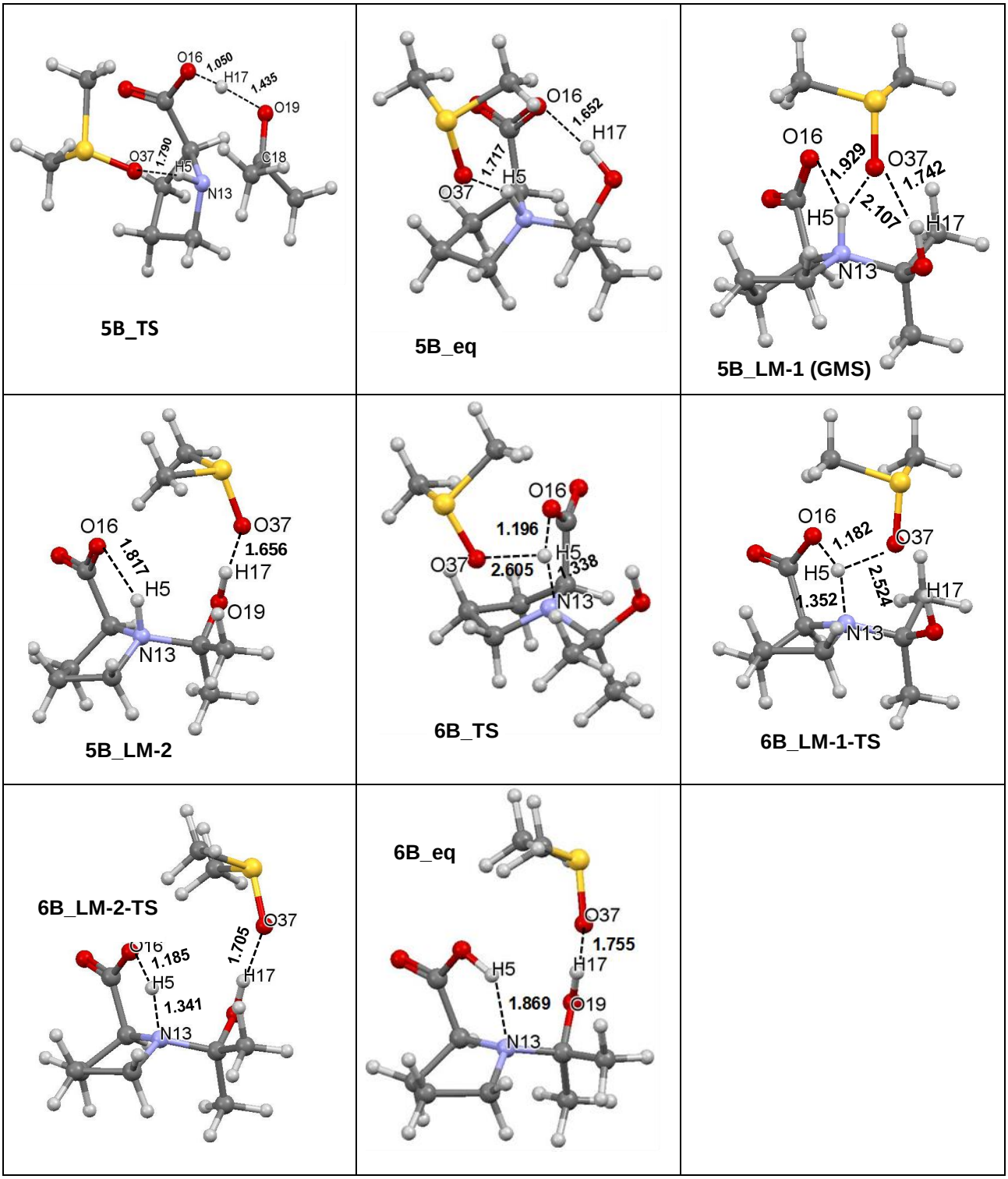

Part B

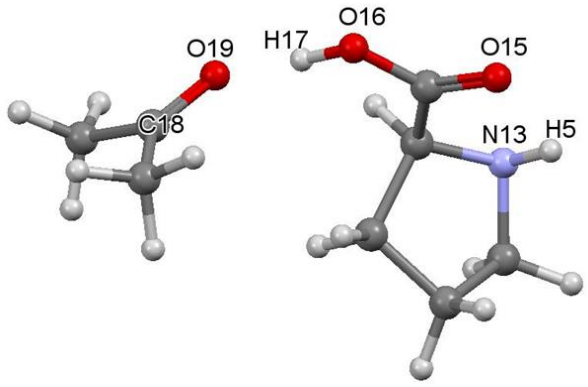

4b_GMS

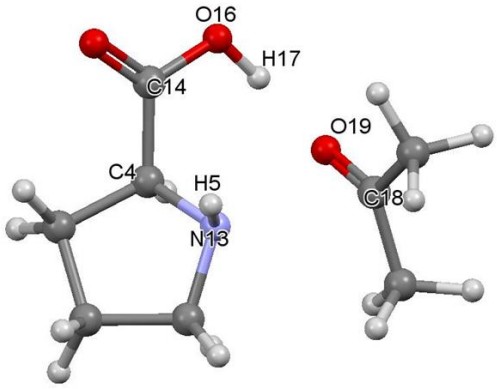

4b_p-org

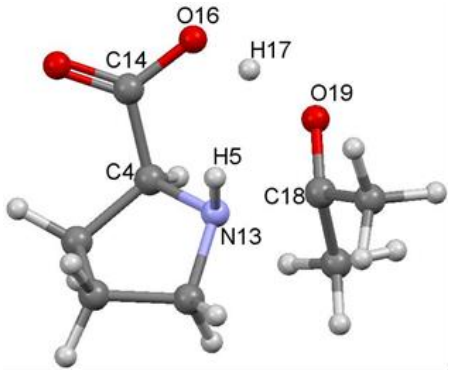

5b_TS

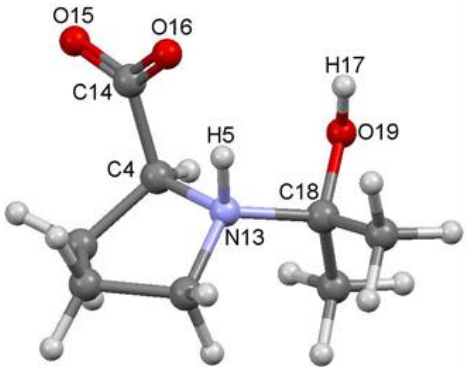

5b_eq

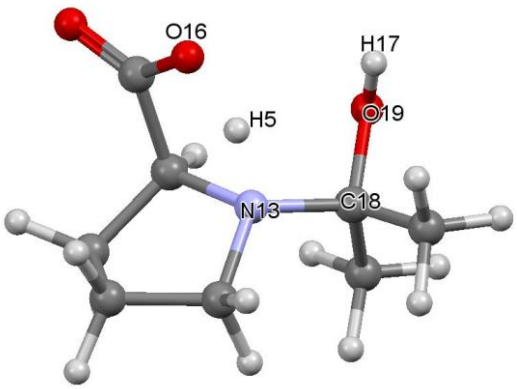

6b_TS

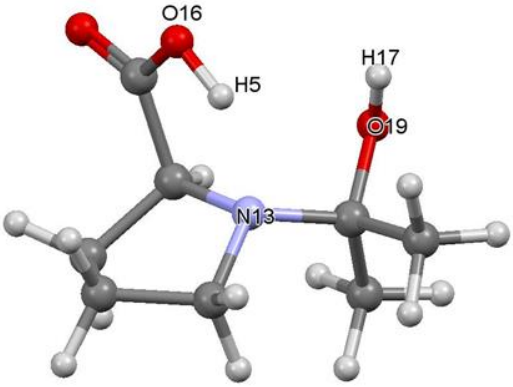

6b_eq

*Conformational search for **5B_GMS**.*

Once the equilibrium structure (**5B_eq**) is formed, the subsequent step in the multi-step mechanism is the 2nd H-transfer of H5 to O16. It was necessary to study **5B_eq** conformer distribution prior to the d(H5,O16) scan, hence the DA(C4,N13,C18,O19) was chosen and scanned in steps of 10° resulting in complex **5B_LM-1**. In another experiment, the d(H5,O37) reaction coordinate made of atoms of proline and the DMSO solvent was scanned in steps of –0.1Å resulting in complex **5B_LM-2** (Figure B15). The **5B_LM-1** is the lowest energy structure found, hence **5B_GMS**

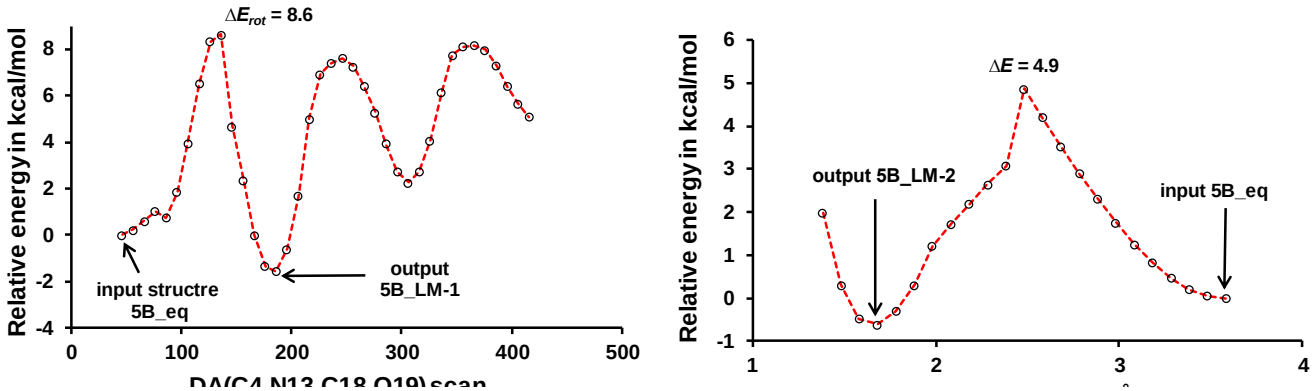

Figure B13. Data for scan of DA(C4,N13,C18,O19) dihedral angle and d(H5,O16) reaction coordinate using complex **5B_eq** as the input (in an effort to search the conformer distribution) leading to complexes **5B_LM-1 (GMS)** and **5B_LM-2**.

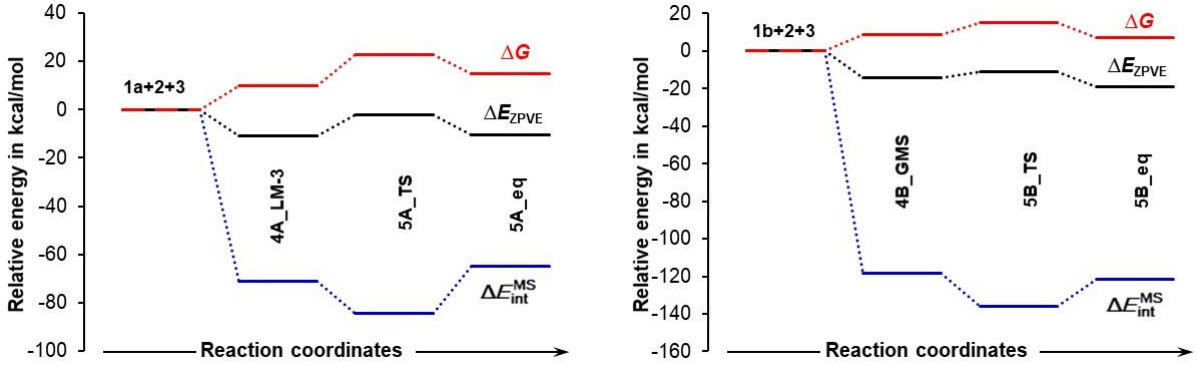

Figure B14. Relative to the energy of reactants, energy changes ΔE_{ZPVE} and ΔG and $\Delta E_{\mathrm{int}}^{\mathrm{MS}}$ computed for the formation of a N13–C18 bond from **4A_LM-3** and **4B_GMS** through transition states **5_TS**.

Appendix C

Supporting Information for Chapter 5

PART C1

Formation of proline higher energy conformer (1b) from the lowest energy conformer (1a) showing

Consecutive steps undertaken to obtain proline active conformer **1b** shown in Tables 1-4, starting from either conformer **1a** in the implicit solvation model or a complex of **1a** with indicated solvent molecules.

Structural change in the implicit solvation model

In Figure C1, we anticipated that the puckering of the pyrrolidine ring would result in the turning of H5 from the *anti* orientation in **1a** to the *syn* orientation in **1b**, thus DA(H12,C4,N13,H5) was scanned in steps of +6° this resulted in the re-orientation of H5 and formation of conformer **1b** as we had hoped.

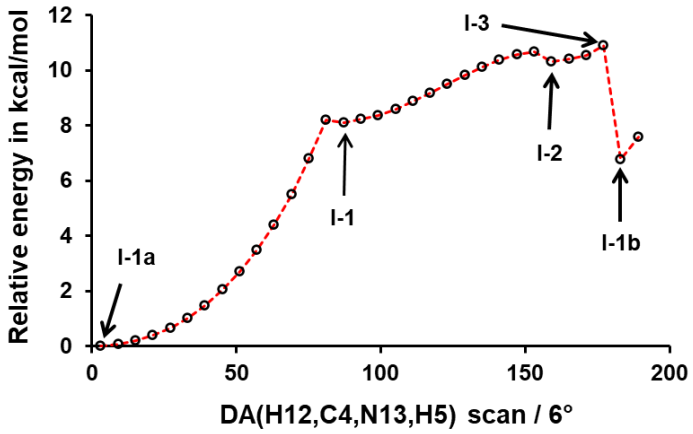

Figure C1. Data for scan of DA(H12,C4,N13,H5) in **I-1a** showing the associated intermediate conformers (shown in Table 1) leading to the formation of the active conformer **I-1b**

Structural change in the presence of an explicit solvent molecule of acetone

The influence of an explicit solvent molecule of acetone on the structural change of proline from **1a** to **1b** was established by conducting the DA(H12,C4,N13,H5) scan using complex **A-1a** (shown in Table 2). The data obtained (Figure C2) shows that an additional DA(12,C4,C14,O15) must be scanned to rotate the carboxylic group about the C4–C14 single bond before the active conformer **1b** is formed. A scan of DA(H12,C4,N13,H5) resulted in the formation of complex **A-3**, after energy optimisation **A-3** was further submitted for (DA(12,C4,C14,O15) scan. Notably data from the two DA scans show two turning points (**A-1** and **A-4**) which are not stationary points within the potential energy surface, and their energy terms was estimated using single point frequency calculation.

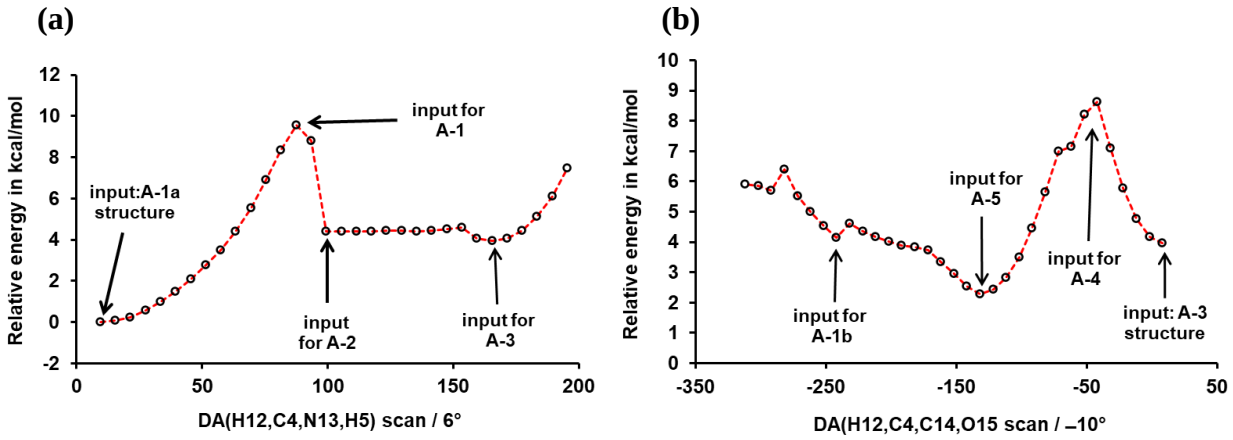

Figure C2. Data for scan of: (a) DA(H12,C4,N13,H5) using **A-1a** as the input structure and (b) DA(H12,C4,C14,O15) using **A-3** as the input structure, and the associated intermediate complexes (shown in Table 2.) along the change from **A-1a** to **A-1b**

Structural change in the presence of an explicit solvent molecule of DMSO

The effect of an explicit solvent molecule of DMSO was investigated by replacing the molecule of acetone in **A-1a** with a molecule of DMSO, the resulting energy optimised complex **D-1a** (Table 3) was submitted for DA(H12,C4,N133,H5) scan as in the case of acetone and data obtained resembles the data obtained when acetone was used. It shows that two DAs needed to be scanned before the formation of **D-1b**. When compared to structures obtained when a molecule of acetone is present, the complexes obtained in the presence of a molecule of DMSO have lower relative energies, indicating that DMSO has a better facilitating effect than acetone.

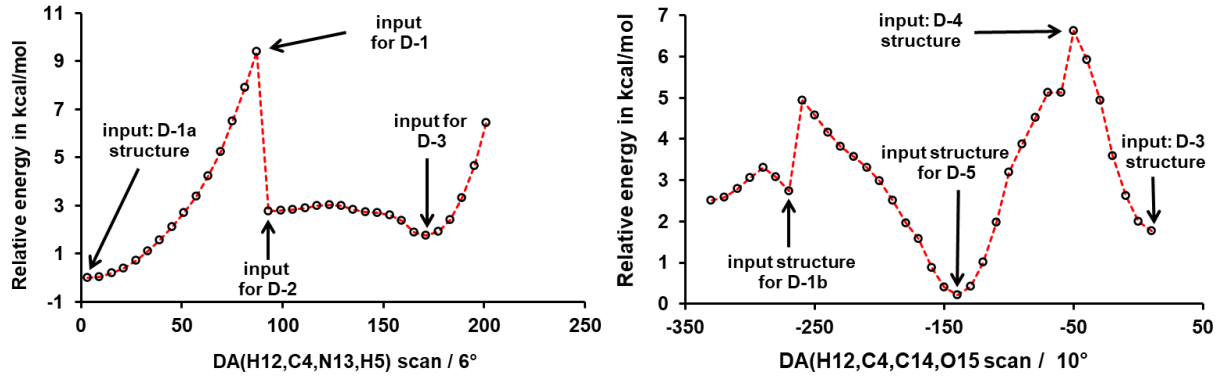

Figure C3. Data for scan of: (a) DA(H12,C4,N13,H5) using **D-1a** and (b) DA(H12,C4,C14,O15) using **D-3** as input structures, respectively and the associated intermediate complexes (shown in Table 3.) along the change from **D-1a** to **D-1b**

Structural change in the presence of explicit solvent molecule of acetone and DMSO

The effect of solvent molecules of acetone and DMSO on the structural change of proline from **1a** to **1b** was investigated by conducting DA(H12,C4,N13,H5) scan using complex **AD-1a** as in previous cases. When the DA(H12,C4,N13,H5) was scanned complex **AD-2** was located and the calculation terminated. After energy optimisation complex **AD-2** was submitted for DA(H12,C4,C14,O15) and complex **AD-3** was located which is analogous to **A-3** and **D-3**, further scanning of DA(H12,C4,C14,O15) resulted in the termination of the calculation. After energy optimisation, complex **AD-3** was further submitted for DA(H12,C4,C14,O15) scan and data obtained Figure C4c shows formation of a 3-MC of proline **1b**, acetone and DMSO (**AD-1b**).

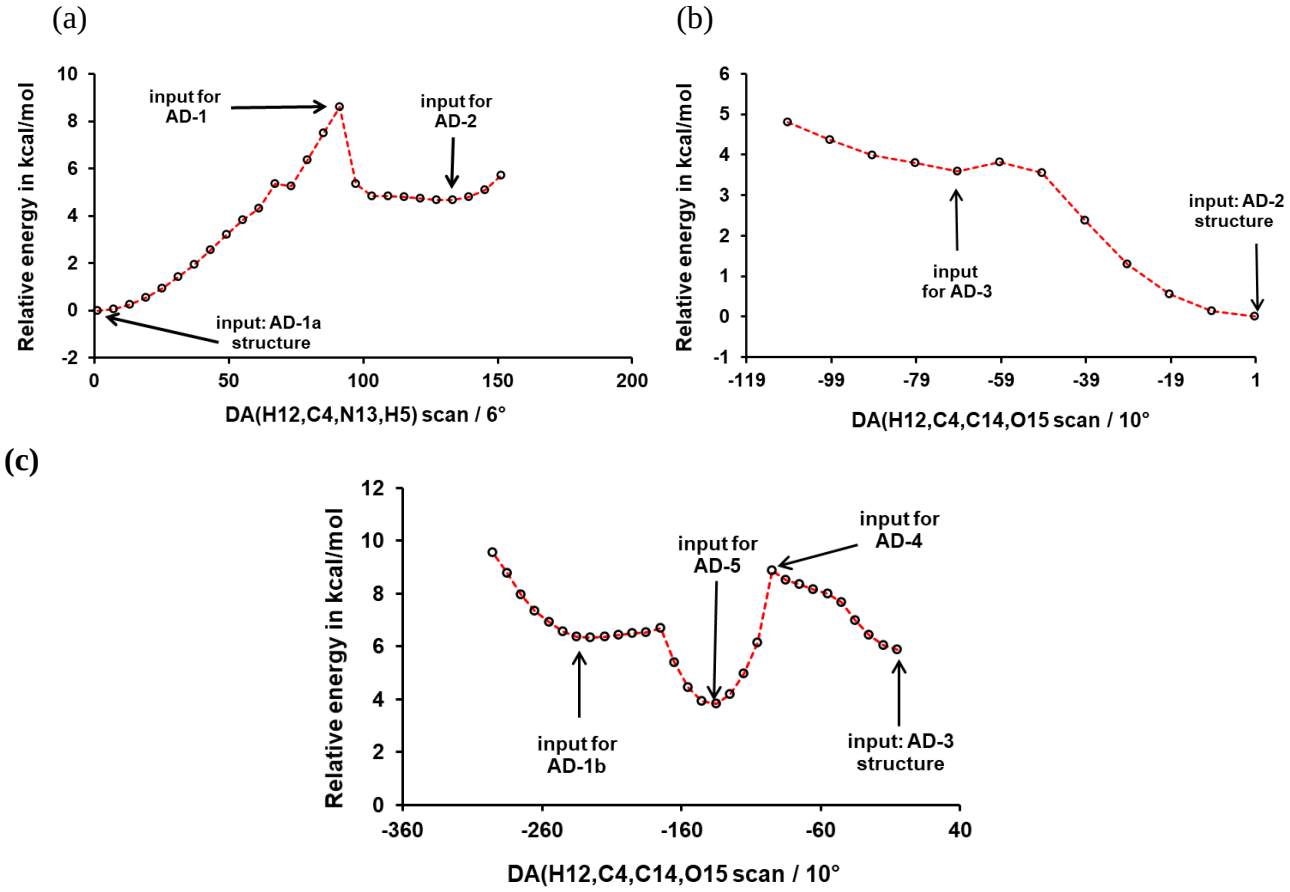

Figure C4. Data for scan of: (a) DA(H12,C4,N13,H5) using input structure **AD-1a**, (b) DA(H12,C4,C14,O15) using **AD-2** as the input structure, and a continuation of scan of DA(H12,C4,C14,O15) using input structure **AD-3**, resulting in the indicated 3-MCs (shown in Table 4.)

Table C1. Energies (in a.u.) and changes in energies (in kcal/mol, relative to the input **I-1a**) for intermediate conformers along the structural change from **1a** to **1b** in the implicit solvation model. Data obtained at the 6-311++G(d,p)/GD3 level.

	E	Δ	E_{ZPVE}	**Δ**	***H***	**Δ**	***G***	**Δ**
I-1a	-401.3116	0.00	-401.1671	0.00	-401.1591	0.00	-401.1991	0.00
I-1	-401.2980	8.54	-401.1543	8.06	-401.1457	8.37	-401.1867	7.76
I-2	-401.2945	10.70	-401.1503	10.54	-401.1418	10.83	-401.1831	10.02
I-3	-401.2936	11.31	-401.1494	11.11	-401.1408	11.44	-401.1823	10.57
I-1b	-401.3009	6.67	-401.1565	6.68	-401.1481	6.88	-401.1890	6.36

Table C2. Energies (in a.u.) and changes in energies (in kcal/mol, relative to the input **A-1a**,) for 2-MCs along the structural change from **A-1a** to **A-1b** in the presence of an explicit solvent molecule of acetone. Data obtained at the 6-311++G(d,p)/GD3 level.

	E	Δ	E_{ZPVE}	**Δ**	***H***	**Δ**	***G***	**Δ**
A-1a	-594.5489	0.00	-594.3202	0.00	-594.3048	0.00	-594.3651	0.00
A-1	-594.5336	9.57	-594.3065	8.65	-594.292	8.12	-594.349	9.77
A-2	-594.5419	4.38	-594.3133	4.33	-594.298	4.30	-594.358	4.73
A-3	-594.5426	3.95	-594.3135	4.23	-594.298	4.25	-594.358	4.56
A-4	-594.5351	8.63	-594.3061	8.87	-594.2908	8.84	-594.3504	9.17
A-5	-594.5453	2.28	-594.3165	2.35	-594.3011	2.34	-594.3613	2.36
A-1b	-594.5429	3.77	-594.3136	4.17	-594.2985	3.98	-594.3566	5.31

Table C3. Energies (in a.u.) and changes in energies (in kcal/mol, relative to the input **D-1a**,) for 2-MCs along the structural change from **D-1a** to **D-1b** in the presence of an explicit solvent molecule of DMSO. Data obtained at the 6-311++G(d,p)/GD3 level.

	E	Δ	E_{ZPVE}	**Δ**	***H***	**Δ**	***G***	**Δ**
D-1a	-954.6091	0.00	-954.3842	0.00	-954.3687	0.00	-954.4283	0.00
D-1	-954.5941	9.41	-954.3708	8.39	-954.3555	8.30	-954.4147	8.53
D-2	-954.6047	2.78	-954.3806	2.30	-954.3649	2.41	-954.4255	1.74
D-3	-954.6063	1.78	-954.3813	1.83	-954.3656	1.93	-954.4256	1.68
D-4	-954.5985	6.63	-954.3741	6.32	-954.3596	5.72	-954.4156	7.94
D-5	-954.6087	0.22	-954.3841	0.08	-954.3685	0.10	-954.4283	-0.04
D-1b	-954.6079	0.76	-954.3829	0.84	-954.3674	0.83	-954.4265	1.11

Table C 4. Energies (in a.u.) and changes in energies (in kcal/mol, relative to the input **AD-1a**,) for 3-MCs along the structural change from **AD-1a** to **AD-1b** Data obtained at the 6-311++G(d,p)/GD3 level.

	E	**Δ**	E_{ZPVE}	**Δ**	***H***	**Δ**	***G***	**Δ**
AD-1a	-1147.8491	0	-1147.5400	0	-1147.5200	0.00	-1147.5900	0.00
AD-1	-1147.8354	8.58	-1147.5270	7.56	-1147.5100	7.40	-1147.5800	8.40
AD-2	-1147.8417	4.62	-1147.5320	4.77	-1147.5100	4.60	-1147.5800	6.20
AD-3	-1147.8400	5.88	-1147.5300	5.98	-1147.5100	4.40	-1147.5800	8.90
AD-4	-1147.8350	8.83	-1147.5300	8.89	-1147.5000	8.90	-1147.5800	9.70
AD-5	-1147.8430	3.81	-1147.5300	4.03	-1147.5100	3.90	-1147.5900	5.50
AD-1b	-1147.8390	6.32	-1147.5300	6.53	-1147.5100	6.50	-1147.5800	7.60

PART C2

Computational details and coordinates for all structures

All calculations were performed in Gaussian 09 Rev. D01 at the RB3LYP/6–311++G(d,p) level of theory with Grimme's empirical correction for dispersion (GD3) in solvent (DMSO) using the implicit default solvation model. Frequency calculations were performed for the B3LYP-optimised local, global and transition state (TS) structures. None and one imaginary frequency were obtained for minimum energy (local and global) and TS structures, respectively. The lowest energy pathway connecting a given transition state with the two associated energy minima (intrinsic reaction coordinate – IRC) was calculated to verify each transition state. Topological calculations were performed in AIMAll (ver. 17.11.14) using B3LYP-generated wave functions

Structural change in the implicit solvation model

I-1a

Atom	X	Y	Z
C1	-0.094582	-1.361651	-0.836534
C2	-0.519069	-1.257337	0.630229
C3	-1.078823	0.170695	0.715158
C4	-0.124681	0.972254	-0.199243
H5	0.328124	0.248080	-2.102555
H6	0.659111	-2.130821	-1.013211
H7	-0.963254	-1.576134	-1.469605
H8	-1.249018	-2.018557	0.907550
H9	0.351123	-1.367125	1.285041
H10	-2.088094	0.204983	0.298301
H11	-1.115513	0.573585	1.727191
H12	-0.646920	1.777708	-0.719826
N13	0.462801	-0.016626	-1.134515
C14	1.009859	1.633409	0.600748
O15	0.830750	2.494407	1.435540
O16	2.218840	1.166547	0.292567
H17	2.019346	0.486584	-0.416837

Zero-point correction=	0.144439 (Hartree/Particle)
Thermal correction to Energy=	0.151574
Thermal correction to Enthalpy=	0.152518
Thermal correction to Gibbs Free Energy=	0.112465
Sum of electronic and zero-point Energies=	–401.167135
Sum of electronic and thermal Energies=	–401.160000
Sum of electronic and thermal Enthalpies=	–401.159056
Sum of electronic and thermal Free Energies=	–401.199110

I-1

Atom	X	Y	Z
C1	1.266280	-1.779280	-0.326890
C2	2.374240	-1.171030	0.534550
C3	2.566940	0.223450	-0.086950
C4	1.141710	0.618230	-0.598410
H5	-0.408610	-0.736370	-1.144410
H6	1.688980	-2.178640	-1.262810
H7	0.731380	-2.591210	0.170020
H8	2.031890	-1.085000	1.569100
H9	3.292390	-1.760100	0.521790
H10	2.955380	0.963300	0.611720
H11	3.265310	0.160590	-0.925720
H12	0.702180	1.385710	0.043850
N13	0.378930	-0.625400	-0.520720
C14	1.270050	1.267660	-1.975430
O15	1.484420	2.447530	-2.129430
O16	1.178190	0.459790	-3.053300
H17	0.988160	-0.449110	-2.775550

Zero-point correction=	0.143667 (Hartree/Particle)
Thermal correction to Energy=	0.151298
Thermal correction to Enthalpy=	0.152242
Thermal correction to Gibbs Free Energy=	0.111215
Sum of electronic and zero-point Energies=	–401.154297
Sum of electronic and thermal Energies=	–401.146666
Sum of electronic and thermal Enthalpies=	–401.145722
Sum of electronic and thermal Free Energies=	–401.186749

I-2

Atom	X	Y	Z
C1	0.975030	-1.674850	0.161950
C2	2.468840	-1.301050	0.240100
C3	2.506050	0.195870	-0.161080
C4	1.059220	0.486560	-0.690970
H5	0.640690	-1.211810	-1.796980
H6	0.796580	-2.726310	-0.066590
H7	0.471500	-1.443080	1.106030
H8	2.891490	-1.476530	1.231040
H9	3.036810	-1.899960	-0.476250
H10	2.728340	0.848220	0.684090
H11	3.267820	0.384410	-0.920750
H12	0.501520	1.026830	0.074960
N13	0.393950	-0.818170	-0.892080
C14	1.015370	1.367260	-1.927990
O15	0.501520	2.458710	-1.959180
O16	1.600940	0.888350	-3.051880
H17	2.052140	0.045650	-2.903010

Zero-point correction=	0.144190 (Hartree/Particle)
Thermal correction to Energy=	0.151779
Thermal correction to Enthalpy=	0.152723
Thermal correction to Gibbs Free Energy=	0.111384
Sum of electronic and zero-point Energies=	–401.150337
Sum of electronic and thermal Energies=	–401.142748
Sum of electronic and thermal Enthalpies=	–401.141804
Sum of electronic and thermal Free Energies=	–401.183143

I-3

Atom	X	Y	Z
C1	0.957400	-1.703620	0.115800
C2	2.415430	-1.251330	0.425420
C3	2.573770	0.102180	-0.316700
C4	1.114380	0.439380	-0.720600
H5	0.877430	-1.259220	-1.847090
H6	0.879200	-2.756490	-0.156520
H7	0.311480	-1.530330	0.980310
H8	2.570870	-1.138530	1.499740
H9	3.141450	-1.979970	0.061050
H10	3.016770	0.884060	0.301610
H11	3.204260	-0.014570	-1.202940
H12	0.619980	0.862780	0.156310
N13	0.467940	-0.859230	-1.003620
C14	0.961830	1.451640	-1.839400
O15	0.444510	2.533040	-1.699380
O16	1.446910	1.111190	-3.056270
H17	1.904190	0.259130	-3.046310

Zero-point correction=	0.144111 (Hartree/Particle)
Thermal correction to Energy=	0.151775
Thermal correction to Enthalpy=	0.152719
Thermal correction to Gibbs Free Energy=	0.111275
Sum of electronic and zero-point Energies=	–401.149435
Sum of electronic and thermal Energies=	–401.141772
Sum of electronic and thermal Enthalpies=	–401.140828
Sum of electronic and thermal Free Energies=	–401.182272

I-1b

Atom	X	Y	Z
C1	-0.409034	-1.241778	-1.036512
C2	-0.667988	-1.544788	0.469564
C3	-0.316231	-0.223429	1.209201
C4	-0.089847	0.767737	0.053782
H5	1.383941	-0.304084	-0.858383
H6	0.086511	-2.056235	-1.565140
H7	-1.349254	-1.026624	-1.551414
H8	-1.705493	-1.840218	0.636219
H9	-0.033680	-2.362083	0.817410
H10	-1.102845	0.109024	1.886810
H11	0.603217	-0.327367	1.789703
H12	-1.060128	1.175332	-0.262867
N13	0.429048	-0.022142	-1.082118
C14	0.773357	1.981069	0.337392
O15	0.900709	2.500917	1.419636
O16	1.383290	2.493824	-0.750523
H17	1.174427	1.920846	-1.512759

Zero-point correction=	0.144477 (Hartree/Particle)
Thermal correction to Energy=	0.151947
Thermal correction to Enthalpy=	0.152891
Thermal correction to Gibbs Free Energy=	0.111845
Sum of electronic and zero-point Energies=	–401.156469
Sum of electronic and thermal Energies=	–401.149000
Sum of electronic and thermal Enthalpies=	–401.148056
Sum of electronic and thermal Free Energies=	–401.189101

A-1a

Atom	X	Y	Z
C1	1.447424	-1.944949	-1.235958
C2	2.770948	-1.183862	-1.336853
C3	3.004681	-0.728297	0.112410
C4	1.578421	-0.408667	0.622558
H5	-0.040227	-1.649759	0.223397
H6	0.925059	-2.031664	-2.190390
H7	1.617168	-2.954279	-0.841488
H8	3.581787	-1.802531	-1.723159
H9	2.658235	-0.319088	-1.998044
H10	3.418920	-1.549197	0.702108
H11	3.677314	0.124652	0.204282
H12	1.444915	-0.706344	1.663677
N13	0.657287	-1.123590	-0.290277
C14	1.261214	1.092497	0.561426
O15	1.808497	1.929556	1.247269
O16	0.309539	1.392712	-0.322878
H17	0.080646	0.489865	-0.704651
C18	-1.782236	1.546244	2.519926
H19	-1.271224	2.286602	1.895705
H20	-2.777196	1.942087	2.739545
H21	-1.219014	1.399954	3.440651
C22	-2.806013	0.247118	0.554162
H23	-2.686581	-0.670937	-0.019819
H24	-3.839520	0.325223	0.907391
H25	-2.618057	1.117486	-0.079868
O26	-1.225413	-0.727516	2.055260
C27	-1.878360	0.256395	1.744145

Zero-point correction=	0.228661 (Hartree/Particle)
Thermal correction to Energy=	0.243110
Thermal correction to Enthalpy=	0.244054
Thermal correction to Gibbs Free Energy=	0.183836
Sum of electronic and zero-point Energies=	–594.320234
Sum of electronic and thermal Energies=	–594.305785
Sum of electronic and thermal Enthalpies=	–594.304841
Sum of electronic and thermal Free Energies=	–594.365059

Structural change in the presence of an explicit solvent molecule of acetone

A-1

Atom	X	Y	Z
C1	1.563180	-2.120600	-1.009930
C2	2.669760	-1.123410	-1.389620
C3	3.147250	-0.597920	-0.025620
C4	1.835010	-0.511330	0.795860
H5	0.067720	-1.635610	0.479810
H6	0.768350	-2.185410	-1.758630
H7	1.979720	-3.128750	-0.895930
H8	3.472200	-1.586280	-1.965510
H9	2.260850	-0.303250	-1.987450
H10	3.807400	-1.323930	0.454960
H11	3.672420	0.355930	-0.079440
H12	2.035850	-0.597110	1.867050
N13	1.059820	-1.628920	0.287750
C14	1.211270	0.881700	0.618910
O15	1.547540	1.845380	1.267450
O16	0.265470	1.010910	-0.333610
H17	0.080680	0.135120	-0.710320
C18	-1.837780	1.427940	2.546990
H19	-1.169360	2.165220	2.088630
H20	-2.772790	1.940030	2.785410
H21	-1.369460	1.041580	3.451510
C22	-2.980280	0.617890	0.393330
H23	-2.940960	-0.180830	-0.346480
H24	-4.003720	0.716750	0.770230
H25	-2.713990	1.573750	-0.065220
O26	-1.498880	-0.759690	1.661780
C27	-2.059030	0.320570	1.548600

Zero-point correction=	0.227185 (Hartree/Particle)
Thermal correction to Energy=	0.240800
Thermal correction to Enthalpy=	0.241744
Thermal correction to Gibbs Free Energy=	0.184153
Sum of electronic and zero-point Energies=	–594.306453
Sum of electronic and thermal Energies=	–594.292838
Sum of electronic and thermal Enthalpies=	–594.291894
Sum of electronic and thermal Free Energies=	–594.349485

A-2

Atom	X	Y	Z
C1	0.745681	-1.337629	-0.622071
C2	1.942492	-1.038456	-1.524372
C3	2.827509	-0.171092	-0.616161
C4	2.586400	-0.754675	0.812936
H5	0.763551	-1.604730	1.463629
H6	0.067436	-0.472673	-0.602999
H7	0.169449	-2.209257	-0.940327
H8	2.454789	-1.967880	-1.787948
H9	1.661020	-0.525523	-2.445488
H10	3.883889	-0.186768	-0.882116
H11	2.488077	0.867814	-0.658157
H12	3.441688	-1.363100	1.120089
N13	1.392529	-1.594270	0.672193
C14	2.559560	0.401297	1.814689
O15	3.595126	0.888248	2.223688
O16	1.389916	0.915653	2.206043
H17	0.580585	0.444425	1.888832
C18	-1.786091	1.618274	0.367371
H19	-2.140419	1.473313	-0.656712
H20	-2.403707	2.407779	0.807422
H21	-0.743449	1.932712	0.363270
C22	-3.333002	-0.282266	1.140959
H23	-3.381562	-1.111885	1.844391
H24	-4.103433	0.458698	1.370113
H25	-3.534760	-0.646715	0.128206
O26	-1.052610	-0.146182	1.800799
C27	-1.972451	0.354596	1.162251

Zero-point correction=	0.228587 (Hartree/Particle)
Thermal correction to Energy=	0.242990
Thermal correction to Enthalpy=	0.243934
Thermal correction to Gibbs Free Energy=	0.184401
Sum of electronic and zero-point Energies=	–594.313328
Sum of electronic and thermal Energies=	–594.298925
Sum of electronic and thermal Enthalpies=	–594.297981
Sum of electronic and thermal Free Energies=	–594.357514

A-3

Atom	X	Y	Z
C1	1.241542	-2.343343	-0.288372
C2	1.062910	-1.103213	-1.199987
C3	1.888217	0.012750	-0.507166
C4	2.459793	-0.681295	0.769478
H5	0.728341	-1.520135	1.494098
H6	0.352089	-2.972584	-0.232927
H7	2.069586	-2.962087	-0.647942
H8	1.405432	-1.296609	-2.218192
H9	0.009536	-0.821879	-1.255861
H10	2.696026	0.393708	-1.133312
H11	1.254443	0.860573	-0.242056
H12	3.455559	-1.068398	0.545356
N13	1.588437	-1.837138	1.055345
C14	2.646591	0.263152	1.948641
O15	3.743899	0.577841	2.359937
O16	1.552496	0.779145	2.522936
H17	0.697391	0.515130	2.098878
C18	-1.400098	2.055118	0.431297
H19	-1.200374	2.038522	-0.646093
H20	-2.286177	2.676909	0.578816
H21	-0.544474	2.485606	0.949717
C22	-2.956055	0.009144	0.478538
H23	-2.949193	-1.055920	0.704203
H24	-3.771389	0.494328	1.025850
H25	-3.145746	0.176150	-0.584880
O26	-0.840480	0.027354	1.558484
C27	-1.660089	0.646879	0.885742

Zero-point correction=	0.229097 (Hartree/Particle)
Thermal correction to Energy=	0.243572
Thermal correction to Enthalpy=	0.244516
Thermal correction to Gibbs Free Energy=	0.184801
Sum of electronic and zero-point Energies=	–594.313489
Sum of electronic and thermal Energies=	–594.299014
Sum of electronic and thermal Enthalpies=	–594.298070
Sum of electronic and thermal Free Energies=	–594.357785

A-4

Atom	X	Y	Z
C1	1.290770	-2.349220	-0.400340
C2	0.989670	-1.033850	-1.154090
C3	1.846110	0.030620	-0.422210
C4	2.440160	-0.735690	0.803080
H5	0.783490	-1.716420	1.462220
H6	0.453320	-3.048520	-0.392590
H7	2.152070	-2.856870	-0.846650
H8	1.228700	-1.104300	-2.216850
H9	-0.072270	-0.793830	-1.070130
H10	2.655710	0.408720	-1.048690
H11	1.241120	0.888800	-0.134790
H12	3.463750	-0.996290	0.518520
N13	1.646420	-1.968110	0.981470
C14	2.593610	-0.000170	2.137900
O15	3.363810	-0.393570	2.987100
O16	1.803270	1.052350	2.394040
H17	0.973940	1.023080	1.862580
C18	-1.580550	2.152150	0.197510
H19	-1.478030	2.023420	-0.885930
H20	-2.529630	2.665690	0.368180
H21	-0.750920	2.752680	0.568150
C22	-2.812100	-0.060410	0.642050
H23	-2.632910	-1.076640	0.989640
H24	-3.639430	0.380260	1.208470
H25	-3.113370	-0.061800	-0.408820
O26	-0.629530	0.376980	1.475900
C27	-1.588970	0.790680	0.834810

Zero-point correction=	0.229030 (Hartree/Particle)
Thermal correction to Energy=	0.243423
Thermal correction to Enthalpy=	0.244367
Thermal correction to Gibbs Free Energy=	0.184677
Sum of electronic and zero-point Energies=	–594.306096
Sum of electronic and thermal Energies=	–594.291702
Sum of electronic and thermal Enthalpies=	–594.290758
Sum of electronic and thermal Free Energies=	–594.350449

A-5

Atom	X	Y	Z
C1	2.914295	-2.17811	-0.60978
C2	1.453596	-2.416814	-0.994888
C3	0.702707	-1.883788	0.231884
C4	1.554314	-0.648273	0.643559
H5	3.599558	-0.776064	0.759127
H6	3.253493	-2.969018	0.074449
H7	3.586122	-2.165199	-1.471358
H8	1.196572	-1.831491	-1.883135
H9	1.236605	-3.466270	-1.201120
H10	-0.335267	-1.615451	0.039577
H11	0.718060	-2.634141	1.028390
H12	1.095780	0.259911	0.236326
N13	2.883984	-0.850775	0.044532
C14	1.596740	-0.489330	2.159200
O15	2.582421	-0.713036	2.831643
O16	0.459668	-0.094245	2.739535
H17	-0.265466	0.088276	2.084983
C18	-1.044803	2.736432	0.919300
H19	-0.494133	3.021794	0.016334
H20	-1.694871	3.576826	1.173677
H21	-0.337883	2.547064	1.725858
C22	-3.057513	1.684871	-0.283186
H23	-3.468059	0.718096	-0.570049
H24	-3.817310	2.260452	0.256306
H25	-2.790214	2.266688	-1.169186
O26	-1.567980	0.408823	1.059016
C27	-1.862202	1.512481	0.609536

Zero-point correction=	0.228766 (Hartree/Particle)
Thermal correction to Energy=	0.243196
Thermal correction to Enthalpy=	0.244140
Thermal correction to Gibbs Free Energy=	0.183965
Sum of electronic and zero-point Energies=	–594.316491
Sum of electronic and thermal Energies=	–594.302061
Sum of electronic and thermal Enthalpies=	–594.301117
Sum of electronic and thermal Free Energies=	–594.361291

A-1b

Atom	X	Y	Z
C1	1.033092	-0.965687	-1.070823
C2	1.587224	-2.384530	-0.792835
C3	1.340659	-2.604436	0.724832
C4	0.668424	-1.295627	1.194131
H5	1.990538	0.063041	0.411977
H6	1.603294	-0.408555	-1.815625
H7	-0.004200	-1.024968	-1.416141
H8	1.092477	-3.137828	-1.409085
H9	2.655671	-2.426282	-1.016191
H10	0.704542	-3.467728	0.928540
H11	2.278982	-2.748653	1.261357
H12	-0.421073	-1.398686	1.138990
N13	1.039835	-0.245975	0.217336
C14	1.016947	-0.853803	2.616156
O15	1.954278	-1.292738	3.247752
O16	0.228144	0.083718	3.150720
H17	-0.492116	0.374170	2.530291
C18	-0.195239	2.676502	0.793777
H19	-0.736719	3.628113	0.851983
H20	0.305571	2.495182	1.743258
H21	0.537428	2.761715	-0.009316
C22	-1.731739	1.525930	-0.908104
H23	-2.492233	0.751340	-0.994550
H24	-2.148009	2.496082	-1.196019
H25	-0.905728	1.315884	-1.592679
O26	-1.615153	0.838489	1.367281
C27	-1.196681	1.595041	0.493511

Zero-point correction=	0.229286 (Hartree/Particle)
Thermal correction to Energy=	0.243443
Thermal correction to Enthalpy=	0.244387
Thermal correction to Gibbs Free Energy=	0.186282
Sum of electronic and zero-point Energies=	–594.313594
Sum of electronic and thermal Energies=	–594.299436
Sum of electronic and thermal Enthalpies=	–594.298492
Sum of electronic and thermal Free Energies=	–594.356597

Structural change in the presence of an explicit solvent molecule of DMSO

D-1a

Atom	X	Y	Z
C1	1.373131	-1.818602	-0.432468
C2	2.313751	-1.144755	0.575493
C3	2.570291	0.222255	-0.073785
C4	1.203889	0.560840	-0.726847
H5	0.573421	-0.241420	-2.655620
H6	1.950625	-2.262495	-1.250248
H7	0.752054	-2.602077	0.004972
H7	1.808777	-1.019953	1.537782
H8	3.232528	-1.709869	0.745392
H9	2.884093	0.992437	0.630311
H10	3.344925	0.134536	-0.841233
H12	0.614095	1.209616	-0.073185
N13	0.517335	-0.728024	-0.959699
C14	1.371358	1.296382	-2.057827
O15	0.930479	0.590139	-3.098341
O16	1.864259	2.399939	-2.170615
H17	-0.397230	-0.728842	-0.502660
C18	-1.145094	-0.889825	2.786963
H19	-0.295129	-0.277338	2.486939
H20	-1.423852	-0.692539	3.822918
H21	-0.926784	-1.948227	2.651095
C22	-2.577896	1.304077	1.981012
H23	-3.373450	1.714653	1.360626
H24	-2.781768	1.503963	3.033888
H25	-1.609074	1.707052	1.683705
O26	-2.103066	-0.721520	0.271428
S27	-2.573454	-0.500691	1.720531

Zero-point correction=	0.224868 (Hartree/Particle)
Thermal correction to Energy=	0.239447
Thermal correction to Enthalpy=	0.240391
Thermal correction to Gibbs Free Energy=	0.180810
Sum of electronic and zero-point Energies=	–954.384220
Sum of electronic and thermal Energies=	–954.369641
Sum of electronic and thermal Enthalpies=	–954.368697
Sum of electronic and thermal Free Energies=	–954.428278

D-1

Atom	X	Y	Z
C1	1.705350	-2.033100	0.065340
C2	3.096260	-1.345010	-0.054260
C3	2.801000	0.085630	-0.553060
C4	1.371140	0.333060	0.010400
H5	-0.243230	-1.064900	-0.226860
H6	1.579480	-2.848890	-0.652130
H7	1.575040	-2.453780	1.072380
H7	3.582180	-1.306850	0.923180
H8	3.762590	-1.879360	-0.732710
H9	3.522430	0.823200	-0.198590
H10	2.773030	0.118200	-1.645250
H12	1.530870	0.598470	1.067860
N13	0.767780	-0.956840	-0.215150
C14	0.668290	1.455680	-0.720590
O15	0.637270	2.618200	-0.341140
O16	0.102940	1.087370	-1.884900
H17	0.195470	0.114230	-1.949060
C18	-1.614920	-0.676610	2.497120
H19	-0.644640	-0.246170	2.250320
H20	-2.007670	-0.259720	3.425240
H21	-1.543820	-1.760910	2.573570
C22	-2.657350	1.503160	1.184290
H23	-3.279820	1.880660	0.373970
H24	-3.030670	1.865730	2.143100
H25	-1.616760	1.791390	1.032350
O26	-2.132040	-0.777830	-0.151500
S27	-2.801980	-0.315310	1.156610

Zero-point correction=	0.223246 (Hartree/Particle)
Thermal correction to Energy=	0.237679
Thermal correction to Enthalpy=	0.238623
Thermal correction to Gibbs Free Energy=	0.179406
Sum of electronic and zero-point Energies=	–954.370842
Sum of electronic and thermal Energies=	–954.356409
Sum of electronic and thermal Enthalpies=	–954.355465
Sum of electronic and thermal Free Energies=	–954.414682

D-2

Atom	X	Y	Z
C1	1.666985	-1.903656	-0.482075
C2	3.034666	-1.522238	-1.047191
C3	3.105209	-0.010438	-0.768494
C4	2.226999	0.192654	0.513481
H5	0.694827	-1.090137	1.169332
H6	0.869434	-1.630663	-1.190552
H7	1.569796	-2.969280	-0.262899
H7	3.820523	-2.051300	-0.501307
H8	3.137068	-1.754480	-2.108662
H9	4.120261	0.355762	-0.617466
H10	2.678375	0.544698	-1.607376
H12	2.851665	0.485828	1.361575
N13	1.621467	-1.118574	0.760266
C14	1.306566	1.397082	0.280415
O15	1.754554	2.527784	0.314061
O16	0.018700	1.203902	-0.007777
H17	-0.326277	0.271906	0.106511
C18	-2.093116	0.257922	2.748997
H19	-1.466178	1.092391	2.434119
H20	-2.980008	0.606091	3.279324
H21	-1.531380	-0.436786	3.372042
C22	-3.397183	0.706068	0.364320
H23	-3.718302	0.307903	-0.597254
H24	-4.259423	1.056757	0.932337
H25	-2.659330	1.497477	0.230633
O26	-1.320931	-0.996424	0.499643
S27	-2.626754	-0.670540	1.274528

Zero-point correction=	0.224102 (Hartree/Particle)
Thermal correction to Energy=	0.238851
Thermal correction to Enthalpy=	0.239795
Thermal correction to Gibbs Free Energy=	0.179147
Sum of electronic and zero-point Energies=	–954.380555
Sum of electronic and thermal Energies=	–954.365806
Sum of electronic and thermal Enthalpies=	–954.364862
Sum of electronic and thermal Free Energies=	–954.425510

D-3

Atom	X	Y	Z
C1	2.185310	-1.929580	0.654920
C2	2.367698	-1.710399	-0.874573
C3	2.333521	-0.170466	-1.056608
C4	2.351739	0.363114	0.403602
H5	0.677681	-0.629746	1.000874
H6	1.500278	-2.744391	0.894765
H7	3.148758	-2.153911	1.122475
H7	3.307987	-2.140046	-1.226052
H8	1.558735	-2.180931	-1.436310
H9	3.173554	0.213757	-1.637485
H10	1.409904	0.134329	-1.552751
H12	3.386381	0.432217	0.747386
N13	1.672390	-0.662404	1.218089
C14	1.775965	1.764807	0.550709
O15	2.478881	2.725692	0.798732
O16	0.465611	1.931704	0.364827
H17	-0.041194	1.098240	0.134572
C18	-2.292863	-0.720023	2.049344
H19	-1.741433	0.101912	2.506273
H20	-3.304489	-0.788744	2.450677
H21	-1.769943	-1.664988	2.190556
C22	-3.187396	1.201122	0.280808
H23	-3.250138	1.537699	-0.753120
H24	-4.187701	1.096601	0.702473
H25	-2.577431	1.881870	0.874966
O26	-0.940765	-0.196722	-0.212047
S27	-2.402823	-0.441002	0.253425

Zero-point correction=	0.224955 (Hartree/Particle)
Thermal correction to Energy=	0.239681
Thermal correction to Enthalpy=	0.240625
Thermal correction to Gibbs Free Energy=	0.180651
Sum of electronic and zero-point Energies=	–954.381297
Sum of electronic and thermal Energies=	–954.366571
Sum of electronic and thermal Enthalpies=	–954.365627
Sum of electronic and thermal Free Energies=	–954.425601

D-4

Atom	X	Y	Z
C1	2.529000	-1.828310	0.865150
C2	1.640610	-1.690550	-0.376000
C3	2.046290	-0.309400	-0.908470
C4	2.426270	0.503680	0.361630
H5	1.799230	-0.385380	2.118290
H6	2.164710	-2.553380	1.595330
H7	3.543090	-2.124520	0.573320
H7	1.791620	-2.487640	-1.107390
H8	0.586690	-1.682220	-0.090150
H9	2.933960	-0.395630	-1.540010
H10	1.269250	0.158360	-1.511230
H12	3.381640	1.004630	0.181610
N13	2.579580	-0.482080	1.476490
C14	1.496710	1.627330	0.833730
O15	1.860970	2.379320	1.718890
O16	0.278590	1.766700	0.317680
H17	-0.070540	1.029830	-0.270380
C18	-2.009520	-0.941810	1.338580
H19	-1.318290	-0.254030	1.825840
H20	-2.922250	-1.063650	1.922780
H21	-1.540800	-1.910620	1.173250
C22	-3.105200	1.335290	0.246730
H23	-3.371320	1.888530	-0.653020
H24	-3.992020	1.162550	0.857420
H25	-2.329030	1.856910	0.806960
O26	-1.112730	0.024380	-1.007740
S27	-2.458310	-0.278590	-0.298760

Zero-point correction=	0.224381 (Hartree/Particle)
Thermal correction to Energy=	0.238005
Thermal correction to Enthalpy=	0.238950
Thermal correction to Gibbs Free Energy=	0.182908
Sum of electronic and zero-point Energies=	–954.374144
Sum of electronic and thermal Energies=	–954.360519
Sum of electronic and thermal Enthalpies=	–954.359575
Sum of electronic and thermal Free Energies=	–954.415617

D-5

Atom	X	Y	Z
C1	3.616430	-1.369624	0.184160
C2	2.412937	-2.139113	0.747221
C3	1.246921	-1.174347	0.478462
C4	1.921985	0.248240	0.494614
H5	3.673591	0.189811	1.505413
H6	4.578999	-1.701940	0.577126
H7	3.648377	-1.464467	-0.907326
H7	2.264605	-3.115818	0.280984
H8	2.545386	-2.290707	1.822893
H9	0.812106	-1.349573	-0.506960
H10	0.444514	-1.264641	1.212012
H12	1.641484	0.780972	-0.416251
N13	3.380329	0.043067	0.542420
C14	1.436438	1.066042	1.684614
O15	2.088493	1.211975	2.701793
O16	0.222792	1.597851	1.575068
H17	-0.201835	1.423861	0.677438
C18	-2.506903	-0.784414	0.015987
H19	-2.327640	-0.471994	1.044951
H20	-3.532222	-1.131473	-0.116632
H21	-1.806159	-1.562835	-0.280562
C22	-3.430008	1.782677	-0.349865
H23	-3.337031	2.726669	-0.885077
H24	-4.432166	1.373078	-0.482296
H25	-3.191364	1.909989	0.706340
O26	-0.834236	1.186848	-0.755570
S27	-2.237606	0.629577	-1.100431

Zero-point correction=	0.224658 (Hartree/Particle)
Thermal correction to Energy=	0.239267
Thermal correction to Enthalpy=	0.240212
Thermal correction to Gibbs Free Energy=	0.180403
Sum of electronic and zero-point Energies=	–954.384085
Sum of electronic and thermal Energies=	–954.369475
Sum of electronic and thermal Enthalpies=	–954.368531
Sum of electronic and thermal Free Energies=	–954.428339

D-1b

Atom	X	Y	Z
C1	1.122184	-2.309201	0.656675
C2	1.603036	-2.231318	2.135835
C3	1.869498	-0.725609	2.384755
C4	1.199828	-0.038085	1.175122
H5	2.309150	-0.924102	-0.276967
H6	1.637068	-3.073581	0.073068
H7	0.051201	-2.529323	0.620060
H7	0.839041	-2.620509	2.812033
H8	2.509607	-2.818819	2.292533
H9	1.468039	-0.370265	3.335677
H10	2.940214	-0.511807	2.363609
H12	0.132957	0.093994	1.369126
N13	1.346051	-0.980142	0.047615
C14	1.822618	1.304190	0.802433
O15	3.018413	1.424036	0.616563
O16	1.005736	2.344191	0.674706
H17	0.031812	2.087745	0.732115
C18	-1.460863	1.924300	-1.960259
H19	-0.418648	1.607531	-1.921627
H20	-1.956667	1.536346	-2.850915
H21	-1.539056	3.010169	-1.930000
C22	-1.938532	-0.477427	-0.708233
H23	-2.339912	-0.996007	0.161763
H24	-2.440039	-0.827748	-1.611684
H25	-0.855084	-0.602576	-0.777014
O26	-1.520145	1.767374	0.730654
S27	-2.339290	1.286351	-0.497117

Zero-point correction=	0.224990 (Hartree/Particle)
Thermal correction to Energy=	0.239559
Thermal correction to Enthalpy=	0.240503
Thermal correction to Gibbs Free Energy=	0.181373
Sum of electronic and zero-point Energies=	–954.382886
Sum of electronic and thermal Energies=	–954.368317
Sum of electronic and thermal Enthalpies=	–954.367372
Sum of electronic and thermal Free Energies=	–954.426503

Structural change in the presence of explicit solvent molecule of acetone and DMSO

AD-1a

Atom	X	Y	Z
C1	1.102264	-0.003492	-1.014833
C2	2.464308	-0.703684	-1.031605
C3	2.417608	-1.559799	0.243206
C4	1.664771	-0.648548	1.239699
H5	-0.134751	0.225415	0.657415
H6	1.093104	0.926218	-1.586882
H7	0.328046	-0.663153	-1.425821
H8	2.621345	-1.293284	-1.935826
H9	3.269590	0.034758	-0.965178
H10	1.828536	-2.463646	0.068982
H11	3.398017	-1.860880	0.612900
H12	1.051820	-1.229997	1.933235
N13	0.857796	0.274358	0.419529
C14	2.635963	0.172393	2.104371
O15	3.408645	-0.316016	2.903572
O16	2.553501	1.482993	1.889125
H17	1.831489	1.551145	1.192869
C18	-0.164147	3.266478	0.213133
O19	0.974852	3.606019	-0.067615
C20	-1.163268	2.871931	-0.845740
H21	-0.702581	2.880495	-1.832948
H22	-1.567306	1.882509	-0.613706
H23	-2.005896	3.571147	-0.826696
C24	-0.653355	3.228091	1.640953
H25	-1.443358	3.975749	1.769147
H26	-1.097966	2.252712	1.854068
H27	0.162328	3.438711	2.331855
C28	-2.225950	-2.143646	-0.356504
H29	-1.177973	-2.360004	-0.148181
H30	-2.816296	-3.060341	-0.389635
H31	-2.329823	-1.597346	-1.293145
C32	-2.428252	-2.105537	2.382342
H33	-2.731065	-1.568045	3.279993
H34	-2.960278	-3.055383	2.315344
H35	-1.348255	-2.256177	2.368963
S36	-2.897073	-1.069823	0.957295
O37	-1.977395	0.165042	1.012333

Zero-point correction=	0.309537 (Hartree/Particle)
Thermal correction to Energy=	0.331147
Thermal correction to Enthalpy=	0.332091
Thermal correction to Gibbs Free Energy=	0.254836
Sum of electronic and zero-point Energies=	–1147.539532
Sum of electronic and thermal Energies=	–1147.517922
Sum of electronic and thermal Enthalpies=	–1147.516978
Sum of electronic and thermal Free Energies=	–1147.594233

AD-1

Atom	X	Y	Z
C1	1.338190	-0.095170	-1.906060
C2	2.885060	-0.173690	-1.737530
C3	3.113260	-0.761620	-0.320650
C4	1.718970	-1.363670	0.029870
H5	-0.119560	-0.261060	-0.286380
H6	0.995280	0.889030	-2.232100
H7	1.009260	-0.825380	-2.663550
H8	3.325270	-0.814480	-2.503930
H9	3.345620	0.811410	-1.827490
H10	3.905450	-1.511300	-0.287690
H11	3.354930	0.030530	0.391810
H12	1.704420	-2.358110	-0.447780
N13	0.841870	-0.404900	-0.582710
C14	1.538600	-1.547840	1.518830
O15	1.746910	-2.602660	2.081890
O16	1.170560	-0.475570	2.230010
H17	1.008540	0.326320	1.684370
C18	-0.504390	2.635370	1.137880
O19	0.249520	2.055930	1.907290
C20	-0.188200	2.779720	-0.325310
H21	0.819820	2.427140	-0.530890
H22	-0.906850	2.176630	-0.887140
H23	-0.307310	3.819430	-0.641630
C24	-1.799730	3.237260	1.616050
H25	-1.827090	4.305780	1.383990
H26	-2.624320	2.764910	1.074880
H27	-1.922700	3.087650	2.687850
C28	-2.200880	-2.417940	1.126230
H29	-1.150830	-2.450310	1.416330
H30	-2.806990	-3.028610	1.796980
H31	-2.327800	-2.752480	0.097460
C32	-2.274090	-0.330050	2.906020
H33	-2.568450	0.696230	3.117880
H34	-2.783980	-1.013410	3.586500
H35	-1.191330	-0.439330	2.963510
S36	-2.816040	-0.700510	1.204490
O37	-1.912010	0.132100	0.276720

Zero-point correction=	0.307923 (Hartree/Particle)
Thermal correction to Energy=	0.329287
Thermal correction to Enthalpy=	0.330231
Thermal correction to Gibbs Free Energy=	0.254624
Sum of electronic and zero-point Energies=	–1147.527492
Sum of electronic and thermal Energies=	–1147.506129
Sum of electronic and thermal Enthalpies=	–1147.505185
Sum of electronic and thermal Free Energies=	–1147.580791

AD-2

Atom	X	Y	Z
C1	1.403947	-0.201037	-1.777753
C2	2.917261	-0.375955	-1.581276
C3	3.050428	-0.536334	-0.061130
C4	1.815697	-1.405013	0.270697
H5	-0.021811	-0.550362	-0.301080
H6	1.126727	0.851127	-1.666006
H7	1.080101	-0.539956	-2.766170
H8	3.267781	-1.282124	-2.085277
H9	3.488535	0.468654	-1.971031
H10	3.983279	-1.007617	0.253257
H11	2.974303	0.440093	0.423833
H12	2.077619	-2.459359	0.141189
N13	0.779660	-1.024833	-0.713404
C14	1.367202	-1.295360	1.724354
O15	1.364357	-2.252209	2.474918
O16	0.971373	-0.104164	2.182439
H17	0.978932	0.628003	1.510899
C18	-0.276983	2.592158	0.582372
O19	0.777896	1.967902	0.519897
C20	-0.886792	3.195523	-0.648299
H21	-0.161580	3.239762	-1.459812
H22	-1.712453	2.535452	-0.935466
H23	-1.305186	4.183739	-0.445516
C24	-1.001433	2.795383	1.882430
H25	-0.821132	3.825872	2.209475
H26	-2.077045	2.680884	1.743358
H27	-0.638224	2.110016	2.645883
C28	-2.196206	-2.403946	0.903455
H29	-1.185306	-2.466959	1.305933
H30	-2.879775	-3.042572	1.464649
H31	-2.207453	-2.676984	-0.150722
C32	-2.449161	-0.427377	2.784711
H33	-2.800285	0.570015	3.043839
H34	-2.995127	-1.175874	3.360393
H35	-1.372668	-0.509212	2.936385
S36	-2.803700	-0.684944	1.012593
O37	-1.793784	0.184970	0.241999

Zero-point correction=	0.309740 (Hartree/Particle)
Thermal correction to Energy=	0.331114
Thermal correction to Enthalpy=	0.332058
Thermal correction to Gibbs Free Energy=	0.257330
Sum of electronic and zero-point Energies=	–1147.531934
Sum of electronic and thermal Energies=	–1147.510560
Sum of electronic and thermal Enthalpies=	–1147.509616
Sum of electronic and thermal Free Energies=	–1147.584345

AD-3

Atom	X	Y	Z
C1	1.257580	-0.606634	-1.980610
C2	2.579095	0.136141	-1.620620
C3	2.732098	-0.052757	-0.100016
C4	1.981187	-1.382043	0.128989
H5	0.027050	-0.860911	-0.341321
H6	0.466929	0.077744	-2.293872
H7	1.430539	-1.306148	-2.803298
H8	3.422874	-0.320667	-2.143208
H9	2.554934	1.190154	-1.904253
H10	3.773224	-0.095567	0.225787
H11	2.237292	0.757427	0.441176
H12	2.628948	-2.212996	-0.164679
N13	0.816091	-1.344655	-0.772363
C14	1.574779	-1.677412	1.564841
O15	1.876430	-2.704514	2.134905
O16	0.830534	-0.768037	2.210921
H17	0.681647	0.075474	1.728639
C18	-0.519961	2.429138	0.907185
O19	0.223051	1.799745	1.649631
C20	-0.308213	2.474553	-0.580254
H21	0.706314	2.176070	-0.835317
H22	-1.013268	1.764529	-1.022208
H23	-0.527086	3.465633	-0.982743
C24	-1.696973	3.192426	1.450488
H25	-1.547306	4.262383	1.274239
H26	-2.602388	2.904312	0.908800
H27	-1.818878	3.010035	2.517027
C28	-2.076525	-2.597868	1.389693
H29	-1.099945	-2.503119	1.862403
H30	-2.770165	-3.149327	2.025873
H31	-1.992419	-3.082254	0.417851
C32	-2.567413	-0.293007	2.790969
H33	-2.916267	0.738153	2.785592
H34	-3.183607	-0.892300	3.462515
H35	-1.513784	-0.346086	3.062799
S36	-2.768031	-0.934124	1.094819
O37	-1.739492	-0.181431	0.231062

Zero-point correction=	0.310005 (Hartree/Particle)
Thermal correction to Energy=	0.331499
Thermal correction to Enthalpy=	0.332443
Thermal correction to Gibbs Free Energy=	0.257733
Sum of electronic and zero-point Energies=	–1147.529718
Sum of electronic and thermal Energies=	–1147.508224
Sum of electronic and thermal Enthalpies=	–1147.507279
Sum of electronic and thermal Free Energies=	–1147.581990

AD-4

Atom	X	Y	Z
C1	2.028915	-1.839374	-1.809560
C2	1.962471	-0.292903	-1.897533
C3	1.891966	0.175892	-0.422179
C4	1.914784	-1.150968	0.393846
H5	0.446261	-2.124869	-0.558804
H6	1.491657	-2.343176	-2.614836
H7	3.071198	-2.174335	-1.842505
H8	2.824542	0.120452	-2.425524
H9	1.064271	0.019998	-2.433878
H10	2.721942	0.830302	-0.149814
H11	0.960924	0.703814	-0.241343
H12	2.959209	-1.347748	0.676045
N13	1.460110	-2.218720	-0.504319
C14	1.153134	-1.159787	1.707168
O15	0.579713	-2.131072	2.148960
O16	1.178944	-0.034971	2.444922
H17	1.445868	0.759907	1.949299
C18	-0.160672	3.022587	1.307416
O19	0.940252	2.639830	1.680590
C20	-0.568499	2.960335	-0.140728
H21	0.306231	3.017748	-0.788203
H22	-1.047435	1.984737	-0.298074
H23	-1.288760	3.740185	-0.393618
C24	-1.178082	3.551247	2.284524
H25	-1.260477	4.635271	2.148095
H26	-2.166920	3.134678	2.074470
H27	-0.880426	3.336311	3.309973
C28	-2.400640	-2.694509	0.670245
H29	-1.479285	-2.946601	1.194552
H30	-3.281224	-3.030786	1.219364
H31	-2.404929	-3.112833	-0.335865
C32	-2.388242	-0.455978	2.260327
H33	-2.368210	0.630834	2.324547
H34	-3.281484	-0.841449	2.753932
H35	-1.480179	-0.887048	2.679385
S36	-2.485076	-0.880200	0.487294
O37	-1.142977	-0.454741	-0.136727

Zero-point correction=	0.309593 (Hartree/Particle)
Thermal correction to Energy=	0.331240
Thermal correction to Enthalpy=	0.332184
Thermal correction to Gibbs Free Energy=	0.256104
Sum of electronic and zero-point Energies=	–1147.525359
Sum of electronic and thermal Energies=	–1147.503712
Sum of electronic and thermal Enthalpies=	–1147.502768
Sum of electronic and thermal Free Energies=	–1147.578848

AD-5

Atom	X	Y	Z
C1	2.591490	-2.055831	-1.495142
C2	1.179046	-1.486954	-1.672951
C3	1.194108	-0.294175	-0.709814
C4	2.095439	-0.794984	0.469816
H5	2.576324	-2.763590	0.425554
H6	2.694567	-3.097858	-1.804052
H7	3.309820	-1.462965	-2.072695
H8	0.954409	-1.193601	-2.700967
H9	0.437236	-2.228359	-1.359459
H10	1.681224	0.564306	-1.177437
H11	0.205777	0.033632	-0.387105
H12	2.743252	0.018715	0.806438
N13	2.891724	-1.923577	-0.050712
C14	1.245580	-1.222983	1.663404
O15	1.003781	-2.383097	1.934106
O16	0.740542	-0.244161	2.416799
H17	0.934764	0.661158	2.052564
C18	0.006460	2.829346	1.185547
O19	1.012073	2.128150	1.262944
C20	-0.261380	3.656163	-0.036394
H21	0.628768	3.728241	-0.659900
H22	-1.054973	3.140905	-0.588092
H23	-0.632970	4.648905	0.227432
C24	-0.997510	2.901145	2.300258
H25	-0.894908	3.875966	2.789992
H26	-2.007806	2.836166	1.895239
H27	-0.830241	2.113028	3.032608
C28	-2.217467	-1.816891	0.092979
H29	-1.252860	-1.937448	0.585395
H30	-2.915092	-2.591502	0.414638
H31	-2.105811	-1.842700	-0.990186
C32	-2.758747	-0.321209	2.323134
H33	-3.159287	0.595568	2.753311
H34	-3.338925	-1.178624	2.667300
H35	-1.700875	-0.431653	2.563099
S36	-2.935768	-0.189240	0.510509
O37	-1.922892	0.872067	0.053279

Zero-point correction=	0.309925 (Hartree/Particle)
Thermal correction to Energy=	0.331254
Thermal correction to Enthalpy=	0.332198
Thermal correction to Gibbs Free Energy=	0.257610
Sum of electronic and zero-point Energies=	–1147.533103
Sum of electronic and thermal Energies=	–1147.511774
Sum of electronic and thermal Enthalpies=	–1147.510830
Sum of electronic and thermal Free Energies=	–1147.585418

AD-1b

Atom	X	Y	Z
C1	2.966385	-1.129861	-1.188409
C2	1.863598	-2.002747	-1.838996
C3	0.638044	-1.838649	-0.899727
C4	1.137612	-0.890997	0.210761
H5	2.863993	-1.877616	0.702591
H6	3.971266	-1.541272	-1.297283
H7	2.963703	-0.126152	-1.625709
H8	1.650052	-1.686838	-2.862382
H9	2.180686	-3.047667	-1.877472
H10	-0.229786	-1.414465	-1.405417
H11	0.337248	-2.794558	-0.468578
H12	0.893581	0.138848	-0.053678
N13	2.617764	-1.002968	0.240996
C14	0.568180	-1.143674	1.600020
O15	-0.015080	-2.159196	1.923711
O16	0.789959	-0.189270	2.508375
H17	1.112708	0.647241	2.090118
C18	0.246000	2.878623	1.251249
O19	1.242773	2.162961	1.269816
C20	-0.091733	3.703049	0.043968
H21	0.754870	3.757940	-0.639305
H22	-0.927706	3.196455	-0.450006
H23	-0.428374	4.703292	0.326459
C24	-0.675001	2.980515	2.435086
H25	-0.433089	3.907079	2.968784
H26	-1.714086	3.050341	2.111911
H27	-0.538860	2.136088	3.108409
C28	-2.938714	-1.525164	0.119694
H29	-2.084986	-2.062138	0.532550
H30	-3.882604	-1.965777	0.443702
H31	-2.891997	-1.498538	-0.968298
C32	-2.856766	-0.151595	2.486675
H33	-2.785008	0.803453	3.004329
H34	-3.791932	-0.648591	2.748794
H35	-1.995303	-0.780408	2.710404
S36	-2.879728	0.207474	0.694984
O37	-1.481810	0.733508	0.336154

Zero-point correction=	0.309891 (Hartree/Particle)
Thermal correction to Energy=	0.331438
Thermal correction to Enthalpy=	0.332382
Thermal correction to Gibbs Free Energy=	0.256907
Sum of electronic and zero-point Energies=	–1147.529127
Sum of electronic and thermal Energies=	–1147.507580
Sum of electronic and thermal Enthalpies=	–1147.506636
Sum of electronic and thermal Free Energies=	–1147.582111

PART C3

Data pertaining to interaction energies of molecular system (sum of covalent bonding, non-covalent bonding or long-distance interactions and inter molecular interaction energies)

Table C5. Variation in intramolecular interaction energy in proline conformers on moving from **1a** to **1b** in (i) the implicit solvation model (Part A) and (ii) in the presence of an explicit solvent molecule of acetone (Part B), (iii) in the presence of an explicit solvent molecule of DMSO Part C and (iv) the presence of explicit solvent molecules of acetone and DMSO Part D.
Part A in the implicit solvation model

	${}_{\text{intra}}E_{\text{int}}^{\text{MS}}$	Δ	C-B ${}_{\text{intra}}E_{\text{int}}^{\text{mol}}$	Δ	L-D ${}_{\text{intra}}E_{\text{int}}^{\text{mol}}$	Δ
I-1a	-4175.9	0.0	-4267.4	0.0	91.5	0.0
I-1	-4147.7	28.2	-4248.4	18.9	100.8	9.3
I-2	-4096.4	79.5	-4200.5	66.9	104.1	12.7
I-3	-4088.4	87.5	-4190.9	76.5	102.5	11.0
I-1b	-4128.7	47.2	-4228.2	39.2	99.5	8.1

Part B in the presence of a molecule of acetone

	C-B ${}_{\text{intra}}E_{\text{int}}^{\text{mol}}$					L-D ${}_{\text{intra}}E_{\text{int}}^{\text{mol}}$				
	Total	**1**	Δ	**2**	Δ	Total	**1**	Δ	**2**	Δ
A-1a	-6236.1	-4271.1	0.0	-1965.0	0.0	25.6	92.36	0.0	-66.75	0.0
A-1	-6232.2	-4268.1	3.0	-1964.1	0.8	34.8	102.5	10.2	-67.8	-1.0
A-2	-6228.6	-4278.1	-7.0	-1950.4	14.5	53.5	121.9	29.5	-68.36	-1.6
A-3	-6196.7	-4250.0	21.1	-1946.7	18.2	58.3	127.00	34.6	-68.68	-1.9
A-4	-6194.7	-4242.5	28.6	-1952.2	12.7	57.4	126.2	33.8	-68.8	-2.0
A-1b	-6212.4	-4263.9	7.2	-1948.5	16.5	51.0	119.5	27.2	-68.5	-1.8
A-5	-6197.8	-4251.1	20.1	-1946.8	18.2	50.2	120.6	28.2	-70.36	-3.6

Part C in the presence of a molecule of DMSO

	C-B ${}_{\text{intra}}E_{\text{int}}^{\text{mol}}$					L-D ${}_{\text{intra}}E_{\text{int}}^{\text{mol}}$				
	Total	**1**	Δ	**3**	Δ	Total	**1**	Δ	**3**	Δ
D-1a	-6268.8	-4281.1	0.0	-1987.7	0.0	106.1	98.3	0.0	7.8	0
D-1	-6270.1	-4286.4	-5.3	-1983.7	4.0	114.4	106	7.7	8.4	0.6
D-2	-6238.9	-4282.3	-1.2	-1956.6	31.1	136.1	126	27.7	10.1	2.3
D-3	-6215.4	-4258.7	22.4	-1956.7	31.0	142.9	132.8	34.5	10.1	2.3
D-4	-6209.1	-4248.7	32.4	-1960.4	27.3	135.8	125.3	27.0	10.5	2.7
D-5	-6234.0	-4268.0	13.1	-1966.0	21.7	133.5	123.8	25.5	9.7	1.9
D-1b	-6222.9	-4264.1	17.0	-1958.8	28.9	137.7	124.1	25.8	13.6	5.8

Part D in the presence of explicit solvent molecules of acetone and DMSO

	$^{\text{C-B}}_{\text{intra}}E^{\text{mol}}_{\text{int}}$							
	total		**1**		**2**		**3**	
		Δ		Δ		Δ		Δ
AD-1a	-8244.1	0.0	-4289.4	0.0	-1967.3	0.0	-1987.5	0.0
AD-1	-8289.9	-45.8	-4340.5	-51.1	-1960.8	6.5	-1988.6	-1.1
AD-2	-8208.0	36.1	-4267.1	22.3	-1951.3	16.0	-1989.7	-2.2
AD-3	-8208.0	36.1	-4259.6	29.7	-1959.0	8.3	-1989.3	-1.9
AD-4	-8197.7	46.4	-4247.1	42.2	-1963.0	4.3	-1987.6	-0.2
AD-5	-8201.3	42.8	-4258.0	31.3	-1947.7	19.6	-1995.5	-8.1
AD-1b	-8197.4	46.7	-4249.0	40.4	-1951.3	16.0	-1997.2	-9.7

	$^{\text{L-D}}_{\text{intra}}E^{\text{mol}}_{\text{int}}$							
	Total		**1**		**2**		**3**	
		Δ		Δ		Δ		Δ
AD-1a	44.3	0.0	98.7	0.0	-62.7	0.0	8.3	0.0
AD-1	65.4	21.1	123.6	24.9	-67.2	-4.5	9.0	0.7
AD-2	71.0	26.6	130.2	31.5	-68.7	-6.1	9.5	1.2
AD-3	70.0	25.7	127.6	28.9	-66.9	-4.2	9.2	0.9
AD-4	70.4	26.1	125.1	26.4	-65.3	-2.7	10.6	2.3
AD-5	63.2	18.8	121.8	23.1	-68.7	-6.1	10.1	1.8
AD-1b	61.9	17.5	120.9	22.2	-69.0	-6.3	9.9	1.6

Table C6. Strongest attractive and repulsive diatomic intermolecular interactions (in kcal/mol) in the indicated **2**-MCs involving proline (**1**), and a molecule of acetone (**2**)

A-1a

Atom A of **1**	Atom B of **2**	E_{int}(A,B)
Most attractive interactions		
C14	O26	-165.1
O16	C27	-113.3
N131	C27	-97.7
O15	C27	-96.2
H17	O26	-70.8
H5	O26	-61.4
C4	O26	-38.9
C1	O26	-32.8
Most repulsive interactions		
C1	C27	25.6
C4	C27	29.1
H5	C27	43.1
H17	C27	60.5
O15	O26	114.6
N13	O26	120.5
O16	O26	127.6
C14	C27	138.4
Total		-16.7

A-1

Atom A of **1**	Atom B of **2**	E_{int}(A,B)
Most attractive interactions		
C14	O26	-169.5
O16	C27	-118.8
O15	C27	-98.6
N13	C27	-95.2
H17	O26	-76.9
H5	O26	-69.2
C4	O26	-43.5
C1	O26	-34.5
Most repulsive interactions		
C1	C27	26.0
C4	C27	32.7
H5	C27	44.5
H17	C27	63.0
O15	O26	117.1
N13	O26	124.9
O16	O26	135.6
C14	C27	140.3
Total		-22.1

A-2

Atom A of **1**	Atom B of **2**	E_{int}(A,B)
Most attractive interactions		
C14	O26	-151.0
H17	O26	-138.3
O16	C27	-113.0
N13	C27	-87.6
O15	C27	-71.5
H5	O26	-56.3
C1	O26	-43.3
C4	O26	-36.7
Most repulsive interactions		
C4	C27	26.9
C1	C27	31.4
H5	C27	36.8
H17	C27	83.6
O15	O26	94.9
C14	C27	111.1
N13	O26	116.6
O16	O26	148.7
Total		-47.6

A-3

Atom A of **1**	Atom B of **2**	E_{int}(A,B)
Most attractive interactions		
C14	O26	-157.0
H17	O26	-142.1
O16	C27	-111.9
N13	C27	-79.2
O15	C27	-71.8
H5	O26	-58.7
C4	O26	-36.1
C1	O26	-36.1
Most repulsive interactions		
C4	C27	25.9
C1	C27	26.2
H5	C27	36.0
H17	C27	83.5
O15	O26	96.4
N13	O26	108.1
C14	C27	114.0
O16	O26	149.9
Total		-52.9

A-4

Atom A of **1**	Atom B of **2**	E_{int}(A,B)
Most attractive interactions		
C14	O26	-163.6
H17	O26	-133.7
O16	C27	-108.9
N13	C27	-74.3
O15	C27	-74.2
H5	O26	-49.4
C4	O26	-35.3
C1	O26	-34.5
Most repulsive interactions		
C4	C27	25.2
C1	C27	25.6
H5	C27	32.5
H17	C27	80.1
N13	O26	100.8
O15	O26	102.2
C14	C27	116.1
O16	O26	147.5
Total		-43.9

A-5

Atom A of **1**	Atom B of **2**	E_{int}(A,B)
Most attractive interactions		
C14	O26	-157.8
H17	O26	-143.4
O16	C27	-114.6
O15	C27	-74.1
N13	C27	-59.1
C4	O26	-30.8
H5	O26	-26.2
C1	O26	-24.7
Most repulsive interactions		
C1	C27	19.0
H5	C27	20.4
C4	C27	22.9
N13	O26	75.8
H17	C27	85.7
O15	O26	97.3
C14	C27	117.3
O16	O26	150.0
Total		-42.6

A-1b

Atom A of **1**	Atom B of **2**	E_{int}(A,B)
Most attractive interactions		
C14	O26	-165.6
H17	O26	-146.4
O16	C27	-120.7
N13	C27	-112.9
O15	C27	-79.0
C4	O26	-40.4
H5	O26	-36.6
C1	O26	-36.0
Most repulsive interactions		
C1	C27	30.7
H5	C27	31.4
C4	C27	31.5
H17	C27	90.3
O15	O26	100.4
N13	O26	120.3
C14	C27	127.4
O16	O26	153.3
Total		-52.1

Table C7. Strongest attractive and repulsive diatomic intermolecular interactions (in kcal/mol) in the indicated **2**-MCs involving proline (**1**), and a molecule of DMSO (**3**)

D-1a

Atom A of **1**	Atom B of **3**	E_{int}(A,B)
Most attractive interactions		
C14	O26	-126.4
N13	S27	-109.9
H17	O26	-95.7
O15	S27	-79.9
O16	S27	-76.2
H5	O26	-59.0
C1	O26	-39.4
C4	O26	-36.4
C14	C22	-10.6
C14	C18	-10.1
Most repulsive interactions		
N13	C18	10.3
C4	S27	29.4
C1	S27	31.7
H5	S27	46.8
H17	S27	60.4
O16	O26	88.6
O15	O26	98.2
C14	S27	106.0
N13	O26	134.6
Total		-37.4

D-1

Atom A of **1**	Atom B of **3**	E_{int}(A,B)
Most attractive interactions		
C14	O26	-163.3
N13	S27	-124.9
O16	S27	-108.4
O15	S27	-102.0
H5	O26	-96.8
H17	O26	-77.1
C4	O26	-45.2
C1	O26	-42.7
C14	C22	-15.9
C14	C18	-13.2
Most repulsive interactions		
O15	C18	10.0
N13	C22	10.6
O16	C22	11.2
O15	C22	11.4
N13	C18	12.0
C1	S27	35.4
C4	S27	37.9
H17	S27	59.8
H5	S27	63.9
O15	O26	111.7
O16	O26	131.9
C14	S27	141.2
N13	O26	147.6
Total		-4.9

D-2

Atom A of **1**	Atom B of **3**	E_{int}(A,B)
Most attractive interactions		
C14	O26	-166.6
H17	O26	-158.3
O16	S27	-143.9
N13	S27	-98.2
O15	S27	-90.0
H5	O26	-72.0
C1	O26	-43.9
C4	O26	-39.9
C14	C18	-14.1
C14	C22	-13.3
O16	H25	-11.7
O16	H19	-10.2
Most repulsive interactions		
O16	C18	12.8
O16	C22	12.8
C4	S27	30.8
C1	S27	31.5
H5	S27	46.6
H17	S27	102.5
O15	O26	104.7
N13	O26	126.6
C14	S27	138.3
O16	O26	166.0
Total		-89.6

D-3

Atom A of **1**	Atom B of **3**	E_{int}(A,B)
Most attractive interactions		
C14	O26	-171.2
H17	O26	-162.1
O16	S27	-135.6
N13	S27	-96.4
O15	S27	-85.2
H5	O26	-73.2
C4	O26	-39.4
C1	O26	-38.3
C14	C22	-12.5
C14	C18	-12.3
Most repulsive interactions		
O16	C18	11.4
O16	C22	12.3
C1	S27	29.4
C4	S27	29.8
H5	S27	47.2
H17	S27	100.1
O15	O26	104.9
N13	O26	120.3
C14	S27	134.3
O16	O26	165.1
	Total	-71.4

D-4

Atom A of **1**	Atom B of **3**	E_{int}(A,B)
Most attractive interactions		
C14	O26	-168.1
H17	O26	-162.9
O16	S27	-145.3
O15	S27	-90.2
N13	S27	-69.7
H5	O26	-31.2
C1	O26	-30.0
C4	O26	-29.3
C14	C18	-14.1
C14	C22	-13.9
O16	H25	-12.6
Most repulsive interactions		
O16	C18	12.7
O16	C22	13.0
C4	S27	24.3
C1	S27	25.1
H5	S27	27.1
N13	O26	81.7
O15	O26	103.8
H17	S27	105.0
C14	S27	140.8
O16	O26	166.4
Total		-67.5

D-5

Atom A of **1**	Atom B of **3**	E_{int}(A,B)
Most attractive interactions		
C14	O26	-175.7
H17	O26	-165.6
O16	S27	-136.6
O15	S27	-87.1
N13	S27	-65.9
C4	O26	-33.6
H5	O26	-28.3
C1	O26	-27.5
C14	C18	-13.3
C14	C22	-11.7
Most repulsive interactions		
O16	C22	11.4
O16	C18	12.1
C1	S27	22.3
H5	S27	22.8
C4	S27	25.0
N13	O26	82.8
H17	S27	102.0
O15	O26	107.1
C14	S27	138.0
O16	O26	165.7
Total		-56.1

D-1b

Atom A of **1**	Atom B of **3**	E_{int}(A,B)
Most attractive interactions		
C14	O26	-176.6
H17	O26	-166.0
O16	S27	-137.2
O15	S27	-90.4
N13	S27	-89.8
C4	O26	-37.0
H5	O26	-30.4
C1	O26	-29.5
N13	H25	-20.7
C14	C22	-16.1
C14	C18	-14.2
O16	H25	-10.5
Most repulsive interactions		
O15	C22	10.7
N13	C22	11.7
O16	C18	12.7
C14	H25	12.9
O16	C22	13.4
C1	S27	26.9
H5	S27	27.6
C4	S27	30.6
N13	O26	97.0
H17	S27	101.9
O15	O26	107.1
C14	S27	143.6
O16	O26	165.5
Total		-56.9

Table C8. Top eight strongest attractive and repulsive diatomic intermolecular interactions (in kcal/mol) in the indicated 3-MCs involving **1** (proline), **2** (acetone) and **3** (DMSO solvent molecule), upon moving from AD-1a (in **LEC**) to AD-1b (in **HEC**).
Part A. Molecules **1** and **2** in **AD-1a**

Atom A of 1	Atom B of 2	E_{int}(A,B)
Most attractive interactions		
C14	O19	-132.6
N13	C18	-111.0
O16	C18	-104.9
H17	O19	-89.5
O15	C18	-69.8
H5	O19	-47.2
C1	O19	-36.6
C4	O19	-30.9
Most repulsive interactions		
C4	C18	26.0
C1	C18	30.5
H5	C18	42.2
H17	C18	70.3
O15	O19	85.6
C14	C18	107.7
N13	O19	123.9
O16	O19	129.7
Total		-6.6

Part B. Molecules **1** and **3** in **AD-1a**

Atom A of **1**	Atom B of **3**	E_{int}(A,B)
Most attractive interactions		
C14	O37	-123.9
N13	S28	-112.3
H5	O37	-95.8
O16	S28	-79.5
O15	S28	-75.2
H17	O37	-58.5
C1	O37	-39.7
C4	O37	-37.1
C14	C33	-10.6
C14	C29	-10.1
Most repulsive interactions		
N13	C29	10.6
C4	S28	30.4
C1	S28	32.5
H17	S28	46.9
H5	S28	60.9
O15	O37	86.9
O16	O37	97.0
C14	S28	104.7
N13	O37	136.1
Total		-36.7

Part C. Molecules **2** and **3** in **AD-1a**

Atom A of **2**	Atom B of **3**	E_{int}(A,B)
Most attractive interactions		
C18	O37	-94.8
O19	S28	-80.1
H22	O37	-15.6
H26	O37	-13.7
Most repulsive interactions		
C18	S28	73.2
O19	O37	101.7
Total		-29.3

Part D. Molecules **1** and **2** in **AD-1**

Atom A of **1**	Atom B of **2**	E_{int}(A,B)
Most attractive interactions		
C14	O19	-147.1
H17	O19	-122.7
O16	C18	-111.5
N13	C18	-102.9
O15	C18	-71.9
H5	O19	-53.1
C4	O19	-38.2
C1	O19	-36.4
Most repulsive interactions		
C1	C18	30.4
C4	C18	30.4
H5	C18	44.2
H17	C18	80.3
O15	O19	93.0
C14	C18	111.6
N13	O19	124.4
O16	O19	144.8
Total		-43.4

Part E. Molecules **1** and **3** in **AD-1**

Atom A of **1**	Atom B of **3**	E_{int}(A,B)
Most attractive interactions		
C14	O37	-150.1
N13	S36	-119.0
O16	S36	-116.9
O15	S36	-96.4
H5	O37	-95.6
H17	O37	-78.3
C4	O37	-44.2
C1	O37	-43.8
C14	C32	-15.5
O16	H35	-15.5
C14	C28	-15.2
Most repulsive interactions		
N13	C32	10.4
O15	C28	10.8
O15	C32	11.1
O16	C28	11.4
N13	C28	11.4
C14	H35	11.7
O16	C32	12.2
C1	S36	34.5
C4	S36	36.7
H5	S36	61.6
H17	S36	67.0
O15	O37	101.8
O16	O37	128.9
C14	S36	138.0
N13	O37	145.8
Total		2.6

Part F. Molecules **2** and **3** in **AD-1**

Atom A of **2**	Atom B of **3**	E_{int}(A,B)
Most attractive interactions		
C18	O37	-130.3
O19	S36	-119.3
C18	C32	-11.5
H22	O37	-11.3
O19	H35	-10.3
Most repulsive interactions		
O19	C32	13.3
C18	S36	102.3
O19	O37	143.0
Total		-24.2

Part G. Molecules **1** and **2** in **AD-2**

Atom A of **1**	Atom B of **2**	E_{int}(A,B)
Most attractive interactions		
C14	O19	-156.2
H17	O19	-146.3
O16	C18	-121.4
N13	C18	-86.7
O15	C18	-75.3
H5	O19	-53.7
C1	O19	-39.8
C4	O19	-36.1
Most repulsive interactions		
C4	C18	26.9
C1	C18	28.5
H5	C18	40.8
H17	C18	90.6
O15	O19	97.3
N13	O19	112.6
C14	C18	118.2
O16	O19	154.0
Total		-46.7

Part H. Molecules **1** and **3** in **AD-2**

Atom A of **1**	Atom B of **3**	E_{int}(A,B)
Most attractive interactions		
C14	O37	-160.2
O16	S36	-124.2
N13	S36	-109.4
O15	S36	-103.8
H5	O37	-84.2
H17	O37	-82.4
C4	O37	-38.1
C1	O37	-37.7
C14	C32	-16.5
C14	C28	-15.8
O16	H35	-15.1
Most repulsive interactions		
N13	C28	11.1
O15	C28	11.3
O16	C28	11.7
C14	H35	12.1
O15	C32	12.2
O16	C32	12.8
C1	S36	29.9
C4	S36	32.1
H5	S36	56.0
H17	S36	67.7
O15	O37	109.1
N13	O37	129.4
O16	O37	140.5
C14	S36	145.8
Total		-5.5

Part I. Molecules **2** and **3** in **AD-2**

Atom A of **2**	Atom B of **3**	E_{int}(A,B)
Most attractive interactions		
C18	O37	-133.3
O19	S36	-113.5
H22	O37	-12.6
C18	C32	-9.7
Most repulsive interactions		
O19	C32	11.1
C18	S36	98.5
O19	O37	145.7
Total		-13.9

Part J. Molecules **1** and **2** in **AD-3**

Atom A of **1**	Atom B of **2**	E_{int}(A,B)
Most attractive interactions		
C14	O19	-150.5
H17	O19	-131.4
O16	C18	-112.1
N13	C18	-75.8
O15	C18	-71.6
H5	O19	-44.2
C4	O19	-32.2
C1	O19	-29.1
Most repulsive interactions		
C1	C18	23.7
C4	C18	25.1
H5	C18	35.7
H17	C18	82.7
O15	O19	94.1
N13	O19	94.2
C14	C18	112.1
O16	O19	147.8
Total		-31.5

Part K. Molecules **1** and **3** in **AD-3**

Atom A of **1**	Atom B of **3**	E_{int}(A,B)
Most attractive interactions		
C14	O37	-157.5
O16	S36	-129.4
N13	S36	-106.5
O15	S36	-95.7
H17	O37	-89.5
H5	O37	-83.7
C4	O37	-38.3
C1	O37	-37.8
C14	C28	-16.3
C14	C32	-14.4
O16	H35	-13.5
O16	H29	-11.3
Most repulsive interactions		
C14	H29	9.9
O15	C32	9.9
C14	H35	10.0
N13	C28	10.9
O15	C28	11.4
O16	C28	12.4
O16	C32	12.4
C1	S36	29.4
C4	S36	31.5
H5	S36	54.2
H17	S36	74.8
O15	O37	103.3
N13	O37	128.5
C14	S36	141.8
O16	O37	143.2
Total		-10.4

Part L. Molecules **2** and **3** in **AD-3**

Atom A of **2**	Atom B of **3**	E_{int}(A,B)
Most attractive interactions		
C18	O37	-134.2
O19	S36	-123.5
H22	O37	-15.7
C18	C32	-11.2
O19	H35	-9.5
Most repulsive interactions		
O19	C28	9.8
O19	C32	13.1
C18	S36	103.9
O19	O37	149.8
Total		-17.6

Part M. Molecules **1** and **2** in **AD-4**

Atom A of **1**	Atom B of **2**	E_{int}(A,B)
Most attractive interactions		
C14	O19	-151.6
H17	O19	-116.4
O16	C18	-112.6
O15	C18	-75.9
N13	C18	-52.9
C4	O19	-26.7
H5	O19	-26.1
C1	O19	-23.1
Most repulsive interactions		
C1	C18	18.4
C4	C18	20.9
H5	C18	21.0
N13	O19	66.5
H17	C18	77.5
O15	O19	96.3
C14	C18	116.8
O16	O19	144.1
Total		-24.0

Part N. Molecules **1** and **3** in **AD-4**

Atom A of **1**	Atom B of **3**	E_{int}(A,B)
Most attractive interactions		
C14	O37	-200.9
O15	S36	-134.1
O16	S36	-113.5
N13	S36	-93.6
H17	O37	-71.3
H5	O37	-62.0
C4	O37	-42.4
C1	O37	-37.7
C14	C32	-18.8
C14	C28	-17.3
O15	H29	-16.8
O15	H35	-16.6
O16	H35	-11.7
Most repulsive interactions		
N13	C28	10.4
O16	C28	10.5
O16	C32	12.9
C14	H29	13.1
O15	C32	13.5
O15	C28	13.5
C14	H35	14.8
C1	S36	29.5
C4	S36	32.8
H5	S36	44.1
H17	S36	58.6
N13	O37	114.6
O16	O37	133.1
O15	O37	147.2
C14	S36	169.5
Total		-18.6

Part O. Molecules **2** and **3** in **AD-4**

Atom A of 2	Atom B of 3	Eint(A,B)
Most attractive interactions		
C18	O37	-98.8
O19	S36	-95.4
H22	O37	-18.1
Most repulsive interactions		
O19	C32	11.0
C18	S36	81.5
O19	O37	115.4
Total		-4.3

Part P. Molecules **1** and **2** in **AD-5**

Atom A of **1**	Atom B of **2**	E_{int}(A,B)
Most attractive interactions		
C14	O19	-161.6
H17	O19	-147.3
O16	C18	-120.6
O15	C18	-76.5
N13	C18	-56.6
C4	O19	-30.3
H5	O19	-26.4
C1	O19	-25.2
Most repulsive interactions		
C1	C18	19.1
H5	C18	19.9
C4	C18	21.5
N13	O19	75.4
H17	C18	89.9
O15	O19	99.9
C14	C18	120.7
O16	O19	154.2
Total		-43.8

Part Q. Molecules **1** and **3** in **AD-5**

Atom A of **1**	Atom B of **3**	E_{int}(A,B)
Most attractive interactions		
C14	O37	-150.2
O16	S36	-117.8
O15	S36	-101.9
H17	O37	-73.6
N13	S36	-62.5
C4	O37	-26.1
H5	O37	-25.6
C1	O37	-24.8
C14	C32	-16.6
C14	C28	-16.1
O16	H35	-15.8
H11	O37	-14.6
O15	H29	-10.2
Most repulsive interactions		
O15	C28	11.6
O16	C28	12.0
C14	H35	12.1
O15	C32	12.3
O16	C32	12.7
C1	S36	22.1
C4	S36	23.3
H5	S36	23.6
H17	S36	63.3
N13	O37	69.2
O15	O37	105.0
O16	O37	128.9
C14	S36	140.6
Total		-19.0

Part R. Molecules **2** and **3** in **AD-5**

Atom A of **2**	Atom B of **3**	E_{int}(A,B)
Most attractive interactions		
C18	O37	-125.1
O19	S36	-109.4
H22	O37	-14.3
H26	O37	-9.8
C18	C32	-9.8
Most repulsive interactions		
O19	C32	11.3
C18	S36	94.9
O19	O37	137.4
Total		-24.8

Part S. Molecules **1** and **2** in 3-MC **AD-1b**

Atom A of **1**	Atom B of **2**	E_{int}(A,B)
Most attractive interactions		
C14	O19	-164.6
H17	O19	-140.9
O16	C18	-121.5
O15	C18	-80.3
N13	C18	-72.3
C4	O19	-35.8
C1	O19	-30.2
H5	O19	-29.3
H12	O19	-11.4
Most repulsive interactions		
H5	C18	21.8
C1	C18	22.4
C4	C18	25.6
H17	C18	89.0
N13	O19	98.5
O15	O19	101.4
C14	C18	127.2
O16	O19	152.5
Total		-47.8

Part T. Molecules **1** and **3** in 3-MC **AD-1b**

Atom A of **1**	Atom B of **3**	E_{int}(A,B)
Most attractive interactions		
C14	O37	-198.5
O15	S36	-127.9
O16	S36	-121.5
H17	O37	-80.4
N13	S36	-68.5
C4	O37	-35.8
C1	O37	-27.8
H5	O37	-27.0
C14	C32	-18.5
C14	C28	-17.4
O15	H29	-14.8
O15	H35	-14.5
H12	O37	-11.8
O16	H35	-10.7
Most repulsive interactions		
O16	C28	11.1
C14	H29	12.1
O16	C32	13.2
C14	H35	13.2
O15	C32	13.2
O15	C28	13.2
H5	S36	22.8
C1	S36	22.9
C4	S36	27.3
H17	S36	64.3
N13	O37	83.0
O15	O37	138.0
O16	O37	143.3
C14	S36	170.0
Total		-27.8

Part U. Molecules **2** and **3** in 3-MC **AD-1b**

Atom A of **2**	Atom B of **3**	E_{int}(A,B)
Most attractive interactions		
C18	O37	-131.1
O19	S36	-110.0
H22	O37	-12.7
Most repulsive interactions		
O19	C32	10.5
C18	S36	96.6
O19	O37	142.7
Total		-4.0

Appendix D

Supporting Information for Chapter 6

PART D1

Data pertaining to the relative stability of the zwitterion relative to the non-ionic conformer in the implicit solvent model

Table D1. Atomic charges on the zwitterion **1c** and the lower energy conformer of proline **1a**, the charge in atomic charge Δ represents (**1c** minus **1a**).

Atom A	Q(A)		Δ(1c–1a)
	1a	**1c**	
O15	-1.194	-1.246	-0.052
O16	-1.137	-1.232	-0.094
N13	-0.990	-0.948	0.042
C4	0.302	0.223	-0.078
C1	0.322	0.273	-0.049
H5	0.370	0.435	0.065
H17	0.602	0.472	-0.130
C14	1.525	1.645	0.120
Total:	-0.200	-0.377	-0.177

Table D2. Diatomic interaction energies $E_{\text{int}}^{\text{A,B}}$ and their components ($V_{\text{XC}}^{\text{A,B}}$ and $V_{\text{cl}}^{\text{A,B}}$) between covalently bonded atoms in the zwitterion (**1c**) and the lower energy conformer (**1c**) of *S*-proline also showing changes in these energy components on structural transformation from **1c** to **1c**.. All values in kcal mol^{-1}.

Atom		$E_{\text{int}}^{\text{A,B}}$		$V_{\text{XC}}^{\text{A,B}}$		$V_{\text{cl}}^{\text{A,B}}$		**1c** *minus* **1a**		
A	B	**1c**	**1a**	**1c**	**1a**	**1c**	**1a**	$\Delta E_{\text{int}}^{\text{A,B}}$	$\Delta V_{\text{XC}}^{\text{A,B}}$	$\Delta V_{\text{cl}}^{\text{A,B}}$
C1	C2	-168.6	-166.9	-184.4	-182.9	15.8	15.9	-1.7	-1.5	-0.2
C1	H6	-146.3	-148.4	-173.4	-173.9	27.0	25.5	2.1	0.6	1.5
C1	H7	-146.0	-149.4	-174.1	-173.1	28.1	23.7	3.4	-1.0	4.4
C1	N13	-259.6	-274.8	-161.8	-177.7	-97.9	-97.0	15.2	16.0	-0.8
C2	C3	-171.3	-171.5	-183.0	-182.9	11.7	11.5	0.2	0.0	0.2
C2	H8	-153.1	-153.3	-174.3	-175.2	21.1	21.9	0.1	0.9	-0.8
C2	H9	-152.2	-153.6	-174.5	-174.3	22.2	20.7	1.4	-0.2	1.6
C3	C4	-166.3	-162.9	-180.2	-177.3	13.9	14.3	-3.4	-2.9	-0.4
C3	H10	-152.4	-153.3	-174.8	-174.4	22.3	21.1	0.9	-0.3	1.2
C3	H11	-152.6	-152.7	-173.7	-174.6	21.0	21.9	0.1	0.9	-0.8
C4	H12	-146.5	-144.0	-172.5	-170.8	26.0	26.8	-2.5	-1.7	-0.8
C4	N13	-245.7	-269.3	-158.2	-182.0	-87.5	-87.3	23.6	23.8	-0.2
C4	C14	-100.1	-80.3	-166.8	-174.2	66.7	93.9	-19.8	7.4	-27.3
H5	N13	-257.5	-247.1	-151.0	-161.8	-106.5	-85.3	-10.4	10.8	-21.2
N13	H17	-258.4		-131.4		-127.1		-258.4	-131.4	-127.1
C14	O15	-840.3	-862.3	-227.1	-244.1	-613.2	-618.3	22.0	17.0	5.1
C14	O16	-814.1	-665.4	-219.1	-180.1	-595.0	-485.4	-148.6	-39.0	-109.6
O16	H17		-312.1		-100.5		-211.6	312.1	100.5	211.6
	Total:	-4331.3	-4267.4	-2980.0	-2979.7	-1351.4	-1287.7	-63.9	-0.3	-63.7

Table D3. Intramolecular non-covalent (long-distance) diatomic interaction energies $E_{\text{int}}^{\text{A,B}}$ and their components ($V_{\text{XC}}^{\text{A,B}}$ and $V_{\text{cl}}^{\text{A,B}}$) in the zwitterion (**1c**) and the lower energy conformer (**1a**) of *S*-proline. All values in kcal mol^{-1}.

Atom		$E_{\text{int}}^{\text{A,B}}$		$V_{\text{XC}}^{\text{A,B}}$		$V_{\text{cl}}^{\text{A,B}}$		**1c** minus **1a**		
A	B	**1c**	**1a**	**1c**	**1a**	**1c**	**1a**	$\Delta E_{\text{int}}^{\text{A,B}}$	$\Delta V_{\text{XC}}^{\text{A,B}}$	$\Delta V_{\text{cl}}^{\text{A,B}}$
C1	C3	-2.23	-1.68	-5.80	-5.55	3.58	3.86	-0.54	-0.26	-0.28
C1	C4	16.88	21.84	-2.29	-2.77	19.17	24.61	-4.97	0.48	-5.45
C1	H5	29.43	28.27	-1.30	-1.67	30.73	29.94	1.16	0.36	0.79
C1	H8	-1.91	-1.22	-3.92	-3.59	2.01	2.38	-0.69	-0.33	-0.36
C1	H9	-1.27	-2.05	-3.81	-3.73	2.54	1.68	0.78	-0.08	0.86
C1	H10	1.22	0.68	-0.49	-0.50	1.71	1.18	0.54	0.01	0.53
C1	H11	0.69	1.15	-0.51	-0.48	1.20	1.63	-0.47	-0.03	-0.44
C1	H12	2.88	2.88	-0.15	-0.19	3.03	3.08	0.00	0.05	-0.05
C1	C14	48.32	50.66	-0.17	-0.21	48.49	50.86	-2.33	0.04	-2.37
C1	O15	-28.63	-32.45	-0.09	-0.08	-28.53	-32.36	3.82	-0.01	3.83
C1	O16	-37.05	-40.51	-0.25	-0.19	-36.81	-40.31	3.45	-0.05	3.50
C1	H17	31.17	27.11	-1.00	-0.19	32.16	27.30	4.06	-0.80	4.86
C2	C4	-2.11	-1.81	-5.21	-5.10	3.10	3.29	-0.30	-0.11	-0.19
C2	H5	3.49	2.34	-0.09	-0.36	3.58	2.70	1.15	0.27	0.88
C2	H6	-1.23	-2.12	-3.06	-3.29	1.84	1.17	0.90	0.23	0.67
C2	H7	-0.91	-2.50	-2.78	-3.54	1.87	1.04	1.60	0.77	0.83
C2	H10	-2.10	-2.59	-3.27	-3.61	1.17	1.02	0.49	0.34	0.15
C2	H11	-2.54	-2.08	-3.57	-3.20	1.03	1.12	-0.46	-0.37	-0.09
C2	H12	0.37	0.15	-0.24	-0.36	0.60	0.51	0.22	0.12	0.09
C2	N13	-17.69	-16.37	-7.41	-7.80	-10.27	-8.57	-1.32	0.38	-1.70
C2	C14	8.85	6.89	-0.31	-0.37	9.16	7.26	1.96	0.06	1.90
C2	O15	-5.94	-5.11	-0.19	-0.12	-5.76	-4.99	-0.83	-0.06	-0.76
C2	O16	-6.47	-5.30	-0.14	-0.29	-6.33	-5.01	-1.17	0.16	-1.32
C2	H17	3.73	2.97	-0.20	-0.03	3.93	3.01	0.76	-0.17	0.93
C3	H5	3.48	2.65	-0.16	-0.20	3.63	2.84	0.83	0.04	0.79
C3	H6	0.08	-0.19	-0.50	-0.48	0.58	0.29	0.27	-0.02	0.29
C3	H7	0.14	-0.25	-0.46	-0.49	0.61	0.24	0.39	0.03	0.37
C3	H8	-2.57	-2.47	-3.59	-3.45	1.02	0.99	-0.11	-0.14	0.03
C3	H9	-2.15	-2.90	-3.30	-3.74	1.15	0.85	0.75	0.44	0.30
C3	H12	-1.14	-1.34	-2.97	-2.99	1.83	1.65	0.20	0.02	0.18
C3	N13	-16.45	-15.57	-6.39	-6.40	-10.07	-9.17	-0.88	0.02	-0.90
C3	C14	10.14	5.98	-3.23	-4.43	13.38	10.41	4.17	1.20	2.97

Table D3 Continues

Atom		$E_{int}^{A,B}$		$V_{XC}^{A,B}$		$V_{cl}^{A,B}$		**1c** minus **1a**		
A	B	**1c**	**1a**	**1c**	**1a**	**1c**	**1a**	$\Delta E_{int}^{A,B}$	$\Delta V_{XC}^{A,B}$	$\Delta V_{cl}^{A,B}$
C3	O15	-9.39	-8.34	-2.15	-2.07	-7.24	-6.27	-1.05	-0.07	-0.97
C3	O16	-8.43	-6.95	-0.77	-0.54	-7.66	-6.42	-1.48	-0.24	-1.24
C3	H17	3.78	3.79	-0.09	-0.03	3.88	3.82	-0.01	-0.06	0.05
C4	H5	25.57	26.00	-1.27	-1.77	26.85	27.77	-0.43	0.50	-0.92
C4	H6	2.45	1.15	-0.11	-0.43	2.56	1.58	1.31	0.32	0.98
C4	H7	2.35	1.03	-0.31	-0.12	2.67	1.14	1.32	-0.20	1.52
C4	H8	0.63	0.74	-0.40	-0.49	1.03	1.23	-0.11	0.08	-0.20
C4	H9	0.95	0.25	-0.48	-0.31	1.43	0.56	0.70	-0.16	0.86
C4	H10	-1.59	-2.04	-3.71	-3.88	2.11	1.85	0.44	0.18	0.27
C4	H11	-2.12	-1.10	-3.75	-3.31	1.62	2.20	-1.02	-0.44	-0.58
C4	O15	-42.83	-57.56	-13.15	-9.67	-29.69	-47.89	14.73	-3.48	18.21
C4	O16	-50.41	-63.57	-11.12	-8.16	-39.28	-55.42	13.17	-2.97	16.14
C4	H17	28.57	33.58	-1.15	-0.53	29.71	34.11	-5.02	-0.61	-4.40
H5	H6	3.92	1.88	-0.25	-0.05	4.17	1.93	2.04	-0.20	2.24
H5	H7	4.78	0.92	-0.28	-0.31	5.06	1.22	3.86	0.03	3.84
H5	H8	1.02	0.97	-0.02	-0.06	1.04	1.03	0.05	0.03	0.02
H5	H9	1.99	0.40	-0.01	-0.02	2.01	0.42	1.59	0.00	1.59
H5	H10	1.90	0.74	-0.02	-0.01	1.92	0.75	1.15	-0.01	1.17
H5	H11	1.22	1.30	-0.01	-0.03	1.23	1.33	-0.08	0.01	-0.09
H5	H12	4.41	3.42	-0.35	-0.35	4.76	3.77	0.99	0.00	0.99
H5	C14	74.89	58.64	-0.10	-0.15	74.99	58.79	16.25	0.06	16.20
H5	O15	-44.54	-37.21	-0.05	-0.05	-44.48	-37.16	-7.33	0.00	-7.33
H5	O16	-57.29	-47.40	-0.15	-0.14	-57.14	-47.26	-9.89	-0.01	-9.88
H5	H17	47.70	32.23	-0.71	-0.14	48.41	32.37	15.46	-0.57	16.03
H6	H7	-0.12	-1.85	-2.63	-3.10	2.51	1.25	1.73	0.47	1.26
H6	H8	-0.09	0.18	-0.50	-0.09	0.41	0.27	-0.28	-0.42	0.14
H6	H9	0.25	-0.18	-0.37	-0.44	0.62	0.26	0.44	0.08	0.36
H6	H10	0.30	0.06	-0.03	-0.03	0.33	0.09	0.24	0.00	0.24
H6	H11	-0.06	0.08	-0.31	-0.06	0.25	0.14	-0.14	-0.25	0.11
H6	H12	0.46	0.16	-0.02	-0.05	0.48	0.21	0.29	0.03	0.26
H6	N13	-17.26	-11.62	-5.36	-5.43	-11.90	-6.19	-5.64	0.06	-5.70
H6	C14	8.25	3.20	-0.02	-0.01	8.27	3.21	5.06	0.00	5.06
H6	O15	-5.11	-2.08	-0.02	-0.02	-5.09	-2.06	-3.04	0.00	-3.04
H6	O16	-6.43	-2.38	-0.25	-0.04	-6.18	-2.34	-4.06	-0.21	-3.84
H6	H17	4.47	1.52	-0.29	-0.05	4.75	1.57	2.95	-0.24	3.18

Table D3 Continues

Atom		$E_{int}^{A,B}$		$V_{XC}^{A,B}$		$V_{cl}^{A,B}$		**1c** *minus* **1a**		
A	B	**1c**	**1a**	**1c**	1a	1c	**1a**	$\Delta E_{int}^{A,B}$	$\Delta V_{XC}^{A,B}$	$\Delta V_{cl}^{A,B}$
H7	H8	0.11	-0.16	-0.39	-0.44	0.49	0.28	0.26	0.05	0.21
H7	H9	0.55	-0.37	-0.07	-0.51	0.62	0.14	0.92	0.44	0.48
H7	H10	0.28	-0.18	-0.07	-0.33	0.35	0.15	0.45	0.26	0.20
H7	H11	0.19	0.05	-0.03	-0.03	0.21	0.08	0.14	0.00	0.13
H7	H12	0.49	0.13	-0.02	-0.01	0.51	0.13	0.37	-0.01	0.38
H7	N13	-18.00	-10.18	-5.02	-5.62	-12.99	-4.56	-7.83	0.61	-8.43
H7	C14	9.16	1.96	-0.02	-0.04	9.19	2.00	7.20	0.01	7.19
H7	O15	-5.72	-1.15	-0.02	-0.01	-5.70	-1.13	-4.58	-0.01	-4.57
H7	O16	-7.03	-1.79	-0.02	-0.08	-7.01	-1.71	-5.24	0.06	-5.30
H7	H17	4.96	1.15	-0.04	-0.07	4.99	1.23	3.80	0.04	3.77
H8	H9	-1.50	-1.98	-3.03	-3.19	1.53	1.21	0.49	0.16	0.32
H8	H10	0.00	-0.11	-0.39	-0.41	0.39	0.30	0.11	0.02	0.09
H8	H11	-0.27	0.22	-0.51	-0.08	0.24	0.30	-0.48	-0.43	-0.06
H8	H12	0.11	0.15	-0.13	-0.05	0.24	0.20	-0.04	-0.08	0.04
H8	N13	-3.72	-4.11	-0.43	-0.59	-3.30	-3.53	0.39	0.16	0.23
H8	C14	3.19	3.52	-0.02	-0.04	3.21	3.55	-0.33	0.01	-0.34
H8	O15	-2.05	-2.36	-0.02	-0.02	-2.04	-2.34	0.31	0.00	0.31
H8	O16	-2.24	-2.61	-0.03	-0.03	-2.21	-2.58	0.37	0.00	0.37
H8	H17	1.24	1.54	-0.01	0.00	1.26	1.54	-0.29	-0.01	-0.28
H9	H10	0.37	-0.38	-0.08	-0.53	0.45	0.16	0.75	0.45	0.29
H9	H11	-0.01	-0.13	-0.40	-0.39	0.38	0.26	0.12	-0.01	0.13
H9	H12	0.32	0.07	-0.02	-0.02	0.34	0.09	0.25	0.00	0.25
H9	N13	-5.71	-1.86	-0.60	-0.54	-5.11	-1.32	-3.86	-0.06	-3.80
H9	C14	5.22	-0.81	-0.04	-0.22	5.27	-0.58	6.03	0.18	5.85
H9	O15	-3.49	0.30	-0.01	-0.05	-3.48	0.35	-3.79	0.03	-3.83
H9	O16	-3.63	0.38	-0.05	-0.57	-3.58	0.94	-4.01	0.52	-4.53
H9	H17	1.95	-0.38	-0.03	-0.03	1.98	-0.35	2.34	0.00	2.34
H10	H11	-1.49	-1.71	-3.03	-3.09	1.54	1.38	0.22	0.06	0.16
H10	H12	0.17	-0.20	-0.50	-0.62	0.66	0.42	0.37	0.12	0.24
H10	N13	-5.61	-3.04	-0.46	-0.24	-5.15	-2.80	-2.57	-0.23	-2.34
H10	C14	7.68	3.74	-0.09	-0.39	7.78	4.13	3.95	0.30	3.65
H10	O15	-5.45	-2.97	-0.48	-0.11	-4.98	-2.86	-2.48	-0.37	-2.11
H10	O16	-4.73	-2.49	-0.06	-0.09	-4.67	-2.41	-2.24	0.03	-2.27
H10	H17	2.11	1.31	-0.02	0.00	2.13	1.31	0.80	-0.01	0.81
H11	H12	0.02	0.39	-0.40	-0.07	0.43	0.46	-0.37	-0.33	-0.04
H11	N13	-3.53	-4.71	-0.18	-0.51	-3.35	-4.20	1.18	0.33	0.84

Table D3 Continues

Atom		$E_{\text{int}}^{\text{A,B}}$		$V_{\text{XC}}^{\text{A,B}}$		$V_{\text{cl}}^{\text{A,B}}$		**1c** *minus* **1a**		
A	B	**1c**	**1a**	**1c**	**1a**	**1c**	**1a**	$\Delta E_{\text{int}}^{\text{A,B}}$	$\Delta V_{\text{XC}}^{\text{A,B}}$	$\Delta V_{\text{cl}}^{\text{A,B}}$
H11	C14	2.86	4.08	-0.99	-0.74	3.85	4.83	-1.22	-0.25	-0.97
H11	O15	-3.18	-4.94	-0.80	-2.13	-2.38	-2.81	1.76	1.33	0.43
H11	O16	-2.19	-3.18	-0.34	-0.07	-1.85	-3.11	0.99	-0.28	1.26
H11	H17	1.18	1.81	0.00	0.00	1.19	1.81	-0.63	0.00	-0.62
H12	N13	-17.54	-15.82	-5.12	-4.80	-12.42	-11.03	-1.72	-0.32	-1.40
H12	C14	17.18	11.38	-2.72	-4.12	19.89	15.50	5.80	1.41	4.39
H12	O15	-12.84	-10.79	-1.35	-1.37	-11.49	-9.43	-2.05	0.01	-2.06
H12	O16	-11.27	-9.23	-0.66	-0.54	-10.61	-8.70	-2.03	-0.12	-1.91
H12	H17	4.83	4.85	-0.13	-0.04	4.96	4.89	-0.02	-0.09	0.07
N13	C14	-198.51	-188.16	-4.42	-5.99	-194.10	-182.17	-10.35	1.58	-11.93
N13	O15	107.56	108.96	-0.97	-0.86	108.53	109.82	-1.40	-0.11	-1.29
N13	O16	139.93	140.88	-9.07	-11.94	149.00	152.82	-0.95	2.87	-3.82
C14	H17	109.30	175.62	-0.54	-1.03	109.84	176.65	-66.32	0.50	-66.81
O15	O16	201.04	178.90	-30.24	-28.42	231.28	207.32	22.14	-1.82	23.96
O15	H17	-56.63	-86.29	-0.18	-0.50	-56.45	-85.79	29.66	0.32	29.35
O16	H17	-111.83		-14.22		-97.61		-111.83	-14.22	-97.61
N13	H17		-132.83		-19.08		-113.75	132.83	19.08	113.75
Total:		136.48	91.47	-205.54	-212.00	342.02	303.47	45.01	6.46	38.55

Table D4. Interaction energies ($E_{\text{int}}^{\text{A},\mathcal{R}}$ in kcal mol^{-1}) between atom A and the remaining atoms of *S*-proline constituting a molecular fragment R (R is made of all the atoms of *S*-proline except A) computed for **1a** and **1c**. $\Delta E_{\text{int}}^{\text{A},\mathcal{R}}$ = { $E_{\text{int}}^{\text{A},\mathcal{R}}$ in **1c**} – { $E_{\text{int}}^{\text{A},\mathcal{R}}$ in **1b**}.

	$E_{\text{int}}^{\text{A},\mathcal{R}}$		$\Delta V_{\text{XC}}^{\text{A},\mathcal{R}}$		$\Delta V_{\text{cl}}^{\text{A},\mathcal{R}}$		**1c** *minus* **1a**		
Atom	**1c**	**1a**	**1c**	**1a**	**1c**	**1a**	$\Delta E_{\text{int}}^{\text{A},\mathcal{R}}$	$\Delta V_{\text{XC}}^{\text{A},\mathcal{R}}$	$\Delta V_{\text{cl}}^{\text{A},\mathcal{R}}$
C1	-661.05	-684.72	-713.52	-726.91	52.47	42.18	23.67	13.39	10.28
C2	-667.78	-670.30	-742.65	-743.48	74.86	73.18	2.51	0.84	1.68
C3	-667.32	-668.19	-741.12	-739.69	73.80	71.50	0.87	-1.43	2.30
C4	-680.36	-697.68	-720.69	-740.95	40.33	43.27	17.32	20.25	-2.94
H5	-155.52	-171.93	-155.77	-167.06	0.25	-4.88	16.41	11.29	5.12
H6	-156.46	-160.66	-187.09	-187.53	30.63	26.86	4.20	0.43	3.76
H7	-154.79	-162.58	-186.23	-187.76	31.44	25.18	7.79	1.53	6.26
H8	-161.20	-161.08	-187.63	-187.69	26.44	26.61	-0.12	0.05	-0.17
H9	-158.40	-163.32	-186.75	-188.58	28.36	25.26	4.93	1.83	3.10
H10	-159.39	-162.52	-187.44	-188.25	28.05	25.73	3.13	0.81	2.32
H11	-161.88	-161.53	-188.52	-188.79	26.64	27.25	-0.35	0.27	-0.62
H12	-158.08	-157.87	-187.28	-186.33	29.19	28.46	-0.22	-0.95	0.73
N13	-1078.01	-945.61	-647.84	-591.43	-430.17	-354.18	-132.40	-56.41	-75.99
C14	-1647.83	-1470.34	-625.72	-616.26	-1022.11	-854.08	-177.49	-9.46	-168.03
O15	-757.76	-826.16	-276.82	-289.45	-480.94	-536.71	68.40	12.63	55.77
O16	-782.31	-842.71	-286.47	-331.66	-495.84	-511.05	60.40	45.19	15.21
H17	-181.89	-244.17	-149.95	-122.25	-31.95	-121.92	62.28	-27.70	89.98
Total:	-8390.04	-8351.38	-6371.49	-6384.06	-2018.54	-1967.32	-38.66	12.57	-51.22

Table D5. Diatomic interaction energies $E_{\text{int}}^{\text{A,B}}$ and their components ($V_{\text{XC}}^{\text{A,B}}$ and $V_{\text{cl}}^{\text{A,B}}$) between covalently bonded atoms in the zwitterion (**1c**) and the lower energy energy conformer of *S*-proline (**1a**) in the presence of a single solvent molecule of water **4**. All values in kcal mol^{-1}.

Atom		$E_{\text{int}}^{\text{A,B}}$		$V_{\text{XC}}^{\text{A,B}}$		$V_{\text{cl}}^{\text{A,B}}$		**1c** *minus* **1a**		
A	**B**	**1c**	**1a**	**1c**	**1a**	**1c**	**1a**	$\Delta E_{\text{int}}^{\text{A,B}}$	$\Delta V_{\text{XC}}^{\text{A,B}}$	$\Delta V_{\text{cl}}^{\text{A,B}}$
C1	C2	-168.8	-166.9	-184.6	-182.5	15.8	15.7	-1.9	-2.0	0.2
C1	H6	-146.2	-148.9	-173.3	-173.1	27.1	24.1	2.8	-0.2	3.0
C1	H7	-145.8	-147.6	-174.0	-174.0	28.2	26.4	1.8	0.0	1.8
C1	N13	-259.6	-274.1	-161.5	-177.7	-98.2	-96.4	14.5	16.3	-1.8
C2	C3	-171.3	-171.4	-183.0	-183.0	11.7	11.5	0.1	-0.1	0.2
C2	H8	-153.1	-153.5	-174.2	-174.3	21.1	20.8	0.5	0.1	0.3
C2	H9	-152.1	-153.2	-174.4	-174.9	22.3	21.8	1.1	0.5	0.5
C3	C4	-166.0	-161.6	-179.7	-175.1	13.7	13.5	-4.3	-4.6	0.2
C3	H10	-152.4	-153.3	-174.7	-175.3	22.3	22.0	0.9	0.6	0.3
C3	H11	-152.6	-153.2	-173.7	-174.1	21.1	20.9	0.6	0.4	0.2
C4	H12	-146.0	-143.8	-172.2	-170.5	26.2	26.7	-2.2	-1.7	-0.5
C4	N13	-245.2	-266.7	-158.3	-182.1	-86.9	-84.6	21.5	23.8	-2.3
C4	C14	-99.7	-82.1	-168.7	-176.7	69.0	94.6	-17.6	8.0	-25.6
H5	N13	-257.7	-246.7	-150.5	-161.7	-107.1	-85.1	-10.9	11.1	-22.1
N13	H17	-259.1		-132.8	0.0	-126.3	0.0	-259.1	-132.8	-126.3
C14	O15	-845.2	-865.0	-229.6	-245.9	-615.5	-619.1	19.8	16.3	3.5
C14	O16	-800.6	-657.5	-213.8	-176.1	-586.7	-481.4	-143.0	-37.8	-105.3
O16	H17		-314.3		-98.3		-215.9	314.3	98.3	215.9
O18	H19	-323.5	-321.4	-105.2	-115.7	-218.3	-205.7	-2.1	10.5	-12.6
O18	H20	-319.4	-318.0	-133.4	-131.3	-186.0	-186.8	-1.4	-2.1	0.7
Total		-4964.1		-3217.7	-3217.7	-3222.5	-4899.5	-64.7	4.8	-69.5

Table D6. Intramolecular non-covalent (long-distance) diatomic interaction energies $E_{\text{int}}^{\text{A,B}}$ and their components ($V_{\text{XC}}^{\text{A,B}}$ and $V_{\text{cl}}^{\text{A,B}}$) in the zwitterion (**1c**) and the lower energy conformer of *S*-proline (**1a**) in the presence of a molecule of water **4**. All values in kcal mol^{-1}.

Atom		$E_{\text{int}}^{\text{A,B}}$		$V_{\text{XC}}^{\text{A,B}}$		$V_{\text{cl}}^{\text{A,B}}$		**1c** *minus* **1a**		
A	B	**1c**	**1a**	**1c**	1a	1c	**1a**	$\Delta E_{\text{int}}^{\text{A,B}}$	$\Delta V_{\text{XC}}^{\text{A,B}}$	$\Delta V_{\text{cl}}^{\text{A,B}}$
C1	C3	-2.2	-5.8	3.6	-2.0	-5.7	3.7	-0.2	-0.1	0.0
C1	C4	16.9	-2.3	19.2	21.5	-2.9	24.4	-4.6	0.6	-5.2
C1	H	29.6	-1.3	30.9	28.2	-1.8	30.0	1.4	0.5	0.9
C1	H8	-1.8	-3.9	2.1	-2.0	-3.8	1.7	0.2	-0.2	0.4
C1	H9	-1.2	-3.8	2.6	-1.3	-3.5	2.2	0.1	-0.3	0.4
C1	H10	1.3	-0.5	1.8	1.1	-0.5	1.6	0.1	0.0	0.1
C1	H11	0.8	-0.5	1.3	0.6	-0.5	1.1	0.2	0.0	0.2
C1	H12	3.1	-0.2	3.2	3.0	-0.2	3.2	0.0	0.0	0.0
C1	C1	48.2	-0.2	48.4	50.6	-0.2	50.8	-2.4	0.1	-2.4
C1	O15	-28.5	-0.1	-28.4	-32.3	-0.1	-32.2	3.8	0.0	3.8
C1	O16	-36.9	-0.2	-36.6	-40.9	-0.3	-40.7	4.0	0.0	4.0
C	H17	31.3	-1.0	32.4	27.6	-0.2	27.8	3.7	-0.8	4.5
C2	C4	-2.1	-5.2	3.1	-1.7	-5.0	3.3	-0.4	-0.2	-0.2
C2	H5	3.5	-0.1	3.6	2.5	-0.1	2.7	1.0	0.0	0.9
C2	H6	-1.2	-3.1	1.9	-2.6	-3.6	1.0	1.4	0.5	0.9
C2 -	H7	-0.9	-2.8	1.9	-2.0	-3.2	1.1	1.2	0.4	0.8
C2	H10	-2.1	-3.3	1.2	-2.1	-3.3	1.1	0.1	0.0	0.1
C2	H11	-2.5	-3.5	1.1	-2.5	-3.6	1.0	0.1	0.0	0.0
C2	H12	0.4	-0.2	0.6	0.4	-0.2	0.6	0.1	0.0	0.1
C2	N13	-17.8	-7.5	-10.3	-16.4	-7.9	-8.5	-1.4	0.4	-1.7
C2	C14	8.9	-0.3	9.2	7.4	-0.4	7.7	1.5	0.0	1.5
C2	O15	-6.0	-0.2	-5.8	-5.4	-0.2	-5.3	-0.5	0.0	-0.5
C2	O16	-6.4	-0.1	-6.3	-5.4	-0.1	-5.3	-1.0	0.0	-1.0
C2	H17	3.7	-0.2	3.9	3.2	-0.1	3.2	0.5	-0.2	0.7
C3	H5	3.6	-0.1	3.7	2.6	-0.2	2.8	0.9	0.0	0.9
C3	H6	0.1	-0.5	0.6	-0.3	-0.5	0.3	0.3	0.0	0.3
C3	H7	0.2	-0.5	0.6	-0.2	-0.5	0.3	0.3	0.0	0.3
C3	H8	-2.6	-3.6	1.0	-3.0	-3.8	0.8	0.4	0.2	0.2
C3	H9	-2.1	-3.3	1.2	-2.7	-3.5	0.9	0.5	0.2	0.3
C3	H12	-1.0	-2.9	1.9	-1.4	-3.0	1.6	0.4	0.1	0.3
C3	N13	-16.4	-6.2	-10.2	-14.5	-6.0	-8.6	-1.8	-0.2	-1.6
C3	C14	10.3	-3.3	13.6	5.6	-4.6	10.2	4.7	1.3	3.4

Table D6 Continues

Atom		$E_{\text{int}}^{\text{A,B}}$		$V_{\text{XC}}^{\text{A,B}}$		$V_{\text{cl}}^{\text{A,B}}$		**1c** *minus* **1a**		
A	B	**1c**	**1a**	**1c**	**1a**	**1c**	**1a**	$\Delta E_{\text{int}}^{\text{A,B}}$	$\Delta V_{\text{XC}}^{\text{A,B}}$	$\Delta V_{\text{cl}}^{\text{A,B}}$
C3	O15	-9.6	-2.2	-7.4	-8.1	-2.2	-5.9	-1.5	-0.1	-1.5
C3	O16	-8.4	-0.7	-7.7	-6.8	-0.6	-6.2	-1.6	-0.1	-1.5
C3	H17	3.8	-0.1	3.9	3.6	0.0	3.6	0.2	-0.1	0.3
C4	H5	25.7	-1.3	27.0	25.7	-1.8	27.5	0.1	0.6	-0.5
C4	H6	2.5	-0.1	2.6	1.1	-0.1	1.2	1.4	0.0	1.4
C4	H7	2.4	-0.3	2.7	1.5	-0.4	1.9	0.9	0.1	0.9
C4	H8	0.7	-0.4	1.1	0.3	-0.3	0.7	0.4	0.0	0.4
C4	H9	1.0	-0.5	1.5	0.6	-0.5	1.1	0.4	0.0	0.4
C4	H10	-1.6	-3.7	2.1	-1.5	-3.6	2.1	-0.1	-0.1	0.0
C4	H11	-2.1	-3.7	1.7	-2.1	-3.6	1.5	0.0	-0.1	0.1
C4	O15	-43.3	-12.8	-30.6	-57.1	-9.5	-47.6	13.8	-3.2	17.0
C4	O16	-50.5	-10.6	-39.9	-63.5	-8.1	-55.4	13.0	-2.5	15.5
C4	H17	28.7	-1.1	29.8	33.8	-0.5	34.3	-5.1	-0.6	-4.5
H5	H6	4.0	-0.3	4.3	1.2	-0.3	1.5	2.8	0.1	2.7
H5	H7	5.0	-0.3	5.2	2.0	-0.4	2.4	2.9	0.1	2.8
H5	H8	1.1	0.0	1.1	0.2	0.0	0.3	0.9	0.0	0.9
H5	H9	2.1	0.0	2.1	1.1	0.0	1.1	1.0	0.0	1.0
H5	H10	2.0	0.0	2.0	1.3	0.0	1.3	0.7	0.0	0.7
H5	H11	1.3	0.0	1.4	0.8	0.0	0.8	0.5	0.0	0.5
H5	H12	4.8	-0.3	5.2	3.6	-0.4	4.0	1.3	0.1	1.2
H5	C14	74.4	-0.1	74.5	58.1	-0.2	58.3	16.2	0.1	16.2
H5	O15	-44.2	-0.1	-44.1	-36.8	-0.1	-36.8	-7.3	0.0	-7.3
H5	O16	-56.7	-0.1	-56.6	-47.1	-0.1	-47.0	-9.6	0.0	-9.6
H5	H17	48.1	-0.7	48.8	32.3	-0.1	32.4	15.9	-0.6	16.4
H6	H7	0.0	-2.6	2.6	-1.7	-3.0	1.4	1.7	0.4	1.2
H6	H8	-0.1	-0.5	0.4	-0.4	-0.5	0.2	0.3	0.0	0.3
H6	H9	0.3	-0.4	0.6	-0.1	-0.4	0.3	0.4	0.0	0.4
H6	H10	0.3	0.0	0.4	0.1	0.0	0.1	0.3	0.0	0.3
H6	H11	0.0	-0.3	0.3	-0.2	-0.3	0.1	0.1	0.0	0.1
H6	H12	0.5	0.0	0.5	0.1	0.0	0.2	0.4	0.0	0.4
H6	N13	-17.5	-5.4	-12.1	-10.6	-5.8	-4.8	-6.9	0.4	-7.3
H6	C14	8.5	0.0	8.5	1.3	0.0	1.3	7.3	0.0	7.3
H6	O15	-5.3	0.0	-5.2	-0.8	0.0	-0.8	-4.5	0.0	-4.4
H6	O16	-6.6	-0.3	-6.4	-0.9	-0.2	-0.7	-5.8	-0.1	-5.7
H6	H17	4.6	-0.3	4.9	0.6	-0.1	0.6	4.1	-0.2	4.3
H7	H8	0.1	-0.4	0.5	-0.1	-0.4	0.3	0.3	0.0	0.2

Table D6 Continues

Atom		$E_{int}^{A,B}$		$V_{XC}^{A,B}$		$V_{cl}^{A,B}$		**1c** *minus* **1a**		
A	B	**1c**	**1a**	**1c**	**1a**	**1c**	**1a**	$\Delta E_{int}^{A,B}$	$\Delta V_{XC}^{A,B}$	$\Delta V_{cl}^{A,B}$
H7	H9	0.6	-0.1	0.7	0.2	-0.1	0.3	0.4	0.0	0.4
H7	H10	0.3	-0.1	0.4	0.1	-0.1	0.2	0.2	0.0	0.2
H7	H11	0.2	0.0	0.2	0.1	0.0	0.1	0.1	0.0	0.1
H7	H12	0.5	0.0	0.6	0.3	0.0	0.3	0.3	0.0	0.3
H7	N13	-18.3	-5.0	-13.3	-12.7	-5.2	-7.5	-5.6	0.2	-5.8
H7	C14	9.5	0.0	9.5	4.4	0.0	4.4	5.1	0.0	5.1
H7	O15	-5.9	0.0	-5.9	-2.9	0.0	-2.8	-3.0	0.0	-3.0
H7	O16	-7.2	0.0	-7.2	-3.5	0.0	-3.5	-3.7	0.0	-3.7
H7	H17	5.1	0.0	5.2	2.3	0.0	2.3	2.8	0.0	2.8
H8	H9	-1.4	-3.0	1.6	-2.0	-3.2	1.2	0.5	0.2	0.4
H8	H10	0.0	-0.4	0.4	-0.2	-0.4	0.3	0.2	0.0	0.1
H8	H11	-0.2	-0.5	0.3	-0.4	-0.5	0.2	0.1	0.0	0.1
H8	H12	0.2	-0.1	0.3	0.0	-0.1	0.1	0.1	0.0	0.1
H8	N13	-3.9	-0.5	-3.5	-2.2	-0.6	-1.5	-1.8	0.2	-1.9
H8	C14	3.4	0.0	3.4	1.2	0.0	1.2	2.2	0.0	2.2
H8	O15	-2.2	0.0	-2.2	-0.7	0.0	-0.7	-1.4	0.0	-1.4
H8	O16	-2.4	0.0	-2.3	-0.9	0.0	-0.9	-1.5	0.0	-1.5
H8	H17	1.3	0.0	1.3	0.5	0.0	0.5	0.8	0.0	0.8
H9	H10	0.4	-0.1	0.5	0.2	-0.1	0.3	0.2	0.0	0.2
H9	H11	0.0	-0.4	0.4	-0.2	-0.4	0.3	0.2	0.0	0.1
H9	H12	0.4	0.0	0.4	0.2	0.0	0.2	0.2	0.0	0.2
H9	N13	-5.9	-0.6	-5.3	-3.9	-0.7	-3.2	-2.0	0.1	-2.1
H9	C14	5.5	0.0	5.5	2.6	0.0	2.6	2.9	0.0	2.9
H9	O15	-3.6	0.0	-3.6	-1.8	0.0	-1.7	-1.9	0.0	-1.9
H9	O16	-3.8	0.0	-3.7	-1.8	0.0	-1.8	-1.9	0.0	-1.9
H9	H17	2.0	0.0	2.1	1.1	0.0	1.1	0.9	0.0	1.0
H10	H11	-1.4	-3.0	1.6	-1.8	-3.1	1.3	0.4	0.1	0.2
H10	H12	0.2	-0.5	0.7	0.0	-0.6	0.5	0.3	0.1	0.2
H10	N13	-5.7	-0.4	-5.3	-4.5	-0.4	-4.1	-1.2	0.0	-1.2
H10	C14	8.0	-0.1	8.1	5.3	-0.1	5.4	2.7	0.0	2.7
H10	O15	-5.7	-0.4	-5.2	-3.8	-0.3	-3.5	-1.8	-0.1	-1.7
H10	O16	-4.9	-0.1	-4.8	-3.4	0.0	-3.3	-1.5	0.0	-1.5
H10	H17	2.2	0.0	2.2	1.9	0.0	1.9	0.3	0.0	0.3
H11	H12	0.1	-0.4	0.5	0.0	-0.4	0.3	0.1	0.0	0.1
H11	N13	-3.8	-0.2	-3.6	-2.6	-0.2	-2.4	-1.2	0.0	-1.2
H11	C14	3.3	-1.0	4.3	0.6	-1.2	1.8	2.7	0.2	2.6
H11	O15	-3.6	-0.9	-2.7	-1.9	-1.0	-0.9	-1.7	0.1	-1.7

Table D6 Continues

Atom		$E_{int}^{A,B}$		$V_{XC}^{A,B}$		$V_{cl}^{A,B}$		**1c** *minus* **1a**		
A	B	**1c**	**1a**	**1c**	**1a**	**1c**	**1a**	$\Delta E_{int}^{A,B}$	$\Delta V_{XC}^{A,B}$	$\Delta V_{cl}^{A,B}$
H11	O16	-2.5	-0.3	-2.2	-1.0	-0.2	-0.8	-1.5	-0.1	-1.4
H11	H17	1.3	0.0	1.3	0.6	0.0	0.6	0.7	0.0	0.7
H12	N13	-18.3	-5.1	-13.2	-16.3	-4.9	-11.4	-2.0	-0.2	-1.8
H12	C14	18.4	-2.8	21.2	12.0	-4.2	16.2	6.3	1.3	5.0
H12	O15	-13.6	-1.3	-12.3	-11.1	-1.2	-9.9	-2.5	-0.1	-2.5
H12	O16	-12.0	-0.6	-11.3	-9.7	-0.5	-9.2	-2.3	-0.1	-2.2
H12	H17	5.2	-0.1	5.3	5.2	0.0	5.2	0.0	-0.1	0.1
N13	C14	-196.5	-4.4	-192.0	-186.4	-5.8	-180.5	-10.1	1.4	-11.5
N13	O15	106.3	-0.9	107.3	107.6	-0.9	108.4	-1.3	-0.1	-1.2
N13	O16	138.5	-8.7	147.3	140.8	-12.0	152.8	-2.3	3.3	-5.6
N13	H17	0.0	0.0	0.0	-133.9	-18.9	-115.0	133.9	18.9	115.0
C14	H17	108.0	-0.5	108.5	175.9	-1.0	176.8	-67.9	0.5	-68.3
O15	O16	199.1	-29.6	228.7	179.5	-27.9	207.4	19.6	-1.7	21.3
O15	H17	-56.1	-0.2	-56.0	-86.8	-0.5	-86.3	30.7	0.3	30.4
O16	H17	-109.2	-12.8	-96.5	0.0	0.0	0.0	-109.2	-12.8	-96.5
H19	H20	83.3	-0.6	83.8	83.8	-0.6	84.4	-0.5	0.1	-0.6
Total		221.6	-202.4	423.9	176.9	-210.7	387.5	44.7	8.3	36.4

PART D2

Data pertaining to the relative stability of the zwitterion 1c with respect to the non-ionic conformer 1a, in the presence of either an explicit solvent molecule of DMSO 3 or solvent molecule/s of water 4.

Table D7. Relative to the Zw (**1c**) energies of the LEC **1a** and associated transition states (TS) in implicit solvation model and in the presence of solvent molecule/s of water and DMSO. Energies (in au) and associated changes in kcal mol^{-1} computed at the B3LYP/6-311++G(d,p)/GD3,

	E	Δ	E_{ZPVE}	**Δ**	***H***	***Δ***	***G***	**Δ**
1c	-401.3134	0.0	-401.1675	0.0	-401.1593	0.0	-401.1999	0.0
1a_TS	-401.3067	4.2	-401.1653	1.4	-401.1577	1.0	-401.1965	2.1
1a	-401.3109	1.6	-401.1665	0.7	-401.1583	0.6	-401.1987	0.7
1c_1w	-477.7918	0.0	-477.6217	0.0	-477.6102	0.0	-477.6601	0.0
1a_1w-TS	-477.7799	7.5	-477.6152	4.1	-477.6038	4.0	-477.6540	3.8
1a_1w	-477.7837	5.1	-477.6161	3.6	-477.6040	3.9	-477.6565	2.3
1c_2w	-554.2746	0.0	-554.0789	0.0	-554.0650	0.0	-554.1201	0.0
1a_2w-TS	-554.2611	8.4	-554.0707	5.1	-554.0571	5.0	-554.1115	5.4
1a_2w	-554.2642	6.5	-554.0708	5.1	-554.0565	5.3	-554.1128	4.6
1c_3w	-630.7529	0.0	-630.5337	0.0	-630.5161	0.0	-630.5808	0.0
1a_3w-TS	-630.7352	11.1	-630.5216	7.6	-630.5039	7.7	-630.5699	6.8
1a_3w	-630.7368	10.1	-630.5204	8.4	-630.5020	8.8	-630.5692	7.3
1c_1D	-954.6196	0.0	-954.3928	0.0	-954.3775	0.0	-954.4364	0.0
1a_1D-TS	-954.6058	8.6	-954.3841	5.4	-954.3691	5.3	-954.4272	5.8
1a_1D	-954.6091	6.6	-954.3842	5.4	-954.3687	5.5	-954.4283	5.1

Table D8. Atomic charges on 2-MCs of water with **1a** and **1c**, where Δ represents atomic charges on **1c** 2-MC minus **1a** 2-MC.

	1a 2-MC	**1c** 2-MC	
Atom A	Q(A)		Δ
O15	-1.185	-1.232	-0.047
O18	-1.185	-1.218	-0.032
O16	-1.142	-1.216	-0.074
N13	-0.985	-0.945	0.039
C4	0.298	0.225	-0.072
C1	0.321	0.272	-0.049
H5	0.369	0.438	0.068
H20	0.564	0.553	-0.048
H19	0.601	0.613	0.001
H17	0.611	0.474	-0.090
C14	1.523	1.640	0.117
Total:	-0.210	-0.397	-0.187

Table D9. Atomic charges on 3-MCs involving two molecules of water and proline conformers **1a** and **1c**, where Δ represents atomic charges on **1c** 3-MC minus 1a 3-MC.

	Q(A)		
Atom A	**1a** 3-MC	**1c** 3-MC	Δ
O18	-1.220	-1.252	-0.032
O21	-1.190	-1.207	-0.017
O15	-1.184	-1.219	-0.035
O16	-1.140	-1.213	-0.072
N13	-0.985	-0.943	0.042
C4	0.300	0.230	-0.071
C1	0.320	0.270	-0.050
H5	0.372	0.440	0.068
H23	0.573	0.564	-0.009
H19	0.581	0.599	0.019
H20	0.597	0.588	-0.010
H17	0.611	0.471	-0.140
H22	0.613	0.619	0.006
C14	1.528	1.641	0.113
Total	-0.224	-0.412	-0.188

Table D10. Atomic charges on 4-MCs involving three molecules of water and proline conformers **1a** and **1c**, where Δ represents atomic charges on **1c** 4-MC minus **1a** 4-MC.

	Q(A)		
Atom A	**1a** 4-MC	**1c** 4-MC	Δ
O18	-1.222	-1.253	-0.032
O21	-1.191	-1.208	-0.017
O15	-1.187	-1.222	-0.035
O24	-1.145	-1.149	-0.004
O16	-1.143	-1.216	-0.073
N13	-1.014	-0.978	0.036
C4	0.301	0.238	-0.063
C1	0.322	0.276	-0.046
H5	0.417	0.489	0.072
H23	0.572	0.563	-0.009
H19	0.582	0.600	0.018
H25	0.583	0.595	0.013
H26	0.583	0.596	0.013
H20	0.597	0.587	-0.010
H17	0.608	0.458	-0.150
H22	0.614	0.619	0.006
C14	1.526	1.635	0.109
Total	-0.198	-0.370	-0.172

Table D11. Atomic charges on 2-MCs of a solvent molecule of DMSO and proline conformers **1a** and **1c**, where Δ represents atomic charges on **1c** 2-MC minus **1a** 2-MC.

	Q(A)		
Atom A	**1a**	**1c**	Δ
O26	-1.244	-1.241	0.003
O16	-1.198	-1.253	-0.054
O15	-1.140	-1.240	-0.100
N13	-1.028	-0.991	0.038
C18	-0.123	-0.122	0.002
C22	-0.123	-0.121	0.002
C4	0.303	0.239	-0.064
C1	0.325	0.279	-0.047
H17	0.431	0.503	0.073
H5	0.601	0.451	-0.150
S27	1.133	1.127	-0.005
C14	1.524	1.639	0.115
Total:	-0.540	-0.728	-0.189

Table D12. Most strongest attractive and repulsive diatomic intermolecular interactions (in kcal/mol) in the indicated 2-MCs involving a water molecule **4** with either **1a** (proline), or **1c** (the zwitterion)

Part A Molecules of **1a** and **4** in **1a-1w**

Atom A of **1a**	Atom B of **4**	E_{int}(A,B)
Most attractive diatomic interaction		
C14	O18	-169.9
O16	H19	-115.3
O15	H19	-76.2
H17	O18	-67.3
O16	H20	-64.9
O15	H20	-61.7
N13	H19	-44.3
N13	H20	-32.6
H5	O18	-24.8
C4	O18	-23.7
C1	O18	-22.0
Most repulsive diatomic interaction		
C4	H20	10.7
H5	H20	11.1
C1	H19	13.0
C4	H19	14.4
H5	H19	14.7
H17	H20	28.8
H17	H19	44.8
N13	O18	73.4
C14	H20	79.4
C14	H19	110.0
O15	O18	124.2
O16	O18	143.7
Total		-34.3

Table D13. Part B Molecules of **1c** and **4** in **1c-1w**

Atom A of **1a**	Atom B of **4**	E_{int}(A,B)
Most attractive diatomic interaction		
C14	O18	-203.1
O16	H19	-142.9
O15	H19	-88.1
O16	H20	-72.1
O15	H20	-69.8
N13	H19	-43.4
H17	O18	-41.5
N13	H20	-30.8
H5	O18	-30.4
C1	O18	-19.4
C4	O18	-18.0
Most repulsive diatomic interaction		
C4	H19	10.8
C1	H19	11.5
H5	H20	13.1
H17	H20	17.4
H5	H19	18.0
H17	H19	25.8
N13	O18	71.9
C14	H20	90.8
C14	H19	135.2
O15	O18	142.7
O16	O18	164.8
Total		-57.5

Table D14. Strongest attractive and repulsive diatomic intermolecular interactions (in kcal/mol) in the indicated 3-MCs involving two water molecule **4** with proline conformers **1a** and **1c**.

Part A Two molecules of water **4** and a molecule of proline **1a**

Atom A of **1a**	Atom B of **4**	E_{int}(A,B)
Most attractive diatomic interaction		
C14	O21	-179.0
C14	O18	-169.7
O15	H22	-129.5
H20	O21	-126.7
O16	H19	-102.1
O18	H22	-83.4
H19	O21	-75.7
O16	H22	-73.5
O16	H20	-70.3
O18	H23	-69.9
O15	H23	-68.4
O15	H19	-67.5
H17	O18	-67.3
O15	H20	-66.2
H17	O21	-52.2
O16	H23	-50.4
N13	H19	-41.7
N13	H22	-38.2
N13	H20	-35.0
N13	H23	-29.0
H5	O18	-25.4
C4	O18	-24.1
C4	O21	-22.9
H5	O21	-22.7
C1	O18	-22.0
C1	O21	-19.7
Most repulsive diatomic interaction		
C4	H23	10.1
H5	H23	10.1
C1	H20	10.4
C1	H22	11.5
C4	H20	11.7
H5	H20	12.0
C1	H19	12.1
H5	H22	13.2
C4	H19	13.5
C4	H22	13.9
H5	H19	14.0
H11	H23	22.7
H17	H20	30.9
H17	H22	31.2

Table D14 Part A continues

Atom A of **1a**	Atom B of **4**	E_{int}(A,B)
Most repulsive diatomic interaction		
H19	H23	31.3
H19	H22	40.6
H17	H19	41.7
H20	H23	45.8
H20	H22	53.5
N13	O21	64.8
N13	O18	74.1
C14	H23	76.3
C14	H20	86.4
C14	H19	98.6
O16	O21	118.4
C14	H22	121.2
O15	O18	123.2
O16	O18	143.9
O15	O21	152.8
O18	O21	159.1
Total		-83.1

Table D14. Part B Two molecules of water 4 and a molecule of the zwitterion 1c

Atom A	Atom B	E_{int}(A,B)
Most attractive diatomic interaction		
C14	O18	-199.9
C14	O21	-194.1
O15	H22	-144.9
O16	H19	-130.9
H20	O21	-123.6
O18	H22	-88.6
O16	H22	-81.3
H19	O21	-80.4
O15	H19	-78.2
O16	H20	-76.5
O15	H23	-72.1
O18	H23	-70.2
O15	H20	-69.7
O16	H23	-53.8
H17	O18	-42.0
N13	H19	-41.6
N13	H22	-37.0

Table D14 Part B continues

Atom A of **1c**	Atom B of **4**	E_{int}(A,B)
Most attractive diatomic interaction		
H17	O21	-33.4
N13	H20	-32.6
H5	O18	-31.2
N13	H23	-27.3
H5	O21	-27.1
C1	O18	-19.5
C4	O18	-18.6
C1	O21	-16.9
C4	O21	-16.6
Most repulsive diatomic interaction		
C4	H19	10.6
C1	H19	11.0
H5	H23	11.8
H5	H20	14.0
H17	H23	14.5
H5	H22	15.9
H5	H19	17.5
H17	H20	18.4
H17	H22	19.7
H17	H19	24.7
H19	H23	32.3
H20	H23	43.6
H19	H22	44.6
H20	H22	53.7
N13	O21	62.5
N13	O18	72.8
C14	H23	80.9
C14	H20	94.7
C14	H19	123.5
O16	O21	129.1
C14	H22	132.1
O15	O18	137.0
O15	O21	163.4
O18	O21	165.2
O16	O18	165.7
Total		-148.7

Table D 15. Strongest attractive and repulsive diatomic intermolecular interactions (in kcal/mol) in the indicated 4-MCs involving three water molecule **4** with proline conformers **1a** and **1c**.

Part A Three molecules of water **4** and a molecule of proline **1a**

Atom A of **1a**	Atom B of **4**	E_{int}(A,B)
Most attractive diatomic interaction		
C14	O21	-179.1
C14	O18	-170.4
O15	H22	-130.3
H20	O21	-126.6
C14	O24	-112.9
O16	H19	-103.5
O18	H22	-83.6
H5	O24	-81.7
H19	O21	-76.0
O16	H22	-73.9
O16	H20	-70.6
O18	H23	-70.1
O15	H23	-68.5
O15	H19	-68.1
H17	O18	-66.9
O15	H20	-66.4
N13	H25	-56.9
N13	H26	-56.9
H17	O24	-53.0
H17	O21	-51.8
O16	H23	-50.8
N13	H19	-43.3
O16	H26	-42.8
O15	H26	-40.5
O16	H25	-40.1
N13	H22	-39.3
O15	H25	-36.3
N13	H20	-36.1
C1	O24	-35.5
C4	O24	-32.7
H19	O24	-32.0
H22	O24	-31.2
O18	H26	-30.0
N13	H23	-29.9

Table D15 Part A continues

Atom A of **1a**	Atom B of **4**	E_{int}(A,B)
Most attractive diatomic interaction		
H20	O24	-28.7
O18	H25	-28.6
H5	O18	-28.5
O21	H26	-28.1
O21	H25	-26.0
H5	O21	-25.3
H23	O24	-24.7
C4	O18	-24.2
C4	O21	-23.0
C1	O18	-22.1
C1	O21	-19.8
Most repulsive diatomic interaction		
C4	H23	10.2
C1	H20	10.5
H5	H23	11.3
C1	H22	11.6
C4	H20	11.7
H23	H25	11.7
C1	H19	12.2
H23	H26	12.6
H5	H20	13.4
H20	H25	13.6
C4	H19	13.6
C4	H22	14.0
H20	H26	14.4
H22	H25	14.6
C4	H25	14.7
H5	H22	14.8
H19	H25	15.1
C4	H26	15.7
H5	H19	15.7
H19	H26	15.8
H22	H26	16.0
C1	H26	16.1
C1	H25	17.1
H17	H23	22.6
H17	H25	24.3

Table D15 Part A continues

Atom A of **1a**	Atom B of **4**	E_{int}(A,B)
Most repulsive diatomic interaction		
H17	H26	25.2
H17	H20	30.7
H17	H22	31.0
H5	H26	31.0
H5	H25	31.1
H19	H23	31.5
H19	H22	40.8
H17	H19	41.5
H20	H23	45.7
C14	H25	51.8
H20	H22	53.5
O21	O24	55.0
C14	H26	56.9
O18	O24	60.4
N13	O21	66.8
C14	H23	76.3
N13	O18	76.7
O15	O24	78.8
C14	H20	86.4
O16	O24	87.3
C14	H19	99.3
O16	O21	119.0
N13	O24	119.6
C14	H22	121.4
O15	O18	124.0
O16	O18	145.0
O15	O21	153.4
O18	O21	159.5
	Total	-104.0

Table D16. Part B Three molecules of water **4** and a molecule of the zwitterion **1c**

Atom A of **1c**	Atom B of **4**	E_{int}(A,B)
Most repulsive diatomic interaction		
C14	O18	-199.7
C14	O21	-193.9
O15	H22	-146.3
O16	H19	-132.0
C14	O24	-128.9
H20	O21	-123.7
H5	O24	-109.6
O18	H22	-88.8
O16	H22	-81.8
H19	O21	-80.7
O15	H19	-78.6
O16	H20	-76.8
O15	H23	-72.2
O18	H23	-70.2
O15	H20	-69.8
N13	H25	-59.6
N13	H26	-59.5
O16	H23	-54.0
H17	O24	-52.3
O16	H26	-49.4
O16	H25	-45.1
O15	H26	-43.5
N13	H19	-42.9
O15	H25	-42.1
H17	O18	-40.5
N13	H22	-38.3
H19	O24	-34.8
H5	O18	-34.3
O18	H26	-34.3
N13	H20	-33.6
H22	O24	-33.2
C1	O24	-32.8
H17	O21	-32.3
O18	H25	-31.2
O21	H26	-30.5
H5	O21	-29.9
C4	O24	-29.4
H20	O24	-29.3
O21	H25	-28.9
N13	H23	-28.2
H23	O24	-25.4
C1	O18	-19.8
C4	O18	-19.3
C4	O21	-17.3
C1	O21	-17.3
Most repulsive diatomic interaction		
C1	H22	10.1
C4	H22	10.3
C4	H19	11.0

Table D16 Part B continues

Atom A of **1c**	Atom B of **4**	E_{int}(A,B)
Most repulsive diatomic interaction		
C1	H19	11.1
H23	H25	12.7
H5	H23	13.0
H23	H26	13.2
C4	H26	13.5
C4	H25	13.8
H17	H23	14.0
H20	H25	14.2
C1	H26	14.7
H5	H20	15.4
H20	H26	15.5
C1	H25	15.5
H22	H25	16.4
H19	H25	16.6
H22	H26	17.3
H5	H22	17.5
H17	H20	17.7
H19	H26	18.3
H17	H22	19.1
H5	H19	19.2
H17	H25	23.6
H17	H19	23.8
H17	H26	25.3
H19	H23	32.3
H5	H25	40.5
H5	H26	40.6
H20	H23	43.5
H19	H22	44.8
H20	H22	53.7
O21	O24	58.2
C14	H25	62.1
N13	O21	64.6
O18	O24	64.8
C14	H26	65.6
N13	O18	75.1
C14	H23	80.5
O15	O24	85.1
C14	H20	94.4
O16	O24	95.9
N13	O24	123.1
C14	H19	123.5
O16	O21	129.9
C14	H22	132.2
O15	O18	137.5
O15	O21	164.3
O18	O21	165.6
O16	O18	166.5
0.0	TotaI	-164.4

Table D17. Strongest attractive and repulsive diatomic intermolecular interactions (in kcal/mol) in 2-MCs of the DMSO molecule and proline conformers **1a** and **1c**.

Part A. Molecules of DMSO **2** and proline **1a**

Atom A of **1a**	Atom B of **4**	E_{int}(A,B)
Most attractive diatomic interaction		
C14	O26	-126.4
N13	S27	-109.9
H17	O26	-95.7
O15	S27	-79.9
O16	S27	-76.2
H5	O26	-59.0
C1	O26	-39.4
C4	O26	-36.4
C14	C22	-10.6
C14	C18	-10.1
Most repulsive diatomic interaction		
N13	C18	10.3
C4	S27	29.4
C1	S27	31.7
H5	S27	46.8
H17	S27	60.4
O16	O26	88.6
O15	O26	98.2
C14	S27	106.0
N13	O26	134.6
Total		-37.4

Table D17. Part B. Molecules of DMSO **2** and proline **1c**

Atom A of **1c**	Atom B of **4**	E_{int}(A,B)
Most attractive diatomic interaction		
C14	O26	-140.2
H17	O26	-127.9
N13	S27	-111.3
O15	S27	-87.0
O16	S27	-80.7
H5	O26	-57.1
C1	O26	-37.1
C4	O26	-31.8
C14	C22	-11.7
C14	C18	-10.9
Most repulsive diatomic interaction		
N13	C18	10.0
C4	S27	25.1
C1	S27	28.7
H5	S27	43.5
H17	S27	76.1
O16	O26	93.5
O15	O26	106.9
C14	S27	117.1
N13	O26	137.2
Total		-57.7

PART D3

Data pertaining to the catalytic activity of the zwitterion of proline 1c.

Table D18. Energies (in au) and changes in energies relative to either **2c_GMS** for **2-MCs** of proline **1c** and acetone **2** or **2C_pre-org** for 3-MCs as proline **1c**, acetone **2**, and DMSO **3**.

	E	Δ	E_{ZPVE}	**Δ**	***H***	**Δ**	***G***	**Δ*G***
Data pertaining to 22-MCs of proline **1c** and acetone **2**								
2c_GMS	-594.55672	0.0	-594.32617	0.0	-594.31097	0.0	-594.37043	0.0
2c_GMS-TS	-594.50639	31.6	-594.27445	32.5	-594.26059	31.6	-594.31402	35.4
2a_1	-594.54675	6.3	-594.31786	5.2	-594.30246	5.3	-594.36275	4.8
2c_pre-org	-594.55170	3.2	-594.32130	3.1	-594.30584	3.2	-594.36628	2.6
2c_TS	-594.48957	42.1	-594.25805	42.7	-594.24500	41.4	-594.29680	46.2
2a_TS	-594.53029	16.6	-594.30086	15.9	-594.28823	14.3	-594.33865	19.9
3a	-594.54427	7.8	-594.30957	10.4	-594.29687	8.8	-594.34707	14.7
Data pertaing to 3-MCs of proline **1c**, acetone **2** and the solvent molecule of DMSO **3**								
2C_pre-org	-1147.8590	0.0	-1147.54819	0.0	-1147.52552	0.0	-1147.60383	0.0
2C_TS	-1147.7957	39.7	-1147.48339	40.7	-1147.46403	38.6	-1147.53001	46.3
2A_TS	-1147.8356	14.7	-1147.52503	14.5	-1147.50477	13.0	-1147.57437	18.5
3A	-1147.8532	3.6	-1147.53835	6.2	-1147.51825	4.6	-1147.58741	10.3

Table D19. Strongest attractive and repulsive diatomic intermolecular interactions (in kcal/mol) in complex 2c_GMS of proline **1c** and acetone **2**

Atom A of 1c	Atom B of 2	E_{int}(A,B)
Most attractive diatomic interaction		
C14	O19	-143.4
O16	C18	-103.6
H17	O19	-89.2
N13	C18	-86.2
O15	C18	-68.1
H5	O19	-50.9
C1	O19	-36.1
C4	O19	-25.6
O16	H21	-17.5
H6	O19	-9.9
Most repulsive diatomic interaction		
C14	H21	11.0
C4	C18	18.5
C1	C18	24.2
H5	C18	36.3
H17	C18	56.5
O15	O19	86.4
C14	C18	111.7
N13	O19	116.3
O16	O19	130.7
Total		-39.0

Table D20. Most strongest attractive and repulsive diatomic intermolecular interactions (in kcal/mol) in complex **2c_pre-org** of proline **1c** and acetone **2**

Atom A of **1c**	Atom B of **2**	E_{int}(A,B)
Most attractive diatomic interaction		
C14	O19	-143.4
O16	C18	-103.6
H17	O19	-89.2
N13	C18	-86.2
O15	C18	-68.1
H5	O19	-50.9
C1	O19	-36.1
C4	O19	-25.6
O16	H21	-17.5
H6	O19	-9.9
Most repulsive diatomic interaction		
C14	H21	11.0
C4	C18	18.5
C1	C18	24.2
H5	C18	36.3
H17	C18	56.5
O15	O19	86.4
C14	C18	111.7
N13	O19	116.3
O16	O19	130.7
Total		-39.0

Table D21. Most strongest attractive and repulsive diatomic intermolecular interactions (in kcal/mol) in transition state **2c_TS** made of atoms of proline **1c** and acetone **2**

Atom A of **1c**	Atom B of **2**	E_{int}(A,B)
Most attractive diatomic interaction		
N13	C18	-164.5
C14	O19	-143.5
O16	C18	-107.2
H17	O19	-89.7
O15	C18	-73.2
H5	O19	-64.0
C1	O19	-45.2
C4	O19	-23.8
H7	O19	-12.2
O16	H21	-12.0
Most repulsive diatomic interaction		
C4	C18	20.6
C1	C18	36.3
H5	C18	58.8
H17	C18	77.9
O15	O19	86.3
C14	C18	122.2
O16	O19	126.8
N13	O19	142.8
Total		-63.6

Table D22. Strongest attractive and repulsive diatomic intermolecular interactions (in kcal/mol) in complex **2a_GMS** of proline **1a** and acetone **2**

Atom A of **1a**	Atom B of **2**	E_{int}(A,B)
Most attractive diatomic interaction		
C14	O19	-161.3
O16	C18	-113.4
O15	C18	-98.6
N13	C18	-76.9
H17	O19	-65.6
C1	O19	-34.4
C4	O19	-29.7
H5	O19	-29.5
Most repulsive diatomic interaction		
H5	C18	24.0
C4	C18	24.0
C1	C18	26.2
H17	C18	56.9
N13	O19	94.3
O15	O19	115.1
O16	O19	125.1
C14	C18	138.3
Total		-5.3

Table D23. Strongest attractive and repulsive diatomic intermolecular interactions (in kcal/mol) in complex **2a_pre-org** of proline **1a** and acetone **2**

Atom A of **1a**	Atom B of **2**	E_{int}(A,B)
Most attractive diatomic interaction		
C14	O19	-139.6
O16	C18	-104.5
N13	C18	-103.4
H17	O19	-102.7
O15	C18	-69.9
H5	O19	-38.7
C1	O19	-37.9
C4	O19	-32.0
Most repulsive diatomic interaction		
C4	C18	26.0
C1	C18	31.0
H5	C18	33.2
H17	C18	73.4
O15	O19	88.9
C14	C18	108.1
N13	O19	119.8
O16	O19	135.0
Total		-13.1

Table D24. Strongest attractive and repulsive diatomic intermolecular interactions (in kcal/mol) in transition state **2a_TS** made of atoms of proline **1a** and acetone **2**

Atom A of **1a**	Atom B of **2**	E_{int}(A,B)
Most attractive diatomic interaction		
H17	O19	-217.6
N13	C18	-207.6
C14	O19	-194.0
O16	C18	-125.4
O15	C18	-81.2
H5	O19	-50.0
C1	O19	-45.8
C4	O19	-36.4
H6	O19	-9.5
Most repulsive diatomic interaction		
C4	C18	29.9
C1	C18	36.9
H5	C18	45.7
H17	C18	101.6
O15	O19	111.9
N13	O19	128.0
C14	C18	137.2
O16	O19	171.9
Total		-204.5

Table D25. Strongest attractive and repulsive diatomic intermolecular interactions (in kcal/mol) in complex **2b_GMS** of proline **1b** and acetone **2**

Atom A of **1b**	Atom B of **2**	E_{int}(A,B)
Most attractive diatomic interaction		
C14	O19	-159.8
H17	O19	-143.9
O16	C18	-114.2
O15	C18	-73.9
N13	C18	-58.0
C4	O19	-30.7
H5	O19	-26.4
C1	O19	-25.5
Most repulsive diatomic interaction		
C1	C18	19.7
H5	C18	20.1
C4	C18	21.9
N13	O19	76.4
H17	C18	85.6
O15	O19	97.8
C14	C18	117.8
O16	O19	150.0
Total		-43.2

Table D26. Strongest attractive and repulsive diatomic intermolecular interactions (in kcal/mol) in complex **2b_pre-org** of proline **1b** and acetone **2**

Atom A of **1b**	Atom B of **2**	E_{int}(A,B)
Most attractive diatomic interaction		
C14	O19	-165.3
H17	O19	-146.5
O16	C18	-120.5
N13	C18	-112.2
O15	C18	-78.8
C4	O19	-40.4
H5	O19	-36.5
C1	O19	-35.9
Most repulsive diatomic interaction		
C1	C18	30.6
H5	C18	31.2
C4	C18	31.4
H17	C18	90.3
O15	O19	100.2
N13	O19	120.1
C14	C18	127.2
O16	O19	153.1
Total		-51.8

Table D27. Strongest attractive and repulsive diatomic intermolecular interactions (in kcal/mol) in transition state **2a_TS** made of atoms of proline **1a** and acetone **2**

Atom A of **1b**	Atom B of **2**	E_{int}(A,B)
Most attractive diatomic interaction		
N13	C18	-224.8
H17	O19	-198.0
C14	O19	-197.4
O16	C18	-119.0
O15	C18	-78.7
H5	O19	-60.1
C4	O19	-43.3
C1	O19	-38.2
H12	O19	-14.3
Most repulsive diatomic interaction		
C4	C18	33.6
C1	C18	34.3
H5	C18	52.4
H17	C18	92.6
O15	O19	113.4
N13	O19	129.7
C14	C18	133.4
O16	O19	172.0
Total		-212.5

PART D4

Computational details and coordinates for all structures

All calculations were performed in Gaussian 09 Rev. D01 at the RB3LYP/6–311++G(d,p) with Grimme's empirical correction for dispersion (GD3) in solvent (DMSO) using the implicit default solvation model. Frequency calculations were performed on these structures while none and one imaginary frequency was obtained for minimum energy (local and global) and TS structures, respectively. The intrinsic reaction coordinate IRC was calculated using the TS in order to locate the respective energy minima (reactants or products). Topological calculations were performed using AIMAll (ver. 17.11.14) using B3LYP-generated wavefunctions.

1a

Atom	X	Y	Z
C1	-0.094582	-1.361651	-0.836534
C2	-0.519069	-1.257337	0.630229
C3	-1.078823	0.170695	0.715158
C4	-0.124681	0.972254	-0.199243
H5	0.328124	0.248080	-2.102555
H6	0.659111	-2.130821	-1.013211
H7	-0.963254	-1.576134	-1.469605
H8	-1.249018	-2.018557	0.907550
H9	0.351123	-1.367125	1.285041
H10	-2.088094	0.204983	0.298301
H11	-1.115513	0.573585	1.727191
H12	-0.646920	1.777708	-0.719826
N13	0.462801	-0.016626	-1.134515
C14	1.009859	1.633409	0.600748
O15	0.830750	2.494407	1.435540
O16	2.218840	1.166547	0.292567
H17	2.019346	0.486584	-0.416837

Zero-point correction =	0.144439 (Hartree/Particle)
Thermal correction to Energy =	0.151574
Thermal correction to Enthalpy =	0.152518
Thermal correction to Gibbs Free Energy =	0.112465
Sum of electronic and zero-point Energies =	–401.167135
Sum of electronic and thermal Energies =	–401.160000
Sum of electronic and thermal Enthalpies =	–401.159056
Sum of electronic and thermal Free Energies =	–401.199110

1a_TS

Atom	X	Y	Z
C1	1.926439	-0.645644	-0.118279
C2	1.590808	0.684438	-0.797902
C3	0.685805	1.380415	0.232033
C4	-0.160469	0.227168	0.794179
H5	0.819593	-1.535345	1.439995
H6	2.202960	-1.439067	-0.812203
H7	2.726774	-0.519615	0.614369
H8	2.486550	1.258422	-1.035336
H9	1.045418	0.507330	-1.729334
H10	1.287968	1.817876	1.031985
H11	0.061911	2.165834	-0.194085
H12	-0.431944	0.363346	1.840217
N13	0.659032	-1.011390	0.585933
C14	-1.449383	-0.050651	-0.028045
O15	-2.359841	0.763726	-0.103539
O16	-1.394081	-1.220645	-0.590907
H17	-0.295701	-1.500340	-0.153476

Zero-point correction=	0.141391 (Hartree/Particle)
Thermal correction to Energy=	0.148035
Thermal correction to Enthalpy=	0.148980
Thermal correction to Gibbs Free Energy=	0.110156
Sum of electronic and zero-point Energies=	–401.165276
Sum of electronic and thermal Energies=	–401.158632
Sum of electronic and thermal Enthalpies=	–401.157688
Sum of electronic and thermal Free Energies=	–401.196511

1b

Atom	X	Y	Z
C1	-0.40903	-1.24178	-1.03651
C2	-0.66799	-1.54479	0.469564
C3	-0.31623	-0.22343	1.209201
C4	-0.08985	0.767737	0.053782
H5	1.383941	-0.30408	-0.85838
H6	0.086511	-2.05623	-1.56514
H7	-1.34925	-1.02662	-1.55141
H8	-1.70549	-1.84022	0.636219
H9	-0.03368	-2.36208	0.81741
H10	-1.10285	0.109024	1.88681
H11	0.603217	-0.32737	1.789703
H12	-1.06013	1.175332	-0.26287
N13	0.429048	-0.02214	-1.08212
C14	0.773357	1.981069	0.337392
O15	0.900709	2.500917	1.419636
O16	1.38329	2.493824	-0.75052
H17	1.174427	1.920846	-1.51276

Zero-point correction =	0.144477 (Hartree/Particle)
Thermal correction to Energy =	0.151947
Thermal correction to Enthalpy =	0.152891
Thermal correction to Gibbs Free Energy =	0.111845
Sum of electronic and zero-point Energies =	–401.156469
Sum of electronic and thermal Energies =	–401.149000
Sum of electronic and thermal Enthalpies =	–401.148056
Sum of electronic and thermal Free Energies =	–401.189101

1c

Atom	X	Y	Z
C1	-0.094582	-1.361651	-0.836534
C2	-0.519069	-1.257337	0.630229
C3	-1.078823	0.170695	0.715158
C4	-0.124681	0.972254	-0.199243
H5	0.328124	0.248080	-2.102555
H6	0.659111	-2.130821	-1.013211
H7	-0.963254	-1.576134	-1.469605
H8	-1.249018	-2.018557	0.907550
H9	0.351123	-1.367125	1.285041
H10	-2.088094	0.204983	0.298301
H11	-1.115513	0.573585	1.727191
H12	-0.646920	1.777708	-0.719826
N13	0.462801	-0.016626	-1.134515
C14	1.009859	1.633409	0.600748
O15	0.830750	2.494407	1.435540
O16	2.218840	1.166547	0.292567
H17	2.019346	0.486584	-0.416837

Zero-point correction=	0.145904 (Hartree/Particle)
Thermal correction to Energy=	0.153163
Thermal correction to Enthalpy=	0.154107
Thermal correction to Gibbs Free Energy=	0.113521
Sum of electronic and zero-point Energies=	–401.167520
Sum of electronic and thermal Energies=	–401.160261
Sum of electronic and thermal Enthalpies=	–401.159316
Sum of electronic and thermal Free Energies=	–401.199903

1c_1w

Atom	X	Y	Z
C1	0.800534	-1.910348	0.851917
C2	2.152725	-1.302382	1.211926
C3	2.194524	-0.025500	0.360304
C4	0.751035	0.513407	0.409116
H5	-0.631457	-0.558395	1.603197
H6	0.821250	-2.383319	-0.129482
H7	0.390322	-2.604752	1.581348
H8	2.185971	-1.059990	2.277637
H9	2.971164	-1.987770	0.991340
H10	2.901478	0.714142	0.732108
H11	2.468756	-0.266793	-0.669774
H12	0.621524	1.243333	1.206388
N13	-0.104626	-0.702326	0.743377
C14	0.250395	1.112483	-0.927309
O15	0.822809	2.140634	-1.318851
O16	-0.687702	0.470208	-1.489627
H17	-0.773208	-0.765199	-0.045844
O18	-1.485146	1.497432	-3.902985
H19	-1.187760	1.138729	-3.034276
H20	-0.916291	2.259738	-4.051299

Zero-point correction=	0.170089 (Hartree/Particle)
Thermal correction to Energy=	0.180705
Thermal correction to Enthalpy=	0.181649
Thermal correction to Gibbs Free Energy=	0.131706
Sum of electronic and zero-point Energies=	–477.621715
Sum of electronic and thermal Energies	–477.611100
Sum of electronic and thermal Enthalpies=	–477.610156
Sum of electronic and thermal Free Energies=	–477.660098

1c_1w-TS

Atom	X	Y	Z
C1	0.743286	-1.853618	0.733210
C2	2.128862	-1.376914	1.176416
C3	2.262571	-0.016692	0.473421
C4	0.832051	0.564780	0.538040
H5	-0.663978	-0.521950	1.530435
H6	0.777499	-2.267211	-0.277467
H7	0.285651	-2.588511	1.393604
H8	2.150979	-1.248873	2.262565
H9	2.918671	-2.076002	0.897522
H10	2.985576	0.645853	0.947312
H11	2.566989	-0.156833	-0.567156
H12	0.713878	1.269315	1.360814
N13	-0.085150	-0.609669	0.701837
C14	0.367197	1.228121	-0.774129
O15	0.881674	2.230672	-1.238916
O16	-0.624541	0.548779	-1.297118
H17	-0.687260	-0.270778	-0.437551
O18	-1.616239	1.148006	-3.874935
H19	-1.271846	0.954856	-2.983141
H20	-1.119575	1.920001	-4.165553

Zero-point correction=	0.164689 (Hartree/Particle)
Thermal correction to Energy=	0.175162
Thermal correction to Enthalpy=	0.176106
Thermal correction to Gibbs Free Energy=	0.125885
Sum of electronic and zero-point Energies=	–477.615214
Sum of electronic and thermal Energies=	–477.604741
Sum of electronic and thermal Enthalpies=	–477.603797
Sum of electronic and thermal Free Energies=	–477.654018

1a_1w

Atom	X	Y	Z
C1	0.771821	-1.881945	0.819023
C2	2.173585	-1.378150	1.179143
C3	2.238514	-0.033771	0.440040
C4	0.786506	0.506866	0.560654
H5	-0.560992	-0.565604	1.704741
H6	0.770654	-2.320325	-0.183782
H7	0.371162	-2.621730	1.512302
H8	2.249757	-1.223631	2.259868
H9	2.965037	-2.064967	0.873304
H10	2.962339	0.663808	0.859670
H11	2.496983	-0.192934	-0.610408
H12	0.709827	1.235560	1.370465
N13	-0.084805	-0.667270	0.816626
C14	0.326409	1.207883	-0.716828
O15	0.843357	2.196885	-1.183996
O16	-0.721541	0.603713	-1.292857
H17	-0.918350	-0.161499	-0.673018
O18	-1.528966	1.205457	-4.006409
H19	-1.264825	1.012339	-3.092554
H20	-1.040175	2.002646	-4.236775

Zero-point correction=	0.167636 (Hartree/Particle)
Thermal correction to Energy=	0.178762
Thermal correction to Enthalpy=	0.179707
Thermal correction to Gibbs Free Energy=	0.127183
Sum of electronic and zero-point Energies=	–477.616050
Sum of electronic and thermal Energies=	–477.604924
Sum of electronic and thermal Enthalpies=	–477.603979
Sum of electronic and thermal Free Energies=	–477.656503

1c_2w

Atom	X	Y	Z
C1	0.893454	-1.944025	0.733324
C2	2.194259	-1.272074	1.163605
C3	2.140035	0.081698	0.442252
C4	0.662205	0.505201	0.545694
H5	-0.663950	-0.788358	1.563565
H6	0.957163	-2.330565	-0.283203
H7	0.529413	-2.725088	1.396407
H8	2.208593	-1.133438	2.248056
H9	3.062810	-1.868085	0.883390
H10	2.792763	0.831414	0.885825
H11	2.422963	-0.036697	-0.606882
H12	0.481045	1.115366	1.428638
N13	-0.101601	-0.800914	0.714401
C14	0.123721	1.230396	-0.706072
O15	0.620214	2.356621	-0.925000
O16	-0.737735	0.606500	-1.379203
H17	-0.742224	-0.834796	-0.097814
O18	-1.722976	1.709910	-3.768715
H19	-1.423414	1.269356	-2.948079
H20	-1.212290	2.538208	-3.755406
O21	-0.011677	3.887619	-3.080894
H22	0.236407	3.348833	-2.289425
H23	0.810748	4.038293	-3.558318

Zero-point correction=	0.195714 (Hartree/Particle)
Thermal correction to Energy=	0.208602
Thermal correction to Enthalpy=	0.209546
Thermal correction to Gibbs Free Energy=	0.154466
Sum of electronic and zero-point Energies=	–554.078872
Sum of electronic and thermal Energies=	–554.065984
Sum of electronic and thermal Enthalpies=	–554.065040
Sum of electronic and thermal Free Energies=	–554.120120

1c_2w-TS

Atom	X	Y	Z
C1	0.850352	-1.881230	0.591658
C2	2.172361	-1.346725	1.148404
C3	2.209709	0.094286	0.615008
C4	0.730330	0.539718	0.681297
H5	-0.693118	-0.776971	1.477963
H6	0.955311	-2.166585	-0.457735
H7	0.437106	-2.725393	1.141441
H8	2.145893	-1.348065	2.241919
H9	3.030256	-1.938209	0.825311
H10	2.852236	0.754834	1.195472
H11	2.562709	0.106096	-0.419549
H12	0.521099	1.134587	1.570080
N13	-0.083508	-0.716599	0.669474
C14	0.254837	1.305830	-0.565566
O15	0.706643	2.399671	-0.884502
O16	-0.651104	0.624132	-1.207986
H17	-0.680410	-0.286552	-0.462648
O18	-1.851632	1.582231	-3.682959
H19	-1.548158	1.139598	-2.874700
H20	-1.304071	2.388176	-3.698461
O21	-0.066469	3.738109	-3.187296
H22	0.256922	3.297544	-2.371840
H23	0.712629	3.866897	-3.738638

Zero-point correction=	0.190459 (Hartree/Particle)
Thermal correction to Energy=	0.203126
Thermal correction to Enthalpy=	0.204070
Thermal correction to Gibbs Free Energy=	0.149607
Sum of electronic and zero-point Energies=	–554.070671
Sum of electronic and thermal Energies=	–554.058004
Sum of electronic and thermal Enthalpies=	–554.057060
Sum of electronic and thermal Free Energies=	–554.111523

1a_2w

Atom	X	Y	Z
C1	0.884834	-1.917003	0.680839
C2	2.215892	-1.339306	1.173574
C3	2.195401	0.079624	0.586854
C4	0.696092	0.477987	0.681593
H5	-0.606090	-0.824126	1.621339
H6	0.971212	-2.238378	-0.361653
H7	0.518965	-2.760221	1.266783
H8	2.225155	-1.299844	2.267092
H9	3.080132	-1.918146	0.842712
H10	2.831628	0.785315	1.119402
H11	2.516950	0.060414	-0.458050
H12	0.514219	1.105937	1.556152
N13	-0.076855	-0.785554	0.758640
C14	0.232929	1.265066	-0.540898
O15	0.688595	2.346696	-0.861667
O16	-0.714748	0.644757	-1.236494
H17	-0.870403	-0.196403	-0.703625
O18	-1.835887	1.664486	-3.824610
H19	-1.607624	1.169626	-3.025903
H20	-1.268238	2.454566	-3.756053
O21	-0.058463	3.767514	-3.152019
H22	0.257361	3.311613	-2.345473
H23	0.728872	3.930754	-3.682389

Zero-point correction=	0.193370 (Hartree/Particle)
Thermal correction to Energy=	0.206683
Thermal correction to Enthalpy=	0.207627
Thermal correction to Gibbs Free Energy=	0.151416
Sum of electronic and zero-point Energies=	–554.070800
Sum of electronic and thermal Energies=	–554.057487
Sum of electronic and thermal Enthalpies=	–554.056543
Sum of electronic and thermal Free Energies=	–554.112754

1c_3w

Atom	X	Y	Z
C1	0.836985	-2.072350	0.345909
C2	1.798049	-1.288183	1.235973
C3	1.729182	0.128897	0.650076
C4	0.240572	0.312447	0.294705
H5	-1.078210	-1.272312	0.748642
H6	1.286601	-2.306642	-0.618732
H7	0.433288	-2.980732	0.787897
H8	1.446009	-1.295925	2.271245
H9	2.802843	-1.710373	1.213246
H10	2.066487	0.898767	1.341905
H11	2.340662	0.193865	-0.253878
H12	-0.311082	0.761775	1.119658
N13	-0.289024	-1.095019	0.101393
C14	-0.005263	1.131786	-0.988775
O15	0.327760	2.337093	-0.924727
O16	-0.494974	0.506993	-1.964993
H17	-0.639346	-1.123939	-0.867836
O18	-0.932024	1.815500	-4.406187
H19	-0.806408	1.301127	-3.582671
H20	-0.590854	2.691260	-4.154059
O21	0.129979	4.063730	-3.007258
H22	0.226316	3.446549	-2.239200
H23	1.017829	4.386325	-3.193253
O24	-2.349943	-1.541641	1.969633
H25	-2.140405	-1.368396	2.895246
H26	-3.207653	-1.126905	1.817571

Zero-point correction=	0.219120 (Hartree/Particle)
Thermal correction to Energy=	0.235804
Thermal correction to Enthalpy=	0.236748
Thermal correction to Gibbs Free Energy=	0.172013
Sum of electronic and zero-point Energies=	630.533734
Sum of electronic and thermal Energies=	630.517051
Sum of electronic and thermal Enthalpies=	630.516107
Sum of electronic and thermal Free Energies=	630.580842

1c_3w-TS

Atom	X	Y	Z
C1	0.789197	-1.942067	0.249255
C2	1.776558	-1.310431	1.235473
C3	1.748659	0.174175	0.838414
C4	0.269459	0.408180	0.449126
H5	-1.094474	-1.155490	0.697499
H6	1.260341	-2.098490	-0.724912
H7	0.367043	-2.889332	0.583767
H8	1.412964	-1.436691	2.259567
H9	2.774679	-1.746623	1.169644
H10	2.065139	0.843796	1.637139
H11	2.399550	0.348162	-0.022655
H12	-0.294844	0.873176	1.258601
N13	-0.294280	-0.928899	0.103365
C14	0.089757	1.247356	-0.825389
O15	0.443711	2.416670	-0.915771
O16	-0.467184	0.537321	-1.770676
H17	-0.584228	-0.429149	-1.163210
O18	-1.040132	1.627715	-4.416248
H19	-0.919279	1.129967	-3.592581
H20	-0.642510	2.490764	-4.199967
O21	0.173018	3.911196	-3.236546
H22	0.311762	3.419998	-2.398079
H23	1.048830	4.196930	-3.517420
O24	-2.538991	-1.559547	1.915995
H25	-2.508535	-2.415111	2.359780
H26	-2.708836	-0.919882	2.617356

Zero-point correction=	0.213541 (Hartree/Particle)
Thermal correction to Energy=	0.230366
Thermal correction to Enthalpy=	0.231310
Thermal correction to Gibbs Free Energy=	0.165221
Sum of electronic and zero-point Energies=	630.521629
Sum of electronic and thermal Energies=	630.504804
Sum of electronic and thermal Enthalpies=	630.503859
Sum of electronic and thermal Free Energies=	630.569948

1a_3w

Atom	X	Y	Z
C1	0.785267	-1.982819	0.285138
C2	1.747483	-1.307406	1.269333
C3	1.691196	0.162594	0.828169
C4	0.208630	0.341762	0.398737
H5	-1.091626	-1.227138	0.728397
H6	1.281543	-2.155608	-0.675219
H7	0.386949	-2.935343	0.636529
H8	1.370240	-1.412417	2.291211
H9	2.757552	-1.719900	1.231475
H10	1.971538	0.867378	1.610100
H11	2.355624	0.326887	-0.024609
H12	-0.371485	0.822948	1.189803
N13	-0.320468	-1.009188	0.099792
C14	0.067624	1.205987	-0.851593
O15	0.418837	2.370070	-0.919011
O16	-0.471766	0.549500	-1.871911
H17	-0.648743	-0.364809	-1.466220
O18	-0.975886	1.757629	-4.556269
H19	-0.900529	1.197548	-3.771239
H20	-0.577413	2.596306	-4.258188
O21	0.205284	3.954974	-3.209617
H22	0.328103	3.442566	-2.384248
H23	1.084317	4.260164	-3.458531
O24	-2.494050	-1.611240	2.099775
H25	-2.346966	-2.416222	2.609790
H26	-2.623881	-0.920523	2.759936

Zero-point correction=	0.216377 (Hartree/Particle)
Thermal correction to Energy=	0.233787
Thermal correction to Enthalpy=	0.234731
Thermal correction to Gibbs Free Energy=	0.167554
Sum of electronic and zero-point Energies=	630.520381
Sum of electronic and thermal Energies=	630.502971
Sum of electronic and thermal Enthalpies=	630.502026
Sum of electronic and thermal Free Energies=	630.569203

1a_1D

Atom	X	Y	Z
C1	0.732689	-2.046891	0.626258
C2	1.718061	-1.408826	1.605372
C3	2.007483	-0.044575	0.965336
C4	0.639569	0.404114	0.420660
H5	-0.242203	-0.885023	-0.876443
H6	1.245739	-2.472062	-0.236216
H7	0.078100	-2.798456	1.063456
H8	1.250533	-1.281944	2.585516
H9	2.611673	-2.020686	1.732722
H10	2.413805	0.683523	1.665774
H11	2.719074	-0.157617	0.142293
H12	0.082039	0.959427	1.174479
N13	-0.102388	-0.885145	0.146363
C14	0.718995	1.238555	-0.884587
O15	0.311649	0.664154	-1.929127
O16	1.199626	2.383831	-0.760562
H17	-1.039874	-0.889775	0.613551
C18	-1.772702	-1.060877	3.907058
H19	-0.921729	-0.428345	3.655239
H20	-2.145249	-0.835860	4.907281
H21	-1.510141	-2.115262	3.832232
C22	-3.195206	1.045987	2.861919
H23	-3.948519	1.391574	2.155432
H24	-3.491504	1.299166	3.880713
H25	-2.216998	1.462461	2.620987
O26	-2.535998	-1.058491	1.318511
S27	-3.121899	-0.767571	2.718461

Zero-point correction=	0.226772 (Hartree/Particle)
Thermal correction to Energy=	0.241102
Thermal correction to Enthalpy=	0.242046
Thermal correction to Gibbs Free Energy=	0.183189
Sum of electronic and zero-point Energies=	954.392784
Sum of electronic and thermal Energies=	954.378454
Sum of electronic and thermal Enthalpies=	954.377510
Sum of electronic and thermal Free Energies=	954.436367

1a_1D-TS

Atom	X	Y	Z
C1	0.743109	-2.009025	0.606036
C2	1.700399	-1.383754	1.626768
C3	1.966353	0.010417	1.038022
C4	0.605596	0.402058	0.419513
H5	-0.115386	-0.549734	-1.159752
H6	1.295189	-2.411676	-0.247496
H7	0.115259	-2.800641	1.015014
H8	1.208043	-1.298616	2.599711
H9	2.612276	-1.968769	1.759006
H10	2.298330	0.737632	1.778385
H11	2.732620	-0.048794	0.259946
H12	0.024962	1.038802	1.088687
N13	-0.108658	-0.877658	0.143213
C14	0.721038	1.084051	-0.960918
O15	0.223101	0.315487	-1.890248
O16	1.230291	2.185183	-1.120152
H17	-1.035695	-0.895721	0.589649
C18	-1.784330	-1.136410	3.883860
H19	-0.908106	-0.551255	3.605734
H20	-2.089387	-0.921486	4.908914
H21	-1.592446	-2.201927	3.764680
C22	-3.128478	1.087016	2.994755
H23	-3.898568	1.505681	2.348277
H24	-3.350220	1.314421	4.038405
H25	-2.142821	1.457561	2.711261
O26	-2.668026	-0.985849	1.339201
S27	-3.16982	-0.72161	2.772204

Zero-point correction=	0.221702 (Hartree/Particle)
Thermal correction to Energy=	0.235766
Thermal correction to Enthalpy=	0.236710
Thermal correction to Gibbs Free Energy=	0.178632
Sum of electronic and zero-point Energies=	–954.384113
Sum of electronic and thermal Energies=	–954.370049
Sum of electronic and thermal Enthalpies=	–954.369105
Sum of electronic and thermal Free Energies=	–954.427184

1a_1D

Atom	X	Y	Z
C1	1.373131	-1.818602	-0.432468
C2	2.313751	-1.144755	0.575493
C3	2.570291	0.222255	-0.073785
C4	1.203889	0.560840	-0.726847
H5	0.573421	-0.241420	-2.655620
H6	1.950625	-2.262495	-1.250248
H7	0.752054	-2.602077	0.004972
H8	1.808777	-1.019953	1.537782
H9	3.232528	-1.709869	0.745392
H10	2.884093	0.992437	0.630311
H11	3.344925	0.134536	-0.841233
H12	0.614095	1.209616	-0.073185
N13	0.517335	-0.728024	-0.959699
C14	1.371358	1.296382	-2.057827
O15	0.930479	0.590139	-3.098341
O16	1.864259	2.399939	-2.170615
H17	-0.397230	-0.728842	-0.502660
C18	-1.145094	-0.889825	2.786963
H19	-0.295129	-0.277338	2.486939
H20	-1.423852	-0.692539	3.822918
H21	-0.926784	-1.948227	2.651095
C22	-2.577896	1.304077	1.981012
H23	-3.373450	1.714653	1.360626
H24	-2.781768	1.503963	3.033888
H25	-1.609074	1.707052	1.683705
O26	-2.103066	-0.721520	0.271428
S27	-2.573454	-0.500691	1.720531

Zero-point correction=	0.224868 (Hartree/Particle)
Thermal correction to Energy=	0.239447
Thermal correction to Enthalpy=	0.240391
Thermal correction to Gibbs Free Energy=	0.180810
Sum of electronic and zero-point Energies=	954.384220
Sum of electronic and thermal Energies=	954.369641
Sum of electronic and thermal Enthalpies=	954.368697
Sum of electronic and thermal Free Energies=	954.428278

2c_inp

Atom	X	Y	Z
C1	-0.690672	-1.849803	1.911015
C2	-2.063187	-1.952947	2.569084
C3	-2.937960	-1.026230	1.708199
C4	-2.382355	-1.168078	0.276074
H5	-1.015630	-2.771628	0.046846
H6	-0.209979	-0.900188	2.142857
H7	-0.009579	-2.672204	2.118177
H8	-2.426928	-2.983231	2.525102
H9	-2.028028	-1.647898	3.615228
H10	-3.994029	-1.288314	1.750040
H11	-2.841817	0.007825	2.039241
H12	-2.999153	-1.821698	-0.338928
N13	-1.023197	-1.831237	0.438258
C14	-2.162699	0.172404	-0.484222
O15	-3.160508	0.913523	-0.568988
O16	-0.997749	0.361023	-0.924279
H17	-0.390123	-1.226606	-0.120934
C18	1.995108	-3.247562	-2.449906
O19	1.102684	-2.893918	-1.695153
C20	1.806565	-3.246664	-3.948645
H21	2.168990	-4.181557	-4.384660
H22	0.760060	-3.086742	-4.206251
H23	2.412649	-2.441373	-4.377568
C24	3.327864	-3.727170	-1.936545
H25	3.333654	-4.822069	-1.997011
H26	4.147058	-3.356533	-2.557370
H27	3.467856	-3.431970	-0.897431

2c_1

Atom	X	Y	Z
C1	-0.280888	-2.037195	1.774049
C2	-1.563701	-2.861393	1.673020
C3	-2.534313	-1.905276	0.966010
C4	-1.660648	-1.197035	-0.085651
H5	0.397521	-1.683131	-0.200944
H6	-0.329601	-1.320565	2.593566
H7	0.633862	-2.620393	1.859304
H8	-1.393337	-3.754855	1.065922
H9	-1.915121	-3.180053	2.654795
H10	-3.377634	-2.414076	0.501780
H11	-2.929359	-1.175086	1.677978
H12	-1.662387	-1.738260	-1.031167
N13	-0.255513	-1.257660	0.481410
C14	-2.039575	0.287562	-0.331203
O15	-3.136130	0.475438	-0.895145
O16	-1.209322	1.139603	0.084390
H17	0.001798	-0.264445	0.612622
C18	1.557268	-3.313082	-2.129320
O19	1.514760	-2.301807	-1.438947
C20	0.592284	-4.451652	-1.932206
H21	1.097483	-5.414243	-2.036284
H22	0.097516	-4.386415	-0.964582
H23	-0.163698	-4.397933	-2.723569
C24	2.579020	-3.460687	-3.223021
H25	3.304503	-4.224503	-2.922921
H26	2.106006	-3.817606	-4.141705
H27	3.095094	-2.518313	-3.399936

Zero-point correction=	0.230752 (Hartree/Particle)
Thermal correction to Energy=	0.244954
Thermal correction to Enthalpy=	0.245898
Thermal correction to Gibbs Free Energy=	0.186604
Sum of electronic and zero-point Energies=	–594.325538
Sum of electronic and thermal Energies=	–594.311335
Sum of electronic and thermal Enthalpies=	–594.310391
Sum of electronic and thermal Free Energies=	–594.369686

2c_pre-org

Atom	X	Y	Z
C1	0.784860	1.995643	-0.093251
C2	2.224723	2.140458	0.394210
C3	2.626142	0.695847	0.716997
C4	2.021424	-0.117846	-0.438473
H5	0.733491	0.801183	-1.831819
H6	0.080827	1.903466	0.731489
H7	0.443400	2.778584	-0.766055
H8	2.858102	2.545460	-0.399917
H9	2.288477	2.806179	1.255417
H10	3.703020	0.548227	0.778615
H11	2.183338	0.382552	1.667366
H12	2.688504	-0.115922	-1.299718
N13	0.776129	0.665759	-0.823638
C14	1.654988	-1.576077	-0.063494
O15	2.633519	-2.331545	0.116825
O16	0.429461	-1.831470	0.042908
H17	-0.058249	0.110256	-0.560892
C18	-3.004402	0.031117	0.015357
O19	-2.020903	0.688150	-0.295518
C20	-2.934812	-1.463747	0.187767
H21	-1.899725	-1.801113	0.175997
H22	-3.433114	-1.764337	1.113618
H23	-3.488168	-1.933036	-0.633446
C24	-4.342872	0.688038	0.240594
H25	-5.126765	0.155405	-0.304598
H26	-4.594456	0.620245	1.304388
H27	-4.315486	1.734638	-0.060073

Zero-point correction=	0.230409 (Hartree/Particle)
Thermal correction to Energy=	0.244923
Thermal correction to Enthalpy=	0.245867
Thermal correction to Gibbs Free Energy=	0.185428
Sum of electronic and zero-point Energies=	–594.321296
Sum of electronic and thermal Energies=	–594.306782
Sum of electronic and thermal Enthalpies=	–594.305837
Sum of electronic and thermal Free Energies=	–594.366277

2c_GMS

Atom	X	Y	Z
C1	1.526410	-1.921791	-0.829866
C2	2.276772	-2.000082	0.500419
C3	2.510449	-0.525090	0.854090
C4	1.191260	0.155758	0.456513
H5	-0.335122	-0.923319	-0.517357
H6	2.207143	-1.752288	-1.663514
H7	0.895653	-2.780463	-1.050136
H8	1.652365	-2.480673	1.258726
H9	3.201080	-2.570884	0.406848
H10	2.737059	-0.363941	1.906789
H11	3.335833	-0.119063	0.262026
H12	0.466713	0.106084	1.269533
N13	0.661966	-0.691024	-0.684391
C14	1.331859	1.622949	-0.026328
O15	1.676071	2.445462	0.844939
O16	1.093092	1.819724	-1.248512
H17	0.705169	-0.060673	-1.502554
C18	-2.844459	-0.201492	0.072978
O19	-2.038762	-1.116715	-0.057938
C20	-4.269413	-0.476653	0.465473
H21	-4.917580	-0.252530	-0.388408
H22	-4.396331	-1.518414	0.755893
H23	-4.575845	0.187867	1.277713
C24	-2.455107	1.237666	-0.138373
H25	-3.231211	1.769351	-0.693618
H26	-2.380707	1.718419	0.843426
H27	-1.497719	1.329272	-0.650519

Zero-point correction=	0.230544 (Hartree/Particle)
Thermal correction to Energy=	0.244804
Thermal correction to Enthalpy=	0.245748
Thermal correction to Gibbs Free Energy=	0.186287
Sum of electronic and zero-point Energies=	–594.326174
Sum of electronic and thermal Energies=	–594.311914
Sum of electronic and thermal Enthalpies=	–594.310970
Sum of electronic and thermal Free Energies=	–594.370431

2c_GMS-TS

Atom	X	Y	Z
C1	-0.040800	-1.655444	0.584979
C2	-1.290705	-2.339763	0.045772
C3	-2.266195	-1.173206	-0.160647
C4	-1.372548	-0.010432	-0.630105
H5	0.578455	-0.582451	-1.114605
H6	-0.177924	-1.329514	1.616211
H7	0.874957	-2.232207	0.502010
H8	-1.066202	-2.834096	-0.903571
H9	-1.665292	-3.091725	0.740864
H10	-3.045392	-1.392613	-0.889150
H11	-2.751394	-0.912254	0.782641
H12	-1.409300	0.133127	-1.708670
N13	0.076705	-0.403740	-0.255367
C14	-1.628353	1.340224	0.087942
O15	-2.740497	1.864065	-0.054752
O16	-0.634104	1.750533	0.765691
H17	0.271087	0.490536	0.290736
C18	2.239896	0.087645	-0.155795
O19	2.578624	-0.984026	-0.639138
C20	2.122482	1.327274	-1.027757
H21	3.112522	1.794352	-1.010422
H22	1.892348	1.061550	-2.060456
H23	1.405833	2.054215	-0.645262
C24	2.336416	0.327734	1.340012
H25	3.327254	0.764562	1.504768
H26	1.602158	1.043900	1.711310
H27	2.280616	-0.609970	1.890343

Zero-point correction=	0.231939 (Hartree/Particle)
Thermal correction to Energy=	0.244854
Thermal correction to Enthalpy=	0.245798
Thermal correction to Gibbs Free Energy=	0.192368
Sum of electronic and zero-point Energies=	–594.274452
Sum of electronic and thermal Energies=	–594.261537
Sum of electronic and thermal Enthalpies=	–594.260593
Sum of electronic and thermal Free Energies=	–594.314024

2a_1

Atom	X	Y	Z
C1	-0.300349	-1.542403	0.630363
C2	-1.565278	-2.349324	0.318233
C3	-2.593304	-1.246781	0.025996
C4	-1.750268	-0.160758	-0.698222
H5	0.235737	-0.575442	-1.117725
H6	-0.330440	-1.169419	1.659332
H7	0.628610	-2.096525	0.498150
H8	-1.404690	-2.966628	-0.571094
H9	-1.868766	-3.001747	1.139273
H10	-3.432483	-1.578262	-0.584568
H11	-2.996594	-0.850445	0.962117
H12	-1.871373	-0.236176	-1.781073
N13	-0.339312	-0.389543	-0.304828
C14	-2.169722	1.254700	-0.297480
O15	-3.267103	1.722761	-0.513128
O16	-1.208071	1.932602	0.332608
H17	-0.442452	1.289285	0.331537
C18	2.758507	0.191163	-0.305172
O19	2.668363	-0.719129	-1.113269
C20	2.596809	1.634228	-0.717851
H21	3.585788	2.105771	-0.727270
H22	2.158327	1.702403	-1.712698
H23	1.989964	2.184467	0.005090
C24	3.034842	-0.068967	1.154884
H25	3.823179	0.592784	1.523381
H26	2.129953	0.162424	1.726708
H27	3.306847	-1.111281	1.316284

Zero-point correction=	0.228890 (Hartree/Particle)
Thermal correction to Energy=	0.243346
Thermal correction to Enthalpy=	0.244290
Thermal correction to Gibbs Free Energy=	0.183997
Sum of electronic and zero-point Energies=	–594.317857
Sum of electronic and thermal Energies=	–594.303401
Sum of electronic and thermal Enthalpies=	–594.302456
Sum of electronic and thermal Free Energies=	–594.362749

2c_TS

Atom	X	Y	Z
C1	-0.040021	-1.540287	-0.765281
C2	1.036436	-2.385211	-0.098188
C3	2.099948	-1.355565	0.309264
C4	1.295969	-0.090526	0.664580
H5	-0.713016	-0.474775	0.929168
H6	0.267984	-1.185383	-1.748857
H7	-1.009730	-2.016775	-0.856696
H8	0.623932	-2.888349	0.780941
H9	1.420431	-3.148797	-0.775253
H10	2.709876	-1.686890	1.148493
H11	2.768636	-1.144586	-0.527817
H12	1.219759	0.073422	1.738349
N13	-0.140233	-0.312811	0.112518
C14	1.787605	1.206679	-0.031284
O15	2.930611	1.600040	0.234985
O16	0.931356	1.712829	-0.821437
H17	-0.157435	0.605929	-0.436314
C18	-2.159636	0.320346	-0.069744
O19	-2.244439	0.160281	-1.277077
C20	-1.952106	1.704867	0.530151
H21	-1.418666	2.354577	-0.160488
H22	-2.958249	2.104765	0.690683
H23	-1.450072	1.691232	1.499779
C24	-2.784926	-0.705032	0.879769
H25	-2.378280	-0.684299	1.894900
H26	-3.836654	-0.414038	0.958659
H27	-2.746722	-1.713171	0.469457

Zero-point correction=	0.231512 (Hartree/Particle)
Thermal correction to Energy=	0.243622
Thermal correction to Enthalpy=	0.244567
Thermal correction to Gibbs Free Energy=	0.192766
Sum of electronic and zero-point Energies=	594.258054
Sum of electronic and thermal Energies=	594.245943
Sum of electronic and thermal Enthalpies=	594.244999
Sum of electronic and thermal Free Energies=	594.296799

2a_TS

Atom	X	Y	Z
C1	-0.108795	-1.944959	-0.306892
C2	1.323118	-2.409745	-0.066249
C3	2.098710	-1.089730	-0.047517
C4	1.121739	-0.069899	0.611253
H5	-0.493751	-0.995959	1.475096
H6	-0.266548	-1.644553	-1.345825
H7	-0.867363	-2.672687	-0.027603
H8	1.395785	-2.919204	0.898781
H9	1.672868	-3.092801	-0.841375
H10	3.037356	-1.137328	0.502315
H11	2.322608	-0.777600	-1.070835
H12	1.349956	0.050589	1.668064
N13	-0.252197	-0.716793	0.527649
C14	1.383377	1.304834	-0.032949
O15	2.348250	1.923462	0.396989
O16	0.683497	1.719743	-1.052911
H17	-0.298388	1.234060	-1.207302
C18	-1.757274	0.298658	-0.049394
O19	-1.468337	0.635601	-1.264147
C20	-1.776629	1.385668	1.019967
H21	-0.923330	2.057055	0.941886
H22	-2.681075	1.978404	0.855248
H23	-1.823214	0.969373	2.027619
C24	-2.879009	-0.714463	0.097692
H25	-2.915641	-1.165628	1.090939
H26	-3.816790	-0.173890	-0.060287
H27	-2.804242	-1.488262	-0.665048

Zero-point correction=	0.229426 (Hartree/Particle)
Thermal correction to Energy=	0.241109
Thermal correction to Enthalpy=	0.242053
Thermal correction to Gibbs Free Energy=	0.191640
Sum of electronic and zero-point Energies=	594.300861
Sum of electronic and thermal Energies=	594.289178
Sum of electronic and thermal Enthalpies=	594.288234
Sum of electronic and thermal Free Energies=	594.338647

3a

Atom	X	Y	Z
C1	-0.100166	-1.748118	-0.578977
C2	1.417714	-1.979691	-0.474910
C3	1.842781	-1.228556	0.797435
C4	0.932508	0.005361	0.798344
H5	-0.699730	-1.103701	1.286316
H6	-0.418473	-1.400081	-1.556490
H7	-0.686650	-2.619786	-0.299329
H8	1.656640	-3.041759	-0.430057
H9	1.918999	-1.556679	-1.347005
H10	1.654982	-1.833807	1.688843
H11	2.890707	-0.936124	0.799474
H12	0.817002	0.445625	1.786498
N13	-0.411812	-0.638461	0.424408
C14	1.486526	1.106663	-0.154057
O15	2.545083	1.611580	0.253484
O16	0.870423	1.381533	-1.223171
H17	-0.668922	1.033678	-1.399032
C18	-1.663903	0.262745	0.051160
O19	-1.575584	0.625467	-1.278255
C20	-1.667217	1.458922	1.002066
H21	-0.824028	2.121696	0.809821
H22	-2.585990	2.019373	0.825172
H23	-1.651808	1.145136	2.048114
C24	-2.897618	-0.614525	0.231949
H25	-3.005602	-0.950477	1.265218
H26	-3.773473	-0.019301	-0.028236
H27	-2.863161	-1.478119	-0.432808

Zero-point correction=	0.234700 (Hartree/Particle)
Thermal correction to Energy=	0.246455
Thermal correction to Enthalpy=	0.247399
Thermal correction to Gibbs Free Energy=	0.197197
Sum of electronic and zero-point Energies=	594.309569
Sum of electronic and thermal Energies=	594.297814
Sum of electronic and thermal Enthalpies=	594.296869
Sum of electronic and thermal Free Energies=	594.347071

2C_pre-org

Atom	X	Y	Z
C1	1.173882	-2.053919	0.290459
C2	2.634589	-1.935969	0.719757
C3	3.096445	-0.660345	0.000189
C4	1.884647	0.286909	0.104859
H5	0.222092	-0.418293	1.203281
H6	1.087215	-2.435861	-0.726991
H7	0.543325	-2.644699	0.952278
H8	2.699939	-1.812207	1.804808
H9	3.211851	-2.818366	0.441884
H10	3.987710	-0.215921	0.440500
H11	3.311460	-0.878152	-1.049730
H12	1.956031	0.915210	0.993026
N13	0.695595	-0.627410	0.294857
C14	1.669868	1.190591	-1.136693
O15	2.566758	2.037896	-1.337412
O16	0.631040	0.971629	-1.811590
H17	0.035087	-0.432322	-0.471236
C18	-2.634858	0.033209	0.528048
O19	-2.211269	-0.841745	-0.213504
C20	-2.150465	1.458090	0.428104
H21	-1.412478	1.561599	-0.367326
H22	-2.997990	2.124937	0.243539
H23	-1.709612	1.743866	1.387199
C24	-3.632695	-0.268893	1.616074
H25	-3.096319	-0.206087	2.568125
H26	-4.434030	0.473801	1.635447
H27	-4.043931	-1.270693	1.495621
S28	0.248125	-0.176179	4.041692
C29	-0.854836	0.701525	5.190594
H30	-1.847835	0.255216	5.135198
H31	-0.440582	0.624786	6.196482
H32	-0.878817	1.742498	4.871519
C33	0.013494	-1.863405	4.680599
H34	0.399265	-1.908603	5.699860
H35	-1.048553	-2.108152	4.646172
H36	0.584910	-2.527328	4.033017
O37	-0.496348	-0.145764	2.684576

Zero-point correction=	0.310796 (Hartree/Particle)
Thermal correction to Energy=	0.332522
Thermal correction to Enthalpy=	0.333466
Thermal correction to Gibbs Free Energy=	0.255157
Sum of electronic and zero-point Energies=	1147.548194
Sum of electronic and thermal Energies=	1147.526468
Sum of electronic and thermal Enthalpies=	1147.525524
Sum of electronic and thermal Free Energies=	1147.603833

2C_TS

Atom	X	Y	Z
C1	-1.119723	0.271719	1.805550
C2	-0.377270	-0.964614	2.294580
C3	-0.802402	-2.053545	1.301064
C4	-0.981643	-1.308254	-0.033360
H5	-0.056695	0.498240	-0.045255
H6	-2.185145	0.221655	2.029804
H7	-0.726984	1.206794	2.186838
H8	0.702027	-0.795369	2.248695
H9	-0.634728	-1.202970	3.327196
H10	-0.069309	-2.854742	1.213610
H11	-1.751108	-2.499600	1.606698
H12	-0.153302	-1.468159	-0.719347
N13	-0.992910	0.216828	0.304060
C14	-2.314554	-1.594711	-0.766983
O15	-2.524980	-2.770490	-1.108641
O16	-3.047831	-0.575710	-0.933948
H17	-1.891004	0.406466	-0.207491
C18	-1.169533	2.248545	-0.237285
O19	-2.260189	2.442406	0.287076
C20	-1.062527	1.965083	-1.733130
H21	-1.916219	1.386589	-2.083946
H22	-1.083772	2.946468	-2.216549
H23	-0.126630	1.476401	-2.006623
C24	0.083548	2.844629	0.395188
H25	0.983986	2.253437	0.239160
H26	0.230335	3.797653	-0.124823
H27	-0.074726	3.058679	1.450630
S28	2.682828	-0.596123	-0.073497
C29	3.726645	-1.027776	-1.497278
H30	4.014769	-0.110263	-2.010900
H31	4.599698	-1.571351	-1.134123
H32	3.128033	-1.665526	-2.145974
C33	3.837489	0.518534	0.782215
H34	4.706534	-0.059145	1.099215
H35	4.120528	1.322297	0.102063
H36	3.311752	0.913243	1.650751
O37	1.580114	0.324007	-0.653918

Zero-point correction= 0.312309 (Hartree/Particle)
Thermal correction to Energy= 0.330720
Thermal correction to Enthalpy= 0.331665
Thermal correction to Gibbs Free Energy= 0.265685
Sum of electronic and zero-point Energies= –1147.483389
Sum of electronic and thermal Energies= –1147.464978
Sum of electronic and thermal Enthalpies= –1147.464034
Sum of electronic and thermal Free Energies= –1147.530014

2A_TS

Atom	X	Y	Z
C1	-0.660052	-0.373270	1.672921
C2	-0.750834	-1.917884	1.582750
C3	-0.533734	-2.222715	0.089358
C4	-1.115290	-0.968406	-0.597142
H5	0.344935	0.305623	-0.003974
H6	-1.526012	0.060794	2.177504
H7	0.238757	-0.032248	2.185937
H8	-0.013823	-2.410047	2.218024
H9	-1.739811	-2.259001	1.898441
H10	0.532387	-2.282891	-0.144408
H11	-1.012252	-3.140877	-0.247546
H12	-0.718190	-0.828696	-1.603622
N13	-0.630786	0.130326	0.272799
C14	-2.641828	-1.122974	-0.766118
O15	-3.050643	-2.087124	-1.391366
O16	-3.480312	-0.251495	-0.244274
H17	-3.094460	0.633130	0.157123
C18	-1.420965	1.983486	0.155991
O19	-2.567931	1.858712	0.698343
C20	-1.334333	2.140983	-1.353256
H21	-2.054836	1.498342	-1.859831
H22	-1.590083	3.179875	-1.586811
H23	-0.329386	1.941655	-1.727717
C24	-0.354039	2.723490	0.939341
H25	0.647409	2.542659	0.546990
H26	-0.574032	3.792998	0.855780
H27	-0.400185	2.449204	1.993431
S28	3.121120	-0.445023	-0.486255
C29	4.638282	0.367723	-1.079203
H30	4.800030	1.277126	-0.499620
H31	5.471583	-0.327087	-0.967761
H32	4.482153	0.602017	-2.131308
C33	3.595666	-0.626756	1.263464
H34	4.453270	-1.297718	1.326579
H35	3.830953	0.357469	1.669887
H36	2.741575	-1.062725	1.780365
O37	2.030854	0.648613	-0.513490

Zero-point correction=	0.310536 (Hartree/Particle)
Thermal correction to Energy=	0.329847
Thermal correction to Enthalpy=	0.330791
Thermal correction to Gibbs Free Energy=	0.261194
Sum of electronic and zero-point Energies=	1147.525030
Sum of electronic and thermal Energies=	1147.505719
Sum of electronic and thermal Enthalpies=	1147.504774
Sum of electronic and thermal Free Energies=	–1147.574372

3A

Atom	X	Y	Z
C1	-0.678372	-0.193303	1.748137
C2	-0.789241	-1.726689	1.680276
C3	-0.518595	-2.074081	0.207401
C4	-1.134586	-0.893802	-0.557093
H5	0.345148	0.362646	0.038170
H6	-1.519880	0.275317	2.249748
H7	0.247196	0.145196	2.209307
H8	-0.085223	-2.210001	2.357387
H9	-1.796494	-2.039848	1.960891
H10	0.554866	-2.126527	0.010158
H11	-0.964603	-3.015823	-0.105992
H12	-0.689749	-0.764332	-1.541848
N13	-0.665561	0.277428	0.304891
C14	-2.664039	-1.101501	-0.752862
O15	-2.936570	-2.029692	-1.534623
O16	-3.484785	-0.372069	-0.125284
H17	-3.017264	1.053800	0.410286
C18	-1.237088	1.712919	0.077332
O19	-2.468478	1.834143	0.709622
C20	-1.321391	1.940295	-1.433173
H21	-2.079465	1.302865	-1.888710
H22	-1.606092	2.979410	-1.602676
H23	-0.358160	1.759072	-1.915223
C24	-0.269128	2.691609	0.737545
H25	0.731493	2.607251	0.312790
H26	-0.645652	3.701622	0.570758
H27	-0.221844	2.520587	1.813665
S28	3.049505	-0.509958	-0.445720
C29	4.473934	0.332455	-1.197482
H30	4.650575	1.265248	-0.661406
H31	5.338395	-0.329854	-1.138942
H32	4.215735	0.524336	-2.237853
C33	3.671066	-0.613308	1.261664
H34	4.548941	-1.260274	1.274448
H35	3.912384	0.391113	1.610595
H36	2.875105	-1.051354	1.862738
O37	1.931933	0.562863	-0.413224

Zero-point correction=	0.314861 (Hartree/Particle)
Thermal correction to Energy=	0.334022
Thermal correction to Enthalpy=	0.334966
Thermal correction to Gibbs Free Energy=	0.265804
Sum of electronic and zero-point Energies=	–1147.538351
Sum of electronic and thermal Energies=	–1147.519190
Sum of electronic and thermal Enthalpies=	–1147.518246
Sum of electronic and thermal Free Energies=	1147.587409

Appendix E

Supporting Information for Chapter 7

6b

Atom	X	Y	Z
C1	-0.309377	1.039727	-1.420743
C2	-1.830458	0.997887	-1.295387
C3	-2.046074	1.007819	0.223785
C4	-0.946406	0.078558	0.751397
H5	0.160495	-0.836719	-0.604461
H6	0.083031	0.654418	-2.358997
H7	0.067776	2.047550	-1.258357
H8	-2.294088	1.843607	-1.803067
H9	-2.222391	0.077570	-1.736200
H10	-1.909097	2.017811	0.618265
H11	-3.029979	0.653205	0.527195
H12	-0.564582	0.367516	1.725898
N13	0.169613	0.162722	-0.284529
C14	-1.365321	-1.423872	0.826027
O15	-2.268693	-1.697529	1.634028
O16	-0.732298	-2.199140	0.053038
H17	1.843209	-1.405418	0.952936
C18	1.588153	0.417199	0.266404
O19	1.774689	-0.509408	1.309758
C20	1.698905	1.801849	0.885844
H21	1.583081	2.589080	0.142444
H22	0.962983	1.943623	1.677595
H23	2.693234	1.891497	1.323821
C24	2.579161	0.197417	-0.872477
H25	2.452294	0.936572	-1.664080
H26	3.588762	0.290951	-0.471432
H27	2.466480	-0.801394	-1.303003

Zero-point correction=	0.234061 (Hartree/Particle)
Thermal correction to Energy=	0.246190
Thermal correction to Enthalpy=	0.247135
Thermal correction to Gibbs Free Energy=	0.195918
Sum of electronic and zero-point Energies=	–594.313838
Sum of electronic and thermal Energies=	–594.301708
Sum of electronic and thermal Enthalpies=	–594.300764
Sum of electronic and thermal Free Energies=	–594.351981

7b

Atom	X	Y	Z
C1	-0.582384	2.015630	-0.027401
C2	0.834851	2.620406	0.058961
C3	1.790500	1.411410	0.130338
C4	0.939998	0.227546	-0.362509
H5	-0.631246	-0.077236	1.307802
H6	-1.268121	2.417508	0.714361
H7	-1.015457	2.163891	-1.019587
H8	1.035410	3.230081	-0.822526
H9	0.942461	3.259376	0.935254
H10	2.685818	1.527857	-0.476742
H11	2.102199	1.224094	1.160591
H12	0.875614	0.249021	-1.455643
N13	-0.404454	0.553019	0.205031
C14	1.609478	-1.110689	-0.002881
O15	2.725472	-1.311835	-0.444491
O16	1.000447	-1.994781	0.763438
H17	0.014194	-1.746819	0.977660
C18	-1.568555	-0.429140	-0.048708
O19	-1.331796	-1.139969	1.169693
C20	-2.912839	0.285805	0.010265
H21	-3.002260	0.872782	0.925019
H22	-3.073952	0.932198	-0.854870
H23	-3.693212	-0.477001	0.020777
C24	-1.441571	-1.268868	-1.312320
H25	-2.291033	-1.952462	-1.359625
H26	-1.467005	-0.633075	-2.200501
H27	-0.533360	-1.869009	-1.333536

Zero-point correction=	0.227604 (Hartree/Particle)
Thermal correction to Energy=	0.239352
Thermal correction to Enthalpy=	0.240297
Thermal correction to Gibbs Free Energy=	0.189767
Sum of electronic and zero-point Energies=	–594.264718
Sum of electronic and thermal Energies=	–594.252969
Sum of electronic and thermal Enthalpies=	–594.252025
Sum of electronic and thermal Free Energies=	–594.302554

8b

Atom	X	Y	Z
C1	-0.269658	0.548704	-1.646086
C2	-1.806810	0.535247	-1.574412
C3	-2.118716	1.211977	-0.232402
C4	-0.973604	0.704657	0.664624
H5	0.271793	-1.504201	0.652201
H6	0.112106	-0.387641	-2.069279
H7	0.096668	1.369199	-2.269978
H8	-2.264943	1.041945	-2.424366
H9	-2.174194	-0.494863	-1.563353
H10	-2.039685	2.298317	-0.316612
H11	-3.100191	0.963482	0.167816
H12	-0.822977	1.374618	1.514200
N13	0.163671	0.746633	-0.247387
C14	-1.371683	-0.656335	1.292085
O15	-2.385634	-0.753452	1.954335
O16	-0.593900	-1.720256	1.098342
H17	1.964696	-1.310273	-0.745449
C18	1.512635	0.464071	0.136767
O19	1.761062	-1.013797	0.150392
C20	1.797354	0.894633	1.573579
H21	1.592332	1.959459	1.694276
H22	1.190052	0.335119	2.287011
H23	2.845199	0.705351	1.805806
C24	2.513544	1.089325	-0.835789
H25	2.383235	2.172693	-0.855188
H26	3.530090	0.858555	-0.514924
H27	2.380860	0.710131	-1.851207

Zero-point correction=	0.232386 (Hartree/Particle)
Thermal correction to Energy=	0.244493
Thermal correction to Enthalpy=	0.245437
Thermal correction to Gibbs Free Energy=	0.194947
Sum of electronic and zero-point Energies=	–594.309785
Sum of electronic and thermal Energies=	–594.297678
Sum of electronic and thermal Enthalpies=	–594.296733
Sum of electronic and thermal Free Energies=	–594.347224

LM-2

Atom	X	Y	Z
C1	-0.245614	-0.088477	-1.623930
C2	-1.746937	0.195076	-1.596121
C3	-1.848629	1.308558	-0.546832
C4	-0.813557	0.876670	0.516132
H5	-0.505257	-1.288300	0.850097
H6	0.000092	-1.079298	-2.005835
H7	0.258706	0.657456	-2.250920
H8	-2.129625	0.492571	-2.572926
H9	-2.297520	-0.692793	-1.271569
H10	-1.535482	2.262549	-0.977702
H11	-2.845327	1.437617	-0.124996
H12	-0.361776	1.746612	0.994910
N13	0.164901	0.024469	-0.200948
C14	-1.481251	0.054570	1.631348
O15	-2.243785	0.526411	2.446735
O16	-1.161999	-1.238656	1.603800
H17	2.438538	-0.507507	-1.557479
C18	1.611813	0.282230	0.048629
O19	2.346950	-0.740194	-0.626385
C20	1.921504	0.091451	1.532292
H21	1.375449	0.801461	2.154990
H22	1.664194	-0.922652	1.841915
H23	2.988511	0.246319	1.696939
C24	2.068318	1.664779	-0.439635
H25	1.534749	2.463319	0.079627
H26	3.135353	1.784168	-0.244782
H27	1.900880	1.785093	-1.512254

Zero-point correction=	0.232253 (Hartree/Particle)
Thermal correction to Energy=	0.244465
Thermal correction to Enthalpy=	0.245410
Thermal correction to Gibbs Free Energy=	0.194468
Sum of electronic and zero-point Energies=	594.310337
Sum of electronic and thermal Energies=	–594.298124
Sum of electronic and thermal Enthalpies=	–594.297180
Sum of electronic and thermal Free Energies=	–594.348122

LM-2

Atom	X	Y	Z
C1	-0.303033	-0.864642	-0.977222
C2	-1.784072	-0.576529	-1.208032
C3	-1.816211	0.955316	-1.240241
C4	-0.792519	1.347135	-0.151076
H5	-0.610995	0.053468	1.645589
H6	-0.122214	-1.853631	-0.556107
H7	0.254481	-0.774404	-1.916484
H8	-2.155400	-1.030126	-2.127718
H9	-2.382886	-0.958110	-0.375405
H10	-1.459037	1.319236	-2.206368
H11	-2.799668	1.388052	-1.057160
H12	-0.286594	2.275073	-0.422523
N13	0.126175	0.188714	-0.018226
C14	-1.487237	1.604950	1.195324
O15	-2.205717	2.557237	1.407128
O16	-1.246195	0.666544	2.111472
H17	1.772140	1.944958	-1.319786
C18	1.572456	0.482661	0.007629
O19	2.021893	1.015901	-1.256915
C20	2.356864	-0.815278	0.196469
H21	2.002494	-1.347883	1.080456
H22	2.255538	-1.463725	-0.674039
H23	3.414465	-0.580887	0.323309
C24	1.897791	1.468341	1.134902
H25	1.620668	1.051360	2.104487
H26	2.970086	1.667542	1.134529
H27	1.379928	2.422231	1.011112

Zero-point correction=	0.232540 (Hartree/Particle)
Thermal correction to Energy=	0.244709
Thermal correction to Enthalpy=	0.245653
Thermal correction to Gibbs Free Energy=	0.194854
Sum of electronic and zero-point Energies=	–594.313310
Sum of electronic and thermal Energies=	–594.301141
Sum of electronic and thermal Enthalpies=	–594.300197
Sum of electronic and thermal Free Energies=	–594.350996

12b

Atom	X	Y	Z
C1	0.129817	1.680084	-0.921967
C2	-1.383495	1.902583	-0.806147
C3	-1.686664	1.568477	0.659637
C4	-0.768832	0.363895	0.928451
H5	0.229742	-1.536493	-0.692920
H6	0.413316	1.268639	-1.892205
H7	0.689049	2.605397	-0.760617
H8	-1.670152	2.917306	-1.083020
H9	-1.915847	1.210176	-1.464065
H10	-1.392421	2.395390	1.311177
H11	-2.730682	1.328878	0.850842
H12	-0.537910	0.280434	1.991381
N13	0.440510	0.719745	0.165895
C14	-1.461219	-0.968725	0.525699
O15	-2.530423	-1.230617	1.074133
O16	-0.899019	-1.741104	-0.348972
H17	1.945990	-2.050147	-0.801569
C18	1.609244	0.043933	0.223997
O19	1.375661	-1.292781	-0.987543
C20	2.814851	0.725487	-0.377613
H21	2.625620	1.066149	-1.393179
H22	3.073034	1.589381	0.242424
H23	3.662535	0.041946	-0.392302
C24	1.882921	-0.734103	1.493025
H25	2.803056	-1.307836	1.388922
H26	2.010965	-0.027084	2.317479
H27	1.074249	-1.419169	1.742714

Zero-point correction=	0.227060 (Hartree/Particle)
Thermal correction to Energy=	0.239096
Thermal correction to Enthalpy=	0.240040
Thermal correction to Gibbs Free Energy=	0.189728
Sum of electronic and zero-point Energies=	–594.304853
Sum of electronic and thermal Energies=	–594.292816
Sum of electronic and thermal Enthalpies=	–594.291872
Sum of electronic and thermal Free Energies=	–594.342185

13b

Atom	X	Y	Z
C1	0.300082	1.782640	-0.454488
C2	-1.196152	1.819820	-0.764182
C3	-1.834581	1.278158	0.520299
C4	-0.891098	0.136280	0.925038
H5	0.734686	-1.034869	-1.673156
H6	0.923768	1.594824	-1.325779
H7	0.633627	2.690443	0.053520
H8	-1.527188	2.826567	-1.017448
H9	-1.418826	1.161951	-1.607632
H10	-1.843383	2.047840	1.296613
H11	-2.850648	0.912024	0.385680
H12	-0.888107	-0.027978	2.000681
N13	0.442756	0.643198	0.500418
C14	-1.272053	-1.216773	0.229701
O15	-2.344927	-1.701936	0.633929
O16	-0.490992	-1.678450	-0.642212
H17	1.170072	-0.849092	-3.148011
C18	1.582849	0.150743	0.856871
O19	1.454570	-0.678807	-2.244840
C20	2.848680	0.742897	0.330141
H21	2.940000	0.464195	-0.725205
H22	2.840625	1.832668	0.391854
H23	3.707495	0.355932	0.874994
C24	1.696358	-1.015767	1.775707
H25	2.342810	-1.760092	1.302376
H26	2.208580	-0.688475	2.686368
H27	0.751703	-1.481052	2.037146

Zero-point correction=	0.229201 (Hartree/Particle)
Thermal correction to Energy=	0.243433
Thermal correction to Enthalpy=	0.244378
Thermal correction to Gibbs Free Energy=	0.188205
Sum of electronic and zero-point Energies=	–594.326416
Sum of electronic and thermal Energies=	–594.312183
Sum of electronic and thermal Enthalpies=	–594.311239
Sum of electronic and thermal Free Energies=	–594.367411

14b

Atom	X	Y	Z
C1	-0.461584	1.227739	-1.732649
C2	-1.792564	0.498889	-1.540558
C3	-2.123558	0.751944	-0.064918
C4	-0.759074	0.620580	0.622473
H5	0.714289	-3.039686	1.055629
H6	0.193970	0.759653	-2.465075
H7	-0.607343	2.275974	-2.002911
H8	-2.554250	0.874193	-2.223238
H9	-1.664749	-0.570446	-1.723649
H10	-2.517566	1.762261	0.073163
H11	-2.834857	0.042081	0.352415
H12	-0.704587	1.203363	1.539872
N13	0.177596	1.186034	-0.383728
C14	-0.403407	-0.867113	0.967799
O15	-1.177653	-1.400871	1.788176
O16	0.605555	-1.365277	0.407194
H17	-0.242986	-3.620283	2.045412
C18	1.403493	1.524679	-0.160618
O19	0.546210	-3.873921	1.549564
C20	2.027105	1.438815	1.188750
H21	2.288678	2.452147	1.510907
H22	1.409911	0.964020	1.943788
H23	2.965756	0.885724	1.096254
C24	2.258890	2.021342	-1.281811
H25	3.158641	2.494498	-0.893163
H26	2.561541	1.170593	-1.902553
H27	1.725942	2.726168	-1.921527

Zero-point correction=	0.228788 (Hartree/Particle)
Thermal correction to Energy=	0.243249
Thermal correction to Enthalpy=	0.244193
Thermal correction to Gibbs Free Energy=	0.186040
Sum of electronic and zero-point Energies=	–594.324422
Sum of electronic and thermal Energies=	–594.309961
Sum of electronic and thermal Enthalpies=	–594.309017
Sum of electronic and thermal Free Energies=	–594.367170

Imine and water at infinite separation

Atom	X	Y	Z
C1	-0.288923	2.601455	-2.350288
C2	-1.522702	1.721998	-2.141598
C3	-1.797865	1.853584	-0.638925
C4	-0.392242	1.830094	-0.026980
H5	-1.361045	-14.360865	6.305179
H6	0.372039	2.251863	-3.141911
H7	-0.559889	3.641494	-2.546245
H8	-2.355300	2.049547	-2.763504
H9	-1.291495	0.685074	-2.395912
H10	-2.288804	2.806175	-0.421222
H11	-2.407778	1.048717	-0.233882
H12	-0.349086	2.363059	0.920858
N13	0.422562	2.551660	-1.039020
C14	0.143076	0.364953	0.209927
O15	-0.540303	-0.281830	1.034438
O16	1.164033	0.014849	-0.418606
H17	-2.412817	-14.013157	7.352233
C18	1.617495	3.005502	-0.856719
O19	-1.837865	-14.728401	7.057784
C20	2.318090	2.916172	0.454311
H21	2.485278	3.933351	0.824210
H22	1.795288	2.335375	1.206407
H23	3.304551	2.475868	0.286142
C24	2.350764	3.655665	-1.986791
H25	3.235245	4.173023	-1.620248
H26	2.673148	2.886379	-2.696928
H27	1.717944	4.361498	-2.527705

Zero-point correction=	0.226429 (Hartree/Particle)
Thermal correction to Energy=	0.241813
Thermal correction to Enthalpy=	0.242757
Thermal correction to Gibbs Free Energy=	0.178100
Sum of electronic and zero-point Energies=	–594.313662
Sum of electronic and thermal Energies=	–594.298278
Sum of electronic and thermal Enthalpies=	–594.297334
Sum of electronic and thermal Free Energies=	–594.361991

15b

Atom	X	Y	Z
C1	-0.014346	1.813987	0.520568
C2	1.498020	1.808955	0.788377
C3	2.089326	1.092027	-0.434218
C4	1.034645	0.019067	-0.744682
H5	-0.865681	-1.159056	1.374806
H6	-0.593867	1.638620	1.429607
H7	-0.358644	2.750621	0.073637
H8	1.889793	2.817221	0.922150
H9	1.714130	1.240729	1.696318
H10	2.167209	1.776855	-1.282662
H11	3.068393	0.652571	-0.252028
H12	1.072866	-0.288490	-1.788760
N13	-0.223766	0.716715	-0.448622
C14	1.254777	-1.263429	0.116651
O15	2.292449	-1.893516	-0.116416
O16	0.381443	-1.584982	0.996644
H17	-1.883802	-0.549011	2.565408
C18	-1.434232	0.317462	-0.844309
O19	-1.882577	-0.942811	1.682686
C20	-2.603678	0.776121	-0.224118
H21	-2.596447	1.713819	0.320781
H22	-3.544182	0.523691	-0.699122
H23	-2.325992	-0.193758	0.886000
C24	-1.509098	-0.798500	-1.851340
H25	-2.546089	-1.045719	-2.069002
H26	-1.017917	-0.501542	-2.781706
H27	-1.006776	-1.696089	-1.482202

Zero-point correction=	0.223733 (Hartree/Particle)
Thermal correction to Energy=	0.235959
Thermal correction to Enthalpy=	0.236903
Thermal correction to Gibbs Free Energy=	0.185678
Sum of electronic and zero-point Energies=	–594.294389
Sum of electronic and thermal Energies=	–594.282163
Sum of electronic and thermal Enthalpies=	–594.281219
Sum of electronic and thermal Free Energies=	–594.332444

16b

Atom	X	Y	Z
C1	0.538114	1.797696	0.730305
C2	2.014015	1.388524	0.779888
C3	2.231271	0.691402	-0.568342
C4	0.926527	-0.107202	-0.745828
H5	-1.027790	-1.665218	0.989222
H6	0.057544	1.767848	1.709088
H7	0.419430	2.802418	0.316105
H8	2.667180	2.248197	0.930567
H9	2.183514	0.684614	1.598636
H10	2.317002	1.428461	-1.371560
H11	3.105814	0.044417	-0.595256
H12	0.711727	-0.294436	-1.798629
N13	-0.081089	0.807536	-0.185353
C14	1.044006	-1.496844	-0.047707
O15	1.907807	-2.250877	-0.504645
O16	0.294858	-1.761048	0.961942
H17	-2.486022	-2.496885	0.814550
C18	-1.370504	0.829727	-0.538647
O19	-2.127180	-1.606869	0.933483
C20	-2.216988	1.935867	0.032979
H21	-1.833872	2.910737	-0.280075
H22	-3.246936	1.840855	-0.304699
H23	-2.205347	1.915154	1.125680
C24	-1.983182	-0.181286	-1.286995
H25	-2.229568	-1.007032	-0.055117
H26	-2.958289	0.041757	-1.703926
H27	-1.376992	-0.874804	-1.860928

Zero-point correction=	0.223261 (Hartree/Particle)
Thermal correction to Energy=	0.235573
Thermal correction to Enthalpy=	0.236518
Thermal correction to Gibbs Free Energy=	0.184532
Sum of electronic and zero-point Energies=	–594.292571
Sum of electronic and thermal Energies=	–594.280258
Sum of electronic and thermal Enthalpies=	–594.279314
Sum of electronic and thermal Free Energies=	–594.331300

17b

Atom	X	Y	Z
C1	-0.226053	1.865850	0.359109
C2	1.281159	1.939354	0.622532
C3	1.898751	1.276538	-0.615620
C4	0.938578	0.120543	-0.902665
H5	-0.545169	-1.293925	1.781668
H6	-0.803772	1.744401	1.274155
H7	-0.587267	2.745312	-0.181149
H8	1.618353	2.964811	0.772789
H9	1.530563	1.363643	1.517798
H10	1.895662	1.966694	-1.462931
H11	2.914268	0.919459	-0.457905
H12	0.926427	-0.139444	-1.964576
N13	-0.378910	0.667494	-0.500980
C14	1.286922	-1.182983	-0.121861
O15	2.436609	-1.418626	0.206940
O16	0.282501	-1.993389	0.136375
H17	-0.902685	-1.146211	3.266644
C18	-1.538062	0.076544	-0.784386
O19	-0.988545	-0.705956	2.414627
C20	-2.775500	0.642559	-0.151347
H21	-2.871960	1.706795	-0.380902
H22	-3.661233	0.123587	-0.511099
H23	-2.713528	0.538078	0.935475
C24	-1.572745	-1.142076	-1.494392
H25	-2.555294	-1.552790	-1.691890
H26	-0.862525	-1.283919	-2.306977
H27	-0.704559	-1.760595	-0.549023

Zero-point correction=	0.223573 (Hartree/Particle)
Thermal correction to Energy=	0.237327
Thermal correction to Enthalpy=	0.238271
Thermal correction to Gibbs Free Energy=	0.182840
Sum of electronic and zero-point Energies=	–594.294231
Sum of electronic and thermal Energies=	–594.280477
Sum of electronic and thermal Enthalpies=	–594.279533
Sum of electronic and thermal Free Energies=	–594.334964

13

Atom	X	Y	Z
C1	0.364232	1.888120	-0.402470
C2	-1.151571	2.083224	-0.308342
C3	-1.556276	1.179741	0.863360
C4	-0.677830	-0.058215	0.655346
H5	0.746027	1.933862	-1.420535
H6	0.904358	2.604097	0.219415
H7	-1.407821	3.130951	-0.153814
H8	-1.631514	1.745254	-1.229430
H9	-1.316832	1.656579	1.817905
H10	-2.610535	0.910613	0.863520
H11	-0.494276	-0.600478	1.581408
N12	0.594425	0.520924	0.159113
C13	-1.302649	-1.073457	-0.381581
O14	-2.395561	-1.549857	-0.004983
O15	-0.660606	-1.297460	-1.429385
C16	1.728703	-0.096246	0.163977
C17	2.966058	0.523512	-0.388166
H18	2.862203	1.567518	-0.668705
H19	3.768214	0.422419	0.347603
H20	3.273056	-0.054868	-1.266536
C21	1.836528	-1.474094	0.736199
H22	2.837494	-1.872822	0.584214
H23	1.630976	-1.451648	1.811029
H24	1.107451	-2.134939	0.264679

Zero-point correction=	0.204429 (Hartree/Particle)
Thermal correction to Energy=	0.215787
Thermal correction to Enthalpy=	0.216731
Thermal correction to Gibbs Free Energy=	0.166831
Sum of electronic and zero-point Energies=	–517.869070
Sum of electronic and thermal Energies=	–517.857712
Sum of electronic and thermal Enthalpies=	–517.856768
Sum of electronic and thermal Free Energies=	–517.906668

13-*syn*-ts

Atom	X	Y	Z
C1	-0.34962	1.861052	0.347147
C2	1.171351	2.035659	0.361413
C3	1.642092	1.155648	-0.80369
C4	0.730014	-0.0677	-0.7122
H5	-0.79459	1.946305	1.338112
H6	-0.83268	2.585033	-0.31533
H7	1.460174	3.081134	0.254189
H8	1.582885	1.662731	1.302977
H9	1.473446	1.662825	-1.75715
H10	2.69043	0.872963	-0.73685
H11	0.562774	-0.51852	-1.69404
N12	-0.54621	0.496814	-0.1998
C13	1.270913	-1.19713	0.221395
O14	2.461061	-1.23976	0.505284
O15	0.398477	-2.07481	0.63222
C16	-1.69668	-0.16887	-0.20242
C17	-2.86941	0.462963	0.490315
H18	-3.08847	1.439346	0.049193
H19	-3.75147	-0.16681	0.39952
H20	-2.657	0.625221	1.550839
C21	-1.76236	-1.49141	-0.69992
H22	-2.73793	-1.96149	-0.6654
H23	-1.20406	-1.71214	-1.60905
H24	-0.72483	-1.94635	0.115947

Zero-point correction=	0.199709 (Hartree/Particle)
Thermal correction to Energy=	0.209914
Thermal correction to Enthalpy=	0.210858
Thermal correction to Gibbs Free Energy=	0.164087
Sum of electronic and zero-point Energies=	–517.842780
Sum of electronic and thermal Energies=	–517.832575
Sum of electronic and thermal Enthalpies=	–517.831630
Sum of electronic and thermal Free Energies=	–517.878401

13-*syn*

Atom	X	Y	Z
C1	0.435974	1.812742	-0.375437
C2	-1.074122	2.018912	-0.446344
C3	-1.585827	1.157343	0.715507
C4	-0.631587	-0.064921	0.717879
H5	0.939898	2.018130	-1.319252
H6	0.878267	2.448816	0.402009
H7	-1.353212	3.068251	-0.346879
H8	-1.461349	1.652602	-1.401425
H9	-1.469111	1.691110	1.660792
H10	-2.631541	0.864805	0.622562
H11	-0.398668	-0.364237	1.742967
N12	0.559473	0.380729	-0.016326
C13	-1.280181	-1.278445	0.041050
O14	-2.132651	-1.953903	0.570228
O15	-0.866655	-1.523439	-1.209114
C16	1.810089	-0.194889	0.265128
C17	2.986795	0.475429	-0.397400
H18	3.112780	1.503674	-0.047231
H19	3.903385	-0.072535	-0.182261
H20	2.853666	0.514174	-1.482827
C21	1.962906	-1.307313	1.009077
H22	2.949274	-1.732290	1.136240
H23	1.141896	-1.830043	1.481105
H24	-0.154749	-0.873192	-1.392105

Zero-point correction=	0.204953 (Hartree/Particle)
Thermal correction to Energy=	0.215731
Thermal correction to Enthalpy=	0.216676
Thermal correction to Gibbs Free Energy=	0.168394
Sum of electronic and zero-point Energies=	–517.856303
Sum of electronic and thermal Energies=	–517.845524
Sum of electronic and thermal Enthalpies=	–517.844580
Sum of electronic and thermal Free Energies=	–517.892862

13-*anti*

Atom	X	Y	Z
C1	-0.988148	1.684135	0.432796
C2	0.069855	2.525532	-0.286061
C3	1.301564	1.617741	-0.291953
C4	0.694897	0.212526	-0.525078
H5	-0.973218	1.843840	1.515802
H6	-1.995858	1.901309	0.073536
H7	-0.251425	2.726536	-1.311789
H8	0.252650	3.480361	0.208398
H9	2.033108	1.863963	-1.060328
H10	1.801360	1.654870	0.680388
H11	0.644050	-0.003835	-1.595264
N12	-0.626446	0.285369	0.110646
C13	1.606838	-0.831022	0.115017
O14	1.292230	-1.167885	1.376802
O15	2.580632	-1.290936	-0.432899
C16	-1.627293	-0.671615	-0.115758
C17	-1.213322	-1.915217	-0.865246
H18	-0.427015	-2.464764	-0.339815
H19	-2.066103	-2.583650	-0.974424
H20	-0.837298	-1.678327	-1.864234
C21	-2.890219	-0.523260	0.333040
H22	-3.618878	-1.299546	0.143526
H23	-3.217967	0.335738	0.902440
H24	0.452806	-0.717549	1.596191

Zero-point correction=	0.204613 (Hartree/Particle)
Thermal correction to Energy=	0.215567
Thermal correction to Enthalpy=	0.216511
Thermal correction to Gibbs Free Energy=	0.167840
Sum of electronic and zero-point Energies=	–517.852869
Sum of electronic and thermal Energies=	–517.841915
Sum of electronic and thermal Enthalpies=	–517.840971
Sum of electronic and thermal Free Energies=	–517.889642

10B

Atom	X	Y	Z
C1	-1.337084	0.929934	-2.333583
C2	-0.652816	0.097297	-3.418780
C3	-0.858077	-1.335075	-2.910330
C4	-0.654666	-1.181777	-1.389548
H5	0.740183	0.339327	-0.474595
H6	-0.972143	1.956784	-2.288312
H7	-2.418405	0.961984	-2.517514
H8	-1.083902	0.269939	-4.405751
H9	0.413985	0.336394	-3.468561
H10	-1.883820	-1.660581	-3.101385
H11	-0.180454	-2.067449	-3.349205
H12	-1.238704	-1.909246	-0.825719
N13	-1.027205	0.214030	-1.070037
C14	0.808300	-1.434902	-1.001331
O15	1.357746	-2.509498	-1.127899
O16	1.441362	-0.368066	-0.517577
H17	-0.625357	0.333862	1.475518
C18	-1.978655	0.395780	0.060925
O19	-1.395721	-0.212796	1.205527
C20	-2.176795	1.897122	0.299610
H21	-2.766857	2.031500	1.208004
H22	-1.209793	2.385122	0.433167
H23	-2.707971	2.372974	-0.526639
C24	-3.324891	-0.303070	-0.159206
H25	-3.197781	-1.383149	-0.250902
H26	-3.976882	-0.111377	0.694942
H27	-3.818894	0.069305	-1.058385
S28	1.954253	1.115059	2.674434
C29	2.041067	-0.703114	2.792538
H30	2.959950	-0.970145	3.316103
H31	1.174883	-1.024373	3.369806
H32	2.017472	-1.119136	1.786425
C33	3.385426	1.363635	1.574354
H34	3.428466	2.428462	1.348656
H35	4.285408	1.058343	2.109963
H36	3.237962	0.776111	0.669280
O37	0.705215	1.426302	1.816465

Zero-point correction=	0.313339 (Hartree/Particle)
Thermal correction to Energy=	0.332540
Thermal correction to Enthalpy=	0.333484
Thermal correction to Gibbs Free Energy=	0.264890
Sum of electronic and zero-point Energies=	–1147.537170
Sum of electronic and thermal Energies=	–1147.517969
Sum of electronic and thermal Enthalpies=	–1147.517025
Sum of electronic and thermal Free Energies=	–1147.585618

11B

Atom	X	Y	Z
C1	-0.372424	1.664339	-1.461672
C2	0.177455	0.909037	-2.666374
C3	-0.825837	-0.241333	-2.804156
C4	-1.132443	-0.616654	-1.347068
H5	-0.999582	-1.409052	0.907669
H6	0.373339	2.301178	-0.983313
H7	-1.213953	2.301918	-1.773093
H8	0.241476	1.535236	-3.557387
H9	1.176441	0.521254	-2.444987
H10	-1.741464	0.118469	-3.280736
H11	-0.451035	-1.089629	-3.374150
H12	-2.182710	-0.905975	-1.239439
N13	-0.804987	0.593075	-0.542009
C14	-0.327688	-1.831746	-0.852454
O15	0.366404	-2.528277	-1.563653
O16	-0.469633	-2.121757	0.443018
H17	-0.817030	0.151923	2.136761
C18	-1.723895	0.964990	0.550507
O19	-1.610301	-0.051275	1.574912
C20	-3.202021	0.996795	0.144716
H21	-3.341049	1.642783	-0.725493
H22	-3.576112	0.000193	-0.092435
H23	-3.801346	1.388044	0.968513
C24	-1.314053	2.314968	1.147140
H25	-1.513212	3.133620	0.454686
H26	-1.898887	2.484344	2.052561
H27	-0.257934	2.317504	1.415553
S28	2.024631	0.178619	2.788603
C29	2.185844	-1.616999	2.524774
H30	3.207752	-1.822062	2.202216
H31	1.995946	-2.093075	3.486232
H32	1.459827	-1.940332	1.779159
C33	2.254463	0.713379	1.060461
H34	2.269495	1.802539	1.062211
H35	3.210931	0.328999	0.704661
H36	1.416877	0.343006	0.466180
O37	0.534469	0.435338	3.117685

Zero-point correction=	0.314300 (Hartree/Particle)
Thermal correction to Energy=	0.332913
Thermal correction to Enthalpy=	0.333857
Thermal correction to Gibbs Free Energy=	0.267935
Sum of electronic and zero-point Energies=	–1147.534686
Sum of electronic and thermal Energies=	–1147.516073
Sum of electronic and thermal Enthalpies=	–1147.515129
Sum of electronic and thermal Free Energies=	–1147.581051

12B

Atom	X	Y	Z
C1	0.851672	0.140018	1.789006
C2	1.313326	-1.312783	1.968434
C3	2.623615	-1.378570	1.173420
C4	2.314169	-0.504203	-0.052590
H5	0.019856	0.309541	-1.333887
H6	-0.233908	0.222915	1.704154
H7	1.176298	0.767685	2.624276
H8	1.432004	-1.580104	3.018976
H9	0.584111	-1.998833	1.528830
H10	3.440882	-0.926945	1.742354
H11	2.913610	-2.387618	0.886548
H12	3.234406	-0.109883	-0.487780
N13	1.520793	0.583491	0.543151
C14	1.619724	-1.334861	-1.175263
O15	2.233928	-2.327128	-1.588199
O16	0.474161	-0.952657	-1.613708
H17	-1.039411	1.231836	-0.443508
C18	-2.246469	-1.694249	0.532226
O19	-1.843589	-1.759060	1.541723
C20	-2.886404	-2.555167	0.334225
H21	-1.446498	-1.614209	-0.206086
H22	-3.809177	-0.315188	-1.267529
H23	-2.936533	-0.417045	-1.912368
C24	-4.467683	-1.179470	-1.361341
H25	-4.356823	0.598626	-1.493868
H26	-2.294533	1.001368	0.538320
H27	-3.279390	-0.194508	0.471177
S28	1.111275	1.705611	-0.141221
C29	-0.245805	1.319422	-1.054651
H30	2.052191	2.168873	-1.238817
H31	1.627833	3.035391	-1.743555
H32	3.009903	2.448877	-0.794590
C33	2.224076	1.390527	-1.982035
H34	0.599300	2.834929	0.734563
H35	1.424397	3.209045	1.344775
H36	0.225365	3.646001	0.110530
O37	-0.203539	2.506872	1.393792

Zero-point correction=	0.311450 (Hartree/Particle)
Thermal correction to Energy=	0.329788
Thermal correction to Enthalpy=	0.330732
Thermal correction to Gibbs Free Energy=	0.265425
Sum of electronic and zero-point Energies=	–1147.529952
Sum of electronic and thermal Energies=	–1147.511615
Sum of electronic and thermal Enthalpies=	–1147.510671
Sum of electronic and thermal Free Energies=	–1147.575978

13B

Atom	X	Y	Z
C1	0.895287	0.132548	1.797597
C2	1.278316	-1.340128	1.958985
C3	2.642675	-1.434639	1.266144
C4	2.468599	-0.530708	0.038133
H5	-0.313867	0.541244	-1.675498
H6	-0.171436	0.306278	1.656406
H7	1.248618	0.738289	2.634716
H8	1.307596	-1.633052	3.008084
H9	0.556157	-1.977920	1.446308
H10	3.430942	-1.038089	1.911799
H11	2.914220	-2.445968	0.969527
H12	3.418313	-0.130018	-0.307765
N13	1.624557	0.572861	0.570637
C14	1.789800	-1.289247	-1.153336
O15	2.503909	-2.178847	-1.653833
O16	0.619926	-0.957860	-1.476277
H17	-1.357537	1.342721	-0.888985
C18	-2.207282	-1.670582	0.460145
O19	-1.779439	-1.874784	1.440382
C20	-2.852557	-2.497609	0.161369
H21	-1.423334	-1.483489	-0.276793
H22	-3.917036	-0.141434	-1.056541
H23	-3.097583	-0.123132	-1.775183
C24	-4.546211	-1.022982	-1.184342
H25	-4.518403	0.763374	-1.136641
H26	-2.227078	1.009357	0.700980
H27	-3.228463	-0.169562	0.631660
S28	1.517169	1.759714	0.070833
C29	-0.866606	1.347294	-1.732658
H30	2.231351	2.174858	-1.167296
H31	1.468774	2.497789	-1.880438
H32	2.856091	3.043489	-0.938889
C33	2.837353	1.397709	-1.622647
H34	0.678584	2.783213	0.766731
H35	1.150727	3.046053	1.719830
H36	0.594337	3.682074	0.160060
O37	-0.318615	2.397574	0.982680

Zero-point correction=	0.311358 (Hartree/Particle)
Thermal correction to Energy=	0.332170
Thermal correction to Enthalpy=	0.333115
Thermal correction to Gibbs Free Energy=	0.260888
Sum of electronic and zero-point Energies=	–1147.547674
Sum of electronic and thermal Energies=	–1147.526861
Sum of electronic and thermal Enthalpies=	–1147.525917
Sum of electronic and thermal Free Energies=	–1147.598143

11B'

Atom	X	Y	Z
C1	-1.514040	1.568794	-2.216619
C2	-1.526269	0.295790	-3.063542
C3	-1.533315	-0.805744	-1.996390
C4	-0.593318	-0.243203	-0.920835
H5	1.377071	0.779274	-0.038741
H6	-1.121001	2.432281	-2.756739
H7	-2.537748	1.810655	-1.893782
H8	-2.383896	0.251774	-3.736443
H9	-0.615035	0.233860	-3.666680
H10	-2.535944	-0.911786	-1.573540
H11	-1.207846	-1.779184	-2.359977
H12	-0.901486	-0.562431	0.082226
N13	-0.644516	1.227616	-1.074796
C14	0.852136	-0.756697	-1.056483
O15	1.146355	-1.812089	-1.580899
O16	1.798801	0.002802	-0.497117
H17	0.078755	0.932450	1.604621
C18	-0.780302	2.024982	0.155534
O19	0.335816	1.667866	0.997188
C20	-2.093050	1.779473	0.914831
H21	-2.946490	2.069554	0.299293
H22	-2.201264	0.729583	1.191278
H23	-2.111344	2.375924	1.829461
C24	-0.608237	3.505058	-0.178481
H25	-1.430240	3.874294	-0.793795
H26	-0.586623	4.079568	0.748816
H27	0.331140	3.656562	-0.714041
S28	0.604260	-1.515519	3.151886
C29	0.700627	-2.897556	1.967112
H30	1.367626	-3.654429	2.382068
H31	-0.307191	-3.300000	1.873375
H32	1.067180	-2.540008	1.005325
C33	2.302910	-0.887040	2.945420
H34	2.387017	0.007633	3.561066
H35	2.997279	-1.651205	3.297177
H36	2.470061	-0.655203	1.893154
O37	-0.320131	-0.460309	2.498867

Zero-point correction=	0.313302 (Hartree/Particle)
Thermal correction to Energy=	0.332421
Thermal correction to Enthalpy=	0.333365
Thermal correction to Gibbs Free Energy=	0.265178
Sum of electronic and zero-point Energies=	–1147.535121
Sum of electronic and thermal Energies=	–1147.516001
Sum of electronic and thermal Enthalpies=	–1147.515057
Sum of electronic and thermal Free Energies=	–1147.583245

12B'

Atom	X	Y	Z
C1	-0.744648	1.811991	-2.253348
C2	-0.660945	0.768184	-3.377256
C3	-1.661160	-0.312133	-2.945274
C4	-1.467700	-0.363038	-1.420359
H5	0.670871	0.411857	0.098848
H6	0.232691	2.246211	-2.029043
H7	-1.429549	2.625583	-2.508848
H8	-0.888400	1.197261	-4.353714
H9	0.346354	0.345394	-3.422267
H10	-2.684599	0.001482	-3.168531
H11	-1.487029	-1.282212	-3.407899
H12	-2.363991	-0.746896	-0.930467
N13	-1.273194	1.059102	-1.091195
C14	-0.309072	-1.333031	-1.039521
O15	-0.479696	-2.528249	-1.314243
O16	0.737334	-0.855587	-0.468523
H17	0.632717	1.176480	1.574091
C18	-1.142313	1.540565	0.191116
O19	0.482235	1.343104	0.589840
C20	-1.889553	0.752606	1.253415
H21	-2.962630	0.857716	1.078287
H22	-1.636035	-0.305720	1.236682
H23	-1.652360	1.141845	2.242600
C24	-1.301881	3.041355	0.336021
H25	-2.332089	3.313515	0.093556
H26	-1.093551	3.339017	1.363810
H27	-0.627698	3.584161	-0.323904
S28	1.583543	-0.608149	3.477079
C29	0.454844	-1.899196	2.859401
H30	0.882456	-2.868283	3.120459
H31	-0.496475	-1.761088	3.371170
H32	0.349294	-1.796982	1.779164
C33	2.948554	-0.902258	2.305300
H34	3.684604	-0.117077	2.471959
H35	3.382125	-1.876741	2.534426
H36	2.560334	-0.877836	1.286550
O37	0.954362	0.750436	3.070413

Zero-point correction=	0.310538 (Hartree/Particle)
Thermal correction to Energy=	0.329226
Thermal correction to Enthalpy=	0.330170
Thermal correction to Gibbs Free Energy=	0.263477
Sum of electronic and zero-point Energies=	–1147.529339
Sum of electronic and thermal Energies=	–1147.510651
Sum of electronic and thermal Enthalpies=	–1147.509706
Sum of electronic and thermal Free Energies=	–1147.576400

13B'

Atom	X	Y	Z
C1	-0.878512	1.789193	-2.168516
C2	-0.521817	0.777527	-3.258055
C3	-1.491153	-0.381380	-2.993668
C4	-1.519744	-0.474713	-1.459332
H5	1.235372	0.848943	-0.131587
H6	-0.032554	2.377775	-1.817068
H7	-1.681480	2.460007	-2.482747
H8	-0.630438	1.206948	-4.253634
H9	0.510709	0.444669	-3.135887
H10	-2.489009	-0.138992	-3.369031
H11	-1.177278	-1.323924	-3.439686
H12	-2.464812	-0.867653	-1.091912
N13	-1.386465	0.950541	-1.044900
C14	-0.362140	-1.375873	-0.921021
O15	-0.591461	-2.598335	-0.997867
O16	0.676251	-0.809218	-0.491041
H17	1.349891	1.528381	1.220848
C18	-1.642818	1.420739	0.131766
O19	1.532004	1.689349	0.274407
C20	-2.041680	0.552348	1.269384
H21	-2.967869	0.934152	1.706871
H22	-2.158869	-0.497894	1.019461
H23	-1.254608	0.657384	2.026700
C24	-1.489538	2.882584	0.396963
H25	-2.007152	3.478618	-0.357994
H26	-1.874242	3.134825	1.382839
H27	-0.424102	3.128591	0.356291
S28	1.468745	-0.438512	3.399267
C29	0.319451	-1.746551	2.857503
H30	0.746482	-2.710834	3.136388
H31	-0.619870	-1.589631	3.386124
H32	0.189989	-1.668753	1.778354
C33	2.836900	-0.858562	2.267555
H34	3.600813	-0.092123	2.391975
H35	3.230878	-1.832175	2.562816
H36	2.453676	-0.876334	1.247217
O37	0.874197	0.892272	2.881012

Zero-point correction=	0.311531 (Hartree/Particle)
Thermal correction to Energy=	0.332124
Thermal correction to Enthalpy=	0.333068
Thermal correction to Gibbs Free Energy=	0.261429
Sum of electronic and zero-point Energies=	–1147.547838
Sum of electronic and thermal Energies=	–1147.527246
Sum of electronic and thermal Enthalpies=	–1147.526301
Sum of electronic and thermal Free Energies=	–1147.597940

14B

Atom	X	Y	Z
C1	-1.461901	1.536425	-2.148082
C2	-1.354173	0.252421	-2.971903
C3	-1.284057	-0.830447	-1.887299
C4	-0.415155	-0.170082	-0.797850
H5	1.169888	1.257295	-1.324699
H6	-1.135082	2.421893	-2.694496
H7	-2.501111	1.693958	-1.833886
H8	-2.197283	0.124650	-3.652016
H9	-0.435929	0.258604	-3.566986
H10	-2.279883	-1.020578	-1.478985
H11	-0.871269	-1.779432	-2.230167
H12	-0.695475	-0.507188	0.201042
N13	-0.574721	1.291612	-0.984160
C14	1.068533	-0.527589	-0.959476
O15	1.512649	-1.644768	-0.776671
O16	1.830873	0.498979	-1.316913
H17	0.075553	1.011990	1.660421
C18	-0.818889	2.088300	0.253234
O19	0.256478	1.827628	1.145364
C20	-2.159236	1.751144	0.924965
H21	-2.999436	1.971728	0.264199
H22	-2.202035	0.698981	1.211277
H23	-2.269263	2.352692	1.829507
C24	-0.738124	3.571775	-0.101134
H25	-1.543805	3.870028	-0.773679
H26	-0.817439	4.160174	0.814249
H27	0.220426	3.787090	-0.578398
S28	0.616133	-1.522404	3.166821
C29	0.393569	-3.016950	2.149178
H30	1.095258	-3.775644	2.499020
H31	-0.629987	-3.354715	2.307000
H32	0.571885	-2.763338	1.103602
C33	2.311200	-1.107848	2.637227
H34	2.553275	-0.142718	3.080433
H35	2.983919	-1.875813	3.021585
H36	2.347568	-1.063755	1.549088
O37	-0.305199	-0.450710	2.538391

Zero-point correction=	0.313498 (Hartree/Particle)
Thermal correction to Energy=	0.332577
Thermal correction to Enthalpy=	0.333521
Thermal correction to Gibbs Free Energy=	0.265888
Sum of electronic and zero-point Energies=	–1147.537779
Sum of electronic and thermal Energies=	–1147.518700
Sum of electronic and thermal Enthalpies=	–1147.517756
Sum of electronic and thermal Free Energies=	–1147.585389

15B

Atom	X	Y	Z
C1	-1.464742	1.631625	-2.279366
C2	-1.380992	0.535477	-3.338077
C3	-1.504068	-0.740263	-2.497067
C4	-0.693204	-0.414625	-1.233831
H5	0.953658	0.702834	0.320967
H6	-1.035441	2.577125	-2.613640
H7	-2.516804	1.811005	-2.007450
H8	-2.159755	0.631913	-4.096191
H9	-0.407953	0.571319	-3.837649
H10	-2.551573	-0.906596	-2.229199
H11	-1.127218	-1.633887	-2.990852
H12	-1.172880	-0.864932	-0.357421
N13	-0.695722	1.071921	-1.151688
C14	0.758049	-0.982836	-1.221755
O15	1.030317	-1.969691	-1.921488
O16	1.570403	-0.409528	-0.410881
H17	0.330995	0.951333	1.838143
C18	-0.829547	1.711512	0.132954
O19	0.443770	1.360864	0.865226
C20	-2.003801	1.246442	0.998788
H21	-2.932804	1.487266	0.477792
H22	-1.978329	0.174596	1.189214
H23	-2.002326	1.762224	1.960389
C24	-0.804760	3.230075	0.009846
H25	-1.729409	3.599337	-0.435818
H26	-0.706328	3.665403	1.004933
H27	0.041876	3.545835	-0.600930
S28	0.993568	-0.947773	3.526765
C29	0.329866	-2.211346	2.398932
H30	0.799870	-3.162568	2.651731
H31	-0.742758	-2.264462	2.578864
H32	0.551546	-1.926373	1.371370
C33	2.678528	-0.849029	2.846057
H34	3.175149	-0.023002	3.353048
H35	3.182815	-1.787981	3.079239
H36	2.626165	-0.688738	1.768378
O37	0.291595	0.388908	3.130473

Zero-point correction=	0.311241 (Hartree/Particle)
Thermal correction to Energy=	0.329212
Thermal correction to Enthalpy=	0.330156
Thermal correction to Gibbs Free Energy=	0.265289
Sum of electronic and zero-point Energies=	–1147.518024
Sum of electronic and thermal Energies=	–1147.500054
Sum of electronic and thermal Enthalpies=	–1147.499110
Sum of electronic and thermal Free Energies=	–1147.563976

13B-*syn*-ts

Atom	X	Y	Z
C1	-0.555625	0.328807	-2.153705
C2	-0.209997	-1.139755	-2.399212
C3	-1.472531	-1.871804	-1.928671
C4	-1.878194	-1.088015	-0.664947
H5	-0.525632	0.027996	2.146334
H6	0.319805	0.946686	-1.961785
H7	-1.094666	0.755651	-3.005446
H8	0.033904	-1.330477	-3.444580
H9	0.647728	-1.431831	-1.787809
H10	-2.261029	-1.789487	-2.681881
H11	-1.314698	-2.927579	-1.713138
H12	-2.958232	-1.111209	-0.511967
N13	-1.451246	0.288168	-0.973876
C14	-1.224994	-1.711793	0.606478
O15	-1.726767	-2.781298	0.986184
O16	-0.233158	-1.108694	1.133062
H17	0.026852	1.490271	2.517355
C18	-1.891624	1.372311	-0.331307
O19	-0.791561	0.894405	2.605083
C20	-2.692843	1.322369	0.817876
H21	-3.207316	2.239924	1.082180
H22	-3.232888	0.409281	1.050666
H23	-1.616707	1.222806	1.845886
C24	-1.397780	2.707251	-0.822440
H25	-1.652551	2.851449	-1.875608
H26	-1.839283	3.514415	-0.241608
H27	-0.310392	2.776150	-0.735918
S28	2.668980	1.533808	1.804640
C29	2.748715	-0.095440	2.618508
H30	3.628885	-0.614221	2.236254
H31	2.861087	0.091313	3.685645
H32	1.840540	-0.659105	2.403726
C33	2.224806	0.956109	0.136619
H34	2.082399	1.846812	-0.473513
H35	3.058686	0.370706	-0.253380
H36	1.317286	0.353144	0.205631
O37	1.397787	2.234251	2.358463

Zero-point correction=	0.306101 (Hartree/Particle)
Thermal correction to Energy=	0.325215
Thermal correction to Enthalpy=	0.326159
Thermal correction to Gibbs Free Energy=	0.258446
Sum of electronic and zero-point Energies=	–1147.520334
Sum of electronic and thermal Energies=	–1147.501220
Sum of electronic and thermal Enthalpies=	–1147.500276
Sum of electronic and thermal Free Energies=	–1147.567989

14B-*syn*

Atom	X	Y	Z
C1	-0.429754	0.553560	-1.555683
C2	-0.058889	-0.863105	-1.991716
C3	-1.426197	-1.541257	-2.133815
C4	-2.227592	-0.961114	-0.942895
H5	-1.043141	-0.731539	1.342021
H6	0.356303	1.044897	-0.983126
H7	-0.666823	1.173665	-2.429692
H8	0.520842	-0.873989	-2.915420
H9	0.530277	-1.358153	-1.214506
H10	-1.907518	-1.229584	-3.063930
H11	-1.389118	-2.629926	-2.118223
H12	-3.288392	-0.868395	-1.196675
N13	-1.626091	0.344420	-0.716378
C14	-2.177857	-1.935635	0.246357
O15	-2.795335	-2.982075	0.198782
O16	-1.417488	-1.654136	1.297924
H17	0.260414	1.140596	1.726451
C18	-2.332675	1.379572	-0.128459
O19	-0.446397	0.640015	2.203434
C20	-3.481499	1.196901	0.564912
H21	-3.983413	2.047858	1.004448
H22	-3.939620	0.226743	0.706965
H23	-1.227881	1.207570	2.187665
C24	-1.721189	2.752374	-0.271861
H25	-1.670445	3.049351	-1.323521
H26	-2.318894	3.489050	0.263957
H27	-0.700924	2.777715	0.119004
S28	2.984614	1.494062	0.928486
C29	3.306596	0.947237	2.636611
H30	4.301016	0.500935	2.674706
H31	3.268887	1.835242	3.265965
H32	2.539862	0.230715	2.932681
C33	2.999816	-0.145911	0.133579
H34	2.767489	0.006925	-0.919045
H35	3.998828	-0.570829	0.237830
H36	2.250309	-0.779346	0.608513
O37	1.509627	1.958975	0.904452

Zero-point correction=	0.310422 (Hartree/Particle)
Thermal correction to Energy=	0.331021
Thermal correction to Enthalpy=	0.331965
Thermal correction to Gibbs Free Energy=	0.260017
Sum of electronic and zero-point Energies=	–1147.532111
Sum of electronic and thermal Energies=	–1147.511513
Sum of electronic and thermal Enthalpies=	–1147.510569
Sum of electronic and thermal Free Energies=	–1147.582516

13B-*anti*-ts

Atom	X	Y	Z
C1	-0.940734	1.789852	-2.215270
C2	-0.535671	0.802983	-3.319981
C3	-1.423427	-0.423724	-3.064305
C4	-1.495633	-0.482399	-1.531073
H5	0.810061	0.911673	0.214270
H6	-0.085746	2.342315	-1.820720
H7	-1.688670	2.512508	-2.553278
H8	-0.672527	1.228367	-4.314241
H9	0.517110	0.533127	-3.209755
H10	-2.426404	-0.263822	-3.469093
H11	-1.024876	-1.346109	-3.484161
H12	-2.391842	-0.998587	-1.190103
N13	-1.538615	0.940974	-1.160491
C14	-0.261693	-1.230069	-0.929303
O15	-0.242867	-2.458055	-1.110868
O16	0.620194	-0.546550	-0.318006
H17	1.244252	1.564448	1.621321
C18	-1.880297	1.406273	0.038175
O19	0.941547	1.801500	0.687589
C20	-2.483023	0.441561	1.022366
H21	-2.625252	0.922079	1.988069
H22	-3.454448	0.096272	0.657331
H23	-1.851312	-0.437307	1.160142
C24	-1.544475	2.706825	0.455311
H25	-1.374073	3.478425	-0.288490
H26	-2.002467	3.052510	1.375042
H27	-0.173674	2.277452	0.712037
S28	1.977914	-0.395217	3.451297
C29	0.437741	-1.278462	3.042544
H30	0.572554	-2.330936	3.295801
H31	-0.349905	-0.843453	3.656104
H32	0.237426	-1.152267	1.978734
C33	3.021491	-1.107931	2.137774
H34	3.975489	-0.583431	2.172678
H35	3.168231	-2.165292	2.363748
H36	2.522681	-0.977251	1.176163
O37	1.738687	1.085108	3.052436

Zero-point correction=	0.306153 (Hartree/Particle)
Thermal correction to Energy=	0.325419
Thermal correction to Enthalpy=	0.326363
Thermal correction to Gibbs Free Energy=	0.257686
Sum of electronic and zero-point Energies=	–1147.522281
Sum of electronic and thermal Energies=	–1147.503015
Sum of electronic and thermal Enthalpies=	–1147.502071
Sum of electronic and thermal Free Energies=	–147.570748

14B-*anti*

Atom	X	Y	Z
C1	-0.990340	1.882876	-2.147283
C2	-0.435747	0.960494	-3.236637
C3	-1.290932	-0.304839	-3.092701
C4	-1.482777	-0.426049	-1.563645
H5	0.576282	0.240988	-0.155827
H6	-0.227170	2.551148	-1.740677
H7	-1.820365	2.499375	-2.515756
H8	-0.502079	1.406345	-4.229333
H9	0.615604	0.733447	-3.038465
H10	-2.270523	-0.157854	-3.553661
H11	-0.839936	-1.197593	-3.524885
H12	-2.422321	-0.930410	-1.334781
N13	-1.474057	0.959641	-1.112209
C14	-0.382711	-1.318874	-0.958572
O15	-0.420307	-2.523429	-1.109716
O16	0.618442	-0.753347	-0.290928
H17	1.437201	1.543867	1.345373
C18	-2.044661	1.414805	0.057467
O19	0.982225	1.724969	0.484993
C20	-2.597048	0.363735	0.988463
H21	-2.909743	0.817965	1.927403
H22	-3.463758	-0.135535	0.545749
H23	-1.856800	-0.407866	1.214833
C24	-2.085372	2.729786	0.389710
H25	-1.737430	3.514417	-0.268495
H26	-2.529513	3.028716	1.328999
H27	0.153926	2.180978	0.707846
S28	2.267422	-0.295301	3.410987
C29	0.585833	-0.980266	3.242339
H30	0.589390	-1.994743	3.643456
H31	-0.076633	-0.346049	3.829613
H32	0.307105	-0.976487	2.189591
C33	3.085589	-1.363542	2.180613
H34	4.120278	-1.030897	2.109205
H35	3.047121	-2.391456	2.544120
H36	2.570321	-1.264522	1.224871
O37	2.221227	1.118894	2.787735

Zero-point correction=	0.310285 (Hartree/Particle)
Thermal correction to Energy=	0.330785
Thermal correction to Enthalpy=	0.331729
Thermal correction to Gibbs Free Energy=	0.259131
Sum of electronic and zero-point Energies=	–1147.535070
Sum of electronic and thermal Energies=	–1147.514570
Sum of electronic and thermal Enthalpies=	–1147.513626
Sum of electronic and thermal Free Energies=	–1147.586224

Table E1. Energies (in au) and associated changes relative to **6b** (in kcal mol^{-1}) computed for the indicated structures at the B3LYP/6-311++G(d,p)/GD3

	E	Δ	E_{ZPVE}	**Δ**	***H***	**Δ**	***G***	**Δ**
10b	-594.5456	0.0	-594.3130	0.0	-594.3000	0.0	-594.3506	0.0
11b	-594.5420	2.3	-594.3099	2.0	-594.2968	2.0	-594.3475	1.9
12b	-594.5319	8.6	-594.3049	5.1	-594.2919	5.1	-594.3422	5.3
13b	-594.5556	-6.3	-594.3264	-8.4	-594.3112	-7.1	-594.3674	-10.6
14b	-594.5532	-4.7	-594.3244	-7.2	-594.3090	-5.7	-594.3672	-10.4
imine+H2O	-594.5401	3.5	-594.3137	-0.4	-594.2973	1.7	-594.3620	-7.2
13	-518.0735	0.0	-517.8691	0.0	-517.8568	0.0	-517.9067	0.0
13-*syn*-ts	-518.0425	19.5	-517.8428	16.5	-517.8316	15.8	-517.8784	17.7
13-*syn*	-518.0613	7.7	-517.8563	8.0	-517.8446	7.6	-517.8929	8.7
13-*anti*	-518.0575	10.1	-517.8529	10.2	-517.8410	9.9	-517.8896	10.7

Table E2. Energies (in au) and associated changes relative to **10B** (in kcal mol^{-1}) computed for the indicated structures at the B3LYP/6-311++G(d,p)/GD3.

	E	Δ	E_{ZPVE}	**Δ**	***H***	**Δ**	***G***	**Δ**
10B	-1147.8505	0.0	-1147.5370	0.0	-1147.5169	0.0	-1147.5850	0.0
11B	-1147.8490	1.0	-1147.5347	1.5	-1147.5151	1.1	-1147.5811	2.5
12B	-1147.8414	5.7	-1147.5300	4.4	-1147.5107	3.9	-1147.5760	5.7
13B	-1147.8590	-5.3	-1147.5477	-6.7	-1147.5259	-5.6	-1147.5981	-8.3
14B	-1147.8513	-0.5	-1147.5378	-0.5	-1147.5178	-0.5	-1147.5854	-0.3
13B-*syn*-ts	-1147.8264	15.1	-1147.5203	10.5	-1147.5003	10.5	-1147.568	10.7
14B-*syn*	-1147.8425	5.0	-1147.5321	3.1	-1147.5106	4.0	-1147.5825	1.5
11B'	-1147.8484	1.3	-1147.5351	1.2	-1147.5151	1.2	-1147.5832	1.1
15B	-1147.8293	13.3	-1147.5180	11.9	-1147.4991	11.2	-1147.5640	13.2
12B'	-1147.8399	6.7	-1147.5293	4.8	-1147.5097	4.5	-1147.5764	5.4
13B'	-1147.8594	-5.5	-1147.5478	-6.8	-1147.5263	-5.9	-1147.5979	-8.1
13B-*anti*-ts	-1147.8284	13.9	-1147.5223	9.3	-1147.5021	9.3	-1147.5707	8.9
14B-*anti*	-1147.8454	3.3	-1147.5351	1.2	-1147.5136	2.1	-1147.5862	-0.8